博士論文

Growth of continents during the Archean and Proterozoic eons:

isotopic and geochemical analyses of 3.4－2.2 billion year old sandstones from southern Africa, North America, and western Australia

（太古代・原生代の大陸成長：アフリカ南部、北アメリカ、および

オーストラリア西部の 34～22 億年前砂岩の同位体および地球化学分析）

Hikaru Sawada 沢田 輝

Index

Chapter 1. General introduction

The occurrence of vast granitic continental crust, as well as continuing active plate subduction, is one of the unique features of the Earth among the planets of our Solar system. In the framework of plate tectonics (Wilson, 1965; Morgan, 1968), plate boundaries of subduction zones are characterized by the production of granitic continental crust through arc magmatism, and also by secondary modification of the crustal rocks through sedimentary and metamorphic processes (Dewey and Bird, 1970; Matsuda and Uyeda, 1971; Fig. 1-1). Oceanic plates, in general, subduct into the mantle beneath other plates, and disappear from the Earth's surface within several hundred million years after their birth at mid-oceanic ridges. In contrast, continental crusts often preserve rocks and minerals of over four billion years-long the Earth's history (Fig. 1-2). Therefore, the growth history of continental crust has been the main topic of discussion on the evolution of solid Earth for years (Fig. 1-3).

Given a unidirectional production process of new granitic continental crusts, age structure of the extant continental crust directly represents the total growth history of the continental crust. The age structure of the extant continents, however, does not record the real growth history of continental crust, mainly because continental crust once-formed have suffered secondary modification and destruction; i.e. reworking and recycling. Technical terms of 'reworking' and 'recycling' of continental crust have been used in different sense, and thus we need to use them under strict definition to avoid confusion. In this study, according to recent common usage (Cawood et al., 2013; Rollinson, 2017), "reworking" is referred to a process, in which pre-existing crust is transformed apparently into younger one within crust by re-melting and/or high-grade metamorphism, whereas "recycling" is used for a process of transportation of pre-existing crust from the surface of the Earth into the mantle (Fig. 1-1).

To demonstrate age structure of the modern continents, Hurley and Rand (1969) compiled available whole-rock geochronological data over the world before 1960's. They showed that older crusts are rarer; for example, >2.3 Ga crusts (i.e. the first half of the Earth history) merely occupy no more than 20 percent of total continental volume, and 3 Ga ones are extremely rare, less than 1 percent of that (Fig. 1-4). Taking into crustal reworking and recycling into the consideration on the age structure of the modern continents, many studies aiming to reconstruct growth history of continental crust appeared by the 1990's (Figure 1-4). Those studies can be classified into two groups; i.e. one is suggesting rapid crustal production on the early Earth and

subsequent significant amount of crustal recycling (Fyfe, 1978; Armstrong, 1981), and the other is proposing progressive growth crust with minor amount of crustal recycling (O'Nions et al., 1979; Dewey and Windley, 1981; Allegre, 1982; McLennan and Taylor, 1982; Reymer and Schubert, 1984).

Material from reworked continental crust is petrologically represented by S-type granitoid, which represents one of the most typical end members of re-melted crustal rocks (Chappell and White, 1974). Isotopic signatures in crustal rocks and minerals, such as Rb-Sr, U-Th-Pb, Sm-Nd, and Lu-Hf systematics, are significant in estimate degree and timing of reworking of continental crust (Hurley et al., 1962; Patterson and Tatsumoto, 1968; DePaolo and Wasserburg, 1976; DePaolo, 1981; Wyllie, 1984). Geologic structures of continental crusts and secular change in mass balance of the crusts had also been investigated on the basis of geological observation (Dewey and Windley, 1981; Reymer and Schubert, 1984). On the other hand, information for recycling of continental crust had been limited because subducted continental crust usually does not leave apparent geological trace on continents. Fyfe (1978) considered that, on the early warmer Earth, a huge amount of continental crust was produced through multiple hotspot-like settings without plate subduction, and that the total amount of continental crust became greater in history in the beginning, then has decreased through sediment subduction since the onset of plate subduction sometime in the Archean (Fig. 1-2). Armstrong (1981) also emphasized rapid production of continental crust during the Hadean and early Archean, and subsequent steady-state balance between new input of juvenile continental crust and crustal recycling (Fig. 1-2). However, from the view of geological evidence at that time, the amount of continental crustal recycling and its secular change was totally unknown. Many other studies during the 1980-1990s considered crustal recycling had been minor simply because the density of granitoids is much smaller than that of mantle peridotite, thus a progressive growth of continental crust has occurred through the history of the Earth (O'Nions et al., 1979; Dewey and Windley, 1981; Allegre, 1982; McLennan and Taylor, 1982; Reymer and Schubert, 1984; Fig. 1-2).

During the 1990s and 2000s, two major progresses in understanding of the growth history of continental crust were achieved; one is the finding of granitic subduction into the mantle, and the other is the development of *in-situ* analytical technique of zircon. The observations of modern trenches along subduction zone clarified that plate subduction can cause significant volume loss of granitic continental crust through sediment subduction, subduction erosion (tectonic erosion) (von Huene and Lallemand, 1990; Scholl and von Huene, 2007; 2009; Clift et al., 2009; Isozaki

et al., 2010) and island arc subduction (Yamamoto et al., 2009; Santosh et al., 2009). Global balance between production and destruction of continental crust for modern continents may indicate that the rate of destruction equals or even exceeds the production (Clift et al., 2009; Stern and Scholl, 2010; Fig. 1-5). As these estimations do not include island arc subduction, the destruction of continental crust is likely more voluminous than production of it on the modern Earth.

Zircon is an accessary mineral commonly contained in crustal rocks, especially in granitoids. The recent technical development in U-Pb dating of single-grain zircon has made it possible to perform precise and rapid *in-situ* by using SHRIMP (Froude et al., 1983; Stern, 1997) and LA-ICPMS (Hirata and Nisbett, 1995). Furthermore, zircon Lu-Hf isotopic analysis combined with the U-Pb age dating is one of the most powerful tools to identify source material of host rock and its degree of crustal reworking (Thirwall and Walder, 1995; Vervoort et al. 1996; Knudsen et al., 2001; Griffin et al., 2004). By U-Pb age dating of many detrital zircon grains from a sandstone, age pattern of continental crust in provenance of the sandstone can be estimated (Gehrels and Dickinson, 1995; Gehrels et al., 1995). Rino et al. (2004) and (2008) performed U-Pb age dating of detrital zircons in river sands from 16 modern large river over the world and estimated igneous age structure of modern extant continents (Fig. 1-5). Through comparison, the age structure by Rino et al. with age pattern of the orogenic belts shown in Fig. 1-3 (Utsunomiya et al., 2009), it is confirmed that the old crust before ca. 2 Ga is rare in the modern continents, even after exclusion effect of intra-crustal sedimentary process. Zircon analysis also contributed significantly for finding the oldest geological record of the Earth; e.g. the 4.03 Ga Acasta gneiss in Slave Craton in northern Canada as the oldest unit (Bowring and Williams, 1999), and 4.37 Ga early Hadean detrital zircon from the Jack Hills meta-conglomerate in the Yilgarn Craton in western Australia as the oldest crustal material (Wilde et al., 2001; Holden et al., 2008; Isozaki et al., 2018). Further Hadean 4.2-4.0 Ga zircon has been found from many localities (Fig. 1-6). These occurrences of Hadean zircon indicate that production of continental crust had prevailed by ca. 4.2 Ga.

These new findings by 2010 require either significant degree of crustal reworking and recycling have been destroyed Hadean and Archean continental crusts or suppressed production mechanism of granitic crust on the early Earth. By compiling of a large number of zircon U-Pb and Lu-Hf isotopic data, possible models for the growth history of continental crust including crustal recycling have been proposed (Belousova et al., 2010; Dhime et al., 2012). Even though these studies took crustal recycling into the account, they treated amount of recycling as a

simplified parameter in their numerical calculation. Though details in method of data reduction and calculation were different between those studies, they commonly concluded that over 70 % volume of the modern continental crust had been formed by ca. 3 Ga, and after that, reworking of those crust has dominated over net production of juvenile crust formation from the mantle (Fig. 1-5). In order to explain the few preservations of the ancient continental crust despite of the active production, they interpreted that plate subduction start at ca. 3 Ga, and that pre-3 Ga crust was dominantly mafic (Fig. 1-6). However, these previous compilation of zircon data did not consider the effect of depositional age. Thus, the results likely reflected superimposing of once-formed and recycled crust and failed to capture actual crustal increase and decrease.

Plate subduction during the Archean has been considered as to be unlikely because of buoyant oceanic plates in regards of thick basaltic crust, approximately five times thicker than the present (Davies, 1992; 1995), or highly depleted and mechanically strong peridotitic lithosphere (Davaille and Jaupart, 1993; Solomatov, 1995). Under a tectonic regime without plate subduction, a single plate on the Earth, i.e. 'stagnant-lid', covered the surface of the Earth, thus crust can be formed only by mantle plume upwelling (Solomatov, 1995). These claims, however, can be reasonably refuted by relatively light low-viscosity asthenosphere by considering slab melting and mineral-phase change in deeper mantle (Nisbet and Fowler, 1983; Komiya et al., 2004). When thick basaltic oceanic crust subduct into high-temperature mantle, granitic magma is produced by slab melting and garnet-bearing residue heavier than mantle peridotite, and forms to promote plate subduction (Komiya et al., 2004). Furthermore, 4.0-3.8 Ga accretionary complexes with oceanic plate stratigraphy and duplex structures have been identified from the Isua Greenstone belt and Nulliak supracrustal rocks in the North Atrantic Craton (Maruyama et al., 1991; Komiya et al., 1999; 2015; 2016; Shimojo et al., 2016). Therefore, recycling of the continental crust into the mantle during the early Earth can be expected.

By assuming onset of plate subduction before 4 Ga, Komiya (2011) estimated production, reworking, and recycling of continental crust on the basis of U-Pb age and Hf model age of detrital zircon from modern river sand (Rino et al., 2008; Iizuka et al., 2010) and mantle potential temperature (Komiya, 2004). He searched values of continental erosion rate (i.e. total sediment flux) to fit the constraint conditions. As a result, he proposed a model of continental growth history in which rapid crustal growth in the Archean and Paleoproterozoic, peak of total amount at ca. 1.8 Ga, and subsequent decrease (Fig. 1-5). The calculation, however, was carried out based on assumption that continental erosion is unrelated to the age of geological bodies; however this assumption appears highly unrealistic because relatively young crusts along subduction zones

are more likely recycled into the mantle as shown in modern active continents (Fig. 1-1, 1-2).

To improve understandings on growth history of the continental crust, this study focuses on secular change in size of individual continental blocks, because it may be a major controlling factor in determine preservation / destruction of continental crust. If the size of continental blocks were smaller than those of modern ones, total length of plate boundary and ratio of plate convergent margin to total area of continental block was larger than present (Fig. 1-7). Oceanic island arc-like smaller continental blocks should have been easily destructed and subducted into the mantle by arc subduction, and they could not stay on the surface of the Earth for a long time (Yamamoto et al., 2009; Santosh et al., 2009). Under this regime, both production of juvenile continental crust and destruction of pre-existing continental crust (i.e. recycling and reworking) could have been occurred.

On the other hand, after the size of continental block increased, preservation of older crust has likely increased. From geological evidences, the Rodinia Supercontinent formed ca. 1.3-1.1 Ga and rifted ca. 1.0-0.7 Ga is the oldest supercontinent of which paleogeography is well constrained by paleomagnetic analysis and similarity of geological units (Moores, 1991; Karlstrom et al., 2001; Li et al., 2008; Evans, 2009). Even though several Proterozoic and Archean continents before 1.3 Ga have been proposed such as Columbia (Rogers and Santosh, 2002), Sclavia, Superia, and Vaalbara (Bleeker, 2003), paleogeography and size of these continents are still not constrained. Nonetheless, the 2.0-1.8 Ga shield of 'Nuna continent' preserved in modern North American continent is the strong evidence for the existence of a continental block > 5,000 km square since ca. 1.8 Ga (Hoffman, 1988).

In short, the size of pre-ca. 2.0 Ga continental blocks and its secular change are yet not well constrained (Fig. 1-8). This study aims to clarify the change in size of continental blocks from the middle Archean to the Paleoproterozoic, i.e. between ca. 3.5 and 2.0 Ga era. After this introduction, results of detrital zircon analyses, such as U-Pb dating and Lu-Hf isotopic analysis, are described in chapters 2-5. In Chapter 2, on the basis of data compilation of detrital zircon U-Pb ages from sandstones, the secular change in average lifespan of continental crust and size of continental blocks since ca. 3 Ga are discussed. To explore continental growth before 3 Ga, this study reports newly obtained U-Pb and Lu-Hf data from the Murmac Bay Group in the Rae Craton, Canada in Chapter 3. Chapter 4 focused on the pre-3 Ga continental growth through zircon U-Pb ages of the Shurugwi Greenstone Belt in the Zimbabwe Craton, southern Africa, whereas Chapter 5 describes detrital zircon U-Pb ages from the ca. 2.2-2.1 Ga Magondi Supergroup in the Zimbabwe Craton. Chapter 6 reports newly obtained whole-rock composition of major, minor

and trace elements in sandstone deposited between ca. 3.4-0.1 Ga to estimate degree of sedimentary sorting, and discusses relationship between sedimentary sorting of minerals in detrital grains and change in size of provenance.

References

Armstrong, R. L.1981. Radiogenic isotopes: the case for crustal recycling on a near-steady-state no-continental-growth Earth [and discussion]. Philosophical Transactions of the Royal Society of London A: Mathematical, Physical and Engineering Sciences, 3011461, 443-472.

Belousova, E. A., Kostitsyn, Y. A., Griffin, W. L., Begg, G. C., O'Reilly, S. Y., and Pearson, N. J. 2010. The growth of the continental crust: constraints from zircon Hf-isotope data. Lithos, 1193, 457-466.

Bleeker, W. 2003. The late Archean record: a puzzle in ca. 35 pieces. Lithos,712, 99-134.

Bowring, S. A., & Williams, I. S. (1999). Priscoan (4.00–4.03 Ga) orthogneisses from northwestern Canada. Contributions to Mineralogy and Petrology, 134(1), 3-16.

Bradley, D. C. (2011). Secular trends in the geologic record and the supercontinent cycle. *Earth-Science Reviews*, *108*(1-2), 16-33.

Byerly, B. L., Lowe, D. R., Drabon, N., Coble, M. A., Burns, D. H., & Byerly, G. R. (2018). Hadean zircon from a 3.3 Ga sandstone, Barberton greenstone belt, South Africa. *Geology*, *46*(11), 967-970.

Clift, P. D., Vannucchi, P., and Morgan, J. P. 2009. Crustal redistribution, crust–mantle recycling and Phanerozoic evolution of the continental crust.Earth-Science Reviews, 971, 80-104.

Compston, W. T., and Pidgeon, R. T. (1986). Jack Hills, evidence of more very old detrital zircons in Western Australia. Nature, 321(6072), 766.

Cui, P.L., Sun, J.G., Sha, D.M., Wang, X.J., Zhang, P., Gu, A.L., and Wang, Z.Y. (2013): Oldest zircon xenocryst (4.17 Ga) from the north China craton.*International Geology Review*, **55**,

1902-1908.

Davies, G.F. (1992): On the emergence of plate tectonics. Geology, 20, 963-966.

Davaille, A. and Jaupart, C. (1993): Transient high-Rayleigh-number thermal convection with large viscosity variations. Journal of Fluid Mechanics, 253, 141-166.

Dewey, J. F., & Bird, J. M. (1970). Mountain belts and the new global tectonics. *Journal of Geophysical Research*, *75*(14), 2625-2647.

Dewey, J. F., & Windley, B. F. (1981). Growth and differentiation of the continental crust. Phil. Trans. R. Soc. Lond. A, 301(1461), 189-206.

de Wit, M. J., and Hart, R. A. 1993. Earth's earliest continental lithosphere, hydrothermal flux and crustal recycling. Lithos, 303, 309-335.

Dhuime, B., Hawkesworth, C. J., Cawood, P. A., and Storey, C. D. (2012). A change in the geodynamics of continental growth 3 billion years ago. Science, 335(6074), 1334-1336.

Diwu, C., Sun, Y., Wilde, S. A., Wang, H., Dong, Z., Zhang, H. and Wang, Q. (2013): New evidence for ~ 4.45 Ga terrestrial crust from zircon xenocrysts in Ordovician ignimbrite in the North Qinling Orogenic Belt, China. Gondwana Research, 23, 1484-1490.

Froude, D. O., Ireland, T. R., Kinny, P. D., Williams, I. S., Compston, W., Williams, I. T., and Myers, J. S. (1983). Ion microprobe identification of 4,100–4,200 Myr-old terrestrial zircons. Nature, 304(5927), 616.

Fyfe, W. S. 1978. The evolution of the Earth's crust: modern plate tectonics to ancient hot spot tectonics?. Chemical Geology, 231, 89-114.

Gehrels, G. E., Dickinson, W. R., Ross, G. M., Stewart, J. H., and Howell, D. G. 1995. Detrital zircon reference for Cambrian to Triassic miogeoclinal strata of western North America. Geology, 239, 831-834.

Gehrels, G. E., and Dickinson, W. R. 1995. Detrital zircon provenance of Cambrian to Triassic miogeoclinal and eugeoclinal strata in Nevada. American Journal of Science, 2951, 18-48.

Hawkesworth, C., Cawood, P., Kemp, T., Storey, C., and Dhuime, B. (2009). A matter of preservation. Science, 323(5910), 49-50.

Hirata, T., & Nesbitt, R. W. (1995). U-Pb isotope geochronology of zircon: Evaluation of the laser probe-inductively coupled plasma mass spectrometry technique. *Geochimica et cosmochimica Acta*, *59*(12), 2491-2500.

Hurley, P. M., and Rand, J. R. 1969. Pre-drift continental nuclei. Science, 1643885, 1229-1242.

Hoffman, P. F. 1988. United Plates of America, the birth of a craton-Early Proterozoic assembly and growth of Laurentia. Annual Review of Earth and Planetary Sciences, 16, 543-603.

Holden, P., Lanc, P., Ireland, T. R., Harrison, T. M., Foster, J. J., and Bruce, Z. (2009). Mass-spectrometric mining of Hadean zircons by automated SHRIMP multi-collector and single-collector U/Pb zircon age dating: The first 100,000 grains. International Journal of Mass Spectrometry, 286(2-3), 53-63.

Iizuka, T., Hirata, T., Komiya, T., Rino, S., Katayama, I., Motoki, A., & Maruyama, S. (2005). U-Pb and Lu-Hf isotope systematics of zircons from the Mississippi River sand: Implications for reworking and growth of continental crust. *Geology*, *33*(6), 485-488.

Iizuka, T., Horie, K., Komiya, T., Maruyama, S., Hirata, T., Hidaka, H., & Windley, B. F. (2006). 4.2 Ga zircon xenocryst in an Acasta gneiss from northwestern Canada: Evidence for early continental crust. Geology, 34(4), 245-248.

Iizuka, T., Komiya, T., Rino, S., Maruyama, S., & Hirata, T. (2010). Detrital zircon evidence for Hf isotopic evolution of granitoid crust and continental growth. Geochimica et Cosmochimica Acta, 74(8), 2450-2472.

Iizuka, T., Campbell, I. H., Allen, C. M., Gill, J. B., Maruyama, S., & Makoka, F. (2013). Evolution of the African continental crust as recorded by U–Pb, Lu–Hf and O isotopes in detrital zircons from modern rivers. Geochimica et Cosmochimica Acta, 107, 96-120.

Isozaki, Y., Aoki, K., Nakama, T., and Yanai, S. 2010. New insight into a subduction-related orogen: a reappraisal of the geotectonic framework and evolution of the Japanese Islands. Gondwana Research, 181, 82-105.

Isozaki, Y., Yamamoto, S., Sakata, S., Obayashi, H., Hirata, T., Obori, K. I., ... and Maruyama, S. (2018). High-reliability zircon separation for hunting the oldest material on Earth: An automatic zircon separator with image-processing/microtweezers-manipulating system and double-step dating. Geoscience Frontiers, 9(4), 1073-1083.

Knudsen, T. L., Griffin, W., Hartz, E., Andresen, A., & Jackson, S. (2001). In-situ hafnium and lead isotope analyses of detrital zircons from the Devonian sedimentary basin of NE Greenland: a record of repeated crustal reworking. *Contributions to Mineralogy and Petrology*, *141*(1), 83-94.

Komiya, T., Maruyama, S., Masuda, T., Nohda, S., Hayashi, M., and Okamoto, K. 1999. Plate tectonics at 3.8–3.7 Ga: field evidence from the Isua accretionary complex, southern West Greenland. The Journal of geology, 1075, 515-554.

Komiya, T., Maruyama, S., Hirata, T., and Yurimoto, H. 2002. Petrology and geochemistry of MORB and OIB in the mid-Archean North Pole region, Pilbara craton, Western Australia: implications for the composition and temperature of the upper mantle at 3.5 Ga. International Geology Review, 4411, 988-1016.

Komiya, T., Maruyama, S., Hirata, T., Yurimoto, H., and Nohda, S. 2004. Geochemistry of the oldest MORB and OIB in the Isua Supracrustal Belt, southern West Greenland: implications for the composition and temperature of early Archean upper mantle. Island Arc, 131, 47-72.

Komiya, T. 2004. Material circulation model including chemical differentiation within the mantle and secular variation of temperature and composition of the mantle. Physics of the Earth and Planetary Interiors, 1461, 333-367.

Komiya, T. (2011). Continental recycling and true continental growth. Russian Geology and Geophysics, 52(12), 1516-1529.

Komiya, T., Yamamoto, S., Aoki, S., Sawaki, Y., Ishikawa, A., Tashiro, T., Koshida, K., Shimojo, M., Aoki, K., and Collerson, K. D. 2015. Geology of the Eoarchean,> 3.95 Ga, Nulliak supracrustal rocks in the Saglek Block, northern Labrador, Canada: The oldest geological evidence for plate tectonics. Tectonophysics, 662, 40-66.

Li, Z. X., Bogdanova, S. V., Collins, A. S., Davidson, A., De Waele, B., Ernst, R. E., ... & Karlstrom, K. E. (2008). Assembly, configuration, and break-up history of Rodinia: a synthesis. Precambrian research, 160(1-2), 179-210.

Li, Z., Chen, B. and Wei, C. (2016): Hadean detrital zircon in the North China Craton. Journal of Mineralogical and Petrological Sciences, 111, 283-291.

Martel, E., van Breemen, O., Berman, R.G. and Pehrsson, S. (2008): Geochronology and

tectonometamorphic history of the Snowbird Lake area, Northwest Territories, Canada: New insights into the architecture and significance of the Snowbird tectonic zone. Precambrian Research, 161, 201-230.

Maruyama, S., Masuda, S., and Appel, P. W. U. 1991. The oldest accretionary complex on the Earth, Isua, Greenland. Geological Society of America Abstract 23, A429-430.

Maruyama, S., Yuen, D. A., and Windley, B. F. 2007. Dynamics of plumes and superplumes through time. In Superplumes: Beyond Plate Tectonics pp. 441-502. Springer Netherlands.

McCulloch, M. T., and Bennett, V. C. 1994. Progressive growth of the Earth's continental crust and depleted mantle: geochemical constraints. Geochimica et Cosmochimica Acta, 5821, 4717-4738.

McLennan, S. M., and Taylor, S. R. 1982. Geochemical constraints on the growth of the continental crust. The Journal of Geology, 347-361.

Mojzsis, S.J. and Harrison, T.M. (2002): Establishment of a 3.83-Ga magmatic age for the Akilia tonalite (southern West Greenland). Earth and Planetary Science Letters, 202, 563-576.

Moores, E. M. 1991. Southwest US-East Antarctic SWEAT connection: a hypothesis. Geology, 195, 425-428.

Morgan, W. J. (1968). Rises, trenches, great faults, and crustal blocks. *Journal of Geophysical Research*, *73*(6), 1959-1982.

Nadeau, S., Chen, W., Reece, J., Lachhman, D., Ault, R., Faraco, M.T.L., Fraga, L.M., Reis, N.J. and Betiollo, L.M. (2013): Guyana: the lost Hadean crust of South America?. Brazilian Journal of Geology, 43, 601-606.

Paquette, J.L., Barbosa, J.S.F., Rohais, S., Cruz, S.C.P., Goncalves, P., Peucat, J.J., Leal, A.B.M., Santos-Pinto, M. and Martin, H. (2015): The geological roots of South America: 4.1 Ga and 3.7 Ga zircon crystals discovered in NE Brazil and NW Argentina. Precambrian Research, 271, 49-55.

Rino, S., Komiya, T., Windley, B. F., Katayama, I., Motoki, A., & Hirata, T. (2004). Major episodic increases of continental crustal growth determined from zircon ages of river sands; implications for mantle overturns in the Early Precambrian. *Physics of the Earth and Planetary*

Interiors, *146*(1-2), 369-394.

Rino, S., Kon, Y., Sato, W., Maruyama, S., Santosh, M., and Zhao, D. 2008. The Grenvillian and Pan-African orogens: world's largest orogenies through geologic time, and their implications on the origin of superplume. Gondwana Research, 141, 51-72.

Rogers, J. J., and Santosh, M. 2003. Supercontinents in Earth history. Gondwana Research, 63, 357-368.

Rollinson, H. (2017). There were no large volumes of felsic continental crust in the early Earth. *Geosphere*, *13*(2), 235-246.

Scholl, D. W., and von Huene, R. 2007. Crustal recycling at modern subduction zones applied to the past—Issues of growth and preservation of continental basement crust, mantle geochemistry, and supercontinent reconstruction. Geological Society of America Memoirs, 200, 9-32.

Scholl, D. W., and von Huene, R. 2009. Implications of estimated magmatic additions and recycling losses at the subduction zones of accretionary non-collisional and collisional suturing orogens. Geological Society, London, Special Publications, 3181, 105-125.

Shimojo, M., Yamamoto, S., Sakata, S., Yokoyama, T.D., Maki, K., Sawaki, Y., Ishikawa, A., Aoki, K., Aoki, S., Koshida, K. and Tashiro, T. (2016): Occurrence and geochronology of the Eoarchean, ~ 3.9 Ga, Iqaluk Gneiss in the Saglek Block, northern Labrador, Canada: Evidence for the oldest supracrustal rocks in the world. Precambrian Research, 278, 218-243.

Solomatov, V.S. (1995): Scaling of temperature- and stress-dependent viscosity convection. Physics of Fluids, 7, 266-274.

Stern, R.A. (1997): The GSC Sensitive High Ion Microprobe (SHRIMP) : analytical techniques of zircon U-Th-Pb age determinations and performance evaluation, Geol. Surv. Can. Curr. Res., 1-31.

Stern, R. J., & Scholl, D. W. (2010). Yin and yang of continental crust creation and destruction by plate tectonic processes. *International Geology Review*, *52*(1), 1-31.

Stern, C. R. 2011. Subduction erosion: rates, mechanisms, and its role in arc magmatism and the evolution of the continental crust and mantle. Gondwana Research, 202, 284-308.

Thirlwall, M. F., & Walder, A. J. (1995). In situ hafnium isotope ratio analysis of zircon by inductively coupled plasma multiple collector mass spectrometry. *Chemical Geology*, *122*(1-4), 241-247.

Yamamoto, S., Senshu, H., Rino, S., Omori, S., and Maruyama, S. 2009. Granite subduction: arc subduction, tectonic erosion and sediment subduction. Gondwana Research, 153, 443-453.

Vervoort, J. D., Patchett, P. J., Gehrels, G. E., & Nutman, A. P. (1996). Constraints on early Earth differentiation from hafnium and neodymium isotopes. *Nature*, *379*(6566), 624.

von Huene, R., and Lallemand, S. 1990. Tectonic erosion along the Japan and Peru convergent margins. Geological Society of America Bulletin, 1026, 704-720.

Wilde, S. A., Valley, J. W., Peck, W. H., and Graham, C. M. (2001). Evidence from detrital zircons for the existence of continental crust and oceans on the Earth 4.4 Gyr ago. Nature, 409(6817), 175.

Wilson, J. T. (1965). A new class of faults and their bearing on continental drift. Nature, 207(4995), 343.

Wyche, S. (2007): Evidence of pre-3100 Ma crust in the Youanmi and south west terranes, and eastern goldfields superterrane, of the Yilgarn craton. Developments in Precambrian Geology, 15, 113-123.

Wyche, S., Nelson, D.R. and Riganti, A. (2004): 4350-3130 Ma detrital zircons in the Southern Cross Granite–Greenstone Terrane, Western Australia: Implications for the early evolution of the Yilgarn Craton. Australian Journal of Earth Sciences, 51, 31-45.

Xing, G.F., Wang, X.L., Wan, Y., Chen, Z.H., Jiang, Y., Kitajima, K., Ushikubo, T. and Gopon, P. (2014): Diversity in early crustal evolution: 4100 Ma zircons in the Cathaysia Block of southern China. Scientific Reports, 4, 5143.

Figures

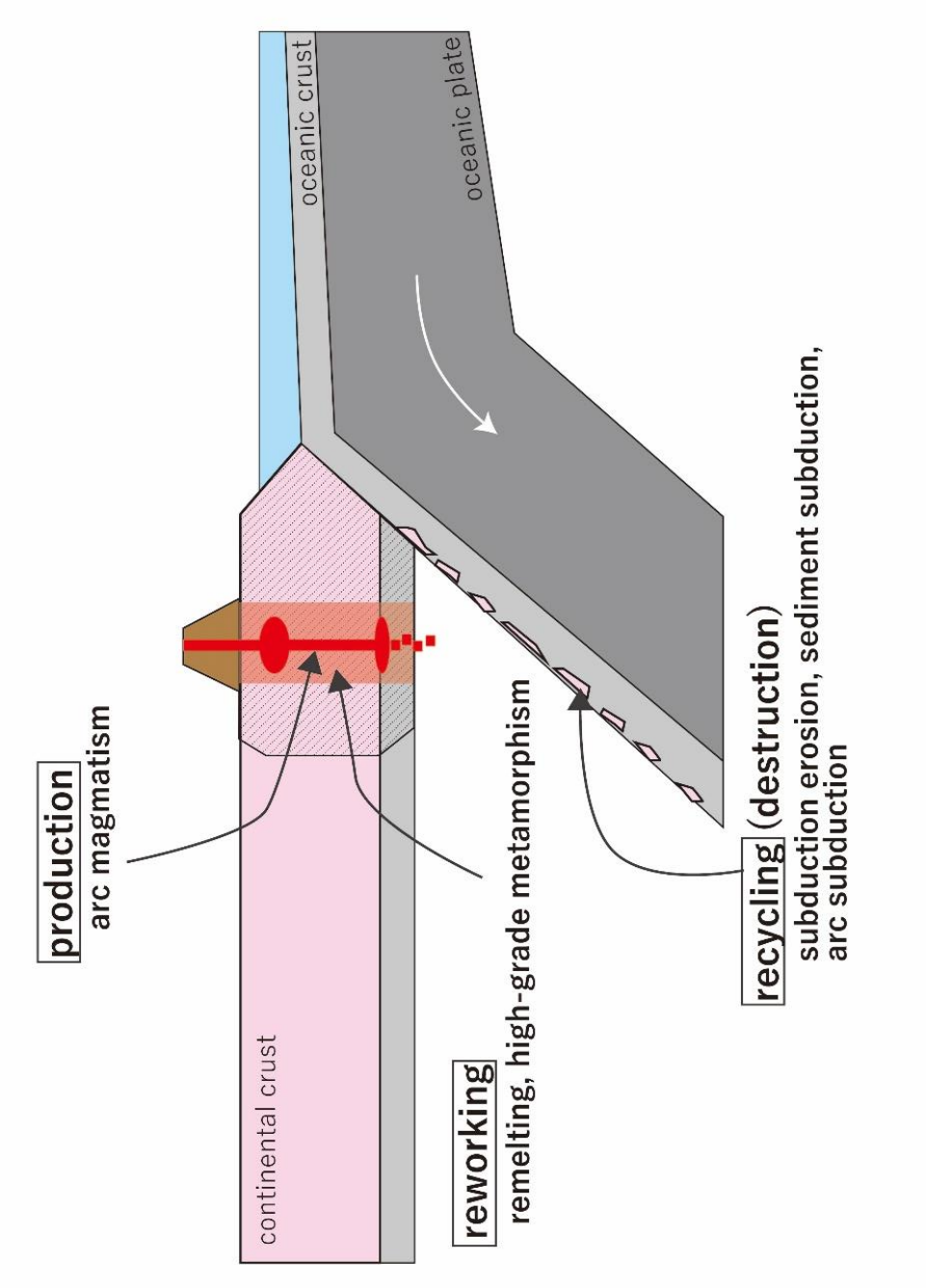

Figure 1-1. Schematic image of production, reworking, and recycling of continental crust in plate subduction zone.

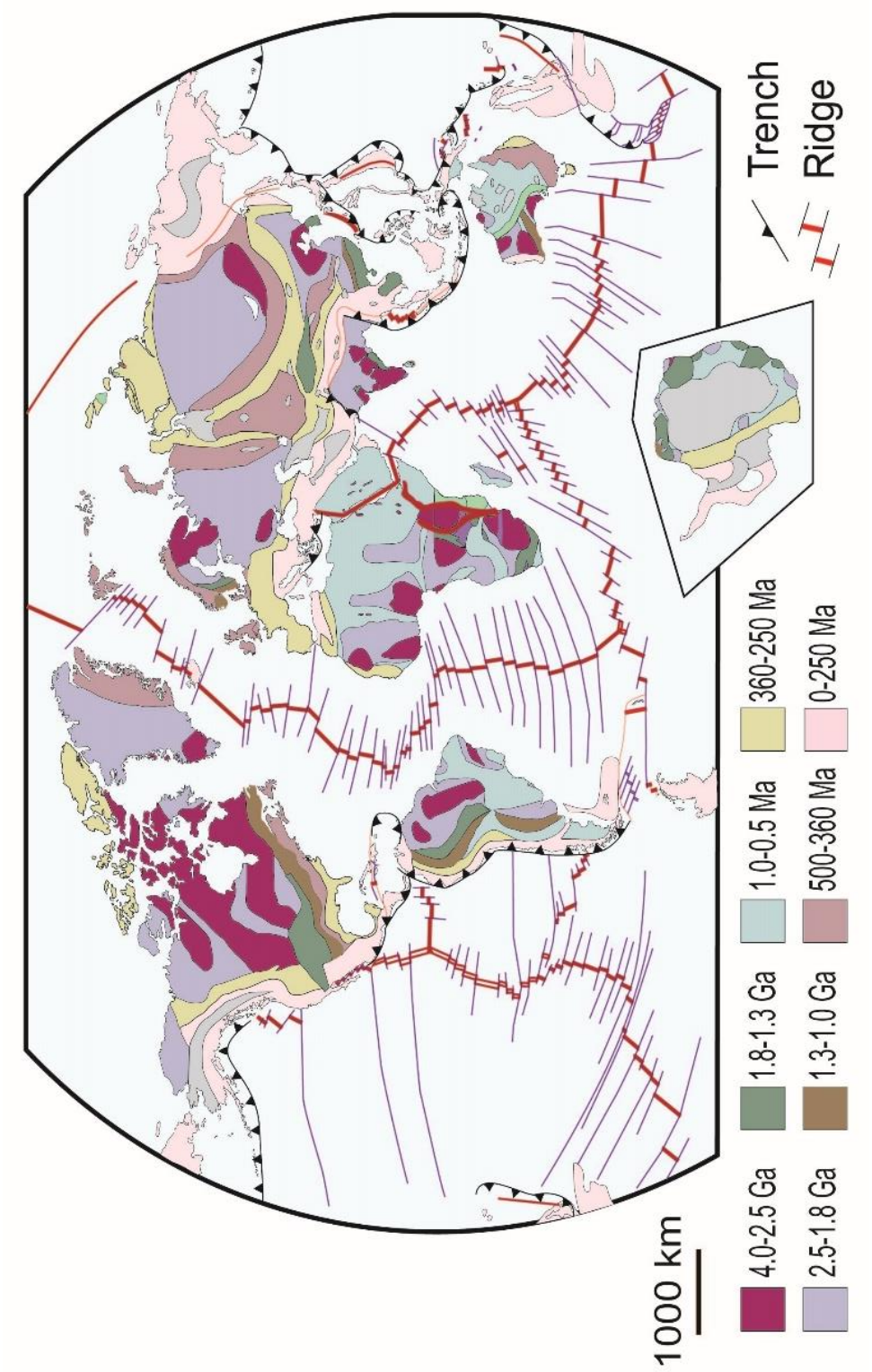

Figure 1-2. World geotectonic map compiled by Maruyama et al. (2007).

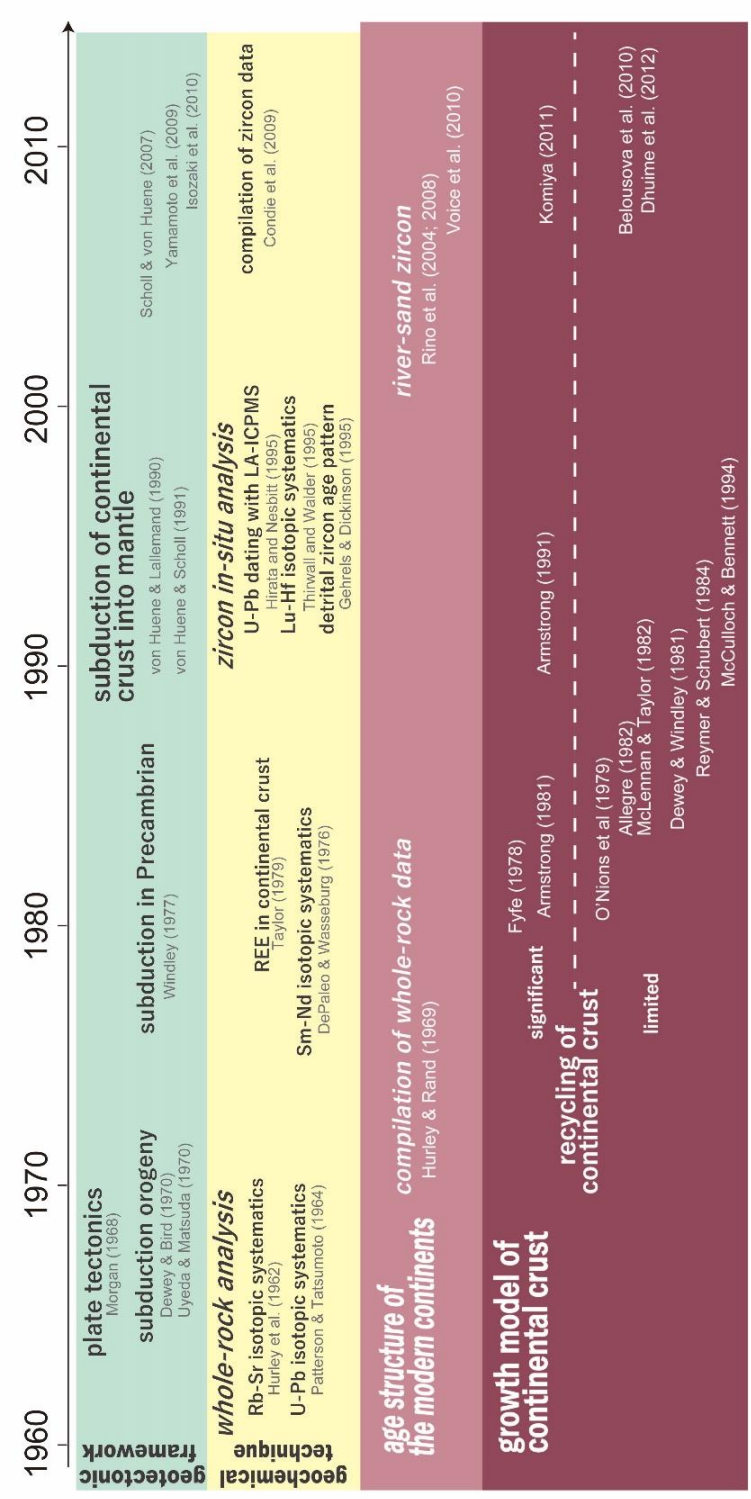

Figure 1-3. A historical review of studies on the growth of continental crust in the last half century.

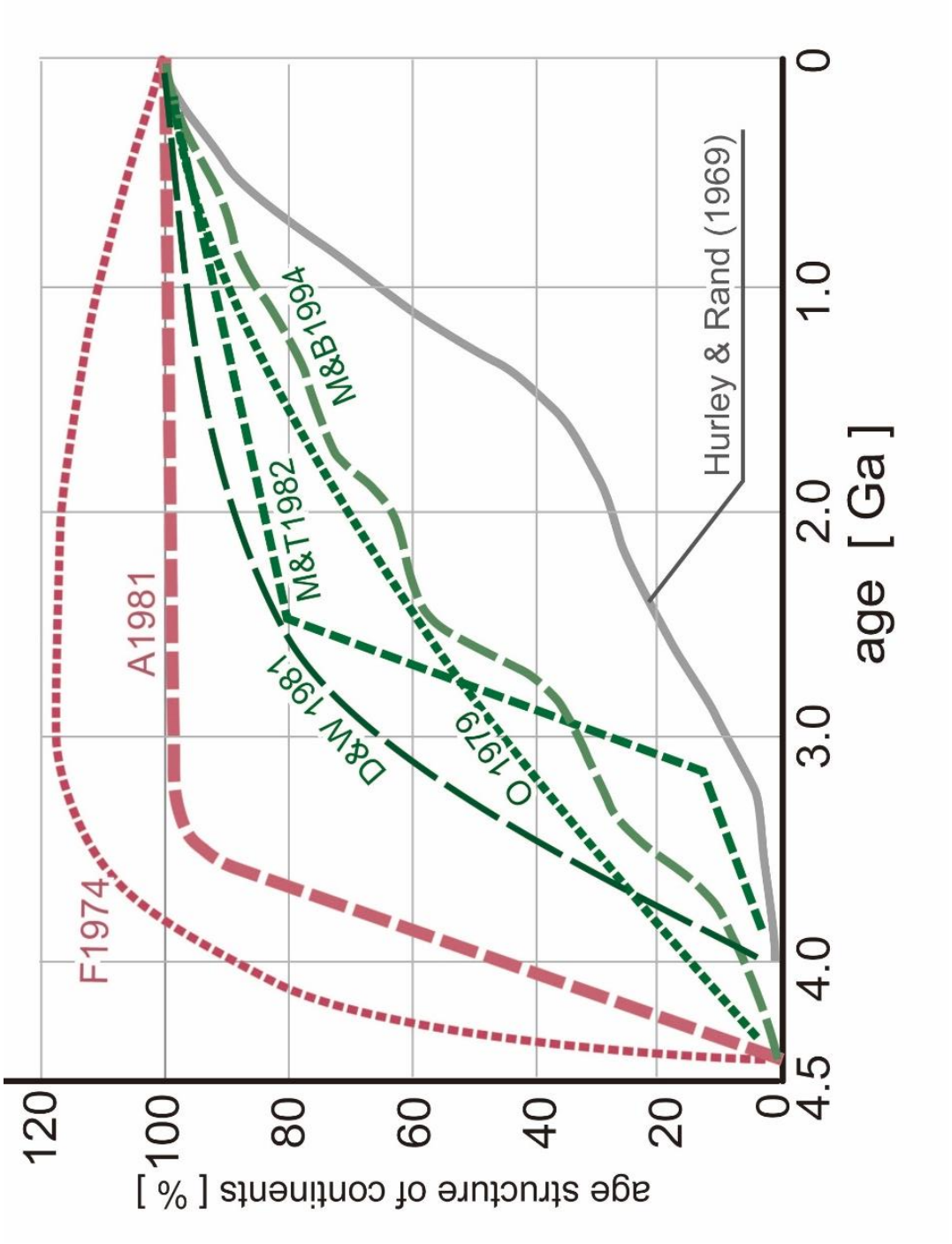

Figure 1-4. Growth model of continental crust before 1990's Estimation of age structure of the modern continents (Hurley and Rand, 1969) and continental growth curves (Fyfe, 1978; Armstrong, 1981; O'Nions et al., 1979; Dewey and Windley, 1981; McLennan and Taylor, 1982).

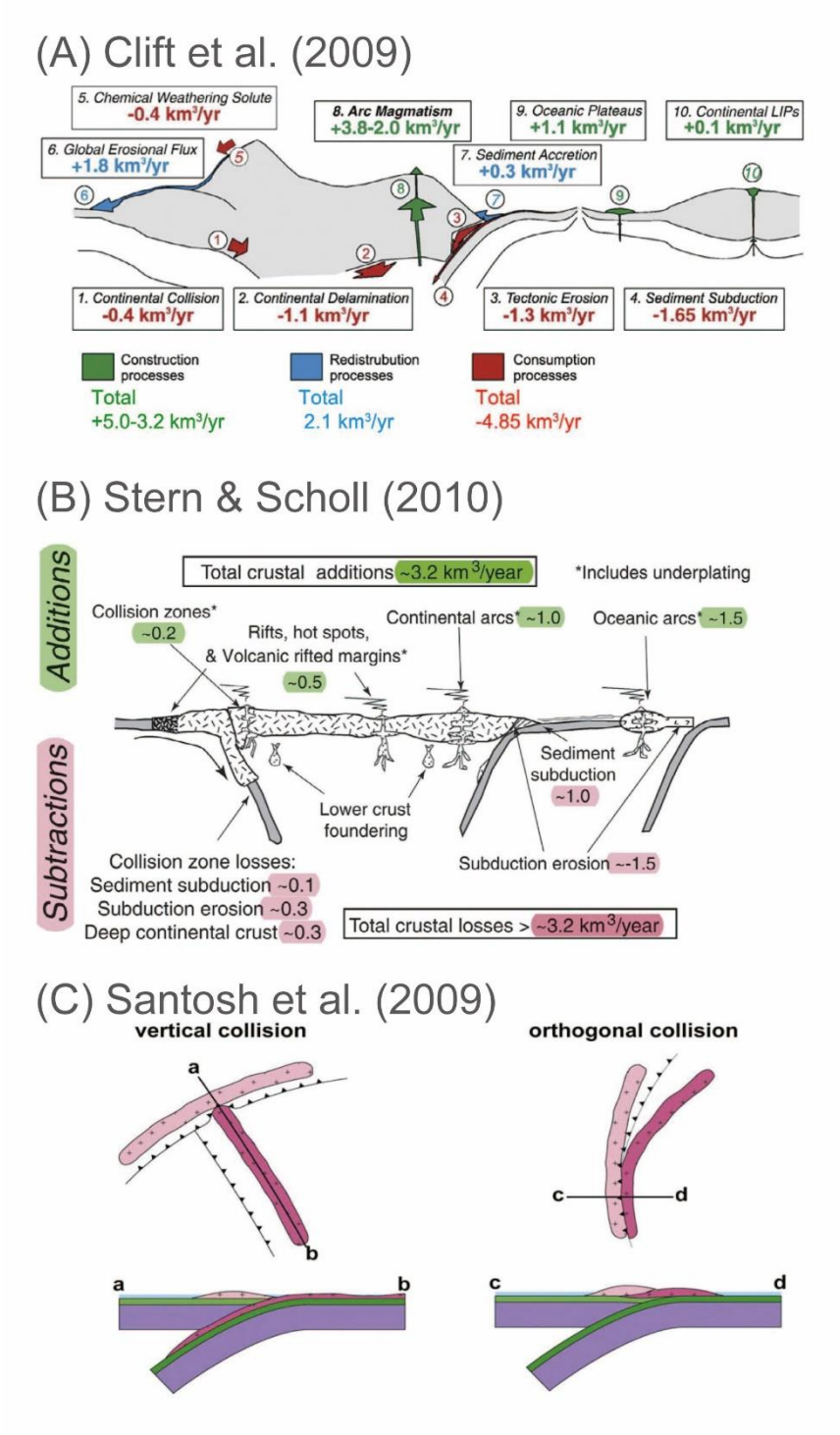

Figure 1-5. Schematic images of processes of granitic subduction into the mantle. (A) and (B) show estimation of global balance between addition and subduction of continental crust on the modern Earth. (C) island arc subduction (Santosh et al. 2009).

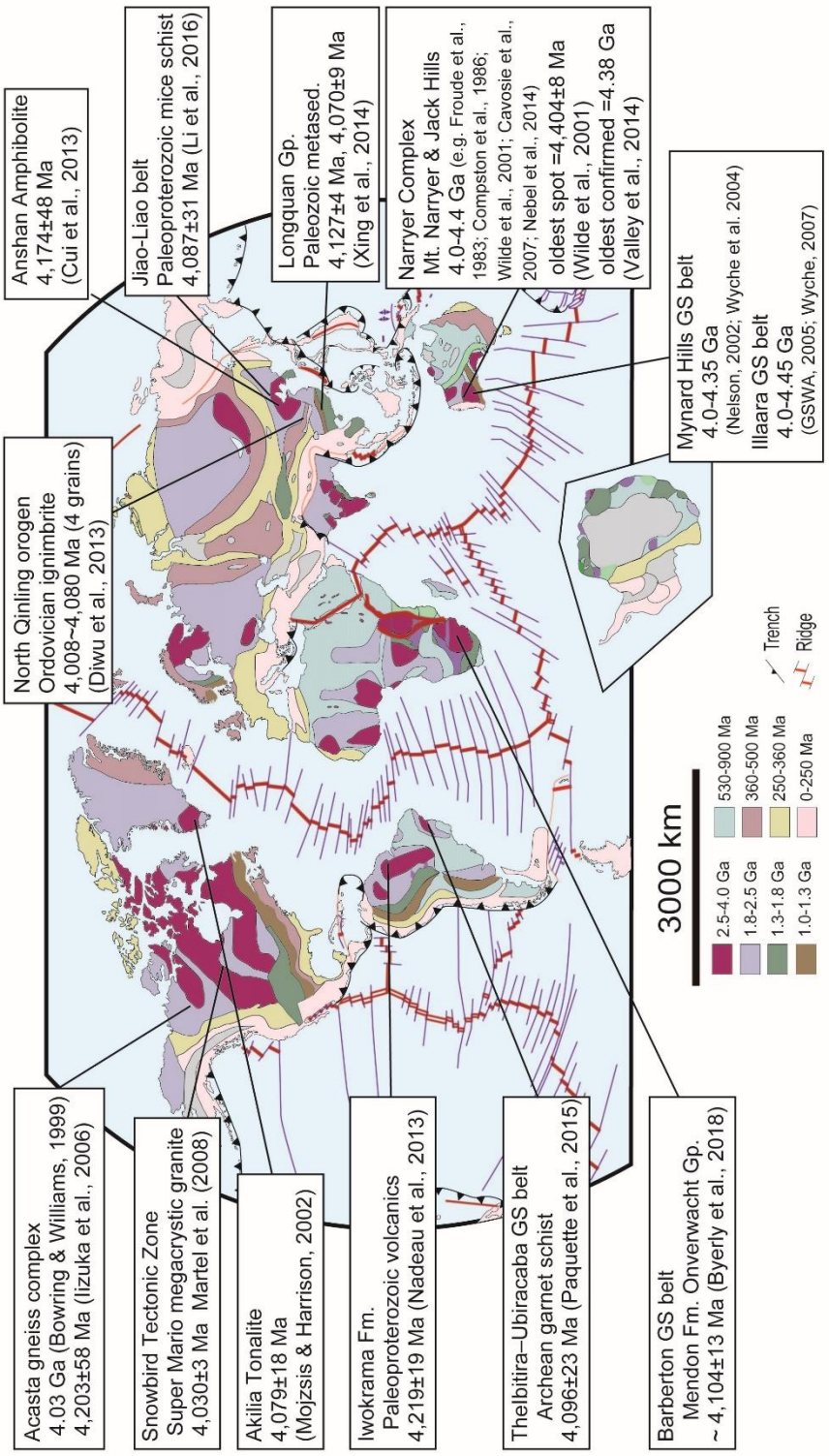

Figure 1-6. Localities of Hadean zircon. (GS: greenstone).

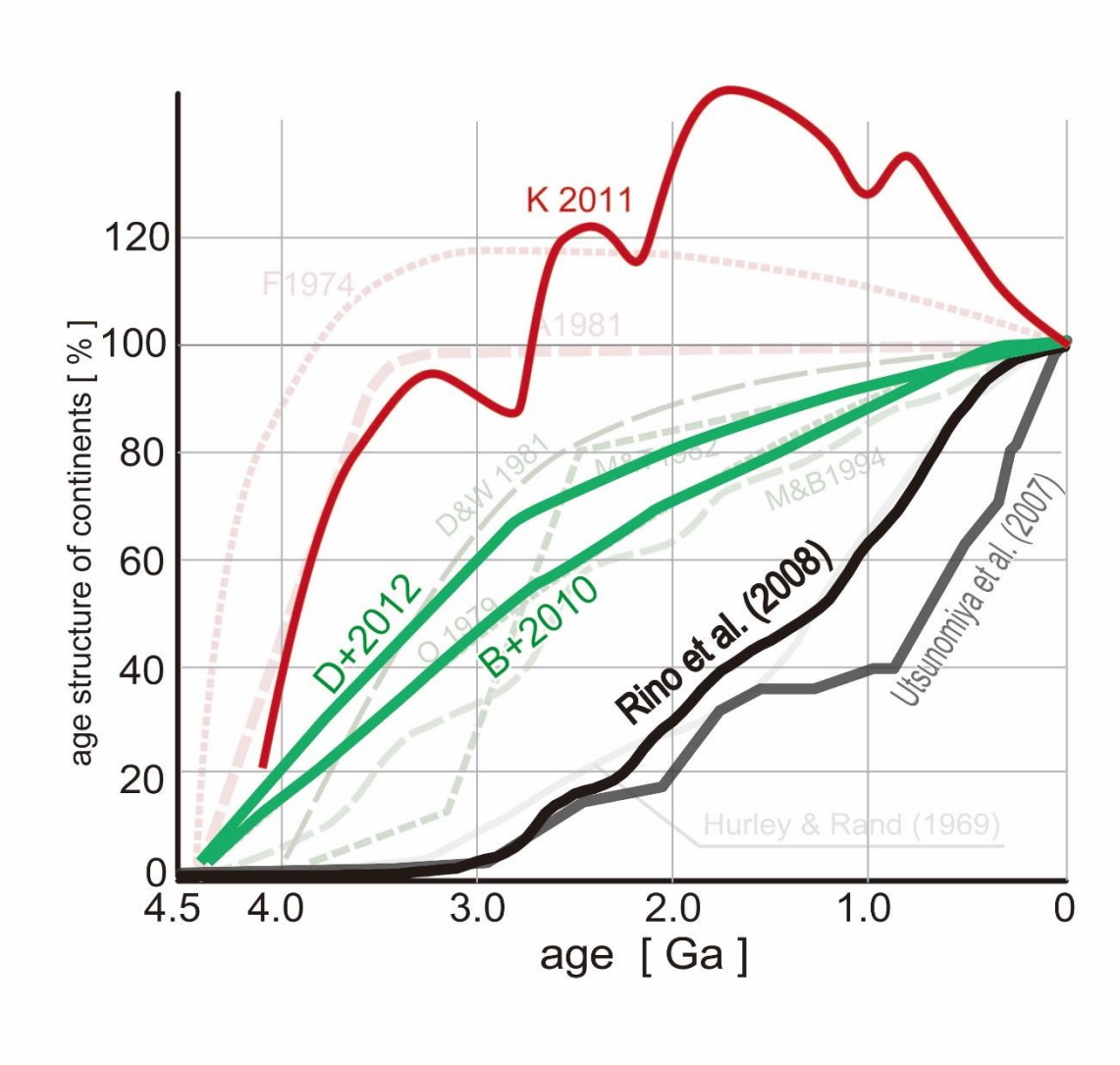

Figure 1-7. Age structure of orogenic belts in the modern continents (Utsunomiya et al., 2007), age frequency pattern of detrital zircons from modern 16 rivers (Rino et al., 2008), and growth model of continental crust After 2000's (Belousova et al., 2010; Komiya, 2011; Dhuime et al., 2012).

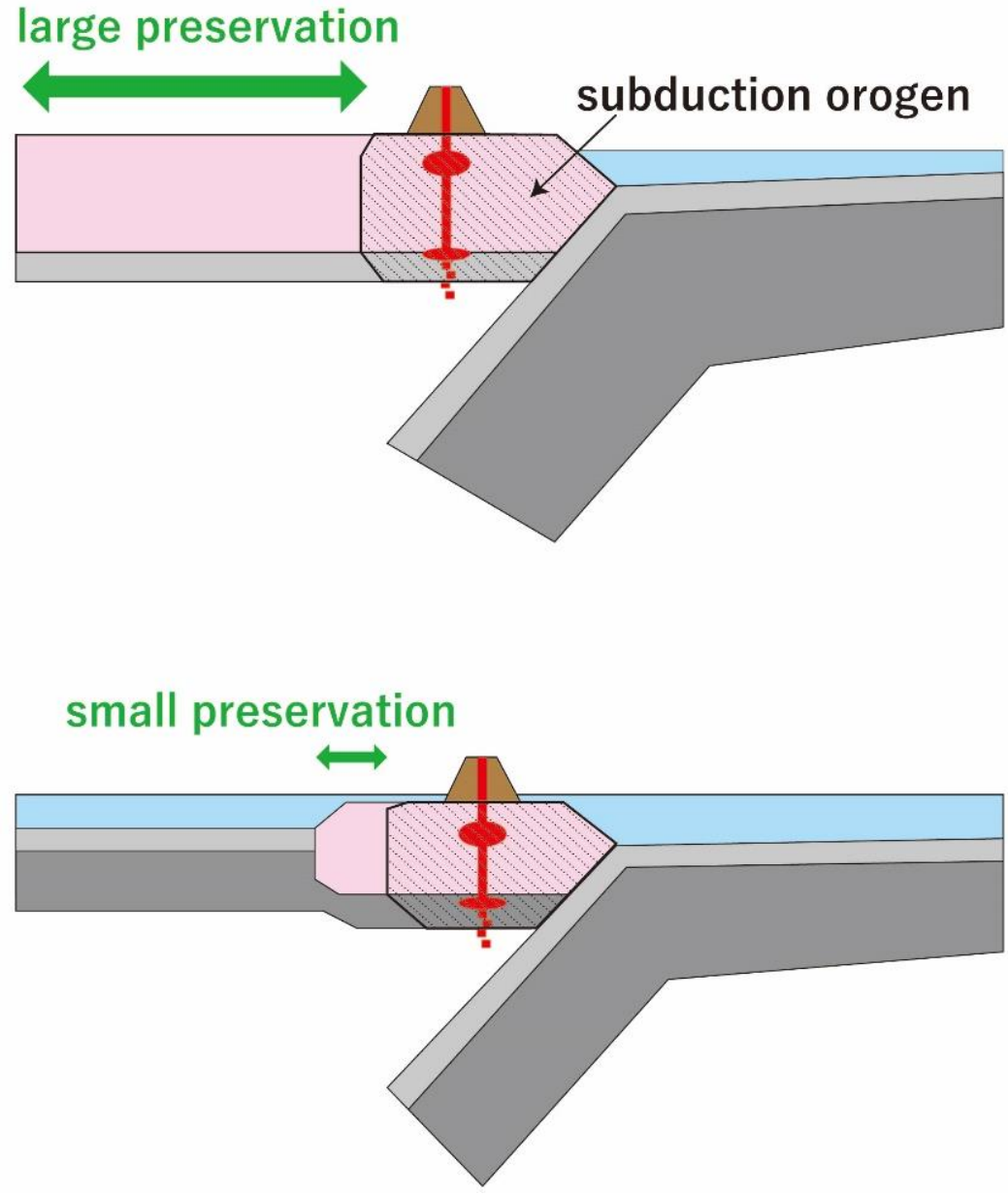

Figure 1-8. Difference in preservation of older continental crust from subduction orogen depending on size of continental blocks.

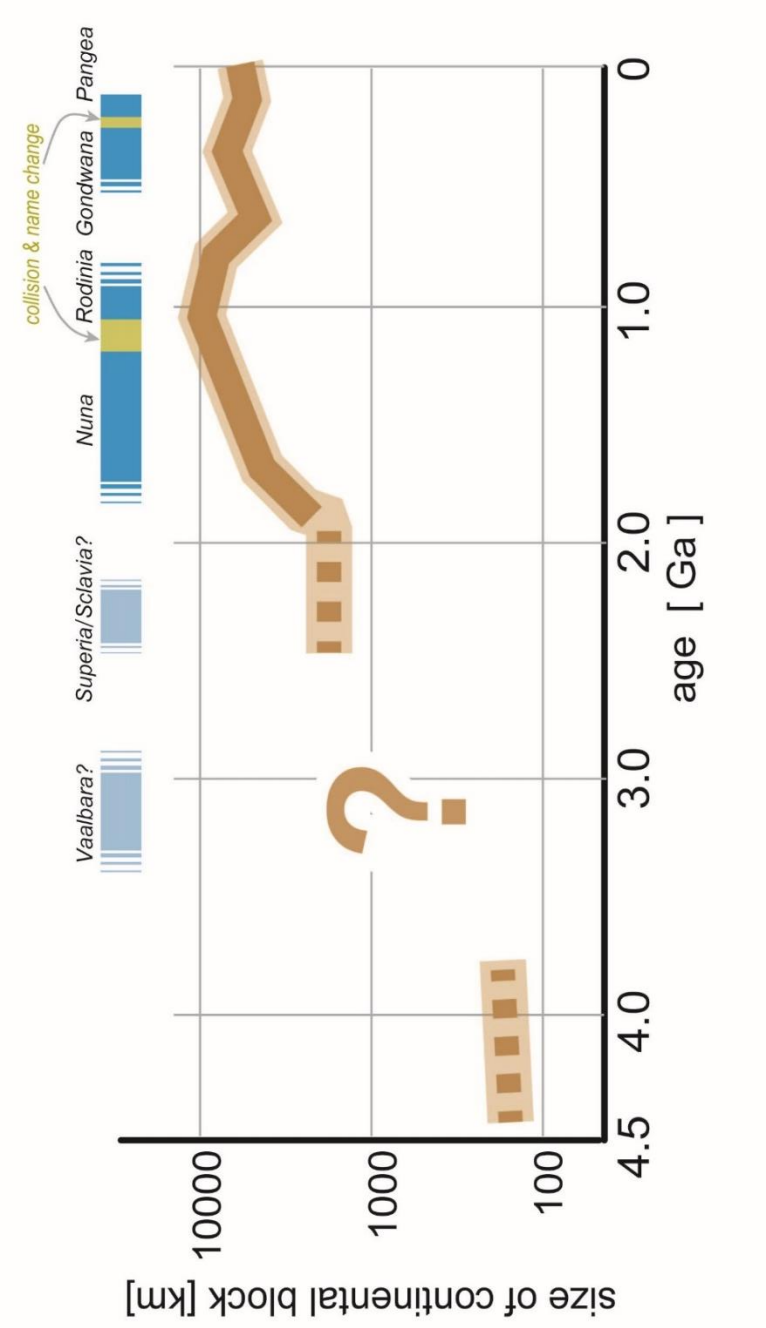

Figure 1-9. Maximum scale of size of continental blocks through time. The size before 2.0 Ga is still not well constrained. Timing of Supercontinents and putative continental blocks in the Paleoproterozoic and Archean is modified after Bradley (2011).

Chapter 2. Secular change in age structure of granitic crust and the continental growth: compilation of detrital zircon U-Pb ages

Abstract

To reveal the secular change in age structure of continents through time, this study compiled the U-Pb age spectra of detrital zircons for 2.9, 2.6, 2.3, 1.0, and 0.6 Ga sandstones and modern river sands. Results of the compilation demonstrated the following episodes in the history of continental crust; 1) low growth rate of the continents due to the short cycle in production/destruction of granitic crust during the Neoarchean to Paleoproterozoic (2.9—2.3 Ga), 2) net increase in volume of the continents during Paleo- to Mesoproterozoic (2.3—1.0 Ga), and 3) net decrease in volume of the continents during the Neoproterozoic and Phanerozoic (after 1.0 Ga). The relatively rapid cycle of production and destruction of continental crust before 2.3 Ga can be caused by size of continental blocks was smaller than that of the modern ones. The difference in size of continental blocks is indeed reflected in the heterogeneous crustal age structure of continents after 1.0 Ga. During the Mesoproterozoic, plural continents amalgamated into larger ones comparable to modern continental blocks in size. Relatively older crusts were preserved in continental interiors, whereas younger crusts were accreted along continental peripheries. In addition to continental arc magmatism, the direct accretion of intra-oceanic island arc around continental peripheries also became important for net continental growth. Since 1.0 Ga, total volume of continents has decreased, and this appears consistent with on-going phenomena along modern active arc-trench system with dominant tectonic erosion and/or arc subduction. Subduction of a huge amount of granitic crusts into the mantle through time is suggested, and this requires re-consideration of the mantle composition and heterogeneity.

2.1. Introduction

For discussions of the growth history of the continental crust, a totally new input was given by age spectra of detrital zircons in the 1990s-2000s, through precise and rapid dating technique has been developed (e.g. Gehrels and Dickinson, 1995; Gehrels et al., 1995). In particular, Rino et al. (2004; 2008) analyzed age spectra of detrital zircons in river sands from extant modern

continents, in particular, U-Pb age spectra of detrital zircons of deltaic river sands from the Mississippi River, and compared the results with the surface crustal age distribution of North American craton with lesser Precambrian sedimentary covers. Consequently, they demonstrated that the river sand composition faithfully reflects the crustal composition of the provenance, regardless of orogenic disturbance by the Rocky Mountains and/or terrigenous noise by the Quaternary glacier-interglacial cycles. This result confirmed that crustal composition of hinterland is by and large reflected in river sands deposited at lower streams of a major river with large drainage system, when the crustal basement is extensively exposed. Essentially similar results were obtained also from other continents (Rino et al., 2008). The curve indicates that continental crusts older than 2.3 Ga (i.e. the first half of the Earth history) merely occupy no more than 20 percent of all continents, and those of > 3 Ga are quite rare (Fig. 2-1A), in good agreement with actual age proportion of crust on extant continents (Fig. 1-1).

Recent compilations of large dataset (over ten-thousands of ages from multiple sources) of detrital zircon ages, for minimizing local bias, recognized some peaks in zircon age (Condie et al., 2009; Belousova et al., 2010; Voice et al., 2011; Roberts and Spencer, 2015; Puetz et al., 2017). These distinct peaks apparently correspond to the timings of supercontinent amalgamation during the Proterozoic and Phanerozoic (Rino et al., 2004; 2008; Condie et al., 2009). Some researchers proposed that episodic production of juvenile crust caused by mantle plumes related to break-up of supercontinents (Rino et al., 2004; Condie et al., 2009). Other researchers pointed out that the continental crust would obtain preservation potential through shielding continental inboard from subduction zones during supercontinental periods (Hawkesworth et al., 2009; Roberts, 2012). These discussions highlighted contrasting views on the process of construction of continental crust, i.e. episodic production versus preservation potential. To date, diverse models have been proposed for the secular change in total continental volume through time (Fig. 1-2); however, it is too crude to interpret the accumulated age spectra without checking depositional ages and/or settings of host sandstones because of significant destruction of older continental crust through time. As such a major obstacle exists in reconstructing precise volume of ancient continents, the secular change in age structure of continental crust through time has not yet been clearly demonstrated.

Age structure is one of the fundamental parameters for population dynamics (Veizer and Jansen, 1985). The evolution of continental crusts indeed occurred not in steady-state but with volatile changes of production and destruction through the Earth's history. In this study, we compiled the age structure of detrital zircons for several time-bins subdivided by depositional

ages of host sandstones. This compilation led us detect a contrasting aspect in age spectra of detrital zircons between pre-2.3 Ga interval and post-1.0 Ga one, which likely suggests that a major change in age structure of continents has occurred sometime in mid-Precambrian time.

2.2. Data compilation

2.2.1. Conditions for a compilation

For the compilation of U-Pb ages of detrital zircons, this study focuses on clastic rocks deposited specifically in extensional tectonic settings. In such settings, steep mountain ranges and other geographical protruding are generally minor and sediment receives matured terrigenous clastics from the wide range of provenances. Age frequency distribution of detrital zircons in such sedimentary rocks likely reflects the rock compositions in provenances in a given time internal. In contrast, clastic rocks accumulated along compressional tectonic settings, such as accretionary complex and forearc basin, would have large bias owing to steep mountain ranges, active volcanic chain, and exposed granitic batholith (e.g. Cawood et al., 2012; Aoki et al., 2014). In this regard, the latter group is unsuitable for the purpose of this study. All of the 16 rivers in Rino et al. (2008), compiling U-Pb ages of detrital zircons in modern river mouths, run on passive continental margins (Table 2-1).

To collect world wide data for the compilation, this study focuses on periods at *ca.* 2.9, 2.6, 2.3, 1.0, and 0.6 Ga which relatively abundant in sedimentary rocks. Note that this compilation of detrital zircon ages includes only crustal ages of continental blocks and does not include the fragmental continental crust, such as oceanic island arcs. Thus, this study estimates “age structure of the continents”, not “age structure of the all continental crust on the Earth’s surface”.

To reduce local bias, this study selected one rock sample on each craton for the compilation at 2.9, 2.6 and 2.3 Ga. For the compilation at 1.0 and 0.6 Ga, localities were selected to cover the whole Earth. In case that more than two age frequency distributions have been reported from several sequences in a locality, this study chooses one of them according to maturity of the sediments and/or width of age spectrum. Nonetheless these criteria may be still flawed to recover precise age structures of continents in the past, they are important to obtain global trend of age structure of continents with bias as few as possible.

2.3.2. Integration of age data set

This study compiled our analytical data described above with previously reported data shown in Fig. 2. This study selected data with the following criteria; i.e. ages 1) dated by *in-situ* analysis with LA-ICP-MS, SIMS, and SHRIMP, 2) of igneous origin guaranteed by oscillatory zoning (no metamorphic zircons), and 3) with discordance less than 10 % in U-Pb isotopic systematics.

Although source rocks of individual detrital zircons cannot be identified by U-Pb dating and other geochemical analysis, this study suppose that all detrital zircons have been derived from granitoids composing continental crust. All localities, references of data sources and age frequency distributions of each data are summarized in Table 1. By adding all these age data, this study obtained averaged age spectra of detrital zircons for five periods (2.9. 2.5, 2.3, 1.0, and 0.6 Ga) individually. Figure 2-1A illustrates the average age spectra for these 5 periods together with that of modern river sands (Rino et al., 2008) in the form of cumulative curves normalized to 100%. Note that the vertical axis of Fig. 2-1A represents not the volume of the continental crust but the percentage in age.

By compiling detrital zircon ages from modern river sands, Rino et al. (2008) integrated individual age frequency distributions after the adjustment according to area of each river's drainage basin. In this study, in contrast, age frequency distributions from each rock sample are regarded as having the same weight as a whole, because it is unfeasible to estimate precise areas of ancient provenance.

2.3.3. Fitting of the result of compilation by linear function

In order to discuss more detailed secular changes in age structure of continent, each curve is fitted to polygonal line function. The function is represented by

$$f(t) = \begin{cases} 0 & (t \geq X) \\ \dfrac{1}{T - X}t + \dfrac{T}{X - T} & (t < X) \end{cases}$$

where t [Ma] means an age (i.e. time), T [Ma] is depositional age of compiled rock samples, and X [Ma] represents an age of the bending point in this function. Parameter X, a fitting parameter for a curve, is computed through a least-square method.

Value of X – T [M.yr.] means a time span for once-produced continental crust being vanished by recycling processes at each period. In this paper, this time span is referred as *"continental average cycle"*. This word does not mean the span in which all continental crust is completely disappeared or replaced, but something like an average lifetime. The fitting lines are shown in Fig. 2-1B. The detailed results of fitting are given in Table 2. As values of asymptotic standard error of the fitting parameter X are between 1 and 2 Ma, these lines are regarded well fitted.

2.4. Discussion

2.4.1. Major change in preservation of continental crust between 2.3 and 1.0 Ga

The results of compilation shown in Fig. 2-1 clearly demonstrate several interesting aspects of age composition of Precambrian continents. First, the three cumulative curves for age structure of continents at 2.9, 2.6 and 2.3 Ga (3 lines in reddish colored in Fig. 2-1) apparently run nearly parallel to each other. This observation suggests that the age structure of continents was rather constant during the late Archean to early Proterozoic (at least between 2.9 and 2.3 Ga). This also indicates that the averaged residence time of crusts has been almost constant between 2.9-2.3 Ga probably because a good balance was kept between the production and destruction of continental crusts. In other words, the pre-2.3 Ga continents have comprised solely young crusts no older than 800 million years old.

Second, post-1.0 Ga crusts had relatively wider age range, over 1300 m.y., with respect to the pre-2.3 Ga crusts (Fig. 2-1B). In particular, the modern river sands have the widest age range of detrital zircon, which reaches ca. 2900 million years, i.e., 3-4 times longer than those of pre-2.3 Ga sandstones. Moreover, the age range of extant continental crusts reaches 4000 million years (Bowring et al., 1988).

Third, the cumulative curves of 2.9, 2.6, and 2.3 Ga are obviously steeper than those of 1.0, 0.6, and 0.0 Ga (Fig. 2-1B). These observations indicate that the pre-2.3 Ga balance between the production and destruction of continental crusts has been lost by the Neoproterozoic, and that the post-1.0 Ga continental crusts tend to be preserved more efficiently than before, in a form of crusts with wider age ranges, such as North America. The present analysis clarified that a major change in the preservation mode of continental crusts has occurred sometime between 2.3 and 1.0 Ga,

probably suggesting a significant shift in tectonic regime during the Paleo- to Mesoproterozoic. In the following sections, more details of the growth pattern of continents though time will be discussed.

2.4.2. Net growth and preservation bias of continents

Crude "continental crust production" is clearly different from the "growth of continents". The former represents the total amount of produced continental crust that simply increases/accumulates along time, regardless of secondary disappearance. The rate of the former has been controlled essentially by the long-term change in mantle temperature, via mantle convection. In contrast, the latter corresponds to the final difference in volume between pre-existing continents and those newly added by arc magmatism and/or secondarily disappeared. Although not much precise, it is easier to estimate the modern rate of continental growth on the basis of direct observations on magmatism and tectonics; however, that of the past appears difficult in general without direct measurements. Nonetheless, we can reconstruct the history of continental growth by checking detrital zircon records in ancient terrigenous clastics.

Age structure of a particular continent recorded its long-term history of the balance between the production and destruction rates of continental crust. Under plate tectonic regime, in general, continental crust is formed mostly by arc magmatism along subduction zones, whereas pre-existing continental crust can be often erased by subduction erosion/sediment subduction (Scholl and von Huene, 2007; 2009; Clift et al., 2009; Yamamoto et al., 2009; Stern, 2011). Without secondary disappearance of the continental crusts, continental volume will increase monotonically as long as subduction-related magmatism continues. In this case, the slope of cumulative curve of crustal age changes simply according to the production rate by magmatism (Fig.2-4A).

On the other hand, in cases with both crustal production and destruction, the following two factors control the age structure of a continent, i.e., "net continental growth" and "preservation bias" according to the heterogeneity in age of crustal rocks. "Net growth" in a continent corresponds to the difference in volume between juvenile continental crust newly formed by arc magmatism and the pre-existing crust secondarily disappearing by subduction erosion. Consequently, the secular change in volume of continental crust can have three options; 1) increase by over-production (Fig.2-4B, left column), 2) no change by balanced production and destruction (Fig.2-4B, middle column), and 3) decrease by over-erosion (Fig.2-4B, right column).

"Preservation bias" represents the degree of vulnerability for variously aged crust to secondary disappearance in regard of spatial arrangement of crusts within a continent. For modern continental blocks, relatively young continental crusts tend to be formed along its peripheries. For example, the North American continent has relatively old continental crusts in its interior (the Canadian shield) surrounded by younger orogenic fronts along the continental peripheries (the Appalachian and Cordilleran belts; Fig. 1-1). With such an uneven distribution of crustal ages in a continent, younger continental crust may easily suffer crustal recycling and reworking processes by active subduction related tectonism, whereas older crust in the interior remain preferentially untouched. Thus "preservation bias" has two end-member options, i.e. 1) with strong bias in spatial distribution of crustal ages, relatively older crusts are selectively preserved (Fig.2-4C), and 2) without bias, continental crusts of various ages are preserved or eroded out proportionally (Fig.2-4B). In general, larger continents tend to have strong bias mostly owing to their longer history with multiple tectonics episodes.

Given these two factors controlling age structure of a continent, Fig.2-4B categorizes possible patterns of continental growth. Figures 2-2B-1, -2, and -3 illustrate three possible options with no preservation bias. In the case of net increase in continental crust (Fig.2-4B-1), the slope of cumulative age gradually turns gentler in the same manner as Fig.2-4A. The starting point of the line at the base indicates the age of the oldest crust, and its position shift toward the younger direction. In the case of no change in continental volume (Fig.2-4B-2), the production and destruction of continental crust balances to keep the line of accumulated age in the same shape (slope) but with gradually shifted toward the younger direction. In the case of net decrease (Fig.2-4B-3), the continental crust disappears much faster than the coeval production. Thus, the young continental crust dominates more, making the slopes much steeper, and shifting the line as a whole toward the younger direction.

When we take "preservation bias" into consideration, cases will be more diverse. Figures 6C-4, -5, and -6 illustrate three options with strong preservation bias. In the case of net increasing or no change in volume of a continent (Figs. 2-2C-4 and -5), secular change in age structures is apparently the same as that of Fig.2-4A. On the contrary, in the case of net decrease (Fig.2-4C-6), a proportion of old continental crust becomes relatively larger through the selective elimination of younger crusts along continental margins. In this case, slopes of accumulated lines become gentler, and the oldest age of crust shift toward the older direction. Consequently, a unique pattern occurs with three lines (t_0, t_1 and t_2) crossing each other in the middle, as shown in Fig.2-4C-6.

2.4.3. Growth of continents since the late Archean

Based on the compilation of age spectra of detrital zircons from 2.9, 2.6, 1.0, and 0.6 Ga sandstones together with that of modern river sands, this study discuss the pattern and change in the growth of continents since the Mesoarchean. On the left-hand side of Fig. 2-3, three cumulative curves for 2.9, 2.6 and 2.3 Ga continental crusts (reddish colored lines) are running almost parallel to each other, and the widths of age variation are relatively narrow. These correspond to the pattern shown in Fig.2-4C-2, suggesting that continents have been produced constantly but at the same time suffering severe destruction during the mid-Archean to the Early Proterozoic time. Consequently, the total volume of continents remained constant or slightly increased (Fig. 2-5). Although the occurrence of 2.9 to 2.3 Ga terrigenous sedimentary rocks has been used as evidence for the extensive exposure of continental landmass(es) in the Archean to early Proterozoic (Ronov, 1964; Rogers, 1996), no data exist for any quantitative estimate of total mass of continental crusts during the Archean and Proterozoic.

The narrow age widths of the three Archean lines (Fig. 2-1) indicate that continental crusts have not been effectively preserved during the Archean, instead they were destructed rapidly in short periods. In other words, rigorous recycling operated for granitic crusts, and most of the Archean continental crusts were likely subducted into the mantle (Fig. 2-4B).

In contrast, the slope of the 1.0 Ga cumulative curve (middle in Fig. 2-1) is gentler than that of 2.3 Ga. This corresponds to the pattern shown in Fig.2-4C-4 or -5, suggesting that net continental growth has occurred during this period. Although destruction had affected both younger and older continental crusts, the preservation potential of older crusts became probably higher around 1.0 Ga. The first large continent appeared between 2.3 and 1.0 Ga and the preservation bias of continental crusts increased after that (Fig. 2-5; Fig. 2-4C).

The present compilations suggest some aspects of continental growth which have not been recognized before; i.e., 1) constant or slight increase in continental volume between ca. 2.9 and 2.3 Ga, 2) net growth of continental crust between ca. 2.3 and 1.0 Ga, 3) net decrease after 1.0 Ga to the present, and 4) total volume of the continents reached maximum during the Proterozoic, particularly between 2.3 Ga and 1.0 Ga.

2.4.4. Post-1.0 Ga decrease of continental crust

As shown in Fig. 5, the slopes of 1.0, 0.6, and 0.0 Ga cumulative curves are gentler than those of 2.9, 2.6 and 2.3 Ga, and more interestingly, they become gentler along time. This observation indicates that the preservation has become more common for older crusts during the Neoproterozoic and Phanerozoic with respect to the Archean and early Proterozoic, as discussed above.

It is also noteworthy that these 3 lines cross each other in the middle (Fig. 2-1B), just like the case of Fig.2-4C-6. This simply indicates that younger crusts occur less abundantly in provenance, but never that older crusts were newly added. As older crusts may naturally decrease or remain the same in amount, these 3 lines should not cross in reality. Instead, the apparent crossing suggests that the total volume of continental crusts may has changed, in particular, has decreased along time after 1.0 Ga. In this regard, for avoiding the mutual crossing of these lines, cumulative curves for 1.0, 0.6, and 0.0 Ga continental crusts need to be modified (Fig. 2-5). The height of the Proterozoic peak between 2.3-1.0 Ga is normalized on the basis of the vertical expansion of the 1.0 and 0.6 Ga cumulative curves.

Based on the above discussion on secular change, this study tentatively places the continental growth curve on about 50-80 % volume of the modern continents, as shown in Fig. 2-3. The results shown in Fig. 2-3 suggest that at 1.0 Ga continents of nearly 150 % volume of modern continents existed, and also at 0.6 Ga 130 %, respectively. The total continental mass likely reached the maximum in the Earth's history, ca. 150% of the modern continents on the planet's surface in volume between 2.3 and 1.0 Ga. On the other hand, this diagram indeed suggests the gradual decrease in total continental mass during the last 1 billion years. Such a notion of decreasing continental mass in the past has never been discussed on the basis of geological data like the present zircon age spectra; however, this appears indeed consistent with on-going phenomena along modern active arc-trench systems with severe tectonics erosion and/or arc subduction rather than the addition of juvenile crusts (Yamamoto et al., 2009).

2.4.5. Pre-3.0 Ga growth of continental crust

The present compilation provided new clues to interpret the growth pattern of continents after 3.0 Ga as discussed above; nonetheless, not much information was available for the pre- 3.0

Ga conditions. On the basis of previously published works, here the current understanding of the Paleoarchean and Hadean continental growth is summarized.

The onset timing of oceanic plate subduction in the Earth's history has been much debated. The main debate against the pre-3.0 Ga plate subduction has been based on the estimated thick Archean basaltic crust with extremely low density with respect to mantle rocks (Davies, 1992, 1995), which was too buoyant to be subducted. In addition, assumed warm Archean mantle was also regarded to suggest the prohibition of oceanic subduction into deeper mantle (Davaille and Jaupart, 1993; Solomatov, 1995). Nevertheless, slab melting and mineral-phase change in deeper mantle were overlooked in these notions (Komiya et al., 2002; Komiya et al., 2004), and the latest actualistic geophysical models (e.g., Ogawa, 2007, 2014; van Hunen and van den Berg, 2008; Sizova et al., 2010; Fischer and Gerya, 2016) instead suggest the earlier operation of plate subduction already in the Eoarchean, and even in the Hadean.

Petrological analysis indicated that the mantle temperature during this period was about 100-200 K warmer than today (Fig. 9A; Komiya, 2004; Herzberg et al., 2010), which may have led a specific tectonic regime like chaotic subduction with small oceanic plates (Yanagisawa and Yamagishi, 2005; Sizova et al., 2010; Ogawa, 2014; Fischer and Gerya, 2016). The putative chaotic subduction of numerous small oceanic plates may explain the geological observations of narrow-shaped Archean crustal blocks, which led some geologists imagine that Archean continental growth essentially has occurred in multiple parallel collision of mid-oceanic island arcs (Fig. 2-4A; de Wit and Hart, 1993; Hoffman, 1989; Santosh et al., 2009).

2.5. Conclusion

This study compiled U-Pb ages of detrital zircon in order to recognize the overall evolutional trend of continents after ca. 3 Ga. The unique approach of this study is in checking and comparing detrital zircon U-Pb age spectra, for 6 distinct time intervals, i.e., 2.9, 2.6, 2.3, 1.0, 0.6, and 0 Ga. The results of the compilations demonstrated the following episodes in the history of continental crust; 1) low growth rate of the continents due to the short cycle in production/destruction of granitic crust during 2.9 to 2.3 Ga, 2) net increase in volume of the continents from 2.3 to 1.0 Ga, and 3) net decrease in volume of the continents from 1.0 Ga to the current. Consequently, the present study documented an alternative history of continental

growth, which is different from the previous models in several aspects.

The Paloproterozoic (ca. 2.3 Ga) and Neoproterozoic (near 1.0 Ga) possibly correspond to the timing of major changes in size of continents. In the Archean and Paleoproterozoic, the embryonic continents were smaller than the modern continents, probably owing to the relatively rapid production and destruction of continental crust. This is indeed reflected in the crustal age structure of modern continents that usually have relatively small amount of Archean crusts with respect to the post-Archean ones. During the Mesoproterozoic, plural continents amalgamated into larger ones comparable to modern continental blocks in size. Relatively older crusts were preserved in continental interiors, whereas younger crusts were accreted along continental peripheries. This created a remarkable heterogeneity in age structure of large continental blocks. and consequently, the preservation bias of older crusts. The total amount of continents reached the maximum around 1.0 Ga, whereas it started to decrease after 1.0 Ga. This appears consistent with on-going phenomena along modern active arc-trench system with dominant subduction erosion and/or arc subduction.

Figures

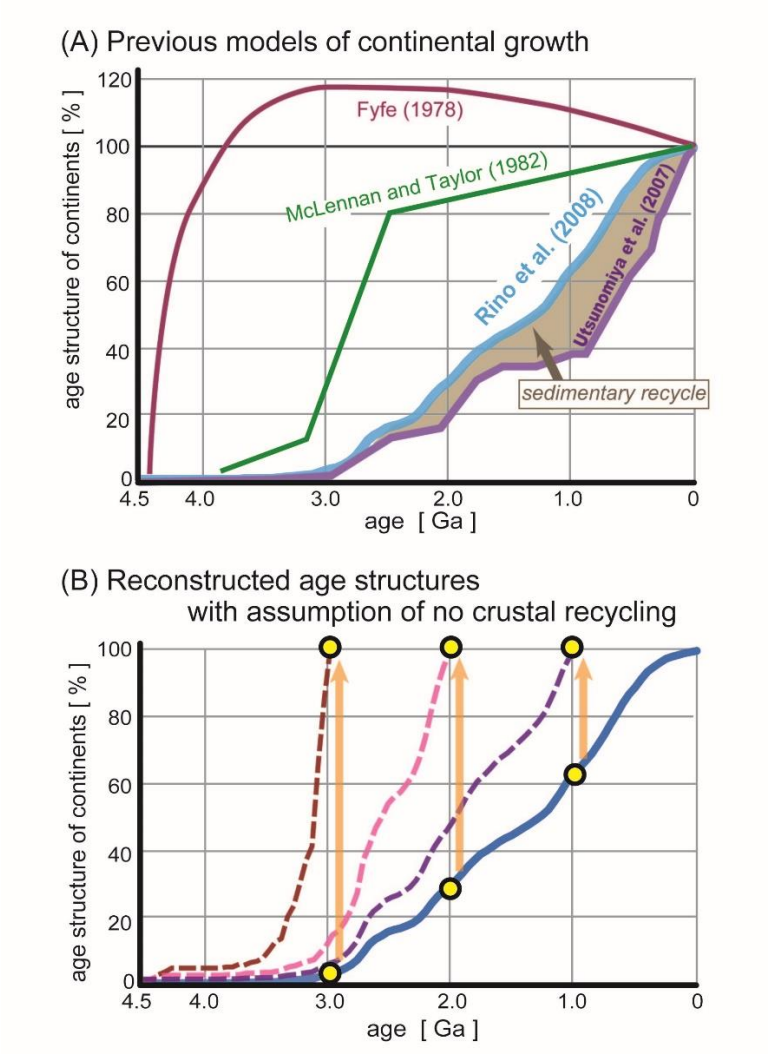

Figure 2-1: (A) Representative continental growth curves (Fyfe, 1978, McLennan and Taylor, 1982) and age structure of continents (Utsunomiya et al., 2007, Rino et al., 2008). The shaded area between the curves by Utsunomiya et al. (2007) and Rino et al. (2008), which represents the difference between the remaining crust mass in map view of Fig. 1-2 and the crustal volume estimated from zircon abundance in river sands. (B) Schematic diagram showing the reconstruction of ancient age structure of continental crust by extrapolating the same pattern from modern river sands into the Proterozoic or Archean time without assuming any recycling in the past; however, such an extreme case never occurred in the real history.

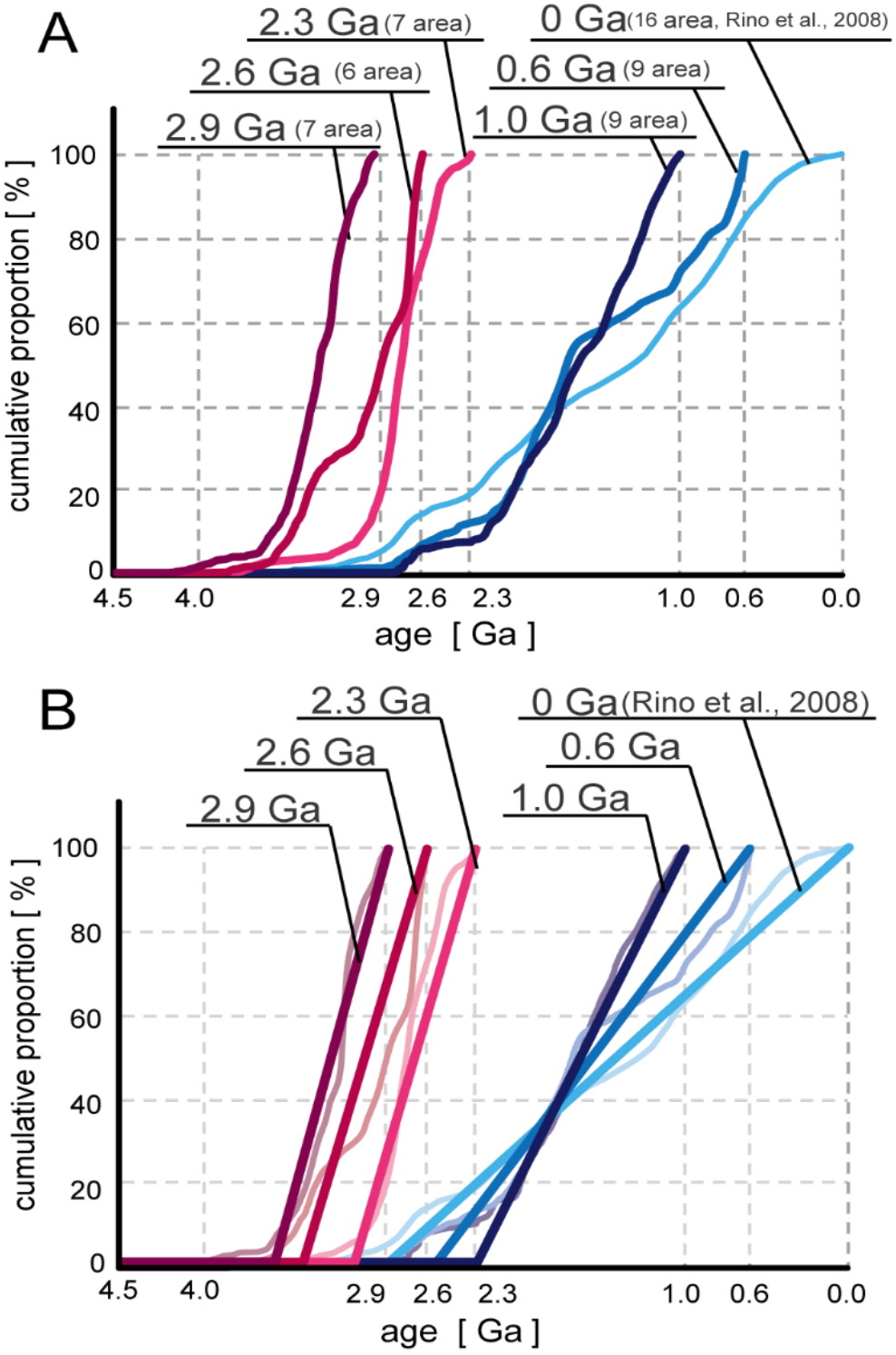

Figure 2-2: Comparison in cumulative curves of averaged detrital zircon age spectra for 6 distinct

time bins, i.e. 2.9, 2.6, 2.3, 1.0, 0.6, and 0 Ga. Vertical axis shows age structure of continents in the form of cumulative age frequency distribution with taking 100 % on a continental volume at each period.

A: cumulative curves of raw data of averaged age spectra.

B: cumulative lines fitted for polygonal line function with original curves of age structure.

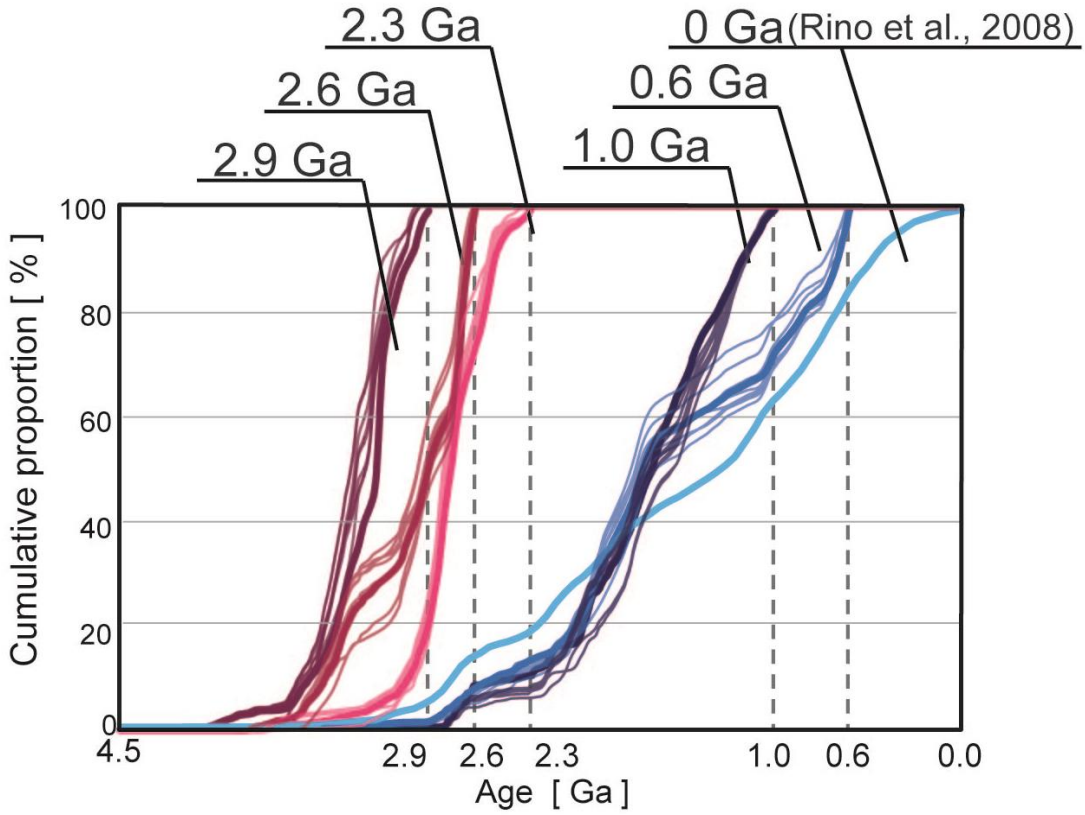

Figure 2-3: Testing of the compilation by repeated integration in different combination of data sources.

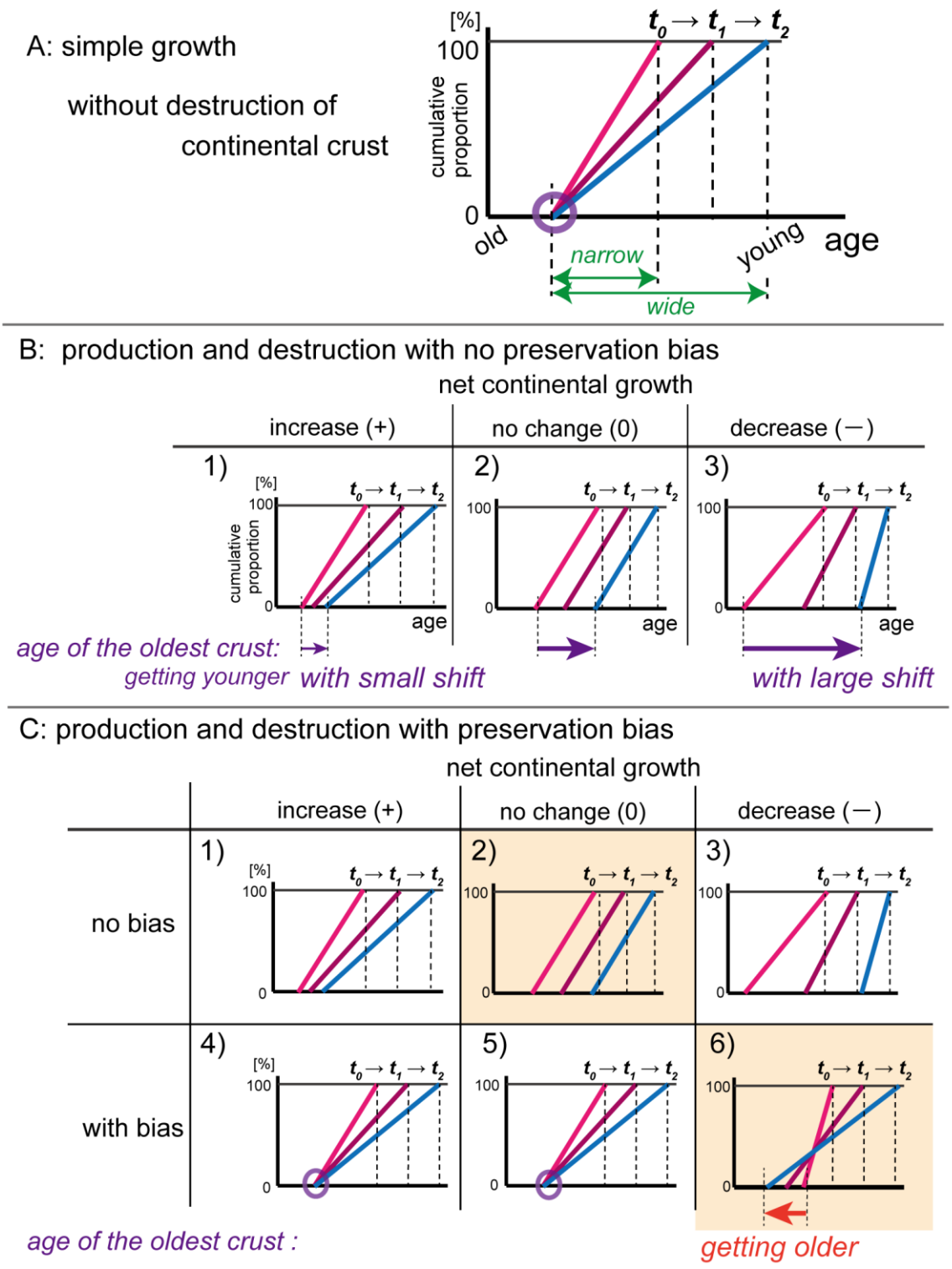

Figure 2-4: Patterns of possible cumulative curves (fitted cumulative lines) and interpretations in

terms of net growth (production minus destruction) of continental crusts and their preservation bias.

A: When crust production is constant without destruction, the cumulative line changes its slope toward gentle, and the age span becomes wider along time (from t0 to t2). B: Three options (1 to 3) may occur according to a balance between the production and destruction of continental crust; i.e., 1) production exceeding destruction, 2) balanced, and 3) destruction exceeds production. The mutual distance (age) between lines and their slopes are different among the three options. C: Six options (1 to 6) may occur according to the production/destruction balance and also to preservation bias. The 2.9, 2.6, and 2.3 Ga cumulative curves correspond to the option 2, whereas those of 1.0, 0.6 and 0 Ga to the option 6.

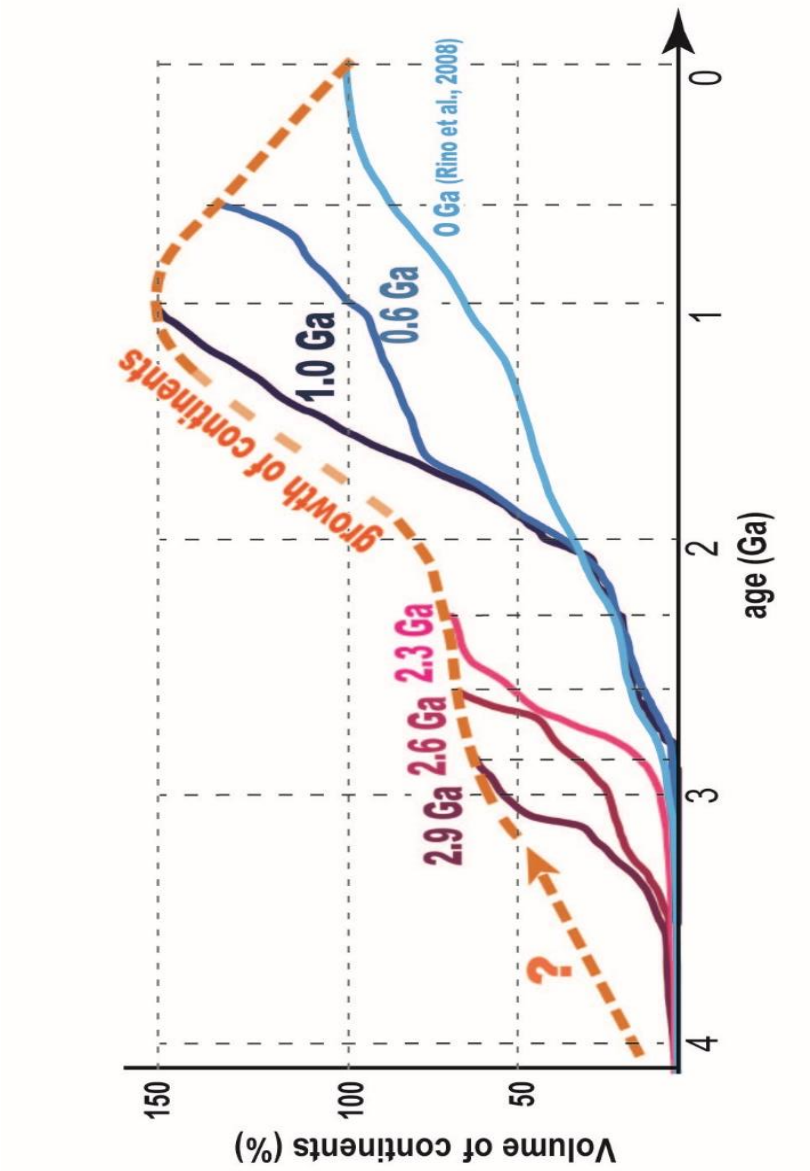

Figure 2-5: Estimated growth history of continents after 3.0 Ga, on the basis of the present compilation of detrital zircon age spectra of sandstones in 6 time-bins and their interpretation.

Tables

Table 2-1: List of area, stratum, references, sample numbers and cumulative age proportions of each sample for compilation.

Table 2-1 List of area, stratum, references, and sample numbers , for compilation.

Age	*No*	*Area*	*Stratum*	*Reference*	*Sample No.*
2.9 Ga	**1**	**Kaapvaal**	**Pongola Gp.**	**This study (Sawada et al., 2018)**	**PP78**
	2	Eastern Slave	Point Lake Quartzite	Sircombe et al. (2001)	
	3	Western Slave	Dwyer Lake Quartzite	Sircombe et al. (2001)	
	4	Dharwar	Dharwar Sgp. Bababudan Gp.	Mishima et al. (2012)	M16-21
	5	Zimbabwe	Buhwa Greenstone Belt, basal quartzite	Dodson et al. (1988)	
	6	Yilgarn	Jack Hills GS belt	Crowly et al. (2005)	Sample26
2.6 Ga	**1**	**Pilbara**	**Mt. Bruce Gp.Jerinaah Fm.**	**This study (Sawada et al., 2018)**	**RM246**
	2	**Zimbabwe**	**Belingwe GS belt Manjeri Fm.**	**This study (Sawada et al., 2016)**	**BW98**
	3	Yilgarn	Eastern Goldfieeld GS belt	Krapez et al. (2000)	KU3
	4	Brazil	Minas Sgp. Caraca Gp.Moeda Fm.	Machado et al. (1996)	M93-2
	5	Superior	Assean Lake Crustal Complex	Bohm et al. (2003)	CB98-83
	6	Dharwar	Hiriyur Fm. Chitradurga Schist Belt	Hokada et al. (2013)	H1102H
2.3 Ga	**1**	**Wyoming**	**Snowy Pass Sgp.**	**This study (Sawada et al., 2018)**	**WY3**
	2	**Rae**	**Lower Murmac Bay Gp**	**Chapter 3**	**UC02**
	3	**Pilbara**	**Turee Creek Gp. Kazput Fm.**	**This study (Sawada et al., 2018)**	**TC255**
	4	Kaapvaal	Postmasburg Gp.Makgenyen Fm.	Mapeo et al. (2006)	RBM2/2001
	5	Superior	Marquette Range Gp.Sturgeon Quartzite	Valini et al. (2006)	StQ
	6	Karelia	Jatulian Quartzite	Kozhevnikov et al. (2010)	S-3976
	7	North China	Wutai Gp.Shizui subgroup	Li et al. (2008)	Jan-28
1.0 Ga	1	Norway	Hadmark Gp.Atna Fm.	Bingen et al., 2011	103 sandstone
	2	NE Greenland	Eleonore Bay Sgp. Nathorst Land Gp.	Dhuime et al., 2007	201728
	3	E Australia	Soldiers Cap Gp.Mt Norna Quartzite	Griffin et al., 2006	P9691
	4	UK	Moin Sgp. Morar Gp.	Kirkland et al., 2008	ARDN-1
	5	South China	Tianli schist	Li et al., 2007	04SC66
	6	Siberia	Uy Gp.Mayamkan Fm.	Rainbird et al., 1998	mm-1
	7	Western Africa	Anti-Atlas Sgp. Taghdout Gp.Mimount Fm.	Abati et al., 2010	AA1
	8	India	Vindhyan Sgp. Bhander Gp.	Malone et al., 2008	I43
	9	Grand Canyon	Unkar Gp. middle Dox Fm.	Timmoos et al., 2005	T02-75-1Z
0.6 Ga	1	Grand Canyon	Upper Bright Angel shale	Gehrels et al. (2011)	
	2	Newfioundland	South Brook Fm.	Cawood and Nemchin (2001)	LM1
	3	South China	Huixiangping Fm. Fanjingshan area	L-J. Wang et al. (2010)	FJS-5
	4	North China	Zhuozi Shan sedimemntary unit	Darby and Gehrels (2006)	Cambrian
	5	Tarim	Yuertus Fm.	Shu et al. (2011)	07A-34
	6	Northeastern Brazil	Serid Gp.Jucurutu gneiss	Van Schmus et al. (2003)	BR/EC-61
	7	United Kingdom	Darladian Sgp. Argyll Gp.	Cawood et al. (2003)	474
	8	Bohemian Massif		Drost et al. (2011)	ja27
	9	Sahara	Aijer Fm., Tassili Ouan Ahaggar basin	Linnemann et al. (2011)	HOG 2

Table 2-2: Fitting for polygonal line function and continental average cycle calculated from the result of fitting.

Age	2.9 Ga	2.6 Ga	2.3 Ga	1.0 Ga	0.6 Ga	0 Ga (Rino et al., 2008)
T [Ma]	3530	3298	3094	2357	2572	2869
Cycle = T-A [Myr.]	630	698	794	1357	1972	2869

Chapter 3. Archean crustal development and plate subduction from detrital zircon U-Pb and Lu-Hf analyses of the Murmac Bay Group in the Rae Craton

Abstract

To understand the timing and mode of crustal development in the Archean, this study performed U-Pb and Hf isotopic analyses of detrital zircon grains from the ca. 2.3 Ga Murmac Bay Group in the Rae Craton, central Canada. The zircon U-Pb ages range from 3.9 to 2.3 Ga with a significant gap in ca. 3.6-3.3 Ga, indicating that granitic magmatism has semi-continuously occurred within the craton since the early Archean. The combined U-Pb and Hf isotopic data define three distinct Hf isotope-age arrays that have slopes equivalent to a typical continental crustal $^{176}Lu/^{177}Hf$ ratio and intersect the mantle evolution curve at 2.6-2.9, 3.2-3.3, and 3.6-3.8 Ga. The Hf isotopic secular trends illustrate episodic crust formation from the depleted mantle during the three periods with subsequent reworking of the crust into younger granitoids. Furthermore, these results show that granitoid crust was rarely reworked more than 800 million years after its formation. This finding is well explained if the Archean craton was developed from the core toward outside by adding new crusts by subduction-related magmatism and/or by secondary accretion of exotic arc crusts. In this framework, younger crusts are more preferentially utilized in crustal melting by subduction-related magmatism. This suggests that plate subduction have operated already in the early Archean, as early as 3.6 Ga Eoarchean.

3.1. Introduction

Detailed history of the crust formation and reworking in the early Archean remains unclear owing to limited geological records on the extant surface crusts. To date, Hadean to earliest Archean geologic units have been reported fragmentarily from several continental fragments within the Laurentia shield; e.g. the Acasta gneiss complex in the Slave Craton (e.g. Bowring and Williams, 1999; Iizuka et al., 2007) and the Nuvvuagittuq Greenstone belt in the Superior Craton (e.g. Cate and Mojzsis, 2007; O'Neil et al., 2008), and Isua-Nuliak supracrustal belts in the North Atlantic Craton (e.g. Nutman and Friend, 2009; Komiya et al., 1998; 2015). The Archean Rae

Craton is in the north-central part of Laurentia and yields early Archean-Hadean zircon grains as detrital zircon (Hartlaub et al., 2004; Ashton et al., 2013; Rainbird et al., 2010; Wodicka et al., 2014) and xenocrystic inherited zircon (Martel et al., 2008) at several localities; however, details of the crustal growth of the craton are still not well known as it suffered by later metamorphism and deformation and was covered by many Proterozoic and Phanerozoic cover sediments. To obtain a signature of regional Archean crust evolution, this study focuses on detrital zircon from the Paleoproterozoic terrigenous clastics (changed into quartzite and psammitic gneisses) in the Murmac Bay Group (MBG) on the Rae Craton (Fig. 3-1). The Paleoproterozoic terrigenous clastics are thought to have been primarily deposited in a sedimentary basin along a continental rift setting or of passive continental margin, and have yielded abundant Archean detrital zircon grains, of which the oldest age reaches 3.9 Ga (Hartlaub et al., 2004; Ashton et al., 2013; Shield et al., 2016). Thus, the Paleoproterozoic meta-sedimentary rocks offer a good opportunity to study the Archean crustal evolution of the (proto-)Rae Craton.

The secular change in the pattern of crustal growth and the degree of reworking can be checked by analyzing preserved crustal rocks and minerals, as reworked crustal materials have distinct isotopic signatures. Among them, a combination of U-Pb age dating and Hf isotopic analysis of zircon grains is effective in documenting secular changes in formation/recycling of ancient continental crusts (e.g., Vervoort et al., 1996; Knudsen et al., 2001; Iizuka et al., 2010). Previous U-Pb and Hf isotope analyses of detrital zircon grains from the MBG (Hartlaub et al., 2006; Shiels et al., 2017) demonstrated that early Archean grains have sub-chondritic $^{176}Hf/^{177}Hf$ indicative of the reworking of pre-existing crust, whereas Paleoproterozoic grains have nearly chondritic to super-chondritic values.

This study reports more comprehensive U-Pb and Hf isotopic data for detrital zircon grains from the MBG with LA-ICP-MS and LA-MC-ICP-MS. The results reveal previously unrecognized secular trends of Hf isotope composition, which provide new insights into the crustal evolution and tectonic regime in the Archean.

3.2. Geological outline

The basement of the Rae Craton is mainly composed of ca. 3.0-2.6 Ga granitoid suites, which are penetrated by late Archean and Proterozoic granitoid intrusive and also covered by

Paleoproterozoic sedimentary sequences (Davis and Zaleski, 1998; Skulski et al., 2003; Hartlaub et al., 2004; Martel et al., 2008). Some zircon grains from a 2.6 Ga granite in the Snowbird Tectonic Zone contain inherited cores with Hadean U-Pb ages (4,043 ± 10 Ma, Martel et al., 2008). In addition, ca. 3.5 Ga zircon grains occur in a granulite xenolith within the Replse Bay kimberlite in the Eastern Rae Craton (Petts et al., 2014). The presence of these ancient zircon grains, although sparse in number even in total, suggests that crust formation in the proto-Rae Craton started by the early Archean.

The 3.0-2.6 Ga granitoid basement of the Rae Craton was overprinted by the late Archean and Paleoproterozoic orogeny accompanied by granitic intrusions and high-grade metamorphism. Based on the geotectonic structures of the late Archean-Paleoproterozoic geological units, it has been suggested that subduction of multiple oceanic plates beneath the Rae Craton caused ca. 2.56-2.4 Ga orogeny, followed by ca. 2.4-2.3 Ga orogeny due to the collisions with the surrounding cratons (Arrowsmith and McQuoid orogenies; Berman et al., 2005; 2013).

After the ca. 2.4 Ga Arrowsmith orogeny, Paleoproterozoic sedimentary basins developed extensively to cover the Archean granitoid basements in the Rae Craton (Wodicka et al., 2014; Rainbird et al, 2010). The oldest sedimentary units occur mainly in the western part of the Rae Craton (Bostock and Breemen, 1994). The Murmac Bay Group (MBG) in the southwest margin of the Rae Craton represents one of the oldest units (Fig. 1). The MBG exposes on the northwest coast of the Athabasca Lake over 100 km in the east-west direction, and the best exposure of the group occurs around Uranium City, Saskatchewan, Canada. The MBG is composed of sedimentary rocks and mafic-ultramafic rocks (Ashton and Card, 1998; Card and Bethune, 1999; Hartlaub et al., 2004). These rocks have been metamorphosed in the amphibolite to granulite facies (Ashton and Card, 1998; Hartlaub and Ashton, 1998; Ashton et al., 2000), and been deformed at least by five episodes (Ashton et al., 2001; Bethune et al., 2013). Its primary stratigraphy and total thickness are unclear except for a few places (e.g. the Crackingstone Peninsula; Hartlaub et al., 2004).

The lower unit of the MBG is mainly composed of quartzite and mafic dykes which intruded both the orthoquartzite and the granitoid basement (Hartlaub et al., 2004). A minor amount of banded iron formation and carbonate rocks are locally associated with the basaltic lava. The previous analysis of the basalt showed MORB-like composition with crustal contamination (Hartlaub et al., 2004). These rock assemblage and geochemical features suggest that the lower MBG deposited in a continental rifted basin (Hartlaub et al., 2004; Ashton et al., 2013). The youngest detrital zircon age of 2.33 Ga for the orthoquartzite, together with the 2.32 Ga quartz-

feldspar porphyry dyke intruding metabasite near the basal unconformity, indicates that the sedimentation of the MBG had started at 2.33-2.32 Ga (Ashton et al., 2013). The upper MBG is composed of pelitic metamorphic rocks, whose age is constrained to be younger than ca. 2.17 Ga from the youngest detrital zircon (Ashton et al., 2013). The depositional age of the upper MBG is younger than the known 1.94-1.92 and 1.91-1.90 Ga metamorphic events (Ashton et al., 2009; Bethune et al., 2013).

In the Rae Craton, ca. 2.1-1.8 Ga sedimentary units are widely distributed in the eastern region (Fig. 1). The basal units of these sedimentary sequences are composed of quartzite. Most detrital zircon grains from those sedimentary units yielded ages between 2.3 and 3.0 Ga, whereas the oldest grain was dated at 3.74 Ga (Rainbird et al., 2010; Wodicka et al., 2014). After continental break-up at ca. 2.1-2.0 Ga, the Rae Craton was metamorphosed and deformed by the 2.0-1.9 Ga Taltson orogeny and the 1.9-1.8 Ga Hudsonian orogeny (Hoffman, 1988; Carson et al., 2004; Berman et al., 2005, 2007; Ashton et al., 2009).

3.3. Samples and methods

3.3.1. Samples

In this study, detrital zircon grains were separated from seven psammitic gneiss (meta-sandstone) samples collected from the Lower Unit of the MBG near Uranium City (Fig. 3-1). All samples were collected from the units mapped as “quartzite” by Asthon et al. (2013), which are composed of mainly quartz with muscovite, biotite, feldspar, and clay minerals. Photomicrographs of thin sections and results of mode count analysis are shown in Fig. 3.2. The volume ratio of quartz diverse between 65 and 95 %.

The WGS84 GPS coordinates of the sample localities are as follows: UC02: 59.49433°N, 108.66552°W; UC03: 59.49302°N, 108.66838°W; UC09: 59.55631°N,108.42908°W; UC11: 59.55574°N, 108.43486°W; UC12: 59.55590°N, 108.43927°W; UC14: 59.55342°N, 108.46904°W; and UC21: 52.12756°N, 108.49379°W.

3.2. U-Pb dating

Detrital zircon grains were concentrated from the disaggregated samples by conventional panning, magnetic separation and using heavy liquid. The separated detrital zircon grains have various colors such as gray, brown, white and colorless, and typically rounded anhedral or subhedral shapes. Approximately 200 to 1,000 zircon grains from each sample were mounted within epoxy resin discs together with the zircon standard FC-1 ($^{206}Pb/^{238}U$ = 0.1859; Paces and Miller, 1993), and the standard glass NIST SRM 610. Cathodoluminescence images were used to check their internal structures and to select the sites for analysis (Figure 3-3). The analysis was carried out on oscillatory- or sector-zoned domains which are considered as magmatic origin. U-Pb dating was performed on 1,163 grains using Agilent 7700x quadrupole ICP-MS (Agilent Technologies) coupled with a NWR213 Nd:YAG laser ablation system (Electro Scientific Industries) at National Museum of Nature and Sciences in Japan. The experimental conditions and the procedures for the measurements were based on the methods described in Tsutsumi et al. (2012). The spot size of the laser was approximately 25 μm in diameter. To remove surface contaminants, regions of interest were pre-ablated using one pulse laser shot with a spot size of 40 μm in diameter prior to analyses. Isotopic composition of common Pb is estimated on the basis of measuring values of ^{204}Pb+^{204}Hg and ^{202}Hg, assuming the isotopic ratio of natural Hg (202Hg/204Hg = 4.369; de Laeter et al., 2003).

3.3. Lu-Hf isotopic analysis

The Lu–Hf isotopic analyses were performed on a LSX-213 Nd:YAG LA system attached to a Thermo Fisher Scientific Neptune plus multiple collector (MC)-ICP-MS at the University of Tokyo. The data were obtained from 30-50 μm ablation pits with a laser repetition rate of 5 Hz and ~60 s ablation time. Helium gas was used to flush the ablation pit. Furthermore, ca. 3–4 ml/min N2 was mixed into the Ar sample carrier gas to enhance the signal intensity (Iizuka and Hirata, 2005). Isotopes of ^{171}Yb, ^{173}Yb, ^{175}Lu, $^{176}(Hf + Yb + Lu)$, ^{177}Hf, ^{178}Hf, ^{179}Hf, ^{180}Hf and ^{182}W were monitored using nine Faraday cups. The contribution of the isobaric interferences by ^{176}Yb and ^{176}Lu on ^{176}Hf was corrected by measuring ^{173}Yb and 175Lu before the mass bias correction for $^{176}Hf/^{177}Hf$. The $^{176}Yb/^{173}Yb$ value of 0.78696 (Thirlwall and Anczkiewicz, 2004) and $^{176}Lu/^{175}Lu$ value of 0.026549 (Chu et al., 2002) were utilized for the interference correction.

Instrumental mass discrimination was corrected using an exponential law. The mass bias factor for Yb was calculated by normalizing the measured $^{173}Yb/^{171}Yb$ to 1.12346 (Thirlwall and Anczkiewicz, 2004), whereas those for Hf and Lu were calculated by normalizing the measured 179Hf/177Hf to 0.7325 (Patchett et al., 1981). Additionally, to enable accurate comparison with literature values, Hf isotopic ratios corrected for mass bias were further normalized to reference values $^{178}Hf/^{177}Hf$ = 1.467168 and $^{176}Hf/^{177}Hf$ = 0.282507 for the Mud Tank zircon standard (normalized to $^{176}Hf/^{177}Hf$ = 0.282160 for JMC-Hf 475; Woodhead and Hergt, 2005). The offset values were determined from the mean Hf isotopic ratios obtained for the standard on any given analytical session.

The zircon standards R33 and FC-1 were analyzed to evaluate the accuracy and precision of data obtained by the present technique. Our data during this study yielded mean initial $^{176}Hf/^{177}Hf$ = 0.282728 ± 0.000026 (2 s.d., n = 70) for R33, and 0.282163 ± 0.000024 (2 s.d., n = 51) for FC-1. These results are consistent with the solution-MC-ICP-MS determinations (0.282753 ± 18 for R33, and 0.282184 ± 16 for FC-1, Woodhead and Hergt, 2005; Fisher et al., 2014).

3.4. Analytical results

The U-Pb isotopic data obtained in this work are listed in Table 3-1 and presented on concordia diagrams in Fig. 3-4. Many zircon grains yielded highly discordant U-Pb ages. The present study has not used the data with %discordances higher than 10% for the following discussion. In addition, the data from zircon domains having Th/U ratios lower than 0.1 or the fraction of common ^{206}Pb in total ^{206}Pb higher than 3% are excluded, given that domains with these characteristics are metamorphic, metamict, or contaminated by inclusions (Hoskin and Ireland, 2000; Rubatto, 2002; Tsutsumi et al., 2012). The selected zircon age populations for each sample are shown in ^{207}Pb-^{206}Pb age histograms (Fig. 3-5). The obtained U-Pb ages range between 3.9 and 2.3 Ga. Among the seven studied samples, four samples (UC02, 09, 11, and 21) have dominant age peaks at 3.0-2.5 Ga, two samples (UC03 and 14) show dominant clusters between 3.4 and 3.0 Ga, and one (UC12) has a prominent peak at 3.9-3.5 Ga with a smaller cluster between 3.0 and 2.6 Ga. The accumulated U-Pb age population of the seven samples (Fig. 3-6B) shows a dominant cluster between 3.4 and 2.5 Ga and a subordinate cluster at 3.9-3.5 Ga, highlighting an age gap in 3.6-3.3 Ga.

The results of the Lu-Hf isotopic analysis are shown in Table 3-2 and graphically presented in Fig. 3-6 as a plot of εHf versus ^{207}Pb-^{206}Pb age. Consistent with the results of Hartlaub et al. (2006), many grains, including early Archean ones, have negative εHf values. A substantial proportion of early Archean grains, together with many late Archean and some middle Archean grains, have positive εHf values. The ^{207}Pb-^{206}Pb age histogram of zircon grains having positive εHf shows prominent clusters at ca. 2.9-2.6 Ga and 3.8-3.6 Ga with a small cluster at 3.3-3.2 Ga (Fig. 3B). In addition, the non-mantle-like (i.e. non-juvenile) Hf isotopic data form three broad εHf-time arrays that intersect with the clusters of mantle-like εHf values and whose slopes are equivalent to 176Lu/177Hf of 0.015 which is typical Precambrian continental crust (Fig. 3A).

3.5. Discussion and implications

The accumulated U-Pb age spectra (Fig. 3-6B) show a dominant cluster at 3.4-2.5 Ga age with a smaller one at 3.9-3.5 Ga. This result indicates that the lower unit of the MBG has a provenance composed of Paleo- to Neoarchean granitoids, probably within the Rae Craton, which is consistent with the previous results by Hartlaub et al. (2004; 2006) and Ashton et al. (2013). Furthermore, this study found that the zircon age patterns are highly variable among the studied samples (Fig. 3-5A-G): dominant age peaks vary from 3.9-3.5 Ga (UC12), 3.5-3.0 Ga (UC03 and 14), to 3.0-2.5 Ga (UC02, 09, 11 and 21). No correlation between mineral assemblage and detrital zircon age pattern is observed among the analyzed samples. The dominant late Archean age cluster of 3.0-2.5 Ga apparently corresponds to the crystalline basement currently exposed in the Rae craton (Davis and Zaleski, 1998; Skulski et al., 2003; Hartlaub et al., 2004; Martel et al., 2008; Ashton et al., 2013). Given that the MBG was deposited in a rift basin in the Rae Craton (Hartlaub et al., 2004; Bethune et al., 2013), the variation in the age pattern may reflect that the major terrigenous source to the MBG has changed significantly, possibly due to topographic changes in the basin caused by active rifting. It is noteworthy that similar age spectra from a single sedimentary package was reported elsewhere in other Paleoproterozoic rift-related basins on other cratons, such as the Huron Supergroup (Craddock et al., 2013) and the Marquette Range Supergroup (Vallini et al., 2006) on the Superior Craton.

The Hf isotopic data (Fig. 3-6) reveal that substantial portions of the 3.8-3.6, 3.3-3.2, and 2.9-2.6 Ga zircon populations have positive εHf values in arc mantle range, whereas most of the analyzed zircon grains formed during other periods exhibit negative εHf values, i.e. enriched

isotopic signatures. Moreover, the depleted and enriched Hf isotopic data define broad arrays that can be explained by successive but discontinuous reworking in the three distinct generations of crust from the depleted mantle. These observations indicate that significant amounts of new crust generation occurred in three steps; i.e., at 3.8-3.6, 3.3-3.2, and 2.9-2.6 Ga, in the (proto-)Rae Craton, followed by the crustal melting to form younger granitic rocks. The 207Pb-206Pb age histograms of all the zircon grains with concordant ages, as well as the subset with positive εHf values (Fig. 3-6B), illustrate that while new crust generation was episodic, intra-crustal reworking was rather continuous after 3.3 Ga. The 3.8-3.6 Ga episodic crust formation is not followed by clear continuous reworking because of the 3.6-3.3 Ga barren interval. The 3.6-3.3 Ga barren interval is recognizable even in the 207Pb-206Pb age spectra of all zircon grains, requiring that both new crust formation and intra-crustal reworking were inactive at that time. Such a barren interval of 3.6-3.3 Ga in zircon ages, especially around 3.4 Ga, has been proposed by Næraa et al. (2012) and Hartlaub et al. (2006) for other regions. The present results confirm the 3.6-3.3 Ga barren interval of crustal formation in the proto-Rae Craton, even though such interval is ambiguous in the "global" U-Pb-Hf data compilation of detrital zircon (Belousova et al., 2010; Dhumie et al., 2012; Roberts and Spencer, 2016).

The secular variation of Hf isotopes in the detrital zircon grains (Fig. 3-6A) further indicates that older crust was usually not reworked 800 million years after its formation. Specifically, crusts formed from the depleted mantle at 3.8-3.6, 3.3-3.2, and 2.9-2.6 Ga were subsequently reworked into enriched magmas generated at 3.6-3.2, 3.2-2.6, and < 2.6 Ga, respectively. Notably, a similar secular trend indicative of crustal rejuvenation was observed in zircon grains from the Phanerozoic circum-Pacific orogens where oceanic plates almost continuously have subducted under continental plates (Collins et al., 2011). The re-depletion in these orogens has been attributed to the emplacement of new continental crust along active continental margins through subduction-related magmatism or island arc accretion. Taking this into account, the repeated crustal rejuvenation trends observed in the Archean zircon records strongly suggest a general pattern of Archean continental growth; a craton grows outward from its interior toward the outer margins mainly by subduction-related magmatism and accretion of continental blocks (Fig. 3-7A, B). In contrast, it is difficult to reconcile our results in the framework of stagnant-lid tectonic regime, under which zoned crustal age distribution would not be observed, as evidenced by the age-space distributions of the Venusian crusts (e.g. Basilevsky and Head, 2000; Tanaka et al., 2014). The 3.8-3.6 Ga crustal formation without such characteristic reworking might have occurred by plume activity without any significant contribution of plate subduction. Another possible explanation for the 3.8-3.6 Ga crustal formation is immature oceanic island arc

with primitive plate subduction, which can prevent continuous reworking of older crust (Collins et al., 2011; Fig. 4C).

These suggest that, in 3.6-3.3 Ga, subduction-related accretion of continental blocks occurred to co-exist continental area of active orogenic region and non-active stable region (Fig. 3-7B). Therefore, we concludes that the Archean proto-Rae Craton has grown under the plate subduction regime, with the implication that the initiation timing of plate subduction goes back as old as ~3.6 Ga.

3.6. Conclusion

U-Pb age and Hf isotopic signature of detrital zircon from the 2.3 Ga Murmac Bay Group in the Rae Craton reveals three major episodes of crustal formation and subsequent crustal reworking in the Archean. The barren interval in U-Pb age and positive εHf values in 3.6-3.3 Ga suggests the proto-Rae Craton was located in continental interior avoiding active crustal formation. Our new results of the εHf -time trend also show that continental crust more than 800 million years after once formed was usually not reworked associated with the later crustal formation. This indicates that the relatively older crust was preserved in interior of a continental block far from active continental margin. The finding implies plate subduction and accretionary growth of a continental block in 3.6-3.3 Ga to build proto-Rae Craton.

Figures

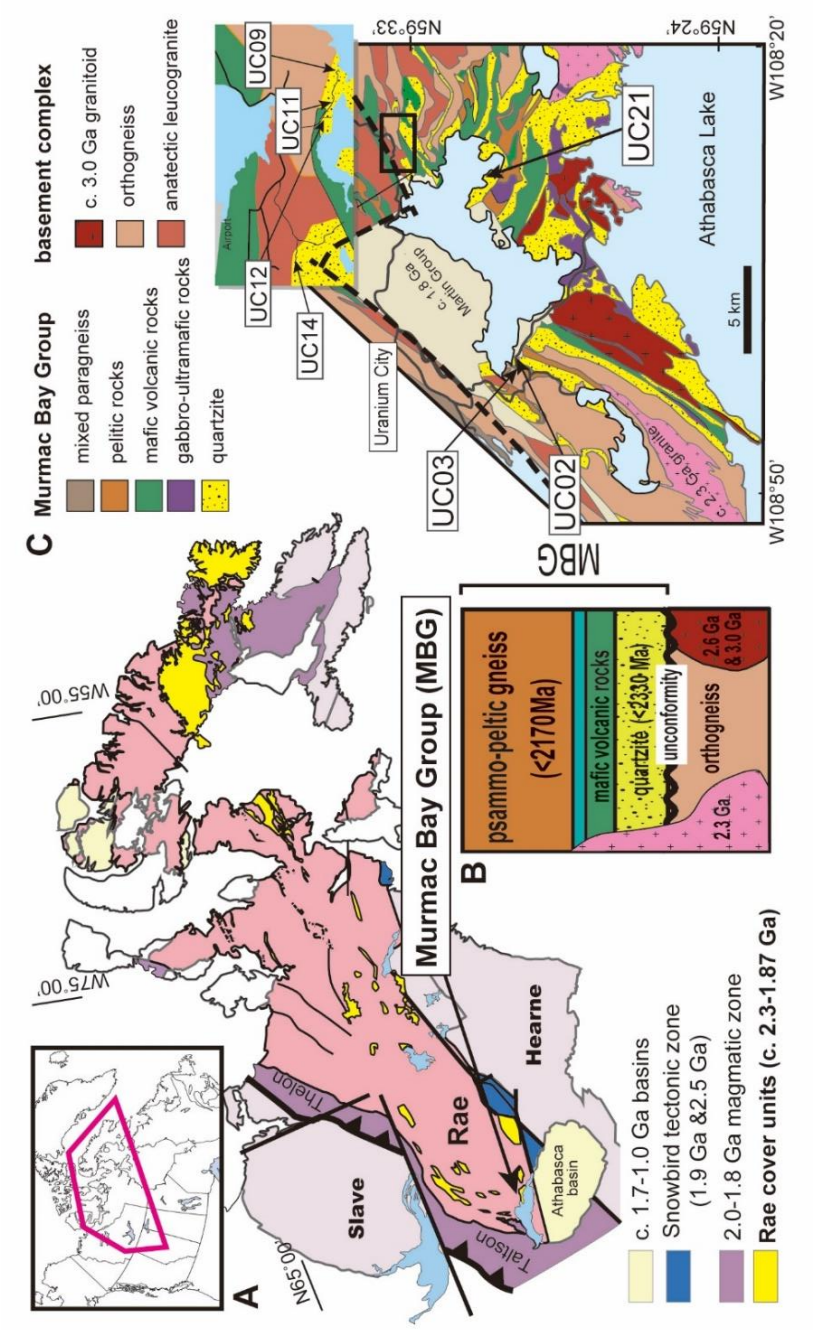

Figure 3-1: Index maps of studied area. A. Geotectonic map of the Rae Craton. B. Schematic stratigraphy of the Murmac Bay Group (Bethune et al., 2013). C. Sample localities on geological map around Uranium City, Saskatchewan (Ashton et al., 2013).

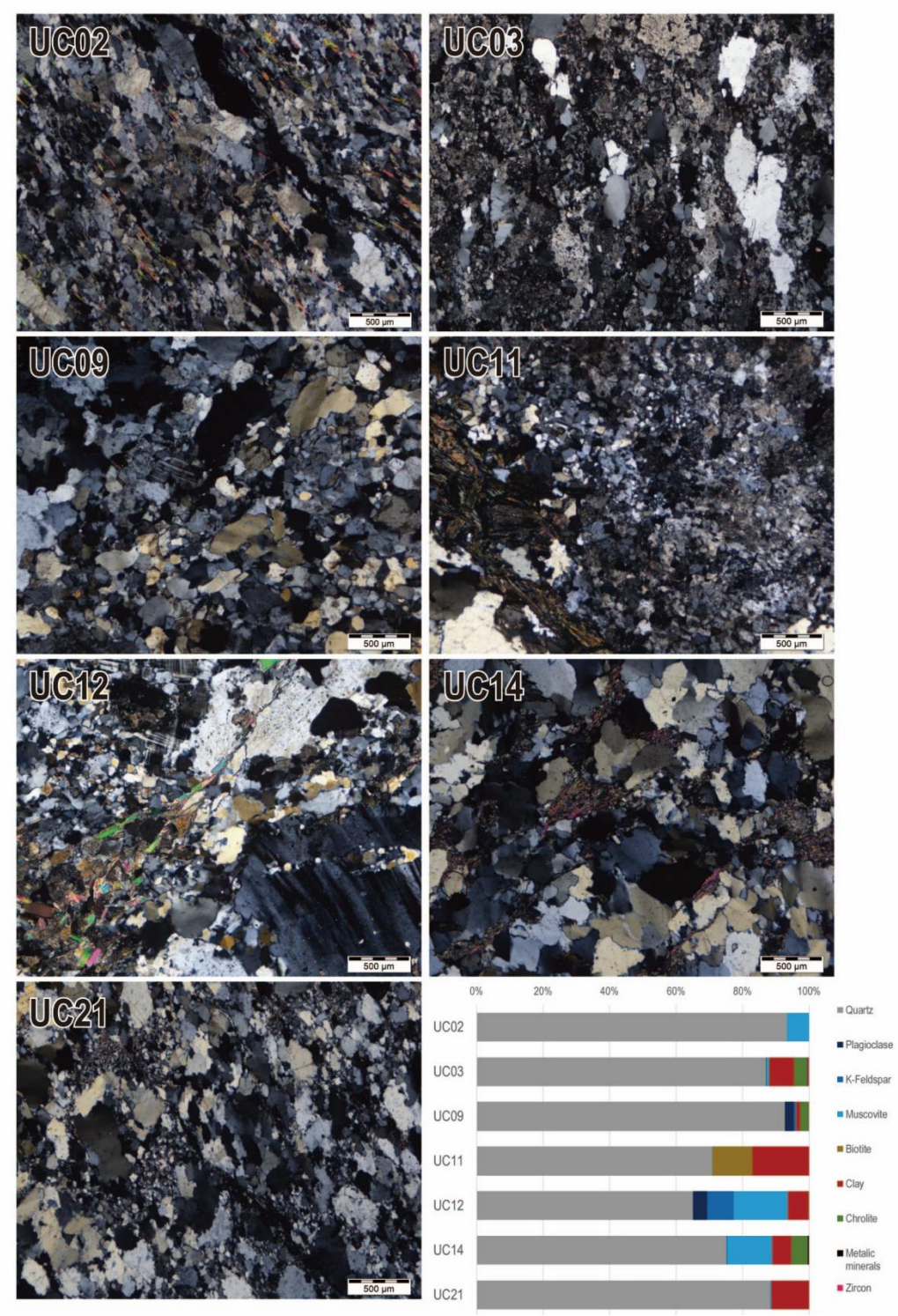

Figure 3-2: Photomicrographs of thin section of analyzed samples.

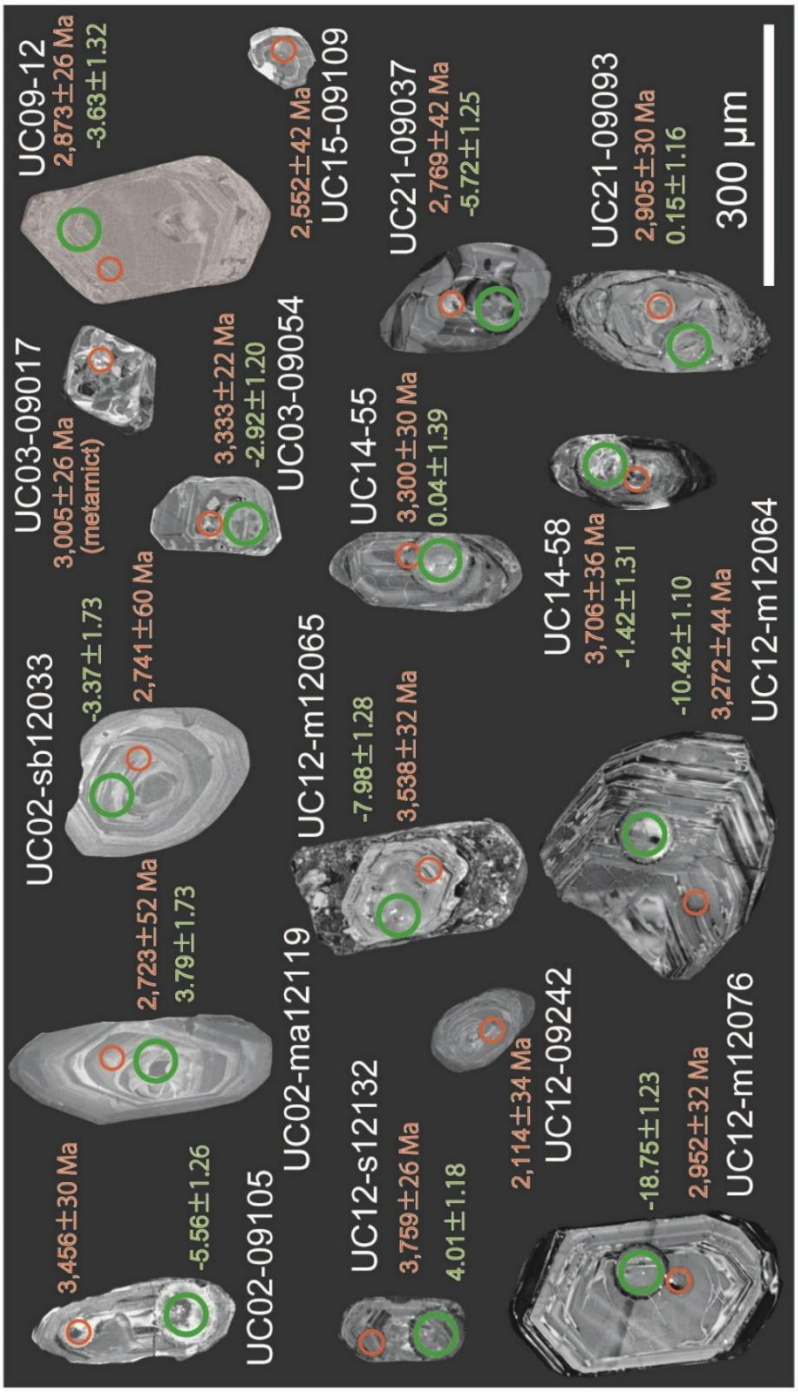

Figure 3-3: Selected CL images with analytical spots and results of U-Pb dating and Hf isotopic analysis.

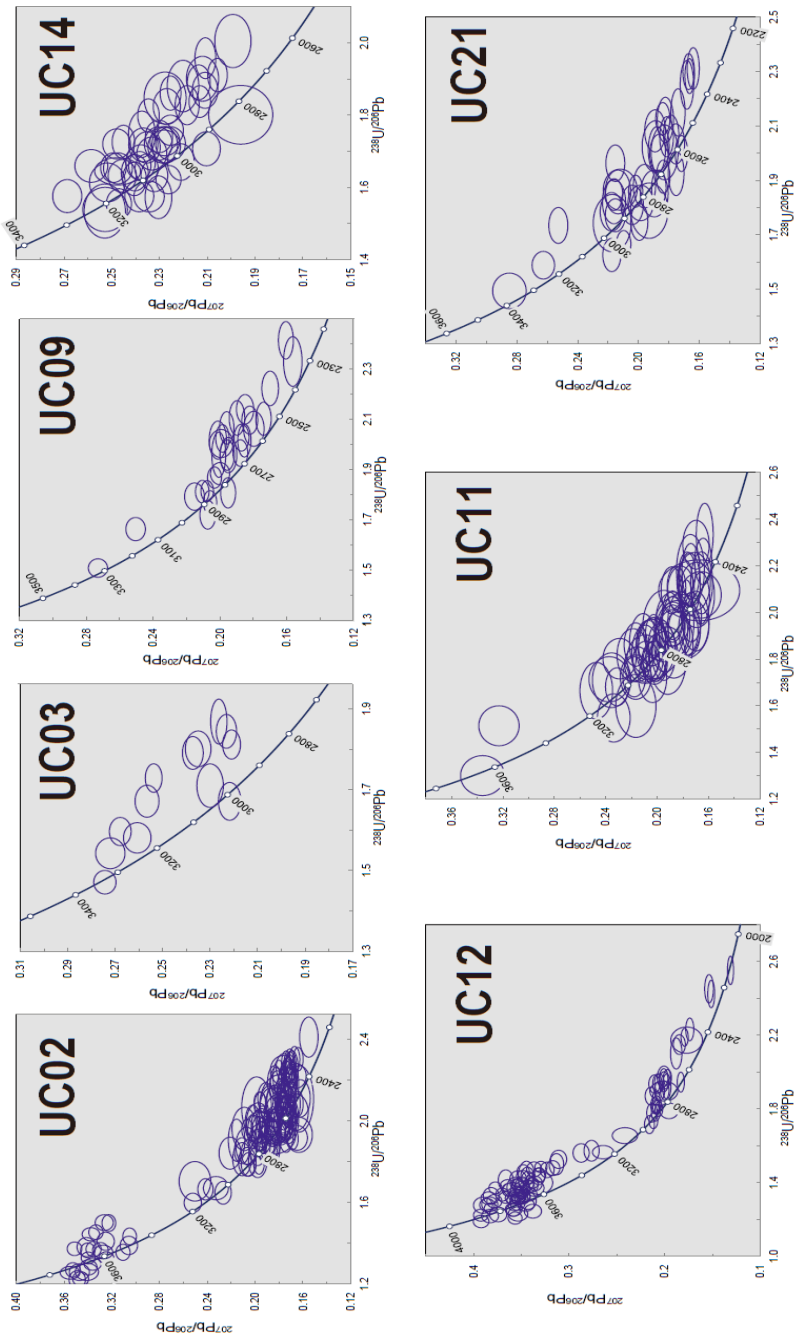

Figure 3-4. Concordia diagrams of the all analyzed samples. These figures were constructed with an ISOPLOT (Ludwig, 2003). Error ellipses on individual spots are at 2σ level.

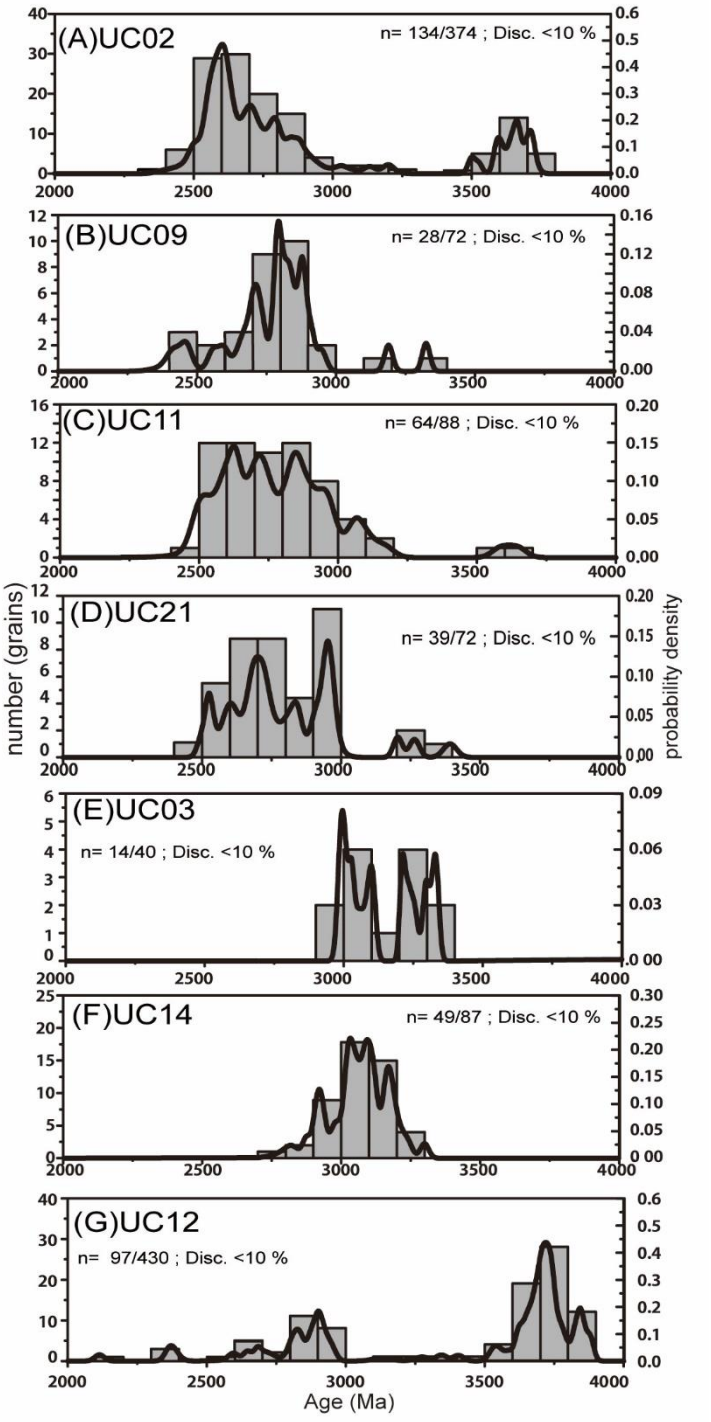

Figure 3-5: (A)-(G) Zircon ^{207}Pb-^{206}Pb age spectra of analyzed seven samples.

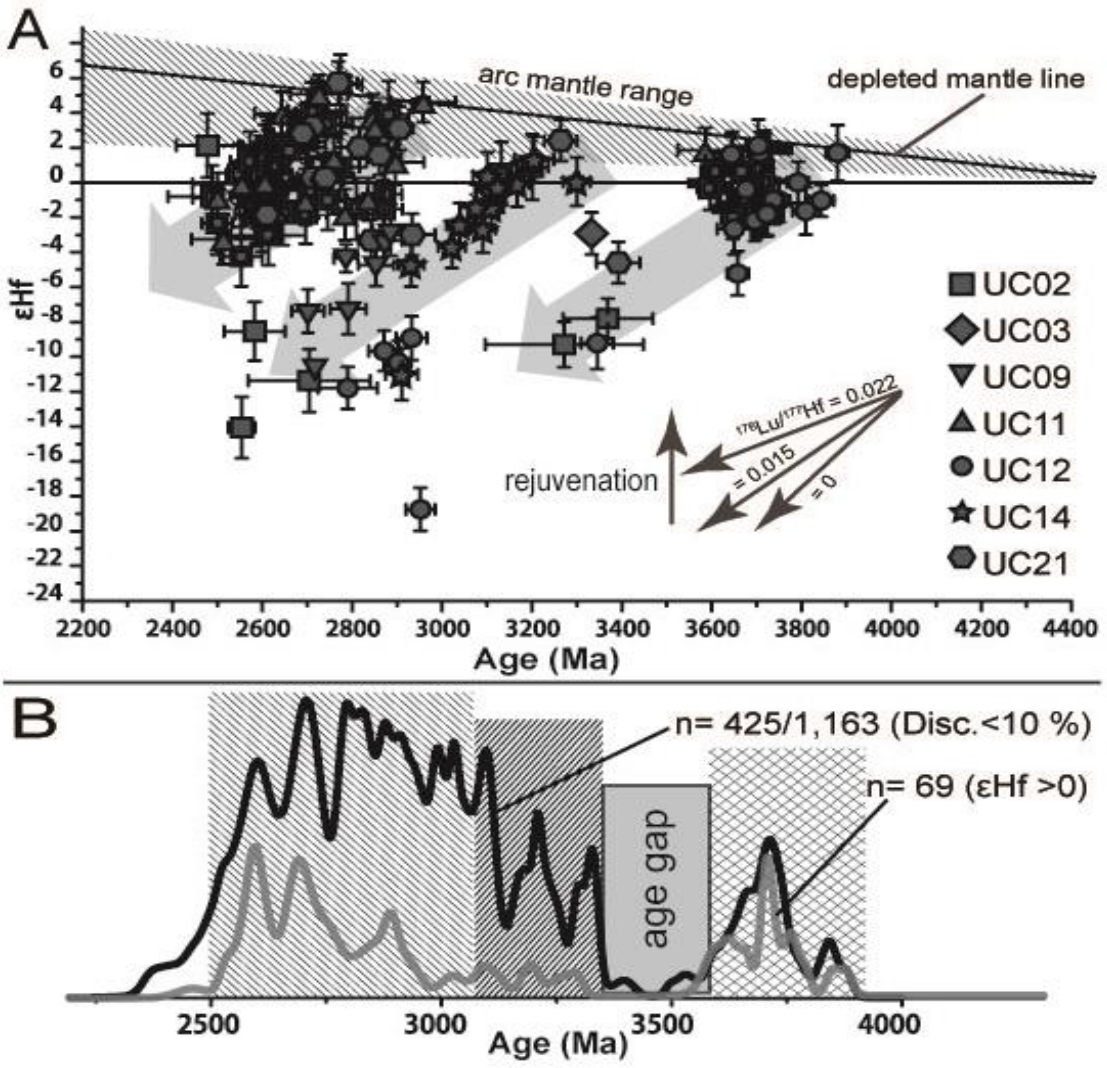

Figure 3-6: A. Plot of εHf value versus ^{207}Pb-^{206}Pb age of zircon grains having discordance less than 5 %. The chondritic uniform reservoir (CHUR), depleted mantle (DM), and arc mantle domain are from Iizuka et al. (2015; 2013). The black arrows are shown for reservoirs with $^{176}Lu/^{177}Hf$ = 0, 0.015, and 0.022, equivalent to zircon, the Precambrian continental crust, and mafic crust (Griffin et al., 2014), respectively. B. Age spectra of all analyzed detrital zircon grains and zircon grains having mantle-like Hf isotope ratios.

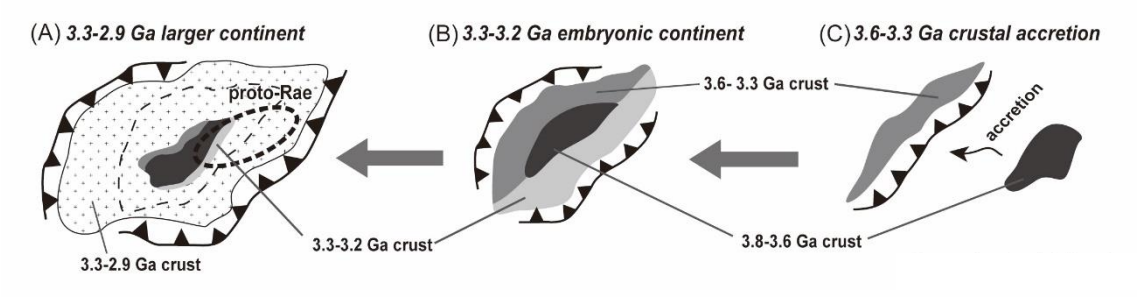

Figure 3-7: Schematic illustration of the development of Archean continental crust.

Tables

Table 3-1: LA-ICPMS U–Pb data and calculated ages of detrital zircons in the Murmac Bay Group. (in Appendix)

Table 3-2: Results from LA-MC-ICPMS Lu-Hf isotopic data for detrital zircons from the Murmac Bay Group. (in Appendix)

Chapter 4. Geochronological constraints to the middle Archean Shurugwi Greenstone Belt in the Zimbabwe Craton and implication for growth of Archean continental block

Abstract

Understanding of repeated formations of greenstone belts and emplacement of granitoid/orthogneiss are significant to reveal crustal evolution on the early Earth. The Shurugwi Greenstone Belt (SGB) in center part of the Zimbabwe Craton has been considered to contain one of the oldest geological units of the craton, but formation age of the belt has not been well constrained. This study performed *in situ* U-Pb dating of zircons from basement orthogneiss of the SGB, meta-sedimentary rocks in the SGB, and late granitic intrusions, as well as whole-rock Re-Os dating of chromitite from the SGB. Most of the detrital zircons from sedimentary rocks in both the Wanderer Formation in the upper unit and the Mont d'Or Formation in the lower unit were highly metamicted. Few numbers of less metamicted ones show concordant ages around ca. 3.6 Ga. Zircons from the granitic intrusion into the SGB show ca. 2.91 Ga, and those from orthogneiss beneath the SGB show ca. 3.02 Ga. Whole rock Os model ages of the ultramafic rocks show ca. 3.0 Ga. In conclusion, the SGB was formed around ca. 3.0 Ga and belongs to the lower Bulawayan unit. Even though the deposition of the SGB occurred ca. 3.0 Ga, meta-sedimentary rocks of the SGB include only ca. 3.6-3.3 Ga zircons. This study envisages that supply of younger detrital zircons from active continental margin to a rift basin of the SGB was prevented because the SGB was formed on center part of a large continental block of the proto-Zimbabwe Craton.

4.1. Introduction

The Zimbabwe Craton has been known as the one of the most representative Archean granitoid-greenstone terrain, which are significant to reveal geotectonic history in the early Earth (Wilson et al., 1978; Fig, 4-1). Although major two Archean cratons are in the southern Africa; i.e. the Zimbabwe and Kaapvaal cratons, they had been different continental blocks before ca. 2.6

Ga late Archean collision (Barton and van Reenen, 1992).

In the Zimbabwe Craton, four generations of greenstone units are recognized; i.e., ca. 2.7-2.6 Ga Shamvaian, ca. 2.8-2.7 Ga upper Bulawayan, ca. 3.0-2.8 Ga lower Bulawayan, and ca. 3.4-3.3 Ga Sebakwian (Wilson et al., 1978; Wilson, 1979). Based on structural geology, lithofacies and geochemistry of igneous rocks, the lower and upper Bulawayan units are interpreted as continental rift basins and passive continental margin deposit (e.g. Blenkinsop et al., 1993; Fedo and Eriksson, 1996; Hunter et al., 1998; Bolhar et al., 2003; Shimizu et al., 2005), whereas the Shamvian unit is considered as deposit in forearc sedimentary basins (Hofmann et al., 2001; 2004). On the other hand, the oldest Sebakwian unit has not been well known about its origin and extent because of a limited distribution compared with other younger greenstone units. The Shurugwi Greenstone belt (SGB) is a unit of greenstone and meta-sediments located in center part of the Zimbabwe Craton (Stowe, 1968; 1974; Cotteril, 1979). The SGB is also well known as economic resource of chromium ore occurred in ultramafic intrusion (Prengargast, 1984). However, several interpretations for the belonging of the SGB has been proposed; i.e. ca. 3.4Ga Sebakwian (Stowe 1968; 1974; Cotterill, 1979), ca. 2.7 Ga upper Bulawayan (Tsomondo et al., 1992), and ca. 3.1-2.9 Ga lower Bulawayan (Nagler et al., 1997).

Ages of granitoid and orthogneiss in the Zimbabwe Craton range one billion years between ca. 3.6 and 2.6 Ga (Hawkesworth et al., 1975; 1979; Jahn and Condie, 1976; Moorbath et al., 1976). Although many studies have reported ages by using whole rock measurements, precise *in situ* dating of zircon are still limited (e.g. Horstwood et al., 1999; Dodson et al., 2001; Jelsma et al., 2004; Rollinson and Whitehouse, 2011; Fig. 1). Therefore, more detailed age dating for granitoid/orthogneiss is necessary to understand of the tectonic history of the SGB and the Zimbabwe Craton.

Recently, Bolhar et al. (2017) reported U-Pb, Lu-Hf, and oxygen isotopic analysis of detrital zircon from the SGB and other supracrustal units in the Zimbabwe Craton, and discuss timing of continental crust production and possible tectonics before 3.3 Ga. This study further added new U-Pb data from different formations of the SGB, and discuss secular change in provenance for sedimentary rocks in greenstone belts and implication for continental growth, especially after 3.3 Ga.

To constrain the formation age of the SGB and associated granitoid/orthogneiss as well as to reveal regional crustal development during the Archean proto-Zimbabwe Craton, this study performed U-Pb dating of zircon grains from meta-sedimentary rocks of the SGB and

granitoid/orthogneiss around the SGB. In addition, this study also performed whole-rock Re-Os dating of chromitite from the SGB.

4.2. Geological outline

4.2.1. Basement granitoid/orthogneiss

The core of the Zimbabwe Craton is composed of the Tokwe and Rhodesdale segments which are the oldest units in the Zimbabwe Craton (Wilson et al, 1978; Fig. 4-1B). The first chronological study of the Tokwe segment is Hawkesworth et al. (1975) which reported Rb-Sr whole rock isochrone age of 3,580 ± 200 Ma for the Tokwe River Gneiss. Afterwards, whole rock Pb-Pb age of the Tokwe River Gneiss were reported as 3,475+87/-93 Ma (Taylor et al., 1991). In addition, zircon in situ dating by using SHRIMP showed 3,455 ± 2 Ma intercept age from the Tokwe River Gneiss (Horstwood et al., 1999). They also recovered zircon intercept age of 3,456 ±6 Ma from the Kwekwe Gneiss and that 3,565 ± 21 Ma from the Sebakwe River Gneiss in the Rhodesdale segment. The Sebakwe River Gneiss is the oldest granitoid/orthogneiss in the Zimbabwe Craton as far as reported. The oldest concordant zircon age of granitoid/orthogneiss in the craton is the Mushandike Granite in the Tokwe segment, of which two samples were dated as 3,374 ± 7 Ma and 3,368 ± 11 Ma (Dodson et al., 2001; Fig. 1). The Shabani Gneiss in southeast part of the Tokwe segment was dated as 3,088 +44/-46 Ma (Taylor et al., 1991).

In the outside of the Tokwe and Rhodesdale segments, younger granitoid between 3.0-2.6 Ga have been reported. Approximately 5 km west from the SGB, there is the Gwenoro Dam gneiss which showed whole rock Rb-Sr age of 2,720 ± 60 Ma (Hawkesworth et al., 1975), whole rock Pb-Pb age of 2,705 + 60/-63 Ma (Taylor et al., 1991), and zircon U-Pb age of 2,769.2 ± 0.2 Ma (Jelsma et al., 2004). Around the SGB, several granitoid intrusions has been recognized; i.e. Mashaba suit 2.7 Ga (Hawkesworth et al., 1979), Somabula Tonalite of 2.9 Ga (Moorbath et al., 1977; Taylor et al., 1991), Chilimanzi Granite of ca. 2.6 Ga (Jelsma et al., 1996).

The Mont d'Or Granite which have been considered to intruded into the SGB was found only from core sample (Stowe, 1974; Cotteril, 1979; Fig. 2C). Moorbath et al. (1976) is the first chronological study of the Mont d'Or Granite, and reported Rb-Sr isochron age of 3,350±120 Ma.

Taylor et al. (1984) also measured the same granite suit by using whole rock Pb-Pb age of 3,345 ± 55 Ma. These chronological studies suggested that the SGB is older than 3.35 Ga and thus belongs to the Sebakwian unit.

4.2.2. Shurugwi Greenstone Belt

Stowe (1968; 1974) separated the SGB into three units; i.e. the Mont d'Or Formation, the Selukwe Formation and the Wanderer Formation (Fig. 4-2B). Through studies of structural geology, he considered the SGB as nappe on allochthonous granite-gneiss basement. The stratigraphic succession is described as the Mont d'Or Formation (mainly quartz arkose), Selukwe Formation (lower greenstone unit with ultramafic intrusion), and Wanderer Formation (clastic rocks with basal unconformity, banded iron formation and upper greenstone unit) with arranged from the oldest (Stowe, 1968; 1974). He described a conformable contact between Mont d'Or and Selukwe formations, as well as unconformity between the ultramafic complex of the Selukwe Formation and basal conglomerate of the Wanderer Formation. According his geological reconstruction, the SGB has been overturned and a nappe on allochthonous on a gneissic basement (Fig. 4-. 2C). He also considered that the intrusion of the Mont d'Or granite minorly occurs in the Mont d'Or Formation, and both are intruded by the late granite (Fig. 4-. 2C).

On the contrary, Cotteril (1979) considered the Mont d'Or and Wanderer formations are same, but differently metasomatised, because they found quartzite including detrital chromite from the Mont d'Or Formation. Also, the Mont d'Or area is dominated by the Mont d'Or granite, and metasedimentary rocks are regarded as minor xenolithic blocks. However, as detrital chromite is commonly observed in the Archean clastic rocks (e.g. Condie, 1989), the observation is still poor to conclude same origin of the Mont d'Or Formation and the Wanderer Formation. In addition, there are no clear evidence of the vast occurrence of the Mont d'Or Granite beneath the area.

Tomondo et al. (1992) re-examined northern part of the SGB that the SGB is part of the 2.7Ga Gweru Greenstone belt which is distribute in the north of the SGB based on similarity in composing rock types (Fig. 4-. 1C). They did not explain geological structure of southern part of the SGB, especially intrusive relationship between the SGB and late granitic intrusions.

Dodson et al. (1988) reported detrital zircon U-Pb age by using SHRIMP. Their data showed variable ages between 3.4 and 3.7 Ga. This result is apparently consistent with the ca. 3.35 Ga

whole rock ages of the Mont d'Or Granite by Moorbath et al. (1976) and Taylor et al. (1991). Therefore, the SGB has been considered as deposited at ca. 3.4-3.3 Ga and belongs to the Sebakwian unit. On the other hand, Nagler et al. (1997) reported detrital zircon Pb-Pb ages of 3.7-3.1Ga from meta-sandstone the Wanderer Formation by using SIMS. They also measured titanite from meta-sandstone and amphibolite of the Wanderer Formation and obtained 2.86 Ga for peak metamorphic age of the SGB. Thus, they concluded the SGB belongs to the lower Bulawayan. However, they did not measure U-Pb age and their zircon dating likely includes discordant ones. Recently, Bolhar et al. (2017) reported U-Pb ages of detrital zircon from conglomerate of the Wanderer Formation. From matrix of the conglomerate sample, they found three i.e., 3.54, 3.64, and 3.70 Ga. On the other hand, from quartzitic pebble of the sample, only 3.3 Ga zircons were found.

4.3. Samples

4.3.1. Basement gneiss (ZW132, 135, 138)

This study analyzed three samples from the basement gneiss beneath the SGB. These samples are orthogneiss composed of quartz, albite, and biotite which show clear banding. Under a microscope, most albite grains are saussuritized. Zircons from those samples show elongated euhedral shape.

4.3.2. Granitoid intrusion (ZW 114, 115, 129)

Two of them are collected from the Mont d'Or granite (Sample ZW114, and 115), and the other is from another granitoid suit which is 1 km south from the Mont d'Or granite unit (Sample ZW129). In Sample ZW114 and 115, subhedral crystals of albite include numbers of small muscovite grains which is approximately 100 μm long (Fig. 4-. 2). This strongly suggests hydrothermal metasomatism of those samples. Zircons of those show euhedral shape, and about 80 % grains of them have oscillatory zoning.

4.3.3. Sedimentary rocks (ZW117, 119, 139)

This study analyzed three samples of sedimentary rocks in the Shurugwi greenstone belt. Samples ZW117 and ZW119 are different in appearance. Sample ZW117 has distinctive coarse quartz grains with pale brown matrix. Sample ZW119 is a gray colored and foliated phyllite (Fig. 4-4). On the other hand, separated zircons are similar subhedral to euhedral crystals with gray in color. Most zircons do not show clear interior structures, except minor ones having unclear core part less metamicted.

Sample ZW139 is phyllite of the Wanderer Formation. This sample is relatively poor in zircon than the other sedimentary rock samples. More than half of zircons are subhedral in shape, and the others are rounded in shape.

4.3.4. Chromitite (ZW185, 191, 195)

Three chromitite samples (ZW185, 191, 195) were analyzed. These samples are composed of chromite with minor amount of kammererite and serepentinite. Sample ZW193 is composed of mostly greenish fibrous serpentinite. Sample ZW195C and ZW195S were cut from one specimen to separate into chromite-rich part and serpentinite-rich part.

4.4 Analytical method

4.4.1. U-Pb dating

For zircon extraction, crushing, sieving, magnetic and heavy-liquid separations were performed at the University of Tokyo. Separated zircon grains were mounted on 10 mm epoxy resin discs and were polished to expose their mid-section. To check the internal structures of zircons, CL images were obtained using a JEOL JSM-5310 scanning electron microprobe

combined with a cathodoluminescence system (Sanyu Electron, Tokyo, Japan).

In situ zircon U–Pb dating was carried out by using an Agilent 8800 single-collector triple quadrupole ICP-MS (Agilent Tech., USA) coupled to a NWR-213 laser-ablation system (ES, Portland, US), that utilizes a 213 nm Nd:YAG laser. The laser was operated with fluence of 4.3 Jcm^{-2}, repetition rate of 5 Hz, and laser spot size diameter of 15 μm.

Data were acquired on six nuclides; ^{202}Hg, ^{204}Pb, ^{206}Pb, ^{207}Pb, $^{232}Th^{16}O$ and ^{238}U. To reduce isobaric interference of ^{204}Hg to ^{204}Pb, small amount of mixed ammonia/helium flowed into collision/reaction cell between the tandem quadropole mass spectrometer (Kasapoğlu et al., 2016). This study succeeded to reduce the gas blank count on 204 amu (^{204}Hg + ^{204}Pb) less than 10 cps in average. Background and ablation data for each analysis were collected over 13 and 15 s, respectively. Data were acquired using multiple groups of 14 unknown samples with FC-1 zircon as secondary standard (Peace and Miller, 1993) bracketed by trio of analyses of the 91500 zircon reference material (Wiedenbeck et al., 1995, 2004) and NIST SRM610 grass standard. As normalization value of 91500, apparent $^{206}Pb/^{238}U$ without common Pb correction is used (Sakata et al., 2017, i.e. $^{206}Pb/^{238}U = 0.17928 \pm 0.00018$). The instrumental mass bias of lead isotope ratios are normalized to compiled values by Jochum and Stoll (2008). Prior to analysis, regions of interest were pre-ablated using a pulse of the laser with spot size diameter of 110 μm to remove potential surface contamination and to avoid metamicted part, cracks, and inclusion minerals. Common Pb correction was made based on ^{204}Pb method (Stern, 1997). Isotopic composition of common Pb is estimated assuming the terrestrial Pb isotope evolution by a two-stage model (Stacey and Kramers, 1975), through a five-step iterative process as follows: if the apparent Pb-Pb age (age without common Pb correction) is older than 3.7 Ga, we assumes that $^{206}Pb/^{204}Pb = 9.307$, $^{207}Pb/^{204}Pb = 10.294$, $^{208}Pb/^{204}Pb = 29.487$, $^{238}U/^{204}Pb = 7.19$, $^{232}Th/^{204}Pb = 33.21$ at the starting age (i.e. age of the Earth is assumed to be 4.57 Ga) as initial parameters. If the apparent age is younger than 3.7 Ga, this study uses $^{206}Pb/^{204}Pb = 11.152$, $^{207}Pb/^{204}Pb = 12.998$, $^{208}Pb/^{204}Pb = 31.23$, $^{238}U/^{204}Pb = 9.74$, $^{232}Th/^{204}Pb = 36.84$, and the starting age of second stage is 3.7 Ga. From these parameters, this study determines the isotopic composition of common Pb and calculate the age with ^{204}Pb method (this is first step). After this procedure, this study can newly calculate the common Pb composition of analyte using the age corrected in first step.

Subsequently, the next common Pb corrected age is also determined in second step. The present study repeats this process five times and determine the final age.

Background intensities were monitored before every analytical spot and subtracted from following signals. The standard deviation of each six measurements of 91500 zircon data bracketing unknown sample groups were calculated, and were applied for uncertainty propagation. Elemental and mass fractionation of U/Pb and Pb/Pb ratio was linearly interpolated by the measured data of each six spot of 91500 zircon and NIST SRM610. The ^{235}U count was calculated from ^{238}U using a $^{238}U/^{235}U$ ratio of 137.88 (Jaffey et al., 1971). Our data obtained during this study yielded mean $^{206}Pb/^{238}U$ value of 0.1872±0.0017 for FC-1. This result agrees with $^{206}Pb/^{238}U$ value of 0.1859 (Peace and Miller, 1993).

4.4.2. Re-Os dating

All samples were sawn and their surfaces were ground off to remove metal contaminants and weathered portions. Approximately, 50 g of each slab samples were disaggregated with a rock hammer by wrapping in plastic sheeting, washed in deionized water, dried, and then powdered in an alumina rod mill.

Highly siderophile element (HSE) concentrations and Os isotope measurements were performed using isotope dilution (ID) mass spectrometry after Carius tube digestion (Shirey and Walker, 1995). The method used for sample digestion, chemical purification and mass spectrometry were based on Ishikawa et al. (2014). Approximately 1 g of powder for each sample was mixed with spike solutions enriched in ^{185}Re and a mixed ^{190}Os-^{191}Ir-^{99}Ru-^{196}Pt-^{105}Pd in a Carius tube. After adding 10 ml of the inverse aqua regia, each Carius tube was frozen in a mixture of ethanol and dry ice, sealed with an oxygen-propane torch. Then, those Carius tubes were heated at 240 °C for more than 72 hours. De-silicification procedures were not applied because extraction of HSEs from ultramafic rocks is largely independent of the use of HF (cf. Ishikawa et al., 2014; Luguet et al., 2015; Day et al., 2016).

Isotopic measurements of the HSE were conducted using two types of mass spectrometer.

Osmium concentrations and isotopic compositions were measured by negative thermal ionisation mass spectrometry (N-TIMS, Thermo Electron Triton) at JAMSTEC, Japan. Purified Os after CCl_4 solvent extraction (Cohen and Waters, 1996) and microdistillation (Birck et al., 1997) was loaded in HBr on baked 99.997% Alfa Aesar Pt wire and covered with a NaOH-$Ba(OH)_2$ activator solution.

All the other HSE were measured by the Quadro-pole ICP-MS (Agilent 7500s) installed in the University of Tokyo at Komaba. Solutions of sample and standard were interspersed throughout the analytical sessions to correct for instrumental fractionation. The monitored masses of analytes and interferences are ^{89}Y, ^{90}Zr, ^{95}Mo, ^{97}Mo, ^{99}Ru, ^{100}Ru, ^{101}Ru, ^{105}Pd, ^{106}Pd, ^{108}Pd, ^{111}Cd, ^{178}Hf, ^{185}Re, ^{187}Re, ^{191}Ir, ^{193}Ir, ^{194}Pt, ^{195}Pt, ^{196}Pt, and ^{202}Hg. Interferences of isobaric-oxide interferences to analyte signals are insignificant (<0.1%).

The accuracy of our analytical methods was evaluated by measuring ultramafic reference materials such as GSJ JP-1 and UB-N. Concentrations and re-productivities have previously been reported in Ishikawa et al. (2014; 2017).

4.5. Results

All results of detrital zircon dating are shown in Fig. 4-4 and. Results of Re-Os dating is summarized in table 1.

4.5.1 The 3.0 Ga gneiss basement (ZW 132, 138)

Two samples of gneiss south from the Shurugwi greenstone belt show ca. 3.0 Ga concordant age. Many zircons from sample ZW132 are highly metamicted and lost their internal structures. Concordant ages of zircons from ZW132 are concentrated around 3 Ga. Other discordant grains array roughly along discordia line from 3.0 Ga to the younger. Distinctively young grains with concordant ages around 2.8 Ga are considered as results of Pb-loss.

Sample ZW138 yielded 9 grains with concordant age of ca. 3.0 Ga and shows relatively clear discordia line. This study selected reliable data according to discordance less than 10%, Th/U ratio higher than 0.1, and less than 0.001 f_{206} values, and calculated weighted mean ^{207}Pb-^{206}Pb ages of 3,006 ± 8 Ma (MSWD = 0.86) for ZW132 and 3,019±15 Ma for ZW138. These ages indicate igneous age of protolith TTG.

4.5.2. The 2.9Ga granitic intrusion (ZW 114, 115)

Most plots of analyses array a discordia line from 2.9 Ga (Fig. 4-5). Analyses selected according to same cut off values as ZW 132 and 138 give ^{207}Pb-^{206}Pb mean ages are 2,912±4 Ma for ZW114 and 2,919±13 Ma for ZW 115. These ages of 2.91 Ga are considered as igneous age of the granite. On the other hand, several grains show older age of 3.4-3.0 Ga. Several grains of them are plotted on the concordant line. These grains are regarded as xenocrysts from pre-existing rocks.

4.5.3. The 2.7 Ga granitoid and gneiss (ZW 129, 135)

Using same cut off value as described above, this study obtained weighted mean ^{207}Pb-^{206}Pb ages of 2,722±14 Ma for ZW129 and 2,718±18 Ma for ZW135.

4.5.4. Detrital zircons in clastic rocks (ZW 117, 119, 139)

Zircons from these three samples show several common aspects. Most analyses show high content of common Pb. Analyses less affected by common Pb show concordant ages of around 3.6 Ga. Those analyses give weighted mean ages of 3,590 ± 12 Ma for ZW117, 3,584 ± 6 Ma for ZW119, and 3,582 ± 11 Ma for ZW139. Those mean that the Mont d'Or Formation and the Wanderer Formation deposited younger than ca. 3.6 Ga. In addition, our data indicates that clastics of these sedimentary rocks are derived from a limited provenance with single age.

4.5.5. Re-Os dating for chromitite (ZW185, 191, 195)

Values of $^{187}Re/^{188}Os$ vary from 0.003 to 0.039, and those of $^{187}Os/^{188}Os$ range between 0.1070 and 0.1088. Concentrations of Os and Re range from 27 to 85 and from 0.08 to 0.22 ppb,

respectively (Table 1). Both T_{MA} model age (Alle`gre and Luck, 1980) and Re depletion T_{RD} age (Walker et al., 1989) were calculated using a ^{187}Re decay constant of $1.666 * 10^{11}$ $year^{-1}$ (Smoliar et al., 1996) relative to the evolution of average chondrite with initial $^{187}Os/^{188}Os = 0.09531$ at 4.558 Ga, and $^{187}Re/^{188}Os = 0.40186$ (Shirey and Walker, 1998) following the recommendation of Puchtel et al. (2014). The T_{MA} shows narrow range in 2.95-2.94 Ga, whereas T_{RD} shows relatively younger 2.92-2.66 Ga (Table 1).

4.6. Discussions

4.6.1. Comparison with previous chronological studies

This study found that basement gneiss south of the SGB is mainly 3.0 Ga, and partly intruded by 2.7 Ga younger granitoid bodies. In addition, the present study confirmed that the late granite intruded into both the SGB and its basement is 2.91 Ga. Previous geological studies have not distinguished the late granitoid of 2.9 Ga and 2.7Ga ones (Stowe, 1968; 1974; Cotterill, 1979).

Age of 2.7 Ga orthogneiss is correspond to the Gwenoro Dam gneiss which is distribute 6 km west from the SGB (Jelsma et al., 2004). In addition, the Mashaba suit, located in approximately 30 km east from the SGB (Fig. 4-1), has whole rock age of 2.7 Ga (Hawkesworth et al., 1979). According geological map of Stowe (1968), locality of Sample ZW129 is recognized as “Syntectonic granodiorite”, but that of Sample ZW135 is in undivided “foliated gneiss”.

The age of 2.9 Ga for the granitoid correspond to whole rock ages of the Somabula Tonalite (Moorbath et al., 1977; Taylor et al., 1991). Zircon U-Pb age of 2.9 Ga for granitoid/gneiss have not been reported in the Ziimbabwe Craton.

Basement orthogneiss around the SGB was previously undivided, and thought to be as a part of the ca. 3.6 Ga Tokwe Gneiss (Wilson, 1990). The 3.0 Ga zircon age of the present study is much younger than the previously believed age. Taylor et al. (1991) reported a Pb-Pb whole rock date of 3,088 ± 45 Ma for the Shabani Gneiss which is ca. 40 km southeast from the SGB,

near the Belingwe GS belt and a part of the Tokwe segment. The present study is the first report of zircon age from the Zimbabwe Craton, even though 3.0 Ga detrital zircon grains have found from the Shamvaian Group on the northwest of the craton (Jelsma et al., 1996).

Age patterns of detrital zircons from meta-sedimentary rocks in the SGB show concentration of concordant ages around ca. 3.6 Ga. This monotonous age pattern is commonly observed in samples from the Mont d'Or and Wanderer formations. Bolhar et al. (2017) also reported three concordant ages of detrital zircon from conglomerate matrix of the Wanderer Formation; i.e. 3.54 Ga, 3.64 Ga and 3.70 Ga. These ages overlap to our analysis within error. Therefore, these detrital zircon ages indicate that provenance for the Mont d'Or and Wanderer formations were almost same. On the other hand, quartzite pebble having only 3.3 Ga detrital zircon grains from conglomerate of the Wanderer Formation was found by Bolhar et al. (2017). This indicates that depositional age of the Wanderer Formation is younger than 3.3 Ga.

4.6.2. Evolutional history of the Shurugwi area

Through zircon U-Pb dating, the present study found 1) 3.0 Ga orthogneiss basement around the SGB, 2) detrital zircons from the Mont d'Or and Wanderer formations having monotonous age pattern with concentration at ca. 3.6 Ga, 3) intrusion of ca. 2.9 Ga granitoids into the SGB and the surrounding orthogneiss basement, and 4) occurrence of minor amount of 2.7 Ga granitoid and orthogneiss. Taking into the ca. 3.3 Ga detrital zircons from conglomerate of the Wanderer Formation recovered by Bolhar et al. (2017), the present study of zircon dating can constrain depositional age of the SGB is between 3.3 and 2.9 Ga.

In addition to the zircon dating, the present Os model ages for chromitite samples from the Selukwe Formation show ca. 3.0-2.9 Ga for ultramafic igneous activity of the SGB, even uncertainty of model ages remains. As this ultramafic unit unconformably contacts with the Wanderer Formation (Stowe, 1968; 1974), these results indicate that depositional age of the formation was ca. 3.0 Ga. Therefore, the Selukwe and Wanderer formations of the SGB likely belongs to the 3.0-2.8 Ga lower Bulawayan Group.

There has been a controversy whether the Mont d'Or Formation is older than the Wanderer Formation (Stowe, 1968; 1974) or both formations are coeval but differently metamorphosed/metasomatized (Cotterill, 1979). From the view of the age pattern of detrital zircons, those two formations are quite similar each other. This result possibly supports the sameness of the two formations. Even if the Mont d'Or Formation is older than the Wanderer Formation, their provenances were quite similar and thus depositional ages of them were also close. Therefore, this study considers that all the SGB including the Mont d'Or Formation belongs to the lower Bulawayan unit.

Both the Mont d'Or and Wanderer formations do not contain any detrital zircon younger than 3.3 Ga even though the neighboring basement gneiss is 3.0 Ga. Therefore, the provenance of the SGB did not include significant amount of 3.3-3.0 Ga granitoid. This possibly supports that the allochthonous origin of the SGB as suggested by Stowe (1974). On the other hand, the "Mont d'Or Granite" is still problematical. Before making conclusion, the whole rock dating should be re-examined by more precise *in-situ* zircon age dating. At the moment, the present study envisages several possibilities, i.e. 1) mixing between the 2.9 Ga granitic intrusion and the old sedimentary rocks of the Mont d'Or Formation, or 2) xenolithic blocks of old granitoid from the basement into the 2.9 Ga granitoid.

4.6.3. Implication for Archean continental growth

Figure 6 shows secular change in detrital zircon age spectra from ca. 3.3-2.7 Ga meta-sedimentary rocks in the Zimbabwe Craton. Age spectra of the ca. 2.7 Ga Majeri Formation in the Belingwe greenstone belt (Fig. 4-6D) show less than 0.5 Ga difference between their depositional age and the youngest major peaks in the spectra. On the other hand, the ca. 3.3 Ga Nijiri quartzite in the Rhodesdale segment (Fig. 4-6A), the ca. 3.0 Ga sediments of the SGB (Fig. 4-6B) and ca. 2.9 Ga quartzite of the Bhuwa greenstone belt (Fig. 4-6C) show over 300 million years intervals between them.

As a possible model for this age pattern is local tectono-magmatic lull between 3.3 and 3.0 Ga in the proto-Zimbabwe Craton. According global compilation of zircon U-Pb and Lu-Hf

isotopic data, crustal production was active during 3.3-3.0 Ga (Belouova et al., 2010; Roberts and Spencer, 2015). On the other hand, in the Zimbabwe Craton, no detrital zircon of those ages has been reported, as well as there are no granitoid/orthogneiss basement. The proto-Zimbabwe Craton during ca. 3.3-3.0 Ga was likely located in tectono-magmatically inactive place of a large continental block. To separate once-formed continental crust from tectono-magmatism, the crust should be in continental interior enough far from active margin. Therefore, during ca. 3.3-2.9 Ga, the proto-Zimbabwe Craton occupied an internal part of a large continental block, and subsequent continental rifting after ca. 2.9 Ga made the proto-Zimbabwe Craton a small continental block. This implication can be supported by the ca. 2.9-2.7 Ga Bulawayan and Belingwean greenstone units which were formed as continental rift basins (Blenkinsop et al., 1993; Fedo and Eriksson, 1996; Hunter et al., 1998; Bolhar et al., 2003; Shimizu et al., 2005). Figure 6E-G summarizes the above implication for the development of the proto-Zimbabwe Craton. Before ca. 3.3 Ga, there were several primitive continental blocks (Fig. 4-6E). The >3.3 Ga crusts are implicated as to have been formed different tectonics from the modern-style subduction on the basis of secular trend in Lu-Hf and oxygen isotope of detrital zircons (Bolhar et al., 2017). Around 3.3 Ga, the primitive continental blocks were possibly amalgamated into together and a relatively larger continental block was formed (Fig. 4-6F). Because the proto-Zimbabwe Craton was far from active continental margin, sedimentary basins on the area do not have supply of 3.3-3.0 Ga detrital grains. After 2.9 Ga, the continental block had been rifted into several smaller blocks (Fig. 4-6G). As a result, relatively young detrital grains from active continental margin were supplied to rift basins.

On the other hand, the ca. 2.7-2.6 Ga Shamvian unit are considered as subduction-related forearc sediments (Hofmann et al., 2001; 2003). After that, ca. 2.6 Ga the Zimbabwe Craton had become stabilized cratonic block through multiple collisions of island arc and continental blocks (Dirks and Jelsma, 1998). The landmass of continental block including the Zimbabwe Craton was likely re-increased through thess collisions during the period. The possible candidates collided with the Zimbabwe Craton are the Yilgarn, Superior and Kola-Karelia cratons according to paleomagnetic studies of radial dyke swarms (Söderlund et al., 2010; Pisarevsky et al., 2014).

6.4.6. Summary

This study reports U-Pb ages of zircons from meta-sedimentary rocks of the SGB and granitoid beneath and intruded into the SGB, as well as Re-Os dating for chromitite in the SGB. The detrital zircons of the SGB shows monotonous age pattern at ca. 3.6 Ga. Granitoid and orthogneiss around the SGB are divided into three generation; i.e. ca. 3.0 Ga basement gneiss, ca. 2.9 Ga granitoid intruded into both the SGB and the 3.0 Ga gneiss, and ca. 2.7 Ga granitoid. As the SGB and 3.0 Ga are bounded with faults according to Stowe (1978), the present zircon U-Pb dating indicates that depositional age of the SGB is between 3.3 and 2.9 Ga. In addition, the Re-Os dating for chromitite show Os model age of ca. 3.0-2.95 Ga. Even though Os model age possesses uncertainty in evolutional model of the mantle composition, these results suggest that the SGB was formed at ca. 3.0 Ga and belongs to the ca. 3.0-2.8 lower Bulawayan unit. Sedimentary rocks of the SGB yielded detrital zircons of ca. 3.6-3.3 Ga and no younger ones, despite of ca. 3.0 Ga deposition. This possibly indicates that the SGB deposited on a large continental block of the proto-Zimbabwe Craton during 3.0-2.9 Ga and supply of younger detrital zircons from active continental margin to the SGB was prevented.

Figures.

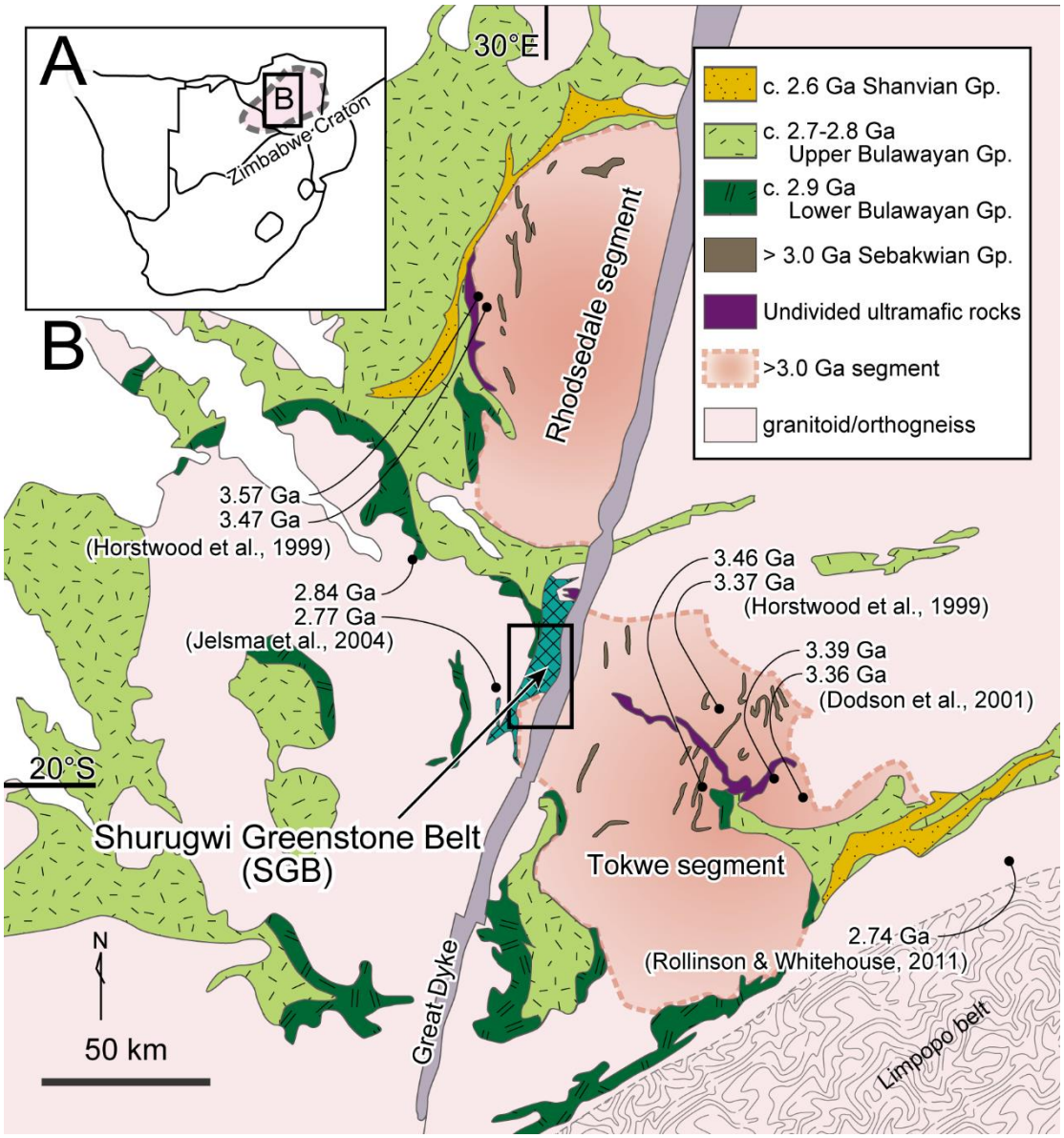

Fig. 4-1:

A. Location of the Zimbabwe Craton in Southern Africa.

B. Geologic map of the center part of the Zimbabwe Craton.

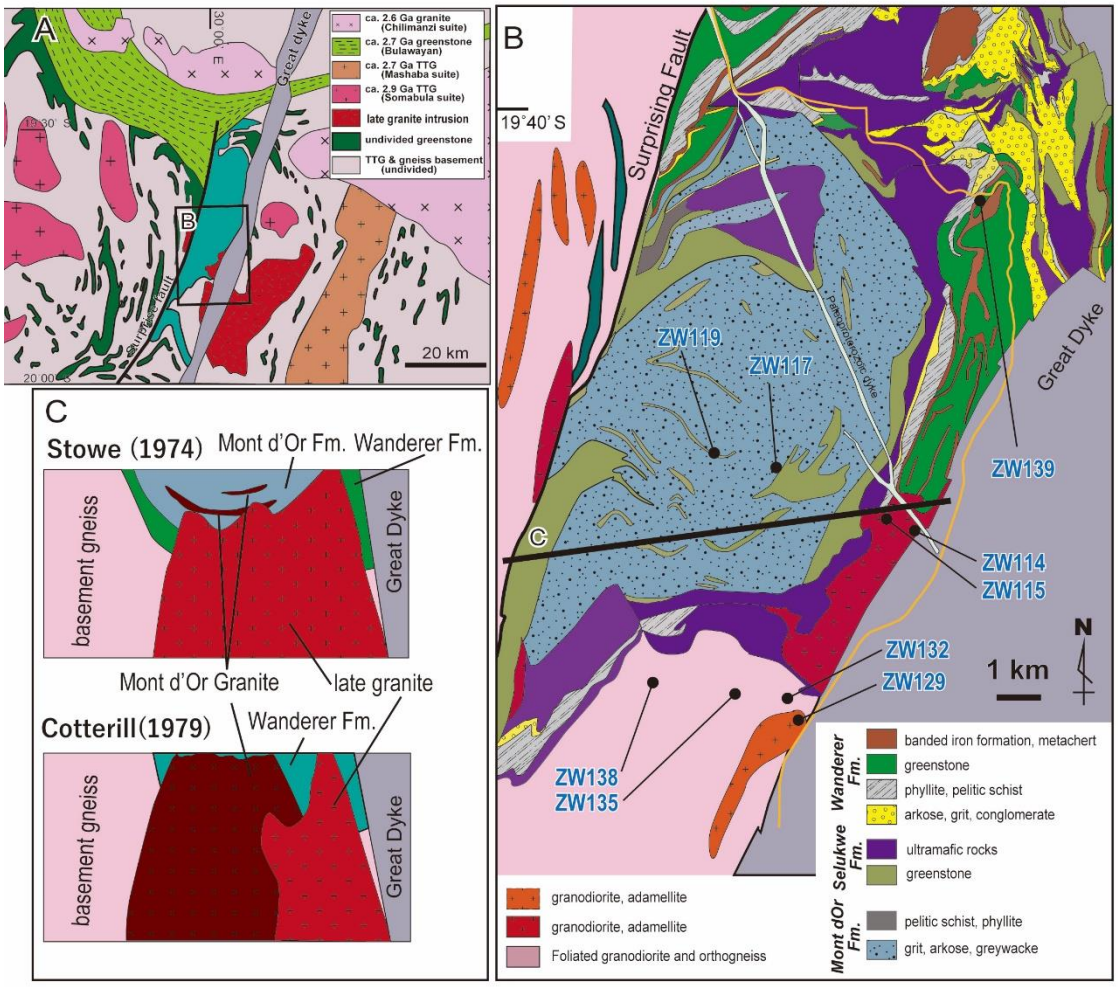

Figure 4-2.

A. Geotectonic map around Shurugwi Greenstone belt (SGB). Mashaba suit of 2.7 Ga (Hawkesworth et al., 1979), Somabula Tobalite of 2.9 Ga (Moorbath et al., 1977; Taylor et al., 1991), Chilimanzi Granite of 2.6 Ga (Jelsma et al., 1996).

B. Geologic map of the SGB area with sample localities modified after Stowe (1968; 1974).

C. Two different models for cross-sectional images of the SGB by Stowe (1974) and Cotterill (1979).

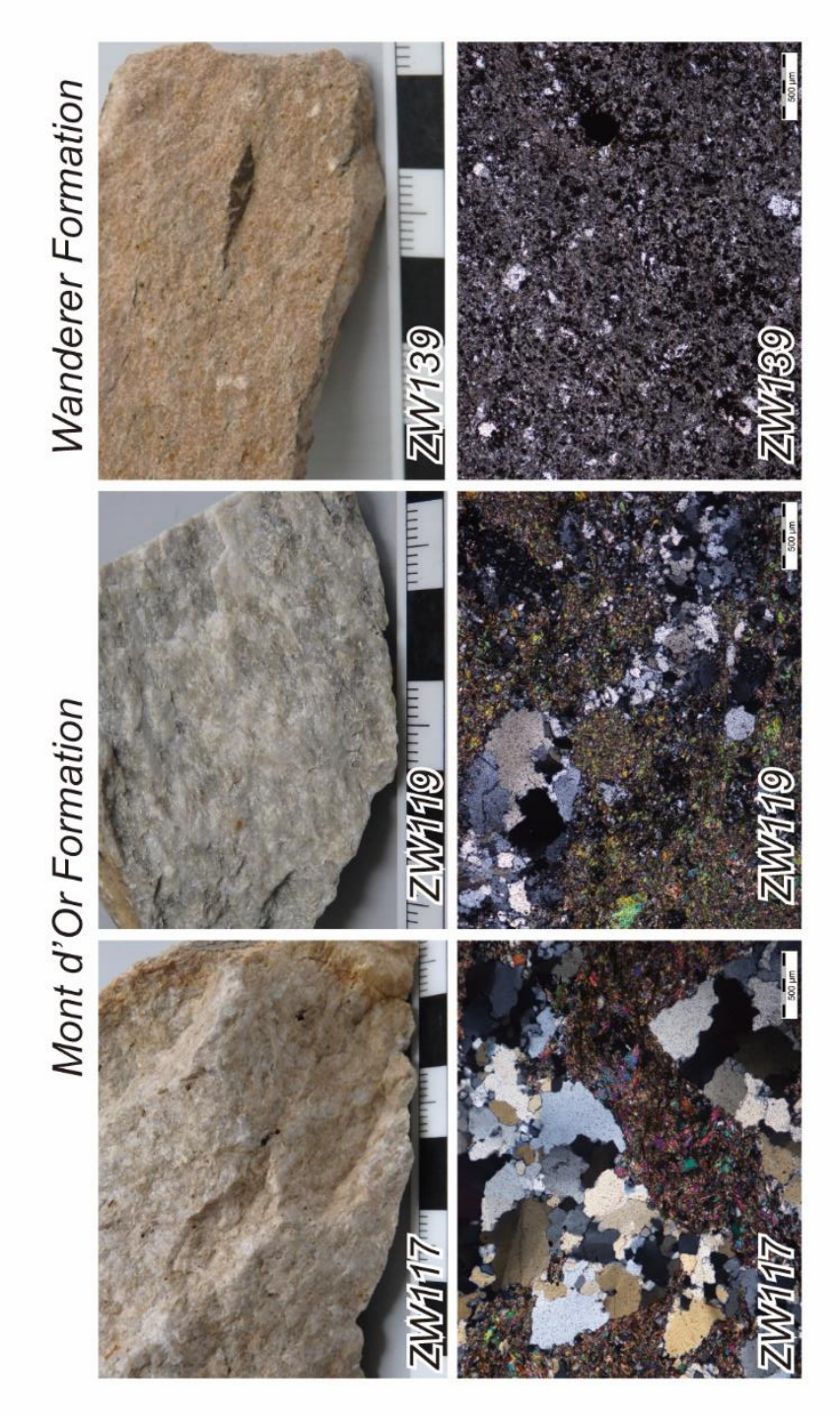

Figure 4-3: Photos of metasedimentary rocks in the Mont d'Or Formation (Z117 and 119) and Wanderer Formation (ZW139).

Figure 4-4. Selected cathodoluminescence images of analyzed zircons with analytical results.

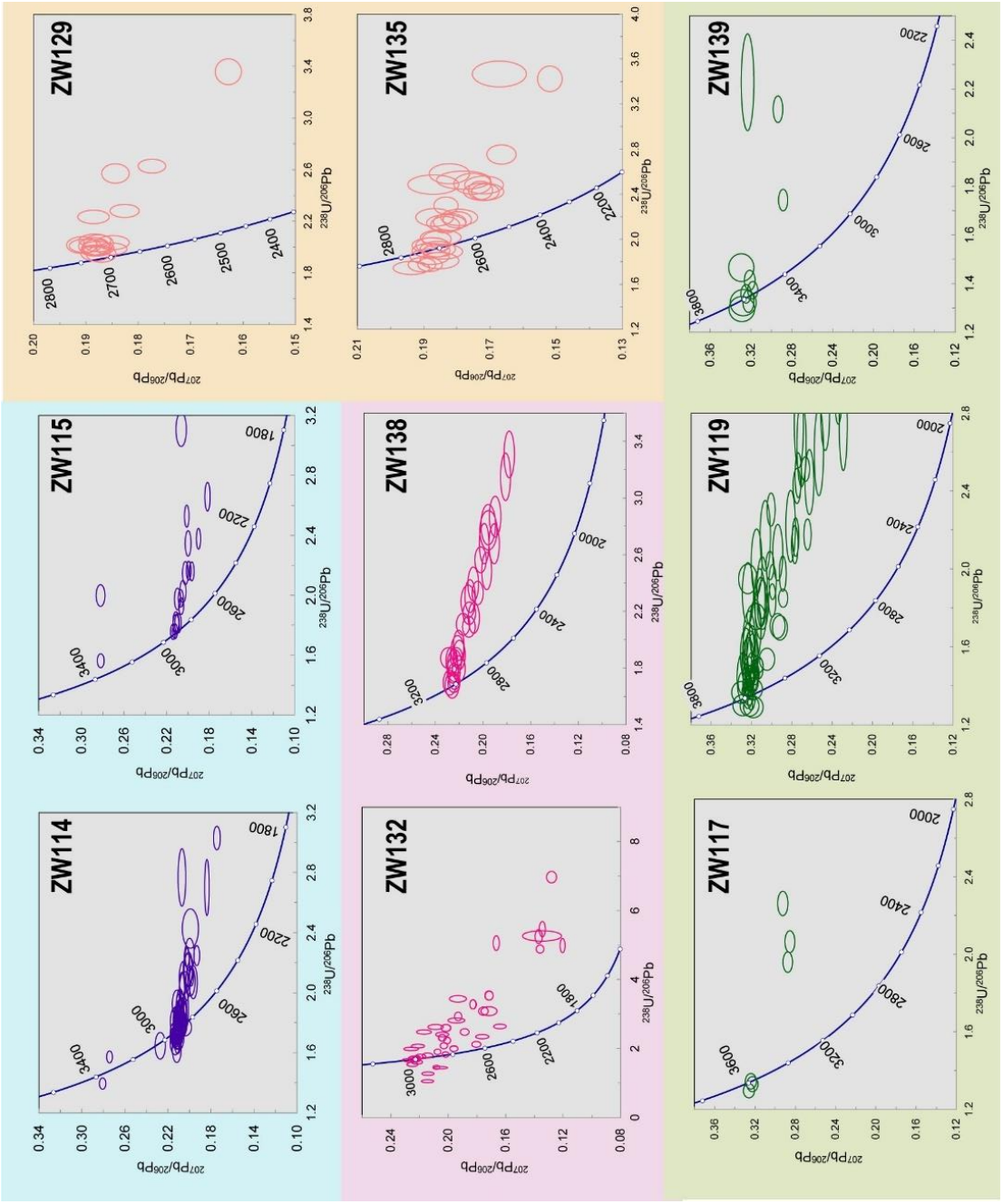

Figure 4-4: Concordia diagrams of the all analyzed samples. These figures were constructed with an ISOPLOT (Ludwig, 2003). Error ellipses on individual spots are at 2σ level.

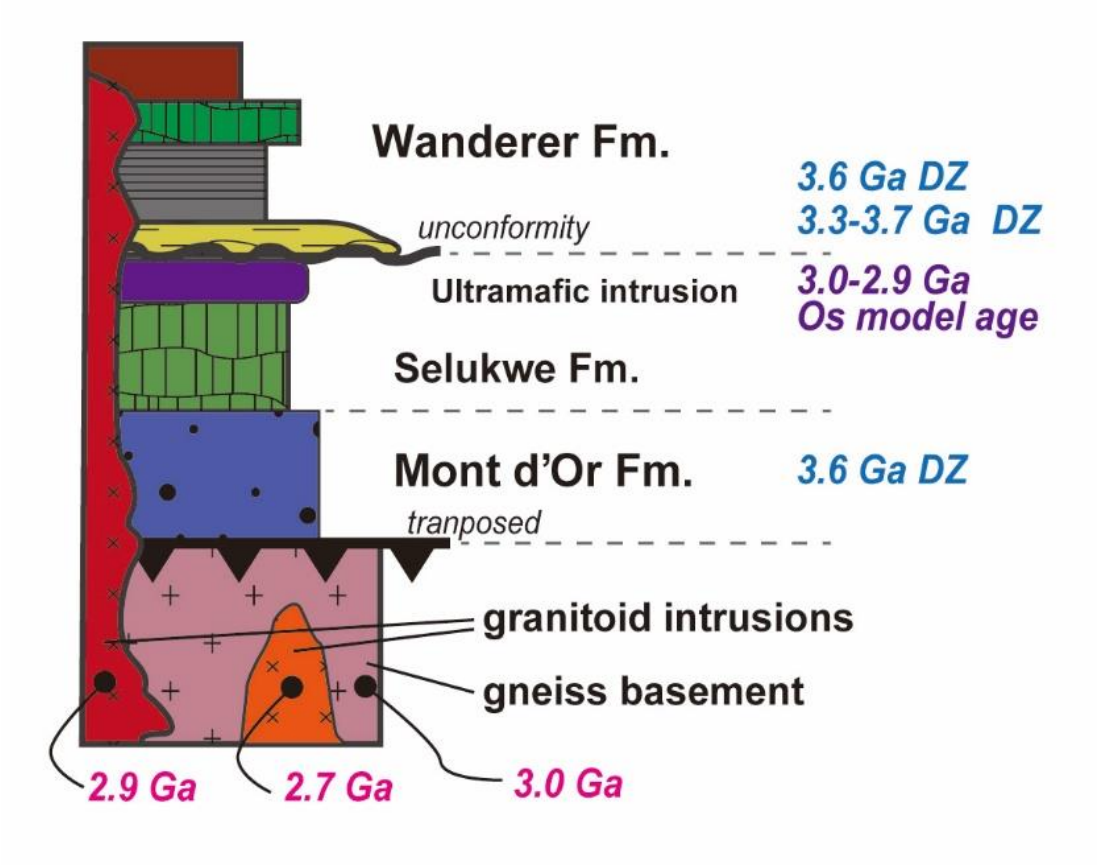

Figure 4-5: Summerly of dating results on schematic geological column of the Shurugwi Greenstone belt.

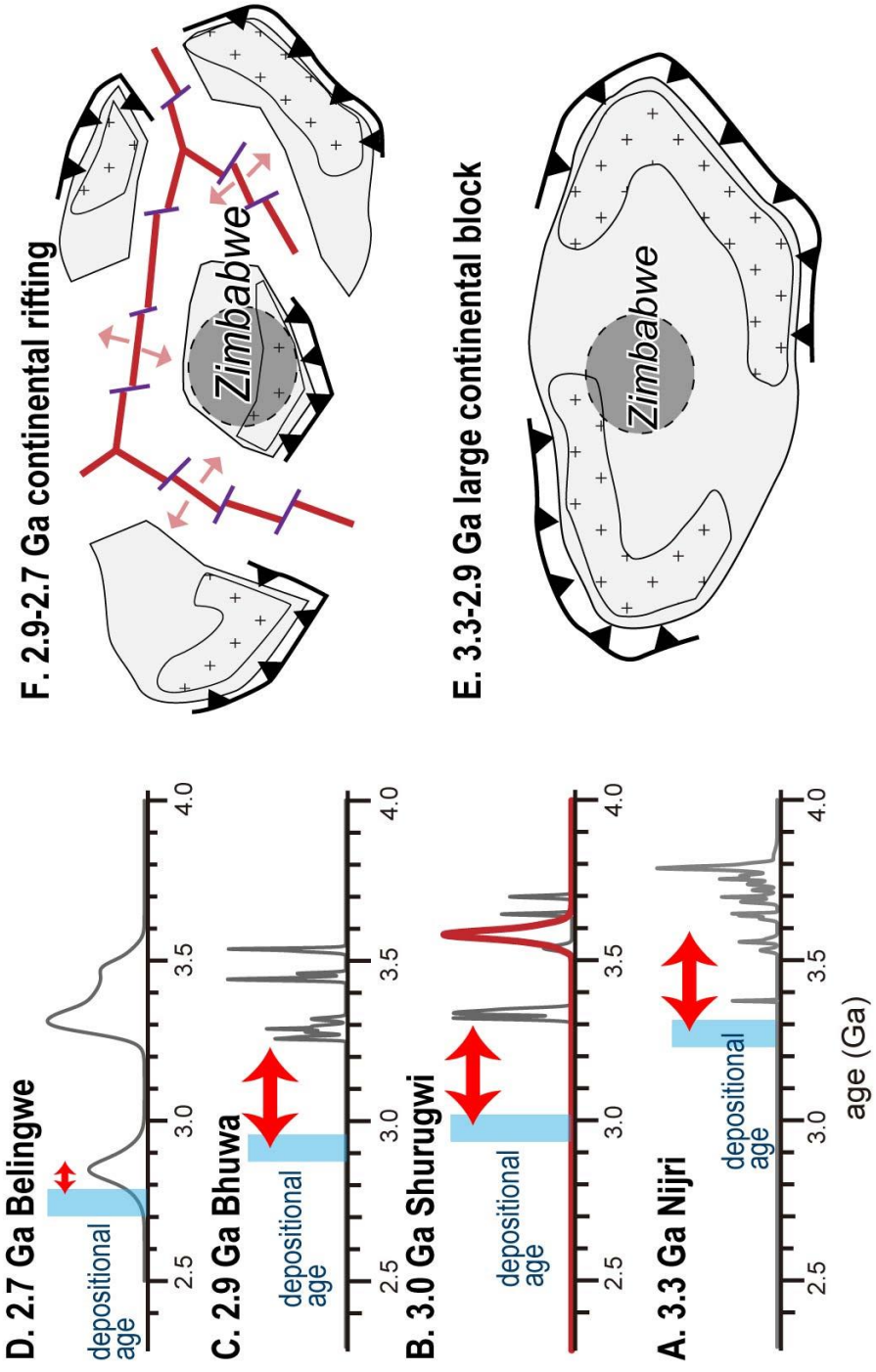

Figure 4- 6: A-D. Comparison of detrital zircon age spectra from meta-sedimentary rocks in the Zimbabwe Craton with various depositional age. A. the ca. 3.3 Ga Nijiri Quartzite (Bolhar et al., 2017). B. the Mont dO'r and Wanderer formations ca. 3.0 Ga Shurugwi GS belt (this study and

Bolhar et al., 2017). C. ca. 2.9 Ga Bhuwa quartzite (Bolhar et al., 2017). D. ca. 2.7 Ga Manjeri Formation of the Belingwe GS belt (Sawada et al., 2016).

E-F. Map view of the proto-Zimbabwe Craton.

Tables

Table 4-1. All results of zircon U-Pb dating. (in Appendix)

Table 4-2 Results of Re-Os dating. (in Appendix)

Chapter 5. Age constraints on the Paleoproterozoic Lomagundi-Jatuli Event in Zimbabwe: zircon geochronology of the Magondi Supergroup

Abstract

The ca. 2.2-2.1 Ga Magondi Supergroup on the Zimbabwe Craton in Southern Africa is mainly composed of sedimentary rocks deposited in a rift basin/passive continental margin, which recorded a unique episode in carbon isotope perturbation called the Lomagundi-Jatuli Event (LJE). This study reports new U-Pb ages of detrital zircons from the Deweras and Lomagundi groups of the Magondi Supergroup, and those of igneous zircons from underlying granitoids, to constrain the timing of the LJE and to identify the provenance of the Magondi Supergroup. Most analyzed detrital zircon grains range in ages between ca. 2.9 and 2.6 Ga. Three ca. 2.3-2.2 Ga detrital zircons from sandstone of the Deweras Group, with the youngest 207Pb-206Pb age of 2,216 ± 22 Ma, indicate the onset of LJE in the Zimbabwe Craton was almost simultaneous to that in Fennoscandia and the Superior Craton, supporting the global simultaneity of the LJE.

5.1. Introduction

The Paleoproterozoic witnessed significant changes in the Earth's surface environment, including the snowball Earth events (Kopp et al., 2005), the great oxygenation of the ocean/atmosphere (Rye and Holland, 1998; Bekker et al., 2004), and the emergence of eukaryotes (Han and Runnegar, 1992; Albani et al., 2010; Edou-Minko et al., 2017). Long-lasting positive carbon isotope excursion (δ13CVPDB >5‰) called the Lomagundi-Jatuli Event (LJE) is another significant phenomenon that is recorded in shallow marine carbonates deposited over the world (e.g., Melezhik et al., 1997; 2005; Bekker et al., 2003). This event is noteworthy with regard to its possible connection to the rise in atmosphere oxygen. Even though the LJE is recorded in sedimentary rocks over the world, the onset and duration of the LJE have been constrained based on U-Pb ages of zircon and baddeleyite mostly from the Fennoscandia and Superior Craton

(Martin et al., 2013). According to those chronological data, the LJE started between 2,306 ± 9 Ma and 2,221 ± 5 Ma, and ended between 2,106 ± 8 Ma and 2,057 ± 1 Ma (Martin et al., 2013). Carbon isotopic change is vaguely assumed to occur simultaneously. However, in the absence of synchronicity of the LJE, it is left with the possibility that each positive carbon isotope excursion reflected discrete phenomena. Therefore, more constraints from other regions are still needed to verify global synchronicity of the LJE. Magondi Supergroup in northwest Zimbabwe is the one of the best candidates for the purpose, because it is also one of the type localities of the event (Galimov et al., 1968; Schidlowski et al., 1975).

Time constraints for the Magondi Supergroup are still not well established because of lack of intrusive igneous rocks or tuff layers. Although baddeleyites in troctolite from the Chimbadzi Hill dyke near the base of the Magondi Supergroup yielded a U-Pb age of 2,262 ± 2 Ma (Manyeruke et al., 2004), the direct contact between the troctolite and Magondi Supergroup is unclear (Master et al., 2013). In addition, there is no report to constrain ages of basement granitoids at the Lomagundi area. This study newly reports U-Pb ages of detrital zircons from terrigenous clastic rocks of the Magondi Supergroup (the Deweras and Lomagundi groups) and igneous zircons in the underlying granitoids to constrain onset of the LJE in Zimbabwe and to discuss the global simultaneity of the LJE.

5.2. Geological outline of the studied area

The northern Zimbabwe Craton is composed of the late Archean granitoids, ca. 2.7–2.65 Ga greenstone units, and the covering ca. 2.2–2.1 Ga Paleoproterozoic sedimentary unit called the Magondi Supergroup (Wilson et al., 1995). Zircon U-Pb ages for the Archean granitoids and felsic volcanics by previous works are summarized in Fig. 1 (Wilson et al., 1995; Horstwood et al., 1999; Jelsma et al., 1996; 2004; Rolinson and Whitehoust, 2011). The Magondi Supergroup is totally ca. 4–5 km thick, and is composed of three units; i.e. the Deweras, Lomagundi, and Piriwiri groups (Master et al., 2010). The Deweras Group exposes on southern and northern sides of Chinhoyi town. Based on lithofacies of the Deweras Group; i.e. sandstone (mainly arenite including cross-, ripple-, and plane-bedded arkose), conglomerate, mudstone, dolostone, and mafic volcanics (Sutton, 1979; Master, 1984; 1991), the depositional environment of the group

is considered to be a rift basin (Master et al., 2010). The Lomagundi Group unconformably overlies on the Deweras Group (Stagman, 1961; Stowe, 1978). The lower part of the group is composed of dolostone and quartzite, and the upper part consists of slate and medium- to fine-grained sandstones with mafic volcanics (Tennick and Phaup, 1976). The Piriwiri Group is comprised of upward coarsening sequences ranging from phyllites and slates to greywacke with mafic volcanics and pyroclastics (Tennick and Phaup, 1976). The Lomagundi Group deposited on shallow-marine in a passive continental margin, and the Piriwiri accumulated in a shelf to continental slope. These groups are probably coeval deposits, because both groups show similar lithofacies change that is characterized by subsidence and following uplift (Leyshon and Tenncik, 1988). The LJE is recorded in the Mangula and Norah formations; i.e. the lower and middle parts of the Deweras Group, and in the Mcheka Formation of the lower half of the Lomagundi Group (Master et al., 1990; 1993; Bekker et al., 2001; Planavsky et al., 2012).

From the Chimbadzi Hill dyke troctolite that intruded into the Archean basement near the Magondi Supergroup, baddeleyites were dated at 2,262 ± 2 Ma by U-Pb dating (Manyeruke et al., 2004). This age was considered coeval to that of basaltic volcanics at the base of the Deweras Group (Manyeruke et al., 2004), but the direct contact between them has not been observed (Master et al., 2010; 2013). The Hurungwe Granite that intruded into the Pirwiri Group is dated at U-Pb age at 1,997.5 ± 2.6 Ma via SHRIMP U-Pb on zircons (McCourt et al., 2001). For the Magondi Supergroup, two direct age constraints were reported; i.e. a whole rock 207Pb-206Pb age of 2,150 ± 50 Ma for a dolostone from the Mcheka Formation of the Lomagundi Group (Schidlowski and Todt, 1998) and a Pb-Pb model age of 2,166–2,112 Ma for a galena in a massive sulfide deposit within the Copper Queen Formation of the Piriwiri Group (Hohndorf and Vetter, 1999). Based on these chronological data, deposition of the Lomagundi Group is estimated at ca. 2.15–2.10 Ga. In addition, detrital zircons from a paragneiss in the Gweta Complex in Botswana, which is regarded to be equivalent to upper part of the Magondi Supergroup, provided a maximum depositional age of 2,125 ± 6 Ma (Mapeo et al., 2001). However, the stratigraphic relationship between the gneiss and the Magondi Supergroup is unknown.

5.3. Samples

This study analyzed three sandstones deposited during the LJE; i.e. two quartz arenaceous sandstones from the Norah Formation of the Deweras Group (ZW5 and ZW68) and one re-crystallized quartzite from the Mcheka Formation of the Lomagundi Group (ZW74). We further dated four granitoids constituting the Archean basement (Zimba unit; ZW79, ZW105, ZW107, and ZW110), which were never dated before (Fig. 5.1). Photomicrographs of the analyzed samples are shown in Fig. 5.2.

ZW5 (17.34761°S, 30.15665°E)

This sample is quartz arenite. Most quartz grains are rounded.

ZW68 (-17.388857°S, 30.049029°E)

This sample is also quartz arenite. Quartz grains are little more angler than sample ZW5. This sample contains more clay minerals as matrix than sample ZW5.

ZW74 (-17.369582°S, 30.100856°E)

This sample is quartzite which consist of mostly recrystallize quartz grains. Minor amount of mica minerals and iron oxide minerals are also observed.

ZW79 (-17.487111°S, 30.545950°E)

This sample is granodiorite. Many of albite grains are suffered by saussuritization.

ZW105 (-17.685517°S, 30.165733°E)

This sample is tonalite.

ZW107 (-17.716508°S, 30.177133°E)

This sample is also tonalite. Each grain is smaller than sample ZW105.

ZW110 (-17.497156°S, 30.141514°E)

This sample is granodiorite which contains phenocrystic K-feldspar grains.

5.4. Methods

In situ zircon U-Pb dating was carried out at Gakushuin University by using an Agilent 8800 single-collector triple quadrupole ICPMS (Agilent Tech., Santa Clara, USA) coupled to a NWR-213 laser-ablation system (ESI, Portland, US), that utilizes a 213 nm Nd:YAG laser. The laser was operated with fluence of 5.0-6.0 Jcm^{-2}, repetition rate of 5 Hz, and laser spot size diameter of 15 μm. Prior to analysis, regions of interest were pre-ablated using a pulse of the laser with spot size diameter of 110 μm to remove potential surface contamination and to avoid cracks, and inclusion minerals.

Data were acquired on six nuclides; ^{202}Hg, ^{204}Pb, ^{206}Pb, ^{207}Pb, ^{208}Pb, $^{232}Th^{16}O$ and $^{238}U^{16}O$. In order to reduce isobaric interference of ^{204}Hg to ^{204}Pb, small amount of mixed ammonia/helium was flowed into collision/reaction cell between the tandem quadropole mass spectrometers (Kasapoğlu et al., 2016). We succeeded to reduce the gas blank count on 204 amu (^{204}Hg + ^{204}Pb) less than 10 cps on average. Background and ablation data for each analysis were collected over 13 and 15 s, respectively. Data were acquired using multiple groups of 15 unknown samples including GJ-1 zircon (Jackson et al., 2004) and Plešovice zircon (Sláma et al., 2008) as secondary standard bracketed by trio of analyses of the 91500 zircon standard (Wiedenbeck et al., 1995, 2004) and NIST SRM610 grass standard. Background intensities were monitored before every analytical spot and subtracted from following signals. As normalization value of 91500 zircon standard, apparent $^{206}Pb/^{238}U$ without common Pb correction is used (Sakata et al., 2017, i.e. $^{206}Pb/^{238}U = 0.17928 \pm 0.00018$). The instrumental mass bias of lead isotope ratios are normalized to compiled values by Jochum and Stoll (2008).

Common Pb correction was made on the basis of ^{204}Pb method (Stern, 1997). Isotopic composition of common Pb is estimated assuming the terrestrial Pb isotope evolution by a two-stage model (Stacey and Kramers, 1975), through a five-step iterative process as follows: if the apparent age is younger than 3.7 Ga, we use $^{206}Pb/^{204}Pb = 11.152$, $^{207}Pb/^{204}Pb = 12.998$, $^{208}Pb/^{204}Pb = 31.23$, $^{238}U/^{204}Pb = 9.74$, $^{232}Th/^{204}Pb = 36.84$, and the starting age of second stage is 3.7 Ga. If the apparent ^{207}Pb-^{206}Pb age (age without common Pb correction) is older than 3.7 Ga, we assume that $^{206}Pb/^{204}Pb = 9.307$, $^{207}Pb/^{204}Pb = 10.294$, $^{208}Pb/^{204}Pb = 29.487$, $^{238}U/^{204}Pb = 7.19$, $^{232}Th/^{204}Pb = 33.21$ at the

starting age (i.e. age of the Earth is assumed to be 4.57 Ga) as initial parameters. From these parameters, we determine the isotopic composition of common Pb and calculate the age with ^{204}Pb method (this is first step). After this procedure, the common Pb composition of analyte can be newly calculated using the age corrected in first step. Subsequently, the next common Pb corrected age is also determined in second step. We repeat this process five times and determine the final age.

We calculated the standard deviation of each six measurements of 91500 standard bracketing unknown samples, and applied it for uncertainty propagation. Mass and elemental fractionation of ^{207}Pb/^{206}Pb and ^{238}U/^{206}Pb ratio was linearly interpolated by the measured data of each six spot of 91500 zircon standard and NIST SRM610. Determination of U and Th content was carried out by using the spots of 91500 zircon. The ^{235}U count was calculated from ^{238}U using a ^{238}U/^{235}U ratio of 137.88 (Jaffey et al., 1971). We obtained weighted mean ^{206}Pb/^{238}U age of 608.1±9.5 Ma for GJ-1 zircon (2σ, n=12), and ^{206}Pb/^{238}U age of 342.7±4.1 Ma for Plešovice zircon (2σ, n=15) as secondary standards. The result of GJ-1 zircon shows excellent coincidence with the reference age of 608.5±1.5 Ma (Jackson et al., 2004), and that of Plešovice zircon overlaps within ca. 1% error range of the reference age of 337.13±0.37 Ma (Sláma et al., 2008).

5.5. Results

Results of U-Pb dating are listed in Appendix 3 and shown in Fig. 2. Selected CL images are shown in Appendix 4. Detrital zircon grains from ZW5 are rounded in shape, whereas those from ZW68 and ZW74 are sub-rounded. Approximately 70% of separated detrital zircon grains have oscillatory zoning, which were selectively dated. Analyzed numbers of zircon grains are 79 for ZW5, 138 for ZW68, and 78 for ZW74. The U-Pb ages of zircons from the two sandstones of the Deweras Group (ZW5 and ZW68) commonly show three distinct clusters; i.e. ca. 2.66–2.64 Ga, ca. 2.74–2.72 Ga, and ca. 2.88–2.86 Ga. The quartzite of the Lomagundi Group (ZW74) has similar age clusters of ca. 2.74–2.72 Ga and ca. 2.88–2.86 Ga, but the cluster around ca. 2.66–2.64 Ga is inconspicuous. Sample ZW5 yields one Mesoarchean grain (ca. 3.01 Ga), whereas ZW68 contains three Paleoproterozoic grains (ca. 2.22–2.21 Ga). Four times of repeated analysis for the youngest grain from ZW68 yielded the weighted mean 207Pb-206Pb age

of 2,216 ± 22 Ma, which means that the Norah Formation started to deposit after this age.

Most zircons from granitoid samples are euhedral in prismatic shapes and with oscillatory zoning. Analyzed number of zircon grains is 12 for ZW79, 10 for ZW105, 50 for ZW107, and 37 for ZW110. Core and rim were separately measured for three grains in ZW107 and two grains in ZW110. Sample ZW107 and ZW110 contain several ca. 2.9–2.8 Ga grains. In view of core-to-rim structure in single grain (Appendix 3), these can be considered as xenocrysts from pre-existing rocks. With the exclusion of such xenocrysts, we calculated weighted mean age by using data plotted on concordia lines in order to constrain igneous age. Igneous age of sample ZW79 is determined at 2.74 Ga, whereas the other samples show igneous ages of ca. 2.65–2.64 Ga.

5.6. Discussion

5.6.1. Depositional age

The carbon isotopic signatures of the LJE were detected both in the Norah and Mangula formations of the Deweras Group and the lowermost part of the Lomagundi Group (Master et al., 1991, 1993). The present study detected for the first time three Paleoproterozoic detrital zircon grains (2,261 ± 26 Ma, 2,252 ± 28 Ma, 2,216 ± 22 Ma) from the sandstone of the Norah Formation (ZW68). The youngest detrital zircon grain shows oscillatory zoning, no metamictic appearance, and its Th/U ratio is higher than 0.1 (Fig. 2; Appendix 4). Furthermore, four ages obtained from the grain overlap within the analytical error. Therefore, Pb-loss is insignificant for the Paleoproterozoic zircon grains, and the age indicate original igneous age. With respect to Pb-Pb ages of dolostone (2,150 ± 50 Ma) from the Lomagundi Group and galena (2,164–2,112 Ma) from the Piriwiri Group (Fig. 3; Schidlowski and Todt, 1998; Hohndorf and Vetter, 1999), the depositional age of the Norah Formation is constrained between 2,216 ± 22 Ma and 2,150 ± 50 Ma.

Many Paleoproterozoic detrital zircon grains were reported from a paragneiss of the Gweta Complex (Mapeo et al., 2001), most of which range in ca. 2.4-2.1 Ga with the youngest age of 2,125 ± 6 Ma. This suggests that the protoliths of the Gweta paragneiss have been deposited after that of the Deweras Group, and are probably correlated with

the Piriwiri Group. Paleoproterozoic detrital zircons are more abundant in the Gweta complex than in the Deweras and Lomagundi groups, therefore, the depositional site of the Gweta protoliths was located relatively close to the extensive exposures of unidentified Paleoproterozoic zircon-bearing basement rocks.

5.6.2. The onset of the LJE

The oldest record of the LJE in the Zimbabwe Craton exists in the Mcheka Formation (Fig. 1). Given the above-mentioned depositional age of the Norah Formation, the LJE likely started before 2,216 ± 22 Ma in Zimbabwe. Estimates for the duration of the LJE are summarized in Fig. 3. The youngest detrital zircon of 2,306 ± 9 Ma from quartzite in the Superior Craton constraints the oldest limit of the LJE (Valini et al., 2006). The onset of the LJE is restricted to be younger than the baddeleyite U-Pb ages of 2,217 ± 4 Ma and 2,221 ± 5 Ma from diabase dykes in the Superior Craton and the Fennoscandia (Perttunen and Vaasjoki, 2001; Noble and Lightfoot, 1992), because these dykes cut the carbonates with the LJE record. With respect to previous data, we conclude that the LJE started at 2,220–2,210 Ma almost simultaneously throughout Fennoscandia area, the Superior, and the Zimbabwe cratons, and probably also in the rest of the globe.

5.6.3. Provenance of the Magondi Supergroup

The newly obtained ages of ca. 2.65–2.64 Ga from the granitoid (ZW105, 107, and 110) near the Magondi Supergroup correspond to that of the Wedza suite in the eastern Zimbabwe Craton (Jelsma et al., 1996; Taylor et al., 1991). Any U-Pb age around 2.7 Ga has never been reported previously from other granitoids near the Magondi Supergroup, except for ca. 2.7 Ga whole-rock Pb-Pb ages of granitoid of the Sesombi suite located at ca. 150 km to the south in the southwestern Zimbabwe Craton (Wilson et al., 1995). The ca. 2.7 Ga granitoid in the Lomagundi area probably corresponds to its northern extension.

Among the three age clusters of the detrital zircons, i.e. ca. 2.88–2.86 Ga, ca. 2.74–2.72 Ga and ca. 2.66–2.64 Ga, the latter two correspond to the ages of the dated granitoids in the studied area (ZW79 for ca. 2.74–2.72 Ga, the others for ca. 2.66–2.64 Ga). Thus, most of detrital zircons were likely derived from the Zimba unit granitoid which occurred

beneath the Magondi Supergroup. A possible candidate for source of the 2.88–2.86 Ga zircons is Chingezi unit, ca. 200 km to the south (Wilson et al., 1995; Fig. 1). In addition, the granitoid sample (ZW110) contains several xenocrystic grains of the ca. 2.9–2.8 Ga. This possibly suggests that another ca. 2.9–2.8 Ga granitoid likely occurred also in the northern Zimbabwe Craton.

Paleoproterozoic felsic rocks have never been reported from the Zimbabwe nor neighboring Kaapvaal and Congo cratons. Given that the Deweras Group was deposited in a rift basin (Master et al., 2010), a certain amount of terrigenous clastics might have been derived from another continental block(s) which had been connected to the Zimbabwe Craton in the pre-rifting stage. Based on the common occurrence of the 2.5–2.4 Ga dyke swarms and paleomagnetic analysis, a possible linkage among the Zimbabwe, Yilgarn (Western Australia), and Superior cratons was pointed out (Söderlund et al., 2010; Pisarevsky et al., 2014). However, the occurrence of ca. 2.3–2.2 Ga granitoids is extremely rare not only in the Yilgarn and Superior but also in other cratons in the world (Spencer et al., 2018), except for the Rio de la Plata Craton in South America (Hartmann et al., 2002). Another possibility for the source is minor felsic volcanics which were associated with the rifting activity and are not left in the Magondi Supergroup.

5.7. Conclusion

Most of terrigenous clastics in the Deweras and Lomagundi groups were derived from the neighboring Archean basement. On the other hand, ca. 2.3–2.2 Ga detrital zircons from the Deweras Group indicates the occurrence of pre-existing Paleoproterozoic rocks near the northern Zimbabwe. Furthermore, the youngest detrital zircon supports simultaneous initiation of the LJE. Because the LJE is recoded also in the Superior, Yilgarn and Rio de la Plata cratons (Martin et al., 2013), more dating of igneous rocks and detrital zircon in these cratons are useful for further constraints on the duration of the LJE.

Figures

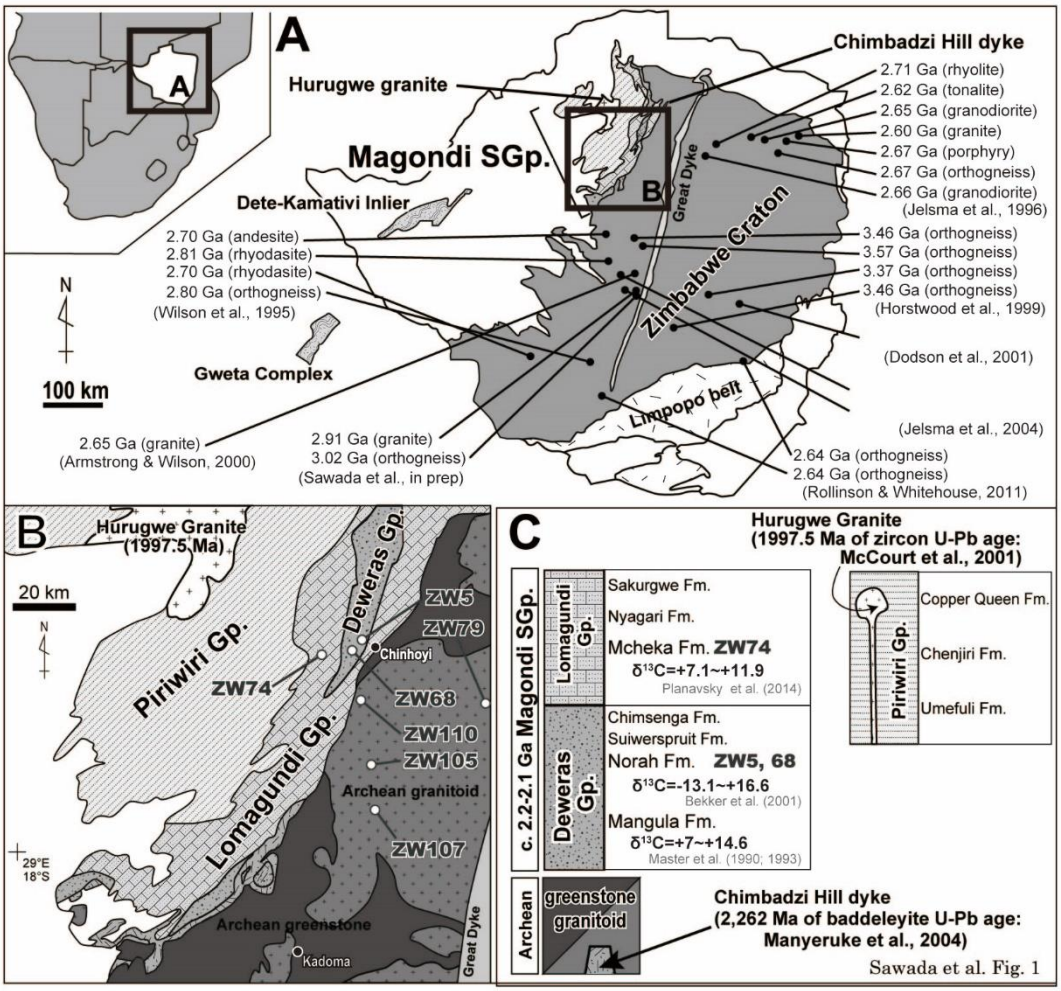

Figure 5-1. (A) Geotectonic map of Zimbabwe with previously reported zircon ages of felsic igneous rocks, (B) geological sketch map of the Lomagundi area in the northern Zimbabwe craton with sample localities (after Master et al., 2010), (C) schematic lithologic column of the major Archean-Proterozoic rocks of the study area. SGp: Supergroup, Gp: Group.

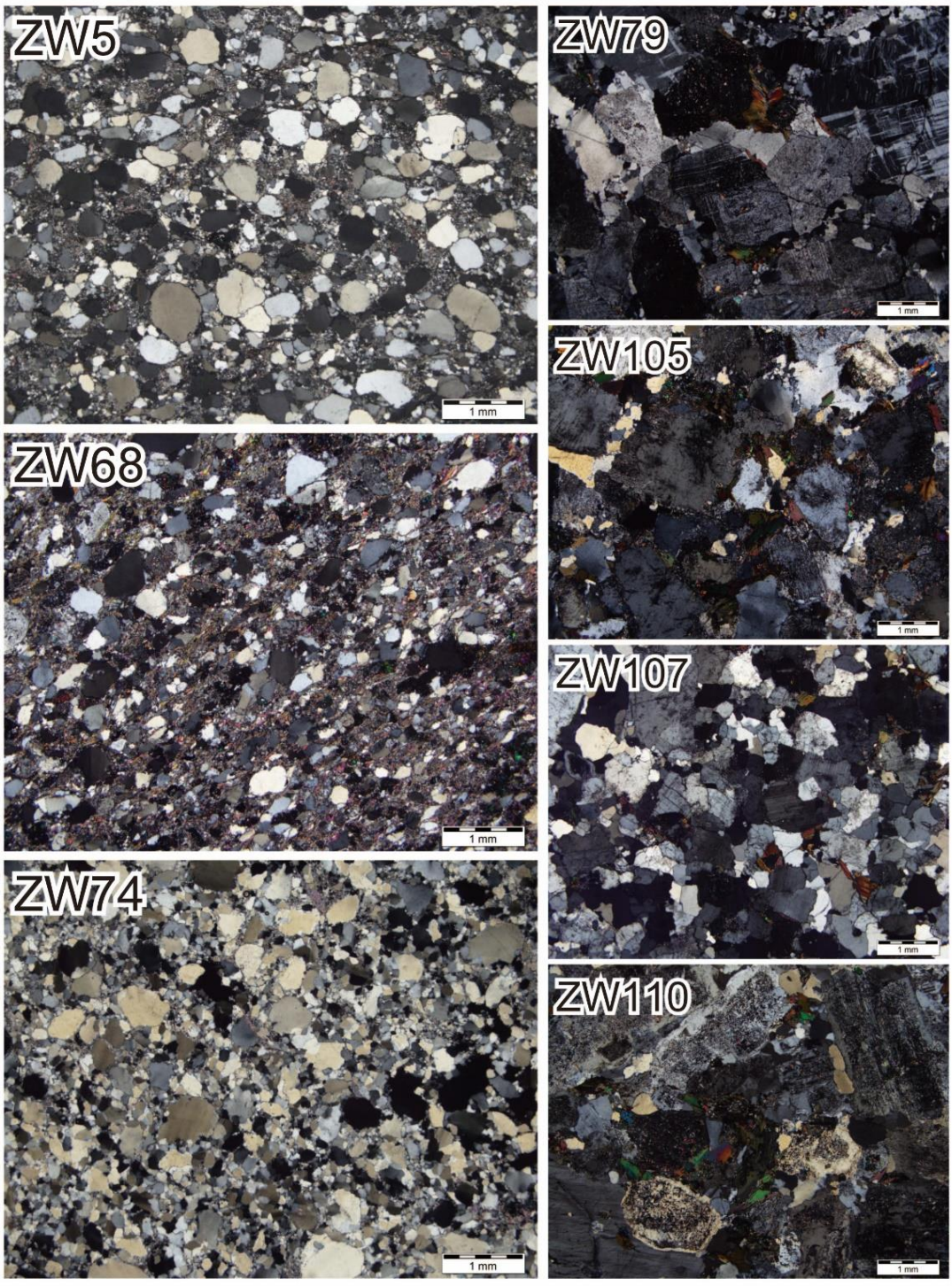

Figure 5-2. Microphotographs of thin sections of analyzed samples.

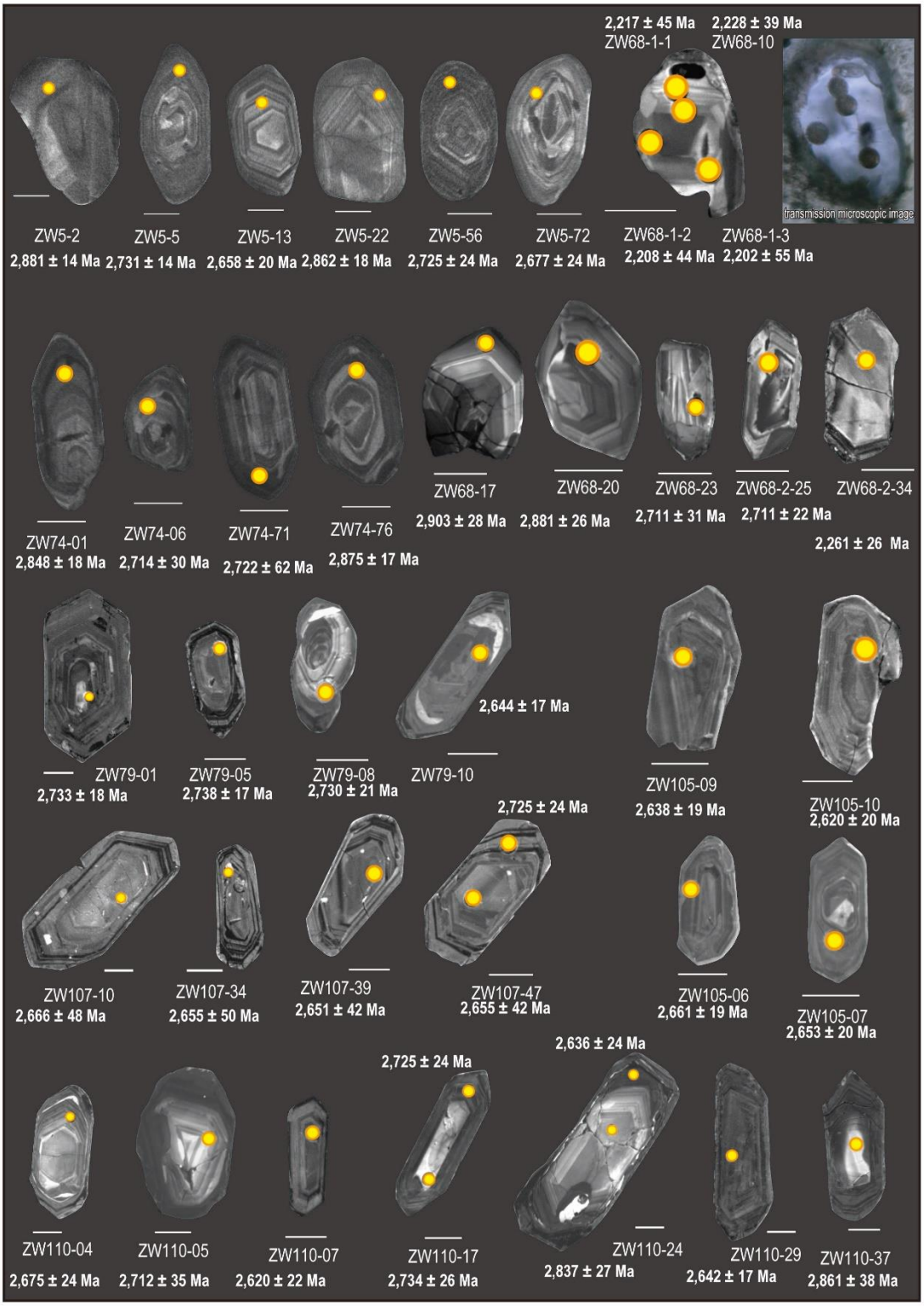

Figure 5-3. Selected cathodoluminescence images of analyzed zircons.

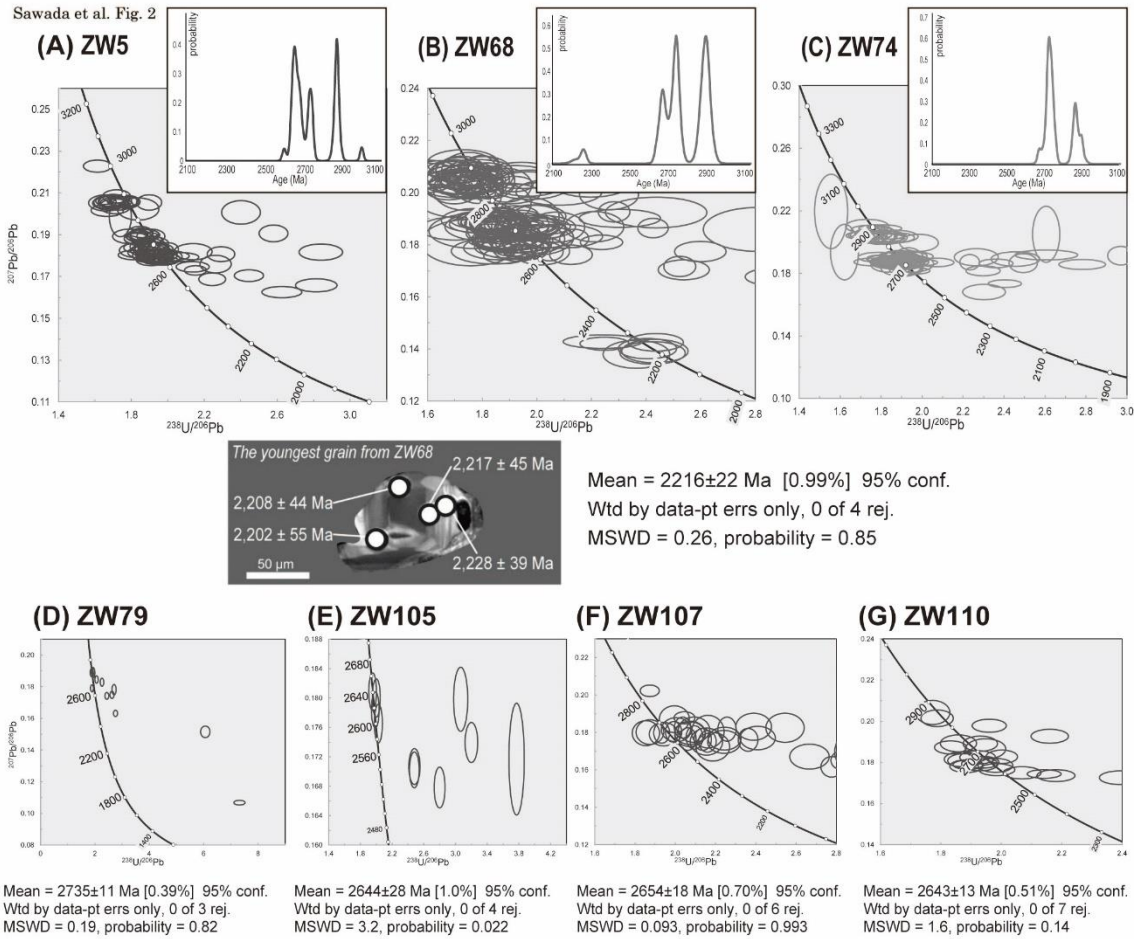

Figure 5-4. (A-C) Tera-Wasserburg concordia diagrams and age frequency diagrams of *in-situ* U-Pb ages of detrital zircons with LA-ICP-MS for sandstone samples. (D-G) Tera-Wasserburg concordia diagrams of *in-situ* U-Pb ages of zircons with LA-ICP-MS for granitoid samples. These figures were constructed with an ISOPLOT (Ludwig, 2003). Error ellipses on individual spots are at 2σ level.

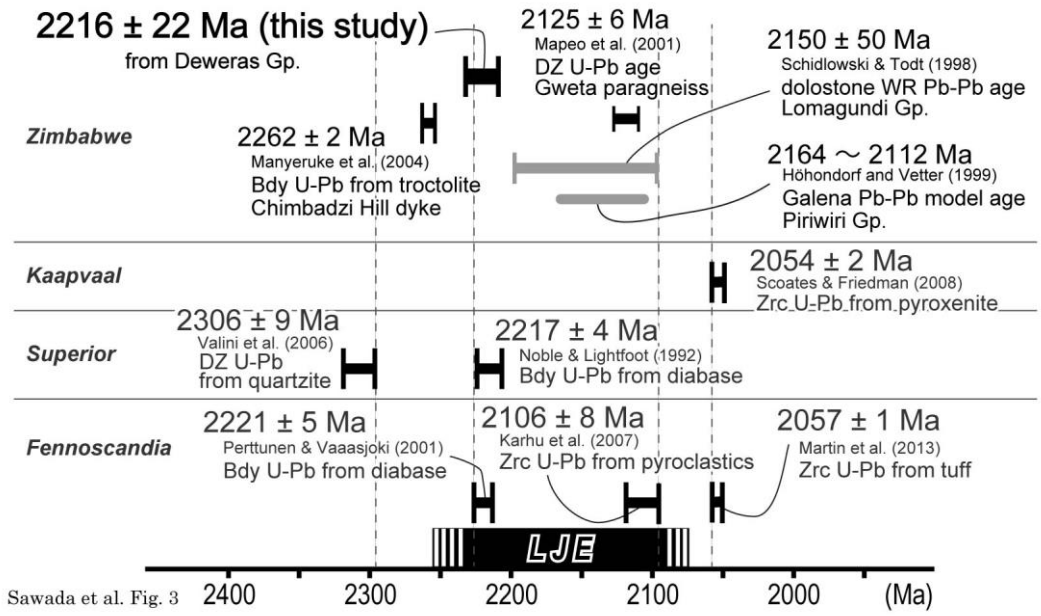

Figure 5-5. Age constraints on the LJE from the Zimbabwe and other cratons (modified after Martin et al., 2013). Bdy; baddeleyite. Zrc; zircon. DZ; detrital zircon. Symbols are at 2σ level.

Table

Table 5-1. Analytical results of zircon U-Pb dating. (in appendix)

Chapter 6. Secular change in size of continental block and sedimentary sorting recovered from sandstone geochemistry

Abstract

Growth history of continental crust has been discussed by many studies; however, forms and sizes of individual continental masses during the Archean to early Paleoproterozoic are still unknown. Chemical composition of sandstones from each continent may reflect its size because of sedimentary sorting of terrigenous clastics. Sandstones composed of ill-sorted grains tend to have similar composition to that of provenance rocks, whereas well-matured sandstones have been fractionated from igneous trend. The pattern of trace elements in sandstone is likely useful in monitoring sedimentary maturity of terrigenous clastics, which potentially reflected the size of provenance continent. In particular, this study focused for the first time on Zr anomaly (=Zr/(Nd*Sm)^0.5) in the primitive mantle-normalized pattern of trace elements to evaluate degree of sedimentary sorting because zircon is concentrated in sandstone through sedimentary sorting more than softer carrier minerals of REEs in granitoids. This study measured whole-rock composition of major, minor and trace elements of 94 Archean-Cenozoic sandstones by using a sector magnetic field type inductively coupled plasma-mass spectrometer (ICP-SFMS). In order to achieve complete digestion, we prepared sample solution from fused-glass bead (sample powder + lithium tetraborate). During the Phanerozoic and Proterozoic (~2.5 Ga), values of Zr anomaly are highly fractionated between 0.2 and 15. On the other hand, in the late Archean (3.0-2.5 Ga), those show less fractionation between 0.7 and 2.5. Furthermore, middle Archean (3.4-3.0 Ga) sandstones yielded values of Zr anomaly between 0.3 and 6, which indicates higher degree of fraction through sedimentary sorting than the middle Archean sandstones. This infers that the general size of late Archean continents had been much smaller than that in the middle Archean (3.4-3.0 Ga), and that the general size of continent likely re-increased after 2.5 Ga. This change in overall trend may have been related to active rifting of continents during the late Archean and subsequent amalgamation in the early Proterozoic.

6.1. Introduction

As reviewed in the first chapter, there is still no generally accepted model for secular change in size of continental block, in particular during Archean and Paleoproterozoic. In order to estimate size of continental blocks through time, this study focused on whole-rock composition of sandstone because mineral composition of detrital grains different from those in provenance of continental crust through degree of sedimentary sorting depend on landform of a continental block (Fig. 6-1). Triangular QFL and QmFLt compositional diagrams is the pioneer to identify tectonic setting of a provenance of sandstone (Dickinson et al., 1983). Especially, quartzose sandstone (e.g., quartz arenite) has been recognized as an indicator of deposition of mature clastics in a cratonic interior setting. As quartzose sandstone have occurred since ca. 3 Ga and sandstones before ca. 3 Ga are dominated by immature volcanic clastics (Ronov, 1964), emergence of large continental blocks has been considered around ca. 3 Ga (Rogers, 1994). However, through a finding in Orinoco River of South American Continent, the recognition was changed that flat topography at least 200 km squares and tropical weather is as the most important to form quartzose sandstone, and tectonic setting itself is not necessarily related (Johnson, 1990; Johnson et al., 1991). Therefore, nonetheless much quartzose sandstone occurs on cratonic interior, occurrence of quartzose sandstone itself cannot inform size of continental block. On the other hand, for bulk chemistry of clastic rocks, several chemical indexes have been proposed for whole-rock composition and utilized for many studies, such as Chemical Index of Alternation (CIA) (Nesbit and Young, 1982), and Weathering Index of Parker (WIP) (Parker, 1970). These indexes, however, require precise contents of K_2O, Na_2O, and CaO, which are fluid mobile elements. Thus, those indexes are not suitable for meta-sandstone, and this study focused on minor and trace elements composition of sandstone.

Trace elements of Zr and Hf are contained by zircon, and well known as immobile during secondary processes, such as weathering, alteration and diagenesis. In addition, REE, Sc and Y are supposed to be immobile during those processes (e.g. Bau and Möller, 1993; Bau and Dulski, 1996). McLennan et al. (1990) measured modern turbidites from oceanic basin in various tectonic setting (Fig. 6- 2A), and proposed a diagram of Zr/Sc vs. Th/Sc to trace provenance of

clastic rocks (Fig. 6- 2B). On the diagram, most sandstones and almost all mudstones are plotted on a line of igneous trend. On the other hand, turbidites off passive continental margins, especially in Atlantic Ocean off N. American Continent, show higher values of Zr/Sc ratio, which considered to have been caused by sedimentary sorting of mineral grains derived from granitic continental crust. Therefore, the diagram of Zr/Sc vs. Th/Sc have been utilized for sandstones to identify their provenance and tectonic setting. However, if we compare Archean granitoids with Phanerozoic and Proterozoic ones (e.g. Condie, 1999; Moyen and Martin, 2012), Archean granitoids are depleted with Sc, as well as Y and heavy REE (HREE) elements. Archean sandstones should have been affected by this compositional difference in granitoids.

Instead, the present study focuses on Zr anomaly in the primitive-mantle (PM) normalized pattern ([Zr]/([Nd]*[Sm])^0.5) of sandstones to evaluate sedimentary sorting of detrital grains. Identical value of Zr anomaly for igneous rocks is 1.0, and most igneous rocks show values between 0.6 and 2.0 (Condie, 1999; Moyen and Martin, 2012). Figure 6-2C shows diagram of Zr/Sc vs. Zr anomaly, which demonstrates proportional relationship between them, and values of Zr anomaly for turbidite from Atlantic Ocean off N. American Continent are up to 5.7 whereas other samples show values between 0.6 and 2.0 same as igneous rocks.

This study measured totally 94 samples of sandstone from ca. 3.4 Ga middle Archean to ca. 0.1 Ga Cenozoic, and discuss secular change in size of continental blocks based on Zr anomaly in PM normalized trace element pattern calculated with the analytical results.

6.2. Analyzed samples and geological background

This study performed whole-rock major, minor and trace elements analyses for totally 94 samples.

6.2.1. 3.4-3.0 Ga middle Archean sandstones

6.2.1.1. Noisy Formation, Onverwacht Group, Barberton Greenstone Belt, Kaapvaal

Craton

The Barberton Greenstone Belt in the Kaapvaal Craton of southern Africa have provided many insights for the Paleoarchean geology because of good preservation without strong metamorphism, as well as greenstone units in the Pilbara Craton. In the greenstone belt, the Onverwacht Group is the oldest group (ca. 3550-3300 Ma). The Noisy Formation is middle part of the group and composed of coarse terrestrial clastics (fluvial sandstone and conglomerate) and felsic airfall tuffs (Viljoen and Viljoen, 1969; de Wit et al., 2011). Depositional age of the Noisy Formation is considered as 3,432±10 Ma based on zircon chronology for the felsic tuff (Grosh et al., 2011).

This study analyzed five samples from the Noisy Formation; i.e. ZW209, 211, 221, 227, and 233. Samples of ZW209 and 221 are fine-grained conglomerates and the others are coarse sandstones.

6.2.1.2. Jack Hills Greenstone belt and Narryer Gneiss Block, Yilgarn Craton

The Jack Hills GS belt and is ca. 3.2 Ga supracrustal rock units in the northern part of the Yilgarn Craton (Myers and Williams, 1985; Spaoggiari et al., 2007). Both the Jack Hills Greenstone belt and Narryer Gneiss Block are well known as the localities yielding abundant Hadean detrital zircons up to 4.4 Ga (Frounde et al., 1983; Compston and Pidgeon, 1986; Wilde et al., 2001). This study measured four quartzite samples from the Narryer Gneiss Block, and two quartzites and three conglomerates from the Jack Hills Greenstone Belt.

6.2.1.3. Beitbridge Group in Limpopo Belt

The Limpopo Belt is a high-grade metamorphic belt between the Zimbabwe and Kaapvaal cratons and comprising Archean to Paleoproterozoic components. The belt had been metamorphosed several times during ca. 2.6-2.5 Ga the late Archean and ca. 2.0 Ga Paleoproterozoic. The central part of the Limpopo belt is composed of orthogneiss of the ca. 3.3-3.2 Ga Sand River Gneisses, supracrustal rocks of the Beitbridge Group (Barton, 1983, 1996). The Beitbridge Group comprises paragneiss, quartzite, BIF, and amphibolite. Based on the sedimentary succession, the Beitbridge Group is assumed to be a continental platform deposit

(e.g., Taylor et al., 1986; Boryta and Condie, 1990; Kro¨ner et al., 1998; Buick et al., 2003). The quartzite of the Beitbridge Group yields >3.9 Ga Eoarchean detrital zircon (Zeh et al., 2008).

This study analyzed two samples from the Beitbridge Group (ZW1, and 199).

6.2.1.4. Quad Creek quartzite, Beartooth Mt. area, Wyoming Craton

In the northwestern part of the Wyoming Craton, the ca. 3.25 Ga Quad Creek metasedimentary enclaves within granitoid gneisses and migmatites are composed of a varied suite of isoclinally folded, sheared and variably deformed chromite-bearing banded and massive quartzites, garnetiferous siliceous paragneisses, amphibolite, quartz–biotite schists and BIF (Maier et al., 2012). Among them, quartzites are well known as host of >3.9 Ga Eoarhcean detrital zircons (Mueller et al., 1992; 1996; Maier et al., 2012). This study analyzed one sample of banded quartzite collected from same outcrop with Mueller et al. (1996).

6.2.1.5. Moodies Group, the Barberton Greenstone Belt, Kaapvaal Craton

The Moodies Group unconformably overlies on the Onverwacht Group and mainly composed of quartz-rich sandstone. The Moodies Group is recognized as the oldest eolian deposits on the Earth preserving wind-ripple strata preserved in the quartz-rich sandstones and interpreted as the first-cycle quartz sandstones produced by eolian abrasion (Simpson et al., 2012). Depositional age of the Moodies Group is considered as ca. 3.2 Ga based on the youngest detrital zircon at 3.19 ± 0.02 Ga (Zeh et al., 2013) and cross-cutting Salisbury Kop Pluton (3,079 ± 6 Ma).

This study measured three samples from the Moodeis Group. Two samples of them are quartz arenite (BE478, and BG266), and the other is greywacke (BE482).

6.2.1.6. Cleaverville Formation, Clearverville Group, Pilbara Craton

The ca. 3.1-3.0 Ga Clearverville Group is volcano-sedimentary sequence occurred in the northwest of the Pilbara Craton (Hickman, 2001). The group is considered as accretionary complex based on lithology and structural geology (Ohta et al., 1996; Shibuya et al., 2007; Kiyokawa et al., 2002). This study analyzed one sample of the Clearverville Formation, which

is considered as forearc deposits (IG220).

6.2.2. ca. 3.0-2.6 Ga late Archean sandstones

6.2.2.1. Mont dO'r Formation, Shurugwi Greenstone Belt, Zimbabwe Craton

Detail of this formation and greenstone belt is described in Chapter 4. This study analyzed one sample from this formation (ZW117).

6.2.2.2. Wagita Formation, Steep Rock Group, Wabigoon Province, Superior Craton

The Steep Rock Group is a volcano-sedimentary unit on 3.0-2.9 Ga continental rift basin and continental platform on the Wabigoon Province, Superior Craton (Wilks and Nisbet, 1987; Tomlinson et al., 2003). Bottom of the Steep Rock Group is the Wagita Formation which is 0-150 m thick and unconformably overlies on >3.0 Ga granitic basement. The Wagita Formation is composed of mainly quatzose meta-sandstone. This study analyzed three samples from the Wagita Formation; i.e. two quartzite (SR01, 03) and one meta-sandstone (SR07).

6.2.2.3. Jutten and Savant groups, Savant Lake Greenstone Belt, Wabigoon Province, Superior Craton

The Savant Lake Greenstone Belt is ca. 2.95-2.70 Ga volcano-sedimentary sequence on the Wabigoon Province of the Superior Craton (Davis et al., 1988; 1991; Sanborn-Barrie, 2000). The GS belt is composed of the Jutten, Handy Lake, and Savant groups from the bottom to the top. The Jutten Group consists of conglomerate and sandstone unconformably on the granitoid basement. The Handy Lake Group overly conformably on the Jutten Group, which are composed of mafic-felsic volcanic rocks. The Savant Group deposited unconformably on those two groups, which are composed of lower matrix-support conglomerate and upper turbidite.

This study analyzed three samples of basal quartzose sandstone (SV12A, 13 and 17) from the Jutten Group, and two samples of turbidite from the Savant Group.

6.2.2.4. Pongola Group, Kaapvaal Craton

The ca. 3.0-2.8 Ga volcano-sedimentary sequences unconformably overlying on the Kaapvaal Craton is called the Pongola Supergroup, and approximately 5 km thick. The sequence consists of two units; the Nsuze Group and the overlying Mozaan Group. The Nsuze Group is dominated by mafic volcanic sequences with shallow-marine clastic rocks and carbonates, whereas the Mozaan Group is comprised of mudstone and sandstones with minor amount of BIF, diamictite and volcanics (Matthews 1967; Watchorn 1980; Gold and von Veh, 1995). Depositional environment of the Mozaan Group is interpreted as wave- or storm-dominated shallow marine shelf sediments, interbedded with marine shelf mudstone and fluvial braid plain sandstone (Beukes and Cairncross, 1991; Gold, 1993). Depositional age of the Mozaan Group is precisely constrained by using U–Pb zircon dating which showed the oldest Pongola volcanic layer in the Nsuze Group at 2,980 ± 10 Ma and the uppermost layer of the Mozaan Group at 2,954 ± 9 Ma (Mukasa et al., 2013).

This study analyzed two samples from Odwoleni Formation which is upper part of the Mozaan Group (PP74 and PP79).

6.2.2.5. Central Slave Cover Group and Duncan Lake Group, Yellowknife Supergroup, Slave Craton

The Yellowknife Supergroup is ca. 2.9-2.6 Ga volcano-sedimentary sequence on the Slave Craton (Bleeker et al., 1999). The lowermost Central Slave Cover Group (CSCG) is a sedimentary sequence composed of quartzite, volcano-clastics, and BIF unconformably deposited on the >3.0 Ga granitoid/gneiss basement of the Slave Craton. The group is conformably covered with basaltic lava flows of the Kam Group. These litho-stratigraphy and geochemistry of basalts from the Kam Group indicates that those groups were formed on a continental margin setting (Cousens, 2000; Mueller et al., 2005).

On the Kam Group and older granitoid/gneiss basement, ca. 2.7 Ga calc-alkaline volcanic rocks erupted, and are overlain by clastic rocks of the Duncan Lake Group (Henderson, 1972). The Duncan Lake Group is composed of ca. 2.68-2.66 Ga turbiditic mudstone and sandstone deposited on back arc setting (Feruson et al., 2005).

In the present study, one sample of the CSCG from Bell Lake (YK10) and two samples of the Burwash Formation which comprises upper part of the Duncan Lake Group (YK04, 07) were analyzed.

6.2.2.7. Fortescue Group, Mt. Bruce Supergroup, Pilbara Craton

The Mount Bruce Supergroup is a ca. 2.78-2.2 Ga volcano-sedimentary unit deposited widely on the Pilbara Craton, and composed of three groups; i.e. the Fortescue, Hamersley, and Turee Creek groups (Thorne and Trendall, 2001). The ca. 2.78-2.63 Ga Fortescue Group unconformably overlying the older granite-greenstone terrane of the craton, is up to 1 km thick. The group is composed of six formations; i.e. the Mt. Roe (mafic lava flows), Hardey (conglomerate and sandstone), Kylene (mafic and felsic volcanics), Tumbiana Formation (clastic rocks and carbonate rocks with stromatolite), Madina Formation (mafic volcanics), and Jeerinah Formation (sandstone and mudstone). Based on lithostratigraphy, the Fortescue Group is considered as a continental rift basin (Thorne and Trendall, 2001).

This study analyzed four samples from the Fortescue Group; i.e. Hardey Formation (FT22), Tumbiana Formation (FT69), and Jeerinah Formation (FT69 and RM10).

6.2.2.8. Manjeri Formation, Belingwe Greenstone Belt, Zimbabwe Craton

The Belingwe Greenstone Belt is situated in the southern part of the Zimbabwe Craton and surrounded by the >2.9 Ga granitoid/gneiss basement. The greenstone belt is divided into the Mtshingwe Group (ca. 2.9–2.8 Ga lower unit mainly composed of ultramafic-mafic volcanic rocks) and the overlying Ngezi Group (ca. 2.8-2.7 Ga upper unit mainly composed of mafic-ultramafic volcanic rocks and clastic rocks and carbonates) (Wilson, 1979; Martin et al., 1980; Abell et al., 1985; Nisbet et al., 1993). The lowest part of the Ngezi Group is called the Manjeri Formation, which unconformably rests on the Archean basement. Conglomerate, sandstone, and carbonates with stromatolitic structure of the Manjeri Formation represent shallow marine facies, whereas the upper part of the Ngezi Group consists of graywacke and mudstone of deeper marine facies (Bickle et al., 1975; Martin, 1978; Martin et al., 1980; Abell et al., 1985). Based on lithofacies, the Manjeri Formation is considered as platform sediment formed in a passive

continental margin. Depositional age of the Manjeri Formation is based on the youngest detrital zircon age of 2,788 ± 87 Ma (Sawada et al., 2016) and whole-rock Pb/Pb isochron age of 2,706 ± 49 Ma for stromatolitic limestone (Bolhar et al., 2002).

This study analyzed two samples from the Manjeri Formation (ZW98 and 335).

6.2.3. Paleoproterozoic sandstones

6.2.3.1. Murmac Bay Group, Rae Craton

Detail of this group is described in Chapter 4.

6.2.3.2. Cascade Quartzite, Deep Lake Group Snowy Pass Supergroup, Wyoming Craton

Paleoproterozoic supracrustal rocks exposed on the southern margin of the Wyoming Craton were deposited on rift basin and passive continental margin, and divided into three groups of the Snowy Pass Supergroup (Karlstorm et al., 1983). The lowermost Phantom Lake Group is composed of mafic volcanics with minor felsic volcanics and terrigenous clastics, and the other three groups, i.e. the Deep Lake, the upper and lower Libby Creek groups, are composed of quartzite (meta-quartzose sandstone), conglomerate including diamictite, pelitic rocks, and carbonates.

6.2.3.3. Turee Creek and lower Wyloo groups, Pilbara Craton

The Turee Creek Group of the Mt. Bruce Supergroup and the Beasley River Quartzite of the lowermost Wyloo Group is Paleoporterozoic sedimentary sequence on a foreland basin (Martin et al., 2000). The Turee Creek Group is composed of three formations; namely the Kungarra Formation (mudstone and siltstone with glacigenic diamictite), the Koolbye Formation (coarse sandstone), and the Kazput Formation (dolomite and sandstone). Depositional ages of the groups are constrained by a zircon U-Pb age of 2,449±3 Ma for the Woongarra Rhyolite in the uppermost Hamersley Group (Barley et al., 1997), a baddeleyite U-Pb age of 2,208±10 Ma for mafic sill in the Kungarra Formation (Mueller et al., 2005), and zircon U-Pb age of 2,209±15 Ma for the

Cheela Springs Basalt conformably overly on the Beasley Quartzite (Martin et al., 1998). This study analyzed seven samples collected near the Hardey Syncline, one from the Koolbye Formation (TC381), four from the middle-upper Kazput Formation (TC96, 144, 179, and 195) and two from the Beasley River Quartzite (TC155 and 266).

6.2.3.4. Magondi Supergroup, Zimbabwe Craton

Detail of this group is described in Chapter 6. This study analyzed two samples; one from the Deweras Group (ZW5) and the other from the Lomagundi Group (ZW74).

6.2.4. Neoproterozoic-Paleozoic sandstones

6.2.4.1. Applercross Formation, Torridon Group, northern Scotland

The Torridon Group is Neoproterozoic upward-fining reddish terrigenous clastics sequence in northern Scotland deposited on foreland basin of the post-Grenvillian orogeny (Stewart, 1969). Depositional age of the group is constrained by the 1,060±18 Ma (Rainbird et al., 2001) and the 997 Ma youngest detrital muscovite (Bluck et al., 1997).

This study analyzed two samples of reddish sandstones; one is a fine-grained sandstone from the upper part of the Applecross Formation (UK2) and the other is coarse-grained sandstone from the basal part of the Applecross Formation (UK4).

6.2.4.2. Darladian Supergroup, Scotland and Ireland

The Neoproterozoic to Cambrian Darladian Supergroup of Ireland and Scotland is composed of silicious clastic rocks and carbonates with minor amount of volcanics deposited on passive continental margin of the eastern Laurentia along Iapetus Ocean (Anderton 1982; 1985; 1988; Harris et al., 1994; Cawood et al., 2003). This study analyzed samples from the Argyll and Southern Highland groups which are upper part of the Darladian Supergroup.

Volcanic rocks of uppermost part of the Argyll Group is dated as 600-595 Ma by using zircon

U-Pb dating (Halliday et al., 1989; Dempster et al., 2002). The youngest detrital zircon from the Southern Highland Group is dated as 553±24 Ma (Cawood et al., 2003).

From Scotland, this study analyzed three samples of the Islay Formation which is the lowermost Argyll Group (ISN1, IS150, IS160), one sample from the Crinan Formation of middle Argyll Group (UKP4), and two samples from the Southern Highland Group (UKP6, and 8). In addition, two samples of the uppermost Argyll Group in Ireland were also analyzed (IR300, 306).

6.2.4.3. South Stack and Gwna groups, Monian Supergroup, Anglesey Island

The South Stack Group occurs in NW Wales and consists of siliciclastic sequence on the passive continental margin of the Laurentia (Barber and Max, 1979; Shackleton, 1954; Phillips, 1991). Depositional age is considered as ca. 500 Ma based on the youngest detrital zircon age of 501±10 Ma (Collins and Buchan, 2004). This study analyzed two quartzite samples from the Holyhead Formation (ANG321 and 331).

The Gwna Group consists of a ca. 610-540 Ma latest Proterozoic volcano-sedimentary trench mélange, which contains oceanic-trench rocks including pillow basalts, cherts, mudstones and sandstones interpreted as ocean plate stratigraphy (Barber and Max, 1979; Shackleton, 1954; Maruyama et al., 2010; Asanuma et al., 2015). This study analyzed two samples analyzed two sandstones of the trench turbidite (IR409; 416).

6.2.4.4. Neoproterozoic-Ordovician sandstones in various tectonic settings, Newfoundland

Newfoundland off the east coast of the North American Continent in NE Canada is composed of ca. 0.62-0.55 Ga rift basin and passive continental margin on ca. >1 Ga Grenville gneissose basement, and 0.51-0.43 Ga sedimentary rocks and igneous rocks of subduction orogen, and ca. 0.43-0.41 Ga post-collisional depostis, which are related with opening and closing of the Iapetous Ocean (Harland and Gayer, 1972; van Staal et al., 1998; Cawood et al., 2001; Pollocketal, 2007). This study analyzed samples from ca. 0.6 Ga Neoproterozoic rift basin sediments near St. John's area (NF2 and 9), ca 0.43 Ga Ordovician trench-fill turbidites of the Barger Group (NF32 and NF33), and the ca. 0.41 Ga Silurian Wigwarn Formation of the Botwood Group composed of forearc shallow marine sandstone near central part of the island (NF28).

6.2.5. Cenozoic sandstones

The SW Japan-arc is well known as a Phanerozoic continental arc-trench system, and orogenic components especially after Cretaceous are well preserved (Isozaki and Maruyama, 1991; Isozaki et al., 2010). This study analyzed totally six Cretaceous sandstones; four samples from forearc side (the Birahu Formation of the Nankai Group: BRH2, BRH3, the Inubouzaki Formation of the Choushi Group: INB, and the Goryo Formation of the Izumi Group: GRY), and two from back arc side (Tedori Group: 14HD2 and 14HD3).

6.3. Method

Rock samples were cut into chips and >100 g of them for each sample was used for analysis to avoid bias caused by heterogeneity in a sample. The chips were rinsed with de-ionized water by an ultrasonic device, dried completely at 120 °C overnight, powdered by an alumina mill, and dried again first at 110 °C then at 950 °C overnight to measure loss on ignition (LOI). Fused-glass beads were prepared with a lithium tetraborate ($Li_2B_4O_7$) flux in a 1:10 dilution ratio at 1050 °C.

Major element compositions (Si, Ti, Al, Fe, Mn, Mg, Ca, Na, K, and P) were determined with an X-ray fluorescence spectrometer (XRF; ZSX Primus II, RIGAKU, Japan) at National Museum of Nature and Science, Japan. The accelerating voltage and the current were set to 50 kV and 50 mA, respectively, during the XRF analysis. Calibration methods using GSJ standards followed Sano et al. (2011).

Minor and trace element composition was analyzed by sector magnetic field type inductively coupled plasma-mass spectrometer (ICP-SFMS; Element, Thermo Fischer, USA) at the University of Tokyo, Komaba. Fragments of the fused-glass beads were properly dissolved into a diluted nitric acid with internal standard elements (In and Bi). This study reports minor (P, Ti, Sc, V, Cr, Co, Ni, Ga) and trace element compositions (Rb, Sr, Y, Zr, Nb, Cs, Ba, REE, Hf, Ta, Th and U). The fused-glass beads can achieve better digestion of Zr and Hf than that with

HF+HClO methods (Koshida et al., 2016). As an analytical standard, solution prepared from basaltic reference material (GSJ JB-3) was utilized. To check analytical accuracy, this study analyzed three granite standard (JG-1a, JG-2 and JG-3) and one chert standard (JCh-1). The differences between the recommended values (Imai et al., 1996; Kunimura et al., 1998) and our averaged values are within 10%, except for extremely low content of Zr in JCh-1 (less than 10 ppm).

6.4. Results

All analytical results of major, minor and trace elements are listed in Table 1. Chondrite-normalized REE patterns and primitive mantle (PM)-normalized trace element patterns are shown in Fig. 6- 3 and 4, respectively.

6.4.1. major elements

Most of the analyzed samples show SiO_2 concentration of between 70 - 95 %. Several extremely quarthose samples have SiO_2 concentration of >95 %. When a result show SiO_2 concentration of 100%, the present study regards the SiO_2 concentration as 99.9 % in discussion below. The second abundant major element is Al_2O_3 (-20 %), except for extremely quarthose samples and the BRH3 of the Cenozoic sample from Japan arc. Concentrations of Fe_2O_3, MgO, CaO, Na_2O, K_2O are less than 10 %, except for MN22 (Fe_2O_3 = 14.7 %) of the and BRH3 (CaO = 11.6 %), and TiO_2, MnO and P_2O_5 are less than 1 % for all samples.

6.4.2. minor and trace elements

Concentration of Co, Ni, Zr, Y, Sc, and REE for most samples are less than those of usual granitoid (e.g. Moyen and Martin, 2012; Imai et al., 1996). This trend can be explained by quartz addition through sedimentary process. As previously reported (e.g. Condie, 1999), concentrations of Cr are enriched in many Archean sandstones compared with Proterozoic and Phanerozoic ones,

but not necessarily all Archean ones show higher content of Cr than Proterozoic and Phanerozoic ones. No clear correlation is observed between depositional age of the samples and concentration of Sc, Y, and REE. On the other hand, Zr-rich samples (>400 ppm) have depositional age of Proterozoic and Phanerozoic except for ca. 3.2 Ga one Archean sample of BT. Sample UC12 and 14 are extremely rich in Ba (2570 ppm for UC12 and 7970 ppm for UC14).

In REE pattern, all samples commonly show LREE enrichment and HREE depletion, which indicates that the detrital grains of all samples were dominantly derived from felsic rocks in the continental crust. Ratios of La/Yb, La/Sm, and Gd/Yb do not show clear secular change, but extremely high La/Yb and Gd/Yb moderate La/Sm ratio for UC09 and 12 indicate strong depletion of HREE for those two samples. Remarkable positive Eu anomalies are found in all samples from the Noisy Formation (ZW209, 211, 221, 223, and 227), two from the Pongola Group (PP74, 79) and one from the Murmac Bay Group (UC14). On the other hand, samples from Jack Hills and Mt. Narryer show negative Eu anomaly. The other samples do not show large Eu anomaly or slightly negative anomaly. Only ZW199 shows clear negative Ce anomaly.

In PM-normalized patterns, negative anomalies of Nb and Ta are detected in all samples. Samples older than 2.8 Ga commonly show negative Sr anomalies, but some of those younger than 2.8 Ga show positive Sr anomalies. Most samples show negative Ti anomaly with several exceptional samples (UC14, UK4, and NF33). Anomalies of Zr and Hf have same trend and values of the ratios vary between 0.2 and 16. Secular change in Zr anomaly is discussed in the next chapter with compilation of data by previous studies.

6.5. Discussion

6.5.1. Secular change in PM normalized pattern and Zr anomaly

Secular change in Zr anomaly in PM-normalized patterns, elemental ratio of Zr/Sc and Zr/Y are summarized in Figure 5. In addition to the present study, this study calculated those values

with data from previous studies listed in Figure 6-3.

As a comprehensive trend, elemental ratio of Zr/Sc and Zr/Y for Archean and Paleoproterozoic samples show higher base values than those for Neoproterozoic and Phanerozoic. This trend can be considered as to be caused depletion of Sc and Y in the Archean granitoid, typically in TTG (Moyen and Martin, 2012). On the other hand, values of Zr anomaly defined by using Zr, Nd, and Sm do not show such a biased trend. More detailed secular trend of Zr anomaly and relationship with composition of the other elements are discussed below.

6.5.1.1. Cenozoic sandstones

Samples from SW Japan arc show values of Zr anomaly between 0.6 and 3.9. The highest value of 3.9 from the Choshi Group of forearc sandstone and the second highest value of 2.8 from the Tedori Group of backarc sandstone, which are comparable to some of modern turbidites along passive continental margin of the N. America (McLennan et al., 1990). Because the SW Japan arc was continental arc before the Miocene opening of Sea of Japan, these high Zr values possibly are caused by suppl of detrital grains from the Eurasian Continent. As a modern analogue, Corolado River over 2,300 km long on the North American Continent flows into subduction margin of the Pacific side. Therefore, this study considers that similar topography possibly occurred in Cenozoic SW Japan, and the sedimentary sorting was caused.

6.5.1.2. Paleozoic-Neoproterozoic and Mesoproterozoic

All samples from Paleozoic forearc basins and accretionary complex show near 1.0 values; IR409, and IR416 (Gwna Group). On the other hand, high values of positive Zr anomaly over 3.0 are yielded from samples of passive continental margin or foreland basin after continental collision; i.e. ISN1, IS150, IS160, IR306 (Darladian Supergroup) and ANG321, ANG 331 (South Stack Group). This result also supports that values of Zr anomaly in sandstones reflects provenance size. On the other hand, as shown by the other samples, sandstones on passive continental margin do not necessarily show such high Zr anomaly.

For the Mesoproterozic, this study analyzed two samples from the Torridon Group (UK2 and UK4), of which values of Zr anomaly are up to 5.5. Fatima and Khan (2012) and Nagrajanetal et

al. (2007) reported trace element composition of India, which shows highly fractionated values of Zr anomaly between 0.3 and 11. These also indicate sedimentary sorting on large continental blocks, in same manner as the Paleozoic-Neoproterozoic sandstones from the passive continental margins.

6.5.1.3. 2.4-2.2 Ga Paleoproterozoic (TC, ZW, UC, WY)

During Paleoproterozoic, values of Zr anomaly show a range between 0.3 and 16 which is the largest diversification through time. Nonetheless, not necessarily all samples show such widely fractionated values of Zr anomaly. Samples from the Magondi Supergroup of the Zimbabwe Craton and the Snowy Pass Supergroup of the Wyoming Craton did not show highly fractionated values of Zr anomaly between 0.4 and 1.4, even though both sedimentary sequences have thick quartzose sandstone layers on continental platforms. From the upper part of the Snowy Pass Supergroup, previous work reported more fractionated values of Zr anomaly between 0.5 and 4.0 (Crichton and Condie, 1993). This possibly indicates that degree of sedimentary sorting increased through development of rift basin continental margin of the Snowy Pass Supergroup. Similarly, more investigation of the Magondi Supergroup may reveal prevailed sedimentary sorting on the Paleoproterozoic Zimbabwe Craton.

Samples from the Turee Creek Group of the Pilbara Craton show highly fractionated values of Zr anomaly between 0.5 and 16. These strongly suggest sedimentary sorting of detrital grains occurred on the foreland basin on the Paleoproterozoic continental block.

Samples from the Murmac Bay Group of the Rae Craton also show wide range of Zr anomaly between 0.3 and 8.8. Several samples of this locality are extremely Ba-rich. Even though reason of the enrichment in Ba is unknown, there are no relation between Ba concentration and Zr anomaly (Fig. 6- 5). Therefore, this study considers that those fractionated values of Zr anomaly also indicates high degree of sedimentary sorting on the Rae Craton.

6.5.1.4. 3.1-2.6 Ga late Archean

During ca. 3.1-2.6 Ga late Archean, analyzed samples show relatively narrow range of Zr anomaly between 0.7 and 2.3. Among them, all relatively high values of Zr anomaly (>2) were

yielded from sandstones formed on continental-rift basins or continental platforms except for sample IG220. On the other hand, all samples of turbidite containing volcanic detritus show values of Zr anomaly near 1.0.

Compilation of data by previous works indicate trend similar as data of the present study. Narrow ranges of Zr anomaly near 1.0 were yielded from arc-related sandstones; i.e. 2.7 Ga forearc turbidite (Polat et al., 1998; Shirey et al., 1986; Wu et al., 2016), 3.1 Ga forearc turbidite (Nesbitt et al., 2009) and 2.98 Ga volcano-clastics (Fralick et al., 2009). On the other hand, relatively wider ranges of Zr anomaly (= 0.3~3.0) were recovered from ca. 3.02 Ga Kenojhar quartzite (E. India: Grosh et al., 2016) and ca. 3.1 Ga Naharmagra quartzite (Raza et al., 2010), both quartzites were considered as continental platform deposits.

These results indicate that, during this era, sedimentary sorting had not occurred so much as the Proterozoic and Phanerozoic, even on continental platform.

6.5.1.5. 3.5-3.1 Ga middle Archean

Both samples from the Beitbridge Group (ZW1 and ZW199) show large values of Zr anomaly; i.e. 4.4 for ZW1 and 5.4 for ZW199. Sample ZW199 is the only sample showing remarkable negative Ce anomaly (Fig. 6- 4). Compared with sample ZW1, ZW199 show relatively higher content of Fe_2O_3, larger negative anomalies of Nb, Ta, and, Ti, smaller La/Yb ratio, and small positive Eu anomaly. These features are possibly related to contribution of chemical sediment, such as BIF and carbonate rock (Boryt and Condie, 1990). Clay minerals occurred on hydrothermal vent after precipitation of Fe oxide grains possibly shows negative Ce anomaly (Shibuya et al., 2010). Given the REE contents of ZW199 were controlled by such chemical sediments, sedimentary sorting before deposition should have occurred to exclude REE abundant minerals except for zircon.

Psammitic gneiss from the Beartooth Mt. of the Wyoming Craton (sample BT) show a high value of Zr anomaly similar to the Beitbrige Group ($Zr/Zr^* = 4.7$). Maier et al. (2014) reported whole-rock composition of several samples of quartzite and psammitic gneiss and those rocks show Zr anomalies of 0.6-3.4. These support that the variation in Zr anomaly have been caused

also by sedimentary sorting between zircon and other minerals.

Samples from the Jack Hills GS belt and Mt. Narryer complex shows values of Zr anomaly between 0.7 and 2.5, which is not so fractionated as the Beartooth Mt. and the Beitbridge Group. Moreover, rocks are considered to have been highly silicified after deposition compared with quartzose sandstones in other localities (Rasmussen et al., 2011). This indicates that the REE composition and values of Zr anomaly did not change through silicification after deposition, and thus the values of Zr anomaly are controlled by sedimentary sorting.

Samples from the Noisy Formation in the Kaapvaal Craton show moderate values of Zr anomaly between 1.3 and 2.0. Whole-rock compositions of shale and fine-grained sandstones in the same locality previously measured by Rouchon et al. (2009) show values of Zr anomaly between 0.7 and 2.7, which indicates relatively larger fraction than samples of the present study. Moreover, fine-grained laminated siltstone associated with chert (silicic chemical deposit) shows much higher values of Zr anomaly over 7.0 (Ledevin et al., 2014). On the other hand, metasomatized dacites of the Hooggenoeg Formation below the Noisy Formation, which are considered as one of the major detrital sources, show Zr anomaly between 1.3 and 2.5 (Rouchon et al., 2009). These suggest that the highly fractionated Zr anomaly were caused by sedimentary sorting. Similarly, from the ca 3.26-3.22 Ga Fig Tree Group on the Onverwacht Group, greywacke samples show relatively wide range of Zr anomaly between 0.6 and 4.7 (Hoffman, 2005). Therefore, this study envisages that the high values of Zr anomaly indicate significant sedimentary fraction on the Kaapvaal Craton during ca. 3.43-3.22 Ga.

The ca. 3.4 Ga Mt. Goldsworthy quartzite in the Pilbara Craton also show wide range of Zr anomaly between 0.1 and 9.0 (Sugitani et al., 2004). Based on lithological similarity and paleomagnetic studies, the pre-3 Ga connection between the Pilbara and Kaapvaal has been considered as continental nuclei (Condie, 1998; Nelson et al., 1999; Erikson et al., 2009). On those cratons, significant degree of sedimentary sorting likely occurred since ca. 3.4 Ga.

6.5.2. Implication for the history of continental growth

Through analysis of whole-rock composition of sandstone as well as compilation of data by previous work, this study found secular trend of Zr anomaly in sandstone as below; 1) wide range of 0.2 ~ >10 throughout after ca. 2.3 Ga Proterozoic and Phanerozoic, 2) narrow range of 0.6 ~ 2.5 during ca. 3.0-2.6 Ga late Archean, and 3) relatively 0.2 ~ 8.0 during ca. 3.5-3.0 Ga middle Archean.

Modern turbidites on passive continental margins show high values of Zr anomaly up to 5.5 (Fig. 6- 2; McLennan et al., 1990). Much higher values of Zr anomaly were recovered from passive continental margin and foreland basin of continental collision zone at ca. 0.6-0.5 Ga, 1.2-1.0 Ga and ca. 2.3-2.2 Ga, which suggests that there have been commonly continental blocks over several thousand kilometers square. Therefore, continental blocks which are thousand-kilometer-long, similar size as the modern ones

The ca. 3.0-2.6 Ga late Archean sandstones do not show fractionated Zr anomaly, which indicates continental blocks of this era was smaller than those of after 2.3 Ga. During the late Archean, amalgamation of small continental blocks has been proposed by many previous studies (e.g. Card, 1990; Kimura et al., 1993; Dirks and Jelsma, 1998; White et al., 2003; Percival et al., 2006; Korsch et al., 2011; Zhai and Santosh, 2011). On the other hand, during the late Archean, many greenstone belts are also considered as continental rifting basins (e.g. Thorne and Trendall, 2001; Nisbet et al., 1993; Bleeker, 1998; Wilks and Nisbet, 1987; Tomlinson et al., 2003; Beules and Cairncross, 1991). Taking these geological observations into account, both collision and rifting of small continental blocks had been occurred frequently during this period. The smaller size of continental blocks should have elongated total length of subduction zones, and possibly lead active production of continental crust as suggested by many detrital zircon chronological studies (Condie et al., 2009; Belousova et al., 2010).

Moreover, the present results suggest that continental blocks during ca. 3.5-3.2 Ga should be larger than the late Archean, even smaller than those after Proterozoic. Figure 6-7 shows simplified schematic image of secular change in continental block through time. On the other

hand, many studies previously have proposed to form production of granitic crust until ca. 3.5 Ga without plate subduction; such as large oceanic plateau model (Van Kranendonk et al., 2007; Reimink et al., 2014), recycling of Hadean proto-crust through heating by mantle plume (Zeh et al., 2014; Kamber, 2015). However, because those processes amount of basaltic crust should be accompanied, production of granite-dominant continental blocks was likely difficult through those processes. Recent analysis of whole-rock δ^{49}Ti isotope in mudstone also indicate that the ca. 3.5 Ga continental block was dominated by granitic crust as the later ones, and difference between them was existence of komatiite in the Archean (Greber et al., 2017). As accretionary complex has been reported as old as 3.95 Ga (Komiya et al., 1999; 2015), plate subduction and production of continental crust is likely started since the Eoarchean and possibly Hadean. Therefore, the granitic continental blocks enough large to induce significant sedimentary sorting had been likely formed by ca. 3.5 Ga, through production and amalgamation of oceanic island arcs over 500 million years.

6.6. Conclusion

Through whole-rock analysis of sandstones as well as data compilation, this study summarizes secular change in size of continental blocks as below; 1) since ca. 2.3 Ga, there have been continental blocks over five thousand kilometer-long, comparable to modern ones. They have formed “supercontinent” several times through continental collision and amalgamation. 2) during the ca. 3.0-2.5 Ga late Archean, size of the continental blocks was much smaller than that of later ones. The reduction in size of the continental blocks elongated total length of the subduction zones. As a result, active production of juvenile continental crust and plural accretion of the arcs occurred around 2.7 Ga as by many previous studies (Rino et al., 2004; 2008; Condie et al., 2009; Belousova et al., 2010). 3) during ca. 3.5-3.0 Ga, there were larger continental blocks than those in the late Archean, even though not comparable to modern ones. 4) Although production of continental crust before 3.5 Ga are still unclear, the >3,5 Ga continental crust is considered as to have been formed in island arcs along boundaries between oceanic plates or large oceanic plateau. Nonetheless, it is difficult to make granitic continents by only plume activity like oceanic plateau.

In addition, to collide continental blocks each other, plate motion driven by subduction is necessary. Therefore, this study supposes that subduction-driven production of continental crust and growth in size of continental blocks through their amalgamation should have occurred before 3.5 Ga early Archean.

Figures

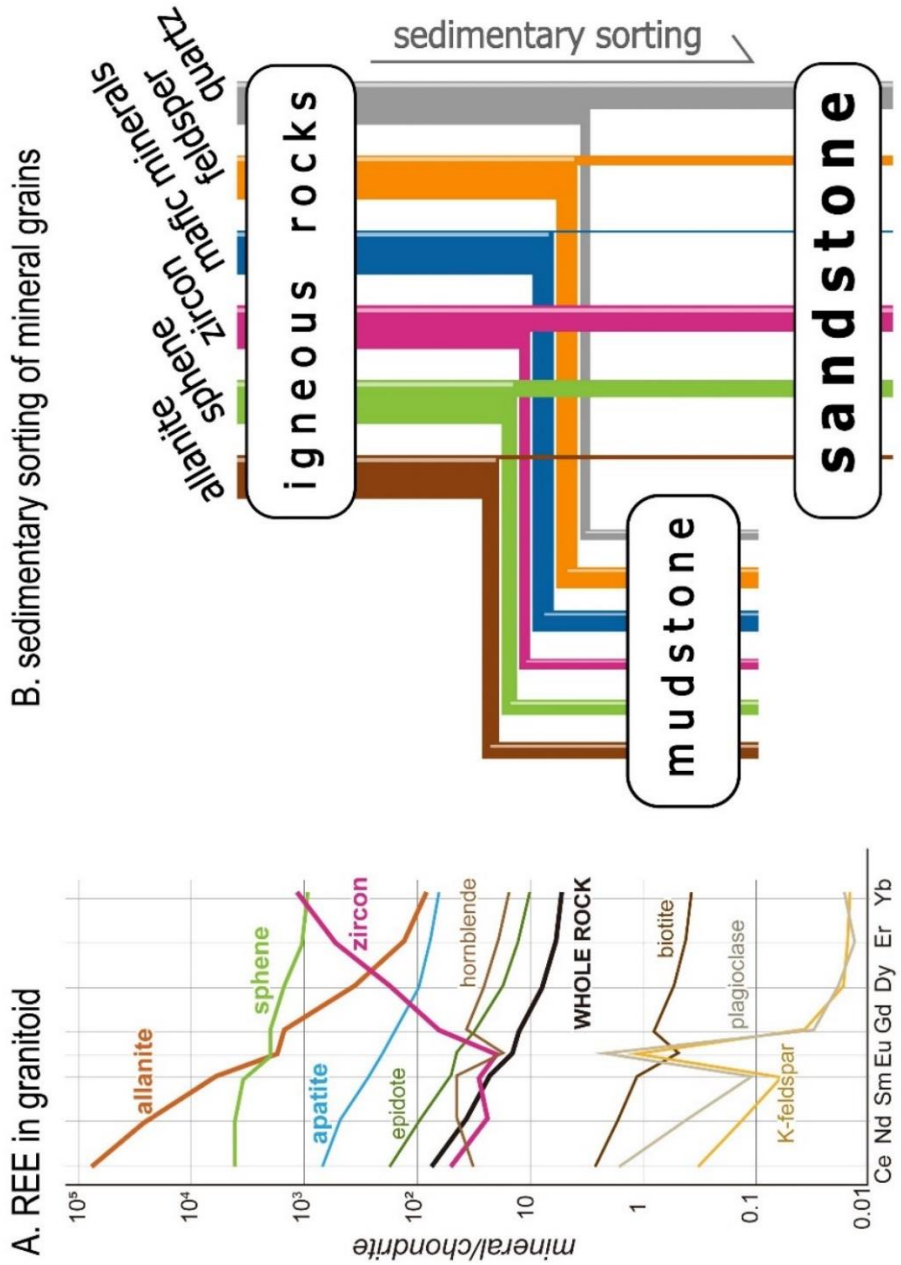

Figure 6-1: A. Chondrite-normalized pattern of REE for typical minerals in granitoid (Cromet and Silver, 1983). B. Schematic images of mineral fraction through sedimentary sorting.

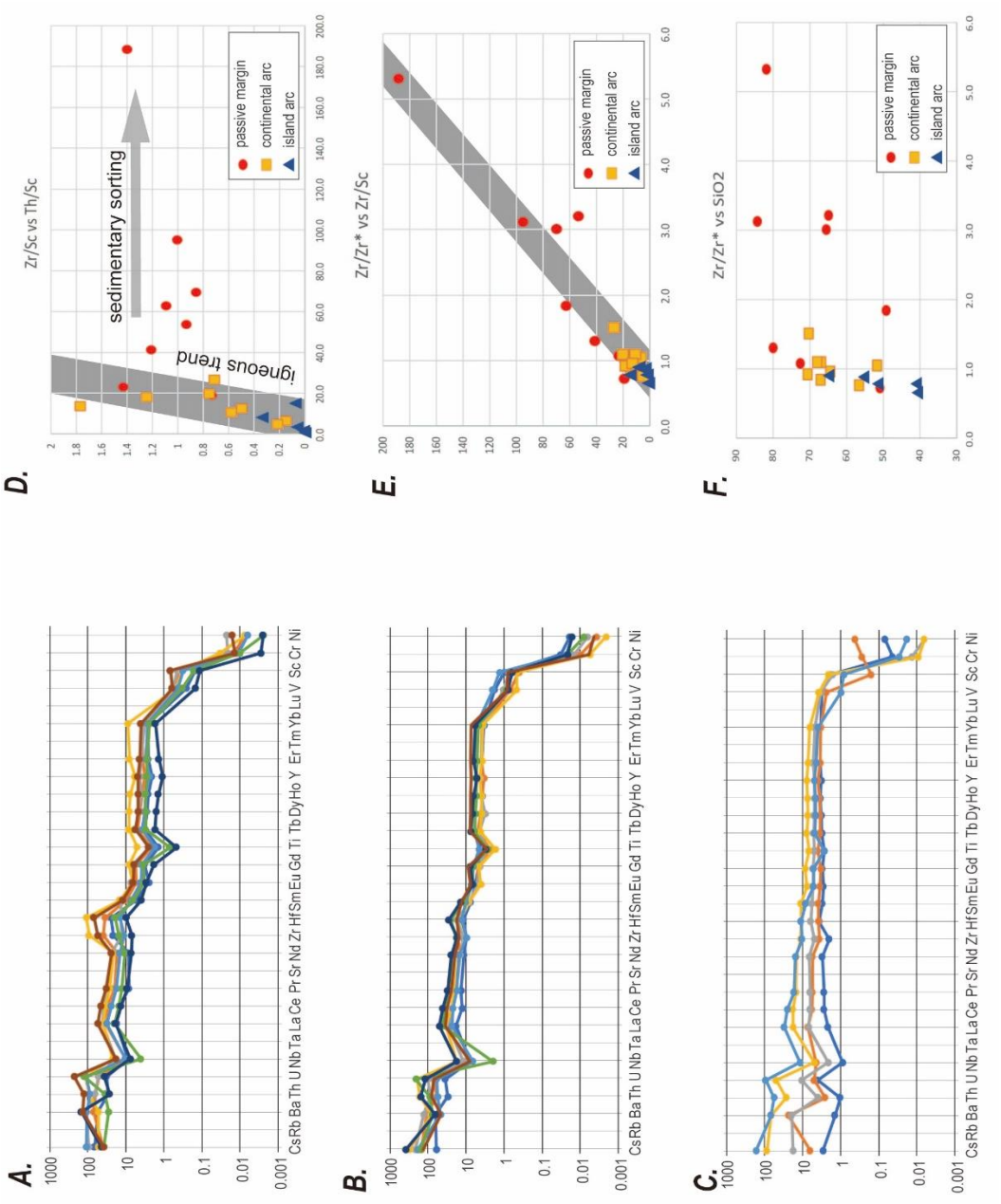

Figure 6-2: A-C. PM normalized pattern of trace elements in turbidite sandstones (data from McLennan et al., 1990). A. passive continental margin B. continental arc, and C. island arc.

D. Zr/Sc vs Th/Sc plot proposed by McLennan et al. (1990), E. Zr/Zr* vs. Zr/Sc, and F. Zr/Sc vs. SiO_2.

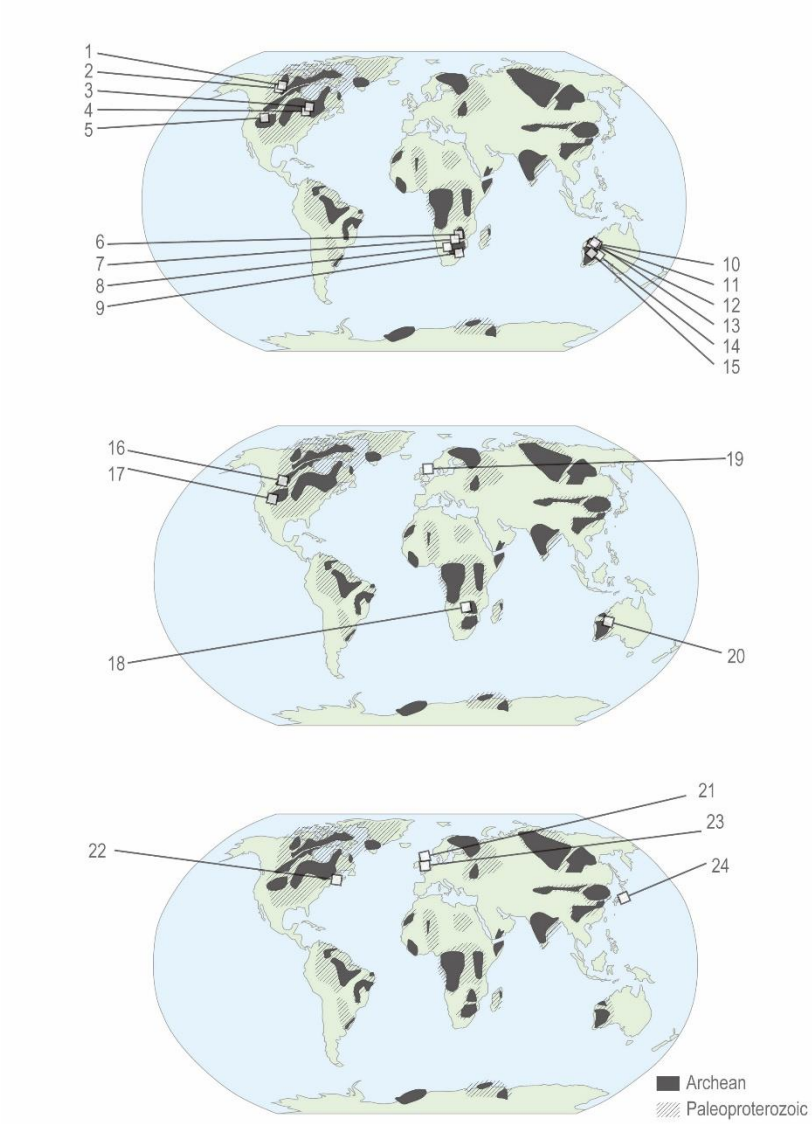

Figure 6-3 Localities of analyzed rock samples.

1. Bell Lake quartzite, Central Slave Cover Group (YK10).

2. Burwash Formation, Duncan Lake Group, Slave Craton (YK04, YK07).

3. Jutten Group (SV06, 12A, 13) and Savant Group (SV17, 25, 26) of the Savant Lake Greenstone Belt, Superior Craton.

4. Steep Rock Group, Superior Craton (SR01, 03, 07)

5. Beartooth Mt. area, Wyoming Craton (BT).

6. Mont dO'r Formation, Shurugwi GS belt, Zimbabwe Craton (ZW117).

7. Manjeri Formation Belingwe GS belt, Zimbabwe Craton (BW98, 335)

8. Beitbridge Group, Limpopo Belt (ZW1, 199).

9. Moodies Group, Barberton Greenstone Belt, Kaapvaal Craton (BG266, BE478, 482).

10. Noisy Formation, Barberton Greenstone Belt, Kaapvaal Craton (ZW209, 211, 221, 227, 233).

11. Pongola Group, Kaapvaal Craton (PP74, 79).

12. Cleaverville Group, Pilbara Craton (IG220)

13. Fortescue Group, Pilbara Craton (RM10, FT22, 61, 69)

14. Jack Hills GS belt, Yilgarn Craton (JH10, 13, 18, 28)

15. Mt. Narryer complex, Yilgarn Craton (MN22, 23, 37, 42)

16. Murmac Bay Group, Rae Craton (UC02, 03, 09, 12, 14, 21)

17. Snowy Pass Supergroup, Wyoming Craton (WY1).

18. Deweras and Lomagundi groups, Zimbabwe Craton (ZW5, 74)

19. Moin Supergroup (UK02, 04)

20. Turee Creek Group, Pilbara Craton (TC96, 144, 155,179, 195, 266, 381)

21. Darladian Supergroup, Ireland and Scotland (UKP4, 6, 8, IR300, 306, ISN1, IS150, 160).

22. Newfoundland (NF02, 09, 28, 32, 33)

23. South Stack Group (ANG321, 331) and Gwna Group (IR409, 416)

24. Cenozoic sandstones from forearc and back arc basins of the Japan arc.

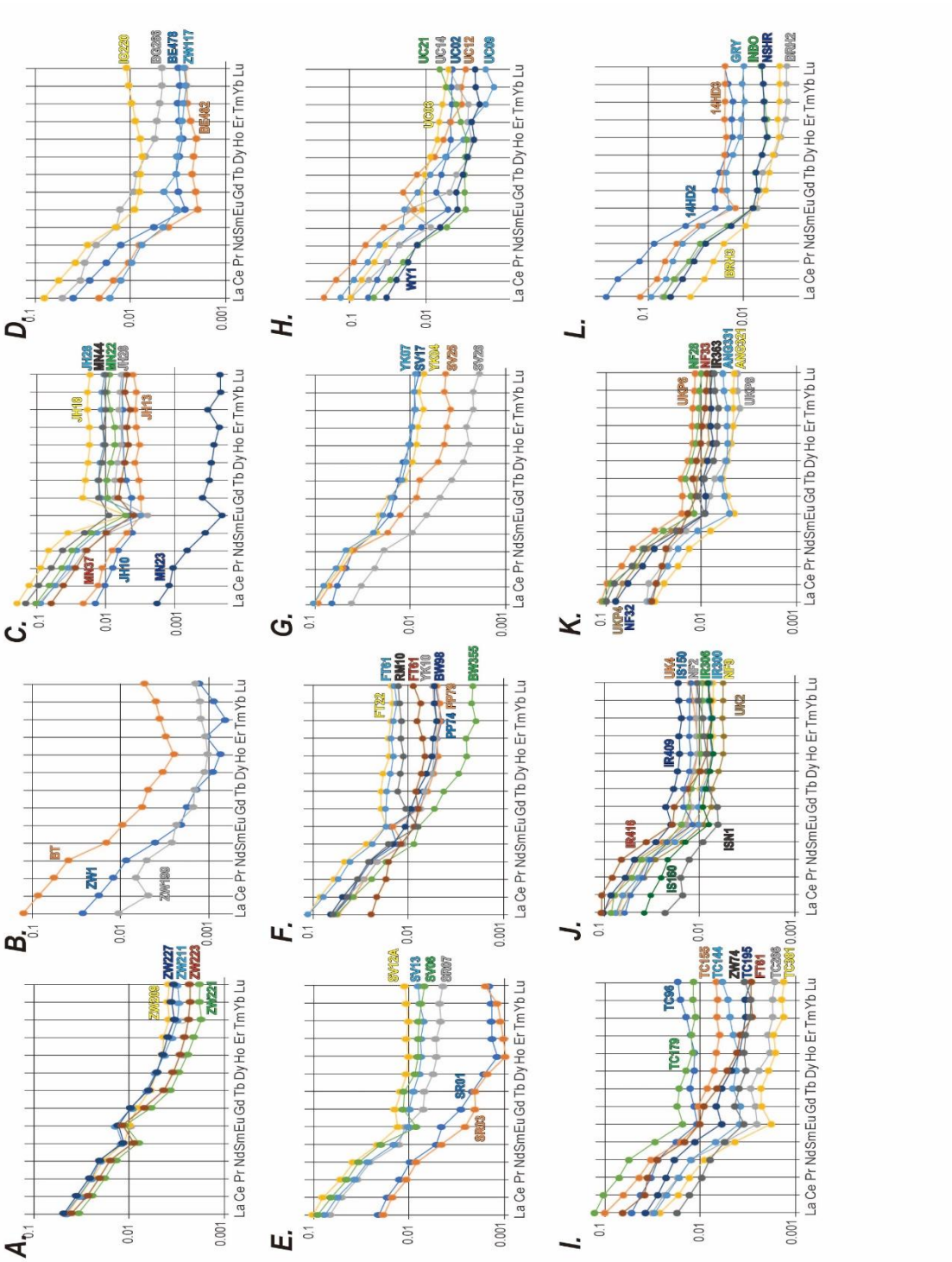

Figure 6-4.Chondrite-normalized REE pattern for all analyzed samples.

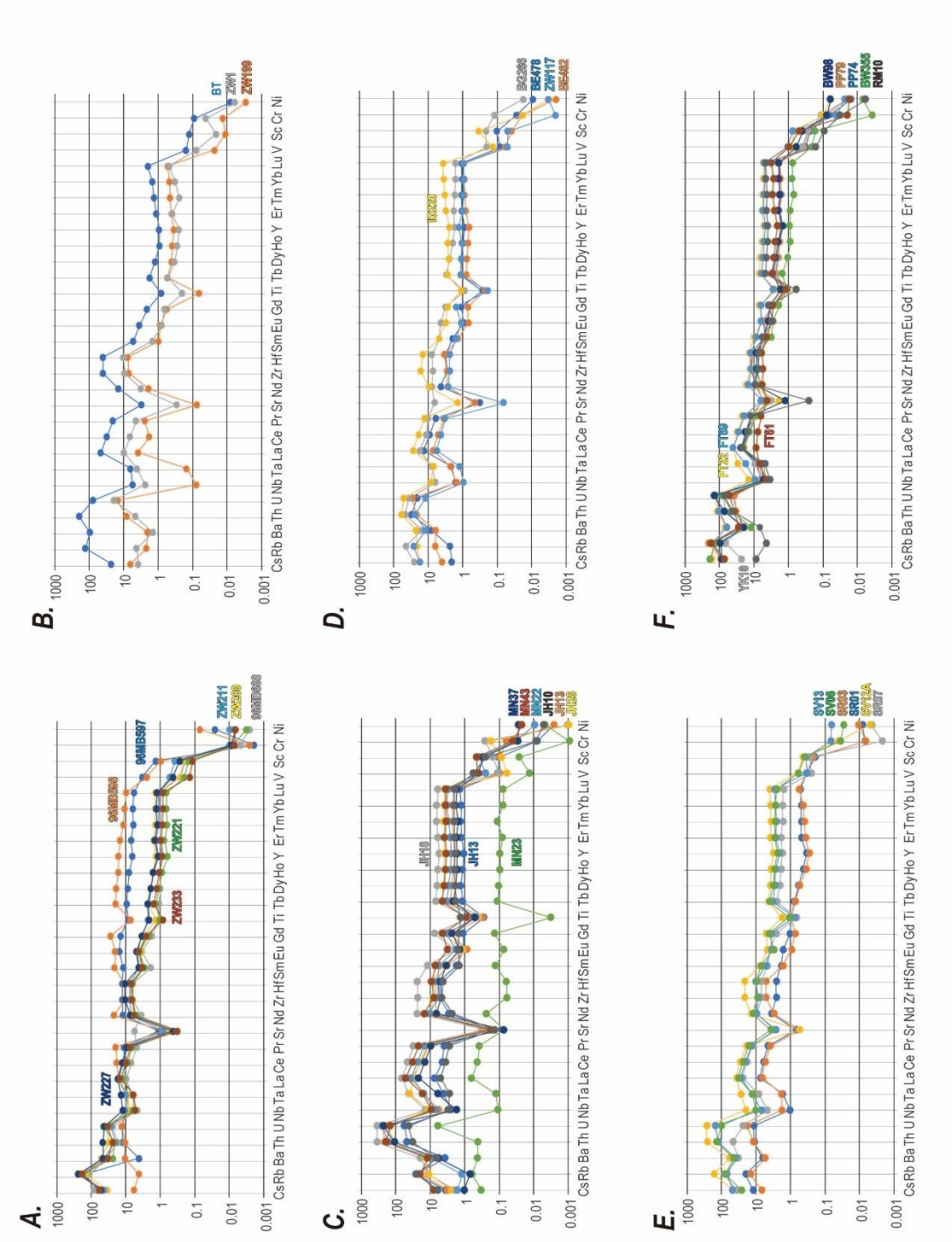

Figure 6-5. Analytical results shown in primitive mantle-normalized trace element pattern.

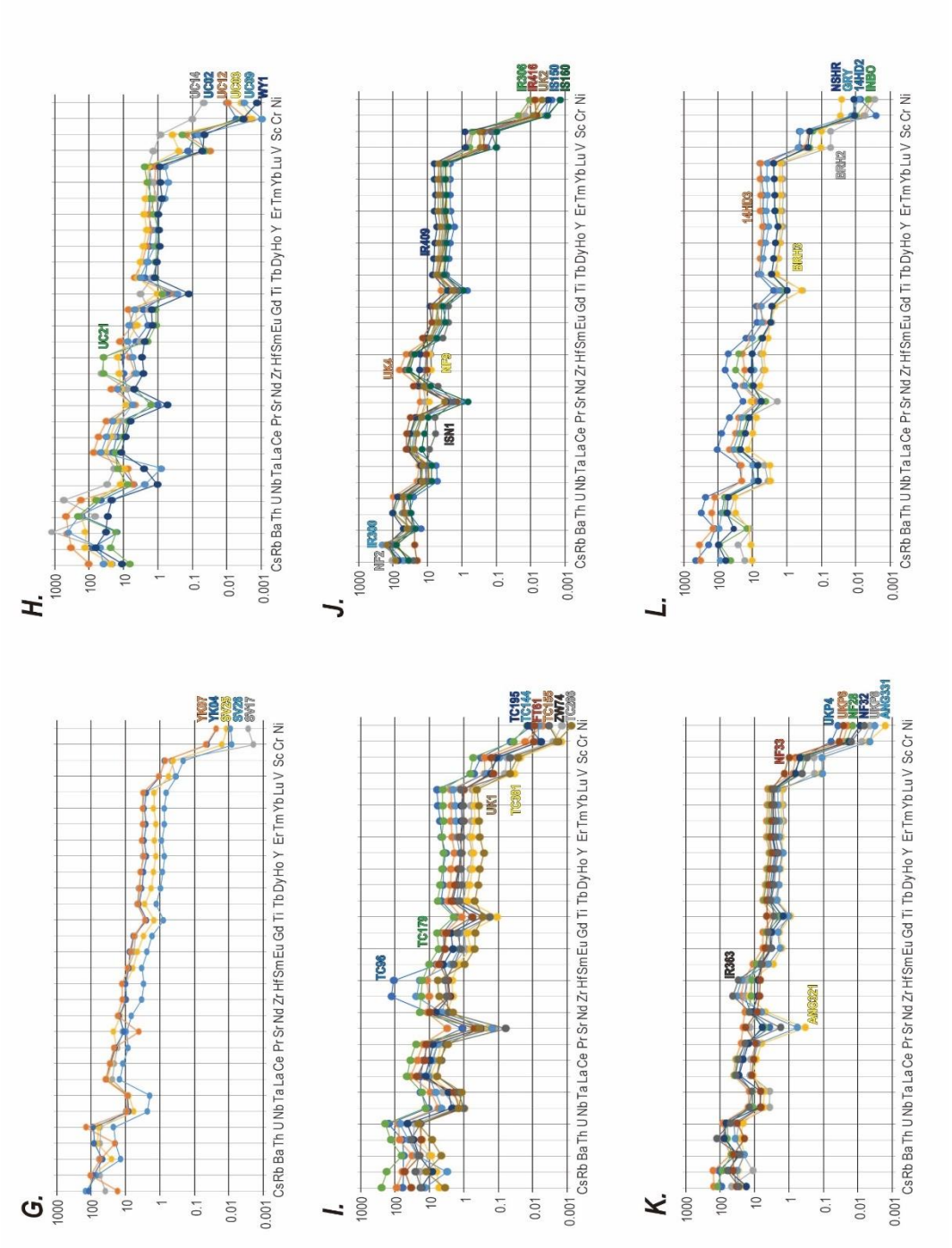

Figure 6-5. (continued)

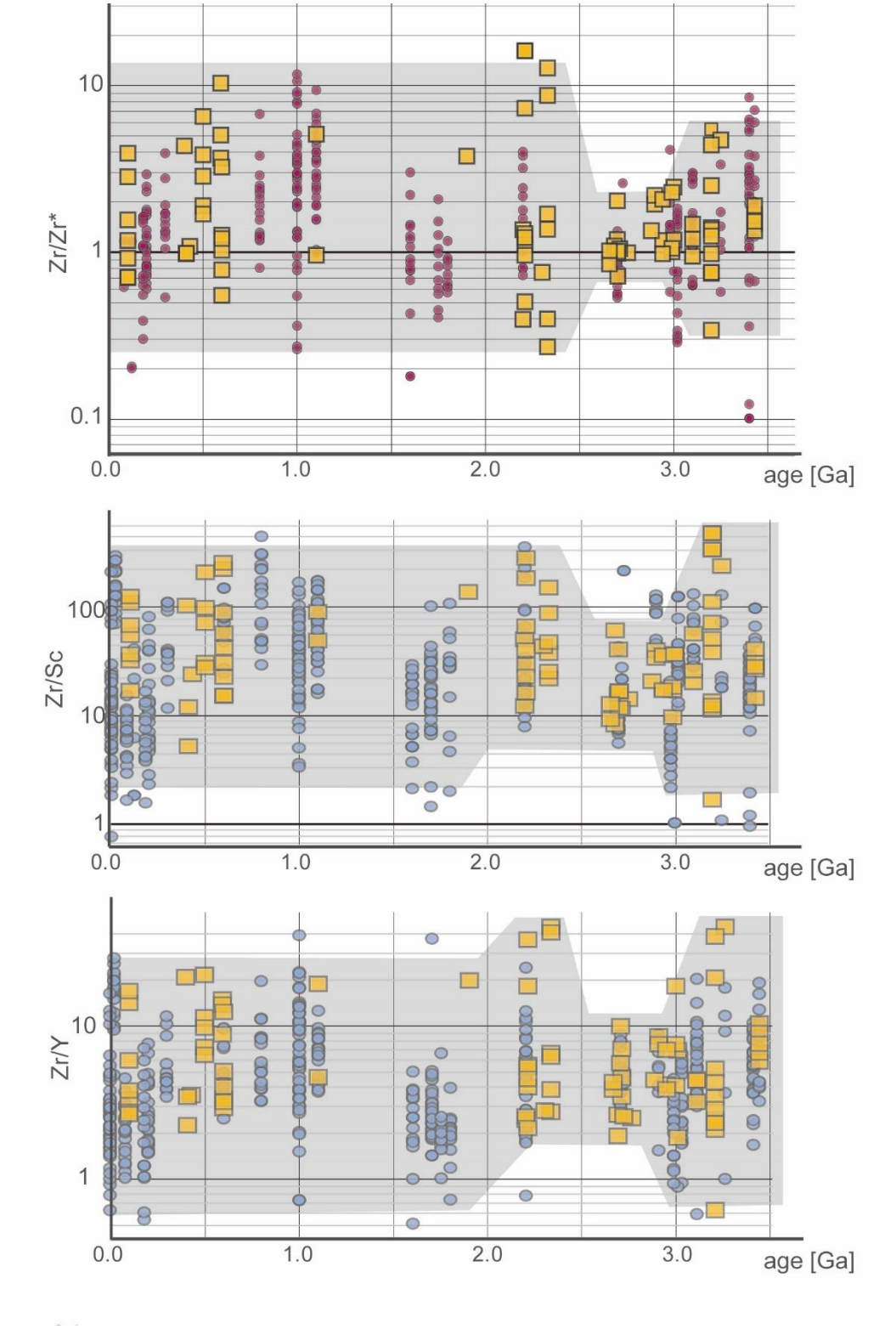

Figure 6-6. Secular change in Zr anomaly, Zr/Sc, and Zr/Y.

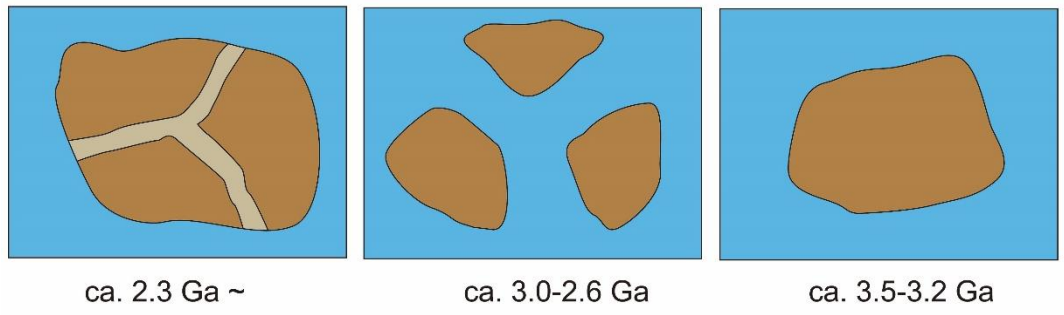

Figure 6-7 Simplified schematic image of change in average size of continental blocks since the ca. 3.5 Ga middle Archean.

Tables

Table 6-1. List of references for compilation of sandstone composition. (in appendix)

Table 6-2. Analytical results of whole-rock sandstone composition with XRF for major elements and ICP-SFMS for minor and trace elements. (in appendix)

Chapter 7. Synthesis

7.1. Secular change in size of continental blocks

Detrital zircon age pattern compiled in Chapter 2, shows that variation in U-Pb age of continental crust is largely different during 2.9-2.3 Ga late Archean-early Proterozoic from 1.0-0 Ga late Proterozoic-Phanerozoic. Continental blocks in 1.0-0 Ga have contain crusts over 3 billion years, in contrast, 2.9-2.3 Ga continental blocks contained crust only less than 1 billion years. The change in variation of crustal age indicates that, during 2.9-2.3 Ga, relatively rapid replacement of crust in continental blocks by production and destruction of continental crust. Taking into preservation bias of older crust in the modern continents, this study considers smaller size of continental block during 2.9-2.3 Ga than 1.0-0 Ga. Therefore, the study in Chapter 2 concluded drastic change in size of continents between 2.3-1.0 Ga.

In Chapter 3, the U-Pb age dating and Lu-Hf isotopic analysis for Archean detrital zircon grains from the Murmac Bay Group illustrates that, during Archean, granitoid crust was rarely reworked more than 800 million years after its formation. This reworking trend is well explained if the Archean craton was developed from the core toward outside by adding new crusts by subduction-related magmatism and/or by secondary accretion of exotic arc crusts. In this framework, younger crusts are more preferentially utilized in crustal melting by subduction-related magmatism. This suggests that accretion of continental blocks dominantly occurred during 3.6-3.3 Ga middle Archean, and finally a continental block was formed at ca. 3.3 Ga relatively large enough to preserve older crust produced between ca. 4.0-3.6 Ga.

In Chapter 4, on the basis of newly determined depositional age of the Shurugwi Greenstone Belt, U-Pb age pattern of detrital zircon from ca. 3.3-2.7 Ga Archean sandstones in the Zimbabwe Craton was compared. By checking differences between depositional age and major peak in age frequency curves, this study found that sandstones deposited ca. 3.3-2.9 Ga show relatively larger age difference over 300 million years and, in contrast, ca. 2.7 Ga sandstones show much smaller difference less than 50 million years. Such a large difference in detrital zircon age pattern between deposition of sandstone and formation of dominant crust in a provenance is observed in only in sandstone formed on passive continental margin setting. Therefore, this result possible suggests that the proto-Zimbabwe Craton during 3.3-2.9 Ga was located in an interior part of a large continental block and young detrital grains were not supplied to the region from active continental margins.

In Chapter 5, detrital zircon U-Pb dating of the ca. 2.2 Ga Deweras Group in the Zimbabwe Craton detected three grains of 2.21-2.23 Ga Paleoproterozoic ones. As no igneous rocks with that age have been found in the extant Zimbabwe and neighboring Kaapvaal cratons, the result indicates that the Zimbabwe Craton connection with other craton during the deposition of the Deweras Group. In other words, the Zimbabwe-Kaapvaal Cratons were a larger continental block than the extant region in the southern Africa.

In chapter 6, this study focused on Zr anomaly in whole-rock composition of sandstones and its secular change since 3.4 Ga to the present. The secular trend suggests that ca. 3.3-3.2 Ga continental blocks were large to fractionate Zr anomaly, possibly several 1,000 km square and those were rifted into smaller blocks during ca. 3.0-2.6 Ga late Archean. The trend of Zr anomaly also indicates that there were continental blocks more than 3,000-5,000 km square, nearly 10,000 km square after ca. 2.3 Ga Paleoproterozoic.

Based on above results of this study, estimated secular change in size of continental block is summarized in Fig. 7-1. When plate subduction and production of continental crust started, the first size of continental block should have been 100-200 km, same as subduction orogenic belt. The first amalgamation to form embryonic continents likely occurred during ca. 3.6-3.3 Ga, as suggested by studies in Chapter 3 and 6. Peak in size was likely at 3.2 Ga as shown in Chapter 6. After that, the embryonic continents were once rifted into smaller continental blocks during ca. 3.0-2.5 Ga late Archean as suggested in Chapter 2, 4, and 6. Note that both rifting and collision were active during the late Archean, and those caused reduction in size of continental blocks. Size of continental blocks was re-increased through collisions of continental block across Archean-Proterozoic boundary, and large continental blocks over 5,000 km scale commonly have existed since then.

7.2. The growth history of continental crust

On the basis of the above discussion combined with previously reported geological evidences, a brief history of continental growth from the Hadean to the present by discriminating five distinct stages; i.e. 1) Stage 1 (4.5-4.2 Ga): formation of primordial crusts, 2) Stage 2 (4.2-3.2 Ga): production of primitive continental crust mostly of oceanic island arc affinity, 3) Stage 3 (3.2-2.3 Ga): emergence of small embryonic continents, 4) Stage 4 (2.3-1.0 Ga): development of

supercontinents, and 5) Stage 5 (1.0-0 Ga): operation of Wilson cycle under modern-style plate tectonics (Fig. 7-3).

Stage 1 (4.5-4.2 Ga): primordial crust after magma ocean

After >4.4 Ga consolidation of the magma ocean, primordial crust was likely covered the Earth's surface in analogy to the Moon's anorthositic crust (Maruyama et al., 2013; Santosh et al., 2017); nonetheless the details are still unknown. Many parts of the primordial continents had been destroyed probably because the putative heavy meteorite bombardment after 4.4 Ga (Abramov et al, 2013; Marchi et al., 2014; Shibaike et al., 2016).

Stage 2 (4.2-3.2 Ga): from initiation of plate subduction to forming of primitive continents

As the surface temperature of the young planet gradually lowered, plate subduction eventually started since ca. 4.2 Ga birth of the ocean. Oxygen isotopic and trace element analyses of Hadean detrital zircon grains from Jack Hills indicates granitic origin of them (Mojzsis et al., 2001; Cavosie et al., 2005; Harrison et al., 2007; 2008). Recent investigations have found many other localities of Hadean zircon (Fig. 1-6) and all of them except for Jack Hills are younger than 4.2 Ga. This probably indicates that production of granitic crust prevailed since ca. 4.2 Ga. More direct evidence for initiation of plate subduction is Eoarchean accretionary complex; i.e. the ca. 3.8 Ga Isua greenstone belt in (Komiya et al., 1999) and the ca. 4.0 Ga Saglek supracrustal rocks (Komiya et al. 2015; Shimojo et al., 2016).

Because Archean mantle potential temperature was >100 K higher than the modern one as petrologically demonstrated (Komiya, 2004; Hertzberg et al. 2010), style of plate subduction in the Archean was different from the modern one; i.e. numerous numbers of small oceanic plates that hosted many subduction zones with intra-oceanic island arcs (Fig. 7-3). Thicker basaltic oceanic crusts and hotter oceanic plates had caused vigorous slab melting and produced granitic continental crust (Komiya, 2004). The Archean island arcs would have been more or less similar sizes (ca. 1,000 km long and 200 km wide or less) to modern island arcs; e.g., Izu-Bonin-Mariana arc (Hoffman, 1989; de Wit and Hart, 1993). However, as the granitic crust was formed as very narrow and possibly thin continental blocks like intra-oceanic island arc, most of them had been subducted soon after their production through arc subduction (Yamamoto et al., 2009; Santosh et al., 2009; Fig. 7-2). Only plural collision of island arcs contributed to increase size of continental blocks, and granitic primitive continents appeared possibly during 3.5-3.3Ga middle

Archean, and peak in size of them was likely at 3.2 Ga. The primitive continents formed during this era might be equivalent to a previously named continental block, Vaalbara (Bleeker, 2003), but this study envisages that not only single continent but several ones were formed by ca. 3.2 Ga.

Stage 3 (3.2-2.3 Ga): breaking-up and re-amalgamation of the primitive continents

After ca. 3.2 Ga, the middle Archean primitive continents had been rifted into smaller continental blocks during the late Archean. Through decomposed to smaller continental blocks, much of the older early-middle Archean continental crust had lost and replaced into younger crust during this period as shown in detrital zircon age pattern in Chapter 2. As most of their peripheries were likely surrounded by subduction zones (Fig. 7-1B), the slow growth rate suggests that subduction itself may have not contributed to net continental growth but induced ubiquitous recycling of the continental crust by continuous subduction erosion. Some of those embryonic continents likely coalesced to form larger masses (Fig. 7-1B), and further accretion of island arcs also added more crusts. Consequently, embryonic continents may have suffered more frequent replacement of older crusts by newer ones than younger continents. This is consistent with previous works of compilation of detrital zircon ages (e.g. Rino et al., 2004; 2008; Condie et al., 2009) showing major age peaks at ca. 2.7-2.6 Ga.

Petrological studies suggest increasing of mantle potential temperature during the late Archean (Komyia, 2004; Herzberg et al., 2010). Traditionally, episodic mantle overturn during Archean-Proterozoic boundary had been expected by numerical simulations (Breuer and Spohn, 1995; Davies, 1995; Moresi and Solomatov, 1998; O'Neill et al., 2007; Ogawa, 2014). The rifting of primitive continents in the late Archean might have been affected by such a mantle episode.

During the early Proterozoic, the fragmented primitive continents re-amalgamated into larger continental blocks with peak in size of them at the at 2.3-2.2 Ga, which are comparable size to modern ones, namely several thousand-kilometer square, as suggested by sandstone geochemistry in Chapter 6. The continents may correspond to previously named Sclavia or Superia (Bleeker, 2003; Bradley, 2011) based on age dating and paleomagnetic analysis of radial dyke swarms. Nonetheless, paleogeography of those continents is still not well constrained as shown in Chapter 5 of this study.

Stage 4 (2.3-1.0 Ga): fragile oceanic plates and large continents

The early Proterozoic continents rifted into smaller continental blocks during ca. 2.3-2.1 Ga, as shown in increased numbers of passive continental margin (Bradley, 2008; Martin et al., 2013). The amalgamated into large continents again during ca. 2.0-1.8 Ga as clearly demonstrated in North American continent (Hoffman, 1988). Name of the continent was originally called Nuna, and later modified to Columbia by several researchers (Rogers and Santosh, 2002; Zhao et al., 2002). Nonetheless large fragments of the continent are preserved in modern extant continents, paleogeography of them is also not well constrained (Bradley, 2011). It is possible to have existed several large continents during this stage.

The Larger continents during the middle Proterozoic had following unique features distinct from younger supercontinents. For example, 1) continental blocks were extremely stable without major break-up for a long period. Activities of dyke swarms recorded the impingement of mantle plume (e.g. Whitmeyer and Karlstrom, 2007; Gladkochub et al., 2010) but no break-up occurred along with these. 2) Continental growth during this period was driven mainly by accretion of plural island arcs composed of granitic crust with depleted mantle-like isotopic signature (e.g. Karlstrom et al., 2001; Geraldes et al., 2001; Whitmeyer and Karlstrom, 2007; Korsch et al., 2011). 4) Ultrahigh- and high-pressure metamorphic rocks are rare (Brown, 2007; Brown and Johnson, 2018). These suggest that major continental rifting and collision had not occurred until the Rodinia supercontinent was formed at ca. 1.3-1.0 Ga.

This study speculates that conditions of oceanic plates were probably similar to those of the Archean ones; many oceanic island arcs were probably generated in a similar way because the assumed higher mantle temperature, ca. 100 ˚C higher than that of modern mantle (Fig 7-1C; Komiya, 2004; Herzberg et al., 2010). On the other hand, older continental crusts were protected from later tectonism around the peripheries and preferentially preserved in the inner part of stable continents. The rapid continental growth suggested by the detrital zircon compilations in Chapter 2 can be explained by accretion of the oceanic island arcs to the stable large continents.

Stage 5 (1.0-0 Ga): modern-style plate tectonics

The last fifth stage is characterized by modern-style plate tectonics and Wilson cycle continuing since ca. 1.0 Ga building of the Rodinia Supercontinent and ca. 0.7 Ga its breaking-up. As decreasing mantle potential temperature (Fig. 7-1A), the size of oceanic plates became larger than previous ones, and number of oceanic island arcs drastically decreased. Most of the

current oceanic island arcs are situated in western Pacific region and Caribbean Sea which occupy only about 5 % of the Earth's surface (Fig. 1-2). Along subduction zones, long-lived Cordillera-type orogeny has been dominant rather than accretion of island arcs. These have caused the decrease in total volume of continental crust.

Reworking of continental crust formed during the stage 4 has been suggested by previous U-Pb and Lu-Hf isotopic analysis of detrital zircon from sand of modern river (Iizuka et al., 2010; 2013). Furthermore, the compilation in Chapter 2 suggests that volume of continents turned to decrease around 1.0 Ga. This estimation is consistent with observations of modern subduction zones and Phanerozoic Pacific-type orogens which are considered as decreasing or equilibrium of the continental mass (Clift et al., 2009; Stern and Scholl, 2010; Isozaki et al., 2010).

7.3. Production, subduction, and preservation of continental crust

Figure 7-4A shows schematic image of secular change in production and subduction of continental crust. Both production and subduction of continental crust was large during stage 2 and 3 of the early Earth. During stage 4 after emergence of large continents, subduction of continental crust would have decreased because effective accretion of island arcs to the large continents occurred. During stage 5 after starting of modern-style plate tectonics, subduction of continental crust is more voluminous than production of continental crust. Figure 7-4B shows growth of total volume of continental blocks which is modified from Figure 2-d in Chapter 2 on the basis of studies in Chapter 3, 4, and 6. The growth of continental blocks can be understood as stacked residual volume between production and subduction of continental crust through time.

Most of the narrow continental crust had subducted into the mantle with basaltic oceanic crust and peridotitic oceanic lithosphere, particularly during stage 2 in the early Archean. A huge amount of granitic material has been incorporated into the mantle ever since the Archean time. Considering the granitic material have subducted with also huge amount of basaltic material, both of them are accumulating in the lowermost mantle as suggested by mantle seismic tomography (Garnero et al., 2016) and computer simulation of mantle convection (Ogawa, 2014). Another possible place for accumulating subducted granitic material is the 270-800 km deep mid-mantle, which was suggested on the basis of the first principle calculation of mineral phase transition of quartz to stishovite in mantle depth (Kawai et al., 2009; 2013). Based on

distribution of observed seismic scatters in the mid-mantle, they also suggested that up to seven times greater volume of extant continents can be stored in the mid-mantle zone as the "second continent" independent of the first continents on the surface. Ever since the Archean, a large amount of ancient continental crusts of granitic composition may have accumulated in mid-mantle depth.

7.4. Progress in understanding of the history of the Earth

Figure 7-5 shows comparison growth of total volumes of continental blocks and production of continental crust by this study with previously proposed 'continental growth curve'. Note that, as explained in the former section, the present study proposed growth of total volume of continental blocks which is different from accumulation of produced continental crust through time.

Most previous studies have not taken into large amount of subduction of continental crust that views resulted into monotonically increasing of continental crust through time (e.g. O'Neil et al., 1979; Dewey and Windley, 1981; Armstrong, 1981; McLennan and Taylor, 1982; McCulloch and Bennet, 1994; Belousova et al., 2010; Dhuime et al., 2012). Fyfe (1978) argued rapid increase of continental crust during Hadean and Archean under hotspot tectonic regime without plate subduction and continental crustal loss.

On the other hand, Komiya (2011) numerically calculated secular change in amount of sediment production (i.e. sediment subduction into the mantle) to estimate the continental growth curve on assumption that higher mantle temperature can produce more granitic crust under plate subduction regime since Hadean. Even though the result of Komiya (2011) shows the most similar curve to the growth of total volume of continental blocks by this study, there are several significantly different points. First, the result of calculation showed almost same amount of sediment subduction have occurred through time. However, it is well known that clastic sediments are very minor in the Archean, especially felsic forearc-trench sedimentary rocks are quite rare (Ronov, 1964). The assumed subduction of continental crust can be modified to be caused island arc subduction proposed by Yamamoto et al. (2009) (Fig. 7-2A) if taking the change in size of continental block by this study as well as the observed distribution of Archean clastic sediment into account. Secondly, the estimated continental growth curve has a peak volume at

ca. 1.8 Ga, which also can be clearly explained from view of size of continental block; namely bimodal size distribution of continental blocks in the middle Proterozoic caused accretion of island arc to large continents (such as Nuna) beside arc subduction.

As discussed in the modern extant subduction zones and Phanerozoic subduction orogen, plate subduction is the only process to produce new granitic continental crust but does not contribute itself for growth in total volume of continental blocks in over 100 Ma-time scale. To increase total volume of continents, there are major two processes; i.e. one is accretion of island arcs to other arc or continental blocks, and the other is preservation of older crust into continental interior far from active subduction orogen. This study concludes that secular change in size of continental blocks can give the best explanation for the growth pattern of continental crust.

The size of continental blocks is possibly related with temperature and thermal structure of the mantle (Figure 7-6). Nonetheless, many things are still not integrated into evolutional model of solid Earth proposed by this study, for example, behavior of terrigenous minerals other than zircon, secular evolution of lower continental crust, mantle, as well as oceanic water volume and atmospheric composition. More investigation of not only granitic continental crust itself but also mantle evolution focusing on size of continental blocks would contribute further understanding entire solid Earth.

Figures

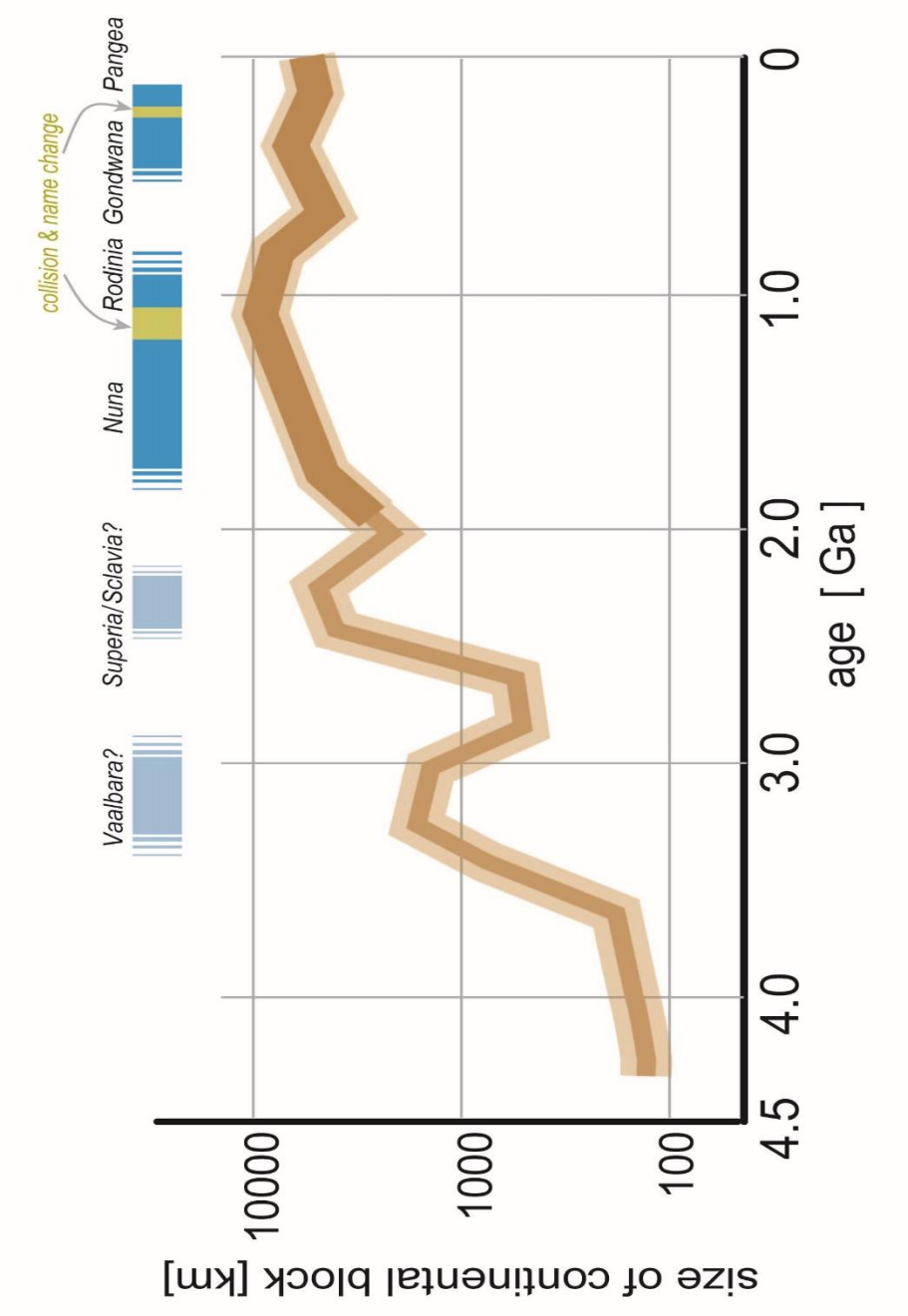

Figure 7-1: Secular change in maximum size-scale of a continental block estimated by this study. Timing of 'Supercontinental period' is modified after Bradley (2011) and Bleeker (2003).

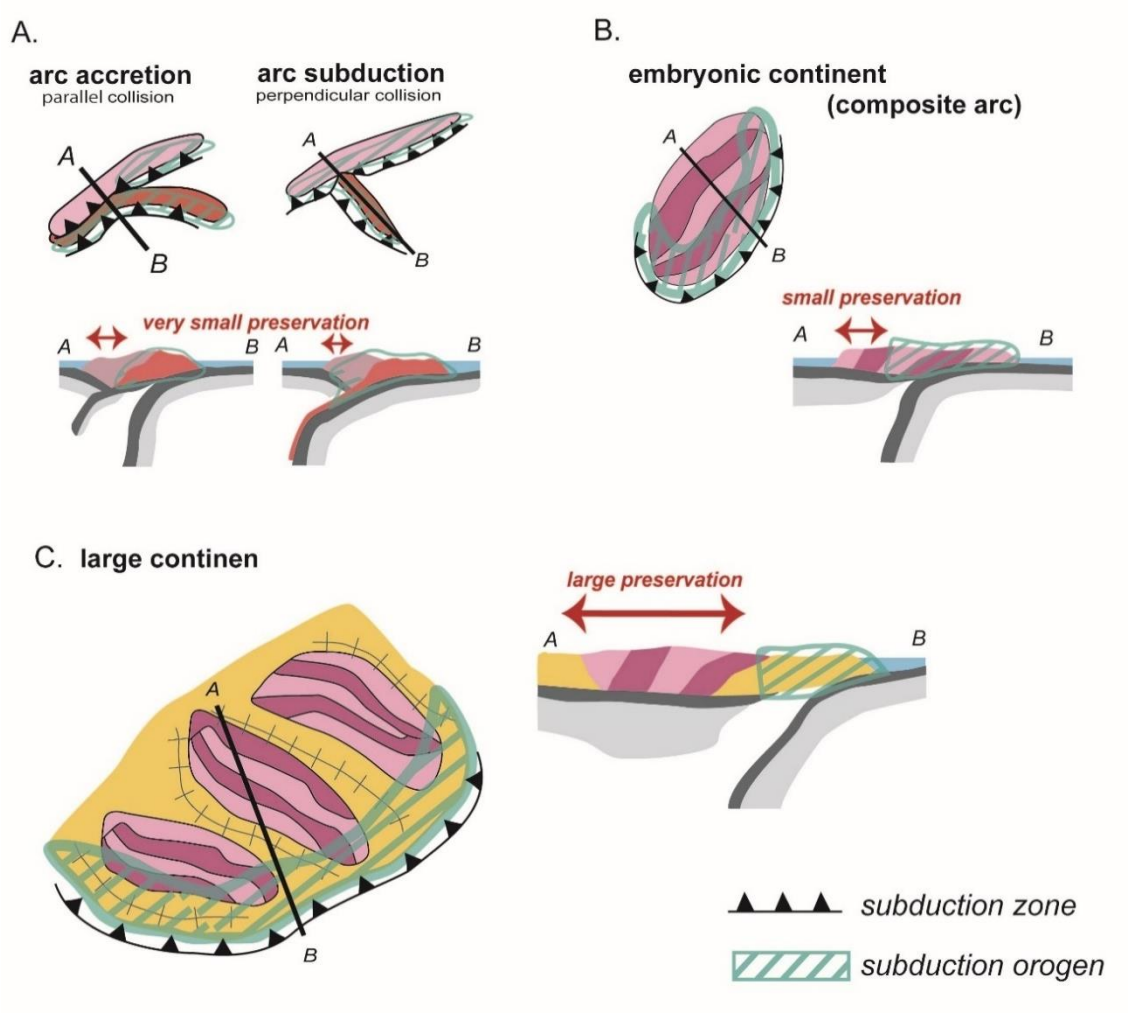

Figure 7-2: Relationship between size of continental block and preservation of older crusts.

A: Before ca. 3.2 Ga, numerous island arcs formed during this time interval and accretion/subduction of island arcs occurred frequently. In the case of parallel collision of two island arcs (left), they easily amalgamated to each other and grew into minor land masses (arc accretion). In contrast, in the case of perpendicular collision of one arc to the other, the crust of the colliding arc likely subducted smoothly into the mantle (arc subduction; middle). Moreover, the subduction erosion also occurred to destruct pre-existing arc crusts. Consequently, the preservation potential of the continental crust was very small.

B: During ca. 3.2−2.3 Ga, some collided composite arcs emerged as embryonic continents, which were larger than individual island arcs but smaller than that of modern continents without having significant amount of older crust. Tectonic recycling occurred along active continental margins

to suppress the net growth of continental crusts.

C: After ca. 2.3 Ga, plural embryonic continents amalgamated to build larger continents comparable to modern ones. Pre-existing crusts in the interiors were protected from the subduction-related tectonism along the active margins, thus the preferential preservation of older crusts started.

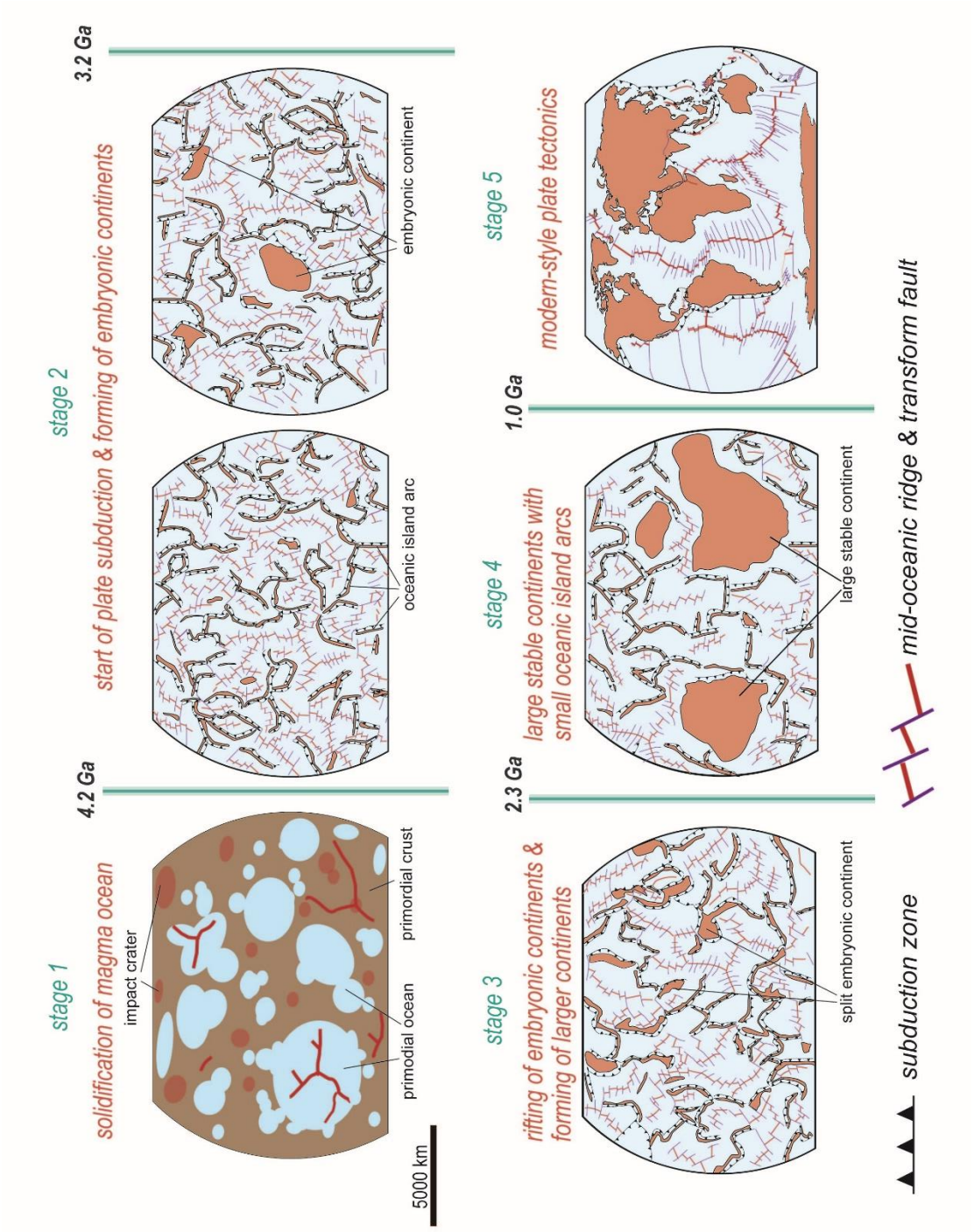

Figure 7-3: World map with continental blocks in five stages; i.e., 4.5–4.2 Ga, 4.2–3.2 Ga, 3.2-2.3 Ga, 2.3–1.0 Ga, and 1.0-0 Ga.

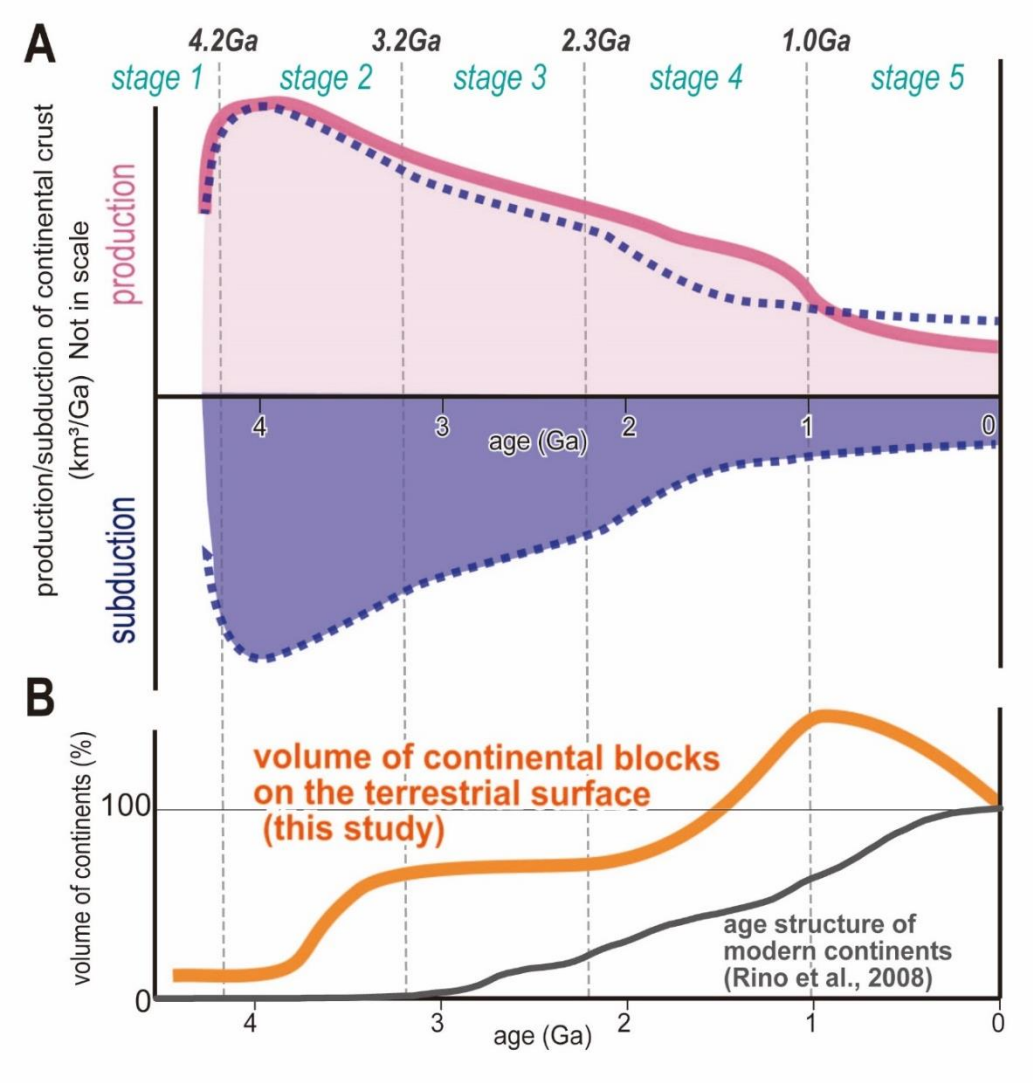

Figure 7-4: showing the secular change in total production of continental crust (red line in A), in total subduction of continental crust (blue line in A), and the resultant growth in volume of continental blocks (orange line in B). The production/subduction of Hadean and early Archean continental crust was huge in magnitude with respect to that of after 1.0 Ga. This suggests the burial of great amount of granitic material into the mantle during stage 2.

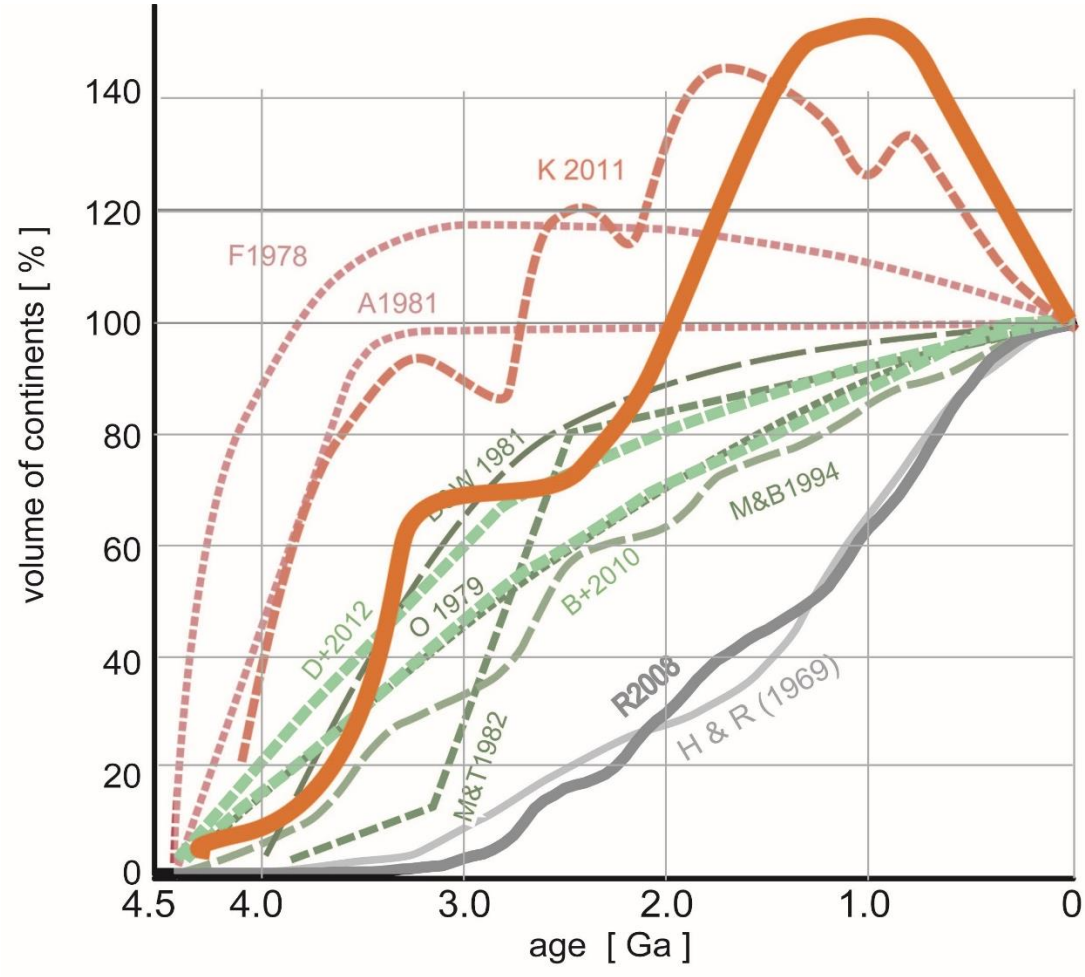

Figure 7-5: Comparison between growth of total volume continental brocks proposed by the present study of chapter 2 and previous studies' growth curve of continental crust (Fyfe, 1978; O'Neil et al., 1979; Dewey and Windley, 1981; Armstrong, 1981; McLennan and Taylor, 1982; McCulloch and Bennet, 1994; Belousova et al., 2010; Komiya, 2011; Dhuime et al., 2012) and also age structure of modern continents (Hurley and Rand, 1969; Rino et al., 2008).

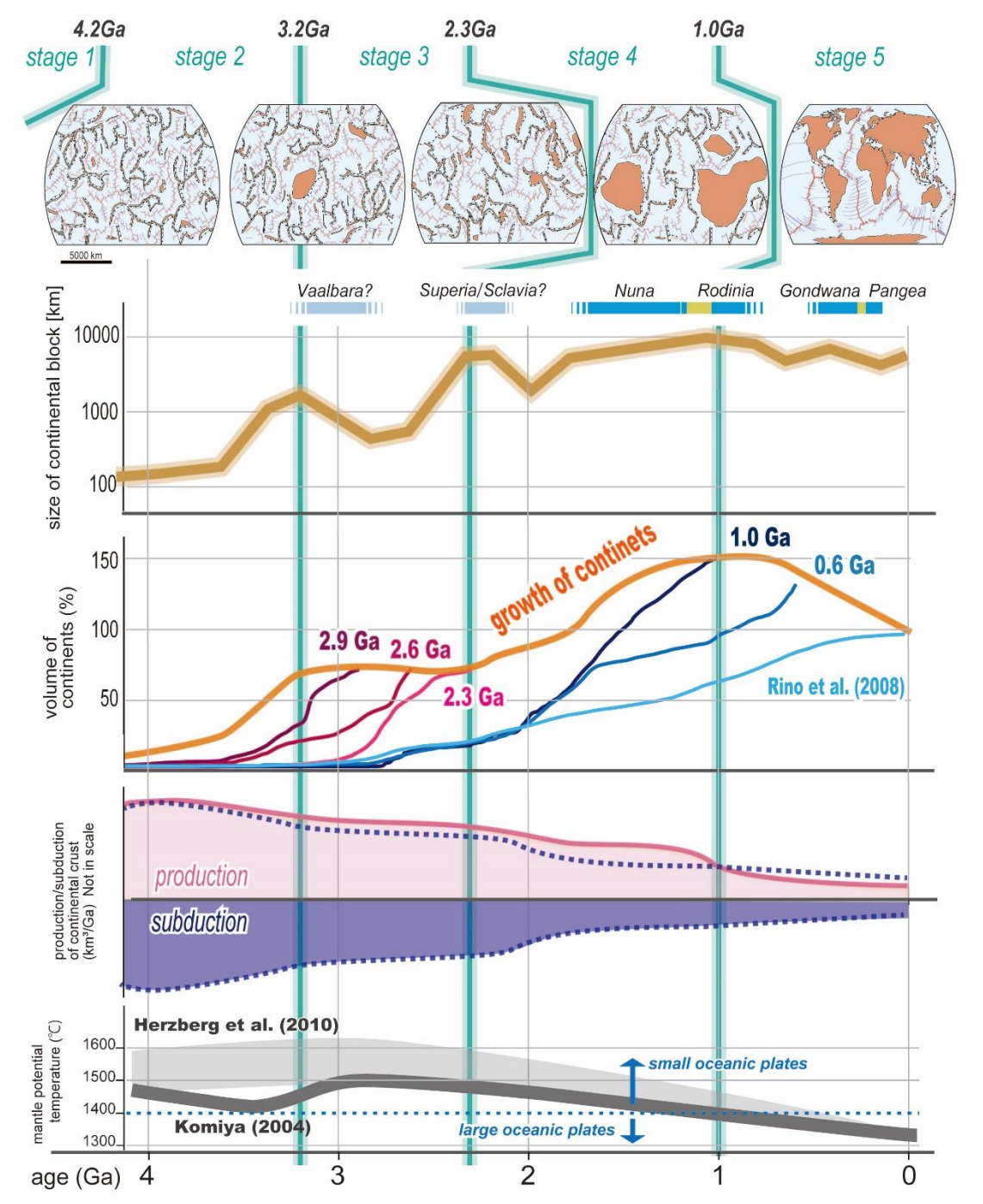

Figure 7-6: Summerly of this study.

References

- Abati, J., Aghzer, A. M., Gerdes, A., and Ennih, N. (2010). Detrital zircon ages of Neoproterozoic sequences of the Moroccan Anti-Atlas belt. Precambrian Research, 1811, 115-128.
- Abramov, O., Kring, D. A., & Mojzsis, S. J. (2013). The impact environment of the Hadean Earth. Chemie der Erde-Geochemistry, 73(3), 227-248.
- Allègre, C. J., and Luck, J. M. (1980). Osmium isotopes as petrogenetic and geological tracers. *Earth and Planetary Science Letters*, *48*(1), 148-154.
- Anderton, R. (1982). Dalradian deposition and the late Precambrian–Cambrian history of the N Atlantic region: a review of the early evolution of the Iapetus Ocean. *Journal of the Geological Society*, *139*(4), 421-431.
- Anderton, R. (1985). Sedimentation and tectonics in the Scottish Dalradian. *Scottish Journal of Geology*, *21*(4), 407-436.
- Aoki, K., Isozaki, Y., Kofukuda, D., Sato, T., Yamamoto, A., Maki, K., Sakata, S., and Hirata, T. 2014. Provenance diversification within an arc-trench system induced by batholith development: the Cretaceous Japan case. Terra Nova,262, 139-149.
- Armstrong, R. (1981). Radiogenic isotopes: the case for crustal recycling on a near-steady-state no-continental-growth Earth. *Philosophical Transactions of the Royal Society of London A: Mathematical, Physical and Engineering Sciences*, *301*(1461), 443-472.
- Asanuma, H., Okada, Y., Fujisaki, W., Suzuki, K., Sato, T., Sawaki, Y., ... and Windley, B. F. (2015). Reconstruction of ocean plate stratigraphy in the Gwna Group, NW Wales: Implications for the subduction–accretion process of a latest Proterozoic trench-forearc. *Tectonophysics*, *662*, 195-207.
- Ashton, K. E., Hartlaub, R. P., Bethune, K. M., Heaman, L. M., Rayner, N., and Niebergall, G. R. (2013), New depositional age constraints for the Murmac Bay Group of the southern Rae Craton , Canada. Precambrian Res., 232, 70-88.
- Ashton, K.E., Boivin, D., and Heggie, G., (2001) Geology of the Southern Black Bay Belt, west

of Uranium City, Rae Province. Sask. Geol. Surv., Misc. Rep. 2001-4.2, 50–63.

- Ashton, K.E., Hartlaub, R.P., Heaman, L.M., Morelli, R.M., Card, C.D., Bethune, K., and Hunter, R.C., (2009) Post-Taltson sedimentary and intrusive history of the south-ern Rae Province along the northern margin of the Athabasca Basin, western Canadian Shield. Precambrian Res. 175, 16-34.

- Ashton, K.E., Kraus, J., Hartlaub, R.P., and Morelli, R., (2000) Uranium City revisited: a new look at the rocks of the Beaverlodge Mining Camp. Sask. Geol. Surv., Misc. Rep. 2000-4.2, 3–15.

- Ashton, K.E., and Card, C.D., (1998) Rae northeast: a reconnaissance of the Rae Province northeast of Lake Athabasca. Sask. Geol. Surv. Misc. Rep. 98-4, 3–16.

- Barber, A. J., and Max, M. D. (1979). A new look at the Mona Complex (Anglesey, North Wales). *Journal of the Geological Society*, *136*(4), 407-432.

- Barley, M. E., Pickard, A. L., and Sylvester, P. J. (1997). Emplacement of a large igneous province as a possible cause of banded iron formation 2.45 billion years ago. *Nature*, *385*(6611), 55.

- Barton Jr, J. M. (1996). The Messina layered intrusion, Limpopo belt, South Africa: an example of in-situ contamination of an Archean anorthosite complex by continental crust. *Precambrian Research*, *78*(1-3), 139-150.

- Barton Jr, J. M., and Van Reenen, D. D. (1992). When was the Limpopo orogeny?. *Precambrian Research*, *55*(1-4), 7-16.

- Barton, J. M. (1983). Rb-Sr and U-Th-Pb isotopic studies of the Sand River Gneiss, Central Zone, Limpopo Mobile Belt. *Spec. Publ Geol. Soc. S. Afr.*, *8*, 9-18.

- Basilevsky, A. T., and Head, J. W. (2000) Rifts and large volcanoes on Venus: Global assessment of their age relations with regional plains. J. Geophys. Res.: Planets, 105, 24583-24611.

- Bau, M., and Möller, P. (1993). Rare earth element systematics of the chemically precipitated component in Early Precambrian iron formations and the evolution of the terrestrial atmosphere-hydrosphere-lithosphere system. *Geochimica et Cosmochimica Acta*, *57*(10), 2239-2249.

- Bekker, A., Holland, H. D., Wang, P. L., Rumble Iii, D., Stein, H. J., Hannah, J. L., Coetzee, L., Beukes, N. J. (2004). Dating the rise of atmospheric oxygen. Nature, 427(6970), 117.
- Bekker, A., Karhu, J.A., Eriksson, K.A., and Kaufman, A.J., (2003). Chemostratigraphy of Paleoproterozoic carbonate successions of the Wyoming Craton: tectonic forcing of biogeochemical change? Precambrian Res. 120, 279–325.
- Belousova, E. A., Kostitsyn, Y. A., Griffin, W. L., Begg, G. C., O'Reilly, S. Y., and Pearson, N. J. 2010. The growth of the continental crust: constraints from zircon Hf-isotope data. Lithos, 1193, 457-466.
- Belousova, E. A., Kostitsyn, Y. A., Griffin, W. L., Begg, G. C., O'Reilly, S. Y., and Pearson, N. J. 2010. The growth of the continental crust: constraints from zircon Hf-isotope data. Lithos, 1193, 457-466.
- Berman, R. G., Pehrsson, S., Davis, W. J., Ryan, J. J., Qui, H., and Ashton, K. E. (2013) The Arrowsmith orogeny: Geochronological and thermobarometric constraints on its extent and tectonic setting in the Rae craton, with implications for pre-Nuna supercontinent reconstruction. Precambrian Res., 232, 44-69.
- Berman, R. G., Sanborn-Barrie, M., Stern, R. A., and Carson, C. J. (2005) Tectonometamorphism at ca. 2.35 and 1.85 Ga in the Rae domain, western Churchill Province, Nunavut, Canada: insights from structural, metamorphic and in situ geochronological analysis of the southwestern Committee Bay Belt. Canadian Mineral., 43, 409-442.
- Berman, R.G., Davis, W.J., Pehrsson, S., (2007) The collisional Snowbird tectonic zone resurrected: growth of Laurentia during the 1.9 Ga accretionary phase of the Trans-Hudson orogeny. Geology, 35, 911–914.
- Bethune, K. M., Berman, R. G., Rayner, N., and Ashton, K. E. (2013) Structural, petrological and U–Pb SHRIMP geochronological study of the western Beaverlodge domain: Implications for crustal architecture, multi-stage orogenesis and the extent of the Taltson orogen in the SW Rae Craton, Canadian Shield. Precambrian Res., 232, 89-118.
- Bickle, M. J., Bettenay, L. F., Boulter, C. A., Groves, D. I., and Morant, P. 1980. Horizontal tectonic interaction of an Archean gneiss belt and greenstones, Pilbara block, Western Australia. Geology, 811, 525-529.

- Bingen, B., Belousova, E. A., and Griffin, W. L. 2011. Neoproterozoic recycling of the Sveconorwegian orogenic belt: detrital-zircon data from the Sparagmite basins in the Scandinavian Caledonides. Precambrian Research, 1893, 347-367.
- Birck, J. L., Barman, M. R., and Capmas, F. (1997). Re-Os isotopic measurements at the femtomole level in natural samples. *Geostandards newsletter*, *21*(1), 19-27.
- Bleeker, W. (2003). The late Archean record: a puzzle in ca. 35 pieces. *Lithos*, *71*(2-4), 99-134.
- Bleeker, W., Ketchum, J. W., Jackson, V. A., and Villeneuve, M. E. (1999). The Central Slave Basement Complex, Part I: its structural topology and autochthonous cover. *Canadian Journal of Earth Sciences*, *36*(7), 1083-1109.
- Blenkinsop, T. G., Fedo, C. M., Bickle, M. J., Eriksson, K. A., Martin, A., Nisbet, E. G., and Wilson, J. F. (1993). Ensialic origin for the Ngezi Group, Belingwe greenstone belt, Zimbabwe. *Geology*, *21*(12), 1135-1138.
- Bluck, B. J., Dempster, T. J., and Rogers, G. (1997). Allochthonous metamorphic blocks on the Hebridean passive margin, Scotland. *Journal of the Geological Society*, *154*(6), 921-924.
- Bolhar, R., Hofmann, A., Kemp, A. I., Whitehouse, M. J., Wind, S., and Kamber, B. S. (2017). Juvenile crust formation in the Zimbabwe Craton deduced from the O-Hf isotopic record of 3.8–3.1 Ga detrital zircons. *Geochimica et Cosmochimica Acta*, *215*, 432-446.
- Bolhar, R., Woodhead, J. D., and Hergt, J. M. (2003). Continental setting inferred for emplacement of the 2.9–2.7 Ga Belingwe Greenstone Belt, Zimbabwe. *Geology*, *31*(4), 295-298.
- Boryta, M., and Condie, K. C. (1990). Geochemistry and origin of the Archaean Beit Bridge complex, Limpopo Belt, South Africa. *Journal of the Geological Society*, *147*(2), 229-239.
- Bostock, H. H., and Breemen, O. V. (1994) Ages of detrital and metamorphic zircons and monazites from a pre-Taltson magmatic zone basin at the western margin of Rae Province. Canadian J. Earth Sci., 31(8) 1353-1364.
- Bowring, S. A., & Williams, I. S. (1999). Priscoan (4.00–4.03 Ga) orthogneisses from northwestern Canada. Contributions to Mineralogy and Petrology, 134(1), 3-16.
- Bradley, D. C. (2011). Secular trends in the geologic record and the supercontinent cycle. Earth-

Science Reviews, 108(1-2), 16-33.

- Bradley, D. C. (2008). Passive margins through earth history. Earth-Science Reviews, 911, 1-26.
- Brasier, M. D., and Lindsay, J. F. (1998). A billion years of environmental stability and the emergence of eukaryotes: new data from northern Australia. Geology, 266, 555-558.
- Breuer, D., & Spohn, T. (1995). Possible flush instability in mantle convection at the Archaean–Proterozoic transition. *Nature*, *378*(6557), 608.
- Brown, M. (2007). Metamorphic conditions in orogenic belts: a record of secular change. International Geology Review, 493, 193-234.
- Brown, M., and Johnson, T. (2018). Secular change in metamorphism and the onset of global plate tectonics. *American Mineralogist*, *103*(2), 181-196.
- Buick, I. S., Williams, I. S., Gibson, R. L., Cartwright, I., and Miller, J. A. (2003). Carbon and U–Pb evidence for a Palaeoproterozoic crustal component in the Central Zone of the Limpopo Belt, South Africa. *Journal of the Geological Society*, *160*(4), 601-612.
- Buick, R., Des Marais, D. J., and Knoll, A. H. (1995). Stable isotopic compositions of carbonates from the Mesoproterozoic Bangemall Group, northwestern Australia. *Chemical Geology*, *123*(1-4), 153-171.
- Byerly, B. L., Lowe, D. R., Drabon, N., Coble, M. A., Burns, D. H., & Byerly, G. R. (2018). Hadean zircon from a 3.3 Ga sandstone, Barberton greenstone belt, South Africa. *Geology*, *46*(11), 967-970.
- Böhm, C. O., Heaman, L. M., Stern, R. A., Corkery, M. T., and Creaser, R. A. 2003. Nature of Assean Lake ancient crust, Manitoba: a combined SHRIMP–ID-TIMS U–Pb geochronology and Sm–Nd isotope study. Precambrian Research, 1261, 55-94.
- Card, C.D., Bethune, K.M., (1999) The Oldman-Bulyea Shear Zone: studies across the Nevins Lake Block-Train Lake Domain boundary in the Rubus-Bulyea lakes and Oldman Lake areas. Sask. Geol. Surv., Misc. Rep. 99, 27–37.
- Card, K. D. (1990). A review of the Superior Province of the Canadian Shield, a product of Archean accretion. *Precambrian Research*, *48*(1-2), 99-156.

- Carley, T. L., Miller, C. F., Wooden, J. L., Padilla, A. J., Schmitt, A. K., Economos, R. C., Bindeman, I. N., and Jordan, B. T. (2014). Iceland is not a magmatic analog for the Hadean: Evidence from the zircon record. Earth and Planetary Science Letters, 405, 85-97.

- Carson, C. J., Berman, R.G., Stern, R.A., Sanborn-Barrie, M., Skulski, T., Sandeman, H.A.I., (2004) Age constraints on the Paleoproterozoic tectono-metamorphic history of the Committee Bay region, western Churchill Province, Canada: evidence from zircon and in situ monazite SHRIMP geochronology. Canadian J. Earth Sci., 41, 1049–1076.

- Cates, N. L., and Mojzsis, S. J. (2007) Pre-3750 Ma supracrustal rocks from the Nuvvuagittuq supracrustal belt, northern Québec. Earth and Planet. Sci. Letter, 255, 9-21.

- Cavosie, A. J., Valley, J. W., & Wilde, S. A. (2005). Magmatic δ18O in 4400–3900 Ma detrital zircons: A record of the alteration and recycling of crust in the Early Archean. *Earth and Planetary Science Letters*, *235*(3-4), 663-681.

- Cawood, P. A., McCausland, P. J., and Dunning, G. R. (2001). Opening Iapetus: constraints from the Laurentian margin in Newfoundland. *Geological Society of America Bulletin*, *113*(4), 443-453.

- Cawood, P. A., Nemchin, A. A., Smith, M., and Loewy, S. (2003). Source of the Dalradian Supergroup constrained by U–Pb dating of detrital zircon and implications for the East Laurentian margin. *Journal of the Geological Society*, *160*(2), 231-246.

- Cawood, P. A., and Hawkesworth, C. J. (2014). Earth's middle age. Geology,426, 503-506.

- Cawood, P. A., and Nemchin, A. A. (2001). Paleogeographic development of the east Laurentian margin: Constraints from U-Pb dating of detrital zircons in the Newfoundland Appalachians. Geological Society of America Bulletin, 1139, 1234-1246.

- Chamberlain, K. R., Frost, C. D., and Frost, B. R. 2003. Early Archean to Mesoproterozoic evolution of the Wyoming Province: Archean origins to modern lithospheric architecture. Canadian Journal of Earth Sciences, 4010, 1357-1374.

- Christensen, U. R., and Yuen, D. A. 1985. Layered convection induced by phase transitions. Journal of Geophysical Research: Solid Earth 1978–2012,90B12, 10291-10300.

- Chu, N. C., Taylor, R. N., Chavagnac, V., Nesbitt, R. W., Boella, R. M., Milton, J. A., German,

C. R., Bayon, G., and Burton, K. (2002) Hf isotope ratio analysis using multi-collector inductively coupled plasma mass spectrometry: an evaluation of isobaric interference corrections. J. Analytical Atomic Spectrometry, 17, 1567-1574.

- Clift, P. D., Vannucchi, P., and Morgan, J. P. (2009). Crustal redistribution, crust–mantle recycling and Phanerozoic evolution of the continental crust.Earth-Science Reviews, 971, 80-104.

- Cohen, A. S., and Waters, F. G. (1996). Separation of osmium from geological materials by solvent extraction for analysis by thermal ionisation mass spectrometry. *Analytica Chimica Acta*, *332*(2-3), 269-275.

- Collins, A., and Buchan, C. (2004). Provenance and age constraints of the South Stack Group, Anglesey, UK: U–Pb SIMS detrital zircon data. *Journal of the Geological Society*, *161*(5), 743-746.

- Collins, W. J., Belousova, E. A., Kemp, A. I., and Murphy, J. B. (2011). Two contrasting Phanerozoic orogenic systems revealed by hafnium isotope data. Nature Geoscience, 4(5), 333.

- Compston, W. T., and Pidgeon, R. T. (1986). Jack Hills, evidence of more very old detrital zircons in Western Australia. Nature, 321(6072), 766.

- Condie, K. C. (1993). Chemical composition and evolution of the upper continental crust: contrasting results from surface samples and shales. *Chemical geology*, *104*(1-4), 1-37.

- Condie, K. C. (1998). Episodic continental growth and supercontinents: a mantle avalanche connection?. *Earth and Planetary Science Letters*, *163*(1-4), 97-108.

- Condie, K. C. (1969). Petrology and geochemistry of the Laramie batholith and related metamorphic rocks of Precambrian age, eastern Wyoming. Geological Society of America Bulletin, 801, 57-82.

- Condie, K. C., Belousova, E., Griffin, W. L., and Sircombe, K. N. (2009). Granitoid events in space and time: constraints from igneous and detrital zircon age spectra. Gondwana Research, 153, 228-242.

- Cornell, D. H., Schütte, S. S., and Eglington, B. L. (1996). The Ongeluk basaltic andesite formation in Griqualand West, South Africa: submarine alteration in a 2222 Ma Proterozoic

sea. Precambrian Research, 791, 101-123.

- Cotterill, P. (1979). The Selukwe schist belt and its chromitite deposits. In *A symposium on mineral deposits and the transportation and deposition of metals: Geological Society of South Africa Special Publication* (No. 5, pp. 229-246).

- Cousens, B. L. (2000). Geochemistry of the archean Kam group, Yellowknife greenstone belt, slave province, Canada. *The Journal of geology*, *108*(2), 181-197.

- Craddock, J. P., Rainbird, R. H., Davis, W. J., Davidson, C., Vervoort, J. D., Konstantinou, A., Boerboom, T., Vorhies, S., Kerber, L., and Lundquist, B. (2013) Detrital Zircon Geochronology and Provenance of the Paleoproterozoic Huron ~2.4-2.2 Ga, and Animikie 2.2-1.8 Ga, Basins, Southern Superior Province. The J. Geology, 121, 623-644.

- Crowley, J. L., Myers, J. S., Sylvester, P. J., and Cox, R. A. (2005). Detrital zircon from the Jack Hills and Mount Narryer, Western Australia: evidence for diverse> 4.0 Ga source rocks. The Journal of Geology, 1133, 239-263.

- Cui, P.L., Sun, J.G., Sha, D.M., Wang, X.J., Zhang, P., Gu, A.L., and Wang, Z.Y. (2013). Oldest zircon xenocryst (4.17 Ga) from the north China craton.*International Geology Review*, **55**, 1902-1908.

- Dalziel, I. W. (1991). Pacific margins of Laurentia and East Antarctica-Australia as a conjugate rift pair: Evidence and implications for an Eocambrian supercontinent. Geology, 196, 598-601.

- Dalziel, I. W., Mosher, S., and Gahagan, L. M. (2000). Laurentia-Kalahari collision and the assembly of Rodinia. The Journal of Geology, 1085, 499-513.

- Darby, B. J., and Gehrels, G. 2006. Detrital zircon reference for the North China block. Journal of Asian Earth Sciences, 266, 637-648.

- Davaille, A. and Jaupart, C. (1993): Transient high-Rayleigh-number thermal convection with large viscosity variations. Journal of Fluid Mechanics, 253, 141-166.

- Davies, G.F. (1992): On the emergence of plate tectonics. Geology, 20, 963-966.

- Davies, G.F., 1995. Punctuated tectonic evolution of the earth. Earth Planet. Sci. Lett. 136, 363–379.

- Davis, D. W., Sutcliffe, R. H., and Trowell, N. F. (1988). Geochronological constraints on the tectonic evolution of a late Archaean greenstone belt, Wabigoon Subprovince, Northwest Ontario, Canada. *Precambrian Research*, *39*(3), 171-191.

- Day, J. M., Waters, C. L., Schaefer, B. F., Walker, R. J., and Turner, S. (2016). Use of hydrofluoric acid desilicification in the determination of highly siderophile element abundances and Re-Pt-Os isotope systematics in mafic-ultramafic rocks. *Geostandards and Geoanalytical Research*, *40*(1), 49-65.

- Dempster, T. J., Rogers, G., Tanner, P. W. G., Bluck, B. J., Muir, R. J., Redwood, S. D., ... and Paterson, B. A. (2002). Timing of deposition, orogenesis and glaciation within the Dalradian rocks of Scotland: constraints from U–Pb zircon ages. *Journal of the Geological Society*, *159*(1), 83-94.

- Dewey, J. F., & Bird, J. M. (1970). Mountain belts and the new global tectonics. *Journal of Geophysical Research*, *75*(14), 2625-2647.

- Dewey, J. F., & Windley, B. F. (1981). Growth and differentiation of the continental crust. Phil. Trans. R. Soc. Lond. A, 301(1461), 189-206.

- Dhuime, B., Bosch, D., Bruguier, O., Caby, R., and Pourtales, S. (2007). Age, provenance and post-deposition metamorphic overprint of detrital zircons from the Nathorst Land group NE Greenland—A LA-ICP-MS and SIMS study. Precambrian Research, 1551, 24-46.

- Dhuime, B., Hawkesworth, C. J., Cawood, P. A., and Storey, C. D. (2012). A change in the geodynamics of continental growth 3 billion years ago. Science, 335(6074), 1334-1336.

- Dickinson, W. R., Beard, L. S., Brakenridge, G. R., Erjavec, J. L., Ferguson, R. C., Inman, K. F., Knepp, R. A., Lindberg, F. A. and Ryberg, P. T. 1983. Provenance of North American Phanerozoic sandstones in relation to tectonic setting. Geological Society of America Bulletin, 942, 222-235.

- Dickinson, W. R., Beard, L. S., Brakenridge, G. R., Erjavec, J. L., Ferguson, R. C., Inman, K. F., ... and Ryberg, P. T. (1983). Provenance of North American Phanerozoic sandstones in relation to tectonic setting. *Geological Society of America Bulletin*, *94*(2), 222-235.

- Dickinson, W. R., and Suczek, C. A. (1979). Plate tectonics and sandstone compositions. *Aapg Bulletin*, *63*(12), 2164-2182.

- Dirks, P. H., and Jelsma, H. A. (1998). Horizontal accretion and stabilization of the Archean Zimbabwe Craton. *Geology*, *26*(1), 11-14.
- Diwu, C., Sun, Y., Wilde, S. A., Wang, H., Dong, Z., Zhang, H. and Wang, Q. (2013): New evidence for ~ 4.45 Ga terrestrial crust from zircon xenocrysts in Ordovician ignimbrite in the North Qinling Orogenic Belt, China. Gondwana Research, 23, 1484-1490.
- Dodson, M. H., Compston, W., Williams, I. S., and Wilson, J. F. (1988). A search for ancient detrital zircons in Zimbabwean sediments. *Journal of the Geological Society*, *145*(6), 977-983.
- Dodson, M. H., Williams, I. S., Kramers, J. D. (2001). The Mushandike granite: further evidence for 3.4 Ga magmatism in the Zimbabwe craton. Geological Magazine, 138(1), 31-38.
- Drost, K., Gerdes, A., Jeffries, T., Linnemann, U., and Storey, C. 2011. Provenance of Neoproterozoic and early Paleozoic siliciclastic rocks of the Teplá-Barrandian unit Bohemian Massif: evidence from U–Pb detrital zircon ages. Gondwana Research, 191, 213-231.
- Edou-Minko, A., Moussavou, M., Sato, T., Sawaki, Y., Ondo, S. N., Maire, R., Guillaume Fleury, Michel Mbina Mounguengui1, Anders Kaestner, Richard Ortega, Stéphane Roudeau, Asuncion Carmona, Makaya Mvoubou1, Benjamin Musavu Moussavou, Sasaki, O., and Roudeau, S. (2017). Growth, duplication and lateral mutual compressive deformation of Akouemma hemisphaeria on the Seafloor of Okondja Basin at 2.2 Ga (Gabon). International Journal of Geosciences, 8(09), 1172.
- Eggins, S. M., Kinsley, L. P. J., and Shelley, J. M. G. 1998. "Deposition and element fractionation processes during atmospheric pressure laser sampling for analysis by ICP-MS." Applied Surface Science, 127, 278-286.
- El Albani, A., Bengtson, S., Canfield, D. E., Bekker, A., Macchiarelli, R., Mazurier, A., Emma U. Hammarlund, Philippe Boulvais, Jean-Jacques Dupuy, Claude Fontaine, Franz T. Fürsich, François Gauthier-Lafaye, Philippe Janvier, Emmanuelle Javaux, Frantz Ossa Ossa, Anne-Catherine Pierson-Wickmann, Armelle Riboulleau, Paul Sardini, Daniel Vachard, Martin Whitehouse Fürsich, F. T. (2010). Large colonial organisms with coordinated growth in oxygenated environments 2.1 Gyr ago. Nature, 466(7302), 100.
- Elkins-Tanton, L. T. (2008). Linked magma ocean solidification and atmospheric growth for Earth and Mars. Earth and Planetary Science Letters, 2711, 181-191.

- Eriksson, P. G., Banerjee, S., Nelson, D. R., Rigby, M. J., Catuneanu, O., Sarkar, S., ... and Raju, P. S. (2009). A Kaapvaal craton debate: Nucleus of an early small supercontinent or affected by an enhanced accretion event?. *Gondwana Research*, *15*(3-4), 354-372.

- Fedo, C. M., Eriksson, K. A., and Krogstad, E. J. (1996). Geochemistry of shales from the Archean (~ 3.0 Ga) Buhwa Greenstone Belt, Zimbabwe: implications for provenance and source-area weathering. *Geochimica et Cosmochimica Acta*, *60*(10), 1751-1763.

- Ferguson, M. E., Waldron, J. W., and Bleeker, W. (2005). The Archean deep-marine environment: turbidite architecture of the Burwash Formation, Slave Province, Northwest Territories. *Canadian Journal of Earth Sciences*, *42*(6), 935-954.

- Fischer, R., and Gerya, T. (2016). Early Earth plume-lid tectonics: A high-resolution 3D numerical modelling approach. Journal of Geodynamics.

- Fisher, C. M., Vervoort, J. D., and Hanchar, J. M. (2014) Guidelines for reporting zircon Hf isotopic data by LA-MC-ICPMS and potential pitfalls in the interpretation of these data. Chem. Geol., 363, 125-133.

- Froude, D. O., Ireland, T. R., Kinny, P. D., Williams, I. S., Compston, W., Williams, I. T., and Myers, J. S. (1983). Ion microprobe identification of 4,100–4,200 Myr-old terrestrial zircons. Nature, 304(5927), 616.

- Fyfe, W. S. (1978). The evolution of the Earth's crust: modern plate tectonics to ancient hot spot tectonics?. *Chemical Geology*, *23*(1-4), 89-114.

- Galimov, I.M., Kuznetsova, N.G., Prokhorov, V.S., (1968). The problem of the composition of the Earth's ancient atmosphere in connection with results of isotopic analyses of carbon from Precambrian carbonates. Geochemistry 11, 1376–1381 (in Russian).

- Garnero, E. J., McNamara, A. K., & Shim, S. H. (2016). Continent-sized anomalous zones with low seismic velocity at the base of Earth's mantle. *Nature Geoscience*, *9*(7), 481.

- Gaschnig, R. M., Rudnick, R. L., McDonough, W. F., Kaufman, A. J., Valley, J. W., Hu, Z., Gao, S., and Beck, M. L. 2016. Compositional evolution of the upper continental crust through time, as constrained by ancient glacial diamictites.Geochimica et Cosmochimica Acta, 186, 316-343.

- Gehrels, G. E., Blakey, R., Karlstrom, K. E., Timmons, J. M., Dickinson, B., and Pecha, M.

(2011). Detrital zircon U-Pb geochronology of Paleozoic strata in the Grand Canyon, Arizona. Lithosphere, 33, 183-200.

- Gehrels, G. E., Dickinson, W. R., Ross, G. M., Stewart, J. H., and Howell, D. G. (1995). Detrital zircon reference for Cambrian to Triassic miogeoclinal strata of western North America. Geology, 239, 831-834.

- Geraldes, M. C., Van Schmus, W. R., Condie, K. C., Bell, S., Teixeira, W., and Babinski, M. (2001). Proterozoic geologic evolution of the SW part of the Amazonian Craton in Mato Grosso state, Brazil. Precambrian Research, 1111, 91-128.

- Gladkochub, D. P., Donskaya, T. V., Wingate, M. T. D., Mazukabzov, A. M., Pisarevsky, S. A., Sklyarov, E. V., and Stanevich, A. M. (2010). A one-billion-year gap in the Precambrian history of the southern Siberian Craton and the problem of the Transproterozoic supercontinent. American Journal of Science, 3109, 812-825.

- Greber, N. D., Dauphas, N., Bekker, A., Ptáček, M. P., Bindeman, I. N., and Hofmann, A. (2017). Titanium isotopic evidence for felsic crust and plate tectonics 3.5 billion years ago. *Science*, *357*(6357), 1271-1274.

- Griffin, W. L., Belousova, E. A., O'Neill, C., O'Reilly, S. Y., Malkovets, V., Pearson, N. J., Spetsius, S. and Wilde, S. A. (2014) The world turns over: Hadean–Archean crust–mantle evolution. Lithos, 189, p. 2-15.

- Griffin, W. L., Belousova, E. A., Walters, S. G., and O'Reilly, S. Y. (2006). Archaean and Proterozoic crustal evolution in the Eastern Succession of the Mt Isa district, Australia: U–Pb and Hf-isotope studies of detrital zircons*.Australian Journal of Earth Sciences, 531, 125-149.

- Grosch, E. G., Kosler, J., McLoughlin, N., Drost, K., Slama, J., and Pedersen, R. B. (2011). Paleoarchean detrital zircon ages from the earliest tectonic basin in the Barberton Greenstone Belt, Kaapvaal craton, South Africa. *Precambrian Research*, *191*(1-2), 85-99.

- Günther, D., and Heinrich, C. A. (1999). Comparison of the ablation behaviour of 266 nm Nd: YAG and 193 nm ArF excimer lasers for LA-ICP-MS analysis. Journal of Analytical Atomic Spectrometry, 149, 1369-1374.

- Halliday, A. N., Graham, C. M., Aftalion, M., and Dymoke, P. (1989). Short paper: the depositional age of the Dalradian Supergroup: U-Pb and Sm-Nd isotopic studies of the Tayvallich

Volcanics, Scotland. *Journal of the Geological Society*, *146*(1), 3-6.

- Han, T. M., Runnegar, B. (1992). Megascopic eukaryotic algae from the 2.1-billion-year-old Negaunee Iron-Formation, Michigan. Science, 257(5067), 232-235.
- Harland, W.B., and Gayer, R.A., 1972, The Arctic Caledonides and earlier oceans: Geological Magazine, 109, 289–314.
- Harrison, T. M., Blichert-Toft, J., Müller, W., Albarede, F., Holden, P., and Mojzsis, S. J. (2005). Heterogeneous Hadean hafnium: evidence of continental crust at 4.4 to 4.5 Ga. Science, 3105756, 1947-1950.
- Harrison, T. M., Schmitt, A. K., McCulloch, M. T., and Lovera, O. M. (2008). Early ≥ 4.5 Ga formation of terrestrial crust: Lu–Hf, δ 18 O, and Ti thermometry results for Hadean zircons. Earth and Planetary Science Letters, 2683, 476-486.
- Hartlaub, R. P., Heaman, L. M., Ashton, K. E., and Chacko, T. (2004), The Archean Murmac Bay Group: evidence for a giant Archean rift in the Rae Province, Canada. Precambrian Res., 131, 345-372.
- Hartlaub, R. P., Heaman, L. M., Chacko, T., and Ashton, K. E. (2007), Circa 2.3 Ga Magmatism of the Arrowsmith Orogeny, Uranium City Region, Western Churchill craton, Canada. The J. Geol., 1152, 181-195.
- Hartlaub, R. P., Heaman, L. M., Simonetti, A., and Böhm, C. O. (2006), Relicts of Earth's earliest crust: U-Pb and morphological characteristics of > 3.7 Ga detrital zircon of the western Canadian Shield. Geol. Soc. America Special Papers, 405, 75-89.
- Hartmann, L. A., Santos, J. O. S., Bossi, J., Campal, N., Schipilov, A., McNaughton, N. J. (2002). Zircon and titanite U–Pb SHRIMP geochronology of Neoproterozoic felsic magmatism on the eastern border of the Rio de la Plata Craton, Uruguay. Journal of South American Earth Sciences, 15, 229-236.
- Hawkesworth, C. J., Bickle, M. J., Gledhill, A. R., Wilson, J. F., and Orpen, J. L. (1979). A 2.9-by event in the Rhodesian Archaean. *Earth and Planetary Science Letters*, *43*(2), 285-297.
- Hawkesworth, C. J., Moorbath, S., O'nions, R. K., and Wilson, J. F. (1975). Age relationships between greenstone belts and “granites” in the Rhodesian Archaean craton. *Earth and Planetary*

Science Letters, *25*(3), 251-262.

- Hawkesworth, C., Cawood, P., Kemp, T., Storey, C., and Dhuime, B. (2009). A matter of preservation. Science, 323(5910), 49-50.
- Hawkesworth, C., Cawood, P., Kemp, T., Storey, C., and Dhuime, B. 2009. Geochemistry: A matter of preservation. Science, 323, 49-50.
- Henderson, J. B. (1972). Sedimentology of Archean turbidites at Yellowknife, Northwest Territories. *Canadian Journal of Earth Sciences*, *9*(7), 882-902.
- Herzberg, C., Condie, K., and Korenaga, J. (2010). Thermal the Earth history and its petrological expression. Earth and Planetary Science Letters, 2921, 79-88.
- Hickman, H. (2001). Geology of the Dampier 1:100 000 sheet: Geological Survey of Western Australia, 1:100 000 Geological Series Explanatory Notes,
- Hirata, T., & Nesbitt, R. W. (1995). U-Pb isotope geochronology of zircon: Evaluation of the laser probe-inductively coupled plasma mass spectrometry technique. *Geochimica et cosmochimica Acta*, *59*(12), 2491-2500.
- Hoffman, P. F. (1988). United plates of America, the birth of a craton: Early Proterozoic assembly and growth of Laurentia. Annual Review of Earth and Planetary Sciences, 16(1), 543-603.
- Hoffman, P. F. 1988. United Plates of America, the birth of a craton-Early Proterozoic assembly and growth of Laurentia. Annual Review of Earth and Planetary Sciences, 16, 543-603.
- Hoffman, P. F. (1989). Precambrian geology and tectonic history of North America. The geology of North America—an overview, 447-512.
- Hofmann, A., Dirks, P. H., and Jelsma, H. A. (2001). Late Archaean foreland basin deposits, Belingwe greenstone belt, Zimbabwe. *Sedimentary Geology*, *141*, 131-168.
- Hofmann, A., Dirks, P. H., and Jelsma, H. A. (2004). Clastic sedimentation in a late Archaean accretionary terrain, Midlands greenstone belt, Zimbabwe. *Precambrian Research*, *129*(1-2), 47-69.
- Hokada, T., Horie, K., Satish-Kumar, M., Ueno, Y., Nasheeth, A., Mishima, K., and Shiraishi, K. (2013). An appraisal of Archaean supracrustal sequences in Chitradurga schist belt, western

Dharwar craton, southern India. Precambrian Research, 227, 99-119.

- Holden, P., Lanc, P., Ireland, T. R., Harrison, T. M., Foster, J. J., and Bruce, Z. (2009). Mass-spectrometric mining of Hadean zircons by automated SHRIMP multi-collector and single-collector U/Pb zircon age dating: The first 100,000 grains. International Journal of Mass Spectrometry, 286(2-3), 53-63.

- Horstwood, M. S., Nesbitt, R. W., Noble, S. R., Wilson, J. F. (1999). U-Pb zircon evidence for an extensive early Archean craton in Zimbabwe: A reassessment of the timing of craton formation, stabilization, and growth. Geology, 27(8), 707-710.

- Hoskin, P. W., and Ireland, T. R. (2000) Rare earth element chemistry of zircon and its use as a provenance indicator. Geology, 28(7), 627-630.

- Houston, R. S., and Karlstrom, K. E. 1992. Geologic Map of Precambrian Metasedimentary Rocks of the Medicine Bow Mountains, Albany and Carbon Counties, Wyoming. US Geological Survey.

- Hunter, M. A., Bickle, M. J., Nisbet, E. G., Martin, A., and Chapman, H. J. (1998). Continental extensional setting for the Archean Belingwe greenstone belt, Zimbabwe. *Geology*, *26*(10), 883-886.

- Hurley, P. M., and Rand, J. R. (1969). Pre-drift continental nuclei. *Science*, *164*(3885), 1229-1242.

- Höhndorf, A., Vetter, U. (1999). The Sanyati Ore Deposits in Zimbabwe: Pb-isotopic investigation of sulfide and oxide ores. Zeitschrift für angewande Geologie, 45, 11-13.

- Ichikawa, H., Kameyama, M., and Kawai, K. (2013). Mantle convection with continental drift and heat source around the mantle transition zone. Gondwana Research, 243, 1080-1090..

- Iizuka, T., Campbell, I. H., Allen, C. M., Gill, J. B., Maruyama, S., & Makoka, F. (2013). Evolution of the African continental crust as recorded by U–Pb, Lu–Hf and O isotopes in detrital zircons from modern rivers. Geochimica et Cosmochimica Acta, 107, 96-120.

- Iizuka, T., Hirata, T., Komiya, T., Rino, S., Katayama, I., Motoki, A., & Maruyama, S. (2005). U-Pb and Lu-Hf isotope systematics of zircons from the Mississippi River sand: Implications for reworking and growth of continental crust. *Geology*, *33*(6), 485-488.

- Iizuka, T., Horie, K., Komiya, T., Maruyama, S., Hirata, T., Hidaka, H., & Windley, B. F. (2006). 4.2 Ga zircon xenocryst in an Acasta gneiss from northwestern Canada: Evidence for early continental crust. Geology, 34(4), 245-248.

- Iizuka, T., Komiya, T., Rino, S., Maruyama, S., & Hirata, T. (2010). Detrital zircon evidence for Hf isotopic evolution of granitoid crust and continental growth. Geochimica et Cosmochimica Acta, 74(8), 2450-2472.

- Iizuka, T., Komiya, T., Ueno, Y., Katayama, I., Uehara, Y., Maruyama, S. and Dunkley, D. J. (2007) Geology and zircon geochronology of the Acasta Gneiss Complex, northwestern Canada: new constraints on its tectonothermal history. Precambrian Res., 153, 179-208.

- Iizuka, T., Yamaguchi, T., Hibiya, Y., and Amelin, Y. (2015) Meteorite zircon constraints on the bulk Lu− Hf isotope composition and early differentiation of the Earth. Proc. Nat. Academy. Sci., 112, 5331-5336.

- Iizuka, T., and Hirata, T. (2005) Improvements of precision and accuracy in in situ Hf isotope microanalysis of zircon using the laser ablation-MC-ICP-MS technique. Chem. Geol., 220, 121-137.

- Imai, N., Terashima, S., Itoh, S., and Ando, A. (1996). 1996 compilation of analytical data on nine GSJ geochemical reference samples,"Sedimentary rock series". *Geostandards Newsletter*, *20*(2), 165-216.

- Isachsen, C. E., and Bowring, S. A. (1997). The Bell Lake group and Anton Complex: a basement–cover sequence beneath the Archean Yellowknife greenstone belt revealed and implicated in greenstone belt formation. *Canadian Journal of Earth Sciences*, *34*(2), 169-189.

- Ishikawa, A., Senda, R., Suzuki, K., Dale, C. W., and Meisel, T. (2014). Re-evaluating digestion methods for highly siderophile element and 187Os isotope analysis: Evidence from geological reference materials. *Chemical Geology*, *384*, 27-46.

- Ishikawa, A., Suzuki, K., Collerson, K. D., Liu, J., Pearson, D. G., and Komiya, T. (2017). Rhenium-osmium isotopes and highly siderophile elements in ultramafic rocks from the Eoarchean Saglek Block, northern Labrador, Canada: implications for Archean mantle evolution. *Geochimica et Cosmochimica Acta*, *216*, 286-311.

- Isozaki, Y. (2014). Memories of pre-Jurassic lost oceans: how to retrieve them from extant lands.

Geoscience Canada 41, 283-311.

- Isozaki, Y., Aoki, K., Nakama, T., and Yanai, S. (2010). New insight into a subduction-related orogen: a reappraisal of the geotectonic framework and evolution of the Japanese Islands. Gondwana Research, 181, 82-105.

- Isozaki, Y., Maruyama, S., and Furuoka, F. (1990). Accreted oceanic materials in Japan. Tectonophysics, 1811, 179-205.

- Isozaki, Y., Yamamoto, S., Sakata, S., Obayashi, H., Hirata, T., Obori, K. I., ... and Maruyama, S. (2018). High-reliability zircon separation for hunting the oldest material on Earth: An automatic zircon separator with image-processing/microtweezers-manipulating system and double-step dating. Geoscience Frontiers, 9(4), 1073-1083.

- Isozaki, Y., and Maruyama, S. (1991). Studies on orogeny based on plate tectonics in Japan and new geotectonic subdivision of the Japanese Islands. *Journal of Geography (Chigaku Zasshi)*, *100*(5), 697-761.

- Jackson, S. E., Pearson, N. J., Griffin, W. L., and Belousova, E. A. (2004). The application of laser ablation-inductively coupled plasma-mass spectrometry to in situ U–Pb zircon geochronology. Chemical Geology, 2111, 47-69.

- Jackson, S. E., Pearson, N. J., Griffin, W. L., and Belousova, E. A. (2004). The application of laser ablation-inductively coupled plasma-mass spectrometry to in situ U–Pb zircon geochronology. *chemical Geology*, *211*(1), 47-69.

- Jaffey, A. H., Flynn, K. F., Glendenin, L. E., Bentley, W. T., and Essling, A. M. (1971). Precision measurement of half-lives and specific activities of U 235 and U 238. *Physical Review C*, *4*(5), 1889.

- Jahn, B. M., and Condie, K. C. (1976). On the age of Rhodesian greenstone belts. Contributions to Mineralogy and Petrology; 57, 1957.

- Jelsma, H. A., Vinyu, M. L., Wijbrans, J. R., Verdurmen, E. A. T., Valbracht, P. J., and Davies, G. R. (1996). Constraints on Archaean crustal evolution of the Zimbabwe craton: a U-Pb zircon, Sm-Nd and Pb-Pb whole-rock isotope study. *Contributions to Mineralogy and Petrology*, *124*(1), 55-70.

- Jelsma, H. A., Vinyu, M. L., Wijbrans, J. R., Verdurmen, E. A. T., Valbracht, P. J., Davies, G. R. (1996). Constraints on Archaean crustal evolution of the Zimbabwe craton: a U-Pb zircon, Sm-Nd and Pb-Pb whole-rock isotope study. Contributions to Mineralogy and Petrology, 124(1), 55-70.

- Jelsma, H., Kröner, A., Bozhko, N., Stowe, C. (2004). Single zircon ages for two Archean banded migmatitic gneisses from central Zimbabwe. South African Journal of Geology, 107(4), 577-586.

- Jelsma, H., Kröner, A., Bozhko, N., and Stowe, C. (2004). Single zircon ages for two Archean banded migmatitic gneisses from central Zimbabwe. South African Journal of Geology, 107(4), 577-586.

- Jochum, K. P., & Stoll, B. (2008). Reference materials for elemental and isotopic analyses by LA-(MC)-ICP-MS: Successes and outstanding needs. *Laser Ablation ICP-MS in the Earth Sciences: Current practices and outstanding issues*, *40*, 147-168.

- Johnson, M. J. (1990). Overlooked sedimentary particles from tropical weathering environments. *Geology*, *18*(2), 107-110.

- Johnsson, M. J., Stallard, R. F., and Lundberg, N. (1991). Controls on the composition of fluvial sands from a tropical weathering environment: Sands of the Orinoco River drainage basin, Venezuela and Colombia. *Geological Society of America Bulletin*, *103*(12), 1622-1647.

- Kamber, B. S. (2015). The evolving nature of terrestrial crust from the Hadean, through the Archaean, into the Proterozoic. *Precambrian Research*, *258*, 48-82.

- Karlstrom, K. E., Flurkey, A. J., and Houston, R. S. (1983). Stratigraphy and depositional setting of the Proterozoic Snowy Pass Supergroup, southeastern Wyoming: Record of an early Proterozoic Atlantic-type cratonic margin. *Geological Society of America Bulletin*, *94*(11), 1257-1274.

- Karlstrom, K. E., Åhäll, K. I., Harlan, S. S., Williams, M. L., McLelland, J., and Geissman, J. W. (2001). Long-lived 1.8–1.0 Ga convergent orogen in southern Laurentia, its extensions to Australia and Baltica, and implications for refining Rodinia. Precambrian Research, 1111, 5-30.

- Kasapoğlu, B., Ersoy, Y. E., Uysal, İ., Palmer, M. R., Zack, T., Koralay, E. O., and Karlsson, A. (2016). The petrology of Paleogene volcanism in the Central Sakarya, Nallıhan Region: Implications for the initiation and evolution of post-collisional, slab break-off-related magmatic

activity. *Lithos*, *246*, 81-98.

- Kawai, K., Tsuchiya, T., Tsuchiya, J., and Maruyama, S. (2009). Lost primordial continents. Gondwana Research, 163, 581-586.

- Kawai, K., Yamamoto, S., Tsuchiya, T., and Maruyama, S. (2013). The second continent: existence of granitic continental materials around the bottom of the mantle transition zone. Geoscience Frontiers, 41, 1-6.

- Kimura, G., Ludden, J. N., Desrochers, J. P., and Hori, R. (1993). A model of ocean-crust accretion for the Superior Province, Canada. *Lithos*, *30*(3-4), 337-355.

- Kirkland, C. L., Strachan, R. A., and Prave, A. R. (2008). Detrital zircon signature of the Moine Supergroup, Scotland: contrasts and comparisons with other Neoproterozoic successions within the circum-North Atlantic region. Precambrian Research, 1633, 332-350.

- Kiyokawa, S., Taira, A., Byrne, T., Bowring, S., and Sano, Y. (2002). Structural evolution of the middle Archean coastal Pilbara terrane, Western Australia. *Tectonics*, *21*(5).

- Knudsen, T. L., Griffin, W., Hartz, E., Andresen, A., & Jackson, S. (2001). In-situ hafnium and lead isotope analyses of detrital zircons from the Devonian sedimentary basin of NE Greenland: a record of repeated crustal reworking. *Contributions to Mineralogy and Petrology*, *141*(1), 83-94.

- Komiya, T. (2011). Continental recycling and true continental growth. Russian Geology and Geophysics, 52(12), 1516-1529.

- Komiya, T. (2004). Material circulation model including chemical differentiation within the mantle and secular variation of temperature and composition of the mantle. Physics of the Earth and Planetary Interiors, 1461, 333-367.

- Komiya, T., Maruyama, S., Hirata, T., Yurimoto, H., and Nohda, S. (2004). Geochemistry of the oldest MORB and OIB in the Isua Supracrustal Belt, southern West Greenland: implications for the composition and temperature of early Archean upper mantle. Island Arc, 131, 47-72.

- Komiya, T., Maruyama, S., Hirata, T., and Yurimoto, H. (2002). Petrology and geochemistry of MORB and OIB in the mid-Archean North Pole region, Pilbara craton, Western Australia: implications for the composition and temperature of the upper mantle at 3.5 Ga. International

Geology Review, 4411, 988-1016.

- Komiya, T., Maruyama, S., Masuda, T., Nohda, S., Hayashi, M., and Okamoto, K. (1999). Plate tectonics at 3.8–3.7 Ga: field evidence from the Isua accretionary complex, southern West Greenland. The Journal of geology, 1075, 515-554.

- Komiya, T., Yamamoto, S., Aoki, S., Koshida, K., Shimojo, M., Sawaki, Y., ... and Ishikawa, A. (2017). A prolonged granitoid formation in Saglek Block, Labrador: Zonal growth and crustal reworking of continental crust in the Eoarchean. *Geoscience Frontiers*, *8*(2), 355-385.

- Komiya, T., Yamamoto, S., Aoki, S., Sawaki, Y., Ishikawa, A., Tashiro, T., Koshida, K., Shimojo, M., Aoki, K., and Collerson, K. D. (2015). Geology of the Eoarchean,> 3.95 Ga, Nulliak supracrustal rocks in the Saglek Block, northern Labrador, Canada: The oldest geological evidence for plate tectonics. Tectonophysics, 662, 40-66.

- Kopp, R. E., Kirschvink, J. L., Hilburn, I. A., Nash, C. Z. (2005). The Paleoproterozoic snowball Earth: a climate disaster triggered by the evolution of oxygenic photosynthesis. Proceedings of the National Academy of Sciences, 102(32), 11131-11136.

- Korsch, R. J., Kositcin, N., and Champion, D. C. (2011). Australian island arcs through time: geodynamic implications for the Archean and Proterozoic. Gondwana Research, 193, 716-734.

- Koshida, K., Ishikawa, A., Iwamori, H., and Komiya, T. (2016). Petrology and geochemistry of mafic rocks in the Acasta Gneiss Complex: Implications for the oldest mafic rocks and their origin. *Precambrian Research*, *283*, 190-207.

- Kozhevnikov, V. N., Skublov, S. G., Marin, Y. B., Medvedev, P. V., Systra, Y., and Valencia, V. (2010), March. Hadean-archean detrital zircons from Jatulian quartzites and conglomerates of the Karelian craton. In Doklady Earth Sciences Vol. 431, No. 1, pp. 318-323. SP MAIK Nauka/Interperiodica.

- Kramers, J. D. (2007). Hierarchical Earth accretion and the Hadean Eon. Journal of the Geological Society, 1641, 3-17.

- Krapez, B., Brown, S. J. A., Hand, J., Barley, M. E., and Cas, R. A. F. 2000. Age constraints on recycled crustal and supracrustal sources of Archaean metasedimentary sequences, Eastern Goldfields Province, Western Australia: evidence from SHRIMP zircon dating. Tectonophysics, 322.1 89-133.

- Kroner, A., Jaeckel, P., Hofmann, A., Nemchin, A. A., and Brandl, G. (1998). Field relationships and age of supracrustal Beit Bridge Complex and associated granitoid gneisses in the Central Zone of the Limpopo Belt, South Africa. *South African Journal of Geology*, *101*(3), 201-213.

- Kunimaru, T., Shimizu, H., Takahashi, K., & Yabuki, S. (1998). Differences in geochemical features between Permian and Triassic cherts from the Southern Chichibu terrane, southwest Japan: REE abundances, major element compositions and Sr isotopic ratios. *Sedimentary geology*, *119*(3-4), 195-217.

- Kusky, T. M., Windley, B. F., Safonova, I., Wakita, K., Wakabayashi, J., Polat, A., and Santosh, M. (2013). Recognition of ocean plate stratigraphy in accretionary orogens through Earth history: A record of 3.8 billion years of sea floor spreading, subduction, and accretion. Gondwana Research, 242, 501-547.

- Leyshon, P.R., Tennick, F.P., (1988). The Proterozoic Magondi Mobile Belt in Zimbabwe–a review. South African Journal of Geology 91, 114–131.

- Li, Q., Liu, S., Wang, Z., Chu, Z., Song, B., Wang, Y., and Wang, T. (2008). Contrasting provenance of Late Archean metasedimentary rocks from the Wutai Complex, North China Craton: detrital zircon U–Pb, whole-rock Sm–Nd isotopic, and geochemical data. International Journal of Earth Sciences, 973, 443-458.

- Li, Z. X., Bogdanova, S. V., Collins, A. S., Davidson, A., De Waele, B., Ernst, R. E., Fitzsimonsg, I.C.W., Fuckh, R.A., Gladkochubi, D.P., Jacobsj, J., Karlstromk, K.E., Lul, S., Natapovm, L.M., Peasen, V., Pisarevskya, S.A., Thraneo, K., and Vemikovsky, V. (2008). Assembly, configuration, and break-up history of Rodinia: a synthesis. Precambrian Research, 1601, 179-210.

- Li, Z. X., Wartho, J. A., Occhipinti, S., Zhang, C. L., Li, X. H., Wang, J., and Bao, C. (2007). Early history of the eastern Sibao Orogen South China during the assembly of Rodinia: new mica 40 Ar/39 Ar dating and SHRIMP U–Pb detrital zircon provenance constraints. Precambrian Research, 1591, 79-94.

- Li, Z., Chen, B. and Wei, C. (2016): Hadean detrital zircon in the North China Craton. Journal of Mineralogical and Petrological Sciences, 111, 283-291.

- Linnemann, U., Ouzegane, K., Drareni, A., Hofmann, M., Becker, S., Gärtner, A., and Sagawe,

A. (2011). Sands of West Gondwana: An archive of secular magmatism and plate interactions—A case study from the Cambro-Ordovician section of the Tassili Ouan Ahaggar Algerian Sahara using U–Pb–LA-ICP-MS detrital zircon ages. Lithos, 1231, 188-203.

- Ludwig, K. R., (2003). User's manual for Isoplot 3.00: a geochronological toolkit for Microsoft Excel (No. 4). Kenneth R. Ludwig.

- Luguet, A., Nowell, G. M., and Pearson, D. G. (2008). 184Os/188Os and 186Os/188Os measurements by Negative Thermal Ionisation Mass Spectrometry (N-TIMS): effects of interfering element and mass fractionation corrections on data accuracy and precision. *Chemical Geology*, *248*(3-4), 342-362.

- Machado, N., Schrank, A., Noce, C. M., and Gauthier, G. (1996). Ages of detrital zircon from Archean-Paleoproterozoic sequences: Implications for Greenstone Belt setting and evolution of a Transamazonian foreland basin in Quadrilátero Ferrífero, southeast Brazil. Earth and Planetary Science Letters, 1411, 259-276.

- Maier, A. C., Cates, N. L., Trail, D., and Mojzsis, S. J. (2012). Geology, age and field relations of Hadean zircon-bearing supracrustal rocks from Quad Creek, eastern Beartooth Mountains (Montana and Wyoming, USA). *Chemical Geology*, *312*, 47-57.

- Malone, S. J., Meert, J. G., Banerjee, D. M., Pandit, M. K., Tamrat, E., Kamenov, G. D., V.R., Pradhan and Sohl, L. E. (2008). Paleomagnetism and detrital zircon geochronology of the Upper Vindhyan Sequence, Son Valley and Rajasthan, India: a ca. 1000Ma closure age for the Purana Basins?. Precambrian Research, 1643, 137-159.

- Manyeruke, T.D., Blenkinsop, T.G., Buchholz, P., Love, D., Oberthür, T., Vetter, U.K., Davis, D.W., (2004). The age and petrology of the Chimbadzi Hill Intrusion, NW Zimbabwe: first evidence for early Paleoproterozoic magmatism in Zimbabwe. J. Afr. Earth Sci. 40, 281–292.

- Mapeo, R.B.M., Armstrong, R.A., Kampunzu, A.B., (2001). SHRIMP U–Pb zircon geochronology of gneisses from the Gweta borehole, northeast Botswana: implications for the Palaeoproterozoic Magondi Belt in southern Africa. Geol. Mag. 138, 299–308.

- Marchi, S., Bottke, W. F., Elkins-Tanton, L. T., Bierhaus, M., Wuennemann, K., Morbidelli, A., and Kring, D. A. (2014). Widespread mixing and burial of Earth/'s Hadean crust by asteroid impacts. Nature, 5117511, 578-582.

- Marsh, B. D. (1979), Island arc development: Some observations, experiments, and speculations. J. Geol. 687-713.
- Martel, E., van Breemen, O., Berman, R.G. and Pehrsson, S. (2008): Geochronology and tectonometamorphic history of the Snowbird Lake area, Northwest Territories, Canada: New insights into the architecture and significance of the Snowbird tectonic zone. Precambrian Research, 161, 201-230.
- Martin, A. P., Condon, D. J., Prave, A. R., Lepland, A. (2013). A review of temporal constraints for the Palaeoproterozoic large, positive carbonate carbon isotope excursion (the Lomagundi–Jatuli Event). Earth-Science Reviews, 127, 242-261.
- Martin, A. P., Condon, D. J., Prave, A. R., and Lepland, A. (2013). A review of temporal constraints for the Palaeoproterozoic large, positive carbonate carbon isotope excursion (the Lomagundi–Jatuli Event). Earth-Science Reviews, 127, 242-261.
- Martin, D. M., Li, Z. X., Nemchin, A. A., and Powell, C. M. (1998). A pre-2.2 Ga age for giant hematite ores of the Hamersley Province, Australia?. *Economic Geology*, *93*(7), 1084-1090.
- Martin, D. M., Powell, C. M., and George, A. D. (2000). Stratigraphic architecture and evolution of the early Paleoproterozoic McGrath Trough, Western Australia. *Precambrian Research*, *99*(1-2), 33-64.
- Maruyama, S., Ikoma, M., Genda, H., Hirose, K., Yokoyama, T., and Santosh, M. 2013. The naked planet Earth: most essential pre-requisite for the origin and evolution of life. Geoscience Frontiers, 42, 141-165.
- Maruyama, S., Kawai, T., and Windley, B. F. (2010). Ocean plate stratigraphy and its imbrication in an accretionary orogen: the Mona complex, Anglesey–Lleyn, Wales, UK. *Geological Society, London, Special Publications*, *338*(1), 55-75.
- Maruyama, S., Masuda, S., and Appel, P. W. U. (1991). The oldest accretionary complex on the Earth, Isua, Greenland. Geological Society of America Abstract 23, A429-430.
- Maruyama, S., Santosh, M., and Azuma, S. (2018). Initiation of plate tectonics in the Hadean: eclogitization triggered by the ABEL Bombardment. *Geoscience Frontiers*,9,1033-1048.
- Maruyama, S., Yuen, D. A., and Windley, B. F. (2007). Dynamics of plumes and superplumes

through time. In Superplumes: Beyond Plate Tectonics pp. 441-502. Springer Netherlands.

- Master, S., (1984). The Stratigraphy of the Deweras Group at the Mangula and Norah Mines, Mhangura, Zimbabwe. B.Sc. (Honours) Dissertation. University of the Witwatersrand, Johannesburg, 75 pp.

- Master, S., (1991). Stratigraphy, tectonic setting, and mineralization of the early Proterozoic Magondi Supergroup, Zimbabwe: a review. Econ. Geol. Res. Unit Inform. Circular: No. 238, Department of Geology, University of the Witwatersrand, Johannesburg, 75 pp.

- Master, S., Bekker, A., Hofmann, A. (2010). A review of the stratigraphy and geological setting of the Palaeoproterozoic Magondi Supergroup, Zimbabwe–Type locality for the Lomagundi carbon isotope excursion. Precambrian Research, 182(4), 254-273.

- Master, S., Verhagen, B.Th., Bassot, J.P., Beukes, N.J., Lemoine, S., (1993). Stable Isotopic signatures of Palaeoproterozoic carbonate rocks from Guinea, Senegal, South Africa and Zimbabwe: Constraints on the timing of the c.2 Ga "Lomagundi" δ13C excursion. In: Dia, A. (Ed.), Symposium on the Early Proterozoic: Geochemical and Structural constraints, Metallogeny. CIFEG Occ. Publ.: 1993/23, Orleans (France), pp. 38–41.

- Matsuda, T., and Isozaki, Y. (1991). Well-documented travel history of Mesozoic pelagic chert in Japan: from remote ocean to subduction zone. Tectonics, 102, 475-499.

- Matsuda, To., and Uyeda, S. (1971). On the Pacific-type orogeny and its model—extension of the paired belts concept and possible origin of marginal seas. Tectonophysics, 111, 5-27.

- McCourt, S., Hilliard, P., Armstrong, R.A., Munyanyiwa, H., (2001). SHRIMP U–Pb zircon geochronology of the Hurungwe granite northwest Zimbabwe: age constraints on the timing of the Magondi orogeny and implications for the correlation between the Kheis and Magondi Belts. S. Afr. J. Geol. 104, 39–46.

- McCulloch, M. T., & Bennett, V. C. (1994). Progressive growth of the Earth's continental crust and depleted mantle: geochemical constraints. Geochimica et Cosmochimica Acta, 58(21), 4717-4738.

- McGregor, V. R., Friend, C.R. L, and Nutman, A. P. (1991). The late Archean mobile belt through Godthabsfjord, southern West Greenland: a continent-continent collision zone?. Bulletin of Geological Society of Dennmark, 39, 179-197.

- McLennan, S. M., Taylor, S. R., McCulloch, M. T., and Maynard, J. B. (1990). Geochemical and Nd and Sr isotopic composition of deep-sea turbidites: crustal evolution and plate tectonic associations. Geochimica et Cosmochimica Acta, 54(7), 2015-2050.

- McLennan, S. M., and Taylor, S. R. (1982). Geochemical constraints on the growth of the continental crust. The Journal of Geology, 347-361.

- McNicoll, V. J., Thériault, R. J., and McDonough, M. R. (2000) Taltson basement gneissic rocks: U Pb and Nd isotopic constraints on the basement to the Paleoproterozoic Taltson magmatic zone, northeastern Alberta. Canadian J. Earth Sci., 37, 1575-1596.

- Meert, J. G. (2012). What's in a name? The Columbia Paleopangaea/Nuna supercontinent. Gondwana Research, 214, 987-993.

- Melezhik, V.A., Fallick, A.E., Clark, T., (1997). Two billion year old isotopically heavy carbon: evidence from the Labrador Trough, Canada. Can. J. Earth Sci. 34, 271–285.

- Melezhik, V.A., Fallick, A.E., Hanski, E., Kump, L., Lepland, A., Prave, A., Strauss, H., (2005). Emergence of the aerobic biosphere during the Archaean–Proterozoic transition: challenges for future research. Geol. Soc. Am. Today 15, 4–11.

- Mishima K., Yamazaki, R., Kumar, M.S., Hokada, T., and Ueno, Y., (2012). Litho-, Chrono- and S-Mif-Chemo-Stratigraphy of Late Archean Dharwar Supergroup, South India. Mineralogical Magazine, 766 2115

- Mojzsis, S. J., Harrison, T. M., and Pidgeon, R. T. (2001). Oxygen-isotope evidence from ancient zircons for liquid water at the Earth's surface 4,300 Myr ago. Nature, 4096817, 178-181.

- Mojzsis, S.J. and Harrison, T.M. (2002): Establishment of a 3.83-Ga magmatic age for the Akilia tonalite (southern West Greenland). Earth and Planetary Science Letters, 202, 563-576.

- Moorbath, S., Wilson, J. F., Goodwin, R., and Humm, M. (1977). Further Rb-Sr age and isotope data on early and late Archaean rocks from the Rhodesian Craton. *Precambrian Research*, *5*(3), 229-239.

- Moorbath, S., Wilson, J., and Cotterill, P. (1976). Early Archaean age for the Sebakwian group at Selukwe, Rhodesia. *Nature*, 536-538.

- Moores, E. M. (1991). Southwest US-East Antarctic SWEAT connection: a hypothesis. Geology, 195, 425-428.
- Moresi, L., & Solomatov, V. (1998). Mantle convection with a brittle lithosphere: thoughts on the global tectonic styles of the Earth and Venus. Geophysical Journal International, 133(3), 669-682.
- Morgan, W. J. (1968). Rises, trenches, great faults, and crustal blocks. *Journal of Geophysical Research*, *73*(6), 1959-1982.
- Mortensen, J.K., Thorpe, R.I., Padgham, W.A., King, J.E., and Davis, W.J. (1988). U–Pb zircon ages for felsic volcanism in the Slave Province, NWT. *In* Radiogenic age and isotope studies: Report 2. Geological Survey of Canada, Paper 88-2, pp. 85–95.
- Moyen, J. F., and Martin, H. (2012). Forty years of TTG research. *Lithos*, *148*, 312-336.
- Mueller, P. A., Wooden, J. L., Mogk, D. W., Nutman, A. P., and Williams, I. S. (1996). Extended history of a 3.5 Ga trondhjemitic gneiss, Wyoming Province, USA: evidence from U□ Pb systematics in zircon. *Precambrian Research*, *78*(1-3), 41-52.
- Mueller, P. A., Wooden, J. L., and Nutman, A. P. (1992). 3.96 Ga zircons from an Archean quartzite, Beartooth Mountains, Montana. *Geology*, *20*(4), 327-330.
- Mueller, W. U., Corcoran, P. L., and Pickett, C. (2005). Mesoarchean continental breakup: evolution and inferences from the> 2.8 Ga Slave craton-cover succession, Canada. *The Journal of geology*, *113*(1), 23-45.
- Mukasa, S. B., Wilson, A. H., and Young, K. R. (2013). Geochronological constraints on the magmatic and tectonic development of the Pongola Supergroup (Central Region), South Africa. Precambrian Research, 224, 268-286.
- Müller, S. G., Krapez, B., Barley, M. E., and Fletcher, I. R. (2005). Giant iron-ore deposits of the Hamersley province related to the breakup of Paleoproterozoic Australia: New insights from in situ SHRIMP dating of baddeleyite from mafic intrusions. *Geology*, *33*(7), 577-580.
- Myers, J. S., and Williams, I. R. (1985). Early Precambrian crustal evolution at Mount Narryer, Western Australia. *Precambrian research*, *27*(1-3), 153-163.

- Nadeau, S., Chen, W., Reece, J., Lachhman, D., Ault, R., Faraco, M.T.L., Fraga, L.M., Reis, N.J. and Betiollo, L.M. (2013): Guyana: the lost Hadean crust of South America?. Brazilian Journal of Geology, 43, 601-606.
- Nagler, T. F., Kramers, J. D., Kamber, B. S., Frei, R., and Prendergast, M. D. A. (1997). Growth of subcontinental lithospheric mantle beneath Zimbabwe started at or before 3.8 Ga: Re-Os study on chromites. *Geology*, *25*(11), 983-986.
- Nakano, K. (2015). Direct measurement of trace rare earth elements in high purity REE oxides, Agilent 8800 ICP-QQQ Application Handbook 2nd edition. pp. 58-59.
- Nebel, O., Rapp, R. P., and Yaxley, G. M. (2014). The role of detrital zircons in Hadean crustal research. Lithos, 190, 313-327.
- Nelson, D. R., Trendall, A. F., and Altermann, W. (1999). Chronological correlations between the Pilbara and Kaapvaal cratons. Precambrian Research, 973, 165-189.
- Noble, S. R., Lightfoot, P. C. (1992). U–Pb baddeleyite ages of the Kerns and Triangle Mountain intrusions, Nipissing diabase, Ontario. Canadian Journal of Earth Sciences, 29(7), 1424-1429.
- Nutman, A. P., and Friend, C. R. (2009) New 1: 20,000 scale geological maps, synthesis and history of investigation of the Isua supracrustal belt and adjacent orthogneisses, southern West Greenland: a glimpse of Eoarchaean crust formation and orogeny. Precambrian Res., 172(3), 189-211
- Næraa, T., Scherstén, A., Rosing, M. T., Kemp, A. I. S., Hoffmann, J. E., Kokfelt, T. F., and Whitehouse, M. J. (2012) Hafnium isotope evidence for a transition in the dynamics of continental growth 3.2 Gyr ago. Nature, 485, 627-630.
- O'Neil, J., Carlson, R. W., Francis, D., and Stevenson, R. K. (2008) Neodymium-142 evidence for Hadean mafic crust. Science, 321, 1828-1831.
- O'Neill, C., Jellinek, A. M., and Lenardic, A. (2007). Conditions for the onset of plate tectonics on terrestrial planets and moons. Earth and Planetary Science Letters, 2611, 20-32.
- Ogawa, M. (2007). Superplumes, plates, and mantle magmatism in two-dimensional numerical models. Journal of Geophysical Research: Solid Earth, 112B6.

- Ogawa, M. (2014). Two-stage evolution of the Earth's mantle inferred from numerical simulation of coupled magmatism-mantle convection system with tectonic plates. Journal of Geophysical Research: Solid Earth, 1193, 2462-2486.

- Ohta, H., Maruyama, S., Takahashi, E., Watanabe, Y., and Kato, Y. (1996). Field occurrence, geochemistry and petrogenesis of the Archean mid-oceanic ridge basalts (AMORBs) of the Cleaverville area, Pilbara craton, Western Australia. *Lithos*, *37*(2-3), 199-221.

- Paces, J. B., and Miller, J. D. (1993) Precise U-Pb ages of Duluth complex and related mafic intrusions, northeastern Minnesota: Geochronological insights to physical, petrogenetic, paleomagnetic, and tectonomagmatic processes associated with the 1.1 Ga midcontinent rift system. J. Geophys. Res.: Solid Earth, 98(B8), 13997-14013.

- Paquette, J.L., Barbosa, J.S.F., Rohais, S., Cruz, S.C.P., Goncalves, P., Peucat, J.J., Leal, A.B.M., Santos-Pinto, M. and Martin, H. (2015): The geological roots of South America: 4.1 Ga and 3.7 Ga zircon crystals discovered in NE Brazil and NW Argentina. Precambrian Research, 271, 49-55.

- Patchett P. J., Kouvo O., Hedge C. E. and Tatsumoto M. (1981) Evolution of continental crust and mantle heterogeneity: evidence from Hf isotopes. Contrib. Mineral. Petrol. 78, 279–297.

- Pehrsson, S. J., Berman, R. G., and Davis, W. J. (2013) Paleoproterozoic orogenesis during Nuna aggregation: a case study of reworking of the Rae Craton , Woodburn Lake, Nunavut. Precambrian Res., 232, 167-188.

- Percival, J. A., McNicoll, V., and Bailes, A. H. (2006). Strike-slip juxtaposition of ca. 2.72 Ga juvenile arc and> 2.98 Ga continent margin sequences and its implications for Archean terrane accretion, western Superior Province, Canada.Canadian Journal of Earth Sciences, 437, 895-927.

- Perttunen, V., Vaasjoki, M. (2001). U-Pb geochronology of the Peräpohja schist belt, northwestern Finland. Special Paper-Geological survey of Finland, 45-84.

- Phillips, E. (1991). Progressive deformation of the South Stack and New Harbour Groups, Holy Island, western Anglesey, North Wales. *Journal of the Geological Society*, *148*(6), 1091-1100.

- Pilot, J., Werner, C. D., Haubrich, F., and Baumann, N. (1998). Palaeozoic and proterozoic zircons from the Mid-Atlantic ridge. Nature, 3936686, 676-679.

- Pisarevsky, S. A., De Waele, B., Jones, S., Söderlund, U., and Ernst, R. E. (2015). Paleomagnetism and U–Pb age of the 2.4 Ga Erayinia mafic dykes in the south-western Yilgarn, Western Australia: Paleogeographic and geodynamic implications. *Precambrian Research*, *259*, 222-231.

- Planavsky, N.J., Bekker, A., Hofmann, A., Owens, J.D., Lyons, T.W., (2012). Sulfur record of rising and falling marine oxygen and sulfate levels during the Lomagundi event. Proc. Natl. Acad. Sci. 109, 18300–18305.

- Polat, A., Hofmann, A. W., and Rosing, M. T. (2002). Boninite-like volcanic rocks in the 3.7–3.8 Ga Isua greenstone belt, West Greenland: geochemical evidence for intra-oceanic subduction zone processes in the early Earth. Chemical Geology, 1843, 231-254.

- Prendergast, M. D. (2008). Archean komatiitic sill-hosted chromite deposits in the Zimbabwe craton. *Economic Geology*, *103*(5), 981-1004.

- Puetz, S. J., Condie, K. C., Pisarevsky, S., Davaille, A., Schwarz, C. J., and Ganade, C. E. (2017). Quantifying the evolution of the continental and oceanic crust. *Earth-Science Reviews*, *164*, 63-83.

- Rainbird, R. H., Davis, W. J., Pehrsson, S. J., Wodicka, N., Rayner, N., and Skulski, T. (2010) Early Paleoproterozoic supracrustal assemblages of the Rae domain, Nunavut, Canada: Intracratonic basin development during supercontinent break-up and assembly. Precambrian Res., 181, 167-186.

- Rainbird, R. H., Hamilton, M. A., and Young, G. M. (2001). Detrital zircon geochronology and provenance of the Torridonian, NW Scotland. *Journal of the Geological Society*, *158*(1), 15-27.

- Rainbird, R. H., Stern, R. A., Khudoley, A. K., Kropachev, A. P., Heaman, L. M., and Sukhorukov, V. I. 1998. U–Pb geochronology of Riphean sandstone and gabbro from southeast Siberia and its bearing on the Laurentia–Siberia connection. Earth and Planetary Science Letters, 1643, 409-420.

- Rasmussen, B., Fletcher, I. R., Muhling, J. R., Gregory, C. J., and Wilde, S. A. (2011). Metamorphic replacement of mineral inclusions in detrital zircon from Jack Hills, Australia: Implications for the Hadean Earth. *Geology*, *39*(12), 1143-1146.

- References

- Reimink, J. R., Chacko, T., Stern, R. A., and Heaman, L. M. (2014). Earth's earliest evolved crust generated in an Iceland-like setting. *Nature Geoscience*, *7*(7), 529.
- Reimink, J. R., Chacko, T., Stern, R. A., and Heaman, L. M. 2014. Earth [rsquor] s earliest evolved crust generated in an Iceland-like setting. Nature Geoscience, 77, 529-533.
- Reymer, A., and Schubert, G. 1984. Phanerozoic addition rates to the continental crust and crustal growth. Tectonics, 31, 63-77.
- Rino, S., Komiya, T., Windley, B. F., Katayama, I., Motoki, A., & Hirata, T. (2004). Major episodic increases of continental crustal growth determined from zircon ages of river sands; implications for mantle overturns in the Early Precambrian. *Physics of the Earth and Planetary Interiors*, *146*(1-2), 369-394.
- Rino, S., Kon, Y., Sato, W., Maruyama, S., Santosh, M., and Zhao, D. (2008). The Grenvillian and Pan-African orogens: world's largest orogenies through geologic time, and their implications on the origin of superplume. Gondwana Research, 141, 51-72.
- Roberts, N. M. (2012). Increased loss of continental crust during supercontinent amalgamation. Gondwana Research, 214, 994-1000.
- Roberts, N. M. (2013). The boring billion?–Lid tectonics, continental growth and environmental change associated with the Columbia supercontinent. Geoscience Frontiers, 46, 681-691.
- Roberts, N. M., and Spencer, C. J. (2015) The zircon archive of continent formation through time. Geological Society, London, Special Publications,3891,197-225.
- Rogers, J. J. (1996). A history of continents in the past three billion years. *The journal of geology*, *104*(1), 91-107.
- Rogers, J. J., and Santosh, M. (2003). Supercontinents in Earth history. Gondwana Research, 63, 357-368.
- Rollinson, H. (2017). There were no large volumes of felsic continental crust in the early Earth. *Geosphere*, *13*(2), 235-246.
- Rollinson, H. R., Whitehouse, M. (2011). The growth of the Zimbabwe Craton during the late Archaean: an ion microprobe U–Pb zircon study. Journal of the Geological Society, 168(4), 941-

952.

- Ronov, A. B. (1964). Common tendencies in the chemical evolution of the earth's crust, ocean and atmosphere. *Geokhimiya*, *1964*, 715-743.

- Rubatto, D. (2002) Zircon trace element geochemistry: partitioning with garnet and the link between U–Pb ages and metamorphism. Chem. Geol., 184(1-2), 123-138.

- Rudnick, R. L. (1995). Making continental crust. Nature, 3786557, 571-577.

- Rye, R., Holland, H. D. (1998). Paleosols and the evolution of atmospheric oxygen: a critical review. American Journal of Science, 298(8), 621-672.

- Sakata, S., Hirakawa, S., Iwano, H., Danhara, T., Guillong, M., and Hirata, T. (2017). A new approach for constraining the magnitude of initial disequilibrium in Quaternary zircons by coupled uranium and thorium decay series dating. *Quaternary Geochronology*, *38*, 1-12.

- Sanborn-Barrie, M. (2000). Structural Geology, Savant Lake greenstone belt, western Superior Province, Ontario; Geological Survey of Canada, Open File 3947, compilation at 1:100 000 scale, 1.

- Sano, T., Fukuoka, T., and Ishimoto, M (2011). Petrological constraints on magma evolution of the Fuji Volcano: A Cases study for the 1707 Hoei eruption. Studies on the Origin and Biodiversity in the Sagami Sea Fossa Magna Element and the Izu-Ogasawara (Bonin) Arc, Memoirs of National Museum of Nature and Science, 47, 471-496.

- Santosh, M., Arai, T., and Maruyama, S. (2017). Hadean Earth and primordial continents: the cradle of prebiotic life. *Geoscience Frontiers*, *8*(2), 309-327.

- Santosh, M., Maruyama, S., and Yamamoto, S. (2009). The making and breaking of supercontinents: some speculations based on superplumes, super downwelling and the role of tectosphere. Gondwana Research, 153, 324-341.

- Sawada, H., Isozaki, Y., Sakata, S., Hirata, T., and Maruyama, S. (2018). Secular change in lifetime of granitic crust and the continental growth: a new view from detrital zircon ages of sandstones. Geoscience Frontiers. 9, 1099-1115.

- Sawada, H., Maruyama, S., Sakata, S., and Hirata, T. (2016). Detrital zircon geochronology by

LA-ICP-MS of the Neoarchean Manjeri Formation in the Archean Zimbabwe craton–the disappearance of Eoarchean crust by 2.7 Ga?. *Journal of African Earth Sciences, 113*, 1-11.

- Schidlowski, M., Eichmann, R., Junge, C.E., 1975. Precambrian sedimentary carbonates: carbon and oxygen isotope geochemistry and implications for the terrestrial oxygen budget. Precambrian Res. 2, 1–69.

- Schidlowski, M., Todt, W. (1998). The proterozoic Lomagundi carbonate province as paragon of a 13 C-enriched carbonate facies: Geology, radiometric age and geochemical significance. Chinese Science Bulletin, 43, 114-114.

- Scholl, D. W., and von Huene, R. 2007. Crustal recycling at modern subduction zones applied to the past—Issues of growth and preservation of continental basement crust, mantle geochemistry, and supercontinent reconstruction. Geological Society of America Memoirs, 200, 9-32.

- Scholl, D. W., and von Huene, R. 2007. Crustal recycling at modern subduction zones applied to the past—Issues of growth and preservation of continental basement crust, mantle geochemistry, and supercontinent reconstruction.Geological Society of America Memoirs, 200, 9-32.

- Scholl, D. W., and von Huene, R. 2007. Crustal recycling at modern subduction zones applied to the past—Issues of growth and preservation of continental basement crust, mantle geochemistry, and supercontinent reconstruction. Geological Society of America Memoirs, 200, 9-32.

- Scholl, D. W., and von Huene, R. (2009). Implications of estimated magmatic additions and recycling losses at the subduction zones of accretionary non-collisional and collisional suturing orogens. Geological Society, London, Special Publications, 3181, 105-125.

- Shackleton, R. M. (1953). The structural evolution of North Wales. *Geological Journal*, *1*(3), 261-297.

- Shibaike, Y., Sasaki, T., and Ida, S. (2016). Excavation and melting of the Hadean continental crust by Late Heavy Bombardment. Icarus, 266, 189-203.

- Shibuya, T., Kitajima, K., Komiya, T., Terabayashi, M., and Maruyama, S. (2007). Middle Archean ocean ridge hydrothermal metamorphism and alteration recorded in the Cleaverville area, Pilbara Craton, Western Australia. *Journal of Metamorphic Geology*, *25*(7), 751-767.

- Shibuya, T., Komiya, T., Nakamura, K., Takai, K., and Maruyama, S. (2010). Highly alkaline,

high-temperature hydrothermal fluids in the early Archean ocean. *Precambrian Research*, *182*(3), 230-238.

- Shiels, C., Partin, C. A., and Eglington, B. M. (2016) Provenance approaches in polydeformed metasedimentary successions: Determining nearest neighboring cratons during the deposition of the Paleoproterozoic Murmac Bay Group. Lithosphere, 8, 519-532.

- Shiels, C., Partin, C. A., and Stern, R. A. (2017) An integrated U-Pb, Hf, and O isotopic provenance analysis of the Paleoproterozoic Murmac Bay Group, northern Saskatchewan, Canada. Precambrian Res., 302, 18-32.

- Shimizu, K., Nakamura, E., and Maruyama, S. (2005). The geochemistry of ultramafic to mafic volcanics from the Belingwe Greenstone Belt, Zimbabwe: magmatism in an Archean continental large igneous province. *Journal of Petrology*, *46*(11), 2367-2394.

- Shimojo, M., Yamamoto, S., Sakata, S., Yokoyama, T.D., Maki, K., Sawaki, Y., Ishikawa, A., Aoki, K., Aoki, S., Koshida, K. and Tashiro, T. (2016). Occurrence and geochronology of the Eoarchean, ~ 3.9 Ga, Iqaluk Gneiss in the Saglek Block, northern Labrador, Canada: Evidence for the oldest supracrustal rocks in the world. Precambrian Research, 278, 218-243.

- Shirey, S. B., and Walker, R. J. (1995). Carius tube digestion for low-blank rhenium-osmium analysis. *Analytical Chemistry*, *67*(13), 2136-2141.

- Shu, L. S., Deng, X. L., Zhu, W. B., Ma, D. S., and Xiao, W. J. (2011). Precambrian tectonic evolution of the Tarim Block, NW China: new geochronological insights from the Quruqtagh domain. Journal of Asian Earth Sciences, 425, 774-790.

- Simpson, E. L., Eriksson, K. A., and Mueller, W. U. (2012). 3.2 Ga eolian deposits from the M ycle quartz sandstones. *Precambrian Research*, *214*, 185-191.oodies Group, Barberton Greenstone Belt, South Africa: Implications for the origin of first-c

- Sircombe, K. N., Bleeker, W., and Stern, R. A. (2001). Detrital zircon geochronology and grain-size analysis of a~ 2800 Ma Mesoarchean proto-cratonic cover succession, Slave Province, Canada. Earth and Planetary Science Letters, 1893, 207-220.

- Sizova, E., Gerya, T., Brown, M., and Perchuk, L. L. (2010). Subduction styles in the Precambrian: insight from numerical experiments. Lithos, 1163, 209-229.

- Sleep, N. H., and Windley, B. F. (1982). Archean plate tectonics: constraints and inferences. The Journal of Geology, 363-379.
- Sláma, J., Košler, J., Condon, D. J., Crowley, J. L., Gerdes, A., Hanchar, J. M., Horstwoodd, M.S.A., Morrish, G. A., Nasdalai, L., Norbergi, N., Schalteggerj, U., Schoenej, B., Tubrettk, M. N., and Whitehouse, M. J. 2008. "Plešovice zircon—a new natural reference material for U–Pb and Hf isotopic microanalysis." Chemical Geology, 2491, 1-35.
- Sláma, J., Košler, J., Condon, D. J., Crowley, J. L., Gerdes, A., Hanchar, J. M., Horstwood, M. S. A., Morris, G. A., Norberg N., Schaltegger, U., Schoene, B., Tubrett, M. N., & Whitehouse, M. J. (2008). Plešovice zircon—a new natural reference material for U–Pb and Hf isotopic microanalysis. *Chemical Geology*, *249*(1-2), 1-35.
- Smoliar, M. I., Walker, R. J., and Morgan, J. W. (1996). Re-Os ages of group IIA, IIIA, IVA, and IVB iron meteorites. *Science*, *271*(5252), 1099-1102.
- Snyder, G. A., Taylor, L. A., and Neal, C. R. (1992). A chemical model for generating the sources of mare basalts: Combined equilibrium and fractional crystallization of the lunar magmasphere. Geochimica et Cosmochimica Acta, 5610, 3809-3823.
- Solomatov, V.S. (1995): Scaling of temperature- and stress-dependent viscosity convection. Physics of Fluids, 7, 266-274.
- Spaggiari, C. V., Pidgeon, R. T., and Wilde, S. A. (2007). The Jack Hills greenstone belt, Western Australia: part 2: lithological relationships and implications for the deposition of≥ 4.0 Ga detrital zircons. *Precambrian Research*, *155*(3-4), 261-286.
- Spencer, C. J., Murphy, J. B., Kirkland, C. L., Liu, Y., and Mitchell, R. N. (2018). A Palaeoproterozoic tectono-magmatic lull as a potential trigger for the supercontinent cycle. *Nature Geoscience*, 1.
- Stacey, J. T., and Kramers, 1. (1975). Approximation of terrestrial lead isotope evolution by a two-stage model. *Earth and planetary science letters*, *26*(2), 207-221.
- Stagman, J.G., (1961). The geology of the country around Sinoia and Banket, Lomagundi District. Bulletin of Rhodesia Geological Survey, 49, 107 pp.
- Stern, C. R. (2011). Subduction erosion: rates, mechanisms, and its role in arc magmatism and

the evolution of the continental crust and mantle. Gondwana Research, 202, 284-308.

- Stern, R. J., & Scholl, D. W. (2010). Yin and yang of continental crust creation and destruction by plate tectonic processes. *International Geology Review*, *52*(1), 1-31.

- Stern, R.A. (1997): The GSC Sensitive High Ion Microprobe (SHRIMP) : analytical techniques of zircon U-Th-Pb age determinations and performance evaluation, Geol. Surv. Can. Curr. Res., 1-31.

- Stewart, A. D., and Kay, M. (1969). Torridonian rocks of Scotland reviewed. In *North Atlantic–Geology and Continental Drift: A symposium* (Vol. 12, pp. 595-608).

- Stowe, C. W. (1968). Geology of the country south and west of Selukwe. *Bull. Geol. Surv. Rhodesia*, 59, 209.

- Stowe, C. W. (1974). Alpine-type structures in the Rhodesian basement complex at Selukwe. *Journal of the Geological Society*, *130*(5), 411-425.

- Stowe, C. W. (1978). Structure of the Lomagundi Group in the Sinoia area, Rhodesia. Geological Survey of Southern Rhodesia Special Publication, 4, 449-459.

- Sugitani, K., Yamashita, F., Nagaoka, T., Yamamoto, K., Minami, M., Mimura, K., and Suzuki, K. (2006). Geochemistry and sedimentary petrology of Archean clastic sedimentary rocks at Mt. Goldsworthy, Pilbara Craton, Western Australia: evidence for the early evolution of continental crust and hydrothermal alteration. *Precambrian Research*, *147*(1-2), 124-147.

- Sutton, E. R. (1979). The geology of the Mafungabusi area. Bulletin of Rhodesia Geological Survey, 81.

- Söderlund, U., Hofmann, A., Klausen, M. B., Olsson, J. R., Ernst, R. E., and Persson, P. O. (2010). Towards a complete magmatic barcode for the Zimbabwe craton: Baddeleyite U–Pb dating of regional dolerite dyke swarms and sill complexes. *Precambrian Research*, *183*(3), 388-398.

- Tanaka, K. L., Robbins, S. J., Fortezzo, C. M., Skinner, J. A., and Hare, T. M. (2014) The digital global geologic map of Mars: Chronostratigraphic ages, topographic and crater morphologic characteristics, and updated resurfacing history. Planet. Space Sci., 95, 11-24.

- Taylor, P. N., Kramersb, J. D., Moorbatha, S., Wilson, J. F., Orpen, J. L., and Martin, A. (1991).

Pb/Pb, Sm-Nd and Rb-Sr geochronology in the Archean Craton of Zimbabwe. Chemical Geology: Isotope Geoscience section, 87(3-4), 175-196.

- Taylor, S. R., Rudnick, R. L., McLennan, S. M., and Eriksson, K. A. (1986). Rare earth element patterns in Archean high-grade metasediments and their tectonic significance. *Geochimica et Cosmochimica Acta*, *50*(10), 2267-2279.

- Thirlwall M. F. and Anczkiewicz R. (2004) Multidynamic isotope ratio analysis using MC-ICP-MS and the causes of secular drift in Hf, Nd and Pb isotope ratios. Int. J. Mass Spectrom. 235, 59–81.

- Thirlwall, M. F., & Walder, A. J. (1995). In situ hafnium isotope ratio analysis of zircon by inductively coupled plasma multiple collector mass spectrometry. *Chemical Geology*, *122*(1-4), 241-247.

- Thorne, A.M., and Trendall, A.F. (2001). Geology of the Fortescue Group, Pilbara Craton, Western Australia Bulletin – Geological Survey of Western Australia, 144.

- Timmons, J. M., Karlstrom, K. E., Heizler, M. T., Bowring, S. A., Gehrels, G. E., and Crossey, L. J. (2005). Tectonic inferences from the ca. 1255–1100 Ma Unkar Group and Nankoweap Formation, Grand Canyon: Intracratonic deformation and basin formation during protracted Grenville orogenesis.Geological Society of America Bulletin, 11711-12, 1573-1595.

- Tomlinson, K. Y., Davis, D. W., Stone, D., and Hart, T. R. (2003). U–Pb age and Nd isotopic evidence for Archean terrane development and crustal recycling in the south-central Wabigoon subprovince, Canada. *Contributions to Mineralogy and Petrology*, *144*(6), 684-702.

- Tsomondo, J. M., Wilson, J. F., and Blenkinsop, T. G. (1992). Reassessment of the structure and stratigraphy of the early Archaean Selukwe Nappe, Zimbabwe. *The Archaean: Terrains, processes, and metallogeny: The University of Western Australia Geology Department (Key Centre) and University Extension*, (22), 123-135.

- Tsutsumi, Y., Horie, K., Sano, T., Miyawaki, R., Momma, K., Matsubara, S., Shigeoka, M., and Yokoyama, K. (2012) LA-ICP-MS and SHRIMP ages of zircon grains in chevkinite and monazite tuffs from the Boso Peninsula, Central Japan. Bull. National Museum of Nature and Sci., Series C, 38, 15-32.

- Tunheng, Apinya, and Takafumi Hirata (2004). "Development of signal smoothing device for

precise elemental analysis using laser ablation-ICP-mass spectrometry." Journal of Analytical Atomic Spectrometry, 197, 932-934.

- Ushikubo, T., Kita, N. T., Cavosie, A. J., Wilde, S. A., Rudnick, R. L., and Valley, J. W. (2008). Lithium in Jack Hills zircons: Evidence for extensive weathering of Earth's earliest crust. Earth and Planetary Science Letters, 2723, 666-676.

- Utsunomiya, A., Ota, T., Windley, B. F., Suzuki, N., Uchio, Y., Munekata, K., and Maruyama, S. 2007. History of the Pacific superplume: implications for Pacific paleogeography since the Late Proterozoic. In Superplumes: beyond plate tectonics pp. 363-408. Springer Netherlands.

- Vallini, D. A., Cannon, W. F., Schulz, K. J. (2006). Age constraints for Paleoproterozoic glaciation in the Lake Superior Region: detrital zircon and hydrothermal xenotime ages for the Chocolay Group, Marquette Range Supergroup. Canadian Journal of Earth Sciences, 43(5), 571-591.

- Van Kranendonk, M. J., Smithies, R. H., Hickman, A. H., and Champion, D. C. (2007). .1 Paleoarchean Development of a Continental Nucleus: the East Pilbara Terrane of the Pilbara Craton, Western Australia. *Developments in Precambrian Geology*, *15*, 307-337.

- Van Schmus, W. R., de Brito Neves, B. B., Williams, I. S., Hackspacher, P. C., Fetter, A. H., Dantas, E. L., and Babinski, M. (2003). The Seridó Group of NE Brazil, a late Neoproterozoic pre-to syn-collisional basin in West Gondwana: insights from SHRIMP U–Pb detrital zircon ages and Sm–Nd crustal residence T DM ages. Precambrian Research, 1274, 287-327.

- Van Staal, C. R., Dewey, J. F., Mac Niocaill, C., and McKerrow, W. S. (1998). The Cambrian-Silurian tectonic evolution of the northern Appalachians and British Caledonides: history of a complex, west and southwest Pacific-type segment of Iapetus. *Geological Society, London, Special Publications*, *143*(1), 197-242.

- Veizer, J., and Jansen, S. L. (1985). Basement and sedimentary recycling-2: Time dimension to global tectonics. The Journal of Geology, 625-643.

- Veizer, J., and Mackenzie, F. T. (2003). Evolution of sedimentary rocks. Treatise on geochemistry, 7, 369-407.

- Vervoort, J. D., Patchett, P. J., Gehrels, G. E., and Nutman, A. P. (1996) Constraints on early Earth differentiation from hafnium and neodymium isotopes. Nature, 379, 624.

- Viljoen, R. P., and Viljoen, M. J. (1969). Evidence for the composition of the primitive mantle and its products of partial melting from a study of the rocks of the Barberton Mountain Land. *Geol. Soc. South Africa, Spec. Publ, 2*, 275-296.

- Voice, P. J., Kowalewski, M., and Eriksson, K. A. (2011). Quantifying the timing and rate of crustal evolution: global compilation of radiometrically dated detrital zircon grains. The Journal of Geology, 1192, 109-126.

- Walker, R. J., Carlson, R. W., Shirey, S. B., and Boyd, F. R. (1989). Os, Sr, Nd, and Pb isotope systematics of southern African peridotite xenoliths: implications for the chemical evolution of subcontinental mantle. *Geochimica et Cosmochimica Acta*, *53*(7), 1583-1595.

- Wang, L. J., Griffin, W. L., Yu, J. H., and O'Reilly, S. Y. (2010). Precambrian crustal evolution of the Yangtze Block tracked by detrital zircons from Neoproterozoic sedimentary rocks. Precambrian Research, 1771, 131-144.

- White, D. J., Musacchio, G., Helmstaedt, H. H., Harrap, R. M., Thurston, P. C., Van der Velden, A., and Hall, K. (2003). Images of a lower-crustal oceanic slab: Direct evidence for tectonic accretion in the Archean western Superior province. Geology, 3111, 997-1000.

- Whitmeyer, S. J., and Karlstrom, K. E. (2007). Tectonic model for the Proterozoic growth of North America. Geosphere, 34, 220-259.

- Wiedenbeck, M., Hanchar, J.M., Peck, W.H., Sylvester, P., Valley, J., Whitehouse, M., Kronz, Andreas, Morishita, Yuichi, Nasdala, Lutz, Fiebig, J., Franchi, I., Girard, J.- P., Greenwood, R.C., Hinton, R., Kita, N., Mason, P.R.D., Norman, M., Ogasawara, M., Piccoli, P.M., Rhede, D., Satoh, H., Schulz-Dobrick, B., Skår, O., Spicuzza, M.J., Terada, K., Tindle, A., Togashi, S., Vennemann, T., Xie, Q., Zheng, Y.F., (2004). Further characterisation of the 91500 zircon crystal. Geostandards and Geoanalytical Research 281, 9-39.

- Wiedenbeck, M., P. Alle, F. Corfu, W.L. Griffin, M. Meier, F. Oberli, A. von Quadt, J.C. Roddick, W. Spiegel (1995). Three natural zircon standards for U-Th-Pb, Lu-Hf, trace element and REE analyses Geostandards News Letter, 191, 1-23.

- Wilde, S. A., Valley, J. W., Peck, W. H., and Graham, C. M. (2001). Evidence from detrital zircons for the existence of continental crust and oceans on the Earth 4.4 Gyr ago. *Nature*, *409*(6817), 175.

- Wilks, M. E., and Nisbet, E. G. (1988). Stratigraphy of the Steep Rock Group, northwest Ontario: a major Archaean unconformity and Archaean stromatolites. *Canadian Journal of Earth Sciences*, *25*(3), 370-391.

- Wilson, J. F. (1979). A preliminary reappraisal of the Rhodesian basement complex. *Spec. Publ. Geol. Soc. S. Afr*, *5*, 1-23.

- Wilson, J. F., Nesbitt, R. W., and Fanning, C. M. (1995). Zircon geochronology of Archaean felsic sequences in the Zimbabwe craton: a revision of greenstone stratigraphy and a model for crustal growth. *Geological Society, London, Special Publications*, *95*(1), 109-126.

- Wilson, J. F., Orpen, J. L., Bickle, M. J., Hawkesworth, C. J., Martin, A., and Nisbet, E. G. (1978). Granite-greenstone terrains of the Rhodesian Archaean craton. *Nature*, *271*(5640), 23-27.

- Wilson, J. T. (1965). A new class of faults and their bearing on continental drift. Nature, 207(4995), 343.

- Windley, B. F., and Garde, A. A. (2009). Arc-generated blocks with crustal sections in the North Atlantic craton of West Greenland: crustal growth in the Archean with modern analogues. Earth-Science Reviews, 931, 1-30.

- Wodicka, N., St-Onge, M. R., Corrigan, D., Scott, D. J., and Whalen, J. B. (2014) Did a proto-ocean basin form along the southeastern Rae cratonic margin? Evidence from U-Pb geochronology, geochemistry (Sm-Nd and whole-rock), and stratigraphy of the Paleoproterozoic Piling group, northern Canada. Geol. Soc. America. Bull., 126, 1625-1653.

- Woodhead J. D. and Hergt J. M. (2005) A preliminary appraisal of seven natural zircon reference materials for in situ Hf isotope determination. Geostand. Geoanal. Res. 29, 183–195.

- Wyche, S. (2007): Evidence of pre-3100 Ma crust in the Youanmi and south west terranes, and eastern goldfields superterrane, of the Yilgarn craton. Developments in Precambrian Geology, 15, 113-123.

- Wyche, S., Nelson, D.R. and Riganti, A. (2004): 4350-3130 Ma detrital zircons in the Southern Cross Granite–Greenstone Terrane, Western Australia: Implications for the early evolution of the Yilgarn Craton. Australian Journal of Earth Sciences, 51, 31-45.

- Xing, G.F., Wang, X.L., Wan, Y., Chen, Z.H., Jiang, Y., Kitajima, K., Ushikubo, T. and Gopon,

P. (2014): Diversity in early crustal evolution: 4100 Ma zircons in the Cathaysia Block of southern China. Scientific Reports, 4, 5143.

- Yamamoto, S., Senshu, H., Rino, S., Omori, S., and Maruyama, S. (2009). Granite subduction: arc subduction, tectonic erosion and sediment subduction. *Gondwana Research*, *15*(3-4), 443-453.

- Yanagisawa, T., and Yamagishi, Y. 2005. Rayleigh-Benard convection in spherical shell with infinite Prandtl number at high Rayleigh number. J. Earth Simulator, 4, 11-17.

- Zeh, A., Gerdes, A., Klemd, R., and Barton Jr, J. M. (2008). U–Pb and Lu–Hf isotope record of detrital zircon grains from the Limpopo Belt–evidence for crustal recycling at the Hadean to early-Archean transition. *Geochimica et Cosmochimica Acta*, *72*(21), 5304-5329.

- Zeh, A., Gerdes, A., and Heubeck, C. (2013). U–Pb and Hf isotope data of detrital zircons from the Barberton Greenstone Belt: constraints on provenance and Archaean crustal evolution. *Journal of the Geological Society*, *170*(1), 215-223.

- Zeh, A., Stern, R. A., and Gerdes, A. (2014). The oldest zircons of Africa—Their U–Pb–Hf–O isotope and trace element systematics, and implications for Hadean to Archean crust–mantle evolution. *Precambrian Research*, *241*, 203-230.

- Zhai, M. G., and Santosh, M. (2011). The early Precambrian odyssey of the North China Craton: a synoptic overview. Gondwana Research, 201, 6-25.

- Zhang, S. H., Zhao, Y., and Santosh, M. (2012). Mid-Mesoproterozoic bimodal magmatic rocks in the northern North China Craton: implications for magmatism related to breakup of the Columbia supercontinent. Precambrian Research, 222, 339-367.

- Zhao, T. P., Zhou, M. F., Zhai, M., & Xia, B. (2002). Paleoproterozoic rift-related volcanism of the Xiong'er Group, North China craton: implications for the breakup of Columbia. International Geology Review, 44(4), 336-351.

- de Laeter, J. R., Böhlke, J. K., De Bièvre, P., Hidaka, H., Peiser, H. S., Rosman, K. J. R., and Taylor, P. D. P. (2003). "Atomic weights of the elements. Review 2000 IUPAC Technical Report." Pure and Applied Chemistry, 756, 683-800.

- de Wit, M. J., Furnes, H., and Robins, B. (2011). Geology and tectonostratigraphy of the

Onverwacht Suite, Barberton greenstone belt, South Africa. *Precambrian Research*, *186*(1-4), 1-27.

- de Wit, M. J., and Hart, R. A. (1993). Earth's earliest continental lithosphere, hydrothermal flux and crustal recycling. Lithos, 303, 309-335.
- van Hunen, J. and van den Berg, A. P. (2008). Plate tectonics on the early Earth: limitations imposed by strength and buoyancy of subducted lithosphere. Lithos, 1031, 217-235.
- von Huene, R., and Lallemand, S. (1990). Tectonic erosion along the Japan and Peru convergent margins. Geological Society of America Bulletin, 1026, 704-720.
-

Acknowledgement

I am deeply thankful to Prof. Yukio Isozaki as a supervisor. He gave me the best advice, useful discussions and selfless supports throughout five years since I was a master student. I would like to express my gratitude to Prof. Shigenori Maruyama and Prof. Yuichiro Ueno (Tokyo Institute of Technology) for helpful comments and constructive discussions until acquiring Master degree as former supervisors. I also deeply thank Dr. Yusuke Sawaki for total supporting my studies since I was an undergraduate student. I also thank them for giving me opportunities to join geological fieldwork in Ireland, Wales, United States, Canada, Mongolia, South Africa, and Zimbabwe and teaching me many aspects of geology and Earth science.

I appreciate Prof. Akira Ishikawa (Tokyo Institute of Technology), Dr. Shuhei Sakata, Prof. Tsuyoshi Ono (Gakushuin University), Dr. Yukiyasu Tsutsumi, Prof. Takashi Sano, Prof. Kenichiro Tani (National Museum of Nature and Science), Dr. Shogo Aoki (Okayama University of Science), Prof. Tsuyoshi Iizuka and Prof. Takafumi Hirata (the University of Tokyo) for supporting geochemical analysis and giving me many comments and discussions.

As to field work, I thank a lot Mr. Ernest Tafumanei Mugandani, Mr. Brian Muteta, and Mr. Two Kufahakurambwi (Geological Survey of Zimbabwe), Dr. Tomohiko Sato, Mr. Hisahiro Uyeda (Tokyo Institute of Technology), Dr. Takuya Saito, Dr. Wataru Fujisaki (JAMSTEC), Dr. Hisashi Asanuma, Dr. Yukiyasu Tsutsumi (National Museum of Nature and Science), and Dr. Uyanga Bold (the University of Tokyo).

I wish to thank Prof. Tsuyoshi Komiya and Prof. Masaki Ogawa for giving me a lot of constructive and significant comments which improved greatly my research. I also wish to thank all other members of Komaba Earth Science group; Dr. Keiko Koshida, Ms. Sena Kono, Ms. Tomoyo Tobita, Mr. Ryo Hasegawa, Mr. Hiroki Uehara, Mr. Satoshi Yoshida, Mr. Yechuan Geng, and Mr. Hiroki Sato for discussion, laboratory works, assistance, and encouragement.

Some studies in this thesis were performed using DC2 Research Fellowship for Young Scientist by JSPS (Project/Area Number 17J07214) and financial support from Academy for Global Leadership of Tokyo Institute of Technology.

I would like to thank for Mr. Koya Arikawa (Hotspring, Inc.) who gave me an opportunity to be interested in Earth science fifteen years ago. Finally, I would like to thank my parents and grandparents, Mr. Hideaki Sawada, Mrs. Yoko Sawada, Ms. Seiko Watanabe, Mr. Kazuaki Sawada, Mrs. Tazuko Sawada for financial support and patient cooperation.

Appendix

Table 3-1. LA-ICP-MS U–Pb data and calculated ages of detrital zircons in the Murmac Bay Group.

No.	spot No.	^{206}Pbc (%)	Th (ppm)	U (ppm)	Th/U	^{238}U/^{206}Pb*	1σ	^{207}Pb*/^{206}Pb*	1σ	^{238}U/^{206}Pb* age (Ma)	1σ	^{207}Pb*/^{206}Pb* age (Ma)	1σ	Concordance %
	UC02													
1	02-09059	0.21	245	403	0.62	1.444	0.013	0.3377	0.0030	3391	24	3654	13	92.8
2	02-09060	2.01	253	462	0.56	1.502	0.016	0.3265	0.0031	3290	27	3602	15	91.3
3	02-09061	19.00	123	327	0.38	1.531	0.022	0.2808	0.0091	3241	36	3369	50	96.2
4	02-09062	0.00	163	321	0.52	1.365	0.015	0.3403	0.0025	3542	30	3666	11	96.6
5	02-09063	0.04	110	526	0.21	1.328	0.012	0.3399	0.0024	3618	25	3664	11	98.8
6	02-09064	0.07	83	1196	0.07	2.415	0.023	0.2321	0.0017	2233	18	3068	11	72.8
7	02-09065	0.73	227	867	0.27	1.735	0.015	0.2774	0.0024	2934	20	3350	14	87.6
8	02-09066	3.05	439	1256	0.36	2.785	0.031	0.1772	0.0048	1978	19	2628	45	75.3
9	02-09070	4.56	244	814	0.31	1.953	0.036	0.2299	0.0121	2666	40	3053	82	87.3
10	02-09071	0.40	275	759	0.37	1.727	0.016	0.2819	0.0022	2944	22	3375	12	87.2
11	02-09072	1.03	121	306	0.41	1.390	0.018	0.3058	0.0030	3494	36	3502	15	99.8
12	02-09073	8.54	138	1332	0.11	2.651	0.089	0.1700	0.0200	2063	59	2559	184	80.6
13	02-09074	8.44	666	1372	0.50	2.703	0.029	0.1937	0.0031	2029	19	2775	26	73.1
14	02-09075	0.00	358	850	0.43	2.051	0.023	0.2655	0.0024	2560	24	3281	14	78.0
15	02-09076	0.18	240	575	0.43	1.373	0.014	0.3514	0.0025	3526	27	3714	11	95.0
16	02-09077	0.00	57	196	0.30	1.382	0.019	0.3415	0.0032	3510	37	3671	14	95.6
17	02-09081	0.00	263	420	0.64	1.384	0.016	0.3500	0.0024	3506	31	3708	11	94.5
18	02-09082	0.00	300	451	0.68	1.606	0.019	0.3025	0.0026	3121	30	3485	13	89.5
19	02-09083	0.00	237	490	0.50	1.685	0.023	0.3017	0.0023	3004	32	3481	11	86.3
20	02-09084	0.00	154	485	0.33	1.454	0.015	0.3334	0.0024	3373	27	3635	11	92.8
21	02-09085	0.00	100	585	0.18	1.499	0.017	0.3226	0.0024	3294	29	3584	11	91.9
22	02-09086	0.07	193	418	0.47	1.366	0.015	0.3297	0.0027	3540	31	3617	13	97.9
23	02-09087	0.06	147	319	0.47	1.222	0.018	0.3491	0.0028	3854	42	3705	12	104.0
24	02-09088	7.92	357	1359	0.27	3.004	0.043	0.1873	0.0083	1852	23	2720	71	68.1
25	02-09092	3.34	61	597	0.10	2.156	0.037	0.2554	0.0073	2457	35	3220	45	76.3
26	02-09093	1.45	133	331	0.41	1.357	0.014	0.3272	0.0032	3559	28	3606	15	98.7
27	02-09094	3.31	408	699	0.60	1.899	0.034	0.2753	0.0055	2727	39	3338	31	81.7
28	02-09095	0.00	284	610	0.48	2.018	0.023	0.2677	0.0021	2595	24	3294	12	78.8
29	02-09096	0.47	410	763	0.55	1.988	0.025	0.2752	0.0047	2626	27	3338	26	78.7
30	02-09097	1.59	229	464	0.51	1.819	0.027	0.3000	0.0038	2824	34	3472	19	81.3
31	02-09098	0.90	622	1019	0.63	2.739	0.051	0.2099	0.0032	2007	32	2906	24	69.0
32	02-09099	0.67	192	530	0.37	1.611	0.021	0.3018	0.0030	3113	32	3481	15	89.4
33	02-09103	2.13	112	428	0.27	1.718	0.029	0.2796	0.0037	2957	39	3362	21	88.0
34	02-09104	2.37	290	916	0.32	2.158	0.023	0.2357	0.0030	2454	22	3092	20	79.4
35	02-09105	0.01	250	594	0.43	1.664	0.019	0.2969	0.0030	3033	28	3456	15	87.8
36	02-09106	2.28	95	312	0.31	1.260	0.017	0.3410	0.0040	3766	39	3669	18	102.6
37	02-09107	0.59	341	862	0.41	1.948	0.049	0.2757	0.0051	2671	55	3340	29	80.0
38	02-09108	0.12	175	271	0.66	1.259	0.017	0.3473	0.0035	3769	38	3697	15	101.9
39	02-09109	0.00	324	553	0.60	1.372	0.015	0.3354	0.0026	3530	31	3643	12	96.9
40	02-09110	0.04	186	450	0.42	1.226	0.014	0.3462	0.0027	3845	34	3692	12	104.2
41	02-09114	8.70	122	671	0.19	1.586	0.029	0.2639	0.0153	3152	46	3272	88	96.3
42	02-09115	0.98	998	1585	0.65	3.934	0.099	0.1729	0.0038	1460	33	2587	36	56.4
43	02-09116	2.42	550	999	0.57	2.419	0.038	0.2439	0.0042	2230	29	3147	27	70.9
44	02-09117	0.00	151	399	0.39	1.781	0.022	0.2826	0.0035	2873	29	3379	19	85.0
45	02-09118	0.43	213	431	0.51	1.410	0.018	0.3252	0.0030	3456	34	3596	14	96.1
46	02-09119	0.05	52	469	0.11	1.356	0.016	0.3108	0.0024	3561	33	3526	12	101.0
47	02-09120	0.22	222	627	0.36	1.434	0.017	0.3052	0.0023	3410	31	3498	12	97.5
48	02-09121	1.70	402	640	0.64	1.769	0.030	0.2916	0.0038	2888	39	3428	20	84.3
49	02-09125	7.25	509	711	0.73	2.238	0.047	0.2795	0.0086	2381	42	3362	47	70.8
50	02-09126	4.18	162	568	0.29	1.699	0.013	0.2911	0.0028	2984	18	3425	15	87.1
51	02-09127	0.00	387	814	0.49	2.232	0.024	0.2349	0.0020	2386	21	3087	14	77.3
52	02-09128	7.82	204	1159	0.18	2.649	0.054	0.1956	0.0138	2065	36	2792	111	73.9
53	02-09129	0.58	138	308	0.46	1.298	0.012	0.3362	0.0029	3683	26	3647	13	101.0
54	02-09130	0.11	68	224	0.31	1.282	0.015	0.3397	0.0029	3717	34	3663	13	101.5
55	02-09131	3.33	171	518	0.34	1.581	0.019	0.2889	0.0048	3160	30	3413	25	92.6
56	02-09132	0.07	118	350	0.34	1.329	0.012	0.3247	0.0026	3617	25	3594	12	100.6
57	02-09136	2.21	232	485	0.49	1.689	0.027	0.2871	0.0051	2998	39	3404	27	88.1
58	02-09137	0.00	248	397	0.64	1.270	0.015	0.3528	0.0025	3745	33	3721	10	100.6
59	02-09138	0.97	147	254	0.60	1.255	0.013	0.3551	0.0034	3777	29	3731	14	101.2
60	02-09139	0.00	2901	947	3.14	2.230	0.067	0.2754	0.0031	2389	60	3339	17	71.5
61	02-09140	1.97	508	795	0.65	1.956	0.022	0.2675	0.0053	2662	24	3293	30	80.8
62	02-09141	5.90	230	523	0.45	1.638	0.045	0.2819	0.0160	3072	67	3375	86	91.0
63	02-09142	0.00	344	516	0.68	1.609	0.015	0.3023	0.0024	3116	24	3483	13	89.5
64	02-09143	21.25	535	1202	0.46	1.841	0.118	0.1414	0.0479	2797	145	2245	492	124.6

65	ma-12004	0.82	83	122	0.70	2.061	0.026	0.1752	0.0030	2550	26	2609	28	97.7
66	ma-12005	0.00	1145	1061	1.11	3.039	0.038	0.1811	0.0015	1834	20	2664	14	68.8
67	ma-12006	0.00	3916	271	14.81	3.589	0.041	0.1733	0.0019	1585	16	2591	19	61.2
68	ma-12007	0.00	203	341	0.61	2.091	0.022	0.1961	0.0020	2520	22	2795	17	90.2
69	ma-12008	0.00	328	267	1.26	2.728	0.035	0.1703	0.0018	2013	22	2562	17	78.6
70	ma-12009	0.00	137	194	0.73	2.243	0.026	0.1732	0.0019	2377	23	2590	19	91.8
71	ma-12010	0.00	144	260	0.57	1.788	0.020	0.1968	0.0018	2864	26	2801	15	102.2
72	ma-12011	0.00	64	116	0.57	2.050	0.026	0.1761	0.0026	2561	27	2618	24	97.8
73	ma-12015	0.00	239	960	0.26	3.208	0.088	0.1531	0.0013	1749	42	2382	14	73.4
74	ma-12016	8.86	163	165	1.02	2.077	0.040	0.0932	0.0056	2534	41	1493	110	169.7
75	ma-12017	0.00	939	1249	0.77	4.503	0.040	0.1465	0.0010	1293	10	2307	12	56.0
76	ma-12018	0.00	2346	1072	2.25	4.348	0.079	0.1410	0.0017	1334	22	2240	21	59.6
77	ma-12019	0.12	286	594	0.49	2.400	0.035	0.1698	0.0016	2245	28	2557	15	87.8
78	ma-12020	0.00	1793	1842	1.00	5.982	0.098	0.1281	0.0013	996	15	2073	18	48.1
79	ma-12021	0.00	1094	1154	0.97	3.644	0.052	0.1436	0.0013	1563	20	2272	15	68.8
80	ma-12022	0.00	149	181	0.84	2.442	0.075	0.1859	0.0025	2213	57	2707	23	81.7
81	ma-12026	0.97	487	575	0.87	2.972	0.038	0.1518	0.0029	1870	21	2367	32	79.0
82	ma-12027	0.00	403	571	0.72	2.598	0.026	0.1600	0.0013	2099	18	2457	14	85.4
83	ma-12028	0.00	2920	1446	2.07	11.449	0.142	0.1828	0.0017	540	6	2680	15	20.1
84	ma-12029	11.49	90	152	0.60	2.450	0.081	0.0908	0.0214	2207	62	1443	393	152.9
85	ma-12030	0.00	81	104	0.80	2.069	0.032	0.1738	0.0031	2542	33	2595	30	97.9
86	ma-12031	0.00	989	1027	0.99	4.661	0.073	0.1576	0.0016	1253	18	2431	18	51.5
87	ma-12032	0.00	484	506	0.98	3.351	0.048	0.1674	0.0016	1683	21	2533	16	66.5
88	ma-12033	5.02	59	103	0.59	2.558	0.047	0.1285	0.0042	2127	33	2079	57	102.3
89	ma-12037	0.00	259	221	1.20	2.521	0.031	0.1922	0.0021	2154	22	2763	18	78.0
90	ma-12038	0.00	733	725	1.04	3.412	0.053	0.1626	0.0013	1657	23	2484	14	66.7
91	ma-12039	0.72	158	274	0.59	2.087	0.021	0.1777	0.0023	2523	21	2633	21	95.8
92	ma-12040	0.00	2171	982	2.27	5.131	0.072	0.1612	0.0015	1148	15	2470	15	46.5
93	ma-12041	0.00	1680	1229	1.40	4.494	0.060	0.1495	0.0012	1295	16	2342	13	55.3
94	ma-12042	2.15	636	582	1.12	2.982	0.078	0.1497	0.0066	1864	42	2344	74	79.5
95	ma-12043	0.00	1185	378	3.22	3.663	0.053	0.2224	0.0028	1556	20	3000	20	51.9
96	ma-12044	15.34	720	546	1.35	4.091	0.067	0.0721	0.0125	1410	21	989	318	142.5
97	ma-12048	0.00	2348	2096	1.15	6.857	0.068	0.1276	0.0010	878	8	2067	13	42.5
98	ma-12049	0.00	3209	2411	1.37	8.644	0.105	0.1162	0.0011	706	8	1900	16	37.1
99	ma-12050	0.00	1216	1039	1.20	4.851	0.052	0.1522	0.0013	1208	12	2372	15	50.9
100	ma-12051	0.00	190	218	0.89	2.272	0.033	0.1709	0.0021	2351	29	2568	20	91.5
101	ma-12052	0.00	816	425	1.97	3.830	0.050	0.1823	0.0018	1495	17	2675	17	55.9
102	ma-12053	0.00	153	183	0.86	2.314	0.031	0.1734	0.0020	2315	26	2592	19	89.3
103	ma-12054	0.00	536	1068	0.51	4.666	0.145	0.1535	0.0028	1252	35	2386	31	52.5
104	ma-12055	0.00	575	840	0.70	3.567	0.050	0.1477	0.0013	1593	20	2320	16	68.7
105	ma-12059	0.00	1078	1009	1.10	3.968	0.038	0.1539	0.0011	1449	13	2391	11	60.6
106	ma-12060	0.00	82	254	0.33	2.142	0.025	0.1746	0.0018	2470	24	2603	17	94.9
107	ma-12061	0.23	151	543	0.29	2.432	0.027	0.1730	0.0014	2221	21	2588	14	85.8
108	ma-12062	0.00	216	409	0.54	2.251	0.027	0.1723	0.0015	2370	23	2582	14	91.8
109	ma-12063	0.00	198	292	0.70	2.622	0.033	0.2055	0.0018	2082	23	2872	14	72.5
110	ma-12064	0.00	691	308	2.31	3.448	0.052	0.1932	0.0025	1642	22	2771	21	59.2
111	ma-12065	0.31	189	226	0.86	1.936	0.025	0.1852	0.0043	2684	29	2701	38	99.4
112	ma-12066	0.00	1484	2354	0.65	4.816	0.054	0.1122	0.0008	1216	12	1836	13	66.2
113	ma-12070	0.00	1763	1314	1.38	3.481	0.062	0.1416	0.0014	1628	26	2248	16	72.4
114	ma-12071	3.67	300	608	0.51	3.864	0.080	0.2271	0.0029	1484	27	3033	21	48.9
115	ma-12072	0.00	400	434	0.94	3.604	0.131	0.1767	0.0027	1579	51	2623	25	60.2
116	ma-12073	0.27	800	725	1.13	4.163	0.050	0.1620	0.0024	1388	15	2478	25	56.0
117	ma-12074	1.65	1808	2195	0.85	7.256	0.105	0.1086	0.0025	832	11	1777	42	46.8
118	ma-12075	0.17	149	178	0.86	2.408	0.041	0.1669	0.0034	2239	32	2528	34	88.6
119	ma-12076	0.00	436	356	1.26	2.449	0.037	0.1768	0.0019	2208	28	2624	18	84.1
120	ma-12077	0.00	60	72	0.85	1.799	0.032	0.1978	0.0031	2849	40	2810	25	101.4
121	ma-12081	0.00	0	104	0.00	2.047	0.027	0.1875	0.0029	2564	28	2722	25	94.2
122	ma-12082	0.00	118	131	0.92	1.854	0.026	0.2112	0.0025	2781	32	2916	20	95.4
123	ma-12083	0.00	1454	990	1.51	3.776	0.061	0.1582	0.0012	1515	22	2437	14	62.2
124	ma-12084	2.00	243	382	0.65	2.649	0.033	0.1615	0.0032	2065	22	2472	34	83.5
125	ma-12085	0.00	625	652	0.98	3.705	0.101	0.1656	0.0015	1540	37	2515	15	61.3
126	ma-12086	0.00	3618	2935	1.26	6.418	0.066	0.1065	0.0007	934	9	1742	12	53.6
127	ma-12087	0.00	646	688	0.96	3.943	0.052	0.1783	0.0017	1457	17	2638	16	55.2
128	ma-12088	0.00	418	363	1.18	2.409	0.028	0.1760	0.0015	2239	22	2617	14	85.5
129	ma-12092	0.00	492	458	1.10	2.714	0.035	0.1689	0.0014	2022	23	2548	14	79.4
130	ma-12093	0.00	1205	791	1.56	7.665	0.114	0.1779	0.0018	790	11	2634	17	30.0
131	ma-12094	0.00	5060	1111	4.67	3.846	0.140	0.1738	0.0034	1490	48	2596	32	57.4
132	ma-12095	0.47	81	246	0.34	2.052	0.025	0.2025	0.0023	2559	26	2847	19	89.9
133	ma-12096	0.00	383	554	0.71	2.877	0.031	0.2150	0.0018	1923	18	2945	13	65.3

134	ma-12097	0.00	638	527	1.24	2.672	0.063	0.1966	0.0019	2049	41	2799	16	73.2
135	ma-12098	0.00	327	516	0.65	2.140	0.021	0.1689	0.0013	2472	20	2548	14	97.0
136	ma-12099	0.00	212	158	1.38	1.665	0.021	0.2417	0.0026	3033	31	3132	18	96.8
137	ma-12103	0.00	417	531	0.81	2.585	0.032	0.1682	0.0015	2108	22	2541	15	83.0
138	ma-12104	0.00	351	364	0.99	3.639	0.067	0.1755	0.0017	1565	25	2612	16	59.9
139	ma-12105	0.00	56	76	0.76	1.960	0.035	0.1852	0.0028	2658	39	2701	25	98.4
140	ma-12106	0.00	483	406	1.22	2.490	0.038	0.1682	0.0019	2176	28	2541	19	85.6
141	ma-12107	0.00	56	103	0.56	2.083	0.036	0.1884	0.0031	2527	36	2730	26	92.6
142	ma-12108	0.00	833	1405	0.61	4.045	0.101	0.1518	0.0015	1424	32	2367	17	60.2
143	ma-12109	1.42	292	971	0.31	3.066	0.034	0.1379	0.0019	1820	17	2202	23	82.6
144	ma-12110	0.00	30	51	0.59	1.992	0.040	0.1975	0.0040	2622	43	2807	33	93.4
145	ma-12114	0.38	46	61	0.78	2.011	0.033	0.1756	0.0045	2602	35	2613	42	99.6
146	ma-12115	0.00	202	295	0.70	1.999	0.030	0.1941	0.0019	2615	33	2778	16	94.1
147	ma-12116	0.00	1456	1479	1.01	5.843	0.070	0.1449	0.0012	1018	11	2287	15	44.5
148	ma-12117	0.08	111	322	0.35	2.302	0.024	0.1640	0.0017	2325	20	2499	17	93.0
149	ma-12118	0.00	505	449	1.15	2.499	0.033	0.1754	0.0017	2170	24	2611	16	83.1
150	ma-12119	0.00	52	69	0.77	1.930	0.037	0.1877	0.0030	2691	42	2723	26	98.8
151	ma-12120	0.00	294	135	2.23	2.187	0.031	0.1708	0.0024	2427	28	2566	24	94.6
152	ma-12121	0.00	483	753	0.66	3.156	0.034	0.1552	0.0012	1774	16	2406	13	73.7
153	ma-12125	0.00	180	172	1.07	2.134	0.027	0.1769	0.0021	2477	26	2625	20	94.4
154	ma-12126	0.00	807	1018	0.81	3.674	0.036	0.1566	0.0012	1552	14	2421	13	64.1
155	ma-12127	0.00	548	500	1.13	2.484	0.026	0.1757	0.0015	2181	19	2614	14	83.4
156	ma-12128	0.00	76	120	0.65	2.071	0.043	0.1839	0.0030	2540	44	2690	26	94.4
157	ma-12129	0.00	254	191	1.36	2.495	0.035	0.1873	0.0022	2172	26	2720	20	79.9
158	ma-12130	0.00	214	215	1.02	1.946	0.034	0.2014	0.0020	2673	38	2839	16	94.2
159	ma-12131	0.00	308	280	1.13	1.958	0.020	0.2066	0.0019	2659	23	2880	15	92.3
160	ma-12132	0.00	109	111	1.01	1.845	0.026	0.2053	0.0026	2792	32	2870	21	97.3
161	ma-12136	0.15	515	606	0.87	2.767	0.031	0.1708	0.0030	1989	19	2567	29	77.5
162	ma-12137	0.00	153	86	1.82	2.262	0.028	0.1758	0.0027	2360	24	2615	26	90.2
163	ma-12138	0.00	5857	1611	3.73	15.059	0.212	0.1633	0.0017	414	6	2492	18	16.6
164	ma-12139	0.00	1917	1524	1.29	5.671	0.078	0.1391	0.0012	1047	13	2217	15	47.2
165	ma-12140	0.00	1349	1303	1.06	6.010	0.063	0.1492	0.0013	992	10	2338	15	42.4
166	ma-12141	1.79	391	704	0.57	4.376	0.055	0.1445	0.0021	1327	15	2283	25	58.1
167	ma-12142	0.00	156	93	1.72	2.091	0.033	0.1729	0.0025	2520	33	2587	24	97.4
168	ma-12143	0.00	139	83	1.71	1.982	0.030	0.1730	0.0030	2634	33	2588	29	101.8
169	ma-12147	0.00	181	346	0.53	2.375	0.027	0.1705	0.0017	2265	22	2564	17	88.3
170	ma-12148	0.25	118	228	0.53	2.024	0.018	0.1715	0.0023	2588	19	2573	22	100.6
171	ma-12149	0.00	1447	1434	1.04	4.893	0.075	0.1313	0.0013	1199	17	2116	18	56.6
172	ma-12150	0.42	72	279	0.27	2.084	0.025	0.1640	0.0017	2526	25	2499	17	101.1
173	ma-12151	0.00	488	358	1.40	2.445	0.024	0.1710	0.0016	2210	18	2569	15	86.0
174	ma-12152	0.00	376	650	0.59	3.169	0.039	0.1591	0.0016	1768	19	2448	17	72.2
175	ma-12153	0.00	145	329	0.45	2.140	0.027	0.1938	0.0016	2472	26	2776	14	89.0
176	ma-12154	0.00	68	107	0.65	2.190	0.033	0.1836	0.0024	2424	30	2687	22	90.2
177	ma-12158	0.00	1024	954	1.10	3.971	0.053	0.1589	0.0016	1448	17	2445	17	59.2
178	ma-12159	0.00	969	1194	0.83	3.982	0.049	0.1403	0.0014	1444	16	2232	17	64.7
179	ma-12160	0.00	47	76	0.63	1.914	0.040	0.1855	0.0029	2710	47	2704	26	100.2
180	ma-12161	0.00	407	863	0.48	2.852	0.055	0.1593	0.0015	1938	32	2450	15	79.1
181	ma-12162	2.43	60	125	0.49	2.108	0.066	0.1629	0.0049	2503	65	2488	49	100.6
182	ma-12163	0.23	116	332	0.36	2.230	0.028	0.1709	0.0022	2389	25	2568	21	93.0
183	ma-12164	0.00	111	45	2.54	2.032	0.052	0.1875	0.0038	2580	55	2722	33	94.8
184	ma-12165	0.00	122	137	0.92	2.137	0.030	0.1778	0.0024	2475	28	2634	22	94.0
185	ma-12169	0.72	213	217	1.01	1.963	0.023	0.1756	0.0027	2654	25	2613	25	101.6
186	ma-12170	0.14	68	127	0.56	1.598	0.019	0.2523	0.0030	3132	30	3201	18	97.8
187	ma-12171	0.00	1144	661	1.78	2.733	0.040	0.1715	0.0015	2010	25	2574	14	78.1
188	ma-12172	0.27	177	267	0.68	2.120	0.026	0.1758	0.0025	2491	25	2615	23	95.3
189	ma-12173	2.45	864	958	0.93	9.529	0.158	0.1582	0.0035	643	10	2438	38	26.4
190	ma-12174	0.00	210	355	0.61	1.951	0.021	0.1747	0.0016	2667	23	2605	15	102.4
191	ma-12175	0.00	1895	1166	1.67	3.956	0.150	0.1900	0.0036	1453	49	2743	31	53.0
192	ma-12176	0.00	359	342	1.07	2.285	0.024	0.1741	0.0015	2340	20	2599	15	90.0
193	ma-12180	0.47	103	162	0.65	1.868	0.022	0.1936	0.0025	2764	26	2774	21	99.7
194	ma-12181	0.00	5381	1203	4.59	9.003	0.119	0.2287	0.0024	679	8	3044	17	22.3
195	ma-12182	0.00	178	295	0.62	2.022	0.023	0.1725	0.0018	2591	24	2584	17	100.3
196	ma-12183	0.00	288	678	0.44	2.577	0.031	0.1710	0.0021	2113	21	2569	20	82.3
197	ma-12184	0.00	1957	1073	1.87	3.311	0.055	0.1540	0.0015	1701	25	2392	17	71.1
198	ma-12185	0.00	2703	402	6.90	3.957	0.054	0.1998	0.0023	1452	18	2825	19	51.4
199	ma-12186	0.00	3370	1608	2.15	7.503	0.132	0.1955	0.0021	807	13	2791	17	28.9
200	ma-12187	0.00	267	255	1.08	2.197	0.027	0.1826	0.0019	2418	25	2678	17	90.3
201	ma-12191	0.00	74	83	0.92	1.918	0.032	0.1936	0.0029	2705	37	2774	24	97.5
202	ma-12192	0.00	311	167	1.91	2.557	0.054	0.2080	0.0027	2128	38	2891	22	73.6

203	ma-12193	4.01	181	315	0.59	3.692	0.097	0.1497	0.0040	1545	36	2344	45	65.9
204	ma-12194	0.00	116	177	0.67	2.195	0.027	0.1726	0.0023	2420	25	2584	22	93.6
205	ma-12195	0.00	890	752	1.21	2.604	0.049	0.1692	0.0017	2095	33	2551	17	82.1
206	ma-12196	0.00	85	138	0.63	1.905	0.042	0.2156	0.0028	2720	49	2949	21	92.2
207	ma-12197	0.00	2557	2347	1.12	10.446	0.140	0.1386	0.0014	589	8	2211	17	26.7
208	ma-12198	0.00	1188	673	1.81	3.420	0.071	0.1679	0.0018	1654	30	2538	18	65.2
209	ma-12202	0.00	1524	671	2.33	2.895	0.057	0.1691	0.0013	1913	33	2550	13	75.0
210	ma-12203	0.00	1010	963	1.08	3.330	0.041	0.1509	0.0015	1693	18	2357	17	71.8
211	ma-12204	0.28	98	136	0.74	2.130	0.028	0.1739	0.0032	2481	27	2596	30	95.6
212	ma-12205	0.00	214	617	0.36	2.525	0.039	0.1582	0.0016	2151	28	2438	17	88.2
213	ma-12206	0.00	1823	773	2.42	5.142	0.114	0.1741	0.0022	1146	23	2599	21	44.1
214	ma-12207	3.25	161	258	0.64	2.216	0.031	0.1462	0.0041	2401	28	2303	47	104.2
215	ma-12208	0.00	47	95	0.51	1.989	0.036	0.2021	0.0026	2626	40	2844	21	92.3
216	ma-12209	1.30	59	204	0.29	2.169	0.031	0.1814	0.0026	2444	29	2667	24	91.6
217	mb-12004	0.00	381	172	2.28	2.154	0.025	0.2116	0.0023	2458	23	2919	18	84.2
218	mb-12005	0.00	117	386	0.31	2.043	0.033	0.1695	0.0015	2568	34	2554	15	100.5
219	mb-12006	0.00	541	1360	0.41	3.753	0.047	0.1489	0.0012	1523	17	2334	14	65.2
220	mb-12007	0.00	1232	998	1.27	3.687	0.044	0.1454	0.0013	1547	16	2294	15	67.4
221	mb-12008	0.00	251	266	0.97	2.202	0.027	0.1758	0.0019	2414	25	2615	17	92.3
222	mb-12009	0.00	785	884	0.91	3.372	0.075	0.1634	0.0017	1674	33	2493	17	67.2
223	mb-12010	0.00	65	80	0.83	1.878	0.037	0.2071	0.0038	2752	44	2884	29	95.4
224	mb-12011	0.00	1560	1488	1.08	5.088	0.071	0.1455	0.0013	1157	15	2295	16	50.4
225	mb-12015	0.00	3428	844	4.17	5.212	0.066	0.2058	0.0019	1131	13	2874	15	39.4
226	mb-12016	0.00	298	289	1.06	2.496	0.030	0.1710	0.0018	2172	22	2569	17	84.6
227	mb-12017	0.00	11	26	0.42	1.704	0.040	0.2505	0.0054	2977	55	3189	34	93.3
228	mb-12018	0.00	46	84	0.57	1.980	0.037	0.1847	0.0026	2635	40	2697	23	97.7
229	mb-12019	0.00	189	264	0.73	2.091	0.025	0.1766	0.0017	2520	25	2622	16	96.1
230	mb-12020	0.00	175	184	0.97	2.362	0.032	0.1784	0.0024	2276	26	2639	23	86.2
231	mb-12021	0.00	355	457	0.80	3.151	0.053	0.1919	0.0024	1777	26	2760	20	64.4
232	mb-12022	0.00	835	310	2.76	2.846	0.042	0.1754	0.0018	1941	25	2611	17	74.3
233	mb-12026	0.00	3109	2232	1.43	4.102	0.046	0.1126	0.0009	1406	14	1843	15	76.3
234	mb-12027	0.00	506	507	1.02	2.619	0.036	0.1749	0.0017	2085	25	2606	16	80.0
235	mb-12028	0.00	1414	1647	0.88	5.313	0.110	0.1297	0.0016	1112	21	2095	21	53.1
236	mb-12029	0.00	829	1475	0.58	3.855	0.064	0.1358	0.0015	1487	22	2175	19	68.4
237	mb-12030	0.00	475	496	0.98	3.898	0.095	0.1633	0.0019	1472	32	2492	20	59.1
238	mb-12031	0.00	451	459	1.01	2.642	0.040	0.1750	0.0017	2069	27	2607	16	79.4
239	mb-12032	0.00	22	49	0.46	1.961	0.043	0.2091	0.0042	2657	48	2900	32	91.6
240	mb-12033	0.34	88	141	0.64	2.310	0.035	0.1866	0.0039	2319	29	2714	34	85.4
241	mb-12037	0.00	95	131	0.74	1.936	0.037	0.1741	0.0025	2685	42	2599	23	103.3
242	mb-12038	0.15	126	376	0.34	2.250	0.030	0.1708	0.0017	2370	26	2566	17	92.4
243	mb-12039	0.00	322	399	0.83	2.301	0.026	0.1670	0.0018	2327	22	2529	18	92.0
244	mb-12040	0.00	231	266	0.89	2.274	0.040	0.1774	0.0024	2350	34	2630	22	89.3
245	mb-12041	18.53	766	1058	0.74	9.074	0.473	0.0531	0.0118	674	33	332	438	203.0
246	mb-12042	0.00	1232	922	1.37	3.163	0.057	0.1534	0.0015	1771	28	2385	16	74.3
247	mb-12043	3.00	242	110	2.25	1.922	0.035	0.1855	0.0078	2700	40	2704	68	99.9
248	mb-12044	0.00	209	98	2.19	2.218	0.046	0.1889	0.0033	2399	42	2734	29	87.7
249	mb-12048	0.00	378	309	1.26	5.722	0.285	0.1921	0.0024	1038	48	2762	20	37.6
250	mb-12049	0.00	1083	999	1.11	4.147	0.063	0.1559	0.0015	1393	19	2413	16	57.7
251	mb-12050	0.00	1098	1262	0.89	6.307	0.097	0.1498	0.0017	949	14	2344	20	40.5
252	mb-12051	5.53	166	148	1.15	2.845	0.063	0.1351	0.0073	1942	37	2167	92	89.6
253	mb-12052	0.00	1220	1565	0.80	4.586	0.052	0.1332	0.0012	1272	13	2142	15	59.4
254	mb-12053	0.00	500	526	0.97	3.623	0.053	0.1653	0.0019	1571	20	2512	19	62.6
255	mb-12054	0.00	1008	896	1.15	2.137	0.028	0.2384	0.0021	2474	27	3111	14	79.5
256	mb-12055	0.46	69	118	0.60	1.963	0.032	0.1846	0.0041	2654	35	2696	37	98.4
257	mb-12059	2.47	173	218	0.81	2.410	0.040	0.1551	0.0032	2237	32	2404	34	93.1
258	mb-12060	0.00	356	152	2.40	1.892	0.024	0.1887	0.0023	2736	28	2732	20	100.1
259	mb-12061	5.35	659	1209	0.56	7.452	0.179	0.1117	0.0036	812	18	1829	57	44.4
260	mb-12062	0.00	1965	2115	0.95	5.751	0.084	0.1186	0.0012	1033	14	1937	17	53.4
261	mb-12063	0.00	706	997	0.73	3.297	0.104	0.1435	0.0015	1708	47	2271	18	75.2
262	mb-12064	0.00	684	890	0.79	3.448	0.043	0.1742	0.0019	1642	18	2600	18	63.1
263	mb-12065	0.00	365	418	0.90	2.233	0.024	0.1804	0.0017	2386	22	2658	16	89.8
264	mb-12066	0.00	447	231	1.98	3.190	0.089	0.2004	0.0027	1758	43	2831	22	62.1
265	mb-12069	0.00	892	644	1.42	3.938	0.362	0.1610	0.0018	1459	120	2467	19	59.1
266	mb-12070	0.00	66	115	0.59	2.967	0.274	0.1764	0.0030	1872	150	2621	28	71.4
267	mb-12071	0.00	102	147	0.71	3.461	0.320	0.1872	0.0026	1636	134	2719	23	60.2
268	mb-12072	0.00	402	308	1.34	3.606	0.329	0.1752	0.0017	1578	128	2609	17	60.5
269	sc-12073	5.32	223	452	0.51	6.442	0.595	0.1364	0.0032	930	80	2183	40	42.6
270	sc-12074	0.00	441	450	1.01	3.491	0.321	0.1599	0.0015	1624	132	2456	16	66.1
271	sc-12075	0.00	433	254	1.75	3.261	0.297	0.1748	0.0018	1724	138	2605	18	66.2

272	sc-12076	0.31	97	474	0.21	3.439	0.314	0.1507	0.0017	1646	133	2355	19	69.9
273	sc-12077	0.00	413	368	1.15	6.058	0.580	0.1787	0.0021	985	87	2642	19	37.3
274	sc-12081	0.00	191	305	0.64	3.238	0.302	0.1707	0.0017	1735	142	2566	16	67.6
275	sc-12082	0.00	201	290	0.71	2.999	0.280	0.1895	0.0016	1855	151	2739	14	67.7
276	sc-12083	0.00	40	81	0.51	2.823	0.267	0.1937	0.0032	1955	159	2775	27	70.4
277	sc-12084	0.00	351	208	1.73	3.635	0.340	0.1696	0.0022	1567	130	2555	21	61.3
278	sc-12085	0.00	275	309	0.91	4.122	0.393	0.1701	0.0018	1400	120	2560	18	54.7
279	sc-12086	0.00	1514	1109	1.40	6.021	0.562	0.1568	0.0019	990	86	2423	20	40.9
280	sc-12087	0.00	374	205	1.87	3.904	0.370	0.1714	0.0021	1470	125	2572	20	57.2
281	sc-12088	0.00	36	90	0.41	1.976	0.034	0.1948	0.0035	2640	38	2784	29	94.8
282	sc-12092	0.00	612	978	0.64	4.888	0.053	0.1490	0.0015	1200	12	2336	17	51.4
283	sc-12093	0.00	371	484	0.79	2.283	0.023	0.1707	0.0015	2342	20	2566	15	91.3
284	sc-12094	0.00	401	189	2.17	2.076	0.026	0.1956	0.0021	2535	26	2791	18	90.8
285	sc-12095	0.26	98	225	0.45	2.202	0.029	0.1706	0.0023	2414	27	2565	23	94.1
286	sc-12096	0.00	391	196	2.04	2.065	0.032	0.1776	0.0020	2545	33	2632	19	96.7
287	sc-12097	0.00	828	602	1.41	5.408	0.110	0.1895	0.0022	1094	20	2739	19	39.9
288	sc-12098	0.00	598	382	1.61	3.165	0.039	0.1854	0.0019	1770	19	2703	17	65.5
289	sc-12099	0.00	354	302	1.20	2.644	0.086	0.1867	0.0020	2068	57	2715	17	76.2
290	sc-12103	0.00	460	533	0.88	3.244	0.087	0.1649	0.0017	1732	41	2508	18	69.1
291	sc-12104	0.32	313	408	0.79	2.220	0.025	0.1656	0.0034	2397	22	2515	34	95.3
292	sc-12105	0.00	393	295	1.36	1.948	0.025	0.1861	0.0020	2671	28	2709	17	98.6
293	sc-12106	4.79	99	164	0.62	3.098	0.067	0.1311	0.0116	1803	34	2113	148	85.3
294	sc-12107	0.00	207	317	0.67	1.938	0.034	0.1969	0.0025	2682	39	2802	21	95.7
295	sa-12004	0.00	164	362	0.46	2.465	0.047	0.1710	0.0022	2195	36	2569	21	85.5
296	sa-12005	0.00	365	433	0.87	2.412	0.054	0.1832	0.0026	2236	42	2684	23	83.3
297	sa-12006	0.00	548	573	0.98	3.147	0.086	0.1696	0.0032	1779	43	2555	31	69.6
298	sa-12007	0.29	429	497	0.89	2.739	0.080	0.1629	0.0051	2006	50	2487	52	80.7
299	sa-12008	1.02	384	311	1.27	2.083	0.059	0.1791	0.0069	2528	59	2646	63	95.5
300	sa-12009	0.88	278	190	1.50	2.496	0.062	0.1932	0.0079	2172	46	2771	65	78.4
301	sa-12010	0.00	1456	574	2.60	3.628	0.084	0.1685	0.0027	1569	32	2544	27	61.7
302	sa-12011	0.00	3251	1677	1.99	6.026	0.125	0.1394	0.0019	990	19	2220	23	44.6
303	sa-12015	0.00	882	571	1.59	3.439	0.158	0.2022	0.0032	1645	67	2846	25	57.8
304	sa-12016	0.00	416	357	1.20	2.769	0.059	0.1685	0.0025	1988	36	2544	25	78.1
305	sa-12017	0.00	5159	804	6.58	6.178	0.140	0.1702	0.0020	967	20	2561	19	37.8
306	sa-12018	0.00	627	416	1.55	2.672	0.052	0.1759	0.0024	2049	34	2615	23	78.4
307	sa-12019	0.03	136	273	0.51	2.052	0.032	0.1731	0.0023	2559	33	2589	22	98.9
308	sa-12020	0.00	2272	884	2.64	4.321	0.091	0.1669	0.0022	1342	26	2528	22	53.1
309	sa-12021	0.00	2296	1864	1.26	5.376	0.066	0.1278	0.0012	1100	12	2069	17	53.2
310	sa-12022	1.75	150	237	0.65	2.605	0.047	0.1656	0.0032	2094	32	2514	33	83.3
311	sa-12026	0.00	49	218	0.23	2.030	0.031	0.1761	0.0022	2581	32	2618	20	98.6
312	sa-12027	0.00	106	117	0.94	2.335	0.028	0.1882	0.0022	2298	24	2728	19	84.2
313	sa-12028	0.42	110	237	0.48	1.912	0.022	0.1686	0.0019	2712	25	2545	19	106.5
314	sa-12029	0.00	385	439	0.90	2.871	0.057	0.1592	0.0016	1926	33	2449	17	78.7
315	sa-12030	0.00	258	171	1.55	2.103	0.028	0.1850	0.0021	2508	28	2700	18	92.9
316	sa-12031	0.18	25	49	0.52	1.670	0.023	0.2329	0.0043	3024	34	3073	30	98.4
317	sa-12032	0.00	28	40	0.71	1.842	0.032	0.2211	0.0038	2796	40	2990	27	93.5
318	sa-12033	0.00	903	433	2.14	3.653	0.102	0.2035	0.0033	1560	39	2856	26	54.6
319	sa-12037	0.00	14483	1477	10.06	8.979	0.218	0.1620	0.0016	681	16	2478	17	27.5
320	sa-12038	1.12	88	110	0.82	2.042	0.037	0.1664	0.0045	2569	38	2523	44	101.8
321	sa-12039	0.00	121	104	1.20	1.799	0.029	0.2067	0.0030	2849	37	2881	23	98.9
322	sa-12040	0.00	130	138	0.97	2.111	0.031	0.1912	0.0027	2500	31	2754	23	90.8
323	sa-12041	0.00	1092	752	1.49	2.719	0.032	0.1663	0.0014	2019	21	2522	14	80.0
324	sa-12042	0.00	3071	343	9.17	4.202	0.069	0.1883	0.0021	1376	20	2729	19	50.4
325	sa-12043	0.00	72	89	0.83	1.648	0.023	0.2269	0.0028	3057	34	3031	20	100.9
326	sa-12044	0.00	419	816	0.53	3.038	0.108	0.1715	0.0027	1835	57	2574	26	71.3
327	sa-12048	0.00	831	688	1.24	3.406	0.079	0.1671	0.0026	1659	34	2530	26	65.6
328	sa-12049	0.00	2534	628	4.14	5.415	0.150	0.1823	0.0026	1092	28	2675	23	40.8
329	sa-12050	2.11	2661	3769	0.72	12.486	0.177	0.1051	0.0028	497	7	1718	48	28.9
330	sa-12051	0.00	423	577	0.75	2.924	0.059	0.1757	0.0029	1896	33	2614	27	72.5
331	sa-12052	0.00	108	134	0.83	1.812	0.033	0.2110	0.0032	2832	42	2914	25	97.2
332	sa-12053	0.00	752	298	2.59	3.229	0.070	0.1853	0.0028	1739	33	2703	24	64.3
333	sa-12054	0.00	138	143	0.99	2.528	0.043	0.1693	0.0028	2149	31	2552	28	84.2
334	sa-12055	0.00	608	297	2.10	2.694	0.058	0.1819	0.0017	2035	37	2672	15	76.1
335	sa-12059	0.00	30	682	0.05	1.833	0.021	0.2027	0.0018	2807	25	2849	15	98.5
336	sa-12060	0.00	93	97	0.98	1.870	0.037	0.1979	0.0030	2761	44	2810	25	98.3
337	sa-12061	0.75	218	209	1.07	1.976	0.038	0.1790	0.0044	2640	42	2645	40	99.8
338	sa-12062	0.00	254	311	0.84	2.635	0.097	0.2142	0.0043	2074	65	2939	32	70.6
339	sa-12063	0.00	152	277	0.56	2.725	0.090	0.1747	0.0036	2015	57	2604	35	77.4
340	sa-12064	0.00	330	311	1.09	2.488	0.055	0.1945	0.0030	2178	41	2782	25	78.3

341	sa-12065	0.00	1236	440	2.88	3.094	0.060	0.2176	0.0032	1805	31	2964	23	60.9
342	sa-12066	2.13	67	102	0.67	1.917	0.025	0.1647	0.0035	2706	29	2506	35	108.0
343	sb-12004	0.00	451	446	1.04	2.714	0.045	0.1616	0.0017	2022	29	2473	18	81.8
344	sb-12005	0.00	776	699	1.14	3.544	0.097	0.1660	0.0018	1602	39	2519	18	63.6
345	sb-12006	0.72	295	302	1.00	2.380	0.040	0.1748	0.0043	2261	32	2605	41	86.8
346	sb-12007	0.00	667	859	0.80	3.016	0.069	0.1594	0.0029	1846	37	2451	30	75.3
347	sb-12008	0.00	299	364	0.84	2.157	0.055	0.1736	0.0032	2455	52	2594	30	94.7
348	sb-12009	0.00	1175	455	2.65	2.509	0.055	0.1864	0.0032	2162	41	2712	28	79.7
349	sb-12010	0.00	122	179	0.70	2.008	0.049	0.1724	0.0036	2605	53	2583	34	100.9
350	sb-12011	0.00	1413	446	3.25	4.022	0.097	0.1840	0.0033	1431	31	2690	30	53.2
351	sb-12015	0.67	144	211	0.70	2.018	0.045	0.1811	0.0046	2595	48	2664	42	97.4
352	sb-12016	0.00	55	73	0.77	2.065	0.062	0.1988	0.0051	2546	63	2818	41	90.3
353	sb-12017	0.00	3149	531	6.08	5.282	0.094	0.1807	0.0025	1118	18	2660	23	42.0
354	sb-12018	0.00	49	133	0.38	2.003	0.044	0.1761	0.0033	2610	47	2618	31	99.7
355	sb-12019	0.00	187	236	0.82	1.859	0.031	0.1853	0.0024	2774	37	2702	21	102.7
356	sb-12020	0.00	686	382	1.84	2.506	0.065	0.1721	0.0031	2165	48	2580	30	83.9
357	sb-12021	0.00	664	405	1.68	2.255	0.036	0.1691	0.0021	2366	32	2550	21	92.8
358	sb-12022	0.00	223	334	0.68	1.860	0.033	0.1902	0.0026	2774	40	2745	22	101.1
359	sb-12026	0.00	207	145	1.46	2.213	0.035	0.1801	0.0020	2404	32	2655	18	90.5
360	sb-12027	1.31	68	116	0.60	1.932	0.035	0.1634	0.0046	2689	40	2493	47	107.9
361	sb-12028	0.00	46	58	0.80	1.981	0.036	0.1805	0.0036	2634	40	2659	32	99.1
362	sb-12029	0.00	189	243	0.80	2.396	0.041	0.1935	0.0028	2248	32	2774	23	81.0
363	sb-12030	0.00	222	244	0.93	1.787	0.024	0.2055	0.0025	2865	31	2872	19	99.8
364	sb-12031	1.41	100	124	0.83	1.966	0.032	0.1961	0.0048	2650	36	2795	40	94.8
365	sb-12032	0.00	746	262	2.92	3.769	0.097	0.1995	0.0034	1517	35	2823	28	53.7
366	sb-12033	0.00	84	121	0.72	1.883	0.039	0.1898	0.0035	2746	47	2741	30	100.2
367	sb-12037	1.49	233	435	0.55	2.247	0.030	0.1766	0.0043	2373	26	2623	40	90.5
368	sb-12038	0.00	241	213	1.16	1.975	0.024	0.1755	0.0016	2641	27	2612	15	101.1
369	sb-12039	0.21	65	180	0.37	2.110	0.037	0.1621	0.0034	2500	37	2478	35	100.9
370	sb-12040	0.00	415	248	1.72	2.299	0.046	0.2144	0.0031	2328	39	2941	23	79.2
371	sb-12041	0.00	511	230	2.27	2.180	0.045	0.1694	0.0024	2434	42	2553	23	95.3
372	sb-12042	1.26	816	1066	0.78	3.976	0.098	0.1426	0.0030	1446	32	2261	35	64.0
373	sb-12043	0.00	422	271	1.60	2.560	0.048	0.1754	0.0024	2126	34	2611	23	81.4
374	sb-12044	2.56	358	360	1.02	4.197	0.094	0.1457	0.0051	1378	28	2297	60	60.0

UC03

1	03-09004	0.00	1310	1372	0.98	2.972	0.025	0.1685	0.0011	1869	14	2544	11	73.5
2	03-09005	0.00	703	1254	0.58	2.646	0.038	0.1780	0.0026	2067	26	2636	24	78.4
3	03-09006	0.01	776	1211	0.66	2.467	0.021	0.2075	0.0019	2194	16	2887	15	76.0
4	03-09007	0.00	1006	1533	0.67	2.200	0.027	0.2179	0.0016	2415	25	2967	12	81.4
5	03-09008	1.22	609	1236	0.51	2.779	0.033	0.1999	0.0021	1981	20	2827	17	70.1
6	03-09009	0.00	718	1040	0.71	2.143	0.027	0.2301	0.0020	2468	26	3054	14	80.8
7	03-09010	4.73	398	919	0.44	2.219	0.036	0.2194	0.0035	2398	32	2978	25	80.5
8	03-09011	5.69	1188	1470	0.83	2.128	0.070	0.2105	0.0080	2483	68	2911	61	85.3
9	03-09015	0.23	983	1338	0.75	2.111	0.022	0.2102	0.0017	2500	22	2908	13	86.0
10	03-09016	0.00	594	796	0.77	1.729	0.014	0.2538	0.0014	2942	20	3210	9	91.7
11	03-09017	0.94	30	557	0.06	1.844	0.017	0.2232	0.0017	2793	21	3005	13	92.9
12	03-09018	0.52	401	582	0.71	1.815	0.016	0.2464	0.0019	2829	20	3163	12	89.4
13	03-09019	2.69	177	769	0.24	2.543	0.028	0.1934	0.0019	2138	20	2773	16	77.1
14	03-09020	0.04	838	1279	0.67	2.549	0.022	0.1948	0.0017	2134	16	2784	15	76.6
15	03-09021	0.00	2301	1278	1.85	2.767	0.043	0.1788	0.0019	1989	26	2643	17	75.3
16	03-09022	0.00	125	270	0.48	1.671	0.019	0.2218	0.0019	3023	28	2995	14	101.0
17	03-09026	0.00	525	848	0.64	1.597	0.014	0.2679	0.0019	3135	22	3295	11	95.1
18	03-09027	0.00	58	755	0.08	1.812	0.015	0.2210	0.0015	2833	19	2989	12	94.8
19	03-09028	0.32	459	916	0.51	1.839	0.020	0.2609	0.0019	2800	24	3254	11	86.0
20	03-09029	10.94	519	546	0.98	1.927	0.025	0.2296	0.0046	2695	28	3051	32	88.3
21	03-09030	0.45	666	1260	0.54	1.976	0.020	0.2314	0.0019	2640	22	3063	13	86.2
22	03-09031	0.00	4941	755	6.71	2.152	0.030	0.2147	0.0017	2461	29	2943	12	83.6
23	03-09032	0.18	895	1422	0.65	2.717	0.028	0.1847	0.0016	2020	18	2697	14	74.9
24	03-09033	0.00	1056	1629	0.66	2.852	0.032	0.1853	0.0020	1937	19	2702	18	71.7
25	03-09037	0.00	1264	1674	0.77	1.868	0.023	0.2264	0.0014	2763	27	3028	10	91.3
26	03-09038	3.38	1886	2232	0.87	2.549	0.028	0.1705	0.0053	2133	20	2564	51	83.2
27	03-09039	0.26	655	1102	0.61	1.791	0.017	0.2373	0.0018	2860	21	3104	12	92.1
28	03-09040	1.95	201	669	0.31	1.710	0.022	0.2300	0.0023	2968	31	3054	16	97.2
29	03-09041	0.08	1258	1936	0.67	3.141	0.036	0.1763	0.0016	1782	18	2620	14	68.0
30	03-09042	0.48	225	331	0.70	1.543	0.016	0.2721	0.0025	3221	26	3320	14	97.0
31	03-09043	0.00	382	574	0.68	2.882	0.058	0.1688	0.0023	1920	33	2548	22	75.4
32	03-09044	0.00	940	1427	0.68	2.345	0.038	0.2117	0.0021	2289	31	2920	16	78.4
33	03-09048	0.00	511	777	0.67	1.672	0.016	0.2566	0.0021	3023	23	3228	12	93.6

34	03-09049	1.49	399	815	0.50	1.801	0.018	0.2351	0.0022	2847	23	3088	15	92.2
35	03-09050	0.00	1137	1638	0.71	3.151	0.027	0.1449	0.0010	1777	14	2288	12	77.6
36	03-09051	0.00	2853	799	3.66	2.156	0.033	0.3782	0.0155	2456	31	3826	61	64.2
37	03-09052	0.00	618	987	0.64	1.921	0.020	0.2391	0.0020	2702	23	3115	13	86.7
38	03-09053	0.77	208	312	0.68	1.581	0.015	0.2608	0.0024	3160	24	3253	14	97.1
39	03-09054	0.11	411	695	0.61	1.471	0.012	0.2744	0.0019	3343	21	3333	11	100.3
40	03-09055	0.00	657	1048	0.64	1.804	0.022	0.2479	0.0018	2843	29	3173	11	89.6
	UC09													
1	09-01	1.25	412	1933	0.22	3.650	0.040	0.1113	0.0009	1561	15	1822	15	85.7
2	09-03	0.44	273	2235	0.13	5.300	0.145	0.1051	0.0012	1114	28	1718	20	64.9
3	09-04	0.55	152	693	0.23	1.867	0.017	0.2032	0.0017	2765	21	2853	14	96.9
4	09-05	2.92	511	1711	0.31	2.530	0.023	0.1644	0.0016	2147	17	2502	16	85.8
5	09-06	0.00	365	832	0.45	1.958	0.037	0.2006	0.0017	2659	41	2832	14	93.9
6	09-07	2.16	208	607	0.35	1.883	0.018	0.1998	0.0023	2746	21	2826	19	97.2
7	09-08	1.39	327	1161	0.29	2.268	0.026	0.1790	0.0018	2355	23	2645	16	89.0
8	09-09	1.10	282	958	0.30	2.482	0.027	0.1614	0.0016	2182	20	2471	17	88.3
9	09-10	0.00	148	736	0.21	1.811	0.018	0.2105	0.0017	2834	23	2911	12	97.4
10	09-11	5.28	333	976	0.35	2.685	0.038	0.1358	0.0028	2041	25	2175	36	93.8
11	09-12	1.12	81	841	0.10	1.784	0.020	0.2056	0.0017	2869	26	2873	13	99.9
12	09-13	0.00	382	1233	0.32	3.675	0.065	0.1735	0.0029	1551	24	2593	28	59.8
13	09-14	0.00	644	1209	0.55	3.568	0.073	0.1513	0.0023	1593	29	2362	26	67.4
14	09-15	0.00	496	529	0.96	1.507	0.015	0.2729	0.0024	3281	26	3324	14	98.7
15	09-16	0.00	245	928	0.27	1.957	0.025	0.1956	0.0018	2661	28	2791	14	95.3
16	09-17	4.48	143	388	0.38	1.817	0.019	0.2024	0.0032	2826	24	2847	26	99.3
17	09-18	0.57	259	673	0.40	2.214	0.045	0.1858	0.0025	2403	41	2706	23	88.8
18	09-19	6.21	258	1235	0.21	2.151	0.028	0.1315	0.0029	2461	27	2119	38	116.2
19	09-20	1.88	270	979	0.28	2.062	0.029	0.1796	0.0025	2549	29	2651	23	96.2
20	09-21	0.00	59	942	0.06	1.911	0.020	0.1956	0.0016	2713	23	2791	13	97.2
21	09-22	29.66	771	1530	0.52	2.871	0.155	0.0709	0.0641	1927	90	955	1211	201.7
22	09-23	9.58	286	876	0.33	2.348	0.048	0.1074	0.0079	2287	40	1757	129	130.2
23	09-24	0.16	245	1017	0.25	2.015	0.027	0.1853	0.0016	2598	29	2702	14	96.2
24	09-25	1.99	311	1270	0.25	2.330	0.041	0.1563	0.0023	2302	34	2417	25	95.3
25	09-26	0.12	368	1089	0.35	2.866	0.030	0.1652	0.0018	1930	17	2511	18	76.8
26	09-27	0.03	169	854	0.20	2.065	0.027	0.1958	0.0018	2546	27	2793	15	91.1
27	09-28	22.14	192	292	0.67	2.535	0.040	0.1334	0.0112	2144	29	2144	141	100.0
28	09-29	0.00	230	1276	0.19	3.814	0.075	0.1702	0.0024	1501	26	2561	23	58.6
29	09-30	0.18	62	1125	0.06	2.485	0.036	0.1701	0.0019	2180	27	2560	19	85.2
30	09-31	0.77	275	1293	0.22	2.414	0.031	0.1604	0.0018	2234	24	2462	19	90.8
31	09-32	0.45	181	747	0.25	2.105	0.028	0.1897	0.0019	2506	28	2741	16	91.4
32	09-33	1.31	334	1200	0.29	1.965	0.022	0.1877	0.0018	2652	24	2723	16	97.4
33	09-34	1.10	307	1421	0.22	2.101	0.027	0.1738	0.0019	2509	27	2596	18	96.7
34	09-35	2.64	286	814	0.36	2.139	0.024	0.1849	0.0021	2472	23	2698	19	91.6
35	09-36	6.27	343	1297	0.27	2.640	0.032	0.1128	0.0019	2071	21	1847	31	112.1
36	09-37	33.06	597	1686	0.36	3.063	0.124	0.0868	0.0611	1821	64	1356	967	134.3
37	09-38	0.01	118	592	0.20	1.719	0.023	0.2072	0.0019	2956	32	2885	15	102.4
38	09-39	3.69	512	1518	0.35	4.099	0.052	0.1112	0.0025	1407	16	1821	40	77.3
39	09-40	19.48	384	1399	0.28	2.809	0.053	0.1223	0.0167	1963	32	1991	225	98.6
40	09-41	2.22	76	1248	0.06	2.359	0.029	0.1744	0.0019	2279	24	2601	19	87.6
41	09-42	21.65	465	1187	0.40	2.437	0.103	0.1185	0.0543	2216	79	1935	652	114.5
42	09-43	0.11	515	1400	0.38	2.653	0.032	0.1520	0.0012	2062	21	2369	14	87.0
43	09-44	5.02	367	807	0.47	1.785	0.026	0.2030	0.0078	2868	34	2852	61	100.6
44	09-45	5.10	115	894	0.13	1.875	0.021	0.1618	0.0070	2756	25	2476	71	111.3
45	09-46	0.04	213	688	0.32	1.769	0.019	0.2059	0.0016	2888	25	2875	12	100.5
46	09-47	0.00	435	1362	0.33	2.898	0.037	0.1510	0.0014	1911	21	2358	16	81.0
47	09-48	0.58	91	869	0.11	2.003	0.023	0.1992	0.0029	2611	25	2821	23	92.5
48	09-49	4.71	666	383	1.78	1.509	0.022	0.3029	0.0118	3278	38	3487	59	94.0
49	09-50	12.81	511	855	0.61	2.758	0.062	0.1330	0.0219	1994	39	2139	264	93.2
50	09-51	10.76	232	410	0.58	2.302	0.034	0.1568	0.0053	2326	29	2422	57	96.0
51	09-52	2.07	276	1395	0.20	2.509	0.030	0.1571	0.0014	2162	22	2426	15	89.1
52	09-53	0.00	166	645	0.26	1.814	0.017	0.2075	0.0015	2831	21	2888	12	98.0
53	09-54	1.14	222	1239	0.18	2.494	0.029	0.1758	0.0018	2173	22	2615	17	83.1
54	09-55	6.16	207	1461	0.15	2.890	0.037	0.1139	0.0037	1916	21	1864	57	102.8
55	09-56	0.00	320	671	0.49	2.023	0.023	0.1984	0.0016	2589	24	2814	14	92.0
56	09-57	1.20	80	337	0.24	1.662	0.019	0.2504	0.0024	3036	28	3189	15	95.2
57	09-58	0.17	85	251	0.35	1.792	0.022	0.2152	0.0024	2859	29	2946	18	97.0
58	09-59	31.13	1441	762	1.94	1.487	0.045	0.3300	0.0275	3315	78	3618	123	91.6
59	09-60	1.76	325	984	0.34	2.222	0.028	0.1699	0.0020	2395	25	2558	19	93.6
60	09-61	1.71	354	1076	0.34	2.401	0.042	0.1808	0.0024	2244	33	2661	22	84.3

61	09-62	0.06	141	872	0.17	1.957	0.029	0.1948	0.0021	2661	32	2785	17	95.5
62	09-63	0.18	275	997	0.28	2.192	0.032	0.1883	0.0020	2423	29	2728	18	88.8
63	09-64	0.66	225	687	0.34	2.096	0.023	0.1821	0.0019	2515	23	2673	18	94.1
64	09-65	3.11	261	1480	0.18	2.516	0.035	0.1355	0.0020	2157	25	2172	26	99.3
65	09-66	0.00	3225	1639	2.02	3.205	0.053	0.1394	0.0017	1751	25	2221	21	78.8
66	09-67	5.98	268	925	0.30	2.320	0.035	0.1584	0.0034	2311	29	2440	36	94.7
67	09-68	0.16	111	963	0.12	2.017	0.031	0.2011	0.0021	2596	33	2837	17	91.5
68	09-69	10.26	183	997	0.19	2.550	0.062	0.0867	0.0077	2133	44	1354	162	157.5
69	09-70	1.21	572	1946	0.30	3.314	0.068	0.1294	0.0019	1700	31	2091	25	81.3
70	09-71	0.00	131	578	0.23	2.027	0.022	0.1870	0.0018	2586	23	2717	16	95.2
71	09-72	0.06	156	729	0.22	1.807	0.025	0.1950	0.0018	2840	32	2786	15	101.9
	UC11													
1	11-09004	0.18	49	82	0.62	1.871	0.041	0.2043	0.0044	2760	49	2862	35	103.7
2	11-09005	0.13	72	142	0.52	2.468	0.052	0.1853	0.0036	2193	39	2702	32	123.2
3	11-09006	0.00	262	480	0.56	2.176	0.049	0.1739	0.0028	2437	46	2597	26	106.5
4	11-09007	0.88	108	115	0.97	1.802	0.035	0.2293	0.0053	2846	45	3049	36	107.1
5	11-09008	1.04	112	136	0.84	1.832	0.036	0.1940	0.0040	2808	44	2778	33	98.9
6	11-09009	0.00	116	108	1.10	2.243	0.039	0.1788	0.0033	2376	34	2643	30	111.2
7	11-09010	0.03	32	61	0.54	2.098	0.041	0.1815	0.0042	2513	41	2668	38	106.2
8	11-09011	0.35	59	112	0.54	2.291	0.043	0.1698	0.0042	2335	37	2557	41	109.5
9	11-09015	0.00	573	190	3.09	2.129	0.039	0.1784	0.0025	2482	38	2640	23	106.4
10	11-09016	0.00	76	92	0.85	1.988	0.043	0.1881	0.0033	2626	46	2727	29	103.8
11	11-09017	0.00	115	254	0.47	2.218	0.041	0.1643	0.0027	2399	37	2501	28	104.3
12	11-09018	0.00	19	54	0.36	1.823	0.050	0.2091	0.0044	2819	63	2900	34	102.9
13	11-09019	0.00	55	66	0.86	1.817	0.046	0.2189	0.0050	2827	58	2974	37	105.2
14	11-09020	0.00	352	254	1.42	2.679	0.075	0.2189	0.0058	2045	49	2974	42	145.4
15	11-09021	1.41	312	116	2.75	2.095	0.053	0.1674	0.0129	2516	53	2533	124	100.7
16	11-09022	0.05	65	81	0.82	1.795	0.034	0.2086	0.0042	2855	43	2896	32	101.5
17	11-09026	0.28	26	37	0.71	1.713	0.040	0.2373	0.0064	2964	55	3104	42	104.7
18	11-09027	0.00	109	121	0.93	2.127	0.054	0.1654	0.0035	2484	53	2513	35	101.2
19	11-09028	0.00	106	62	1.74	2.420	0.048	0.1834	0.0041	2229	37	2685	37	120.4
20	11-09029	0.00	138	209	0.68	1.862	0.038	0.2167	0.0037	2771	46	2958	27	106.8
21	11-09030	0.00	123	756	0.17	2.335	0.055	0.1630	0.0027	2298	45	2489	27	108.3
22	11-09031	0.00	175	210	0.86	2.106	0.037	0.1850	0.0030	2505	37	2700	26	107.8
23	11-09032	0.60	21	31	0.70	1.942	0.063	0.1947	0.0067	2678	71	2784	55	104.0
24	11-09033	0.00	1165	295	4.05	2.681	0.059	0.1867	0.0032	2044	39	2715	27	132.8
25	11-09037	0.00	36	51	0.71	1.868	0.052	0.2110	0.0043	2764	63	2914	33	105.4
26	11-09038	0.42	65	48	1.37	1.938	0.057	0.1811	0.0087	2682	65	2664	77	99.3
27	11-09039	0.69	195	229	0.88	1.926	0.046	0.1789	0.0051	2696	52	2644	46	98.1
28	11-09040	0.28	247	231	1.10	2.132	0.051	0.1713	0.0052	2479	49	2571	50	103.7
29	11-09041	1.15	45	152	0.31	2.662	0.067	0.1570	0.0042	2056	44	2425	44	117.9
30	11-09042	0.00	370	558	0.68	2.817	0.053	0.1681	0.0026	1959	32	2540	25	129.7
31	11-09043	0.00	14	66	0.22	1.911	0.038	0.1840	0.0039	2713	44	2691	35	99.2
32	11-09044	0.00	3510	393	9.17	3.802	0.084	0.1889	0.0030	1505	29	2734	26	181.6
33	11-09048	0.00	334	75	4.55	2.095	0.041	0.1887	0.0034	2516	41	2732	30	108.6
34	11-09049	0.00	1606	306	5.39	2.594	0.037	0.2179	0.0030	2102	25	2966	22	141.1
35	11-09050	0.00	62	109	0.58	1.514	0.035	0.3232	0.0064	3269	59	3586	31	109.7
36	11-09051	0.00	42	76	0.57	1.831	0.050	0.1949	0.0038	2809	62	2785	32	99.1
37	11-09052	0.33	58	123	0.48	1.962	0.053	0.1699	0.0042	2655	58	2558	40	96.4
38	11-09053	0.00	14	42	0.33	1.723	0.039	0.2167	0.0049	2950	54	2958	36	100.3
39	11-09054	1.74	1823	2690	0.70	3.289	0.056	0.1460	0.0029	1711	25	2301	34	134.5
40	11-09055	0.00	225	213	1.08	2.061	0.046	0.1662	0.0028	2550	47	2521	28	98.9
41	11-09059	0.02	84	104	0.83	1.800	0.043	0.2095	0.0057	2849	55	2903	43	101.9
42	11-09060	2.05	349	199	1.80	2.416	0.067	0.1646	0.0092	2232	52	2505	91	112.2
43	11-09061	0.00	151	193	0.80	2.019	0.049	0.2220	0.0038	2593	52	2997	27	115.6
44	11-09062	0.00	5009	837	6.14	10.243	0.300	0.1876	0.0030	600	17	2722	26	453.3
45	11-09063	0.00	904	268	3.47	2.687	0.068	0.1698	0.0030	2039	44	2557	29	125.4
46	11-09064	0.00	63	84	0.77	1.878	0.036	0.2070	0.0037	2752	43	2884	29	104.8
47	11-09065	0.00	66	146	0.46	1.724	0.035	0.2179	0.0036	2949	49	2967	26	100.6
48	11-09066	0.07	53	85	0.65	1.785	0.038	0.2022	0.0041	2868	50	2845	33	99.2
49	11-09070	0.00	465	469	1.02	2.660	0.079	0.1770	0.0032	2057	53	2626	30	127.6
50	11-09071	0.00	1445	432	3.43	3.674	0.130	0.1755	0.0034	1552	49	2612	31	168.3
51	11-09072	0.00	375	163	2.35	2.504	0.110	0.1825	0.0044	2166	81	2677	40	123.6
52	11-09073	0.00	88	79	1.14	1.921	0.051	0.1876	0.0046	2702	58	2722	40	100.7
53	11-09074	6.80	218	180	1.24	2.286	0.061	0.1295	0.0121	2339	52	2092	155	89.4
54	11-09075	0.00	146	170	0.88	2.318	0.058	0.1730	0.0032	2312	49	2589	30	112.0
55	11-09076	0.86	93	113	0.84	1.972	0.047	0.1878	0.0054	2644	52	2724	46	103.0
56	11-09077	0.00	24	42	0.59	1.844	0.055	0.2030	0.0048	2793	68	2851	38	102.1

57	11-09081	0.00	97	91	1.10	1.805	0.041	0.2009	0.0032	2842	53	2835	25	99.8
58	11-09082	0.00	672	290	2.38	2.321	0.095	0.2027	0.0037	2310	80	2849	30	123.4
59	11-09083	0.54	34	61	0.57	1.599	0.055	0.2166	0.0064	3131	86	2957	47	94.5
60	11-09084	0.00	992	268	3.80	2.121	0.056	0.1749	0.0034	2490	54	2606	32	104.7
61	11-09085	0.00	62	85	0.75	1.548	0.042	0.2338	0.0052	3213	69	3080	35	95.9
62	11-09086	0.03	61	94	0.67	1.794	0.059	0.1918	0.0058	2856	76	2759	48	96.6
63	11-09087	0.00	420	237	1.82	2.180	0.063	0.1742	0.0044	2434	59	2599	42	106.8
64	11-09088	0.00	28	42	0.68	1.300	0.035	0.3359	0.0070	3677	75	3646	31	99.2
65	11-09092	0.00	339	151	2.31	2.260	0.051	0.1810	0.0037	2362	45	2664	34	112.8
66	11-09093	0.58	78	72	1.11	1.919	0.054	0.1846	0.0067	2703	62	2696	59	99.7
67	11-09094	0.00	103	130	0.82	1.980	0.043	0.1734	0.0032	2636	47	2592	30	98.3
68	11-09095	1.05	260	260	1.02	2.075	0.057	0.1695	0.0057	2535	58	2554	55	100.7
69	11-09096	0.00	488	182	2.76	1.971	0.050	0.2263	0.0049	2646	55	3028	34	114.4
70	11-09097	0.00	545	599	0.93	2.169	0.037	0.1768	0.0027	2444	34	2624	25	107.4
71	11-09098	0.40	75	90	0.85	1.866	0.060	0.1871	0.0062	2767	72	2718	53	98.2
72	11-09099	0.00	68	95	0.73	1.665	0.050	0.2474	0.0052	3033	72	3170	33	104.5
73	11-09103	0.00	56	69	0.82	1.872	0.032	0.1992	0.0030	2759	38	2821	25	102.3
74	11-09104	0.00	243	304	0.82	2.075	0.026	0.1774	0.0018	2536	27	2630	17	103.7
75	11-09105	0.07	42	80	0.54	1.778	0.031	0.2155	0.0041	2877	40	2948	31	102.5
76	11-09106	2.01	39	60	0.66	2.075	0.041	0.1660	0.0065	2536	41	2519	64	99.3
77	11-09107	0.00	229	94	2.51	1.970	0.040	0.1879	0.0033	2646	44	2725	29	103.0
78	11-09108	0.03	70	151	0.48	1.942	0.037	0.1880	0.0037	2677	42	2726	32	101.8
79	11-09109	0.34	13	33	0.42	1.847	0.053	0.2013	0.0062	2789	65	2838	50	101.8
80	11-09110	0.27	56	89	0.64	1.716	0.042	0.2036	0.0045	2961	58	2857	35	96.5
81	11-09114	0.00	151	127	1.22	1.897	0.039	0.2028	0.0027	2730	46	2850	21	104.4
82	11-09115	0.00	48	99	0.50	1.790	0.035	0.2020	0.0037	2861	45	2844	29	99.4
83	11-09116	0.00	666	1016	0.67	3.341	0.057	0.1471	0.0017	1688	25	2313	20	137.0
84	11-09117	0.00	116	111	1.08	1.927	0.046	0.1749	0.0035	2694	52	2606	33	96.7
85	11-09118	0.00	81	89	0.92	1.951	0.056	0.1816	0.0041	2667	63	2669	37	100.1
86	11-09119	0.00	23	179	0.13	1.681	0.033	0.2312	0.0037	3009	48	3062	25	101.8
87	11-09120	0.94	87	184	0.49	1.710	0.048	0.2355	0.0061	2969	67	3091	41	104.1
88	11-09121	0.46	244	309	0.81	3.077	0.119	0.2004	0.0051	1814	61	2831	41	156.0

UC12

1	12-09147	0.59	326	620	0.54	1.503	0.021	0.3654	0.0031	3287	36	3774	12	114.8
2	12-09148	0.00	444	1429	0.32	2.686	0.041	0.1657	0.0021	2040	27	2516	21	123.3
3	12-09149	0.26	122	1089	0.11	2.709	0.041	0.2011	0.0021	2025	26	2837	16	140.1
4	12-09150	0.16	396	664	0.61	1.869	0.021	0.3346	0.0035	2763	25	3640	15	131.8
5	12-09151	0.47	747	2896	0.26	4.429	0.075	0.0955	0.0014	1312	20	1539	28	117.3
6	12-09152	1.48	569	1232	0.47	3.035	0.053	0.2161	0.0038	1836	28	2954	28	160.9
7	12-09153	0.00	364	991	0.38	2.159	0.050	0.2575	0.0042	2454	47	3233	26	131.8
8	12-09154	1.02	646	1440	0.46	2.929	0.038	0.1576	0.0020	1893	21	2431	22	128.4
9	12-09158	0.00	424	1318	0.33	2.552	0.032	0.2208	0.0019	2132	23	2988	14	140.2
10	12-09159	0.09	704	1901	0.38	3.068	0.045	0.1942	0.0020	1819	23	2779	17	152.8
11	12-09160	0.00	804	1537	0.54	3.159	0.030	0.1923	0.0014	1773	15	2763	12	155.9
12	12-09161	0.00	536	505	1.09	1.597	0.018	0.3458	0.0024	3135	27	3690	11	117.7
13	12-09162	0.61	10	292	0.04	1.936	0.022	0.2077	0.0020	2684	25	2889	15	107.6
14	12-09163	0.00	453	1660	0.28	3.170	0.047	0.1827	0.0023	1768	23	2679	21	151.6
15	12-09164	0.00	584	1537	0.39	2.880	0.039	0.2003	0.0028	1921	22	2830	22	147.3
16	12-09165	0.00	500	1446	0.35	2.554	0.024	0.2120	0.0018	2130	17	2922	14	137.2
17	12-09169	3.30	152	362	0.43	2.144	0.027	0.3186	0.0037	2468	25	3565	17	144.4
18	12-09170	4.07	152	289	0.54	1.371	0.018	0.3368	0.0043	3532	35	3650	19	103.3
19	12-09171	0.01	1885	1472	1.31	3.019	0.064	0.2227	0.0054	1844	34	3002	38	162.8
20	12-09172	0.11	163	858	0.19	1.945	0.022	0.1831	0.0015	2674	25	2683	13	100.3
21	12-09173	0.23	366	648	0.58	1.328	0.019	0.3816	0.0034	3618	39	3840	13	106.1
22	12-09174	0.00	828	2151	0.39	4.346	0.063	0.1313	0.0013	1335	18	2117	17	158.6
23	12-09175	0.30	225	407	0.57	1.316	0.014	0.3841	0.0034	3644	29	3850	13	105.6
24	12-09176	0.00	1420	1218	1.20	2.787	0.048	0.2350	0.0022	1977	30	3088	14	156.2
25	12-09181	0.00	402	697	0.59	1.656	0.027	0.3259	0.0027	3046	39	3600	12	118.2
26	12-09182	0.67	267	634	0.43	2.050	0.063	0.2784	0.0045	2562	65	3355	25	131.0
27	12-09183	0.98	198	404	0.50	1.600	0.025	0.3768	0.0035	3129	39	3821	13	122.1
28	12-09184	0.54	229	293	0.80	1.283	0.017	0.3831	0.0034	3716	36	3846	13	103.5
29	12-09185	0.00	415	1331	0.32	2.874	0.035	0.1556	0.0012	1925	20	2410	14	125.2
30	12-09186	0.33	431	704	0.63	2.051	0.038	0.3065	0.0029	2560	39	3505	14	136.9
31	12-09187	0.00	2472	2122	1.20	4.353	0.083	0.1530	0.0020	1333	23	2380	23	178.5
32	12-09191	1.30	398	792	0.51	1.592	0.019	0.3236	0.0031	3143	30	3589	14	114.2
33	12-09192	0.47	258	551	0.48	1.865	0.030	0.3112	0.0030	2768	36	3528	15	127.5
34	12-09193	0.85	293	555	0.54	1.992	0.030	0.2740	0.0027	2622	33	3330	16	127.0
35	12-09194	1.58	255	515	0.51	1.607	0.018	0.3320	0.0028	3119	27	3628	13	116.3

36	12-09195	0.73	197	1164	0.17	2.912	0.033	0.1546	0.0015	1903	19	2399	16	126.1
37	12-09196	1.47	224	526	0.44	1.893	0.034	0.3153	0.0031	2734	40	3548	15	129.8
38	12-09197	0.00	3237	1397	2.38	4.097	0.170	0.3089	0.0044	1408	52	3517	22	249.8
39	12-09198	0.42	138	328	0.43	1.589	0.021	0.3463	0.0031	3147	33	3692	14	117.3
40	12-09202	0.11	213	322	0.68	1.224	0.013	0.3923	0.0032	3851	32	3881	12	100.8
41	12-09203	0.20	112	258	0.45	1.190	0.014	0.3920	0.0034	3933	35	3880	13	98.7
42	12-09204	0.00	700	4128	0.17	5.864	0.101	0.1027	0.0011	1015	16	1675	19	165.0
43	12-09205	3.55	1013	3236	0.32	4.771	0.066	0.0985	0.0018	1227	15	1597	34	130.2
44	12-09206	0.96	180	1078	0.17	2.232	0.025	0.1737	0.0017	2387	23	2595	17	108.7
45	12-09207	0.02	289	545	0.54	1.219	0.015	0.3827	0.0036	3862	36	3844	14	99.5
46	12-09208	1.19	250	1291	0.20	2.514	0.061	0.2090	0.0058	2159	45	2899	44	134.3
47	12-09209	0.00	256	533	0.49	1.377	0.016	0.3439	0.0031	3520	31	3682	13	104.6
48	12-09213	1.88	85	400	0.22	1.934	0.031	0.3083	0.0033	2687	35	3514	17	130.8
49	12-09214	0.23	65	229	0.29	1.573	0.023	0.2765	0.0032	3172	37	3345	18	105.5
50	12-09215	0.22	192	590	0.33	1.366	0.017	0.3490	0.0034	3542	34	3704	15	104.6
51	12-09216	0.00	849	1540	0.57	2.622	0.027	0.2127	0.0018	2083	18	2928	13	140.6
52	12-09217	0.00	574	811	0.73	1.609	0.020	0.3364	0.0027	3115	31	3648	12	117.1
53	12-09218	0.18	641	1787	0.37	3.535	0.048	0.1333	0.0015	1606	19	2143	20	133.4
54	12-09219	4.13	155	378	0.42	2.409	0.031	0.3067	0.0042	2238	24	3506	21	156.6
55	12-09220	1.17	232	509	0.47	1.519	0.019	0.3357	0.0034	3260	31	3645	15	111.8
56	12-09224	0.00	587	1099	0.55	1.936	0.024	0.2654	0.0041	2684	27	3281	24	122.2
57	12-09225	0.14	457	722	0.65	1.561	0.021	0.2874	0.0035	3191	33	3405	19	106.7
58	12-09226	0.10	540	556	1.00	1.252	0.015	0.3584	0.0030	3784	33	3745	12	99.0
59	12-09227	0.72	180	631	0.29	1.812	0.019	0.2761	0.0026	2832	25	3342	15	118.0
60	12-09228	1.38	262	582	0.46	1.641	0.023	0.2947	0.0034	3067	34	3444	18	112.3
61	12-09229	1.32	476	1053	0.46	2.066	0.039	0.2589	0.0049	2545	40	3242	29	127.4
62	12-09230	0.07	269	564	0.49	1.670	0.039	0.3072	0.0055	3025	56	3508	28	116.0
63	12-09231	0.67	161	3118	0.05	5.503	0.069	0.1022	0.0010	1076	12	1666	18	154.8
64	12-09235	11.09	159	313	0.52	1.157	0.036	0.3178	0.0141	4016	92	3561	66	88.7
65	12-09236	0.00	364	966	0.39	1.994	0.028	0.2873	0.0032	2620	30	3404	18	129.9
66	12-09237	0.07	345	966	0.37	1.995	0.028	0.2868	0.0034	2619	30	3402	18	129.9
67	12-09238	1.69	979	2786	0.36	6.731	0.086	0.1167	0.0018	893	11	1908	27	213.7
68	12-09239	1.18	311	531	0.60	1.527	0.020	0.3109	0.0035	3248	34	3527	17	108.6
69	12-09240	0.66	111	306	0.37	1.245	0.015	0.3379	0.0037	3800	36	3655	16	96.2
70	12-09241	0.00	638	714	0.92	2.345	0.055	0.3193	0.0028	2289	45	3568	13	155.8
71	12-09242	0.00	637	2130	0.31	2.552	0.032	0.1311	0.0013	2132	23	2114	17	99.2
72	m12004	0.21	357	3792	0.10	5.778	0.154	0.1102	0.0011	1029	25	1805	18	175.4
73	m12005	2.85	279	1276	0.22	3.102	0.035	0.1561	0.0020	1801	18	2415	22	134.1
74	m12006	0.13	377	773	0.50	1.425	0.015	0.3431	0.0027	3428	27	3678	12	107.3
75	m12007	0.35	122	561	0.22	1.899	0.022	0.2054	0.0022	2728	26	2871	17	105.3
76	m12008	0.00	373	2940	0.13	3.822	0.060	0.1102	0.0015	1498	21	1804	24	120.4
77	m12009	1.35	1419	3111	0.47	5.439	0.060	0.1031	0.0018	1088	11	1681	32	154.5
78	m12010	0.01	308	1078	0.29	2.341	0.027	0.1787	0.0025	2293	22	2642	23	115.2
79	m12011	0.00	172	766	0.23	1.780	0.019	0.2094	0.0018	2874	25	2903	14	101.0
80	m12015	2.96	344	1141	0.31	2.559	0.030	0.1749	0.0033	2126	21	2606	31	122.6
81	m12016	0.00	322	1143	0.29	2.344	0.038	0.1778	0.0021	2290	31	2634	19	115.0
82	m12017	1.27	567	1238	0.47	2.526	0.067	0.1784	0.0053	2150	49	2639	49	122.8
83	m12018	1.19	131	547	0.24	1.870	0.020	0.2145	0.0024	2761	24	2942	18	106.5
84	m12019	1.17	68	416	0.17	1.779	0.021	0.2133	0.0022	2875	28	2932	17	102.0
85	m12020	0.00	201	1820	0.11	3.438	0.048	0.1332	0.0013	1646	20	2142	17	130.2
86	m12021	0.14	48	1769	0.03	3.443	0.043	0.1292	0.0011	1644	18	2088	15	127.0
87	m12022	0.53	135	1056	0.13	2.562	0.040	0.2431	0.0024	2124	28	3142	16	147.9
88	m12026	0.96	359	804	0.46	1.870	0.037	0.3551	0.0037	2761	44	3731	16	135.1
89	m12027	0.16	279	246	1.16	1.364	0.015	0.3593	0.0040	3545	30	3748	17	105.7
90	m12028	0.28	260	505	0.53	1.813	0.023	0.3420	0.0038	2831	29	3673	17	129.7
91	m12029	1.12	165	634	0.27	2.127	0.024	0.3137	0.0033	2484	23	3541	16	142.5
92	m12030	15.25	651	4437	0.15	4.947	0.080	0.0663	0.0038	1187	17	815	117	68.7
93	m12031	1.45	540	1348	0.41	2.477	0.030	0.2809	0.0028	2186	23	3369	16	154.1
94	m12032	0.41	122	2042	0.06	4.148	0.045	0.1435	0.0015	1392	13	2271	18	163.1
95	m12033	0.03	149	1479	0.10	3.279	0.034	0.1369	0.0014	1716	16	2189	17	127.6
96	m12037	0.00	426	1222	0.36	2.561	0.038	0.1686	0.0023	2125	27	2545	23	119.8
97	m12038	0.47	527	1985	0.27	4.121	0.059	0.1195	0.0015	1401	18	1950	22	139.2
98	m12039	0.35	55	1866	0.03	3.157	0.029	0.1278	0.0012	1774	14	2070	16	116.7
99	m12040	0.63	167	3203	0.05	5.625	0.103	0.1030	0.0016	1055	18	1679	28	159.2
100	m12041	0.26	283	860	0.34	2.226	0.040	0.2210	0.0042	2392	36	2989	31	125.0
101	m12042	0.00	86	1042	0.09	2.623	0.026	0.2094	0.0020	2082	18	2902	16	139.4
102	m12043	0.00	32	121	0.27	1.558	0.021	0.3230	0.0036	3196	34	3586	17	112.2
103	m12044	0.00	280	489	0.59	1.279	0.014	0.3857	0.0032	3724	32	3856	13	103.5
104	m12048	0.47	291	3578	0.08	6.478	0.120	0.0906	0.0015	925	16	1440	31	155.6

105	m12049	1.22	285	2504	0.12	4.843	0.095	0.1259	0.0023	1210	22	2043	31	168.8
106	m12050	0.00	156	599	0.27	1.735	0.017	0.2118	0.0018	2934	24	2921	14	99.6
107	m12051	0.47	278	631	0.45	1.750	0.018	0.3199	0.0029	2914	25	3571	14	122.6
108	m12052	0.33	347	1229	0.29	2.873	0.032	0.1548	0.0017	1925	18	2401	18	124.7
109	m12053	0.00	896	1473	0.62	3.158	0.111	0.2322	0.0062	1773	54	3069	42	173.1
110	m12054	1.52	293	538	0.56	1.869	0.038	0.3108	0.0032	2763	46	3526	16	127.6
111	m12055	0.00	405	696	0.60	2.122	0.027	0.1949	0.0020	2489	26	2785	17	111.9
112	m12059	1.24	235	2780	0.09	5.689	0.074	0.1295	0.0020	1044	13	2093	26	200.5
113	m12060	0.00	219	384	0.59	1.706	0.022	0.3073	0.0026	2975	31	3509	13	118.0
114	m12061	0.00	445	1240	0.37	2.890	0.041	0.1616	0.0019	1915	23	2474	20	129.2
115	m12062	0.69	220	767	0.29	2.059	0.027	0.1985	0.0021	2552	28	2815	17	110.3
116	m12063	20.15	621	2386	0.27	4.496	0.084	0.1289	0.0159	1295	22	2083	203	160.9
117	m12064	0.00	155	641	0.25	1.941	0.021	0.2057	0.0020	2679	24	2873	16	107.2
118	m12065	1.37	273	480	0.58	1.500	0.024	0.3132	0.0031	3294	41	3538	16	107.4
119	m12066	0.00	245	1160	0.22	2.640	0.032	0.1689	0.0015	2071	21	2548	15	123.1
120	m12070	0.00	217	2287	0.10	4.941	0.078	0.1191	0.0013	1188	17	1943	20	163.5
121	m12071	0.97	544	1893	0.30	3.973	0.061	0.1314	0.0023	1447	20	2117	31	146.3
122	m12072	15.11	1235	1925	0.66	4.714	0.054	0.1838	0.0060	1240	13	2689	54	216.8
123	m12073	1.71	305	710	0.44	2.458	0.025	0.2846	0.0037	2200	19	3390	20	154.1
124	m12074	3.12	70	2525	0.03	3.158	0.047	0.1241	0.0012	1774	23	2018	17	113.8
125	m12075	1.56	567	1982	0.29	4.308	0.086	0.1149	0.0028	1346	24	1880	44	139.7
126	m12076	0.00	88	423	0.21	1.715	0.020	0.2159	0.0021	2962	28	2952	16	99.7
127	m12077	2.76	749	1785	0.43	4.194	0.047	0.1348	0.0030	1379	14	2162	39	156.8
128	m12081	0.22	59	1192	0.05	2.600	0.045	0.1720	0.0022	2098	31	2579	21	122.9
129	m12082	0.06	338	1336	0.26	2.452	0.032	0.1536	0.0019	2205	24	2387	21	108.3
130	m12083	10.68	214	1030	0.21	2.173	0.029	0.1770	0.0068	2440	27	2626	63	107.6
131	m12084	0.03	279	1043	0.27	2.101	0.035	0.1879	0.0024	2510	34	2725	21	108.6
132	m12085	0.00	995	2948	0.35	6.834	0.126	0.1381	0.0019	880	15	2205	23	250.5
133	m12086	17.58	368	1218	0.31	3.228	0.061	0.1835	0.0060	1739	29	2686	53	154.4
134	m12087	0.00	395	1355	0.30	2.484	0.035	0.1525	0.0016	2181	26	2376	18	109.0
135	m12088	0.00	1945	2401	0.83	3.698	0.076	0.1584	0.0024	1543	28	2440	25	158.1
136	m12092	0.28	56	1960	0.03	4.346	0.048	0.1106	0.0010	1335	13	1811	16	135.7
137	m12093	1.05	224	545	0.42	1.724	0.032	0.3682	0.0035	2949	43	3786	14	128.4
138	m12094	0.00	421	730	0.59	1.601	0.030	0.3350	0.0033	3128	46	3642	15	116.4
139	m12095	0.69	241	563	0.44	1.954	0.041	0.3062	0.0030	2664	45	3503	15	131.5
140	m12096	0.15	384	1616	0.24	3.275	0.032	0.1274	0.0012	1718	15	2064	16	120.2
141	m12097	0.45	83	249	0.34	1.277	0.018	0.3901	0.0041	3728	40	3873	16	103.9
142	m12098	2.16	173	3016	0.06	5.582	0.147	0.1001	0.0017	1062	26	1626	32	153.1
143	m12099	0.24	145	699	0.21	1.948	0.022	0.2008	0.0020	2671	25	2834	16	106.1
144	m12103	3.01	398	1669	0.24	3.580	0.045	0.1300	0.0022	1588	18	2099	29	132.2
145	m12104	2.19	242	3309	0.08	5.634	0.062	0.0919	0.0013	1053	11	1467	26	139.3
146	m12105	0.21	85	2178	0.04	3.692	0.041	0.1148	0.0010	1545	15	1878	16	121.5
147	m12106	0.00	8072	4588	1.80	7.328	0.195	0.1155	0.0014	825	21	1889	22	229.1
148	m12107	2.63	180	279	0.66	1.230	0.016	0.3534	0.0042	3835	37	3723	18	97.1
149	m12108	1.71	259	837	0.32	1.902	0.052	0.2897	0.0056	2724	61	3417	30	125.4
150	m12109	0.68	295	1017	0.30	2.185	0.024	0.1883	0.0016	2429	22	2729	14	112.4
151	m12110	3.53	200	726	0.28	1.896	0.022	0.2009	0.0060	2731	26	2835	47	103.8
152	m12114	0.00	1101	2219	0.51	4.973	0.083	0.1364	0.0014	1181	18	2183	18	184.8
153	m12115	0.41	277	876	0.32	1.619	0.021	0.3233	0.0030	3100	31	3587	14	115.7
154	m12116	0.64	330	1250	0.27	2.424	0.031	0.1513	0.0015	2227	24	2362	16	106.1
155	m12117	2.02	564	850	0.68	1.971	0.029	0.2800	0.0036	2645	32	3364	20	127.2
156	s12118	0.00	370	945	0.40	2.083	0.028	0.2521	0.0025	2528	28	3199	16	126.5
157	s12119	0.00	817	1057	0.79	2.166	0.047	0.2669	0.0042	2447	44	3290	24	134.4
158	s12120	0.37	195	393	0.51	1.400	0.026	0.3317	0.0059	3475	49	3626	28	104.3
159	s12121	1.33	194	754	0.26	2.019	0.019	0.2461	0.0025	2594	21	3162	16	121.9
160	s12125	0.28	65	404	0.16	2.115	0.029	0.2497	0.0034	2495	28	3184	21	127.6
161	s12126	2.43	356	1342	0.27	3.504	0.056	0.1628	0.0024	1618	23	2487	24	153.7
162	s12127	0.00	847	794	1.09	1.437	0.019	0.3436	0.0028	3404	35	3681	12	108.1
163	s12128	0.87	141	231	0.62	1.544	0.021	0.3252	0.0037	3219	34	3596	18	111.7
164	s12129	0.00	1190	2062	0.59	3.816	0.072	0.1661	0.0017	1500	25	2520	17	168.0
165	s12130	2.05	522	1352	0.40	2.965	0.039	0.1643	0.0052	1873	21	2501	53	133.5
166	s12131	0.00	410	1130	0.37	2.363	0.028	0.1660	0.0017	2275	22	2519	17	110.7
167	s12132	0.00	631	741	0.87	1.497	0.019	0.3617	0.0032	3298	33	3759	13	114.0
168	s12136	0.56	168	365	0.47	1.413	0.023	0.3662	0.0032	3450	44	3778	13	109.5
169	s12137	0.23	114	2479	0.05	4.406	0.047	0.1059	0.0010	1319	13	1730	17	131.2
170	s12138	0.05	388	685	0.58	2.675	0.030	0.3264	0.0033	2047	20	3602	15	175.9
171	s12139	0.00	252	476	0.54	1.313	0.013	0.3498	0.0028	3650	27	3708	12	101.6
172	s12140	0.63	253	525	0.50	1.626	0.025	0.3618	0.0033	3089	38	3759	14	121.7
173	s12141	9.08	193	536	0.37	1.837	0.034	0.2610	0.0050	2801	42	3254	30	116.2

174	s12142	2.24	345	839	0.42	2.275	0.043	0.2862	0.0034	2349	37	3399	18	144.7
175	s12143	0.70	359	426	0.86	1.280	0.014	0.3451	0.0035	3721	32	3687	16	99.1
176	s12147	0.09	666	876	0.78	1.798	0.025	0.2871	0.0029	2851	32	3403	16	119.3
177	s12148	2.98	657	2024	0.33	3.353	0.071	0.2208	0.0038	1683	31	2988	27	177.6
178	s12149	0.00	956	1210	0.81	2.376	0.031	0.2616	0.0026	2265	25	3258	15	143.9
179	s12150	1.38	408	484	0.86	1.799	0.023	0.3273	0.0033	2849	29	3606	15	126.6
180	s12151	0.11	343	550	0.64	1.469	0.017	0.3230	0.0030	3346	31	3586	14	107.2
181	s12152	0.00	1171	1531	0.78	3.156	0.046	0.2009	0.0022	1775	23	2835	18	159.8
182	s12153	0.09	249	1704	0.15	3.571	0.035	0.1693	0.0030	1591	14	2552	29	160.4
183	s12154	0.06	189	812	0.24	1.900	0.021	0.2000	0.0019	2726	24	2828	15	103.7
184	s12158	0.75	479	703	0.70	1.372	0.013	0.3771	0.0027	3530	26	3822	11	108.3
185	s12159	0.72	216	330	0.67	1.472	0.023	0.3519	0.0033	3341	41	3717	14	111.2
186	s12160	0.00	142	641	0.23	1.883	0.022	0.3086	0.0026	2746	26	3515	13	128.0
187	s12161	2.50	250	331	0.77	1.657	0.022	0.3378	0.0038	3043	32	3654	17	120.1
188	s12162	0.49	251	791	0.33	1.899	0.044	0.2765	0.0061	2727	52	3345	34	122.7
189	s12163	0.10	318	679	0.48	1.385	0.015	0.3535	0.0025	3503	28	3724	11	106.3
190	s12164	0.76	191	494	0.40	1.607	0.018	0.3065	0.0028	3120	28	3505	14	112.4
191	s12165	0.00	273	605	0.46	1.387	0.016	0.3384	0.0024	3500	31	3657	11	104.5
192	s12169	0.77	473	752	0.65	1.847	0.020	0.3073	0.0028	2790	25	3509	14	125.8
193	s12170	1.27	175	255	0.70	1.302	0.019	0.3429	0.0035	3673	41	3677	16	100.1
194	s12171	0.00	606	2064	0.30	3.976	0.055	0.1199	0.0016	1446	18	1956	24	135.3
195	s12172	1.04	418	867	0.50	2.056	0.020	0.2382	0.0027	2555	21	3110	17	121.7
196	s12173	0.83	457	834	0.56	1.809	0.041	0.3569	0.0035	2836	52	3738	15	131.8
197	s12174	0.80	291	792	0.38	2.095	0.031	0.3079	0.0035	2516	30	3512	18	139.6
198	s12175	0.51	53	141	0.39	1.379	0.021	0.3490	0.0031	3514	42	3704	14	105.4
199	s12176	10.70	367	940	0.40	2.383	0.035	0.2963	0.0046	2258	28	3452	24	152.8
200	s12180	0.00	312	1003	0.32	2.247	0.039	0.1886	0.0022	2373	34	2731	19	115.1
201	s12181	0.15	78	1390	0.06	3.306	0.040	0.1357	0.0013	1703	18	2175	16	127.7
202	s12182	0.61	267	619	0.44	1.787	0.039	0.3070	0.0035	2864	51	3507	18	122.4
203	s12183	0.29	315	965	0.33	2.404	0.032	0.2578	0.0027	2243	25	3235	17	144.3
204	s12184	0.74	195	560	0.36	1.819	0.021	0.2861	0.0027	2824	27	3398	14	120.3
205	s12185	0.71	263	491	0.55	1.319	0.013	0.3658	0.0032	3637	27	3776	13	103.8
206	s12186	0.00	164	336	0.50	1.313	0.014	0.3528	0.0029	3650	29	3721	12	102.0
207	s12187	1.32	139	582	0.24	2.207	0.034	0.3097	0.0030	2409	31	3521	15	146.2
208	s12191	1.61	400	1841	0.22	3.588	0.061	0.2522	0.0033	1585	24	3200	20	201.9
209	s12192	1.08	82	913	0.09	2.718	0.026	0.1881	0.0020	2020	17	2727	17	135.0
210	s12193	0.00	316	536	0.60	1.483	0.016	0.3640	0.0027	3322	27	3768	12	113.4
211	s12194	0.00	362	759	0.49	1.350	0.013	0.3505	0.0024	3574	27	3711	10	103.8
212	s12195	0.93	317	1102	0.30	2.390	0.041	0.2590	0.0036	2253	33	3242	22	143.9
213	s12196	0.29	207	473	0.45	1.515	0.023	0.3441	0.0030	3267	39	3683	13	112.7
214	s12197	0.21	337	653	0.53	1.543	0.020	0.3287	0.0030	3221	33	3613	13	112.2
215	s12198	0.34	496	980	0.52	2.118	0.032	0.2892	0.0030	2493	31	3415	16	137.0
216	s12202	0.02	114	653	0.18	1.688	0.023	0.3855	0.0031	2999	33	3855	12	128.5
217	s12203	0.82	229	356	0.66	1.684	0.028	0.3437	0.0031	3005	40	3681	13	122.5
218	s12204	5.69	143	432	0.34	2.184	0.053	0.3170	0.0090	2430	49	3557	43	146.4
219	s12205	0.30	99	309	0.33	1.452	0.023	0.3528	0.0032	3377	42	3721	13	110.2
220	s12206	0.69	213	577	0.38	1.516	0.022	0.3328	0.0026	3266	37	3632	11	111.2
221	s12207	3.18	230	669	0.35	2.251	0.055	0.1928	0.0035	2370	48	2767	29	116.7
222	s12208	5.49	347	1285	0.28	3.237	0.054	0.1877	0.0041	1735	25	2723	36	156.9
223	s12209	1.13	163	353	0.47	1.689	0.025	0.3355	0.0031	2997	36	3644	14	121.6
224	s12213	1.68	292	506	0.59	1.748	0.023	0.3183	0.0030	2916	31	3563	14	122.2
225	s12214	0.00	348	1305	0.27	2.406	0.036	0.2040	0.0015	2240	28	2860	12	127.7
226	s12215	2.40	412	659	0.64	2.020	0.036	0.3289	0.0031	2592	38	3614	14	139.4
227	s12216	0.31	247	734	0.34	2.002	0.029	0.3062	0.0034	2612	31	3503	17	134.1
228	s12217	0.00	274	1577	0.18	2.828	0.050	0.1565	0.0018	1952	30	2419	20	124.0
229	s12218	0.00	874	1466	0.61	2.602	0.034	0.2342	0.0017	2097	23	3082	12	147.0
230	s12219	0.30	394	1159	0.35	2.588	0.038	0.1905	0.0017	2106	26	2748	15	130.5
231	s12220	0.00	320	553	0.59	1.577	0.031	0.3688	0.0026	3166	50	3788	11	119.6
232	s12224	0.36	91	1847	0.05	3.134	0.048	0.1586	0.0024	1785	24	2442	25	136.8
233	s12225	1.47	171	495	0.36	2.544	0.033	0.2803	0.0033	2137	24	3366	18	157.5
234	s12226	0.00	509	564	0.93	1.398	0.014	0.3820	0.0027	3479	27	3841	11	110.4
235	s12227	0.21	120	245	0.50	1.299	0.015	0.3782	0.0032	3680	32	3826	13	104.0
236	s12228	1.30	338	1247	0.28	2.821	0.048	0.1758	0.0024	1956	29	2615	23	133.7
237	s12229	0.00	474	1393	0.35	2.210	0.024	0.2524	0.0022	2407	22	3201	14	133.0
238	s12230	0.00	152	316	0.49	1.260	0.012	0.3820	0.0028	3767	28	3841	11	102.0
239	s12231	0.00	2973	1550	1.97	2.290	0.037	0.2521	0.0042	2335	32	3199	27	137.0
240	s12235	3.57	263	906	0.30	2.298	0.027	0.1786	0.0037	2329	23	2641	34	113.4
241	s12236	0.00	632	1647	0.39	3.273	0.035	0.1780	0.0023	1719	16	2635	22	153.3
242	s12237	1.26	340	558	0.62	1.693	0.015	0.3361	0.0036	2992	21	3647	16	121.9

243	s12238	0.19	62	1317	0.05	2.286	0.026	0.1849	0.0025	2339	22	2698	23	115.4
244	s12239	0.00	617	1301	0.49	2.789	0.030	0.2377	0.0018	1976	19	3106	12	157.2
245	s12240	1.39	244	520	0.48	1.812	0.027	0.3636	0.0031	2833	34	3766	13	133.0
246	s12241	0.20	385	1229	0.32	2.459	0.032	0.1786	0.0017	2200	24	2641	16	120.0
247	s12242	6.32	74	2827	0.03	6.931	0.101	0.1042	0.0114	869	12	1702	189	195.9
248	s12246	0.31	134	2499	0.06	3.882	0.036	0.1155	0.0009	1478	12	1889	15	127.8
249	s12247	0.75	437	1004	0.45	2.259	0.029	0.2909	0.0027	2363	25	3424	14	144.9
250	s12248	0.00	1053	864	1.25	1.685	0.026	0.3327	0.0024	3003	37	3631	11	120.9
251	s12249	0.46	384	882	0.45	1.861	0.020	0.2685	0.0023	2772	24	3299	13	119.0
252	s12250	0.00	478	1163	0.42	2.391	0.026	0.2674	0.0021	2253	20	3292	12	146.1
253	s12251	1.35	243	371	0.67	1.624	0.019	0.3506	0.0030	3093	29	3711	13	120.0
254	s12252	0.00	1432	3885	0.38	5.435	0.064	0.0893	0.0008	1089	12	1411	17	129.6
255	s12253	10.09	579	1799	0.33	3.873	0.071	0.1308	0.0047	1481	24	2110	62	142.5
256	s12257	0.00	807	1652	0.50	3.074	0.042	0.1763	0.0026	1816	22	2620	24	144.3
257	s12258	2.08	222	388	0.59	1.479	0.017	0.3170	0.0030	3330	29	3557	15	106.8
258	s12259	0.57	618	976	0.65	1.845	0.034	0.3345	0.0029	2792	42	3640	13	130.4
259	s12260	0.77	319	1526	0.21	2.410	0.087	0.2241	0.0053	2238	69	3012	37	134.6
260	s12261	0.29	84	183	0.47	1.292	0.017	0.3540	0.0033	3695	38	3726	14	100.8
261	s12262	0.00	213	652	0.33	1.598	0.014	0.3187	0.0023	3132	22	3565	11	113.8
262	s12263	0.13	80	2380	0.03	3.665	0.054	0.1197	0.0011	1555	20	1952	17	125.5
263	s12264	0.65	483	826	0.60	1.912	0.024	0.2743	0.0040	2712	28	3332	23	122.8
264	s12268	0.61	166	347	0.49	1.396	0.016	0.3356	0.0030	3482	32	3644	14	104.6
265	s12269	1.50	236	459	0.53	1.671	0.039	0.3693	0.0033	3024	56	3790	14	125.3
266	s12270	0.00	257	488	0.54	1.873	0.019	0.3026	0.0033	2758	23	3485	17	126.3
267	s12271	0.43	106	1522	0.07	3.279	0.105	0.2067	0.0017	1716	48	2881	14	167.9
268	s12272	0.00	631	1873	0.35	3.621	0.041	0.1558	0.0014	1572	16	2412	15	153.4
269	s12273	0.00	308	978	0.32	1.969	0.018	0.1971	0.0018	2647	20	2803	15	105.9
270	s12274	1.35	70	916	0.08	2.468	0.051	0.2061	0.0051	2193	39	2876	40	131.1
271	s12275	0.00	380	935	0.42	2.054	0.028	0.3050	0.0032	2557	29	3497	17	136.7
272	s12279	0.00	262	863	0.31	1.805	0.043	0.3071	0.0050	2841	54	3508	25	123.5
273	s12280	1.51	210	646	0.33	2.158	0.055	0.3296	0.0040	2454	52	3617	18	147.4
274	s12281	6.08	34	1597	0.02	2.544	0.026	0.1408	0.0019	2137	18	2238	23	104.7
275	s12282	0.00	87	951	0.09	1.965	0.037	0.2212	0.0043	2652	41	2990	31	112.7
276	s12283	3.74	535	3050	0.18	5.933	0.082	0.2068	0.0026	1004	13	2882	20	287.0
277	s12284	0.07	391	763	0.53	1.437	0.012	0.3482	0.0028	3406	23	3701	12	108.7
278	s12285	1.58	201	539	0.38	1.646	0.023	0.3319	0.0050	3060	34	3628	22	118.5
279	s12286	0.16	541	694	0.80	1.465	0.016	0.3545	0.0034	3354	28	3728	14	111.1
280	s12290	1.48	174	628	0.28	2.089	0.024	0.1962	0.0021	2521	24	2796	18	110.9
281	s12291	0.15	148	889	0.17	2.252	0.030	0.2428	0.0023	2369	26	3140	15	132.6
282	s12292	0.24	190	803	0.24	1.857	0.016	0.2089	0.0016	2777	20	2898	12	104.4
283	s12293	0.42	77	181	0.43	1.340	0.017	0.3541	0.0033	3594	36	3726	14	103.7
284	s12294	0.44	433	1309	0.34	2.359	0.026	0.2342	0.0024	2278	21	3082	16	135.3
285	s12295	0.68	477	1170	0.42	2.659	0.039	0.2757	0.0029	2058	26	3340	17	162.3
286	s12296	0.21	31	1380	0.02	2.609	0.028	0.1410	0.0012	2091	19	2240	15	107.1
287	s12297	0.00	258	1548	0.17	2.950	0.036	0.1913	0.0017	1882	20	2755	14	146.4
288	s2-12004	0.00	757	1628	0.48	2.762	0.050	0.1961	0.0033	1992	31	2795	27	140.3
289	s2-12005	0.25	289	1041	0.28	2.189	0.020	0.1791	0.0016	2426	18	2646	14	109.1
290	s2-12006	0.85	506	1400	0.37	2.726	0.034	0.2506	0.0022	2014	21	3190	14	158.4
291	s2-12007	0.00	1528	2189	0.72	4.007	0.050	0.1435	0.0032	1436	16	2271	38	158.1
292	s2-12008	0.20	77	1867	0.04	3.673	0.038	0.1205	0.0011	1552	14	1964	16	126.5
293	s2-12009	0.66	61	1495	0.04	3.039	0.036	0.1705	0.0015	1834	19	2564	15	139.8
294	s2-12010	0.35	437	475	0.94	1.344	0.013	0.3499	0.0030	3585	26	3708	13	103.4
295	s2-12011	0.00	199	383	0.53	1.320	0.016	0.3535	0.0029	3636	34	3724	12	102.4
296	s2-12015	0.31	348	1055	0.34	2.116	0.019	0.2677	0.0022	2494	18	3294	13	132.1
297	s2-12016	0.74	343	1031	0.34	2.233	0.021	0.2818	0.0021	2386	19	3374	12	141.4
298	s2-12017	0.16	230	1157	0.20	2.545	0.024	0.1612	0.0014	2136	17	2469	15	115.6
299	s2-12018	2.59	140	659	0.22	2.155	0.041	0.2291	0.0038	2457	39	3047	27	124.0
300	s2-12019	0.00	186	1072	0.18	2.207	0.019	0.2083	0.0025	2409	17	2894	20	120.1
301	s2-12020	0.20	375	975	0.39	1.941	0.032	0.2842	0.0036	2679	37	3388	20	126.5
302	s2-12021	0.59	351	688	0.52	1.654	0.027	0.3285	0.0033	3048	39	3612	15	118.5
303	s2-12022	4.69	162	468	0.36	1.585	0.016	0.3176	0.0036	3153	26	3560	17	112.9
304	s2-12026	0.00	994	2004	0.51	4.482	0.074	0.2323	0.0037	1298	20	3070	25	236.5
305	s2-12027	1.33	184	459	0.41	1.619	0.028	0.3431	0.0032	3101	42	3678	14	118.6
306	s2-12028	0.03	388	1162	0.34	2.033	0.022	0.2719	0.0026	2579	23	3318	15	128.7
307	s2-12029	12.34	168	2104	0.08	4.023	0.047	0.1072	0.0044	1431	15	1753	73	122.5
308	s2-12030	1.24	71	230	0.32	2.632	0.048	0.3073	0.0041	2076	33	3509	20	169.0
309	s2-12031	0.21	368	897	0.42	1.683	0.018	0.3080	0.0027	3007	26	3513	13	116.8
310	s2-12032	2.26	123	259	0.49	1.227	0.016	0.3741	0.0037	3842	38	3810	15	99.2
311	s2-12033	6.25	245	1031	0.24	4.146	0.068	0.2574	0.0044	1393	21	3232	27	232.0

312	s2-12037	0.30	307	1010	0.31	2.323	0.030	0.2868	0.0026	2308	25	3402	14	147.4
313	s2-12038	0.50	273	566	0.50	1.500	0.017	0.3766	0.0030	3292	30	3820	12	116.0
314	s2-12039	0.00	606	1406	0.44	2.893	0.040	0.1506	0.0020	1914	23	2354	22	123.0
315	s2-12040	0.25	592	1751	0.35	3.553	0.066	0.1218	0.0016	1599	26	1984	24	124.1
316	s2-12041	0.83	375	1613	0.24	3.194	0.036	0.1342	0.0014	1756	17	2155	18	122.7
317	s2-12042	1.47	239	1427	0.17	3.245	0.067	0.1618	0.0038	1732	31	2476	39	143.0
318	s2-12043	0.02	174	757	0.24	1.800	0.016	0.2060	0.0016	2849	21	2876	12	101.0
319	s2-12044	2.12	132	221	0.61	1.651	0.021	0.3338	0.0038	3053	30	3636	17	119.1
320	s2-12048	0.11	260	1028	0.26	2.025	0.020	0.2396	0.0020	2587	22	3119	13	120.6
321	s2-12049	0.00	99	432	0.23	1.441	0.016	0.3313	0.0028	3397	29	3624	13	106.7
322	s2-12050	0.55	112	444	0.26	1.472	0.017	0.3365	0.0032	3342	30	3649	14	109.2
323	s2-12051	0.00	1623	1158	1.44	2.484	0.027	0.2421	0.0020	2181	20	3135	13	143.8
324	s2-12052	0.00	432	1121	0.40	2.524	0.030	0.2777	0.0025	2151	22	3352	13	155.8
325	s2-12053	0.23	298	1194	0.26	2.325	0.022	0.1682	0.0014	2306	18	2541	14	110.2
326	s2-12054	1.04	129	583	0.23	2.112	0.024	0.3218	0.0026	2499	23	3580	12	143.3
327	s2-12055	0.61	165	776	0.22	1.877	0.023	0.2777	0.0028	2753	27	3351	16	121.7
328	s2-12059	1.06	146	525	0.28	2.016	0.022	0.2732	0.0026	2596	23	3326	15	128.1
329	s2-12060	1.13	212	870	0.25	1.995	0.020	0.2157	0.0042	2620	21	2951	31	112.7
330	s2-12061	0.10	228	413	0.57	1.316	0.013	0.3595	0.0030	3643	27	3750	12	102.9
331	s2-12062	0.16	196	724	0.28	1.694	0.016	0.2856	0.0024	2991	23	3395	13	113.5
332	s2-12064	3.78	406	1060	0.39	2.431	0.023	0.2835	0.0028	2221	18	3384	15	152.4
333	s2-12065	0.96	144	295	0.50	1.584	0.023	0.3346	0.0034	3155	36	3640	15	115.4
334	s2-12066	0.00	232	584	0.41	1.326	0.014	0.3472	0.0027	3623	28	3696	12	102.0
335	s2-12070	0.14	85	886	0.10	1.934	0.019	0.2760	0.0025	2687	22	3342	14	124.4
336	s2-12071	0.23	220	569	0.40	1.275	0.012	0.3572	0.0026	3732	26	3740	11	100.2
337	s2-12072	1.59	128	379	0.35	1.813	0.018	0.3445	0.0028	2831	23	3685	12	130.2
338	s2-12073	0.29	182	751	0.25	1.922	0.028	0.1979	0.0018	2701	32	2810	15	104.0
339	s2-12074	2.80	382	598	0.66	2.067	0.036	0.3163	0.0031	2544	37	3554	15	139.7
340	s2-12075	0.12	413	1126	0.38	2.649	0.024	0.1810	0.0016	2064	16	2663	15	129.0
341	s2-12076	0.00	628	1124	0.57	2.721	0.041	0.2895	0.0039	2018	26	3416	21	169.3
342	s2-12077	1.01	211	706	0.31	1.969	0.020	0.2010	0.0018	2647	22	2835	15	107.1
343	s2-12081	0.53	147	747	0.20	1.895	0.044	0.3107	0.0045	2732	51	3526	22	129.1
344	s2-12082	0.25	835	2890	0.30	4.444	0.040	0.1024	0.0010	1308	11	1670	18	127.6
345	s2-12083	0.06	159	318	0.51	1.361	0.014	0.3628	0.0030	3551	29	3763	13	106.0
346	s2-12084	1.61	113	344	0.34	1.782	0.022	0.2847	0.0054	2871	28	3390	30	118.1
347	s2-12085	1.60	1071	1259	0.87	2.925	0.027	0.1967	0.0028	1896	15	2801	22	147.8
348	s2-12086	1.74	174	373	0.48	1.633	0.025	0.3373	0.0032	3079	37	3652	14	118.6
349	s2-12087	0.33	140	245	0.59	1.421	0.018	0.3533	0.0035	3436	34	3723	15	108.4
350	s2-12088	1.02	131	346	0.39	1.670	0.032	0.3697	0.0033	3025	46	3792	13	125.4
351	s2-12092	2.88	266	904	0.30	4.094	0.103	0.2825	0.0032	1409	32	3378	18	239.8
352	s2-12093	8.33	196	624	0.32	1.655	0.018	0.2416	0.0054	3046	26	3132	35	102.8
353	s2-12094	0.04	1024	1492	0.70	2.295	0.022	0.2256	0.0025	2332	19	3023	17	129.7
354	s2-12095	4.25	214	739	0.30	2.149	0.022	0.1846	0.0026	2463	21	2696	23	109.5
355	s2-12096	0.54	439	726	0.62	1.746	0.022	0.3439	0.0027	2919	30	3682	12	126.1
356	s2-12097	0.47	116	233	0.51	1.545	0.019	0.3561	0.0032	3217	32	3735	13	116.1
357	s2-12098	8.62	201	2446	0.08	5.223	0.071	0.1316	0.0069	1129	14	2121	89	187.8
358	s2-12099	1.05	218	484	0.46	2.144	0.027	0.3218	0.0026	2468	25	3580	12	145.1
359	s2-12103	1.13	273	894	0.31	2.488	0.027	0.1830	0.0019	2178	20	2681	18	123.1
360	s2-12104	7.63	85	620	0.14	3.567	0.111	0.1958	0.0043	1593	44	2792	36	175.3
361	s2-12105	0.20	98	284	0.35	1.208	0.013	0.3565	0.0030	3889	32	3737	12	96.1
362	s2-12106	0.72	402	617	0.67	2.062	0.033	0.3367	0.0049	2549	33	3649	22	143.1
363	s2-12107	0.99	129	602	0.22	1.820	0.019	0.2102	0.0018	2823	23	2908	14	103.0
364	s2-12108	1.83	213	950	0.23	2.668	0.038	0.1676	0.0026	2052	25	2535	26	123.5
365	s2-12109	1.09	60	2102	0.03	3.774	0.046	0.1378	0.0013	1515	16	2201	17	145.3
366	s2-12110	0.15	239	1172	0.21	2.367	0.029	0.1677	0.0016	2272	24	2536	16	111.6
367	s2-12114	18.65	104	666	0.16	3.089	0.070	0.1672	0.0178	1808	36	2531	169	140.0
368	s2-12115	0.85	142	378	0.38	1.669	0.018	0.3765	0.0034	3027	26	3819	14	126.2
369	s2-12116	0.32	48	1086	0.05	2.659	0.035	0.1710	0.0020	2058	23	2568	20	124.8
370	s2-12117	0.55	234	1060	0.23	2.301	0.021	0.2302	0.0019	2327	18	3055	12	131.3
371	s2-12118	0.00	561	4123	0.14	5.157	0.046	0.0949	0.0008	1142	9	1527	15	133.7
372	s2-12119	0.01	126	563	0.23	1.812	0.014	0.2093	0.0019	2832	17	2901	15	102.4
373	s2-12120	1.28	122	329	0.38	1.433	0.034	0.3446	0.0036	3412	63	3685	15	108.0
374	s2-12121	1.74	124	589	0.22	1.970	0.026	0.2007	0.0029	2647	28	2833	24	107.0
375	s2-12125	0.00	332	664	0.51	1.460	0.015	0.3479	0.0027	3364	28	3700	11	110.0
376	s2-12126	0.63	361	2219	0.17	3.866	0.039	0.1164	0.0015	1483	13	1903	23	128.3
377	s2-12127	0.00	792	1581	0.51	2.751	0.026	0.2091	0.0020	1999	16	2900	16	145.1
378	s2-12128	0.00	196	361	0.56	1.336	0.014	0.3698	0.0028	3603	30	3792	12	105.2
379	s2-12129	0.54	161	233	0.71	1.375	0.022	0.3564	0.0035	3524	44	3736	15	106.0
380	s2-12130	0.35	244	1207	0.21	2.328	0.023	0.2142	0.0040	2304	20	2939	30	127.6

381	s2-12131	0.00	51	556	0.09	1.398	0.012	0.3386	0.0027	3478	23	3658	12	105.2
382	s2-12132	4.09	100	412	0.25	1.661	0.020	0.2906	0.0030	3037	29	3422	16	112.7
383	s2-12136	0.41	290	543	0.55	1.659	0.015	0.3497	0.0030	3041	22	3707	13	121.9
384	s2-12137	0.60	176	490	0.37	1.806	0.019	0.3181	0.0030	2841	24	3562	14	125.4
385	s2-12138	0.00	939	1731	0.56	3.444	0.075	0.1356	0.0022	1643	31	2172	29	132.2
386	s2-12139	0.82	459	1331	0.35	2.951	0.034	0.2131	0.0028	1881	19	2931	21	155.8
387	s2-12140	0.86	160	397	0.41	1.754	0.033	0.2795	0.0054	2908	44	3362	30	115.6
388	s2-12141	0.43	75	1056	0.07	2.249	0.024	0.2112	0.0029	2372	21	2916	22	123.0
389	s2-12142	1.00	280	746	0.39	1.935	0.020	0.2108	0.0024	2685	23	2913	18	108.5
390	s2-12143	0.00	523	889	0.60	1.485	0.013	0.3294	0.0026	3319	22	3616	12	108.9
391	s2-12147	0.44	778	803	0.99	1.577	0.017	0.3478	0.0032	3165	27	3699	14	116.9
392	s2-12148	0.00	1126	2623	0.44	4.980	0.073	0.1050	0.0009	1180	16	1716	14	145.5
393	s2-12149	0.45	197	580	0.35	1.392	0.012	0.3543	0.0029	3490	23	3727	13	106.8
394	s2-12150	2.11	55	1699	0.03	2.979	0.027	0.1196	0.0012	1866	15	1952	17	104.6
395	s2-12151	0.80	208	308	0.69	1.531	0.017	0.3483	0.0034	3241	27	3701	15	114.2
396	s2-12152	0.64	203	446	0.47	1.324	0.016	0.3479	0.0029	3627	34	3699	13	102.0
397	s2-12153	0.00	164	650	0.26	1.824	0.019	0.2082	0.0019	2818	24	2893	15	102.7
398	s2-12154	0.00	159	479	0.34	1.306	0.012	0.3584	0.0027	3664	26	3745	11	102.2
399	s2-12158	0.00	249	613	0.42	1.434	0.019	0.3319	0.0027	3411	35	3627	13	106.3
400	s2-12159	0.42	153	324	0.49	1.425	0.016	0.3846	0.0031	3428	30	3851	13	112.3
401	s2-12160	0.42	126	204	0.63	1.327	0.015	0.3542	0.0036	3620	30	3727	15	103.0
402	s2-12161	5.65	86	501	0.18	1.790	0.017	0.1955	0.0039	2861	22	2790	33	97.5
403	s2-12162	0.00	377	1586	0.24	2.928	0.034	0.1402	0.0015	1894	19	2230	19	117.7
404	s2-12163	4.51	61	319	0.20	2.471	0.049	0.2460	0.0052	2191	37	3161	33	144.3
405	s2-12164	0.04	312	1290	0.25	2.511	0.024	0.1575	0.0014	2161	18	2430	15	112.5
406	s2-12165	2.35	57	2704	0.02	3.711	0.035	0.1169	0.0011	1538	13	1911	17	124.3
407	s2-12169	8.34	270	672	0.41	1.565	0.015	0.2645	0.0045	3184	24	3275	27	102.8
408	s2-12170	0.46	139	300	0.47	1.383	0.014	0.3642	0.0033	3507	27	3769	13	107.5
409	s2-12171	4.52	578	1559	0.38	3.679	0.045	0.1472	0.0035	1550	17	2314	41	149.3
410	s2-12172	1.07	151	591	0.26	2.333	0.039	0.2702	0.0029	2300	33	3309	16	143.9
411	s2-12173	0.40	154	296	0.53	1.255	0.015	0.3579	0.0036	3777	33	3743	15	99.1
412	s2-12174	0.46	420	1478	0.29	2.865	0.049	0.2530	0.0023	1930	28	3205	15	166.1
413	s2-12175	10.27	710	1839	0.40	3.990	0.042	0.1504	0.0037	1442	13	2352	41	163.1
414	s2-12176	0.00	425	411	1.06	1.712	0.027	0.3724	0.0033	2966	37	3803	13	128.2
415	s2-12180	0.29	260	432	0.62	1.337	0.015	0.3409	0.0030	3600	31	3669	13	101.9
416	s2-12181	1.10	265	618	0.44	1.807	0.021	0.3324	0.0029	2840	26	3630	13	127.8
417	s2-12182	7.04	357	825	0.44	2.014	0.021	0.2170	0.0047	2599	22	2960	34	113.9
418	s2-12183	1.49	536	1692	0.33	3.733	0.036	0.1350	0.0017	1530	13	2166	21	141.6
419	s2-12184	3.11	290	846	0.35	2.197	0.060	0.2771	0.0041	2418	55	3348	23	138.5
420	s2-12185	8.73	307	790	0.40	1.943	0.056	0.3225	0.0080	2677	63	3584	37	133.9
421	s2-12186	1.40	295	902	0.34	2.831	0.035	0.2165	0.0023	1950	21	2956	18	151.6
422	s2-12187	10.11	661	2594	0.26	4.588	0.066	0.1209	0.0029	1271	17	1971	42	155.1
423	s2-12191	0.48	255	631	0.41	2.106	0.041	0.3230	0.0032	2504	40	3586	15	143.2
424	s2-12192	0.00	431	753	0.59	2.005	0.022	0.2842	0.0029	2608	24	3388	15	129.9
425	s2-12193	0.00	372	819	0.47	1.858	0.019	0.3266	0.0026	2776	23	3603	12	129.8
426	s2-12194	0.12	297	844	0.36	1.682	0.019	0.3264	0.0026	3007	27	3602	12	119.8
427	s2-12195	0.12	40	976	0.04	2.373	0.022	0.1698	0.0015	2266	18	2557	15	112.8
428	s2-12196	0.00	464	857	0.56	1.729	0.039	0.3093	0.0040	2942	54	3519	20	119.6
429	s2-12197	0.00	261	476	0.56	1.600	0.017	0.3134	0.0028	3130	27	3539	14	113.1
430	s2-12198	4.84	226	1028	0.23	3.132	0.049	0.2560	0.0043	1786	24	3224	26	180.5

	UC14													
1	14-01	0.00	255	609	0.43	1.957	0.023	0.2109	0.0018	2660	26	2914	13	91.3
2	14-02	1.18	235	640	0.38	2.237	0.031	0.1974	0.0028	2382	27	2806	23	84.9
3	14-03	0.00	368	524	0.72	1.624	0.019	0.2406	0.0020	3094	29	3125	13	99.0
4	14-04	0.00	361	1001	0.37	2.678	0.029	0.1705	0.0015	2046	19	2564	15	79.8
5	14-05	0.27	129	238	0.56	1.824	0.020	0.2270	0.0023	2818	25	3032	17	92.9
6	14-06	0.56	379	356	1.09	1.713	0.019	0.2281	0.0028	2964	26	3040	20	97.5
7	14-07	0.00	256	474	0.55	1.726	0.019	0.2452	0.0019	2947	26	3155	13	93.4
8	14-08	0.00	349	637	0.56	1.861	0.019	0.2255	0.0018	2773	23	3022	12	91.8
9	14-09	0.38	316	890	0.36	2.305	0.025	0.1838	0.0023	2323	21	2689	21	86.4
10	14-10	0.00	629	778	0.83	2.458	0.035	0.1746	0.0015	2200	26	2603	15	84.5
11	14-11	0.28	532	454	1.20	1.645	0.015	0.2476	0.0039	3062	23	3171	25	96.6
12	14-12	0.22	95	182	0.53	1.669	0.020	0.2380	0.0025	3027	29	3108	17	97.4
13	14-13	0.00	250	377	0.68	1.632	0.018	0.2457	0.0024	3081	28	3159	15	97.5
14	14-14	0.00	889	1178	0.77	3.189	0.037	0.1530	0.0013	1758	18	2381	14	73.9
15	14-15	0.19	132	846	0.16	2.372	0.023	0.1810	0.0015	2268	18	2663	14	85.2
16	14-16	0.21	69	85	0.84	1.539	0.025	0.2529	0.0038	3227	41	3204	24	100.7
17	14-17	0.01	180	362	0.51	1.622	0.016	0.2263	0.0021	3097	24	3028	15	102.3

18	14-18	0.21	348	639	0.56	1.995	0.018	0.2147	0.0020	2620	19	2942	16	89.0
19	14-19	0.01	286	470	0.62	1.573	0.024	0.2305	0.0023	3172	39	3057	16	103.8
20	14-20	1.67	203	337	0.62	1.707	0.019	0.2104	0.0024	2972	27	2910	18	102.1
21	14-21	0.00	243	397	0.63	1.660	0.016	0.2383	0.0019	3039	23	3110	13	97.7
22	14-22	0.00	461	566	0.84	1.846	0.017	0.2400	0.0020	2790	21	3121	13	89.4
23	14-23	0.00	203	262	0.79	1.758	0.017	0.2255	0.0022	2903	23	3022	15	96.1
24	14-24	0.00	621	1215	0.52	3.033	0.040	0.1647	0.0021	1837	21	2506	21	73.3
25	14-25	0.00	319	820	0.40	1.838	0.018	0.2132	0.0018	2801	22	2931	14	95.6
26	14-26	0.17	310	747	0.43	2.191	0.025	0.1936	0.0017	2424	23	2775	14	87.4
27	14-27	0.00	888	473	1.92	1.655	0.017	0.2494	0.0022	3047	25	3182	14	95.8
28	14-28	1.10	129	327	0.40	1.962	0.024	0.2245	0.0026	2656	26	3015	18	88.1
29	14-29	9.05	483	1362	0.36	2.364	0.036	0.1198	0.0033	2274	29	1955	48	116.3
30	14-30	0.70	192	824	0.24	2.260	0.022	0.1855	0.0018	2362	19	2704	16	87.3
31	14-31	0.00	336	655	0.53	1.652	0.016	0.2355	0.0020	3051	24	3091	14	98.7
32	14-32	0.00	487	672	0.74	2.121	0.022	0.2014	0.0016	2490	21	2839	13	87.7
33	14-33	0.00	5010	622	8.27	1.535	0.031	0.2530	0.0035	3234	51	3205	22	100.9
34	14-34	0.53	223	548	0.42	1.902	0.027	0.2417	0.0025	2723	31	3132	17	86.9
35	14-35	0.20	172	451	0.39	1.828	0.022	0.2185	0.0020	2813	28	2971	15	94.7
36	14-36	0.48	135	202	0.68	1.660	0.018	0.2586	0.0028	3040	27	3240	17	93.8
37	14-37	0.00	426	789	0.55	2.106	0.029	0.2153	0.0016	2505	28	2947	12	85.0
38	14-38	0.40	223	338	0.68	1.741	0.018	0.2303	0.0023	2926	25	3055	17	95.8
39	14-39	0.39	191	264	0.74	1.720	0.017	0.2481	0.0024	2954	23	3174	15	93.1
40	14-40	1.15	431	592	0.75	1.728	0.017	0.2278	0.0025	2943	23	3038	18	96.9
41	14-41	0.24	145	980	0.15	2.482	0.030	0.1786	0.0014	2183	22	2641	13	82.6
42	14-42	0.20	222	462	0.49	1.711	0.018	0.2354	0.0023	2967	25	3090	16	96.0
43	14-43	0.00	220	914	0.25	2.760	0.035	0.1676	0.0015	1993	22	2535	15	78.6
44	14-44	0.00	674	567	1.22	1.955	0.021	0.2246	0.0021	2663	23	3015	15	88.3
45	14-45	0.00	490	742	0.68	2.243	0.024	0.2177	0.0017	2377	21	2965	13	80.2
46	14-46	0.00	646	747	0.89	2.118	0.025	0.2231	0.0020	2493	24	3004	15	83.0
47	14-47	0.70	272	1476	0.19	2.803	0.043	0.1621	0.0025	1967	26	2479	26	79.3
48	14-48	0.00	377	591	0.65	1.799	0.019	0.2347	0.0018	2849	24	3086	12	92.3
49	14-49	1.76	321	375	0.88	1.892	0.028	0.2356	0.0034	2736	33	3092	22	88.5
50	14-50	3.27	271	359	0.77	2.406	0.048	0.2220	0.0048	2241	37	2997	34	74.8
51	14-51	1.14	254	1179	0.22	3.089	0.047	0.1414	0.0018	1808	24	2246	21	80.5
52	14-52	0.64	946	1356	0.72	2.775	0.048	0.1582	0.0025	1984	29	2437	27	81.4
53	14-53	0.00	197	367	0.55	1.641	0.020	0.2404	0.0023	3068	30	3124	15	98.2
54	14-54	0.45	321	532	0.62	1.785	0.023	0.2544	0.0027	2868	30	3214	16	89.2
55	14-55	0.00	343	356	0.99	1.576	0.019	0.2687	0.0025	3167	30	3300	15	96.0
56	14-56	0.00	157	661	0.24	2.170	0.024	0.2256	0.0018	2443	23	3023	12	80.8
57	14-57	0.65	302	531	0.58	2.005	0.030	0.1993	0.0031	2609	32	2822	25	92.4
58	14-58	0.09	196	346	0.58	1.694	0.019	0.2333	0.0026	2991	26	3076	18	97.2
59	14-59	1.94	355	602	0.60	1.901	0.025	0.2121	0.0027	2725	30	2923	20	93.2
60	14-60	3.01	130	174	0.77	1.273	0.021	0.2317	0.0035	3736	46	3065	24	121.9
61	14-61	0.00	369	777	0.49	1.717	0.020	0.2279	0.0022	2958	28	3039	15	97.3
62	14-62	0.00	441	575	0.79	1.909	0.023	0.2274	0.0023	2716	27	3035	16	89.5
63	14-63	0.33	127	1208	0.11	2.623	0.027	0.1533	0.0016	2082	18	2384	18	87.3
64	14-64	0.23	379	735	0.53	1.847	0.029	0.2277	0.0036	2789	36	3038	25	91.8
65	14-65	0.23	257	363	0.73	1.576	0.018	0.2385	0.0025	3167	28	3112	16	101.8
66	14-66	0.00	196	373	0.54	1.555	0.017	0.2471	0.0021	3202	28	3167	14	101.1
67	14-67	0.21	242	652	0.38	1.670	0.021	0.2211	0.0023	3025	30	2990	17	101.2
68	14-68	0.00	231	403	0.59	1.653	0.018	0.2475	0.0025	3050	26	3170	16	96.2
69	14-69	0.03	284	563	0.52	1.721	0.019	0.2306	0.0024	2953	26	3057	17	96.6
70	14-70	0.00	473	499	0.97	1.870	0.024	0.2337	0.0024	2762	29	3079	17	89.7
71	14-71	0.15	313	619	0.52	1.633	0.018	0.2322	0.0023	3079	28	3069	15	100.3
72	14-72	0.13	91	579	0.16	1.869	0.020	0.2110	0.0022	2763	25	2914	17	94.8
73	14-73	0.12	197	312	0.65	1.575	0.017	0.2344	0.0026	3169	28	3084	18	102.8
74	14-74	0.16	337	546	0.63	2.081	0.025	0.2103	0.0025	2530	25	2909	20	87.0
75	14-75	0.62	437	1289	0.35	3.034	0.037	0.1394	0.0016	1837	19	2221	19	82.7
76	14-76	0.32	202	488	0.42	1.718	0.019	0.2369	0.0025	2958	26	3101	16	95.4
77	14-77	0.74	164	202	0.83	1.955	0.030	0.2261	0.0036	2663	34	3026	26	88.0
78	14-78	2.03	134	328	0.42	1.721	0.019	0.2255	0.0026	2952	26	3022	18	97.7
79	14-79	0.00	472	1024	0.47	1.911	0.019	0.2058	0.0017	2713	22	2874	13	94.4
80	14-80	1.94	197	245	0.82	1.187	0.026	0.2343	0.0029	3939	64	3083	20	127.8
81	14-81	0.20	202	581	0.36	1.891	0.020	0.2136	0.0020	2737	23	2934	15	93.3
82	14-82	0.47	165	227	0.75	1.614	0.022	0.2519	0.0031	3109	34	3198	19	97.2
83	14-83	1.14	308	521	0.61	2.250	0.028	0.1944	0.0025	2370	25	2781	21	85.2
84	14-84	0.20	434	1030	0.43	2.219	0.025	0.1847	0.0018	2398	22	2697	16	88.9
85	14-85	0.17	404	788	0.53	1.880	0.029	0.2202	0.0027	2749	35	2984	19	92.1
86	14-86	0.00	372	385	0.99	1.747	0.026	0.2375	0.0023	2917	35	3104	16	94.0

87	14-87	2.55	43	332	0.13	1.801	0.033	0.1961	0.0055	2847	42	2795	45	101.9
	UC15													
1	15-09104	0.00	404	443	0.93	2.251	0.029	0.1719	0.0018	2370	26	2577	17	92.0
2	15-09105	0.00	58	70	0.85	1.741	0.030	0.2009	0.0036	2926	41	2835	29	103.2
3	15-09106	0.00	243	843	0.30	2.809	0.036	0.1669	0.0015	1963	22	2528	15	77.7
4	15-09107	0.00	148	228	0.67	1.990	0.025	0.1720	0.0016	2625	27	2578	16	101.8
5	15-09108	0.00	744	558	1.37	2.952	0.035	0.1645	0.0016	1880	19	2503	17	75.1
6	15-09109	0.68	126	321	0.40	2.363	0.049	0.1693	0.0021	2275	40	2552	21	89.1
	UC21													
1	21-09004	0.00	545	451	1.24	1.734	0.027	0.2528	0.0026	2935	37	3204	16	91.6
2	21-09005	0.00	273	238	1.18	2.016	0.033	0.2246	0.0027	2597	35	3015	19	86.1
3	21-09006	0.33	0	13	0.03	1.315	0.043	0.2139	0.0072	3646	91	2937	53	124.1
4	21-09007	0.00	613	230	2.73	2.156	0.040	0.2083	0.0026	2456	38	2894	19	84.9
5	21-09008	0.00	231	134	1.77	1.866	0.031	0.2121	0.0045	2766	37	2923	34	94.6
6	21-09009	0.00	129	209	0.63	1.925	0.033	0.1752	0.0021	2697	38	2610	19	103.3
7	21-09010	0.00	54	88	0.63	1.879	0.033	0.1961	0.0030	2751	39	2795	25	98.4
8	21-09011	0.00	2327	2090	1.14	4.965	0.066	0.1211	0.0010	1183	14	1974	14	59.9
9	21-09015	0.00	3205	945	3.48	3.144	0.046	0.1515	0.0019	1780	23	2364	21	75.3
10	21-09016	0.00	170	233	0.75	2.266	0.039	0.2510	0.0030	2357	34	3193	19	73.8
11	21-09017	0.00	377	673	0.57	2.311	0.031	0.1640	0.0016	2318	27	2499	16	92.7
12	21-09018	0.00	679	465	1.50	2.573	0.031	0.1769	0.0016	2116	22	2626	14	80.6
13	21-09019	0.00	1424	585	2.50	2.498	0.037	0.1730	0.0019	2171	27	2588	18	83.9
14	21-09020	0.00	1400	609	2.36	2.664	0.044	0.1599	0.0017	2055	29	2456	17	83.7
15	21-09021	0.00	562	533	1.08	2.251	0.037	0.1681	0.0018	2369	32	2540	18	93.3
16	21-09022	0.00	1332	515	2.65	2.188	0.038	0.1857	0.0020	2427	35	2706	18	89.7
17	21-09026	0.00	4223	1456	2.97	4.595	0.080	0.1418	0.0015	1269	20	2250	18	56.4
18	21-09027	0.00	182	61	3.07	2.025	0.039	0.1887	0.0037	2587	41	2732	32	94.7
19	21-09028	0.00	90	77	1.20	1.857	0.033	0.2135	0.0034	2777	40	2934	25	94.6
20	21-09029	0.00	267	115	2.37	2.304	0.038	0.1872	0.0028	2324	32	2719	24	85.5
21	21-09030	0.09	971	1599	0.62	3.425	0.040	0.1311	0.0014	1651	17	2114	19	78.1
22	21-09031	0.00	514	261	2.02	2.149	0.036	0.1740	0.0019	2463	34	2598	18	94.8
23	21-09032	0.00	640	211	3.11	2.122	0.034	0.1823	0.0022	2489	33	2675	20	93.1
24	21-09033	0.00	414	359	1.18	1.998	0.027	0.1717	0.0017	2616	29	2576	16	101.5
25	21-09037	0.33	27	38	0.72	1.789	0.042	0.1929	0.0050	2863	54	2769	42	103.4
26	21-09038	0.00	23	28	0.84	1.743	0.043	0.2173	0.0051	2923	58	2962	37	98.7
27	21-09039	0.00	715	639	1.15	3.190	0.070	0.1730	0.0018	1758	34	2588	18	67.9
28	21-09040	0.29	149	265	0.58	1.998	0.029	0.1864	0.0025	2615	31	2712	22	96.4
29	21-09041	0.00	103	56	1.91	2.158	0.051	0.2088	0.0039	2455	48	2898	30	84.7
30	21-09042	0.00	2183	612	3.66	2.625	0.035	0.1628	0.0015	2080	24	2486	15	83.7
31	21-09043	0.00	500	383	1.34	2.310	0.027	0.1792	0.0018	2319	23	2646	17	87.6
32	21-09044	0.00	592	809	0.75	2.283	0.026	0.1664	0.0013	2342	23	2523	12	92.8
33	21-09048	0.00	338	378	0.92	1.914	0.025	0.1838	0.0018	2710	29	2689	16	100.8
34	21-09049	0.00	1690	730	2.37	3.047	0.037	0.1555	0.0016	1830	19	2408	18	76.0
35	21-09050	0.00	3455	559	6.34	3.139	0.045	0.1706	0.0016	1783	22	2565	15	69.5
36	21-09051	0.00	22	91	0.24	1.821	0.033	0.2162	0.0031	2821	42	2954	23	95.5
37	21-09052	0.00	1514	258	6.01	2.339	0.033	0.1922	0.0021	2295	27	2763	17	83.0
38	21-09053	0.00	196	109	1.84	2.082	0.032	0.1891	0.0028	2529	32	2736	24	92.4
39	21-09054	0.00	38	53	0.74	1.494	0.027	0.2850	0.0045	3304	46	3392	24	97.4
40	21-09055	0.00	123	131	0.96	1.771	0.025	0.2153	0.0027	2885	33	2947	20	97.9
41	21-09059	0.00	1987	296	6.90	2.655	0.034	0.1751	0.0019	2060	23	2608	19	79.0
42	21-09060	0.00	1225	439	2.86	3.530	0.044	0.2108	0.0021	1608	18	2913	16	55.2
43	21-09061	0.00	2567	1128	2.33	4.708	0.176	0.1633	0.0017	1242	42	2491	18	49.8
44	21-09062	0.00	1993	1364	1.50	3.397	0.041	0.1350	0.0011	1663	18	2165	14	76.8
45	21-09063	0.00	300	255	1.20	1.848	0.024	0.2161	0.0023	2788	29	2953	17	94.4
46	21-09064	0.00	35	58	0.61	2.003	0.041	0.1828	0.0036	2611	44	2680	33	97.4
47	21-09065	0.00	484	642	0.77	2.300	0.027	0.1670	0.0015	2327	23	2529	16	92.0
48	21-09066	0.20	62	209	0.30	2.034	0.030	0.1754	0.0024	2578	32	2611	23	98.7
49	21-09070	0.00	97	94	1.06	1.810	0.030	0.2042	0.0030	2836	38	2861	24	99.1
50	21-09071	0.00	123	145	0.87	1.963	0.028	0.2153	0.0025	2654	31	2947	19	90.1
51	21-09072	0.00	151	194	0.80	2.069	0.029	0.1785	0.0021	2542	30	2641	19	96.3
52	21-09073	0.00	1079	573	1.93	2.274	0.029	0.1833	0.0017	2349	25	2685	15	87.5
53	21-09074	0.08	123	144	0.87	1.817	0.027	0.1986	0.0034	2827	34	2816	28	100.4
54	21-09075	0.00	436	192	2.33	2.347	0.038	0.1903	0.0025	2288	31	2746	21	83.3
55	21-09076	0.00	1271	322	4.05	1.860	0.024	0.2019	0.0019	2773	29	2843	15	97.6
56	21-09077	0.00	249	757	0.34	2.468	0.031	0.1584	0.0014	2193	24	2439	15	89.9
57	21-09081	0.00	274	757	0.37	2.513	0.031	0.1627	0.0013	2159	23	2485	14	86.9
58	21-09082	0.00	757	448	1.74	2.060	0.030	0.1815	0.0018	2551	31	2668	17	95.6

59	21-09083	0.00	546	213	2.63	1.872	0.027	0.1866	0.0019	2759	32	2714	17	101.7
60	21-09084	0.07	73	87	0.86	1.852	0.035	0.1896	0.0037	2783	43	2740	32	101.6
61	21-09085	0.00	62	123	0.52	1.588	0.021	0.2627	0.0030	3148	33	3264	18	96.5
62	21-09086	0.00	62	94	0.67	1.626	0.025	0.2176	0.0024	3091	38	2964	18	104.3
63	21-09087	0.00	62	85	0.75	1.785	0.029	0.2178	0.0031	2868	38	2965	23	96.7
64	21-09088	0.00	54	115	0.48	1.747	0.028	0.1995	0.0023	2917	37	2823	19	103.3
65	21-09092	0.00	1025	1101	0.96	2.927	0.036	0.1542	0.0013	1894	20	2395	14	79.1
66	21-09093	0.00	661	343	1.98	1.666	0.020	0.2098	0.0019	3030	29	2905	15	104.3
67	21-09094	0.00	660	274	2.47	2.126	0.024	0.1840	0.0019	2485	24	2690	18	92.4
68	21-09095	0.00	3122	663	4.83	2.983	0.049	0.1728	0.0014	1864	26	2586	14	72.1
69	21-09096	0.00	223	126	1.82	2.012	0.035	0.1879	0.0023	2601	37	2725	20	95.5
70	21-09097	0.00	1005	340	3.04	2.467	0.028	0.1771	0.0015	2194	21	2627	14	83.5
71	21-09098	0.00	2738	1048	2.68	2.945	0.033	0.1535	0.0012	1885	18	2387	13	79.0
72	21-09099	0.00	1065	429	2.55	2.465	0.032	0.1933	0.0019	2195	24	2772	16	79.2

Table 3-2. Results from LA-MC-ICPMS Lu-Hf isotopic data for detrital zircons from the Murmac Bay Group.

spot No.	spot No. of U-Pb	spot size [µm]	$^{176}Yb/^{177}Hf$	2se	$^{176}Lu/^{177}Hf$	2se	$^{180}Hf/^{177}Hf$	2σ	$^{178}Hf/^{177}Hf$	2σ	$^{176}Hf/^{177}Hf$	2σ	$^{176}Hf/^{177}Hf(t)$	2σ	Pb-Pb Age [Ma]	2σ	eHf(t)	2σ	T_{DM} [Ga]
UC02																			
UC02_50_1	02-09061	50	0.02154	0.00066	0.00072	0.00002	1.886678	0.000192	1.467193	0.000092	0.280441	0.000032	0.280380	0.000032	3369	50	-7.80	1.15	3.96
UC02_50_2	02-09062	50	0.04712	0.00207	0.00151	0.00007	1.886572	0.000201	1.467146	0.000099	0.280537	0.000043	0.280417	0.000040	3666	11	0.65	1.44	3.77
UC02_50_3	02-09071	50	0.03797	0.00230	0.00120	0.00007	1.886607	0.000184	1.467228	0.000096	0.280492	0.000036	0.280399	0.000035	3375	12	-6.98	1.27	3.92
UC02_50_4	02-09081	50	0.05164	0.00128	0.00153	0.00003	1.886612	0.000183	1.467184	0.000100	0.280517	0.000037	0.280393	0.000037	3708	11	0.81	1.32	3.79
UC02_50_5	02-09065	50	0.02866	0.00043	0.00087	0.00002	1.886660	0.000182	1.467106	0.000090	0.280449	0.000040	0.280378	0.000040	3350	14	-8.31	1.41	3.97
UC02_50_6	02-09076	50	0.03057	0.00128	0.00096	0.00004	1.886696	0.000187	1.467162	0.000098	0.280448	0.000034	0.280367	0.000034	3714	11	0.03	1.21	3.84
UC02_50_7	02-09077	50	0.01916	0.00059	0.00060	0.00002	1.886596	0.000180	1.467119	0.000102	0.280427	0.000034	0.280370	0.000034	3671	14	-0.89	1.22	3.85
UC02_50_8	02-09110	50	0.03558	0.00150	0.00112	0.00005	1.886640	0.000181	1.467189	0.000098	0.280476	0.000034	0.280375	0.000035	3692	12	-0.22	1.26	3.83
UC02_50_9	02-09129	50	0.03651	0.00037	0.00116	0.00001	1.886626	0.000179	1.467136	0.000093	0.280451	0.000034	0.280355	0.000034	3647	13	-2.02	1.23	3.89
UC02_50_10	02-09105	50	0.03912	0.00043	0.00120	0.00002	1.886767	0.000191	1.467226	0.000102	0.280482	0.000035	0.280384	0.000035	3456	15	-5.56	1.24	3.91
UC02_50_11	02-09114	50	0.02876	0.00044	0.00092	0.00001	1.886679	0.000194	1.467211	0.000096	0.280475	0.000037	0.280403	0.000037	3272	88	-9.30	1.31	3.95
UC02_50_12	02-09136	50	0.05003	0.00159	0.00164	0.00005	1.886584	0.000190	1.467163	0.000107	0.280518	0.000036	0.280396	0.000036	3404	27	-6.38	1.27	3.91
UC02_40_1	02-09093	40	0.04442	0.00106	0.00127	0.00003	1.886752	0.000170	1.467232	0.000126	0.280479	0.000034	0.280457	0.000034	3606	15	0.64	1.23	3.72
UC02_40_4	02-09118	40	0.03387	0.00042	0.00114	0.00001	1.886665	0.000207	1.467050	0.000130	0.280457	0.000035	0.280437	0.000035	3596	14	-0.32	1.26	3.76
UC02S_1	sc-12096	40	0.02664	0.00146	0.00065	0.00006	1.886635	0.000196	1.467072	0.000136	0.281097	0.000052	0.281053	0.000052	2632	19	-1.35	1.86	2.99
UC02S_2	sc-12105	40	0.10589	0.00257	0.00213	0.00006	1.886611	0.000170	1.467112	0.000088	0.281269	0.000049	0.281152	0.000049	2709	17	4.02	1.73	2.78
UC02S_3	sa-12019	40	0.02768	0.00066	0.00068	0.00001	1.886520	0.000170	1.467116	0.000098	0.281172	0.000054	0.281130	0.000054	2589	22	0.39	1.92	2.86
UC02S_4	sa-12026	40	0.02279	0.00009	0.00054	0.00000	1.886801	0.000176	1.467164	0.000095	0.281126	0.000051	0.281090	0.000051	2618	20	-0.33	1.81	2.93
UC02S_5	sa-12031	40	0.04721	0.00192	0.00113	0.00006	1.886785	0.000199	1.467160	0.000113	0.281204	0.000049	0.281128	0.000049	3073	30	11.78	1.75	3.07
UC02S_6	sa-12039	40	0.07302	0.01507	0.00158	0.00035	1.886527	0.000301	1.466952	0.000113	0.281114	0.000054	0.281035	0.000054	2881	23	3.90	1.92	2.93
UC02S_7	sa-12043	40	0.09911	0.00382	0.00235	0.00011	1.886381	0.000357	1.466862	0.000137	0.281326	0.000067	0.281181	0.000066	3031	20	12.66	2.36	3.03
UC02S_8	sa-12052	40	0.03473	0.00263	0.00067	0.00005	1.886643	0.000175	1.467155	0.000104	0.281217	0.000050	0.281171	0.000051	2914	25	9.54	1.80	2.91
UC02S_9	sa-12060	40	0.03482	0.00193	0.00075	0.00003	1.886530	0.000166	1.467145	0.000089	0.280984	0.000049	0.280930	0.000050	2810	25	-1.51	1.77	3.15
UC02S_10	sa-12061	40	0.02244	0.00034	0.00058	0.00001	1.886636	0.000191	1.467201	0.000104	0.281070	0.000051	0.281032	0.000052	2645	40	-1.76	1.83	3.02
UC02S_11	sb-12010	40	0.03143	0.00074	0.00071	0.00002	1.886667	0.000185	1.467226	0.000100	0.280927	0.000047	0.280883	0.000047	2583	34	-8.53	1.68	3.32
UC02S_12	sb-12018	40	0.03311	0.00175	0.00072	0.00004	1.886755	0.000180	1.467189	0.000090	0.281203	0.000050	0.281159	0.000050	2618	31	2.10	1.78	2.80
UC02S_13	sb-12019	40	0.01656	0.00043	0.00041	0.00001	1.886824	0.000183	1.467217	0.000113	0.281209	0.000048	0.281178	0.000048	2702	21	4.77	1.70	2.73
UC02S_14	sb-12022	40	0.02669	0.00015	0.00063	0.00000	1.886525	0.000185	1.467126	0.000097	0.281030	0.000049	0.280988	0.000049	2745	22	-0.99	1.73	3.07
UC02S_15	sb-12030	40	0.06457	0.00851	0.00169	0.00029	1.886563	0.000210	1.466975	0.000153	0.281008	0.000071	0.280912	0.000073	2872	19	-0.67	2.61	3.16
UC02S_16	sb-12033	40	0.03658	0.00097	0.00095	0.00003	1.886784	0.000176	1.467155	0.000096	0.281172	0.000049	0.281113	0.000049	2741	30	3.37	1.73	2.84
UC02S_17	sb-12041	40	0.02692	0.00037	0.00064	0.00001	1.886588	0.000172	1.467200	0.000075	0.281064	0.000048	0.281024	0.000048	2553	23	-4.25	1.70	3.08
UC02S_18	sb-12039	40	0.03836	0.00100	0.00096	0.00001	1.886572	0.000185	1.467161	0.000083	0.281306	0.000052	0.281252	0.000052	2478	35	2.12	1.83	2.68
UC02S_19	sb-12028	40	0.02634	0.00020	0.00063	0.00001	1.886624	0.000188	1.467135	0.000088	0.281165	0.000055	0.281124	0.000055	2659	32	1.84	1.96	2.85
UC02S_20	sb-12038	40	0.03556	0.00040	0.00082	0.00001	1.886559	0.000179	1.467197	0.000092	0.281188	0.000049	0.281139	0.000049	2612	15	1.24	1.76	2.84
UC02L_2	ma-12004	40	0.03101	0.00061	0.00072	0.00001	1.886675	0.000187	1.467131	0.000077	0.281210	0.000049	0.281165	0.000049	2609	28	2.10	1.73	2.79
UC02L_4	ma-12011	40	0.03679	0.00122	0.00086	0.00002	1.886671	0.000165	1.467171	0.000086	0.281166	0.000047	0.281113	0.000047	2618	24	0.48	1.67	2.88
UC02L_5	ma-12065	40	0.03446	0.00088	0.00087	0.00001	1.886660	0.000179	1.467197	0.000095	0.281176	0.000047	0.281124	0.000047	2701	38	2.80	1.68	2.83
UC02L_6	ma-12098	40	0.03485	0.00181	0.00078	0.00003	1.886514	0.000187	1.467193	0.000093	0.281206	0.000048	0.281160	0.000049	2548	14	0.48	1.73	2.82
UC02L_7	ma-12099	40	0.03257	0.00055	0.00078	0.00002	1.886840	0.000166	1.467207	0.000089	0.280828	0.000051	0.280772	0.000051	3132	18	0.51	1.81	3.32
UC02L_8	ma-12105	40	0.07404	0.00155	0.00172	0.00004	1.886702	0.000166	1.467182	0.000092	0.281244	0.000050	0.281146	0.000049	2701	25	3.61	1.76	2.79
UC02L_9	ma-12114	40	0.02422	0.00050	0.00052	0.00001	1.886838	0.000177	1.467225	0.000083	0.281053	0.000048	0.281018	0.000048	2613	42	-3.03	1.71	3.06
UC02L_10	ma-12119	40	0.02528	0.00019	0.00067	0.00001	1.886679	0.000165	1.467201	0.000082	0.281176	0.000048	0.281137	0.000049	2723	26	3.79	1.73	2.80
UC02L_11	ma-12132	40	0.03364	0.00112	0.00082	0.00003	1.886646	0.000168	1.467161	0.000086	0.280938	0.000048	0.280889	0.000047	2870	21	-1.54	1.68	3.20
UC02L_12	ma-12148	40	0.04441	0.00163	0.00100	0.00003	1.886673	0.000167	1.467228	0.000077	0.281222	0.000048	0.281164	0.000048	2573	22	1.22	1.71	2.81
UC02L_13	ma-12142	40	0.01373	0.00022	0.00033	0.00000	1.886610	0.000183	1.467143	0.000087	0.281094	0.000048	0.281070	0.000048	2587	24	-1.80	1.69	2.98
UC02L_14	ma-12143	40	0.03467	0.00109	0.00078	0.00002	1.886689	0.000184	1.467132	0.000087	0.281145	0.000048	0.281098	0.000048	2588	29	-0.77	1.72	2.92
UC02L_15	ma-12150	40	0.04637	0.00061	0.00112	0.00001	1.886652	0.000187	1.467178	0.000093	0.281176	0.000051	0.281113	0.000051	2499	17	-2.33	1.81	2.93
UC02L_16	ma-12160	40	0.03746	0.00091	0.00089	0.00002	1.886511	0.000180	1.467124	0.000091	0.281085	0.000052	0.281030	0.000052	2704	26	-0.46	1.86	3.01
UC02L_17	ma-12162	40	0.01607	0.00020	0.00043	0.00000	1.886617	0.000173	1.467174	0.000077	0.281192	0.000050	0.281163	0.000050	2488	49	-0.81	1.79	2.84

UC02L_18	ma-12164	40	0.02187	0.00070	0.00058	0.00002	1.886740	0.000176	1.467150	0.000103	0.281187	0.000051	0.281147	0.000051	2722	33	4.13	1.81	2.78
UC02L_19	ma-12169	40	0.03526	0.00037	0.00082	0.00001	1.886627	0.000178	1.467147	0.000097	0.281204	0.000049	0.281154	0.000049	2613	25	1.82	1.73	2.81
UC02L_20	ma-12170	40	0.02355	0.00144	0.00057	0.00003	1.886718	0.000169	1.467124	0.000089	0.280780	0.000053	0.280736	0.000053	3201	18	0.89	1.88	3.36
UC02L_21	ma-12174	40	0.02613	0.00066	0.00067	0.00001	1.886749	0.000178	1.467203	0.000095	0.281197	0.000047	0.281155	0.000047	2605	15	1.64	1.68	2.81
UC02L_22	ma-12180	40	0.03543	0.00056	0.00083	0.00001	1.886556	0.000179	1.467076	0.000085	0.281075	0.000054	0.281022	0.000054	2774	21	0.91	1.91	2.99
UC02L_23	ma-12182	40	0.03156	0.00023	0.00077	0.00000	1.886726	0.000190	1.467202	0.000082	0.281118	0.000052	0.281072	0.000052	2584	17	-1.81	1.86	2.98
UC02L_24	ma-12191	40	0.03093	0.00032	0.00079	0.00001	1.886670	0.000186	1.467136	0.000108	0.281205	0.000048	0.281154	0.000048	2774	24	5.63	1.72	2.77
UC02L_25	mb-12005	40	0.05577	0.00322	0.00123	0.00007	1.886708	0.000187	1.467153	0.000080	0.280820	0.000050	0.280747	0.000050	2554	15	-14.06	1.77	3.59
UC02L_26	mb-12018	40	0.02604	0.00301	0.00058	0.00006	1.886700	0.000168	1.467189	0.000098	0.281037	0.000049	0.280997	0.000049	2697	23	-1.79	1.73	3.07
UC02L_27	mb-12019	40	0.03472	0.00168	0.00087	0.00005	1.886742	0.000172	1.467180	0.000100	0.281171	0.000052	0.281120	0.000052	2622	16	0.79	1.87	2.87
UC02L_28	mb-12037	40	0.04112	0.00391	0.00100	0.00009	1.886761	0.000171	1.467284	0.000093	0.281111	0.000053	0.281054	0.000053	2599	23	-2.09	1.90	3.00
UC02L_29	mb-12043	40	0.03238	0.00216	0.00077	0.00004	1.886707	0.000179	1.467186	0.000082	0.280772	0.000051	0.280723	0.000051	2704	68	-11.38	1.80	3.57
UC02L_30	mb-12055	40	0.03975	0.00070	0.00107	0.00001	1.886690	0.000165	1.467175	0.000120	0.281185	0.000052	0.281122	0.000052	2696	37	2.61	1.84	2.84
UC03																			
UC03_1	03-09011	50	0.13542	0.00063	0.00316	0.00001	1.886665	0.000124	1.467204	0.000070	0.280787	0.000034	0.280607	0.000034	2911	61	-10.63	1.22	3.71
UC03_2	03-09016	50	0.06918	0.00245	0.00182	0.00005	1.886585	0.000118	1.467131	0.000068	0.280780	0.000031	0.280667	0.000031	3210	9	-1.37	1.12	3.48
UC03_3	03-09015	50	0.05406	0.00106	0.00189	0.00003	1.886715	0.000183	1.467218	0.000075	0.280812	0.000031	0.280703	0.000031	2908	13	-7.26	1.09	3.53
UC03_4	03-09030	50	0.11774	0.00233	0.00280	0.00005	1.886582	0.000117	1.467140	0.000071	0.280790	0.000034	0.280622	0.000033	3063	13	-6.47	1.18	3.63
UC03_5	03-09029	50	0.10719	0.00094	0.00260	0.00003	1.886647	0.000154	1.467195	0.000075	0.280715	0.000033	0.280559	0.000033	3051	32	-9.00	1.16	3.75
UC03_6	03-09054	50	0.11866	0.00373	0.00281	0.00006	1.886712	0.000134	1.467190	0.000073	0.280727	0.000034	0.280541	0.000034	3333	11	-2.92	1.20	3.67
UC03_7	03-09055	50	0.12742	0.00093	0.00318	0.00001	1.886634	0.000114	1.467184	0.000074	0.280790	0.000032	0.280594	0.000032	3173	11	-4.86	1.15	3.64
UC03_8	03-09052	50	0.09461	0.00195	0.00238	0.00004	1.886650	0.000126	1.467133	0.000068	0.280716	0.000035	0.280570	0.000035	3115	13	-7.07	1.23	3.70
UC03_9	03-09039	50	0.10113	0.00249	0.00249	0.00004	1.886673	0.000123	1.467156	0.000069	0.280769	0.000033	0.280618	0.000034	3104	12	-5.63	1.20	3.62
UC03_10	03-09049	50	0.05595	0.00168	0.00143	0.00004	1.886675	0.000129	1.467177	0.000070	0.280684	0.000033	0.280596	0.000033	3088	15	-6.82	1.17	3.66
UC09																			
UC09_50_1	09-04	50	0.02900	0.00097	0.00086	0.00003	1.886507	0.000178	1.467183	0.000099	0.280868	0.000037	0.280807	0.000037	2853	14	-4.88	1.33	3.36
UC09_50_2	09-05	50	0.04253	0.00177	0.00121	0.00006	1.886588	0.000186	1.467117	0.000091	0.280883	0.000037	0.280810	0.000037	2502	16	-13.06	1.30	3.49
UC09_50_3	09-09	50	0.01572	0.00029	0.00043	0.00001	1.886835	0.000181	1.467201	0.000094	0.280828	0.000033	0.280793	0.000033	2471	17	-14.39	1.19	3.53
UC09_50_4	09-12	50	0.03185	0.00080	0.00095	0.00002	1.886675	0.000183	1.467178	0.000110	0.280899	0.000036	0.280829	0.000037	2873	13	-3.63	1.32	3.32
UC09_50_5	09-16	50	0.03379	0.00053	0.00099	0.00001	1.886804	0.000190	1.467231	0.000109	0.280842	0.000035	0.280774	0.000035	2791	14	-7.50	1.26	3.45
UC09_50_6	09-32	50	0.03870	0.00132	0.00116	0.00004	1.886557	0.000181	1.467099	0.000099	0.280857	0.000038	0.280782	0.000037	2741	16	-8.39	1.32	3.45
UC09_50_7	09-38	50	0.03784	0.00092	0.00113	0.00002	1.886676	0.000192	1.467141	0.000106	0.280914	0.000033	0.280838	0.000033	2885	15	-3.02	1.17	3.29
UC09_50_8	09-41	50	0.04963	0.00153	0.00142	0.00005	1.886670	0.000198	1.467145	0.000097	0.280875	0.000034	0.280787	0.000034	2601	19	-11.52	1.20	3.49
UC09_50_9	09-64	50	0.02963	0.00053	0.00088	0.00002	1.886674	0.000215	1.467127	0.000107	0.280889	0.000034	0.280830	0.000034	2673	18	-8.32	1.21	3.39
UC09_40_01	09-24	40	0.04070	0.00084	0.00105	0.00002	1.886722	0.000183	1.467159	0.000124	0.280849	0.000031	0.280830	0.000031	2702	14	-7.63	1.12	3.38
UC09_40_02	09-35	40	0.05920	0.00316	0.00156	0.00008	1.886649	0.000206	1.467184	0.000131	0.280873	0.000035	0.280847	0.000035	2698	19	-7.09	1.24	3.35
UC09_40_03	09-48	40	0.05095	0.00284	0.00133	0.00007	1.886568	0.000190	1.467157	0.000127	0.280841	0.000033	0.280822	0.000033	2821	23	-5.09	1.17	3.35
UC09_40_04	09-56	40	0.01711	0.00089	0.00044	0.00002	1.886701	0.000178	1.467231	0.000130	0.280808	0.000034	0.280798	0.000034	2814	14	-6.12	1.22	3.40
UC09_40_05	09-60	40	0.03684	0.00066	0.00097	0.00002	1.886633	0.000169	1.467164	0.000125	0.280834	0.000033	0.280816	0.000033	2558	19	-11.50	1.18	3.46
UC09_40_06	09-71	40	0.04835	0.00206	0.00142	0.00003	1.886595	0.000228	1.467163	0.000133	0.280755	0.000033	0.280732	0.000033	2717	16	-10.77	1.18	3.55
UC09_40_07	09-72	40	0.04761	0.00026	0.00131	0.00002	1.886625	0.000186	1.467176	0.000127	0.280886	0.000033	0.280863	0.000033	2786	15	-4.45	1.17	3.28
UC11																			
UC11_1	11-09017	40	0.04292	0.00237	0.00123	0.00011	1.886752	0.000180	1.467125	0.000158	0.281242	0.000040	0.281221	0.000040	2501	28	-0.87	1.43	2.77
UC11_2	11-09009	40	0.03503	0.00108	0.00096	0.00002	1.886639	0.000170	1.467157	0.000123	0.281212	0.000035	0.281194	0.000035	2643	30	3.95	1.25	2.72
UC11_3	11-09022	40	0.01937	0.00016	0.00054	0.00000	1.886578	0.000182	1.467171	0.000124	0.280960	0.000037	0.280948	0.000037	2896	32	1.17	1.31	3.08
UC11_4	11-09050	40	0.06309	0.00096	0.00172	0.00003	1.886560	0.000176	1.467159	0.000121	0.280533	0.000036	0.280505	0.000036	3586	31	1.86	1.29	3.64
UC11_5	11-09053	40	0.04315	0.00128	0.00131	0.00005	1.886499	0.000176	1.467208	0.000136	0.281025	0.000032	0.281004	0.000032	2958	36	4.62	1.16	2.96
UC11_6	11-09088	40	0.00936	0.00014	0.00027	0.00000	1.886706	0.000173	1.467227	0.000128	0.280470	0.000032	0.280462	0.000032	3646	31	1.79	1.14	3.69
UC11_7	11-09108	40	0.02045	0.00061	0.00060	0.00001	1.886633	0.000167	1.467136	0.000122	0.281183	0.000031	0.281171	0.000031	2726	32	5.06	1.12	2.74
UC11_8	11-09086	40	0.01515	0.00012	0.00041	0.00000	1.886607	0.000183	1.467216	0.000125	0.281055	0.000038	0.281045	0.000038	2759	48	1.38	1.36	2.96
UC11_9	11-09095	40	0.03190	0.00231	0.00078	0.00005	1.886575	0.000178	1.467166	0.000124	0.281156	0.000038	0.281140	0.000038	2554	55	-0.08	1.36	2.86
UC11_10	11-09093	40	0.04426	0.00034	0.00118	0.00001	1.886717	0.000176	1.467192	0.000132	0.281039	0.000039	0.281018	0.000039	2696	59	-1.07	1.37	3.03
UC11_11	11-09081	40	0.01563	0.00017	0.00044	0.00000	1.886719	0.000172	1.467140	0.000126	0.280939	0.000034	0.280929	0.000034	2835	25	-0.95	1.23	3.14

UC11_12	11-09104	40	0.02704	0.00047	0.00072	0.00001	1.886668	0.000179	1.467222	0.000132	0.281061	0.000037	0.281047	0.000037	2630	17	-1.61	1.32	3.00
UC11_13	11-09117	40	0.02638	0.00154	0.00067	0.00003	1.886681	0.000178	1.467240	0.000131	0.281121	0.000033	0.281108	0.000032	2606	33	0.01	1.16	2.90
UC11_14	11-09115	40	0.03668	0.00082	0.00102	0.00002	1.886568	0.000180	1.467105	0.000134	0.281073	0.000039	0.281054	0.000039	2844	29	3.71	1.38	2.91
UC11_1	11-09027	**50**	0.02215	0.00117	0.00070	0.00004	1.886687	0.000179	1.467197	0.000114	0.281125	0.000040	0.281078	0.000040	2513	35	-3.27	1.42	2.99
UC11_2	11-09032	**50**	0.02049	0.00067	0.00064	0.00002	1.886551	0.000178	1.467169	0.000101	0.280987	0.000041	0.280938	0.000041	2784	55	-1.83	1.47	3.15
UC11_3	11-09077	**50**	0.04670	0.00072	0.00148	0.00002	1.886592	0.000180	1.467215	0.000102	0.281129	0.000039	0.281034	0.000039	2851	38	3.17	1.40	2.94
UC12																			
UC12s_50_1	s2-12049	50	0.04091	0.00062	0.00112	0.00002	1.886702	0.000196	1.467225	0.000092	0.280482	0.000033	0.280388	0.000033	3624	13	-1.40	1.17	3.84
UC12s_50_2	s2-12050	50	0.04233	0.00159	0.00117	0.00003	1.886687	0.000246	1.467148	0.000107	0.280481	0.000037	0.280388	0.000036	3649	14	-0.77	1.29	3.83
UC12s_50_3	s2-12061	50	0.06010	0.00083	0.00171	0.00003	1.886675	0.000208	1.467176	0.000097	0.280451	0.000034	0.280313	0.000034	3750	12	-1.04	1.23	3.93
UC12s_50_4	s2-12062	50	0.07540	0.00510	0.00211	0.00015	1.886624	0.000220	1.467151	0.000102	0.280526	0.000040	0.280371	0.000035	3395	13	-7.49	1.26	3.96
UC12s_50_5	s2-12066	50	0.04474	0.00027	0.00134	0.00001	1.886680	0.000182	1.467179	0.000095	0.280427	0.000033	0.280317	0.000033	3696	12	-2.18	1.17	3.94
UC12s_50_6	s2-12071	50	0.06222	0.00142	0.00170	0.00002	1.886738	0.000172	1.467158	0.000092	0.280456	0.000036	0.280317	0.000035	3740	11	-1.13	1.26	3.92
UC12s_50_7	s2-12083	50	0.03933	0.00089	0.00121	0.00003	1.886598	0.000206	1.467104	0.000094	0.280362	0.000032	0.280260	0.000033	3763	13	-2.60	1.16	4.02
UC12s_50_8	s2-12087	50	0.04897	0.00082	0.00154	0.00003	1.886634	0.000220	1.467034	0.000089	0.280512	0.000036	0.280388	0.000037	3723	15	0.98	1.31	3.80
UC12s_50_9	s2-12131	50	0.04022	0.00094	0.00139	0.00004	1.886736	0.000234	1.467014	0.000112	0.280368	0.000036	0.280258	0.000036	3658	12	-5.21	1.28	4.07
UC12s_50_10	s2-12132	50	0.05529	0.00058	0.00151	0.00002	1.886676	0.000211	1.467155	0.000097	0.280455	0.000035	0.280341	0.000035	3422	16	-7.91	1.24	4.01
UC12s_50_11	s2-12143	50	0.04870	0.00142	0.00136	0.00003	1.886724	0.000209	1.467194	0.000106	0.280431	0.000034	0.280322	0.000034	3616	12	-3.94	1.22	3.96
UC12s_50_12	s2-12161	50	0.03061	0.00034	0.00086	0.00002	1.886581	0.000223	1.467147	0.000097	0.280716	0.000034	0.280654	0.000034	2790	33	-11.79	1.21	3.67
UC12s_50_13	s2-12125	50	0.05834	0.00128	0.00171	0.00002	1.886657	0.000224	1.467174	0.000099	0.280484	0.000032	0.280350	0.000032	3700	11	-0.91	1.13	3.88
UC12s_50_14	s2-12128	50	0.03101	0.00040	0.00090	0.00001	1.886688	0.000183	1.467131	0.000094	0.280394	0.000033	0.280314	0.000033	3792	12	0.01	1.18	3.91
UC12s_50_15	s2-12105	50	0.06525	0.00298	0.00182	0.00007	1.886737	0.000196	1.467192	0.000105	0.280471	0.000036	0.280322	0.000036	3737	12	-1.00	1.29	3.91
UC12s_50_16	s2-12129	50	0.05279	0.00076	0.00152	0.00002	1.886698	0.000186	1.467143	0.000106	0.280443	0.000036	0.280318	0.000036	3736	15	-1.18	1.30	3.92
UC12s_50_17	s2-12151	50	0.03395	0.00032	0.00111	0.00001	1.886723	0.000197	1.467197	0.000100	0.280390	0.000038	0.280296	0.000038	3701	15	-2.83	1.36	3.98
UC12s_50_19	s2-12159	50	0.05289	0.00262	0.00145	0.00006	1.886632	0.000195	1.467156	0.000099	0.280401	0.000037	0.280274	0.000037	3851	13	0.04	1.32	3.96
UC12s_50_20	S2-12182	50	0.02251	0.00055	0.00059	0.00001	1.886627	0.000222	1.467155	0.000109	0.280679	0.000036	0.280631	0.000036	2960	34	-8.61	1.28	3.65
UC12s_50_21	s2-12010	50	0.07846	0.00179	0.00213	0.00006	1.886644	0.000215	1.467113	0.000098	0.280584	0.000035	0.280418	0.000034	3708	13	1.72	1.20	3.75
UC12s_50_22	s2-12011	50	0.05839	0.00044	0.00172	0.00001	1.886640	0.000187	1.467115	0.000094	0.280446	0.000036	0.280311	0.000036	3724	12	-1.72	1.30	3.94
UC12s_50_23	s2-12032	50	0.04662	0.00081	0.00135	0.00002	1.886555	0.000187	1.467119	0.000100	0.280371	0.000038	0.280255	0.000038	3810	15	-1.63	1.35	4.01
UC12s_50_24	s12158	50	0.05097	0.00106	0.00148	0.00002	1.886618	0.000187	1.467168	0.000104	0.280342	0.000035	0.280220	0.000035	3822	11	-2.59	1.25	4.07
UC12s_50_25	s12136	50	0.06339	0.00186	0.00175	0.00004	1.886674	0.000181	1.467198	0.000098	0.280332	0.000036	0.280193	0.000036	3778	13	-4.63	1.30	4.14
UC12s_50_27	s12164	50	0.04731	0.00150	0.00150	0.00007	1.886482	0.000210	1.467036	0.000108	0.280566	0.000042	0.280450	0.000041	3505	14	-2.05	1.45	3.77
UC12m_50_1	m12006	50	0.04463	0.00154	0.00132	0.00005	1.886565	0.000179	1.467152	0.000097	0.280437	0.000032	0.280325	0.000033	3678	12	-2.32	1.16	3.93
UC12m_50_2	m12007	50	0.01182	0.00049	0.00033	0.00001	1.886682	0.000178	1.467196	0.000099	0.280693	0.000032	0.280660	0.000032	2871	17	-9.67	1.16	3.63
UC12m_50_3	m12011	50	0.02171	0.00069	0.00059	0.00002	1.886698	0.000175	1.467205	0.000100	0.280669	0.000035	0.280620	0.000035	2903	14	-10.33	1.26	3.69
UC12m_50_4	m12019	50	0.00872	0.00009	0.00025	0.00000	1.886603	0.000176	1.467183	0.000099	0.280669	0.000035	0.280641	0.000035	2932	17	-8.92	1.26	3.64
UC12m_50_5	m12027	50	0.05200	0.00133	0.00155	0.00004	1.886562	0.000176	1.467156	0.000099	0.280518	0.000035	0.280397	0.000034	3748	17	1.91	1.23	3.77
UC12m_50_6	m12043	50	0.04118	0.00066	0.00122	0.00003	1.886512	0.000183	1.467110	0.000095	0.280568	0.000038	0.280469	0.000039	3586	17	0.58	1.38	3.70
UC12m_50_8	m12064	50	0.00983	0.00023	0.00025	0.00001	1.886708	0.000169	1.467193	0.000093	0.280666	0.000031	0.280638	0.000031	2873	16	-10.42	1.10	3.67
UC12m_50_9	m12065	50	0.04022	0.00094	0.00139	0.00004	1.886736	0.000234	1.467014	0.000112	0.280368	0.000036	0.280261	0.000036	3538	16	-7.98	1.28	4.11
UC12m_50_10	m12076	50	0.04701	0.00075	0.00140	0.00003	1.886718	0.000185	1.467205	0.000094	0.280445	0.000035	0.280351	0.000035	2952	16	-18.75	1.23	4.17
UC12m_50_11	m12109	50	0.02934	0.00069	0.00073	0.00001	1.886742	0.000173	1.467173	0.000108	0.280670	0.000035	0.280617	0.000035	2729	14	-14.55	1.26	3.76
UC12m_50_12	m12107	50	0.05801	0.00341	0.00167	0.00010	1.886681	0.000179	1.467141	0.000094	0.280447	0.000037	0.280310	0.000036	3723	18	-1.80	1.28	3.94
UC12m_50_13	m12082	50	0.03441	0.00145	0.00088	0.00003	1.886732	0.000180	1.467213	0.000088	0.280675	0.000033	0.280619	0.000033	2387	21	-22.54	1.17	3.88
UC12m_50_14	m12087	50	0.02346	0.00057	0.00065	0.00002	1.886650	0.000182	1.467106	0.000101	0.280726	0.000034	0.280682	0.000034	2376	18	-20.56	1.22	3.77
UC12m_50_15	m12116	50	0.04530	0.00103	0.00107	0.00002	1.886644	0.000193	1.467125	0.000092	0.280731	0.000033	0.280669	0.000033	2362	16	-21.33	1.16	3.80
UC12_30_2	12-09170	30	0.04199	0.00080	0.00119	0.00002	1.886660	0.000136	1.467144	0.000099	0.280494	0.000040	0.280414	0.000041	3650	19	-2.67	1.45	3.83
UC12_30_7	12-09220	30	0.08017	0.00138	0.00212	0.00003	1.886659	0.000160	1.467123	0.000119	0.280524	0.000043	0.280383	0.000042	3645	15	-1.05	1.49	3.84
UC12_30_8	12-09191	30	0.03022	0.00086	0.00088	0.00002	1.886866	0.000181	1.467249	0.000134	0.280411	0.000042	0.280350	0.000042	3589	14	-3.57	1.51	3.92
UC12_30_10	12-09203	30	0.04570	0.00109	0.00125	0.00003	1.886674	0.000141	1.467074	0.000114	0.280394	0.000045	0.280301	0.000045	3880	13	1.70	1.61	3.89
UC12_30_11	12-09225	30	0.05129	0.00110	0.00151	0.00002	1.886679	0.000143	1.467189	0.000101	0.280495	0.000039	0.280398	0.000039	3405	19	-6.31	1.38	3.91
UC12_30_13	12-09214	30	0.03578	0.00233	0.00094	0.00006	1.886694	0.000173	1.467095	0.000121	0.280417	0.000041	0.280356	0.000042	3345	18	-9.21	1.49	4.01
UC12_30_15	12-09228	30	0.03433	0.00065	0.00103	0.00004	1.886698	0.000116	1.467073	0.000105	0.280595	0.000037	0.280528	0.000038	3444	18	-0.71	1.34	3.65
UC12_30_16	12-09206	30	0.04437	0.00098	0.00100	0.00002	1.886855	0.000147	1.467159	0.000101	0.280667	0.000043	0.280619	0.000044	2595	17	-17.65	1.55	3.81
UC12_30_17	12-09207	30	0.06025	0.00190	0.00165	0.00003	1.886752	0.000091	1.467211	0.000092	0.280375	0.000027	0.280249	0.000026	3844	14	-1.04	0.92	4.01

UC12s_40_5	s2-12158	40	0.07285	0.00098	0.00177	0.00003	1.886657	0.000172	1.467110	0.000124	0.280471	0.000037	0.280442	0.000036	3627	13	0.62	1.30	3.73
UC12s_40_6	s2-12197	40	0.10197	0.00376	0.00245	0.00009	1.886681	0.000204	1.467169	0.000127	0.280517	0.000035	0.280478	0.000035	3539	14	-0.24	1.24	3.70
UC12s_40_9	s12268	40	0.06973	0.00526	0.00173	0.00011	1.886800	0.000230	1.467124	0.000126	0.280487	0.000034	0.280458	0.000034	3644	14	1.60	1.22	3.70
UC12s_40_10	s12258	40	0.05136	0.00391	0.00139	0.00008	1.886642	0.000201	1.467216	0.000139	0.280496	0.000050	0.280471	0.000050	3557	15	-0.03	1.79	3.71
UC12s_40_11	s12262	40	0.05646	0.00115	0.00145	0.00003	1.886735	0.000250	1.467143	0.000140	0.280414	0.000036	0.280389	0.000036	3565	11	-2.77	1.29	3.86
UC12s_40_13	s12205	40	0.06709	0.00126	0.00174	0.00002	1.886708	0.000211	1.467189	0.000133	0.280467	0.000034	0.280439	0.000034	3721	13	2.75	1.22	3.72
UC12s_40_14	s12206	40	0.09910	0.00149	0.00231	0.00003	1.886600	0.000194	1.467184	0.000127	0.280447	0.000036	0.280411	0.000036	3632	11	-0.39	1.27	3.79
UC12s_40_18	s12193	40	0.06408	0.00232	0.00212	0.00006	1.886705	0.000244	1.467088	0.000137	0.280416	0.000036	0.280382	0.000036	3768	12	1.87	1.28	3.79
UC12s_40_19	s12170	40	0.06110	0.00256	0.00164	0.00005	1.886791	0.000217	1.467148	0.000144	0.280407	0.000040	0.280380	0.000040	3677	16	-0.41	1.42	3.83
UC12s_40_21	s12197	40	0.05665	0.00136	0.00140	0.00004	1.886594	0.000210	1.467095	0.000129	0.280416	0.000036	0.280392	0.000036	3613	13	-1.52	1.30	3.84
UC12s_40_22	s12175	40	0.05935	0.00122	0.00154	0.00002	1.886832	0.000210	1.467206	0.000139	0.280458	0.000042	0.280432	0.000042	3704	14	2.12	1.50	3.72
UC12s_40_26	s12132	40	0.04162	0.00037	0.00111	0.00001	1.886659	0.000186	1.467168	0.000122	0.280467	0.000033	0.280448	0.000033	3759	13	4.01	1.18	3.76
UC14																			
UC14_1	14-12	50	0.01853	0.00013	0.00056	0.00000	1.886651	0.000175	1.467211	0.000098	0.280806	0.000036	0.280759	0.000036	3108	17	-0.54	1.27	3.35
UC14_2	14-08	50	0.02853	0.00034	0.00091	0.00001	1.886667	0.000184	1.467178	0.000103	0.280756	0.000040	0.280689	0.000040	3022	12	-5.05	1.41	3.52
UC14_3	14-15	50	0.03468	0.00097	0.00113	0.00004	1.886735	0.000193	1.467134	0.000100	0.280818	0.000033	0.280741	0.000033	2663	14	-11.71	1.19	3.56
UC14_4	14-05	50	0.02391	0.00065	0.00071	0.00002	1.886566	0.000175	1.467195	0.000101	0.280811	0.000036	0.280755	0.000036	3032	17	-2.46	1.29	3.39
UC14_5	14-03	50	0.03341	0.00206	0.00101	0.00007	1.886746	0.000209	1.467192	0.000114	0.280832	0.000039	0.280752	0.000039	3125	13	-0.35	1.39	3.36
UC14_6	14-18	50	0.03142	0.00086	0.00105	0.00003	1.886744	0.000185	1.467148	0.000102	0.280788	0.000039	0.280715	0.000039	2942	16	-6.05	1.37	3.50
UC14_7	14-20	50	0.02674	0.00027	0.00074	0.00001	1.886595	0.000183	1.467191	0.000103	0.280653	0.000041	0.280597	0.000041	2910	18	-11.00	1.48	3.73
UC14_8	14-21	50	0.04009	0.00076	0.00115	0.00002	1.886755	0.000189	1.467184	0.000103	0.280815	0.000036	0.280732	0.000036	3110	13	-1.44	1.27	3.40
UC14_9	14-25	50	0.02229	0.00036	0.00071	0.00002	1.886666	0.000182	1.467224	0.000107	0.280815	0.000036	0.280760	0.000036	2931	14	-4.70	1.27	3.42
UC14_10	14-23	50	0.02504	0.00127	0.00081	0.00004	1.886728	0.000181	1.467154	0.000103	0.280789	0.000035	0.280728	0.000035	3022	15	-3.67	1.23	3.44
UC14_11	14-31	50	0.04705	0.00140	0.00125	0.00003	1.886787	0.000175	1.467190	0.000091	0.280798	0.000038	0.280710	0.000038	3091	14	-2.68	1.34	3.45
UC14_12	14-33	50	0.03208	0.00111	0.00103	0.00002	1.886572	0.000189	1.467169	0.000103	0.280822	0.000037	0.280746	0.000037	3205	22	1.32	1.31	3.34
UC14_13	14-58	50	0.02236	0.00018	0.00071	0.00001	1.886706	0.000185	1.467185	0.000102	0.280812	0.000037	0.280755	0.000037	3076	18	-1.42	1.31	3.37
UC14_14	14-61	50	0.02831	0.00017	0.00084	0.00000	1.886660	0.000187	1.467155	0.000102	0.280815	0.000036	0.280751	0.000036	3039	15	-2.44	1.27	3.39
UC14_15	14-66	50	0.02580	0.00044	0.00078	0.00001	1.886770	0.000185	1.467142	0.000102	0.280794	0.000037	0.280732	0.000037	3167	14	-0.08	1.30	3.38
UC14_16	14-70	50	0.02494	0.00114	0.00085	0.00003	1.886648	0.000179	1.467109	0.000101	0.280728	0.000036	0.280663	0.000037	3079	17	-4.62	1.31	3.54
UC14_17	14-76	50	0.04568	0.00363	0.00137	0.00011	1.886780	0.000190	1.467251	0.000103	0.280886	0.000040	0.280789	0.000039	3101	16	0.38	1.38	3.30
UC14_18	14-83	50	0.03681	0.00071	0.00110	0.00002	1.886813	0.000183	1.467145	0.000104	0.280752	0.000040	0.280679	0.000040	2781	21	-11.13	1.41	3.63
UC14_19	14-79	50	0.02847	0.00039	0.00083	0.00001	1.886505	0.000187	1.467187	0.000106	0.280859	0.000037	0.280799	0.000037	2874	13	-4.67	1.31	3.37
UC14_20	14-81	50	0.02310	0.00039	0.00070	0.00001	1.886796	0.000184	1.467198	0.000100	0.280633	0.000039	0.280580	0.000039	2934	15	-11.05	1.40	3.75
UC14_21	14-55	50	0.04467	0.00138	0.00137	0.00004	1.886889	0.000184	1.467207	0.000109	0.280752	0.000040	0.280646	0.000039	3300	15	0.04	1.39	3.49
UC14_22	14-48	50	0.02565	0.00033	0.00081	0.00001	1.886632	0.000192	1.467134	0.000099	0.280824	0.000035	0.280766	0.000036	3086	12	-0.81	1.27	3.35
UC14_23	14-53	50	0.02724	0.00021	0.00083	0.00001	1.886597	0.000195	1.467220	0.000109	0.280820	0.000037	0.280756	0.000037	3124	15	-0.26	1.33	3.35
UC21																			
UC21_1	21-09004	50	0.01752	0.00056	0.00046	0.00001	1.886585	0.000112	1.467192	0.000070	0.280610	0.000033	0.280579	0.000033	3204	16	-4.65	1.16	3.65
UC21_2	21-09009	50	0.02141	0.00010	0.00054	0.00000	1.886755	0.000138	1.467188	0.000072	0.281083	0.000032	0.281053	0.000032	2610	19	-1.85	1.14	3.00
UC21_3	21-09017	50	0.02301	0.00026	0.00060	0.00001	1.886622	0.000138	1.467166	0.000079	0.281189	0.000033	0.281157	0.000033	2499	16	-0.76	1.17	2.85
UC21_4	21-09028	50	0.02312	0.00013	0.00061	0.00000	1.886644	0.000145	1.467192	0.000073	0.280844	0.000033	0.280806	0.000033	2934	25	-2.98	1.19	3.33
UC21_5	21-09040	50	0.03177	0.00068	0.00086	0.00002	1.886747	0.000163	1.467194	0.000094	0.281173	0.000032	0.281128	0.000032	2712	22	3.22	1.15	2.82
UC21_6	21-09053	50	0.01732	0.00020	0.00043	0.00001	1.886687	0.000127	1.467196	0.000082	0.281011	0.000034	0.280986	0.000033	2736	24	-1.27	1.19	3.08
UC21_7	21-09054	50	0.02335	0.00077	0.00059	0.00003	1.886553	0.000143	1.467060	0.000104	0.280498	0.000033	0.280454	0.000033	3392	24	-4.59	1.19	3.81
UC21_9	21-09066	50	0.03799	0.00088	0.00100	0.00002	1.886730	0.000116	1.467229	0.000069	0.281100	0.000034	0.281046	0.000034	2611	23	0.28	1.21	2.97
UC21_10	21-09093	50	0.02609	0.00045	0.00065	0.00001	1.886645	0.000142	1.467157	0.000080	0.281061	0.000032	0.281026	0.000033	2905	15	0.15	1.16	3.00
UC21_12	21-09037	50	0.02050	0.00012	0.00058	0.00000	1.886575	0.000141	1.467201	0.000082	0.281197	0.000035	0.281160	0.000035	2769	42	5.72	1.25	2.77
UC21_13	21-09048	50	0.04649	0.00346	0.00120	0.00006	1.886659	0.000102	1.467137	0.000071	0.281199	0.000032	0.281132	0.000032	2689	16	2.81	1.15	2.82
UC21_14	21-09074	50	0.01626	0.00083	0.00053	0.00004	1.886658	0.000126	1.467106	0.000079	0.281056	0.000032	0.281025	0.000032	2816	28	2.02	1.14	2.97
UC21_15	21-09076	50	0.05852	0.00056	0.00143	0.00001	1.886616	0.000124	1.467199	0.000066	0.280938	0.000034	0.280857	0.000034	2843	15	-3.32	1.20	3.27
UC21_16	21-09070	50	0.00966	0.00014	0.00024	0.00000	1.886706	0.000133	1.467249	0.000070	0.280999	0.000031	0.280983	0.000031	2861	24	1.57	1.12	3.03
UC21_17	21-09071	50	0.03372	0.00375	0.00089	0.00009	1.886588	0.000107	1.467206	0.000073	0.281060	0.000034	0.281007	0.000034	2947	19	4.47	1.22	2.95
UC21_18	21-09084	50	0.02338	0.00033	0.00056	0.00000	1.886620	0.000127	1.467193	0.000070	0.281059	0.000033	0.281027	0.000033	2740	32	0.28	1.16	3.00
UC21_19	21-09085	50	0.02450	0.00084	0.00071	0.00001	1.886720	0.000194	1.467168	0.000080	0.280784	0.000033	0.280737	0.000033	3264	18	2.40	1.19	3.33

UC21_20	21-09093	50	0.10313	0.00273	0.00271	0.00010	1.886564	0.000183	1.467165	0.000083	0.281144	0.000034	0.280996	0.000035	2905	15	3.10	1.26	2.99

Table 4-1. Results of U-Pb dat[a] Common Pb correction was made based on ^{204}Pb method (R. A. Stern, 1997, Geological Survey of Canada Current Research, Radiogenic Age and Isotopic Studies: Report 10, 1-32).

Sample name	Fractional amount of common Pb				Isotope ratios						Common Pb-corrected age (Ma)						U	Th	Th/U
	f_{206}	2σ	f_{207}	2σ	^{207}Pb/^{235}U	2σ	^{206}Pb/^{238}U	2σ	^{207}Pb/^{206}Pb	2σ	^{235}U-^{207}Pb	2σ	^{238}U-^{206}Pb	2σ	^{207}Pb-^{206}Pb	2σ	(ppm)	(ppm)	
ZW114-01	0.0001	0.0001	0.0004	0.0007	16.224	0.372	0.559	0.012	0.2107	0.0018	2889.7	21.9	2860.3	49.1	2910.2	13.9	468	150	0.32
ZW114-02	0.0015	0.0018	0.0079	0.0092	16.492	0.387	0.565	0.012	0.2119	0.0020	2898.1	24.2	2881.7	50.2	2909.5	21.6	253	123	0.49
ZW114-03	0.0000	0.0000	0.0000	0.0000	27.750	0.644	0.717	0.015	0.2808	0.0025	3410.3	22.8	3484.1	57.9	3367.3	13.7	240	126	0.52
ZW114-04	0.0004	0.0004	0.0015	0.0019	24.092	0.548	0.636	0.014	0.2746	0.0022	3270.6	22.3	3173.7	53.2	3330.6	13.1	484	385	0.80
ZW114-05	0.0017	0.0020	0.0105	0.0118	8.022	0.185	0.331	0.007	0.1760	0.0016	2224.0	23.4	1838.3	34.1	2601.1	25.2	633	326	0.52
ZW114-06	0.0001	0.0001	0.0004	0.0006	16.737	0.720	0.576	0.023	0.2108	0.0036	2919.5	41.2	2932.0	92.9	2911.0	27.9	767	678	0.88
ZW114-07	0.0056	0.0007	0.0298	0.0037	13.625	0.588	0.484	0.019	0.2040	0.0036	2695.4	40.9	2534.3	82.8	2818.5	29.2	574	252	0.44
ZW114-08	0.0036	0.0006	0.0184	0.0030	15.417	0.666	0.521	0.021	0.2146	0.0038	2823.7	41.3	2695.7	87.1	2916.3	28.8	495	189	0.38
ZW114-09	0.0000	0.0000	0.0000	0.0000	17.082	0.745	0.581	0.023	0.2131	0.0039	2939.4	41.9	2954.1	94.1	2929.4	29.2	244	67	0.28
ZW114-10	0.0001	0.0002	0.0006	0.0008	17.079	0.740	0.586	0.023	0.2113	0.0037	2938.7	41.5	2973.8	94.2	2914.7	28.5	389	138	0.36
ZW114-11	0.0026	0.0006	0.0137	0.0031	16.159	0.701	0.560	0.022	0.2093	0.0037	2873.0	41.6	2859.8	91.5	2882.3	29.3	339	135	0.40
ZW114-12	0.0004	0.0003	0.0021	0.0014	15.794	0.683	0.545	0.022	0.2101	0.0037	2862.4	41.3	2804.2	89.9	2903.6	28.5	471	171	0.36
ZW114-13	0.0000	0.0000	0.0000	0.0000	17.000	0.736	0.588	0.023	0.2097	0.0037	2934.8	41.5	2981.0	94.4	2903.4	28.6	382	152	0.40
ZW114-14	0.0004	0.0002	0.0021	0.0011	12.937	0.557	0.465	0.018	0.2020	0.0035	2673.1	40.6	2458.8	80.6	2839.5	28.3	753	369	0.49
ZW114-15	0.0001	0.0004	0.0007	0.0019	17.128	0.747	0.585	0.023	0.2123	0.0038	2941.3	41.9	2969.5	94.5	2922.2	29.4	240	65	0.27
ZW114-16	0.0084	0.0012	0.0436	0.0060	14.415	0.628	0.494	0.020	0.2116	0.0038	2735.1	41.7	2570.1	84.1	2859.4	31.2	295	131	0.45
ZW114-17	0.0009	0.0004	0.0046	0.0019	16.635	0.723	0.573	0.023	0.2106	0.0038	2909.6	41.6	2917.6	93.0	2904.1	29.0	314	117	0.37
ZW114-18	0.0006	0.0003	0.0032	0.0014	12.250	0.529	0.444	0.018	0.2002	0.0035	2620.7	40.5	2366.2	78.2	2823.7	28.6	637	250	0.39
ZW114-19	0.0001	0.0001	0.0007	0.0008	16.316	0.708	0.561	0.022	0.2108	0.0037	2894.9	41.5	2871.7	91.7	2911.0	28.7	351	116	0.33
ZW114-20	0.0002	0.0001	0.0008	0.0007	17.002	0.790	0.584	0.025	0.2112	0.0034	2934.2	44.6	2964.5	103.6	2913.4	26.0	401	138	0.34
ZW114-21	0.0000	0.0000	0.0000	0.0000	17.994	0.836	0.617	0.027	0.2117	0.0034	2989.4	44.7	3096.3	107.3	2918.3	26.0	381	176	0.46
ZW114-22	0.0046	0.0012	0.0234	0.0062	17.942	0.849	0.599	0.026	0.2173	0.0038	2963.8	45.9	3014.3	106.0	2929.7	30.1	152	87	0.57
ZW114-23	0.0003	0.0006	0.0013	0.0028	19.048	0.898	0.608	0.027	0.2274	0.0039	3043.0	45.6	3059.5	107.1	3032.1	27.8	171	77	0.45
ZW114-24	0.0025	0.0006	0.0136	0.0031	13.029	0.606	0.465	0.020	0.2031	0.0033	2668.9	43.9	2457.9	89.1	2832.9	26.8	471	244	0.52
ZW114-25	0.0000	0.0000	0.0000	0.0000	15.278	0.709	0.535	0.023	0.2070	0.0033	2832.8	44.2	2763.8	97.9	2882.2	25.9	480	216	0.45
ZW114-26	0.0026	0.0006	0.0133	0.0031	15.963	0.743	0.550	0.024	0.2104	0.0034	2861.7	44.5	2820.1	99.7	2891.2	26.8	370	132	0.36
ZW114-27	0.0005	0.0002	0.0025	0.0012	15.954	0.739	0.557	0.024	0.2078	0.0033	2871.6	44.3	2852.6	100.4	2885.0	25.8	532	185	0.35
ZW114-28	0.0006	0.0003	0.0030	0.0013	15.581	0.722	0.539	0.023	0.2096	0.0033	2848.5	44.2	2778.8	98.3	2898.3	25.8	534	172	0.32
ZW114-29	0.0037	0.0007	0.0192	0.0037	16.342	0.760	0.554	0.024	0.2139	0.0035	2878.5	44.6	2833.4	100.0	2910.2	26.9	385	119	0.31
ZW114-30	0.0006	0.0002	0.0032	0.0011	13.132	0.606	0.483	0.021	0.1970	0.0031	2686.2	43.6	2540.7	91.3	2797.5	25.5	1014	617	0.61
ZW114-31	0.0007	0.0004	0.0037	0.0023	16.348	0.763	0.554	0.024	0.2141	0.0035	2893.9	44.7	2839.6	100.4	2931.8	26.9	297	121	0.41
ZW114-32	0.0023	0.0004	0.0124	0.0023	13.680	0.633	0.478	0.021	0.2076	0.0033	2716.0	43.8	2512.9	90.6	2870.8	26.0	675	353	0.52
ZW114-33	0.0505	0.0043	0.2254	0.0196	14.603	0.691	0.434	0.019	0.2440	0.0043	2549.1	50.1	2224.8	83.1	2818.3	50.8	185	102	0.55
zw114-34	0.0000	0.0000	0.0000	0.0000	16.438	0.943	0.567	0.032	0.2101	0.0021	2902.6	54.9	2897.2	131.7	2906.4	16.4	429	131	0.30
zw114-35	0.0456	0.0016	0.2008	0.0072	18.994	1.088	0.553	0.031	0.2493	0.0025	2826.6	55.2	2730.5	125.6	2895.8	21.9	531	238	0.45
zw114-36	0.0215	0.0016	0.1042	0.0079	11.512	0.663	0.369	0.021	0.2262	0.0025	2463.2	53.9	1988.0	96.8	2882.6	23.0	291	119	0.41
zw114-37	0.0003	0.0001	0.0013	0.0005	16.428	0.940	0.559	0.032	0.2130	0.0021	2900.7	54.7	2863.4	130.3	2926.8	15.8	878	417	0.47
zw114-38	0.0060	0.0006	0.0314	0.0033	15.746	0.904	0.543	0.031	0.2103	0.0022	2831.0	54.8	2782.7	127.7	2865.7	17.6	370	131	0.35
zw114-39	0.0004	0.0001	0.0020	0.0008	16.038	0.918	0.552	0.031	0.2106	0.0021	2877.2	54.7	2834.3	129.4	2907.4	16.1	600	263	0.44
zw114-40	0.0000	0.0000	0.0000	0.0000	16.361	0.938	0.560	0.032	0.2117	0.0021	2898.1	54.8	2868.4	130.6	2918.9	16.2	497	193	0.39
zw114-41	0.0003	0.0001	0.0017	0.0008	12.999	0.745	0.465	0.026	0.2027	0.0020	2678.0	54.0	2461.3	115.4	2846.0	16.4	634	244	0.38
zw114-42	0.0001	0.0001	0.0004	0.0005	14.279	0.819	0.500	0.028	0.2070	0.0021	2768.0	54.5	2614.6	121.4	2881.9	16.7	407	130	0.32
zw114-43	0.0094	0.0007	0.0485	0.0037	15.621	0.896	0.535	0.030	0.2119	0.0021	2806.6	54.7	2740.0	126.0	2854.7	17.7	449	143	0.32
zw114-44	0.0007	0.0002	0.0043	0.0011	9.418	0.539	0.370	0.021	0.1844	0.0018	2375.6	52.5	2030.0	98.2	2687.0	16.7	833	381	0.46
zw114-45	0.0001	0.0002	0.0007	0.0009	16.250	0.932	0.559	0.032	0.2109	0.0021	2891.0	54.9	2861.6	130.5	2911.5	16.5	414	123	0.30
zw114-46	0.0001	0.0001	0.0003	0.0005	16.482	0.947	0.564	0.032	0.2120	0.0022	2904.9	55.0	2882.1	131.3	2920.7	16.8	319	99	0.31

zw114-47	0.0004	0.0002	0.0019	0.0011	15.574	0.894	0.537	0.030	0.2103	0.0022	2849.2	54.8	2770.6	127.2	2905.2	16.7	373	77	0.21
zw114-48	0.0046	0.0005	0.0244	0.0024	12.790	0.326	0.449	0.011	0.2067	0.0019	2641.0	24.1	2380.6	47.4	2847.1	15.4	646	320	0.50
zw114-49	0.0031	0.0004	0.0167	0.0022	13.206	0.337	0.476	0.011	0.2011	0.0018	2678.6	24.2	2504.6	49.5	2812.7	15.4	556	180	0.32
zw114-50	0.0002	0.0002	0.0009	0.0009	17.725	0.456	0.609	0.015	0.2110	0.0020	2974.1	24.7	3066.3	58.6	2912.2	15.1	372	116	0.31
zw114-51	0.0038	0.0008	0.0212	0.0044	12.104	0.321	0.447	0.011	0.1965	0.0021	2592.4	25.2	2373.2	48.5	2768.4	18.7	219	146	0.67
ZW115-01	0.0001	0.0001	0.0008	0.0005	14.775	0.376	0.519	0.012	0.2065	0.0019	2800.2	24.2	2694.3	52.4	2877.3	14.6	648	287	0.44
ZW115-02	0.0004	0.0002	0.0022	0.0008	16.662	0.424	0.568	0.014	0.2126	0.0019	2913.5	24.4	2900.5	55.6	2922.5	14.6	589	159	0.27
ZW115-03	0.0002	0.0001	0.0010	0.0006	12.561	0.319	0.463	0.011	0.1966	0.0018	2646.3	23.9	2454.0	48.5	2796.9	14.8	721	267	0.37
ZW115-04	0.0006	0.0002	0.0031	0.0010	14.432	0.368	0.505	0.012	0.2071	0.0019	2775.6	24.2	2635.8	51.5	2878.9	14.8	592	225	0.38
ZW115-05	0.0009	0.0002	0.0053	0.0012	11.091	0.282	0.421	0.010	0.1910	0.0017	2525.9	23.7	2264.2	45.3	2743.4	15.0	830	324	0.39
ZW115-06	0.0048	0.0004	0.0256	0.0023	11.256	0.285	0.397	0.009	0.2054	0.0018	2520.4	23.7	2148.3	43.3	2835.4	15.1	896	410	0.46
ZW115-07	0.0003	0.0002	0.0014	0.0008	12.725	0.323	0.462	0.011	0.1997	0.0018	2658.2	23.9	2448.8	48.4	2821.6	14.8	735	259	0.35
ZW115-08	0.0000	0.0000	0.0000	0.0000	16.790	0.426	0.569	0.014	0.2138	0.0019	2922.9	24.3	2905.6	55.6	2934.9	14.4	671	270	0.40
ZW115-09	0.0003	0.0002	0.0014	0.0010	24.892	0.647	0.640	0.016	0.2821	0.0027	3302.7	25.4	3187.8	61.0	3373.1	14.8	250	159	0.64
ZW115-10	0.0666	0.0025	0.2748	0.0109	12.627	0.402	0.345	0.010	0.2655	0.0030	2353.9	32.2	1799.2	46.8	2876.8	31.0	459	533	1.16
ZW115-11	0.0004	0.0002	0.0021	0.0010	13.018	0.413	0.466	0.014	0.2027	0.0023	2679.0	29.9	2464.4	60.7	2845.1	18.5	516	184	0.36
ZW115-12	0.0006	0.0002	0.0035	0.0010	11.791	0.372	0.426	0.013	0.2005	0.0022	2584.7	29.6	2288.4	56.9	2825.9	18.2	758	461	0.61
ZW115-13	0.0003	0.0002	0.0015	0.0013	16.127	0.520	0.554	0.017	0.2113	0.0025	2882.9	30.8	2839.7	68.9	2913.2	19.2	249	125	0.50
ZW115-14	0.0096	0.0009	0.0378	0.0035	20.236	0.647	0.505	0.015	0.2905	0.0033	3065.4	31.1	2615.5	64.2	3375.2	18.7	312	79	0.25
ZW115-15	0.0007	0.0003	0.0034	0.0018	15.944	0.510	0.551	0.016	0.2097	0.0024	2870.2	30.6	2829.5	68.4	2898.8	19.0	313	167	0.53
ZW115-16	0.0063	0.0004	0.0361	0.0022	9.775	0.307	0.379	0.011	0.1873	0.0020	2380.0	28.9	2058.6	51.9	2667.9	18.4	1733	897	0.52
ZW115-17	0.0011	0.0003	0.0060	0.0014	14.021	0.444	0.494	0.015	0.2058	0.0023	2745.5	30.0	2586.6	63.1	2864.4	18.3	604	176	0.29
ZW115-18	0.0001	0.0001	0.0005	0.0004	16.123	0.513	0.553	0.016	0.2113	0.0024	2883.7	30.4	2838.9	68.3	2915.1	18.3	410	125	0.31
ZW115-19	0.0003	0.0001	0.0014	0.0008	15.999	0.507	0.549	0.016	0.2115	0.0024	2875.3	30.3	2818.9	67.7	2915.1	18.1	528	161	0.31
ZW115-20	0.0004	0.0002	0.0022	0.0011	14.665	0.467	0.506	0.015	0.2101	0.0024	2791.6	30.3	2639.9	64.4	2903.2	18.5	428	121	0.28

ZW117-01	0.0049	0.0004	0.0241	0.0019	9.187	0.219	0.298	0.006	0.2233	0.0028	2334.5	21.9	1675.8	30.0	2973.6	20.4	1167	756	0.65
ZW117-02	0.0025	0.0003	0.0099	0.0011	20.431	0.532	0.512	0.011	0.2897	0.0040	3102.4	25.2	2657.7	48.0	3404.4	21.6	655	73	0.11
ZW117-03	0.0033	0.0004	0.0127	0.0015	18.047	0.476	0.443	0.010	0.2952	0.0041	2979.9	25.4	2359.5	44.2	3430.3	21.8	516	441	0.85
ZW117-04	0.0001	0.0001	0.0003	0.0004	33.445	0.916	0.752	0.018	0.3225	0.0045	3593.5	27.0	3615.1	65.2	3581.4	21.5	274	15	0.05
ZW117-05	0.0000	0.0001	0.0001	0.0003	34.692	0.939	0.772	0.018	0.3260	0.0045	3629.8	26.7	3687.4	65.2	3598.3	21.4	314	216	0.69
ZW117-06	0.0052	0.0004	0.0207	0.0018	19.460	0.511	0.487	0.011	0.2900	0.0040	3044.7	25.4	2545.3	46.9	3393.1	21.9	535	266	0.50
ZW117-07	0.0000	0.0000	0.0000	0.0000	33.254	0.920	0.744	0.018	0.3242	0.0045	3588.2	27.3	3585.2	65.6	3589.8	21.5	246	193	0.78
ZW117-08	0.0044	0.0004	0.0180	0.0018	12.511	0.326	0.326	0.007	0.2781	0.0039	2626.4	24.5	1813.5	34.8	3330.5	22.1	698	507	0.73
ZW117-09	0.0095	0.0010	0.0518	0.0058	4.561	0.122	0.166	0.004	0.1991	0.0029	1698.2	22.6	982.3	20.3	2747.1	26.4	581	455	0.78
ZW117-10	0.0159	0.0018	0.0669	0.0075	6.539	0.183	0.177	0.004	0.2685	0.0041	1990.4	25.4	1033.3	22.5	3213.2	27.4	310	311	1.00
ZW117-12	0.0182	0.0041	0.0870	0.0194	3.886	0.134	0.122	0.003	0.2312	0.0047	1538.0	32.2	728.6	19.5	2943.8	48.0	110	206	1.87
ZW117-13	0.0000	0.0000	0.0000	0.0000	14.317	17.513	0.324	0.304	0.3206	0.2514	2770.9	1161.0	1808.7	1480.8	3572.6	1205.7	0	0	0.00
ZW117-14	0.1515	0.3261	0.4088	0.8871	1.152	0.391	0.020	0.004	0.4267	0.1201	527.4	632.9	106.2	45.2	3456.2	2441.1	3	1	0.48
ZW117-15	0.0564	0.0012	0.2334	0.0059	12.157	0.309	0.330	0.007	0.2669	0.0037	2370.0	24.3	1749.0	32.8	2957.6	25.5	1576	602	0.38
ZW119-01	0.0000	0.0000	0.0000	0.0000	22.890	0.903	0.513	0.016	0.3235	0.0075	3222.3	38.4	2670.0	69.9	3586.7	35.6	243	147	0.60
ZW119-02	0.0134	0.0025	0.0602	0.0112	2.928	0.104	0.085	0.002	0.2503	0.0051	1342.6	28.0	518.2	14.6	3109.7	37.7	3851	558	0.14
ZW119-03	0.0033	0.0016	0.0119	0.0060	25.068	0.966	0.571	0.018	0.3182	0.0071	3299.2	38.1	2905.7	73.9	3547.9	35.5	273	137	0.50
ZW119-04	0.0196	0.0034	0.1423	0.0248	0.571	0.021	0.030	0.001	0.1377	0.0031	404.6	15.6	187.2	5.4	1963.1	65.2	10318	4186	0.41
ZW119-05	0.0020	0.0010	0.0077	0.0040	23.942	0.873	0.587	0.018	0.2959	0.0060	3258.5	35.8	2971.7	72.2	3440.1	32.1	492	210	0.43
ZW119-06	0.0000	0.0000	0.0000	0.0000	33.285	1.382	0.732	0.025	0.3298	0.0080	3589.1	40.9	3540.6	92.0	3616.3	37.1	138	90	0.65
ZW119-07	0.0009	0.0014	0.0032	0.0050	31.843	1.286	0.724	0.024	0.3192	0.0074	3542.3	40.0	3507.1	89.2	3562.3	36.8	167	102	0.61
ZW119-08	0.0017	0.0009	0.0063	0.0034	27.518	1.002	0.652	0.020	0.3062	0.0062	3395.8	35.8	3230.8	77.2	3494.7	31.6	462	174	0.38
ZW119-09	0.0042	0.0013	0.0163	0.0051	24.067	0.873	0.591	0.018	0.2953	0.0059	3255.1	35.7	2984.2	72.2	3426.5	32.3	531	528	0.99

ZW119-10	0.0012	0.0008	0.0051	0.0033	11.363	0.404	0.318	0.009	0.2595	0.0051	2548.6	33.3	1776.0	45.9	3237.5	31.7	1231	301	0.24
ZW119-11	0.0000	0.0000	0.0000	0.0000	33.959	1.447	0.774	0.027	0.3181	0.0080	3608.9	42.0	3696.0	97.1	3560.8	38.5	117	69	0.59
ZW119-12	0.0053	0.0015	0.0249	0.0072	10.843	0.392	0.333	0.010	0.2360	0.0048	2486.3	34.2	1845.4	47.8	3061.4	35.0	948	1052	1.11
ZW119-13	0.0000	0.0000	0.0000	0.0000	34.200	1.411	0.770	0.026	0.3220	0.0077	3615.8	40.7	3682.3	94.4	3579.2	36.7	140	82	0.59
ZW119-14	0.0000	0.0000	0.0000	0.0000	34.842	1.476	0.769	0.026	0.3287	0.0081	3634.2	41.8	3676.5	96.4	3611.0	37.9	120	44	0.37
zw119-1-01	0.0127	0.0008	0.0553	0.0035	12.869	0.742	0.362	0.020	0.2581	0.0036	2616.7	54.2	1968.2	95.0	3165.4	22.7	1130	99	0.09
zw119-1-02	0.0075	0.0008	0.0278	0.0028	6.368	0.367	0.149	0.008	0.3094	0.0044	2003.1	50.5	890.5	46.5	3486.0	22.3	1433	395	0.28
zw119-1-03	0.0084	0.0006	0.0419	0.0030	8.131	0.468	0.267	0.015	0.2210	0.0030	2207.0	51.8	1513.4	75.3	2932.4	22.9	1708	173	0.10
zw119-1-04	0.0114	0.0007	0.0550	0.0035	2.132	0.122	0.068	0.004	0.2288	0.0032	1120.5	38.9	416.9	22.4	2971.5	23.1	6454	691	0.11
zw119-1-05	0.0000	0.0001	0.0001	0.0002	30.023	1.809	0.682	0.040	0.3195	0.0046	3487.5	59.2	3350.3	152.8	3567.2	22.2	187	59	0.32
zw119-1-06	0.0012	0.0003	0.0043	0.0010	23.546	1.369	0.551	0.031	0.3098	0.0043	3245.6	56.6	2827.6	129.2	3515.1	21.4	581	301	0.52
zw119-1-07	0.0002	0.0001	0.0006	0.0005	30.688	1.811	0.689	0.040	0.3228	0.0045	3508.5	58.0	3379.9	150.8	3582.8	21.6	308	236	0.77
zw119-1-08	0.0026	0.0004	0.0100	0.0017	19.638	1.146	0.481	0.027	0.2962	0.0041	3064.0	56.4	2525.7	118.4	3438.8	21.9	489	439	0.90
zw119-1-09	0.0101	0.0007	0.0472	0.0033	9.420	0.543	0.287	0.016	0.2384	0.0033	2335.5	52.7	1609.9	79.7	3048.2	22.8	1360	622	0.46
zw119-1-10	0.0076	0.0006	0.0353	0.0027	11.360	0.655	0.342	0.019	0.2407	0.0033	2519.7	53.7	1885.3	91.5	3079.4	22.5	1160	128	0.11
zw119-1-11	0.0091	0.0006	0.0543	0.0040	5.806	0.334	0.238	0.013	0.1773	0.0025	1899.2	49.5	1362.5	68.6	2549.7	24.3	1767	80	0.05
zw119-1-12	0.0125	0.0008	0.0576	0.0036	9.772	0.563	0.293	0.016	0.2420	0.0033	2359.0	52.9	1637.5	80.9	3058.8	22.9	1369	102	0.07
zw119-1-13	0.0055	0.0005	0.0233	0.0021	15.149	0.876	0.411	0.023	0.2673	0.0037	2802.2	55.0	2209.3	105.0	3261.9	22.0	895	49	0.05
zw119-1-14	0.0107	0.0007	0.0538	0.0037	7.975	0.459	0.265	0.015	0.2179	0.0030	2178.4	51.7	1503.0	74.9	2893.3	23.3	1464	196	0.13
ZW119-1-15	0.0000	0.0000	0.0000	0.0000	31.358	2.336	0.693	0.051	0.3282	0.0048	3530.4	73.3	3393.7	192.7	3608.8	22.7	200	97	0.48
ZW119-1-16	0.0006	0.0002	0.0020	0.0007	28.811	2.091	0.641	0.046	0.3259	0.0046	3445.1	71.2	3192.2	179.2	3595.7	21.7	548	316	0.58
ZW119-1-17	0.0023	0.0006	0.0085	0.0021	24.015	1.771	0.557	0.040	0.3125	0.0046	3260.7	71.9	2850.0	166.4	3523.9	22.9	274	112	0.41
ZW119-1-18	0.0304	0.0015	0.1579	0.0082	0.617	0.044	0.022	0.002	0.2059	0.0029	424.8	25.1	134.4	9.3	2641.8	28.8	15528	1223	0.08
ZW119-1-19	0.0170	0.0009	0.0719	0.0040	6.842	0.491	0.186	0.013	0.2664	0.0037	2025.4	63.1	1083.9	70.2	3194.4	23.3	2360	285	0.12
ZW119-1-20	0.0001	0.0001	0.0005	0.0005	28.619	2.076	0.646	0.046	0.3213	0.0045	3440.0	71.2	3212.0	180.0	3575.6	21.7	562	264	0.47
ZW119-1-21	0.0128	0.0008	0.0593	0.0038	12.239	0.882	0.369	0.026	0.2403	0.0034	2565.6	67.4	2004.5	121.7	3044.7	23.5	1160	62	0.05
ZW119-1-22	0.0000	0.0000	0.0000	0.0000	29.474	2.218	0.661	0.049	0.3233	0.0049	3469.4	73.9	3271.9	189.2	3585.6	23.1	160	105	0.66
ZW119-1-23	0.0107	0.0007	0.0545	0.0036	4.366	0.313	0.147	0.010	0.2153	0.0030	1659.9	58.7	875.7	57.6	2872.6	23.7	3259	291	0.09
ZW119-1-24	0.0019	0.0003	0.0070	0.0013	26.113	1.900	0.596	0.043	0.3177	0.0045	3343.9	71.2	3009.5	171.6	3551.0	22.0	468	311	0.66
ZW119-1-25	0.0000	0.0000	0.0000	0.0000	27.154	2.040	0.611	0.045	0.3222	0.0049	3389.1	73.6	3074.9	179.9	3580.4	23.1	166	82	0.49
ZW119-1-26	0.0119	0.0008	0.0512	0.0034	14.141	1.020	0.389	0.028	0.2636	0.0037	2709.5	68.2	2096.8	126.6	3204.7	23.1	985	62	0.06
ZW119-2-1-01	0.0055	0.0006	0.0224	0.0023	14.013	0.969	0.366	0.025	0.2776	0.0038	2729.1	65.5	2001.4	116.7	3322.8	21.6	924	490	0.53
ZW119-2-1-02	0.0004	0.0002	0.0013	0.0009	27.991	1.986	0.635	0.044	0.3196	0.0045	3417.5	69.6	3169.3	174.2	3566.4	21.6	279	204	0.73
ZW119-2-1-03	0.0088	0.0007	0.0411	0.0033	8.614	0.594	0.260	0.018	0.2401	0.0033	2259.9	62.5	1479.1	89.3	3067.7	22.5	1406	703	0.50
ZW119-2-1-04	0.0000	0.0003	0.0001	0.0011	28.066	2.030	0.630	0.045	0.3231	0.0047	3421.3	70.9	3149.8	176.6	3584.3	22.3	183	71	0.39
ZW119-2-1-05	0.0019	0.0006	0.0070	0.0022	25.882	1.865	0.591	0.042	0.3177	0.0046	3335.2	70.5	2988.5	168.9	3550.7	22.5	196	104	0.53
ZW119-2-1-06	0.0004	0.0002	0.0014	0.0007	23.810	1.670	0.534	0.037	0.3237	0.0045	3259.3	68.3	2755.5	154.2	3585.8	21.2	415	88	0.21
ZW119-2-1-07	0.0048	0.0005	0.0193	0.0020	17.798	1.233	0.453	0.031	0.2852	0.0039	2960.2	66.6	2397.3	136.0	3368.7	21.4	806	163	0.20
ZW119-2-1-08	0.0014	0.0004	0.0053	0.0013	23.406	1.637	0.542	0.037	0.3131	0.0043	3238.8	68.1	2789.6	155.3	3530.0	21.3	458	316	0.69
ZW119-2-1-09	0.0029	0.0004	0.0107	0.0016	19.665	1.367	0.462	0.031	0.3088	0.0042	3064.6	67.2	2442.1	138.6	3502.6	21.2	630	379	0.60
ZW119-2-1-10	0.0014	0.0003	0.0052	0.0011	22.530	1.566	0.526	0.036	0.3107	0.0042	3201.7	67.6	2721.0	151.4	3518.5	21.0	625	161	0.26
ZW119-2-1-11	0.0079	0.0008	0.0302	0.0030	6.338	0.437	0.153	0.010	0.3008	0.0041	1996.9	60.2	910.1	57.3	3438.8	21.9	1647	395	0.24
ZW119-2-1-12	0.0041	0.0005	0.0169	0.0020	14.360	0.994	0.380	0.026	0.2739	0.0037	2757.6	65.7	2069.9	120.2	3308.3	21.6	874	519	0.59
ZW119-2-1-13	0.0006	0.0002	0.0023	0.0008	28.701	2.006	0.651	0.045	0.3197	0.0043	3441.1	68.6	3231.0	174.2	3565.9	20.9	471	494	1.05
ZW119-2-1-14	0.0024	0.0004	0.0088	0.0015	21.508	1.500	0.492	0.034	0.3168	0.0043	3153.2	67.7	2575.8	145.2	3544.6	21.2	529	243	0.46
ZW119-2-2-15	0.0117	0.0006	0.0592	0.0032	5.442	0.209	0.183	0.007	0.2159	0.0021	1839.4	32.8	1070.5	36.7	2870.8	16.7	1957	1164	0.59
ZW119-2-2-16	0.0107	0.0006	0.0467	0.0027	11.624	0.449	0.328	0.012	0.2570	0.0025	2530.0	36.1	1811.7	59.1	3169.9	16.0	931	704	0.76
ZW119-2-2-17	0.0011	0.0002	0.0038	0.0007	30.999	1.212	0.697	0.026	0.3224	0.0031	3515.3	38.5	3407.4	100.3	3577.3	14.8	430	220	0.51
ZW119-2-2-18	0.0059	0.0004	0.0240	0.0018	18.420	0.715	0.473	0.018	0.2822	0.0027	2988.5	37.4	2486.3	77.6	3346.4	15.4	652	74	0.11
ZW119-2-2-19	0.0097	0.0006	0.0377	0.0022	11.193	0.432	0.276	0.010	0.2942	0.0028	2503.6	35.9	1557.3	51.7	3395.5	15.4	1130	1149	1.02
ZW119-2-2-20	0.0026	0.0003	0.0099	0.0011	22.683	0.883	0.545	0.021	0.3018	0.0029	3203.8	37.8	2799.1	85.6	3468.0	15.0	551	446	0.81

ZW119-2-2-21	0.0033	0.0003	0.0128	0.0012	20.434	0.793	0.508	0.019	0.2920	0.0028	3099.6	37.5	2639.3	81.4	3413.1	15.0	656	295	0.45
ZW119-2-2-22	0.0040	0.0004	0.0143	0.0013	33.442	1.313	0.750	0.029	0.3235	0.0031	3579.6	38.7	3595.7	104.9	3570.5	15.0	363	217	0.60
ZW119-2-2-23	0.0038	0.0004	0.0156	0.0016	15.441	0.599	0.405	0.015	0.2768	0.0027	2827.9	37.0	2182.9	69.6	3326.5	15.4	656	77	0.12
ZW119-2-2-24	0.0008	0.0002	0.0030	0.0007	31.889	1.258	0.711	0.027	0.3255	0.0032	3543.9	38.9	3458.1	102.3	3592.8	15.0	314	322	1.03
ZW119-2-2-25	0.0006	0.0001	0.0023	0.0005	30.450	1.186	0.696	0.026	0.3173	0.0030	3499.2	38.3	3403.8	99.9	3554.3	14.7	506	42	0.08
ZW119-2-2-26	0.0033	0.0004	0.0126	0.0015	21.595	0.846	0.519	0.020	0.3018	0.0030	3153.4	38.0	2687.8	83.4	3464.7	15.4	414	188	0.45
ZW119-2-2-27	0.0374	0.0015	0.1304	0.0054	11.904	0.463	0.262	0.010	0.3299	0.0033	2466.7	36.4	1448.4	48.8	3459.8	18.2	674	2588	3.84
ZW119-2-2-28	0.0036	0.0003	0.0148	0.0014	17.862	0.692	0.464	0.017	0.2793	0.0027	2968.0	37.3	2448.9	76.5	3341.4	15.2	701	360	0.51
ZW119-2-2-29	0.0016	0.0002	0.0058	0.0009	29.035	0.940	0.671	0.020	0.3138	0.0034	3449.0	31.8	3305.8	78.8	3533.3	16.9	405	127	0.31
ZW119-2-2-30	0.0003	0.0001	0.0012	0.0005	32.946	1.093	0.740	0.023	0.3228	0.0036	3577.9	32.7	3570.6	85.7	3581.9	17.1	247	213	0.86
ZW119-2-2-31	0.0001	0.0002	0.0004	0.0008	32.033	1.104	0.707	0.023	0.3285	0.0038	3550.9	33.9	3448.1	86.7	3609.4	17.7	155	66	0.43
ZW119-2-2-32	0.0035	0.0004	0.0150	0.0018	17.011	0.550	0.461	0.014	0.2676	0.0030	2921.0	31.0	2436.8	61.6	3274.0	17.7	451	440	0.98
ZW119-2-2-33	0.0055	0.0005	0.0223	0.0020	15.984	0.513	0.414	0.012	0.2798	0.0031	2854.3	30.7	2224.5	56.7	3335.1	17.6	570	409	0.72
ZW119-2-2-34	0.0034	0.0004	0.0130	0.0015	18.222	0.586	0.435	0.013	0.3036	0.0033	2988.9	31.0	2322.9	59.0	3473.7	17.2	509	277	0.54
ZW119-2-2-35	0.0090	0.0005	0.0394	0.0023	6.045	0.190	0.170	0.005	0.2573	0.0028	1947.4	27.3	1006.0	27.4	3180.8	17.7	2077	626	0.30
ZW119-2-2-36	0.0317	0.0013	0.1122	0.0046	11.508	0.366	0.256	0.008	0.3255	0.0036	2454.6	29.8	1429.5	38.3	3462.3	19.0	827	2334	2.82
ZW119-2-2-37	0.0007	0.0002	0.0026	0.0007	30.635	1.002	0.690	0.021	0.3222	0.0035	3504.8	32.2	3379.3	81.0	3577.3	17.0	320	187	0.59
ZW119-2-2-38	0.0030	0.0003	0.0112	0.0011	20.859	0.665	0.497	0.015	0.3043	0.0033	3121.2	30.9	2595.2	64.0	3479.4	16.9	665	483	0.73
ZW119-2-2-39	0.0014	0.0002	0.0052	0.0008	29.995	0.965	0.685	0.021	0.3175	0.0034	3481.6	31.6	3360.3	79.3	3552.0	16.8	467	376	0.80
ZW119-2-2-40	0.0002	0.0001	0.0006	0.0003	33.460	1.086	0.749	0.023	0.3238	0.0035	3593.7	32.0	3605.2	84.4	3587.3	16.8	372	335	0.90
ZW119-2-2-41	0.0056	0.0004	0.0264	0.0019	9.968	0.315	0.306	0.009	0.2359	0.0026	2407.1	29.1	1714.9	44.6	3058.6	17.7	1198	913	0.76
ZW119-2-2-42	0.0001	0.0001	0.0003	0.0003	31.116	1.004	0.702	0.021	0.3216	0.0035	3522.5	31.7	3426.9	80.8	3577.3	16.7	434	416	0.96
ZW119-2-2-43	0.0002	0.0001	0.0006	0.0003	28.705	0.706	0.664	0.014	0.3133	0.0039	3442.9	24.1	3284.0	54.6	3536.7	19.2	486	362	0.74
ZW119-2-2-44	0.1076	0.0024	0.3315	0.0084	8.873	0.211	0.173	0.004	0.3710	0.0046	1965.9	23.4	927.7	17.6	3351.4	28.0	1380	1515	1.10
ZW119-2-2-45	0.0042	0.0003	0.0167	0.0014	21.874	0.532	0.543	0.011	0.2923	0.0036	3161.8	23.6	2785.4	47.2	3410.3	19.5	632	321	0.51
ZW119-2-2-46	0.0002	0.0002	0.0008	0.0005	32.609	0.848	0.729	0.017	0.3246	0.0041	3568.1	25.6	3527.9	61.7	3590.8	19.5	244	234	0.96
ZW119-2-2-47	0.0006	0.0002	0.0021	0.0007	30.805	0.786	0.694	0.015	0.3219	0.0041	3510.8	25.1	3396.9	58.6	3576.4	19.4	298	213	0.71
ZW119-2-2-48	0.0004	0.0001	0.0014	0.0005	30.847	0.778	0.696	0.015	0.3216	0.0040	3512.8	24.8	3403.2	57.8	3575.8	19.3	341	225	0.66
ZW119-2-2-49	0.0083	0.0005	0.0346	0.0023	15.147	0.368	0.401	0.008	0.2738	0.0034	2791.0	23.2	2159.5	38.2	3285.7	20.1	684	649	0.95
ZW139-01	0.0136	0.0044	0.0699	0.0226	4.851	0.214	0.165	0.005	0.2128	0.0070	1733.2	42.0	973.7	27.1	2831.9	67.0	670	411	0.61
ZW139-02	0.0037	0.0021	0.0190	0.0111	6.483	0.287	0.222	0.007	0.2121	0.0069	2026.8	40.1	1286.8	35.0	2896.2	56.0	517	399	0.77
ZW139-03	0.0006	0.0007	0.0021	0.0026	31.059	1.365	0.683	0.022	0.3300	0.0101	3518.9	43.3	3352.6	82.7	3614.9	47.0	190	114	0.60
ZW139-04	0.0064	0.0034	0.0324	0.0173	9.819	0.437	0.327	0.010	0.2175	0.0071	2387.5	44.1	1815.3	48.5	2919.7	60.3	347	294	0.85
ZW139-05	0.0211	0.0056	0.1080	0.0288	4.194	0.186	0.144	0.004	0.2116	0.0070	1580.2	43.9	848.9	24.0	2765.9	76.2	752	528	0.70
ZW139-06	0.0000	0.0000	0.0000	0.0000	7.927	0.351	0.271	0.008	0.2122	0.0069	2222.8	39.9	1545.4	41.3	2922.7	52.5	439	339	0.77
ZW139-09	0.0032	0.0023	0.0176	0.0127	4.740	0.208	0.173	0.005	0.1992	0.0065	1759.5	38.2	1023.4	28.0	2795.6	57.2	732	563	0.77
ZW139-10	0.0172	0.0048	0.0851	0.0241	10.032	0.444	0.328	0.010	0.2221	0.0072	2356.0	47.1	1799.6	48.2	2880.0	68.1	365	582	1.59
ZW139-11	0.0017	0.0014	0.0091	0.0076	5.240	0.231	0.184	0.005	0.2066	0.0067	1851.4	38.1	1086.7	29.7	2867.2	54.5	647	675	1.04
ZW139-12	0.0004	0.0012	0.0014	0.0043	35.074	1.568	0.772	0.025	0.3294	0.0102	3639.4	44.3	3687.8	90.9	3612.9	47.8	154	111	0.72
ZW139-13	0.0070	0.0031	0.0369	0.0163	3.614	0.158	0.126	0.004	0.2081	0.0067	1522.9	36.9	759.9	21.1	2840.8	59.7	987	1463	1.48
ZW139-14	0.0000	0.0000	0.0000	0.0000	34.177	1.576	0.756	0.025	0.3277	0.0104	3615.2	45.5	3631.2	92.5	3606.3	48.9	126	82	0.65
ZW139-2-1	0.0097	0.0006	0.0368	0.0023	19.854	0.486	0.477	0.010	0.3019	0.0038	3048.1	23.7	2494.1	43.5	3436.8	19.8	572	146	0.25
ZW139-2-2	0.0006	0.0003	0.0021	0.0009	31.397	0.856	0.708	0.017	0.3218	0.0042	3529.5	26.9	3448.2	64.1	3576.0	20.0	167	71	0.42
ZW139-2-3	0.0000	0.0000	0.0000	0.0000	32.998	0.866	0.737	0.017	0.3249	0.0041	3580.6	25.9	3557.7	62.8	3593.4	19.6	225	140	0.62
ZW139-2-4	0.0003	0.0001	0.0012	0.0005	32.008	0.799	0.728	0.016	0.3187	0.0040	3549.4	24.6	3526.5	58.6	3562.3	19.2	391	148	0.38
ZW139-2-5	0.0000	0.0000	0.0000	0.0000	33.483	1.049	0.753	0.021	0.3224	0.0044	3594.9	30.9	3619.1	78.0	3581.5	21.1	78	33	0.42
ZW139-2-6	0.0039	0.0003	0.0152	0.0013	23.169	0.565	0.576	0.012	0.2918	0.0036	3219.1	23.8	2922.6	49.3	3409.5	19.5	584	391	0.67
ZW139-1-1	0.0017	0.0006	0.0059	0.0023	20.132	1.505	0.450	0.033	0.3247	0.0050	3091.98	72.31	2390.37	146.13	3585.79	23.74781	191	223	1.1672
zw129-01	0.0003	0.0002	0.0015	0.0012	13.158	0.291	0.507	0.009	0.1883	0.0023	2689.6	20.9	2642.0	39.8	2725.6	20.4	387	136	0.35

zw129-02	0.0169	0.0012	0.1037	0.0076	3.334	0.067	0.142	0.002	0.1700	0.0021	1404.7	16.5	843.8	12.5	2401.8	25.5	1510	653	0.43
zw129-03	0.0002	0.0003	0.0012	0.0017	12.538	0.326	0.491	0.011	0.1850	0.0025	2644.5	24.5	2576.4	47.0	2697.0	22.7	173	73	0.42
zw129-04	0.0016	0.0004	0.0095	0.0023	10.120	0.221	0.398	0.007	0.1842	0.0023	2437.0	20.3	2159.0	32.9	2677.9	21.0	448	189	0.42
zw129-05	0.0018	0.0003	0.0108	0.0021	7.569	0.155	0.306	0.005	0.1795	0.0022	2171.4	18.5	1717.6	24.9	2632.9	20.4	834	284	0.34
zw129-06	0.0006	0.0003	0.0035	0.0017	12.895	0.297	0.504	0.010	0.1856	0.0023	2668.7	21.8	2628.7	41.7	2699.2	21.0	301	99	0.33
zw129-07	0.0051	0.0007	0.0296	0.0043	10.727	0.240	0.421	0.008	0.1849	0.0023	2471.8	21.2	2254.4	35.3	2655.8	22.2	373	140	0.37
zw129-08	0.0005	0.0002	0.0033	0.0010	9.343	0.192	0.381	0.006	0.1779	0.0021	2369.3	18.9	2079.5	29.6	2628.9	20.0	759	228	0.30
zw129-09	0.0000	0.0000	0.0000	0.0000	13.041	0.321	0.497	0.010	0.1901	0.0025	2682.6	23.2	2603.0	44.7	2743.2	21.6	216	64	0.29
zw129-10	0.0009	0.0004	0.0050	0.0023	11.692	0.272	0.448	0.009	0.1893	0.0024	2575.4	21.8	2384.4	38.7	2729.3	21.4	295	91	0.31
zw129-11	0.0000	0.0000	0.0000	0.0000	12.663	0.311	0.488	0.010	0.1883	0.0025	2654.9	23.1	2561.0	43.9	2727.4	21.6	221	64	0.29
zw129-12	0.0004	0.0002	0.0021	0.0013	11.062	0.245	0.439	0.008	0.1829	0.0023	2526.4	20.6	2343.5	35.9	2676.7	20.7	400	114	0.28
zw129-13	0.0023	0.0006	0.0097	0.0026	6.547	0.141	0.176	0.003	0.2704	0.0035	2043.7	19.1	1040.8	16.7	3296.4	20.5	584	63	0.11
zw129-14	0.0000	0.0000	0.0000	0.0000	12.992	0.329	0.502	0.011	0.1877	0.0025	2679.0	23.9	2621.9	46.4	2722.5	22.0	191	66	0.35
zw129-15	0.0000	0.0000	0.0000	0.0000	13.050	0.382	0.496	0.013	0.1908	0.0024	2683.3	27.6	2596.8	56.7	2749.1	20.5	220	67	0.31
zw129-16	0.0000	0.0000	0.0000	0.0000	13.262	0.389	0.514	0.014	0.1871	0.0023	2698.4	27.7	2674.0	58.2	2716.8	20.5	215	70	0.33
zw129-17	0.0041	0.0004	0.0255	0.0024	8.899	0.221	0.375	0.008	0.1720	0.0019	2304.1	22.7	2046.9	39.2	2540.8	18.6	1469	270	0.18
zw129-18	0.0000	0.0000	0.0000	0.0000	12.942	0.389	0.498	0.014	0.1885	0.0024	2675.4	28.3	2605.2	58.4	2729.0	21.0	189	53	0.28
zw129-19	0.0014	0.0004	0.0088	0.0026	5.704	0.150	0.250	0.006	0.1653	0.0020	1924.4	22.7	1438.5	30.1	2497.7	20.6	662	207	0.31
zw129-20	0.0016	0.0004	0.0091	0.0025	11.047	0.300	0.431	0.011	0.1859	0.0022	2518.6	25.4	2307.2	47.5	2693.7	19.9	388	126	0.32
zw129-21	0.0000	0.0000	0.0000	0.0000	12.750	0.376	0.493	0.013	0.1876	0.0023	2661.3	27.8	2583.2	56.9	2721.3	20.6	209	68	0.33
zw129-22	0.0000	0.0000	0.0000	0.0000	12.962	0.351	0.500	0.012	0.1879	0.0022	2676.9	25.5	2615.0	52.7	2724.0	19.0	384	129	0.34
zw129-23	0.0010	0.0004	0.0060	0.0020	13.248	0.361	0.508	0.013	0.1891	0.0022	2691.8	25.8	2646.6	53.5	2725.9	19.4	365	107	0.29
zw129-24	0.0000	0.0000	0.0000	0.0000	13.296	0.376	0.512	0.013	0.1882	0.0023	2700.9	26.7	2666.9	55.9	2726.4	19.7	273	77	0.28
zw129-25	0.0021	0.0007	0.0130	0.0044	8.209	0.233	0.341	0.009	0.1748	0.0022	2242.6	25.9	1886.3	41.5	2585.7	22.4	296	77	0.26
zw129-26	0.0021	0.0005	0.0122	0.0030	11.630	0.327	0.451	0.011	0.1871	0.0023	2563.7	26.4	2394.7	50.9	2700.1	20.6	288	105	0.36
zw129-27	0.0009	0.0004	0.0055	0.0023	6.719	0.183	0.298	0.007	0.1636	0.0020	2070.3	24.2	1679.7	36.0	2485.1	21.1	422	162	0.38
zw129-28	0.0006	0.0003	0.0038	0.0016	9.922	0.263	0.389	0.009	0.1849	0.0021	2424.1	24.5	2117.7	43.2	2692.4	19.3	489	165	0.34
ZW132-01	0.0029	0.0013	0.0146	0.0065	12.232	0.350	0.404	0.009	0.2195	0.0041	2608.6	27.5	2183.2	40.1	2957.7	32.2	379	146	0.39
ZW132-02	0.0040	0.0006	0.0290	0.0045	3.958	0.099	0.206	0.004	0.1396	0.0022	1601.9	20.5	1201.3	21.6	2177.7	28.1	4981	1293	0.26
ZW132-03	0.0258	0.0020	0.1240	0.0097	22.375	0.570	0.711	0.014	0.2282	0.0035	3071.9	26.8	3392.9	53.7	2868.2	31.1	929	2052	2.21
ZW132-04	0.0004	0.0007	0.0018	0.0036	18.820	0.539	0.601	0.013	0.2272	0.0042	3030.8	27.9	3032.5	53.3	3029.8	30.0	282	112	0.40
ZW132-05	0.0009	0.0006	0.0047	0.0032	11.742	0.325	0.416	0.009	0.2049	0.0037	2579.6	26.1	2238.8	39.9	2859.4	29.6	502	250	0.50
ZW132-06	0.0029	0.0014	0.0171	0.0082	10.520	0.306	0.427	0.009	0.1788	0.0035	2465.7	28.0	2285.3	41.8	2617.9	35.2	366	154	0.42
ZW132-07	0.0005	0.0006	0.0024	0.0028	15.691	0.441	0.503	0.011	0.2264	0.0041	2855.9	27.0	2624.3	46.5	3023.7	29.3	368	143	0.39
ZW132-08	0.0125	0.0018	0.0908	0.0129	2.788	0.073	0.145	0.003	0.1391	0.0024	1282.1	21.7	864.7	16.2	2071.8	39.1	2787	1850	0.66
ZW132-09	0.0472	0.0031	0.2169	0.0146	12.135	0.309	0.372	0.007	0.2363	0.0037	2387.8	29.0	1957.6	34.3	2778.4	40.3	1470	490	0.33
ZW132-10	0.0088	0.0019	0.0538	0.0116	9.029	0.250	0.381	0.008	0.1717	0.0031	2290.6	27.5	2066.9	37.1	2496.6	37.0	593	177	0.30
ZW132-11	0.1504	0.0086	0.5725	0.0343	8.255	0.217	0.224	0.005	0.2677	0.0045	1533.7	66.7	1121.4	23.4	2160.2	143.9	1231	126	0.10
ZW132-12	0.0020	0.0013	0.0103	0.0067	11.078	0.326	0.382	0.008	0.2105	0.0041	2520.0	28.1	2080.3	39.0	2896.1	33.8	343	66	0.19
ZW132-13	0.0027	0.0021	0.0152	0.0116	7.870	0.243	0.292	0.006	0.1957	0.0042	2202.5	29.7	1646.1	32.3	2769.8	40.4	337	93	0.28
ZW132-14	0.0018	0.0007	0.0091	0.0033	14.843	0.391	0.483	0.010	0.2227	0.0037	2796.6	25.2	2538.2	43.2	2988.7	27.0	722	212	0.29
ZW132-1-1	0.0012	0.0003	0.0067	0.0017	12.456	0.440	0.448	0.015	0.2017	0.0019	2633.12	33.20	2383.53	67.71	2830.99	15.9	919	607	0.66
ZW132-1-2	0.0007	0.0002	0.0035	0.0012	15.074	0.533	0.525	0.018	0.2080	0.0020	2816.57	33.70	2720.94	75.60	2885.77	15.7	773	481	0.62
ZW132-1-3	0.0008	0.0003	0.0044	0.0016	7.725	0.273	0.305	0.010	0.1834	0.0018	2195.50	31.78	1717.02	51.15	2678.08	16.5	1066	717	0.67
ZW132-1-4	0.0025	0.0004	0.0131	0.0020	15.413	0.543	0.548	0.019	0.2040	0.0019	2828.52	33.61	2810.69	77.35	2841.25	15.7	971	492	0.51
ZW132-1-5	0.0017	0.0005	0.0083	0.0027	18.005	0.650	0.584	0.020	0.2236	0.0023	2982.01	34.84	2961.55	82.32	2995.83	17.0	354	139	0.39
ZW132-1-6	0.0029	0.0003	0.0150	0.0018	19.996	0.703	0.688	0.023	0.2107	0.0019	3076.51	34.02	3368.34	89.01	2891.17	15.3	1018	391	0.38
ZW132-1-7	0.0057	0.0006	0.0354	0.0039	4.707	0.165	0.199	0.007	0.1715	0.0016	1738.32	29.36	1163.73	35.91	2522.04	17.5	2407	562	0.23
ZW132-1-8	0.0228	0.0012	0.1502	0.0078	4.000	0.139	0.188	0.006	0.1546	0.0014	1504.16	28.26	1085.19	33.59	2157.01	22.7	6189	985	0.16
ZW132-2-1	0.0033	0.0006	0.0265	0.0050	3.420	0.121	0.201	0.007	0.1231	0.0013	1487.84	27.91	1179.27	36.47	1960.27	20.6	1505	305	0.20

ZW132-2-2	0.0727	0.0037	0.3269	0.0167	11.419	0.402	0.350	0.012	0.2364	0.0023	2194.95	38.73	1813.10	53.97	2573.55	44.9	1072	757	0.71
ZW132-2-3	0.0015	0.0004	0.0080	0.0022	13.529	0.482	0.480	0.016	0.2044	0.0020	2709.74	33.76	2524.35	71.54	2851.04	16.6	570	239	0.42
ZW132-2-4	0.0025	0.0006	0.0140	0.0033	9.195	0.328	0.341	0.012	0.1953	0.0020	2344.71	32.73	1889.21	55.95	2768.71	17.6	668	500	0.75
ZW132-2-5	0.0009	0.0003	0.0046	0.0019	12.221	0.437	0.433	0.015	0.2049	0.0021	2617.24	33.60	2315.50	66.74	2859.73	16.7	530	284	0.53
ZW132-2-6	0.0118	0.0011	0.0621	0.0059	14.447	0.514	0.507	0.017	0.2065	0.0020	2718.72	34.19	2619.73	73.72	2793.12	19.2	587	302	0.51
ZW132-2-7	0.0002	0.0002	0.0009	0.0008	18.067	0.628	0.585	0.019	0.2240	0.0031	2992.47	33.47	2968.97	75.91	3008.29	22.3	441	189	0.43
ZW132-2-8	0.0104	0.0007	0.0729	0.0050	3.885	0.131	0.193	0.006	0.1462	0.0020	1549.94	27.10	1125.64	31.93	2188.65	25.1	4842	786	0.16
ZW132-2-9	0.0011	0.0003	0.0054	0.0014	17.174	0.586	0.566	0.018	0.2202	0.0030	2939.43	32.75	2887.99	72.98	2974.83	21.8	887	508	0.57
ZW132-2-10	0.0022	0.0005	0.0114	0.0027	16.616	0.579	0.557	0.018	0.2162	0.0030	2901.97	33.44	2850.52	73.56	2937.86	22.9	435	151	0.35
ZW132-2-11	0.0010	0.0004	0.0047	0.0017	18.425	0.639	0.597	0.019	0.2238	0.0031	3007.62	33.44	3016.18	76.69	3001.91	22.3	471	162	0.34
ZW132-2-12	0.0002	0.0002	0.0009	0.0010	20.151	0.701	0.650	0.021	0.2250	0.0031	3097.76	33.67	3226.17	81.07	3015.56	22.2	425	166	0.39
ZW132-2-13	0.0000	0.0000	0.0000	0.0000	18.975	0.675	0.621	0.020	0.2217	0.0032	3040.53	34.30	3113.04	80.42	2992.96	23.0	272	89	0.33
ZW132-2-14	0.0247	0.0017	0.1153	0.0081	31.650	1.106	0.971	0.031	0.2363	0.0032	3419.12	35.41	4296.49	101.07	2938.77	26.6	343	99	0.29
ZW132-2-15	0.0222	0.0016	0.1047	0.0078	25.998	0.906	0.806	0.026	0.2339	0.0032	3238.59	34.95	3747.28	91.17	2937.15	26.3	386	113	0.29
ZW132-2-16	0.0090	0.0004	0.0535	0.0026	7.077	0.237	0.286	0.009	0.1796	0.0023	2072.42	29.68	1607.38	43.86	2572.88	22.3	13518	5591	0.41
ZW132-2-17	0.0012	0.0005	0.0068	0.0027	11.821	0.414	0.472	0.015	0.1815	0.0026	2583.91	32.86	2491.91	66.09	2656.86	24.1	420	218	0.52
ZW132-2-18	0.0192	0.0013	0.1064	0.0073	8.792	0.299	0.331	0.010	0.1926	0.0026	2214.68	31.46	1813.05	49.28	2610.21	26.4	1436	561	0.39
ZW132-2-19	0.0019	0.0002	0.0107	0.0013	10.581	0.356	0.404	0.012	0.1902	0.0025	2477.03	31.22	2181.72	57.30	2729.04	21.8	3066	349	0.11
ZW132-2-20	0.0000	0.0000	0.0000	0.0000	10.686	0.366	0.384	0.012	0.2016	0.0028	2496.25	31.78	2096.73	56.14	2839.47	22.3	887	399	0.45
ZW132-2-21	0.0012	0.0003	0.0067	0.0017	12.453	0.441	0.448	0.015	0.2017	0.0019	2632.90	33.33	2382.95	67.97	2831.09	15.9	919	607	0.66
ZW132-2-22	0.0007	0.0002	0.0035	0.0012	15.071	0.535	0.525	0.018	0.2081	0.0020	2816.35	33.82	2720.29	75.89	2885.86	15.7	773	481	0.62
ZW132-2-23	0.0008	0.0003	0.0044	0.0016	7.723	0.274	0.305	0.010	0.1834	0.0018	2195.28	31.90	1716.59	51.35	2678.13	16.5	1066	717	0.67
ZW132-2-24	0.0025	0.0004	0.0131	0.0020	15.409	0.545	0.548	0.019	0.2040	0.0019	2828.27	33.74	2810.04	77.65	2841.30	15.6	971	492	0.51
ZW132-2-25	0.0017	0.0005	0.0083	0.0027	18.001	0.653	0.584	0.020	0.2236	0.0023	2981.79	34.96	2960.90	82.62	2995.91	17.0	354	139	0.39
ZW132-2-26	0.0029	0.0003	0.0150	0.0018	19.991	0.705	0.688	0.023	0.2107	0.0019	3076.26	34.15	3367.60	89.36	2891.21	15.3	1018	391	0.38
ZW132-2-27	0.0057	0.0006	0.0354	0.0039	4.705	0.166	0.199	0.007	0.1715	0.0016	1738.09	29.47	1163.43	36.05	2522.04	17.5	2407	562	0.23
ZW132-2-28	0.0228	0.0012	0.1502	0.0078	3.999	0.140	0.188	0.006	0.1546	0.0014	1503.95	28.36	1084.91	33.72	2157.05	22.7	6189	985	0.16
ZW132-2-29	0.0033	0.0006	0.0265	0.0050	3.419	0.121	0.201	0.007	0.1232	0.0013	1487.69	28.01	1178.98	36.61	1960.41	20.6	1505	305	0.20
ZW132-2-30	0.0727	0.0036	0.3269	0.0167	11.416	0.404	0.350	0.012	0.2365	0.0023	2194.73	38.82	1812.65	54.18	2573.62	44.9	1072	757	0.71
ZW132-2-31	0.0015	0.0004	0.0080	0.0022	13.526	0.484	0.480	0.017	0.2044	0.0020	2709.55	33.88	2523.79	71.81	2851.15	16.6	570	239	0.42
ZW132-2-32	0.0025	0.0006	0.0140	0.0033	9.193	0.329	0.341	0.012	0.1953	0.0020	2344.48	32.85	1888.76	56.16	2768.76	17.6	668	500	0.75
ZW132-2-33	0.0009	0.0003	0.0048	0.0018	12.218	0.439	0.432	0.015	0.2049	0.0021	2616.82	33.72	2314.90	66.99	2859.51	16.7	530	284	0.53
ZW132-2-34	0.0119	0.0011	0.0625	0.0059	14.444	0.516	0.507	0.017	0.2065	0.0020	2718.17	34.31	2619.01	73.99	2792.72	19.2	587	302	0.51
ZW132-2-35	0.0002	0.0002	0.0009	0.0008	18.063	0.630	0.585	0.019	0.2240	0.0031	2992.25	33.56	2968.37	76.11	3008.33	22.3	441	189	0.43
ZW132-2-36	0.0104	0.0007	0.0729	0.0050	3.884	0.131	0.193	0.006	0.1462	0.0020	1549.74	27.17	1125.37	32.02	2188.65	25.1	4842	786	0.16
ZW132-2-37	0.0011	0.0003	0.0054	0.0014	17.170	0.587	0.566	0.018	0.2202	0.0030	2939.21	32.84	2887.40	73.18	2974.87	21.8	887	508	0.57
ZW132-2-38	0.0022	0.0005	0.0114	0.0027	16.613	0.580	0.557	0.018	0.2162	0.0030	2901.78	33.52	2849.98	73.75	2937.92	23.0	435	151	0.35
ZW132-2-39	0.0010	0.0004	0.0047	0.0017	18.421	0.641	0.597	0.019	0.2238	0.0031	3007.42	33.53	3015.62	76.89	3001.95	22.4	471	162	0.34
ZW132-2-40	0.0002	0.0002	0.0009	0.0010	20.147	0.703	0.649	0.021	0.2250	0.0031	3097.58	33.76	3225.59	81.29	3015.61	22.2	425	166	0.39
ZW132-2-41	0.0000	0.0000	0.0000	0.0000	18.972	0.676	0.621	0.020	0.2217	0.0032	3040.38	34.39	3112.49	80.62	2993.06	23.0	272	89	0.33
ZW132-2-42	0.0247	0.0017	0.1153	0.0081	31.644	1.109	0.971	0.031	0.2363	0.0032	3418.94	35.49	4295.83	101.34	2938.82	26.7	343	99	0.29
ZW132-2-43	0.0222	0.0016	0.1047	0.0078	25.993	0.908	0.806	0.026	0.2339	0.0032	3238.42	35.04	3746.71	91.41	2937.19	26.3	386	113	0.29
ZW132-2-44	0.0090	0.0004	0.0535	0.0026	7.075	0.238	0.286	0.009	0.1796	0.0024	2072.23	29.77	1607.08	43.99	2572.88	22.4	13518	5591	0.41
ZW132-2-45	0.0012	0.0005	0.0068	0.0027	11.819	0.415	0.472	0.015	0.1815	0.0026	2583.77	32.95	2491.52	66.27	2656.94	24.1	420	218	0.52
ZW132-2-46	0.0192	0.0013	0.1064	0.0073	8.790	0.299	0.331	0.010	0.1926	0.0026	2214.53	31.55	1812.75	49.42	2610.24	26.4	1436	561	0.39
ZW132-2-47	0.0019	0.0002	0.0108	0.0013	10.579	0.357	0.403	0.013	0.1902	0.0025	2476.80	31.30	2181.36	57.46	2728.97	21.9	3066	349	0.11
ZW132-2-48	0.0001	0.0002	0.0004	0.0009	10.685	0.367	0.384	0.012	0.2016	0.0028	2495.68	31.87	2096.27	56.29	2838.91	22.4	887	399	0.45
ZW135-01	0.0006	0.0008	0.0036	0.0051	9.829	0.314	0.411	0.011	0.1734	0.0028	2415.5	29.8	2219.2	51.5	2585.4	28.7	432	162	0.38
ZW135-02	0.0013	0.0013	0.0075	0.0073	11.978	0.398	0.470	0.013	0.1847	0.0033	2595.6	31.9	2482.6	58.0	2684.9	31.7	284	100	0.35
ZW135-03	0.0006	0.0008	0.0037	0.0045	11.032	0.347	0.435	0.012	0.1838	0.0029	2522.4	29.5	2328.4	53.4	2682.4	26.8	460	184	0.40

ZW135-04	0.0000	0.0000	0.0000	0.0000	14.626	0.471	0.564	0.016	0.1881	0.0030	2791.2	30.6	2883.1	64.8	2725.5	26.7	306	166	0.54
ZW135-05	0.0028	0.0019	0.0160	0.0110	13.615	0.488	0.525	0.015	0.1882	0.0038	2708.1	35.4	2712.6	65.3	2704.6	38.5	170	55	0.33
ZW135-06	0.0092	0.0020	0.0525	0.0116	12.050	0.374	0.465	0.013	0.1881	0.0028	2557.9	31.2	2441.1	55.4	2651.8	32.3	484	210	0.43
ZW135-07	0.0001	0.0012	0.0005	0.0070	13.285	0.473	0.514	0.015	0.1876	0.0038	2699.6	34.2	2672.0	64.1	2720.3	35.3	179	60	0.33
ZW135-08	0.0025	0.0019	0.0143	0.0111	11.906	0.441	0.457	0.014	0.1889	0.0042	2583.5	36.2	2421.6	60.3	2713.1	41.0	160	74	0.46
ZW135-09	0.0000	0.0000	0.0000	0.0000	14.806	0.498	0.564	0.016	0.1905	0.0034	2802.8	32.0	2882.2	66.3	2746.2	29.3	228	113	0.49
ZW135-10	0.0005	0.0010	0.0028	0.0056	12.871	0.434	0.500	0.014	0.1865	0.0034	2667.6	32.2	2614.7	61.1	2708.0	31.5	247	76	0.31
ZW135-11	0.0138	0.0034	0.0763	0.0186	10.539	0.350	0.393	0.011	0.1946	0.0035	2410.1	35.7	2111.0	50.7	2673.3	44.9	323	140	0.43
ZW135-12	0.0037	0.0015	0.0246	0.0102	6.272	0.201	0.293	0.008	0.1552	0.0026	1992.8	29.4	1651.8	39.6	2367.7	34.2	602	330	0.55
ZW135-13	0.0017	0.0019	0.0094	0.0109	14.208	0.546	0.543	0.017	0.1896	0.0044	2754.7	37.9	2794.0	69.8	2726.0	42.2	122	47	0.39
ZW135-14	0.0026	0.0018	0.0149	0.0103	11.846	0.410	0.466	0.013	0.1844	0.0036	2578.2	33.8	2460.0	58.7	2672.6	36.5	228	92	0.40
ZW135-15	0.0285	0.0049	0.1501	0.0259	11.438	0.381	0.408	0.011	0.2034	0.0043	2408.7	41.6	2151.8	48.3	2633.7	62.0	336	208	0.62
ZW135-16	0.0008	0.0008	0.0050	0.0049	8.379	0.277	0.363	0.009	0.1672	0.0035	2268.4	30.3	1997.0	43.7	2523.0	36.4	430	174	0.41
ZW135-17	0.0067	0.0036	0.0375	0.0200	10.788	0.414	0.405	0.011	0.1931	0.0050	2469.6	40.4	2180.2	52.4	2717.2	55.3	166	74	0.44
ZW135-18	0.0196	0.0049	0.1124	0.0281	7.490	0.265	0.294	0.008	0.1846	0.0044	2065.7	41.9	1633.7	38.6	2529.4	66.9	322	83	0.26
ZW135-19	0.0104	0.0029	0.0611	0.0169	10.164	0.337	0.407	0.010	0.1811	0.0038	2391.6	34.6	2182.0	47.8	2575.3	46.4	371	496	1.34
ZW135-20	0.0015	0.0015	0.0085	0.0087	13.746	0.494	0.527	0.014	0.1891	0.0044	2724.3	35.0	2725.8	60.9	2723.1	41.1	187	62	0.33
ZW135-21	0.0045	0.0021	0.0264	0.0125	11.574	0.397	0.458	0.012	0.1833	0.0040	2545.6	34.1	2421.2	53.3	2646.3	42.3	273	92	0.34
ZW135-22	0.0075	0.0015	0.0445	0.0089	10.220	0.305	0.416	0.010	0.1780	0.0031	2412.9	28.8	2229.9	45.9	2571.0	33.1	1000	850	0.85
ZW135-23	0.0026	0.0022	0.0151	0.0124	12.837	0.466	0.497	0.014	0.1872	0.0045	2653.4	36.2	2597.3	58.8	2696.5	44.6	187	66	0.35
ZW135-24	0.0081	0.0029	0.0484	0.0171	10.287	0.355	0.416	0.011	0.1792	0.0040	2415.2	35.8	2228.5	49.8	2576.5	48.1	286	176	0.61
ZW135-25	0.0000	0.0000	0.0000	0.0000	13.303	0.498	0.514	0.014	0.1878	0.0047	2701.4	35.3	2672.7	61.3	2722.9	40.9	159	56	0.35
ZW135-26	0.0003	0.0010	0.0017	0.0059	11.795	0.447	0.466	0.013	0.1835	0.0047	2586.7	35.9	2466.7	57.5	2682.0	43.3	164	62	0.38
ZW135-27	0.0000	0.0000	0.0000	0.0000	15.322	0.552	0.574	0.016	0.1937	0.0045	2835.5	34.3	2922.6	64.8	2774.1	38.0	173	67	0.39
ZW135-28	0.0000	0.0000	0.0000	0.0000	13.442	0.534	0.529	0.015	0.1843	0.0050	2711.2	37.5	2736.6	65.1	2692.3	44.5	123	35	0.29
ZW135-29	0.0021	0.0024	0.0128	0.0142	9.819	0.366	0.402	0.012	0.1771	0.0039	2406.1	36.8	2174.5	55.7	2608.4	43.9	304	99	0.33
ZW135-30	0.0000	0.0000	0.0000	0.0000	14.116	0.588	0.553	0.018	0.1852	0.0048	2757.5	39.5	2836.2	74.8	2700.4	42.8	136	31	0.22
ZW138-01	0.0059	0.0020	0.0324	0.0108	6.789	0.229	0.250	0.007	0.1972	0.0035	2055.2	31.3	1429.6	36.7	2758.5	34.9	853	487	0.57
ZW138-02	0.0034	0.0014	0.0167	0.0067	17.780	0.603	0.568	0.017	0.2272	0.0039	2961.7	33.2	2890.0	68.2	3010.9	29.7	399	368	0.92
ZW138-03	0.0021	0.0011	0.0111	0.0060	12.241	0.414	0.430	0.012	0.2063	0.0036	2612.6	32.3	2302.8	56.1	2862.3	30.3	522	475	0.91
ZW138-04	0.0045	0.0018	0.0237	0.0094	11.130	0.375	0.392	0.011	0.2060	0.0036	2511.8	32.6	2123.4	52.3	2842.6	32.6	581	316	0.54
ZW138-05	0.0003	0.0005	0.0016	0.0027	18.078	0.605	0.585	0.017	0.2242	0.0037	2992.4	32.3	2967.4	69.1	3009.3	27.0	447	250	0.56
ZW138-06	0.0069	0.0020	0.0348	0.0099	14.473	0.487	0.482	0.014	0.2180	0.0037	2747.6	33.4	2519.6	60.6	2919.7	32.5	487	207	0.43
ZW138-07	0.0000	0.0000	0.0000	0.0000	16.892	0.669	0.535	0.017	0.2290	0.0053	2928.7	38.0	2762.7	71.9	3044.9	37.3	156	84	0.54
ZW138-08	0.0000	0.0000	0.0000	0.0000	18.302	0.640	0.592	0.018	0.2243	0.0041	3005.7	33.7	2996.5	71.4	3011.9	29.4	303	136	0.45
ZW138-09	0.0054	0.0020	0.0316	0.0117	6.612	0.224	0.260	0.007	0.1847	0.0034	2032.7	31.6	1481.0	37.9	2651.1	36.4	827	350	0.42
ZW138-10	0.0040	0.0016	0.0202	0.0084	13.617	0.468	0.459	0.013	0.2151	0.0039	2704.1	33.5	2427.8	59.3	2917.6	32.4	422	221	0.52
ZW138-11	0.0019	0.0018	0.0097	0.0089	14.307	0.512	0.475	0.014	0.2184	0.0043	2761.1	35.0	2502.0	62.2	2956.3	34.9	304	140	0.46
ZW138-12	0.0000	0.0000	0.0000	0.0000	16.349	0.581	0.533	0.016	0.2225	0.0042	2897.4	34.0	2754.2	67.1	2998.5	30.7	292	127	0.44
ZW138-13	0.0134	0.0033	0.0759	0.0189	4.464	0.206	0.172	0.007	0.1885	0.0030	1659.3	41.2	1009.1	40.5	2620.7	43.6	1092	610	0.56
ZW138-14	0.0022	0.0014	0.0142	0.0091	5.698	0.266	0.258	0.011	0.1602	0.0028	1918.8	41.0	1476.9	57.3	2437.0	33.1	707	468	0.66
ZW138-15	0.0059	0.0025	0.0284	0.0119	19.093	0.915	0.599	0.027	0.2311	0.0040	3018.8	47.7	3012.1	107.7	3023.2	34.3	220	86	0.39
ZW138-16	0.0040	0.0018	0.0223	0.0098	10.037	0.464	0.375	0.016	0.1941	0.0030	2417.4	43.6	2046.3	76.4	2746.5	30.6	519	110	0.21
ZW138-17	0.0022	0.0016	0.0107	0.0078	16.210	0.770	0.530	0.023	0.2219	0.0038	2878.9	46.0	2735.9	98.9	2980.6	30.4	267	103	0.38
ZW138-18	0.0090	0.0026	0.0506	0.0145	6.251	0.287	0.236	0.010	0.1917	0.0030	1966.3	42.0	1357.0	53.0	2686.6	36.1	850	333	0.39
ZW138-19	0.0001	0.0013	0.0008	0.0079	7.932	0.371	0.318	0.014	0.1812	0.0031	2222.5	42.8	1777.3	67.7	2662.6	31.1	531	133	0.25
ZW138-20	0.0038	0.0016	0.0205	0.0086	11.152	0.512	0.404	0.018	0.2002	0.0030	2516.7	43.5	2180.3	80.5	2800.4	28.2	538	350	0.65
ZW138-21	0.0009	0.0010	0.0042	0.0051	16.944	0.800	0.541	0.024	0.2270	0.0037	2927.7	45.5	2787.0	100.2	3025.8	27.7	280	102	0.37
ZW138-22	0.0367	0.0053	0.1869	0.0271	6.299	0.286	0.218	0.009	0.2099	0.0030	1839.6	47.8	1227.0	48.6	2626.5	61.0	1057	1197	1.13
ZW138-23	0.0006	0.0007	0.0034	0.0038	10.287	0.479	0.374	0.016	0.1996	0.0032	2457.8	43.2	2045.8	76.5	2818.7	27.1	472	235	0.50

ZW138-24	0.0272	0.0041	0.1296	0.0197	3.410	0.153	0.107	0.005	0.2302	0.0030	1399.4	38.1	640.7	26.3	2874.2	43.0	2489	1636	0.66
ZW138-25	0.0012	0.0011	0.0058	0.0053	15.597	0.733	0.511	0.023	0.2214	0.0036	2846.9	45.1	2657.9	96.1	2983.6	27.6	310	183	0.59
ZW138-26	0.0025	0.0017	0.0122	0.0082	16.073	0.780	0.522	0.023	0.2235	0.0042	2869.4	47.0	2700.1	98.9	2990.4	33.0	219	97	0.44
ZW138-27	0.0060	0.0022	0.0332	0.0121	9.436	0.413	0.351	0.014	0.1952	0.0032	2350.4	41.7	1927.2	67.8	2741.2	33.9	555	315	0.57
ZW138-28	0.0013	0.0011	0.0068	0.0057	12.683	0.556	0.434	0.018	0.2120	0.0034	2650.0	41.6	2320.8	79.6	2912.0	27.3	442	269	0.61
ZW138-29	0.0024	0.0015	0.0118	0.0075	17.121	0.779	0.558	0.023	0.2223	0.0040	2930.3	44.2	2854.8	96.4	2982.5	31.5	243	163	0.67
ZW138-30	0.0022	0.0016	0.0110	0.0078	17.007	0.788	0.546	0.023	0.2260	0.0043	2924.6	45.0	2802.9	95.9	3009.4	33.5	210	165	0.79
ZW138-31	0.0050	0.0024	0.0252	0.0121	13.249	0.605	0.443	0.018	0.2170	0.0041	2673.5	44.6	2353.4	82.2	2925.4	36.8	280	173	0.62
ZW138-32	0.0017	0.0012	0.0088	0.0063	13.405	0.600	0.465	0.019	0.2091	0.0036	2700.2	42.7	2458.0	84.3	2886.8	30.0	337	138	0.41
ZW138-33	0.0016	0.0012	0.0096	0.0073	7.492	0.334	0.303	0.012	0.1794	0.0032	2163.4	40.4	1702.9	61.0	2634.2	32.4	539	330	0.61
ZW138-34	0.0012	0.0011	0.0065	0.0056	12.070	0.536	0.418	0.017	0.2092	0.0036	2603.7	42.0	2250.8	78.0	2891.0	29.1	396	168	0.42
ZW138-35	0.0461	0.0059	0.2097	0.0271	7.120	0.303	0.215	0.009	0.2398	0.0033	1920.2	47.1	1204.4	44.7	2815.2	61.2	1166	1096	0.94
ZW138-36	0.0000	0.0000	0.0000	0.0000	18.509	0.866	0.589	0.025	0.2279	0.0045	3016.6	45.1	2985.3	101.4	3037.5	31.6	186	108	0.58
ZW138-37	0.0559	0.0061	0.2557	0.0281	5.997	0.251	0.185	0.007	0.2356	0.0029	1724.2	46.8	1035.9	38.7	2704.4	66.6	1909	1669	0.87
ZW138-38	0.0049	0.0026	0.0265	0.0144	9.859	0.455	0.357	0.015	0.2000	0.0040	2396.9	44.5	1962.0	70.3	2790.3	41.2	324	337	1.04
ZW138-39	0.0256	0.0045	0.1273	0.0223	11.142	0.483	0.370	0.015	0.2182	0.0033	2409.0	46.3	1986.2	69.8	2788.5	49.3	577	361	0.62
ZW138-40	0.0005	0.0007	0.0026	0.0034	17.472	0.779	0.561	0.023	0.2257	0.0038	2958.6	42.9	2870.9	95.9	3018.8	27.3	297	91	0.31

Table 4-2. Results of Re-Os dating.

	Os [ppm]	Ir [ppm]	Ru [ppm]	Pt [ppm]	Pd [ppm]	Re [ppm]	187Re/188Os	2sm	187/188Os	2sm	T_{Ma} (Ga)	*2sm*	T_{RD} (Ga)	187/188Os at 2.9 Ga
ZW185	84.8	77.9	286.3	10.4	6.02	0.057	0.0033	0.0002	0.107012	0.000034	2.94	0.0050	2.92	0.10685
ZW191	27.4	26.0	177.8	7.33	82.8	0.224	0.0394	0.0016	0.108785	0.000027	2.95	0.0122	2.66	0.10683
ZW195	46.4	30.1	222.3	23.5	8.24	0.080	0.0083	0.0004	0.107192	0.000008	2.95	0.0027	2.89	0.10678

Table 5-1. analytical results of zircon U-Pb dating.

Sample name	Fractional amount of common Pb	Isotope ratios						Common Pb-corrected age (Ma)								
	f206	207Pb/235U	2σ	206Pb/238U	2σ	207Pb/206Pb	2σ	235U-207Pb	2σ	238U-206Pb	2σ	207Pb-206Pb	2σ	U(ppm)	Th(ppm)	Th/U
ZW5-01	0.003	13.861	0.350	0.5329	0.0128	0.1886	0.0015	2724.6	24.1	2747.3	53.6	2707.9	14.3	323	144	0.44
ZW5-02	0.000	16.431	0.438	0.5759	0.0145	0.2069	0.0018	2902.0	25.5	2932.0	59.5	2881.3	13.9	205	211	1.03
ZW5-03	0.000	13.921	0.411	0.5492	0.0152	0.1838	0.0019	2743.5	28.0	2821.4	63.1	2686.6	17.3	119	38	0.32
ZW5-04	0.022	12.581	0.300	0.4749	0.0108	0.1921	0.0014	2530.0	23.5	2460.3	46.6	2586.4	18.2	671	248	0.37
ZW5-05	0.000	14.224	0.371	0.5466	0.0135	0.1887	0.0016	2764.6	24.8	2810.8	56.3	2731.1	13.9	243	71	0.29
ZW5-06	0.079	7.147	0.166	0.2418	0.0054	0.2144	0.0015	1716.3	27.7	1295.7	26.3	2276.1	43.6	1272	618	0.49
ZW5-07	0.000	16.500	0.430	0.5810	0.0144	0.2060	0.0017	2906.3	25.0	2953.0	58.6	2874.1	13.3	239	98	0.41
ZW5-08	0.027	11.808	0.310	0.3984	0.0099	0.2150	0.0019	2451.6	27.8	2111.3	44.8	2747.3	28.4	243	156	0.64
ZW5-09	0.006	13.941	0.350	0.5255	0.0125	0.1924	0.0015	2715.1	24.2	2709.7	52.8	2719.2	15.2	336	169	0.50
ZW5-10	0.111	26.531	0.765	0.6467	0.0178	0.2975	0.0026	2860.8	44.9	2927.8	66.6	2814.0	63.4	121	74	0.61
ZW5-11	0.028	14.783	0.367	0.5145	0.0121	0.2084	0.0016	2651.4	25.6	2613.2	50.9	2680.7	22.7	379	176	0.46
ZW5-12	0.011	13.337	0.338	0.5077	0.0122	0.1905	0.0015	2640.8	24.8	2621.9	51.9	2655.3	18.3	312	208	0.67
ZW5-13	0.000	13.146	0.428	0.5279	0.0159	0.1806	0.0022	2690.2	30.7	2732.7	67.3	2658.4	20.1	80	35	0.44
ZW5-14	0.000	17.135	0.557	0.6040	0.0184	0.2058	0.0023	2940.8	31.3	3045.1	74.1	2870.2	18.6	76	38	0.50
ZW5-15	0.083	8.966	0.361	0.2485	0.0097	0.2617	0.0024	1962.3	43.3	1323.7	47.3	2724.5	51.5	538	187	0.35
ZW5-16	0.000	13.676	0.573	0.5502	0.0224	0.1803	0.0018	2727.5	39.7	2826.1	93.0	2655.3	16.8	198	142	0.72
ZW5-17	0.000	16.839	0.770	0.5957	0.0262	0.2050	0.0025	2925.4	43.9	3012.2	106.0	2866.3	20.3	79	34	0.43
ZW5-18	0.000	16.662	0.753	0.5993	0.0261	0.2016	0.0024	2915.6	43.3	3027.1	105.3	2839.5	19.5	86	29	0.34
ZW5-19	0.000	13.247	0.583	0.5238	0.0222	0.1834	0.0022	2697.4	41.5	2715.4	93.9	2684.0	19.4	113	38	0.33
ZW5-20	0.000	16.585	0.741	0.5838	0.0252	0.2060	0.0024	2910.8	42.8	2964.0	102.5	2874.3	19.1	95	31	0.32
ZW5-21	0.003	12.706	0.511	0.5112	0.0201	0.1803	0.0016	2642.2	37.9	2655.6	85.4	2632.0	15.5	486	254	0.52
ZW5-22	0.000	16.391	0.710	0.5811	0.0244	0.2046	0.0022	2898.8	41.4	2952.8	99.3	2861.6	17.6	128	47	0.37
ZW5-23	0.000	12.527	0.520	0.5075	0.0205	0.1790	0.0018	2643.4	39.1	2645.3	87.5	2641.9	16.7	232	122	0.53
ZW5-24	0.005	12.634	0.515	0.4976	0.0198	0.1841	0.0017	2625.7	38.6	2593.0	84.8	2651.1	17.5	330	131	0.40
ZW5-25	0.034	14.147	0.576	0.4839	0.0192	0.2120	0.0019	2582.7	40.5	2472.8	81.6	2670.1	28.8	343	252	0.73
ZW5-26	0.004	14.332	0.585	0.5398	0.0215	0.1926	0.0018	2751.1	38.9	2773.7	89.6	2734.6	16.5	321	253	0.79
ZW5-27	0.005	12.334	0.498	0.4858	0.0191	0.1841	0.0017	2600.0	38.1	2541.1	82.7	2646.3	16.7	430	294	0.68
ZW5-28	0.000	13.275	0.591	0.5279	0.0223	0.1824	0.0026	2699.4	42.0	2732.7	94.0	2674.5	23.5	61	22	0.37
ZW5-29	0.000	19.032	0.770	0.6196	0.0242	0.2228	0.0024	3043.4	39.0	3108.2	96.1	3001.0	17.3	99	48	0.49
ZW5-30	0.000	14.034	0.497	0.5344	0.0184	0.1905	0.0015	2752.0	33.6	2760.1	77.5	2746.1	13.3	514	260	0.51
ZW5-31	0.000	16.902	0.662	0.5942	0.0225	0.2063	0.0021	2927.9	37.6	3005.9	90.8	2874.7	16.9	127	43	0.34
ZW5-32	0.000	16.161	0.614	0.5685	0.0209	0.2062	0.0020	2884.9	36.4	2901.0	85.8	2873.6	16.1	170	71	0.42
ZW5-33	0.000	13.007	0.489	0.5227	0.0190	0.1805	0.0018	2680.2	35.4	2710.5	80.3	2657.4	16.2	196	137	0.70
ZW5-34	0.044	11.242	0.397	0.3685	0.0126	0.2212	0.0018	2319.4	35.1	1945.0	57.8	2667.7	29.1	618	269	0.43
ZW5-35	0.000	13.053	0.561	0.5173	0.0211	0.1830	0.0024	2682.9	40.6	2687.4	89.8	2679.5	22.4	73	33	0.45
ZW5-36	0.000	13.338	0.587	0.5331	0.0223	0.1815	0.0025	2703.9	41.6	2754.4	93.6	2666.4	22.9	64	22	0.35
ZW5-37	0.000	14.017	0.559	0.5353	0.0205	0.1899	0.0021	2750.9	37.8	2763.7	86.0	2741.5	18.3	115	52	0.45
ZW5-38	0.028	10.111	0.353	0.3916	0.0133	0.1873	0.0015	2289.2	33.2	2079.6	60.6	2482.0	22.6	854	504	0.59
ZW5-39	0.000	16.574	0.636	0.5855	0.0217	0.2053	0.0020	2910.5	36.7	2971.1	88.2	2868.9	16.0	153	70	0.46
ZW5-40	0.000	17.019	0.844	0.6015	0.0283	0.2052	0.0032	2935.9	47.6	3036.0	113.9	2868.0	25.4	37	13	0.35
ZW5-41	0.000	13.151	0.444	0.5265	0.0161	0.1812	0.0026	2690.6	31.8	2726.8	68.2	2663.5	23.3	152	81	0.53
ZW5-42	0.000	13.231	0.430	0.5331	0.0157	0.1800	0.0024	2696.0	30.7	2754.5	66.2	2652.4	22.5	200	142	0.71
ZW5-43	0.001	14.224	0.431	0.5399	0.0149	0.1911	0.0024	2759.1	28.8	2780.5	62.4	2743.6	20.9	406	167	0.41
ZW5-44	0.000	13.675	0.489	0.5241	0.0171	0.1892	0.0028	2727.5	33.8	2716.7	72.1	2735.5	24.5	108	64	0.59
ZW5-45	0.013	11.607	0.394	0.4479	0.0138	0.1880	0.0027	2499.2	33.8	2359.1	60.9	2615.1	32.6	150	52	0.35

ZW5-46	0.000	13.300	0.463	0.5285	0.0167	0.1825	0.0026	2701.2	32.9	2735.3	70.6	2675.7	24.0	125	54	0.43
ZW5-47	0.000	14.171	0.455	0.5429	0.0159	0.1893	0.0025	2760.8	30.5	2795.4	66.3	2735.6	21.9	217	110	0.51
ZW5-48	0.007	10.029	0.298	0.4118	0.0111	0.1766	0.0022	2398.2	27.8	2210.2	50.5	2562.0	22.9	615	332	0.54
ZW5-49	0.000	12.912	0.482	0.5214	0.0177	0.1796	0.0028	2673.2	35.2	2705.3	74.9	2649.1	25.9	88	45	0.51
ZW5-50	0.005	15.298	0.501	0.5294	0.0158	0.2096	0.0028	2810.7	31.6	2728.6	66.5	2870.2	23.6	182	103	0.57
ZW5-51	0.016	11.408	0.338	0.4529	0.0122	0.1827	0.0023	2467.5	28.3	2376.1	53.5	2543.7	24.5	643	296	0.46
ZW5-52	0.028	12.731	0.376	0.4488	0.0120	0.2057	0.0025	2511.4	29.1	2333.3	52.7	2658.6	26.9	669	397	0.59
ZW5-53	0.000	14.224	0.491	0.5412	0.0170	0.1906	0.0027	2764.8	32.7	2788.3	71.2	2747.7	23.4	130	68	0.53
ZW5-54	0.023	9.346	0.328	0.3637	0.0121	0.1864	0.0021	2244.7	32.9	1959.8	56.1	2515.6	25.3	994	1049	1.05
ZW5-55	0.001	15.270	0.823	0.5448	0.0274	0.2033	0.0040	2826.3	51.9	2800.8	114.2	2844.6	34.3	31	10	0.33
ZW5-56	0.006	14.595	0.554	0.5466	0.0196	0.1937	0.0024	2755.8	36.5	2796.8	81.3	2725.9	23.5	199	138	0.69
ZW5-57	0.000	16.394	0.699	0.5842	0.0234	0.2035	0.0029	2900.1	40.8	2965.7	95.3	2854.9	23.5	82	40	0.49
ZW5-58	0.001	16.234	0.601	0.5693	0.0199	0.2068	0.0025	2885.1	35.5	2902.5	81.9	2872.9	19.9	261	149	0.57
ZW5-59	0.005	13.097	0.470	0.5150	0.0175	0.1844	0.0022	2656.5	34.0	2665.9	74.1	2649.3	20.7	458	204	0.45
ZW5-60	0.000	12.763	0.520	0.5152	0.0197	0.1797	0.0025	2662.3	38.3	2678.6	83.7	2650.0	23.5	113	51	0.46
ZW5-61	0.000	13.202	0.500	0.5205	0.0186	0.1840	0.0023	2692.7	35.8	2700.7	78.7	2686.7	21.1	207	128	0.62
ZW5-62	0.000	12.555	0.609	0.5078	0.0229	0.1793	0.0032	2646.8	45.6	2647.1	97.8	2646.7	29.9	47	16	0.34
ZW5-63	0.001	12.941	0.484	0.5241	0.0185	0.1791	0.0022	2668.6	35.4	2714.0	78.2	2634.4	21.2	236	132	0.56
ZW5-64	0.000	12.813	0.511	0.5158	0.0193	0.1802	0.0025	2666.0	37.6	2681.3	82.2	2654.4	22.8	130	75	0.58
ZW5-65	0.000	16.022	0.616	0.5649	0.0205	0.2057	0.0026	2878.1	36.7	2886.9	84.4	2871.9	20.6	172	83	0.48
ZW5-66	0.004	13.039	0.468	0.5202	0.0177	0.1818	0.0021	2661.8	34.0	2691.8	74.7	2639.0	20.3	457	256	0.56
ZW5-67	0.000	12.918	0.518	0.5213	0.0197	0.1797	0.0024	2673.0	37.8	2704.6	83.6	2649.2	22.1	162	92	0.57
ZW5-68	0.000	13.401	0.555	0.5228	0.0204	0.1859	0.0026	2707.9	39.1	2711.0	86.4	2705.6	22.9	124	66	0.53
ZW5-69	0.000	13.780	0.621	0.5466	0.0231	0.1828	0.0028	2732.4	42.7	2810.2	96.4	2675.4	26.0	73	29	0.40
ZW5-70	0.000	16.710	0.643	0.5816	0.0212	0.2084	0.0025	2917.6	36.8	2954.9	86.5	2892.0	19.7	244	86	0.35
ZW5-71	0.000	14.082	0.549	0.5424	0.0200	0.1883	0.0024	2754.5	37.0	2793.3	83.7	2726.2	20.7	210	103	0.49
ZW5-72	0.000	13.207	0.561	0.5233	0.0209	0.1830	0.0026	2692.4	40.2	2712.4	88.6	2677.3	24.1	103	49	0.48
ZW5-73	0.000	16.691	0.697	0.5878	0.0232	0.2060	0.0028	2916.6	40.0	2980.1	94.2	2873.2	22.1	113	35	0.31
ZW5-74	0.000	13.011	0.505	0.5234	0.0192	0.1803	0.0023	2679.7	36.6	2713.4	81.3	2654.5	20.8	227	197	0.87
ZW5-75	0.001	16.137	0.600	0.5674	0.0200	0.2063	0.0024	2881.5	35.6	2895.4	82.4	2871.8	18.9	427	152	0.36
ZW5-76	0.001	11.313	0.414	0.4684	0.0163	0.1752	0.0020	2546.3	34.2	2475.6	71.5	2603.1	19.2	664	370	0.56
ZW5-77	0.000	14.577	0.654	0.5586	0.0236	0.1892	0.0029	2788.0	42.7	2860.9	97.6	2735.6	24.9	74	34	0.46
ZW5-78	0.000	13.415	0.628	0.5275	0.0232	0.1844	0.0030	2708.6	44.3	2730.8	97.8	2692.2	27.4	61	22	0.36
ZW5-79	0.049	14.724	0.555	0.4377	0.0157	0.2440	0.0029	2565.7	39.5	2244.0	68.2	2830.7	37.2	331	307	0.93
ZW68-01	0.000	12.956	0.490	0.5234	0.0174	0.1795	0.0032	2676.4	35.7	2713.6	73.8	2648.5	29.7	161	117	0.73
ZW68-02	0.000	16.264	0.662	0.5702	0.0207	0.2069	0.0038	2892.4	38.9	2908.6	84.8	2881.2	30.0	94	20	0.22
ZW68-03	0.000	13.449	0.524	0.5367	0.0185	0.1818	0.0033	2711.7	36.8	2769.4	77.5	2669.0	30.2	127	70	0.55
ZW68-04	0.016	18.052	1.005	0.5987	0.0304	0.2187	0.0050	2911.0	58.3	2985.3	121.9	2860.0	55.1	26	9	0.33
ZW68-05	0.017	10.396	0.353	0.3915	0.0116	0.1926	0.0032	2379.1	31.8	2098.9	53.1	2628.7	29.8	897	347	0.39
ZW68-06	0.000	16.313	0.576	0.5764	0.0179	0.2052	0.0035	2895.3	33.8	2934.2	73.1	2868.4	27.5	335	151	0.45
ZW68-07	0.000	13.034	0.466	0.5148	0.0161	0.1836	0.0032	2682.2	33.7	2676.9	68.7	2686.1	28.4	288	186	0.65
ZW68-08	0.007	11.904	0.411	0.4739	0.0143	0.1822	0.0031	2559.1	32.5	2486.5	62.3	2617.2	29.1	537	196	0.37
ZW68-09	0.054	7.110	0.240	0.2751	0.0081	0.1874	0.0031	1819.4	32.2	1490.9	39.1	2219.5	42.3	1307	1033	0.79
ZW68-10	0.003	8.235	0.341	0.4172	0.0151	0.1432	0.0029	2234.8	38.6	2241.3	68.6	2228.8	39.2	95	52	0.55
ZW68-11	0.006	16.004	0.583	0.5505	0.0177	0.2109	0.0036	2845.0	35.1	2812.6	73.1	2868.0	29.5	224	195	0.87
ZW68-12	0.010	9.854	0.340	0.3982	0.0120	0.1795	0.0030	2363.6	32.2	2141.7	54.9	2561.1	30.2	558	346	0.62
ZW68-13	0.000	15.611	0.599	0.5475	0.0186	0.2068	0.0037	2852.3	36.6	2814.5	77.5	2879.2	29.1	139	65	0.47

ZW68-14	0.004	12.210	0.309	0.4906	0.0099	0.1805	0.0028	2599.9	24.0	2565.3	42.5	2626.9	26.5	390	235	0.60
ZW68-15	0.023	10.766	0.260	0.4058	0.0076	0.1924	0.0029	2376.0	24.0	2152.1	34.5	2574.1	30.5	646	566	0.88
ZW68-16	0.000	14.300	0.362	0.5508	0.0111	0.1883	0.0029	2769.2	24.0	2828.3	46.2	2726.4	25.2	376	332	0.88
ZW68-17	0.000	16.065	0.554	0.5558	0.0165	0.2096	0.0037	2880.7	33.0	2849.4	68.5	2902.6	28.4	82	35	0.43
ZW68-18	0.012	11.366	0.272	0.4175	0.0078	0.1974	0.0030	2488.3	22.9	2225.6	35.0	2710.4	26.8	714	271	0.38
ZW68-19	0.007	12.097	0.311	0.4411	0.0090	0.1989	0.0031	2575.4	24.6	2341.7	40.3	2764.8	27.2	345	305	0.88
ZW68-20	0.000	16.276	0.476	0.5698	0.0139	0.2072	0.0033	2891.2	28.0	2906.2	57.0	2880.8	26.4	156	62	0.39
ZW68-21	0.000	14.219	0.464	0.5434	0.0151	0.1898	0.0033	2764.4	30.9	2797.5	62.9	2740.3	28.3	101	50	0.50
ZW68-22	0.001	12.799	0.342	0.4930	0.0106	0.1883	0.0030	2661.3	25.2	2582.1	45.9	2722.1	26.2	262	89	0.34
ZW68-23	0.003	13.633	0.471	0.5239	0.0155	0.1887	0.0034	2710.3	33.2	2710.0	65.5	2710.6	31.4	83	47	0.57
ZW68-24	0.000	13.117	0.378	0.5256	0.0125	0.1810	0.0029	2688.1	27.2	2722.9	52.8	2662.0	27.0	172	66	0.39
ZW68-25	0.003	11.947	0.304	0.4692	0.0095	0.1847	0.0029	2586.1	24.0	2474.8	41.6	2674.5	26.2	372	249	0.67
ZW68-26	0.000	16.777	0.736	0.5840	0.0228	0.2084	0.0042	2922.2	42.0	2964.9	92.9	2892.9	32.4	40	21	0.53
ZW68-1-1	0.000	7.887	0.382	0.4110	0.0167	0.1392	0.0036	2218.2	43.6	2219.4	76.5	2217.1	45.2	148	104	0.70
ZW68-1-2	0.000	7.881	0.377	0.4126	0.0167	0.1385	0.0035	2217.5	43.1	2226.8	76.2	2208.9	44.4	176	150	0.85
ZW68-1-3	0.000	8.049	0.406	0.4229	0.0178	0.1380	0.0038	2236.3	47.5	2273.8	80.7	2202.2	54.8	87	51	0.59
ZW68-1-4	0.002	14.953	0.719	0.5309	0.0218	0.2043	0.0051	2803.8	46.2	2741.6	91.7	2848.9	42.4	124	85	0.69
ZW68-1-5	0.007	12.584	0.575	0.4446	0.0174	0.2053	0.0048	2615.0	43.0	2358.0	77.4	2820.5	39.0	807	332	0.41
ZW68-1-6	0.000	13.806	0.680	0.5372	0.0225	0.1864	0.0048	2736.5	46.6	2771.8	94.4	2710.5	42.6	89	45	0.51
ZW68-1-7	0.000	15.395	0.746	0.5475	0.0227	0.2039	0.0051	2840.0	46.2	2814.8	94.4	2858.0	41.0	106	43	0.41
ZW68-1-8	0.012	15.047	0.775	0.5501	0.0241	0.1984	0.0054	2752.9	54.1	2797.8	99.9	2720.1	60.6	53	29	0.54
ZW68-1-9	0.003	11.857	0.557	0.4537	0.0182	0.1895	0.0046	2577.3	44.3	2405.7	80.5	2715.1	41.5	221	72	0.33
ZW68-2-1	0.037	17.410	0.813	0.5507	0.0221	0.2293	0.0055	2771.7	47.1	2742.1	89.7	2793.2	48.3	224	108	0.48
ZW68-2-2	0.000	13.066	0.650	0.5010	0.0212	0.1891	0.0050	2684.4	46.9	2618.2	91.0	2734.7	43.1	78	45	0.58
ZW68-2-3	0.000	15.584	0.740	0.5591	0.0227	0.2021	0.0050	2850.9	45.4	2862.7	93.9	2842.6	40.4	152	63	0.42
ZW68-2-4	0.001	12.467	0.592	0.4828	0.0196	0.1873	0.0046	2637.2	44.9	2538.0	85.1	2714.1	41.7	161	62	0.38
ZW68-2-5	0.000	12.797	0.599	0.5181	0.0208	0.1792	0.0043	2663.8	44.2	2690.5	88.1	2643.6	40.5	222	151	0.68
ZW68-2-6	0.000	15.969	1.002	0.5759	0.0311	0.2011	0.0064	2874.9	59.9	2932.0	127.3	2835.2	51.9	26	11	0.43
ZW68-2-7	0.003	13.568	0.738	0.5095	0.0239	0.1932	0.0053	2705.8	53.5	2648.5	102.2	2748.8	52.1	65	35	0.54
ZW68-2-8	0.004	12.463	0.601	0.4982	0.0209	0.1814	0.0043	2614.8	45.4	2596.5	89.7	2629.0	39.9	693	348	0.50
ZW68-2-9	0.000	16.746	0.858	0.5909	0.0264	0.2055	0.0052	2920.4	49.1	2993.1	106.8	2870.7	41.0	114	34	0.30
ZW68-2-10	0.000	16.622	0.838	0.5804	0.0255	0.2077	0.0051	2913.3	48.3	2950.2	104.0	2887.9	40.2	148	59	0.40
ZW68-2-11	0.000	16.403	0.888	0.5706	0.0269	0.2085	0.0056	2900.6	51.8	2910.1	110.2	2894.0	43.4	63	17	0.28
ZW68-2-12	0.000	13.925	0.732	0.5364	0.0244	0.1883	0.0049	2744.6	49.8	2768.3	102.5	2727.3	43.1	88	48	0.55
ZW68-2-13	0.000	15.544	0.824	0.5502	0.0253	0.2049	0.0054	2849.2	50.6	2826.2	105.4	2865.5	42.6	77	25	0.32
ZW68-2-14	0.000	15.765	0.863	0.5524	0.0263	0.2070	0.0056	2862.7	52.3	2835.0	109.1	2882.2	44.0	58	12	0.20
ZW68-2-15	0.000	16.228	0.858	0.5764	0.0265	0.2042	0.0053	2890.3	50.5	2934.2	108.4	2859.9	42.3	78	25	0.32
ZW68-2-16	0.000	13.326	0.679	0.5155	0.0228	0.1875	0.0047	2703.0	48.1	2680.1	97.1	2720.2	41.6	130	74	0.57
ZW68-2-17	0.000	14.043	0.705	0.5399	0.0236	0.1886	0.0047	2750.5	47.7	2782.2	98.8	2727.3	41.1	162	78	0.48
ZW68-2-18	0.000	13.872	0.725	0.5372	0.0244	0.1873	0.0049	2741.0	49.5	2771.8	102.3	2718.4	42.7	91	43	0.47
ZW68-2-19	0.005	12.943	0.632	0.5028	0.0214	0.1867	0.0045	2648.1	46.2	2615.1	91.4	2673.5	40.8	349	300	0.86
ZW68-2-20	0.000	13.350	0.725	0.5340	0.0283	0.1813	0.0022	2704.7	51.3	2758.1	118.9	2665.1	19.8	240	127	0.53
ZW68-2-21	0.006	11.787	0.639	0.4367	0.0231	0.1958	0.0024	2554.2	51.2	2323.4	103.1	2742.9	24.7	266	76	0.29
ZW68-2-22	0.000	12.903	0.698	0.5201	0.0275	0.1799	0.0021	2672.2	51.1	2699.3	116.5	2651.7	20.5	263	158	0.60
ZW68-2-23	0.000	14.369	0.822	0.5550	0.0307	0.1878	0.0028	2774.4	54.3	2845.9	127.2	2722.8	24.3	102	56	0.55
ZW68-2-24	0.017	10.038	0.605	0.3624	0.0207	0.2009	0.0039	2351.5	62.0	1964.9	97.2	2706.1	60.9	71	14	0.19
ZW68-2-25	0.000	13.424	0.745	0.5222	0.0282	0.1865	0.0025	2710.0	52.5	2708.4	119.3	2711.2	21.7	155	56	0.36
ZW68-2-26	0.000	13.097	0.703	0.5270	0.0277	0.1802	0.0020	2686.7	50.7	2728.9	116.9	2655.0	18.4	319	280	0.88

ZW68-2-27	0.000	16.689	0.906	0.5832	0.0309	0.2076	0.0024	2917.2	52.0	2961.8	126.0	2886.5	18.4	227	116	0.51
ZW68-2-28	0.000	15.961	0.893	0.5619	0.0306	0.2060	0.0027	2874.5	53.5	2874.3	126.2	2874.6	21.3	130	37	0.28
ZW68-2-29	0.000	14.117	0.764	0.5433	0.0288	0.1884	0.0022	2757.6	51.3	2797.4	120.1	2728.6	18.8	249	131	0.53
ZW68-2-30	0.000	13.646	0.760	0.5264	0.0285	0.1880	0.0025	2725.4	52.7	2726.4	120.4	2724.7	21.7	143	77	0.54
ZW68-2-31	0.026	14.540	0.830	0.5133	0.0284	0.2054	0.0029	2649.9	58.7	2614.6	119.2	2676.9	48.5	102	55	0.54
ZW68-2-32	0.000	12.979	0.749	0.5033	0.0280	0.1870	0.0028	2678.1	54.4	2628.1	120.2	2716.0	25.0	92	49	0.53
ZW68-2-33	0.000	15.101	0.963	0.5880	0.0357	0.1863	0.0036	2821.6	60.7	2981.4	145.0	2709.4	32.0	41	25	0.61
ZW68-2-34	0.000	8.784	0.480	0.4462	0.0235	0.1428	0.0021	2315.9	49.8	2378.4	104.6	2261.3	25.7	297	194	0.66
ZW68-2-35	0.000	16.623	0.893	0.5816	0.0303	0.2073	0.0027	2913.3	51.5	2955.5	123.6	2884.4	21.3	382	234	0.61
ZW68-2-36	0.000	12.912	0.686	0.5201	0.0268	0.1801	0.0023	2671.3	50.1	2698.9	113.8	2650.5	21.7	584	207	0.35
ZW68-2-37	0.000	16.224	0.922	0.5693	0.0312	0.2067	0.0032	2890.1	54.4	2904.9	128.0	2879.8	25.0	140	37	0.27
ZW68-2-38	0.000	17.765	0.983	0.6336	0.0339	0.2033	0.0029	2977.1	53.2	3163.9	133.8	2853.3	23.0	200	44	0.22
ZW68-2-39	0.000	16.118	0.925	0.5693	0.0314	0.2053	0.0032	2883.8	54.9	2904.9	129.1	2869.1	25.5	126	48	0.38
ZW68-2-40	0.000	16.091	0.897	0.5587	0.0301	0.2089	0.0030	2882.2	53.3	2861.4	124.3	2896.8	23.6	182	59	0.33
ZW68-2-41	0.000	16.235	0.977	0.5777	0.0333	0.2038	0.0035	2890.7	57.6	2939.6	136.0	2856.9	28.3	81	43	0.54
ZW68-2-42	0.000	16.504	1.019	0.5865	0.0346	0.2041	0.0037	2906.5	59.1	2975.2	140.5	2859.2	29.7	67	21	0.31
ZW68-2-43	0.000	14.192	0.800	0.5455	0.0296	0.1887	0.0029	2762.6	53.5	2806.2	123.5	2730.9	25.5	159	96	0.60
ZW68-2-44	0.005	14.941	0.826	0.5318	0.0284	0.2038	0.0029	2787.5	53.0	2738.6	119.2	2823.0	26.3	208	106	0.51
ZW68-2-45	0.000	14.473	0.816	0.5540	0.0301	0.1895	0.0029	2781.3	53.5	2841.9	124.8	2737.5	24.8	156	79	0.50
ZW68-2-46	0.000	13.312	0.776	0.5151	0.0288	0.1874	0.0031	2702.0	55.1	2678.5	122.5	2719.7	27.4	109	69	0.63
ZW68-2-47	0.000	14.843	0.826	0.5207	0.0280	0.2067	0.0030	2805.2	53.0	2702.3	118.7	2880.0	23.5	185	63	0.34
ZW68-2-48	0.000	13.639	0.658	0.5327	0.0235	0.1857	0.0036	2725.0	45.6	2752.6	98.9	2704.6	32.1	75	30	0.40
ZW68-2-49	0.000	13.115	0.513	0.5244	0.0189	0.1814	0.0028	2687.9	36.9	2717.9	79.8	2665.5	25.5	169	86	0.51
ZW68-2-50	0.001	16.289	0.601	0.5714	0.0195	0.2068	0.0029	2889.7	35.4	2911.4	80.1	2874.6	23.0	223	77	0.34
ZW68-2-51	0.000	13.937	0.562	0.5484	0.0204	0.1843	0.0029	2745.4	38.2	2818.3	84.8	2692.2	25.9	145	114	0.79
ZW68-2-52	0.000	8.712	0.313	0.4449	0.0146	0.1420	0.0021	2308.3	32.7	2372.7	65.1	2251.8	25.3	293	173	0.59
ZW68-2-53	0.000	16.552	0.742	0.5961	0.0248	0.2014	0.0034	2909.2	42.9	3013.9	100.0	2837.6	27.5	92	33	0.36
ZW68-2-54	0.000	15.581	0.747	0.5579	0.0247	0.2025	0.0037	2851.5	45.8	2858.1	102.3	2846.8	29.9	74	22	0.30
ZW68-2-55	0.000	13.675	0.488	0.5275	0.0174	0.1880	0.0025	2727.5	33.8	2731.1	73.5	2724.9	22.3	279	181	0.65
ZW68-2-56	0.000	15.952	0.872	0.5708	0.0289	0.2027	0.0042	2873.9	52.2	2911.3	118.4	2847.8	33.9	49	24	0.48
ZW68-2-57	0.013	8.755	0.283	0.3534	0.0106	0.1797	0.0022	2237.8	30.7	1928.1	49.8	2534.5	27.2	750	423	0.56
ZW68-2-58	0.000	16.366	0.570	0.5770	0.0187	0.2057	0.0026	2897.6	33.4	2936.2	76.4	2871.0	21.2	319	140	0.44
ZW68-2-59	0.000	12.475	0.445	0.5110	0.0168	0.1771	0.0024	2640.9	33.5	2661.0	71.8	2625.5	22.6	283	226	0.80
ZW68-2-60	0.002	15.994	0.614	0.5681	0.0203	0.2042	0.0029	2868.2	37.1	2896.3	83.2	2848.5	25.0	176	68	0.39
ZW68-2-61	0.001	16.014	0.699	0.5686	0.0230	0.2043	0.0033	2874.8	42.0	2900.9	94.6	2856.6	27.8	101	31	0.31
ZW68-2-62	0.000	16.373	0.630	0.5811	0.0209	0.2044	0.0028	2898.8	36.8	2953.2	85.3	2861.3	22.3	166	53	0.32
ZW68-2-63	0.002	14.746	0.466	0.5224	0.0154	0.2047	0.0023	2790.8	30.2	2705.6	65.2	2853.0	19.4	412	171	0.42
ZW68-2-64	0.000	12.879	0.468	0.5309	0.0179	0.1759	0.0024	2669.7	34.4	2744.9	75.5	2613.2	23.1	213	125	0.59
ZW68-2-65	0.001	13.850	0.538	0.5212	0.0188	0.1927	0.0028	2731.9	37.0	2701.3	79.7	2754.6	24.9	165	183	1.11
ZW68-2-66	0.000	14.342	0.635	0.5510	0.0227	0.1888	0.0031	2772.6	42.0	2829.3	94.3	2731.6	26.7	107	52	0.49
ZW68-2-67	0.000	12.773	0.547	0.4977	0.0197	0.1861	0.0030	2662.0	41.0	2603.3	85.0	2706.8	30.0	120	67	0.55
ZW68-2-68	0.000	13.815	0.502	0.5338	0.0181	0.1877	0.0025	2737.1	34.4	2757.5	76.0	2722.0	21.8	210	78	0.37
ZW68-2-69	0.002	8.197	0.302	0.4115	0.0138	0.1445	0.0022	2238.8	34.9	2217.6	63.2	2258.2	32.9	218	122	0.56
ZW68-2-70	0.000	16.183	0.838	0.5781	0.0280	0.2030	0.0037	2887.7	49.5	2941.1	114.4	2850.7	29.8	67	24	0.36
ZW68-2-71	0.000	13.210	0.664	0.5019	0.0234	0.1909	0.0036	2694.8	47.4	2621.9	100.3	2749.9	31.0	75	38	0.51
ZW68-2-72	0.003	11.342	0.347	0.4484	0.0128	0.1835	0.0021	2535.8	28.9	2382.3	56.7	2661.1	20.5	520	365	0.70
ZW68-2-73	0.000	12.624	0.533	0.5121	0.0201	0.1788	0.0028	2652.0	39.7	2665.4	85.5	2641.9	26.1	125	77	0.62
ZW68-2-74	0.000	12.506	0.634	0.4955	0.0232	0.1831	0.0035	2643.2	47.7	2594.5	100.2	2680.7	31.7	74	27	0.36

ZW68-2-75	0.013	13.622	0.530	0.5157	0.0187	0.1916	0.0027	2651.9	39.9	2652.2	79.0	2651.7	36.7	162	78	0.48
ZW68-2-76	0.000	13.992	0.789	0.5388	0.0289	0.1883	0.0033	2747.1	53.5	2777.6	120.9	2724.8	29.5	363	240	0.66
ZW68-2-77	0.000	16.826	1.098	0.5781	0.0358	0.2111	0.0043	2925.0	62.5	2940.9	146.3	2914.0	33.1	113	67	0.60
ZW68-2-78	0.000	14.666	0.918	0.5617	0.0333	0.1894	0.0038	2793.8	59.5	2873.8	137.6	2736.6	32.7	146	75	0.52
ZW68-2-79	0.011	15.110	0.828	0.5137	0.0268	0.2133	0.0036	2765.0	52.6	2647.5	113.2	2852.0	30.6	563	282	0.50
ZW68-2-80	0.000	13.205	0.825	0.5354	0.0317	0.1789	0.0036	2693.9	59.2	2764.0	133.0	2641.8	34.6	148	93	0.63
ZW68-2-81	0.015	13.780	0.771	0.4618	0.0246	0.2164	0.0038	2662.7	53.8	2418.0	107.3	2854.2	34.2	406	425	1.05
ZW68-2-82	0.002	16.168	0.931	0.5670	0.0311	0.2068	0.0037	2874.8	55.3	2890.0	127.6	2864.1	30.2	279	113	0.40
ZW68-2-83	0.000	17.299	1.036	0.6042	0.0344	0.2077	0.0038	2951.6	57.5	3046.7	138.4	2887.3	29.8	194	116	0.60
ZW68-2-84	0.004	16.339	1.300	0.5865	0.0442	0.2021	0.0051	2875.6	78.5	2965.4	179.4	2813.3	53.4	49	18	0.38
ZW68-2-85	0.001	12.914	0.746	0.5219	0.0286	0.1795	0.0033	2668.1	54.6	2705.2	121.2	2640.0	30.8	276	147	0.53
ZW68-2-86	0.001	13.375	0.861	0.5173	0.0315	0.1875	0.0039	2701.7	61.7	2685.7	134.0	2713.6	38.9	123	88	0.71
ZW68-2-87	0.005	13.169	0.761	0.5005	0.0275	0.1908	0.0035	2667.5	55.0	2606.2	117.7	2714.3	32.8	275	181	0.66
ZW68-2-88	0.000	16.632	1.177	0.5830	0.0392	0.2069	0.0046	2913.9	67.8	2961.0	159.7	2881.5	35.9	76	21	0.28
ZW68-2-89	0.002	14.342	0.922	0.5074	0.0310	0.2050	0.0042	2761.0	61.6	2640.7	132.2	2850.1	36.6	123	33	0.27
ZW68-2-90	0.000	13.292	0.957	0.5430	0.0371	0.1775	0.0040	2700.6	68.0	2796.0	154.9	2630.0	37.7	116	47	0.41
ZW68-2-91	0.000	13.084	0.866	0.5233	0.0329	0.1813	0.0037	2685.7	62.4	2713.3	139.3	2665.0	33.9	201	75	0.38
ZW68-2-92	0.000	17.872	1.260	0.6256	0.0421	0.2072	0.0044	2982.9	67.8	3132.3	166.9	2883.6	34.2	126	43	0.34
ZW68-2-93	0.004	13.270	0.807	0.5265	0.0305	0.1828	0.0034	2676.1	57.6	2717.8	128.6	2644.7	32.0	518	271	0.52
ZW68-2-94	0.002	14.499	1.212	0.5632	0.0447	0.1867	0.0049	2773.8	80.4	2875.8	184.1	2700.4	49.4	59	54	0.91
ZW68-2-95	0.001	13.316	0.820	0.5275	0.0310	0.1831	0.0034	2696.4	58.2	2728.4	130.5	2672.5	31.5	426	180	0.42
ZW68-2-96	0.002	14.777	0.928	0.5153	0.0309	0.2080	0.0039	2793.0	59.9	2675.9	131.2	2878.7	31.9	324	313	0.97
ZW68-2-97	0.000	14.028	1.139	0.5444	0.0419	0.1869	0.0048	2751.6	76.9	2801.7	175.1	2715.0	42.1	66	44	0.67
ZW68-2-98	0.000	17.748	1.143	0.6235	0.0384	0.2064	0.0039	2976.2	61.9	3123.9	152.3	2877.8	31.1	244	64	0.26
ZW68-2-99	0.004	14.502	1.296	0.5711	0.0485	0.1842	0.0051	2762.0	89.0	2903.4	198.8	2660.2	66.7	47	28	0.60
ZW68-2-100	0.000	16.442	1.172	0.5860	0.0399	0.2035	0.0044	2902.9	68.2	2973.3	162.0	2854.4	34.8	119	35	0.30
ZW68-2-101	0.000	12.132	0.794	0.4801	0.0299	0.1833	0.0037	2614.6	61.4	2527.9	130.1	2682.5	33.4	220	140	0.63
ZW68-2-102	0.008	11.391	0.747	0.4137	0.0258	0.1997	0.0041	2513.2	62.3	2216.4	117.0	2762.4	40.6	218	111	0.51
ZW68-2-103	0.004	13.530	0.873	0.4823	0.0296	0.2035	0.0040	2699.1	61.3	2529.6	128.6	2828.6	34.1	247	92	0.37
ZW74-01	0.001	15.536	0.783	0.5538	0.0273	0.2035	0.0021	2844.4	48.1	2839.2	113.2	2848.2	17.6	152	45	0.30
ZW74-02	0.000	16.153	0.811	0.5729	0.0282	0.2045	0.0021	2885.1	48.0	2919.5	115.4	2861.3	16.9	160	52	0.33
ZW74-03	0.000	13.194	0.666	0.5112	0.0252	0.1872	0.0020	2692.1	47.7	2661.1	107.5	2715.5	18.3	153	95	0.62
ZW74-04	0.000	13.557	0.681	0.5207	0.0256	0.1888	0.0020	2719.3	47.5	2702.3	108.4	2732.0	17.5	164	139	0.85
ZW74-05	0.000	13.816	0.710	0.5239	0.0262	0.1913	0.0022	2737.2	48.6	2715.7	110.9	2753.1	18.8	120	48	0.40
ZW74-06	0.003	13.906	0.799	0.5324	0.0295	0.1895	0.0030	2727.1	55.0	2744.7	123.7	2714.2	29.8	47	26	0.55
ZW74-07	0.000	16.037	0.774	0.5570	0.0264	0.2088	0.0018	2879.0	46.1	2854.3	109.5	2896.4	14.3	404	250	0.62
ZW74-08	0.000	13.876	0.709	0.5379	0.0268	0.1871	0.0021	2741.3	48.4	2774.7	112.4	2716.8	18.5	127	90	0.71
ZW74-09	0.039	9.651	0.466	0.3112	0.0147	0.2250	0.0021	2214.0	45.5	1686.9	70.4	2745.3	28.9	458	1148	2.51
ZW74-10	0.010	15.846	0.835	0.5418	0.0278	0.2121	0.0026	2819.1	51.2	2769.4	115.6	2854.9	26.6	89	38	0.43
ZW74-11	0.000	13.464	0.702	0.5224	0.0265	0.1869	0.0023	2712.8	49.3	2709.6	112.2	2715.2	19.9	101	57	0.56
ZW74-12	0.013	10.898	0.534	0.3888	0.0187	0.2033	0.0020	2447.5	46.0	2093.5	85.8	2756.3	22.1	282	93	0.33
ZW74-13	0.019	7.918	0.385	0.2763	0.0131	0.2079	0.0021	2127.9	44.4	1545.9	65.4	2749.5	24.8	386	222	0.57
ZW74-14	0.000	13.484	0.630	0.5211	0.0213	0.1877	0.0042	2714.1	44.1	2703.9	90.4	2721.8	37.0	132	65	0.49
ZW74-15	0.000	15.830	0.733	0.5606	0.0228	0.2048	0.0045	2866.6	44.2	2869.2	94.1	2864.8	36.0	141	35	0.25
ZW74-16	0.009	12.195	0.543	0.4457	0.0173	0.1984	0.0043	2571.7	42.2	2358.0	76.7	2744.7	37.9	262	183	0.70
ZW74-17	0.006	14.350	0.642	0.5071	0.0198	0.2052	0.0045	2739.9	42.8	2630.3	84.5	2821.7	36.9	230	239	1.04
ZW74-18	0.315	64.550	2.917	0.9379	0.0374	0.4991	0.0106	3064.6	92.4	3199.1	106.3	2977.6	141.8	172	143	0.83

ZW74-19	0.040	7.462	0.324	0.2382	0.0090	0.2272	0.0049	1983.0	40.4	1328.1	45.3	2757.5	44.8	545	1165	2.14
ZW74-20	0.000	13.128	0.639	0.5119	0.0219	0.1860	0.0043	2688.9	46.0	2664.6	93.5	2707.2	38.3	91	82	0.90
ZW74-21	0.000	13.827	0.689	0.5296	0.0233	0.1893	0.0044	2736.2	47.3	2739.2	98.0	2734.0	39.1	76	30	0.40
ZW74-22	0.034	12.320	0.526	0.4497	0.0167	0.1987	0.0042	2441.0	40.7	2325.1	72.5	2539.1	39.8	992	393	0.40
ZW74-23	0.000	13.517	0.616	0.5221	0.0208	0.1878	0.0041	2715.7	43.1	2707.7	88.2	2721.6	36.4	174	93	0.54
ZW74-24	0.000	15.771	0.754	0.5598	0.0236	0.2043	0.0046	2863.0	45.7	2866.0	97.5	2860.9	36.8	102	39	0.38
ZW74-25	0.000	13.969	0.616	0.5449	0.0210	0.1859	0.0040	2746.5	41.8	2803.5	87.5	2704.9	35.6	305	208	0.68
ZW74-26	0.000	13.336	0.667	0.5259	0.0232	0.1839	0.0043	2700.9	47.4	2723.1	98.0	2684.4	39.5	74	25	0.34
ZW74-27	0.003	16.098	0.523	0.5641	0.0133	0.2070	0.0046	2868.1	31.5	2877.1	54.9	2861.9	37.4	118	47	0.40
ZW74-28	0.222	27.348	0.752	0.4931	0.0087	0.4023	0.0085	2509.9	67.2	2093.8	37.0	2866.0	115.4	319	192	0.60
ZW74-29	0.004	11.810	0.328	0.4496	0.0079	0.1905	0.0041	2569.1	26.3	2386.0	35.0	2716.8	36.3	324	412	1.27
ZW74-30	0.013	11.083	0.354	0.4063	0.0091	0.1978	0.0045	2464.1	32.0	2174.4	41.7	2712.6	43.5	137	185	1.35
ZW74-31	0.000	15.947	0.517	0.5629	0.0132	0.2055	0.0046	2873.7	31.0	2878.8	54.6	2870.0	36.2	119	63	0.53
ZW74-32	0.000	13.451	0.432	0.5264	0.0121	0.1853	0.0042	2711.9	30.3	2726.1	51.1	2701.3	37.0	128	56	0.44
ZW74-33	0.020	9.892	0.278	0.3435	0.0061	0.2089	0.0045	2325.5	27.9	1870.7	29.0	2752.8	41.1	310	279	0.90
ZW74-34	0.001	13.700	0.420	0.5298	0.0113	0.1875	0.0041	2721.7	29.2	2737.7	47.5	2709.8	37.0	160	75	0.47
ZW74-35	0.003	15.697	0.451	0.5501	0.0104	0.2069	0.0045	2843.3	27.6	2818.9	43.3	2860.6	35.7	236	92	0.39
ZW74-36	0.004	13.397	0.396	0.5147	0.0103	0.1888	0.0041	2686.6	28.3	2668.0	43.6	2700.6	37.2	198	123	0.62
ZW74-37	0.001	13.902	0.557	0.5349	0.0170	0.1885	0.0046	2740.2	38.1	2761.1	71.4	2724.8	40.6	55	40	0.74
ZW74-38	0.060	5.311	0.187	0.1652	0.0040	0.2332	0.0059	1600.4	53.0	930.2	22.6	2645.9	102.4	114	249	2.19
ZW74-39	0.002	13.776	0.466	0.5268	0.0132	0.1897	0.0043	2723.1	32.4	2723.4	55.6	2722.9	38.6	101	78	0.78
ZW74-40	0.003	15.089	0.569	0.5334	0.0192	0.2052	0.0023	2807.0	36.1	2749.7	80.7	2848.4	19.7	164	97	0.59
ZW74-41	0.003	16.302	0.663	0.5760	0.0223	0.2053	0.0025	2879.3	39.3	2925.4	91.1	2847.2	22.5	96	32	0.33
ZW74-42	0.000	13.530	0.566	0.5249	0.0208	0.1870	0.0025	2717.4	39.5	2719.9	87.9	2715.5	22.2	85	41	0.48
ZW74-43	0.000	15.891	0.589	0.5633	0.0200	0.2046	0.0022	2870.3	35.4	2880.3	82.4	2863.3	17.4	189	97	0.51
ZW74-44	0.001	13.721	0.613	0.5256	0.0221	0.1893	0.0028	2727.1	42.4	2721.5	93.5	2731.2	25.3	62	37	0.59
ZW74-45	0.000	14.088	0.507	0.5408	0.0187	0.1889	0.0019	2753.9	34.2	2786.2	78.1	2730.2	17.1	259	225	0.87
ZW74-46	0.020	10.296	0.356	0.3668	0.0122	0.2036	0.0020	2359.0	32.9	1979.7	56.7	2705.3	22.9	513	236	0.46
ZW74-47	0.000	14.184	0.517	0.5467	0.0191	0.1882	0.0020	2761.9	34.6	2811.1	79.5	2726.0	17.3	228	170	0.75
ZW74-48	0.000	16.274	0.661	0.5773	0.0223	0.2044	0.0025	2893.0	38.8	2937.8	91.2	2862.0	20.1	97	30	0.31
ZW74-49	0.007	12.978	0.458	0.4866	0.0165	0.1934	0.0019	2639.2	33.6	2540.5	71.1	2715.7	19.2	349	201	0.57
ZW74-50	0.002	14.063	0.563	0.5436	0.0207	0.1876	0.0023	2744.6	38.3	2794.8	86.4	2707.9	22.3	107	102	0.95
ZW74-51	0.001	13.842	0.515	0.5269	0.0187	0.1905	0.0021	2733.7	35.3	2726.4	79.1	2739.1	18.7	185	184	0.99
ZW74-52	0.027	9.916	0.346	0.3283	0.0110	0.2190	0.0022	2294.6	33.7	1786.9	52.3	2783.6	26.6	440	448	1.02
ZW74-53	0.003	15.653	0.612	0.5488	0.0211	0.2069	0.0014	2838.4	37.4	2812.5	87.6	2856.9	13.1	272	127	0.47
ZW74-54	0.001	14.422	0.596	0.5504	0.0222	0.1900	0.0017	2773.7	39.3	2825.0	92.4	2736.7	15.3	147	93	0.63
ZW74-55	0.001	14.044	0.571	0.5428	0.0216	0.1877	0.0016	2748.2	38.6	2793.3	90.1	2715.2	14.8	173	110	0.63
ZW74-56	0.000	12.920	0.549	0.5155	0.0213	0.1818	0.0018	2672.8	40.1	2679.8	90.6	2667.6	16.8	120	95	0.79
ZW74-57	0.000	13.519	0.609	0.5131	0.0223	0.1911	0.0022	2715.7	42.7	2669.4	95.2	2750.4	20.0	83	120	1.45
ZW74-58	0.000	13.945	0.585	0.5388	0.0220	0.1877	0.0018	2746.0	39.8	2778.4	92.3	2722.3	15.5	131	68	0.52
ZW74-59	0.004	13.940	0.565	0.5334	0.0212	0.1896	0.0016	2721.7	38.8	2745.7	88.8	2703.9	17.0	177	132	0.75
ZW74-60	0.001	14.004	0.568	0.5419	0.0215	0.1874	0.0016	2747.1	38.5	2790.3	89.9	2715.5	14.2	177	84	0.47
ZW74-61	0.000	13.769	0.611	0.5309	0.0228	0.1881	0.0021	2734.0	42.0	2745.4	96.0	2725.5	18.2	90	36	0.40
ZW74-62	0.000	14.705	0.649	0.5682	0.0243	0.1877	0.0020	2794.0	42.0	2899.3	100.0	2718.9	18.0	91	64	0.70
ZW74-63	0.030	12.515	0.505	0.4199	0.0166	0.2162	0.0018	2490.2	40.9	2202.0	73.8	2734.4	32.6	190	63	0.33
ZW74-64	0.003	13.643	0.562	0.5170	0.0208	0.1914	0.0017	2711.3	39.2	2680.9	88.2	2734.1	16.6	154	65	0.42
ZW74-65	0.000	14.654	0.712	0.5585	0.0261	0.1903	0.0025	2793.1	46.2	2860.6	107.9	2744.6	21.7	55	24	0.43
ZW74-66	0.247	46.684	1.522	0.8187	0.0260	0.4136	0.0030	2904.4	76.9	3097.2	84.3	2773.4	122.9	153	93	0.61

ZW74-67	0.001	13.849	0.489	0.5338	0.0180	0.1881	0.0020	2736.5	33.5	2756.5	75.4	2721.9	18.3	113	67	0.59
ZW74-68	0.015	11.845	0.348	0.4300	0.0122	0.1998	0.0015	2513.3	28.5	2276.6	54.5	2710.4	19.1	405	225	0.55
ZW74-69	0.015	11.894	0.368	0.4420	0.0131	0.1951	0.0017	2515.0	30.5	2329.8	58.2	2668.0	23.3	252	177	0.70
ZW74-70	0.002	16.306	0.486	0.5749	0.0166	0.2057	0.0015	2887.2	28.6	2924.4	67.8	2861.4	12.7	332	152	0.46
ZW74-71	0.089	20.915	0.703	0.5677	0.0184	0.2672	0.0024	2706.9	46.6	2687.0	72.5	2721.7	62.2	137	113	0.82
ZW74-72	0.000	16.640	0.581	0.5798	0.0194	0.2081	0.0021	2913.0	33.5	2947.3	79.1	2889.4	16.7	117	56	0.48
ZW74-73	0.000	16.713	0.878	0.5770	0.0286	0.2101	0.0037	2918.5	50.3	2936.6	116.8	2906.1	28.4	29	8	0.27
ZW74-74	0.000	16.584	0.564	0.5892	0.0192	0.2041	0.0020	2911.1	32.6	2986.2	78.0	2859.6	15.6	131	45	0.34
ZW74-75	0.000	15.378	0.788	0.5492	0.0264	0.2031	0.0036	2839.0	48.8	2822.0	110.0	2851.0	28.6	31	15	0.49
ZW74-76	0.000	16.235	0.580	0.5712	0.0195	0.2062	0.0022	2890.7	34.1	2912.5	80.0	2875.6	17.0	105	41	0.39
ZW74-77	0.016	10.955	0.313	0.4229	0.0117	0.1879	0.0014	2429.6	27.5	2242.3	52.5	2590.4	18.5	575	883	1.54
ZW74-78	0.000	14.527	0.468	0.5560	0.0172	0.1895	0.0017	2784.7	30.6	2849.9	71.3	2737.7	14.9	183	97	0.53
zw79-g1	0.000	13.836	0.360	0.5310	0.0125	0.1890	0.0021	2738.5	24.7	2745.6	52.7	2733.3	18.3	260	87	0.34
zw79-g2	0.003	10.030	0.253	0.4117	0.0095	0.1767	0.0018	2421.8	23.4	2217.3	43.5	2598.5	17.2	888	260	0.29
zw79-g3	0.000	8.179	0.205	0.3631	0.0084	0.1634	0.0016	2249.3	22.7	1996.3	39.7	2488.2	16.6	1526	854	0.56
zw79-g4	0.006	2.116	0.053	0.1374	0.0032	0.1117	0.0011	1119.4	17.5	825.5	17.9	1745.5	20.9	3071	254	0.08
zw79-g5	0.000	13.580	0.347	0.5185	0.0121	0.1900	0.0020	2718.9	24.2	2691.9	51.4	2738.9	17.3	427	175	0.41
zw79-g6	0.003	9.337	0.235	0.3814	0.0088	0.1775	0.0018	2355.4	23.1	2077.7	41.1	2605.3	16.9	1137	413	0.36
zw79-g7	0.053	4.780	0.121	0.1743	0.0040	0.1989	0.0020	1515.9	23.8	984.7	21.2	2364.3	33.5	1866	970	0.52
zw79-g8	0.000	13.376	0.367	0.5141	0.0124	0.1887	0.0024	2706.6	25.9	2674.1	52.9	2730.9	21.3	124	69	0.56
zw79-g9	0.009	9.598	0.255	0.3736	0.0089	0.1863	0.0023	2347.5	25.6	2030.0	41.3	2636.0	24.7	234	45	0.19
zw79-g10	0.002	13.200	0.335	0.5292	0.0123	0.1809	0.0018	2682.3	24.0	2733.3	51.8	2644.1	17.2	589	112	0.19
zw79-g11	0.001	12.490	0.319	0.4874	0.0114	0.1858	0.0019	2634.2	24.1	2556.5	49.2	2694.4	17.5	493	275	0.56
zw79-g12	0.002	11.325	0.292	0.4440	0.0104	0.1850	0.0020	2537.1	24.2	2363.8	46.3	2678.7	18.6	378	85	0.22
zw105-g1	0.056	10.930	0.278	0.3455	0.0080	0.2295	0.0024	2241.0	27.5	1820.2	37.1	2651.3	32.8	640	217	0.34
zw105-g2	0.010	10.104	0.257	0.4071	0.0095	0.1800	0.0019	2385.7	23.9	2182.1	43.1	2564.3	19.5	672	137	0.20
zw105-g3	0.108	10.975	0.259	0.2972	0.0061	0.2678	0.0031	2015.2	36.1	1516.2	28.6	2574.1	60.4	434	45	0.10
zw105-g4	0.016	9.138	0.212	0.3633	0.0074	0.1824	0.0021	2260.9	22.1	1969.5	34.5	2536.0	22.8	729	312	0.43
zw105-g5	0.009	7.904	0.184	0.3151	0.0064	0.1819	0.0021	2171.8	21.5	1752.0	31.2	2596.0	21.5	679	183	0.27
zw105-g6	0.001	12.799	0.300	0.5120	0.0105	0.1813	0.0021	2662.1	22.1	2663.9	44.6	2660.7	19.2	424	99	0.23
zw105-g7	0.000	12.442	0.293	0.5004	0.0103	0.1803	0.0021	2636.4	22.2	2614.8	44.0	2653.0	19.5	383	123	0.32
zw105-g8	0.000	9.471	0.223	0.4034	0.0082	0.1703	0.0020	2384.4	21.7	2184.6	37.8	2559.9	19.7	477	145	0.30
zw105-g9	0.000	12.391	0.288	0.5032	0.0102	0.1786	0.0020	2633.3	21.8	2627.0	43.9	2638.1	18.7	575	100	0.17
zw105-g10	0.001	12.116	0.287	0.4942	0.0102	0.1778	0.0021	2605.3	22.4	2585.8	43.8	2620.5	20.3	337	56	0.17
zw107-g1	0.034	8.972	0.212	0.3287	0.0067	0.1980	0.0023	2155.4	24.7	1777.9	31.9	2537.3	31.3	485	143	0.29
zw107-g2	0.010	13.427	0.321	0.4938	0.0102	0.1972	0.0024	2654.6	23.5	2564.7	43.8	2723.8	23.1	285	55	0.19
zw107-g3	0.172	12.488	0.285	0.3082	0.0062	0.2938	0.0032	1812.5	44.4	1464.8	27.6	2239.6	84.6	1219	371	0.30
zw107-g4	0.509	30.613	0.692	0.3572	0.0072	0.6216	0.0064	1621.3	146.8	1042.1	31.1	2484.2	306.8	2338	850	0.36
zw107-g5	0.519	34.183	0.773	0.3994	0.0080	0.6207	0.0064	1645.5	161.4	1133.6	34.4	2379.9	338.8	2223	778	0.35
zw107-g6	0.003	15.134	0.360	0.5352	0.0111	0.2051	0.0024	2808.1	22.9	2756.6	46.4	2845.2	20.3	279	114	0.41
zw107-g7	0.546	37.499	1.524	0.4087	0.0121	0.6655	0.0185	1686.6	399.7	1096.1	73.8	2526.7	822.0	2803	7642	2.73
zw107-g8	0.008	10.639	0.437	0.4186	0.0125	0.1843	0.0052	2446.8	38.4	2238.3	56.4	2624.9	48.2	525	110	0.21
zw107-g9	0.029	11.639	0.487	0.4048	0.0122	0.2086	0.0060	2424.4	42.6	2136.5	55.2	2675.8	58.0	204	116	0.57
zw107-g10	0.000	12.479	0.526	0.4987	0.0151	0.1815	0.0053	2641.2	39.6	2608.4	65.1	2666.4	48.4	156	67	0.43
zw107-g11	0.000	11.976	0.491	0.4825	0.0144	0.1800	0.0051	2601.4	38.4	2537.5	62.4	2651.5	46.8	607	208	0.34

zw107-g12	0.190	15.654	0.639	0.3522	0.0104	0.3224	0.0090	1979.9	96.0	1617.7	46.7	2382.7	182.4	1096	184	0.17
zw107-g13	0.000	12.713	0.527	0.5148	0.0154	0.1791	0.0051	2658.6	39.0	2677.1	65.7	2644.6	47.5	279	62	0.22
zw107-g14	0.164	10.732	0.438	0.2747	0.0081	0.2834	0.0079	1707.1	85.0	1332.4	38.3	2203.7	172.1	1260	429	0.34
zw107-g15	0.002	10.973	0.449	0.4463	0.0133	0.1783	0.0050	2511.2	38.1	2375.3	59.0	2623.0	46.9	805	294	0.36
zw107-g16	0.429	14.783	0.602	0.2030	0.0060	0.5280	0.0147	1223.4	239.3	707.1	34.5	2301.6	580.5	2444	1176	0.48
zw107-g17	0.013	11.757	0.515	0.4633	0.0145	0.1840	0.0057	2512.0	44.4	2427.6	63.4	2581.0	60.4	77	31	0.40
zw107-g18	0.120	11.856	0.492	0.3008	0.0090	0.2859	0.0082	2048.3	65.0	1513.4	42.4	2640.3	113.2	325	75	0.23
zw107-g19	0.265	23.201	0.950	0.4181	0.0125	0.4024	0.0113	2119.3	136.2	1728.4	55.2	2523.4	254.6	567	224	0.39
zw107-g20	0.002	10.893	0.448	0.4469	0.0133	0.1768	0.0050	2502.3	38.3	2377.4	59.3	2605.3	47.5	513	188	0.37
zw107-g21	0.006	12.314	0.521	0.4852	0.0145	0.1841	0.0055	2597.9	39.9	2538.4	62.9	2644.7	50.2	487	101	0.21
zw107-g22	0.018	11.704	0.497	0.4262	0.0128	0.1992	0.0060	2485.5	40.8	2253.7	57.3	2680.8	53.1	360	144	0.40
zw107-g23	0.223	9.921	0.417	0.2071	0.0062	0.3475	0.0103	1481.5	102.6	961.3	30.1	2333.6	221.1	1633	199	0.12
zw107-g24	0.000	11.957	0.513	0.4777	0.0145	0.1815	0.0055	2601.1	40.2	2517.4	63.1	2666.9	50.4	212	114	0.54
zw107-g25	0.058	9.930	0.418	0.3359	0.0100	0.2144	0.0064	2122.5	44.5	1771.9	46.6	2481.7	68.1	1059	444	0.42
zw107-g26	0.002	13.078	0.566	0.5022	0.0153	0.1889	0.0058	2674.2	41.1	2618.6	65.7	2716.6	51.4	154	162	1.05
zw107-g27	0.050	15.138	0.644	0.4871	0.0147	0.2254	0.0068	2565.1	46.1	2450.6	61.9	2656.9	65.2	297	204	0.68
zw107-g28	0.137	15.709	0.660	0.3906	0.0117	0.2917	0.0086	2216.8	68.1	1872.7	50.6	2551.9	117.3	951	342	0.36
zw107-g29	0.479	63.323	2.650	0.6248	0.0186	0.7350	0.0216	2827.1	185.8	1816.4	89.6	3655.7	303.7	2598	1370	0.53
zw107-g30	0.106	14.020	0.591	0.3854	0.0115	0.2639	0.0078	2238.5	58.0	1909.2	50.7	2555.0	95.8	698	201	0.29
zw107-g31	0.395	37.173	1.560	0.4811	0.0143	0.5604	0.0165	2271.5	193.6	1647.2	66.5	2893.3	347.5	981	657	0.67
zw107-g32	0.016	12.318	0.532	0.4715	0.0144	0.1895	0.0058	2540.5	42.3	2457.1	62.3	2607.7	56.2	171	101	0.59
zw107-g33	0.002	13.489	0.575	0.5401	0.0163	0.1811	0.0055	2705.7	40.4	2780.4	68.1	2650.4	50.3	269	200	0.74
zw107-g34	0.001	13.304	0.562	0.5339	0.0160	0.1807	0.0054	2698.5	39.9	2756.7	67.2	2655.2	49.5	488	256	0.52
zw107-g35	0.025	10.029	0.423	0.3845	0.0115	0.1892	0.0056	2300.5	40.2	2052.8	52.6	2528.5	54.7	712	224	0.31
zw107-g36	0.032	13.247	0.390	0.4574	0.0074	0.2100	0.0052	2531.9	30.7	2363.8	32.3	2669.4	47.7	278	71	0.26
zw107-g37	0.011	10.993	0.337	0.4284	0.0072	0.1861	0.0048	2460.5	30.4	2276.6	32.5	2616.3	47.1	156	45	0.29
zw107-g38	0.236	22.337	0.636	0.4238	0.0066	0.3823	0.0091	2194.0	62.1	1808.5	26.8	2576.5	113.2	1188	519	0.44
zw107-g39	0.001	12.870	0.387	0.5178	0.0086	0.1803	0.0045	2667.2	28.5	2688.5	36.4	2651.1	42.0	180	114	0.63
zw107-g40	0.001	12.426	0.373	0.4914	0.0081	0.1834	0.0046	2632.0	28.3	2575.0	35.0	2676.2	41.8	193	75	0.39
zw107-g41	0.014	12.362	0.368	0.4747	0.0078	0.1889	0.0047	2554.9	29.5	2474.9	33.8	2619.1	45.0	224	117	0.52
zw107-g42	0.017	12.392	0.363	0.4712	0.0075	0.1908	0.0047	2538.9	28.8	2452.7	32.8	2608.6	44.1	329	69	0.21
zw107-g43	0.006	8.380	0.242	0.3560	0.0056	0.1707	0.0041	2237.6	26.4	1952.6	26.4	2509.5	41.5	776	74	0.10
zw107-g44	0.040	10.219	0.293	0.3753	0.0058	0.1975	0.0048	2234.2	28.4	1983.2	26.7	2473.0	46.3	971	262	0.27
zw107-g45	0.014	12.821	0.385	0.4919	0.0081	0.1890	0.0047	2588.7	30.1	2548.8	35.0	2620.1	45.9	186	87	0.47
zw107-g46	0.494	26.583	0.754	0.3267	0.0050	0.5901	0.0141	1496.3	170.6	986.3	23.0	2318.5	374.3	2118	637	0.30
zw107-g47	0.001	12.517	0.373	0.5024	0.0082	0.1807	0.0045	2641.1	28.2	2622.8	35.3	2655.2	41.6	218	73	0.34
zw107-g48	0.519	48.450	1.375	0.5577	0.0086	0.6301	0.0150	1972.7	194.0	1533.4	36.2	2471.0	377.3	1402	530	0.38
zw107-g49	0.088	13.161	0.379	0.3780	0.0059	0.2525	0.0061	2260.7	34.6	1909.4	26.5	2595.8	58.3	689	333	0.48
zw107-g50	0.036	14.308	0.419	0.4950	0.0079	0.2096	0.0051	2577.7	30.9	2514.4	33.8	2627.9	48.1	309	94	0.31
zw110-01	0.000	9.228	0.254	0.3829	0.0094	0.1748	0.0022	2359.1	25.3	2089.2	43.8	2601.4	21.1	840	562	0.67
zw110-02	0.112	14.100	0.388	0.3986	0.0098	0.2565	0.0032	2189.4	41.9	1953.0	42.3	2418.9	67.9	770	348	0.45
zw110-03	0.278	9.121	0.249	0.1566	0.0038	0.4224	0.0051	1334.5	72.5	690.7	18.7	2601.8	159.3	2044	1229	0.60
zw110-04	0.001	13.166	0.381	0.5209	0.0131	0.1833	0.0026	2686.3	27.4	2700.7	55.5	2675.5	24.2	187	124	0.66
zw110-05	0.000	13.210	0.464	0.5134	0.0143	0.1866	0.0040	2694.8	33.2	2671.2	61.1	2712.6	35.1	40	17	0.43
zw110-06	0.044	10.557	0.296	0.3562	0.0088	0.2149	0.0029	2258.6	30.7	1889.3	40.8	2612.3	38.9	418	193	0.46
zw110-07	0.000	12.270	0.345	0.5038	0.0125	0.1766	0.0023	2624.6	26.4	2629.8	53.5	2620.6	22.1	359	206	0.58
zw110-08	0.192	15.501	0.427	0.3497	0.0086	0.3215	0.0040	1956.8	64.8	1604.0	37.5	2353.9	121.7	751	233	0.31

zw110-09	0.000	13.380	0.408	0.5346	0.0138	0.1815	0.0029	2706.6	28.8	2760.9	58.0	2666.3	26.8	101	26	0.26
zw110-10	0.000	12.816	0.378	0.5186	0.0132	0.1792	0.0027	2666.2	27.8	2693.2	55.9	2645.8	25.0	145	91	0.63
zw110-11	0.070	7.196	0.199	0.2382	0.0058	0.2191	0.0028	1781.5	31.9	1289.4	29.0	2419.0	49.6	1005	412	0.41
zw110-12	0.002	11.804	0.331	0.4843	0.0120	0.1768	0.0023	2577.3	26.4	2541.7	52.0	2605.4	22.8	392	141	0.36
zw110-13	0.007	8.762	0.243	0.3689	0.0091	0.1722	0.0022	2275.2	25.5	2012.7	42.5	2520.3	23.1	749	34	0.05
zw110-14	0.000	14.045	0.449	0.5381	0.0143	0.1893	0.0034	2752.8	30.3	2775.5	59.8	2736.1	29.3	67	37	0.56
ZW110-15	0.000	10.974	0.297	0.4586	0.0108	0.1736	0.0023	2520.9	25.2	2433.2	47.6	2592.3	22.4	354	179	0.51
ZW110-16	0.024	10.472	0.280	0.3991	0.0093	0.1903	0.0025	2344.6	26.7	2120.6	42.3	2545.7	29.6	482	115	0.24
ZW110-17	0.004	13.804	0.387	0.5200	0.0125	0.1925	0.0028	2715.5	27.2	2690.6	52.8	2734.1	26.2	159	47	0.30
ZW110-18	0.001	14.164	0.386	0.5462	0.0129	0.1881	0.0026	2756.3	26.0	2807.6	53.8	2718.9	22.9	246	92	0.38
ZW110-19	0.006	12.895	0.354	0.5080	0.0120	0.1841	0.0026	2637.6	26.6	2634.7	51.3	2639.9	25.8	230	71	0.31
ZW110-20	0.000	13.275	0.377	0.5323	0.0128	0.1809	0.0027	2699.4	26.8	2751.3	54.0	2660.8	25.0	139	163	1.18
ZW110-21	0.014	9.529	0.265	0.3760	0.0089	0.1838	0.0027	2310.4	27.8	2032.2	41.5	2566.3	32.2	237	116	0.49
ZW110-22	0.013	10.748	0.289	0.4233	0.0099	0.1841	0.0024	2429.4	26.0	2250.7	44.5	2582.7	26.2	415	249	0.60
ZW110-23	0.043	6.945	0.189	0.2754	0.0065	0.1829	0.0025	1859.7	30.6	1507.4	31.8	2280.3	47.2	456	191	0.42
ZW110-24	0.000	13.040	0.361	0.5307	0.0126	0.1782	0.0025	2682.5	26.1	2744.4	53.1	2636.2	23.6	201	126	0.63
ZW110-25	0.001	15.628	0.451	0.5600	0.0137	0.2024	0.0031	2848.7	27.9	2864.1	56.4	2837.9	26.5	107	59	0.55
ZW110-26	0.002	14.050	0.376	0.5111	0.0120	0.1994	0.0026	2744.0	25.5	2657.4	51.0	2808.3	21.6	403	38	0.09
ZW110-27	0.004	13.154	0.350	0.5186	0.0121	0.1840	0.0024	2666.5	25.3	2683.6	51.2	2653.6	22.2	493	89	0.18
ZW110-28	0.014	13.284	0.353	0.4695	0.0110	0.2052	0.0026	2627.8	25.8	2452.6	47.6	2765.7	23.8	513	145	0.28
ZW110-29	0.000	13.046	0.311	0.5290	0.0114	0.1789	0.0018	2683.0	22.5	2737.1	48.0	2642.4	16.9	219	112	0.51
ZW110-30	0.026	10.813	0.246	0.4148	0.0087	0.1891	0.0016	2361.7	22.9	2187.3	39.2	2515.9	22.8	578	322	0.56
ZW110-31	0.065	5.306	0.119	0.1783	0.0037	0.2159	0.0018	1554.4	22.9	993.5	19.4	2430.8	34.0	1568	303	0.19
ZW110-32	0.070	10.469	0.239	0.3260	0.0069	0.2329	0.0020	2128.0	27.6	1707.4	32.0	2563.2	38.5	553	258	0.47
ZW110-33	0.000	11.227	0.263	0.4668	0.0100	0.1744	0.0017	2542.2	21.8	2469.6	43.7	2600.6	16.2	304	131	0.43
ZW110-34	0.063	9.390	0.217	0.3057	0.0065	0.2228	0.0021	2055.6	28.5	1623.2	30.8	2522.4	41.5	453	131	0.29
ZW110-35	0.004	9.065	0.210	0.3905	0.0083	0.1684	0.0016	2318.9	21.6	2117.1	38.2	2501.6	17.9	428	199	0.46
ZW110-36	0.023	14.369	0.334	0.5116	0.0109	0.2037	0.0019	2649.6	24.2	2612.0	46.0	2678.4	24.1	297	53	0.18
ZW110-37	0.000	15.918	0.521	0.5642	0.0146	0.2046	0.0041	2869.8	33.3	2882.9	60.2	2860.6	38.3	30	10	0.33

Table 6-2. Analytical results of major, minor, and trace elements.

SAMPLE NAME	**ZW209**	**ZW211**	**ZW221**	**ZW227**	**ZW233**	**BT**	**ZW1**	**ZW199**	**JH10**	**JH13**	**JH15**
depo age [Ga]	3.43	3.43	3.43	3.43	3.43	3.25	3.2	3.2	3.2	3.2	3.2
SiO2	66.97	67.07	73.75	65.39	74.34	83.24	95.71	94.42	94.83	94.83	94.42
TiO2	0.376	0.52	0.294	0.585	0.228	0.182	0.29	0.103	0.099	0.099	0.103
Al2O3	12.83	12.87	14.33	16.77	14.24	8.705	3.255	2.695	3.714	3.714	2.695
Fe2O3	2.47	1.63	0.36	1.15	0.73	0.466	0.315	2.212	0.245	0.245	2.212
MnO	0.207	0.232	0.043	0.17	0.111	0.001	-0.004	0	0	-0.009	-0.011
MgO	3.8	3.43	0.99	2.82	0.74	0.995	0.155	0.141	0.16	0.16	0.141
CaO	6.76	6.24	1.93	4.27	1.74	0.823	0.038	0.038	0.038	0.038	0.038
Na2O	0.116	0.107	0.12	0.113	0.118	1.983	0.045	0.054	0.038	0.038	0.054
K2O	6.388	7.882	8.361	8.517	8.004	3.021	0.939	0.686	0.93	0.93	0.686
P2O5	0.084	0.083	0.067	0.102	0.052	0.012	0.01	0.016	0.005	0.005	0.016
Total	100.0	100.1	100.2	99.9	100.3	99.4	100.8	100.4	100.0	100.5	103.8
P	263.33	323.50	199.37	335.65	159.96	72.95	14.55	9.09	39.63	34.85	79.44
Sc	3.46	6.10	2.43	4.40	1.87	2.05	0.34	0.18	4.16	1.76	1.62
Ti	1638	2704	1253	2575	999	1002	241	78	1665	348	382
V	21.49	42.89	16.33	35.41	11.55	12.62	6.32	1.91	48.60	9.15	8.12
Cr	23.43	27.22	20.86	23.19	19.52	239.26	110.71	35.29	24.79	22.00	158.68
Co	4.52	4.77	0.99	2.51	2.24	4.73	2.40	0.96	7.76	0.55	1.00
Ni	10.57	29.05	41.40	16.16	9.75	126.69	32.89	17.83	18.45	91.20	2.46
Rb	86.92	132.33	105.98	141.56	109.46	79.54	2.58	1.35	15.12	16.57	12.19
Sr	10.61	16.20	6.15	8.48	6.43	62.46	5.91	1.51	2.84	3.73	6.40
Y	5.77	4.86	2.63	5.06	3.69	4.04	1.08	1.52	8.45	4.74	8.85
Zr	82.28	79.67	66.78	111.31	69.24	438.88	101.60	76.59	50.40	60.59	74.08
Nb	5.10	6.81	4.07	8.03	3.49	3.71	1.58	0.05	2.07	1.73	3.92
Cs	0.73	0.91	1.23	1.07	1.23	0.49	0.08	0.14	0.13	0.08	0.07
Ba	56.76	82.98	100.33	84.62	141.30	529.25	27.65	12.58	42.56	203.64	74.02
La	10.34	10.63	7.89	11.18	9.34	30.46	6.48	2.55	3.37	5.01	22.86
Ce	19.73	19.94	14.60	21.43	16.31	53.38	11.12	3.07	6.41	7.90	32.66
Pr	2.21	2.27	1.64	2.38	1.88	5.36	1.14	0.64	0.74	1.04	2.89
Nd	8.45	9.08	6.21	9.27	7.11	18.18	4.00	2.38	3.01	3.72	9.28
Sm	1.66	1.75	1.16	1.68	1.32	2.17	0.61	0.40	0.61	0.74	1.38
Eu	0.60	0.76	0.60	0.72	0.65	0.51	0.12	0.10	0.16	0.13	0.18
Gd	1.16	1.36	0.79	1.34	0.92	1.16	0.36	0.30	0.85	0.63	1.48
Tb	0.21	0.23	0.13	0.22	0.15	0.18	0.05	0.05	0.18	0.12	0.27
Dy	1.25	1.29	0.73	1.25	0.85	0.83	0.23	0.28	1.35	0.93	1.68
Ho	0.24	0.23	0.13	0.24	0.16	0.14	0.04	0.06	0.31	0.18	0.33
Er	0.69	0.57	0.33	0.63	0.42	0.50	0.17	0.18	0.93	0.58	0.96
Tm	0.09	0.08	0.04	0.08	0.06	0.09	0.02	0.03	0.14	0.09	0.16
Yb	0.63	0.48	0.30	0.57	0.37	0.66	0.15	0.21	0.95	0.58	1.01
Lu	0.09	0.08	0.04	0.08	0.06	0.14	0.03	0.04	0.14	0.10	0.15
Hf	2.23	2.08	1.81	2.96	1.96	11.55	2.93	2.19	1.29	1.72	2.24
Ta	0.34	0.37	0.23	0.51	0.22	0.24	0.16	0.01	0.11	0.16	0.60
Th	2.45	1.58	1.67	3.63	1.91	16.08	0.37	0.68	2.75	3.93	17.12
U	0.69	0.55	0.91	0.86	0.68	1.65	0.39	0.31	0.91	1.21	5.43
Zr/Hf	36.97	38.27	36.96	37.62	35.40	37.99	34.63	35.05	39.07	35.13	33.03
Th/U	3.56	2.86	1.83	4.24	2.82	9.72	0.95	2.19	3.02	3.25	3.15
La/Ybn	11.19	15.03	18.14	13.22	17.22	31.42	30.16	8.39	2.42	5.83	15.35
La/Smn	3.89	3.78	4.23	4.14	4.41	8.76	6.65	4.03	3.43	4.25	10.35
Gd/Ybn	1.50	2.29	2.16	1.89	2.02	1.43	2.00	1.19	0.73	0.87	1.19
Ce/Ce*	1.00	0.98	0.98	1.00	0.94	1.01	0.99	0.58	0.98	0.84	0.97
Eu/Eu*	1.31	1.49	1.93	1.47	1.81	0.98	0.76	0.84	0.68	0.58	0.38
Nb/Nb*	0.35	0.57	0.39	0.43	0.28	0.06	0.35	0.01	0.23	0.13	0.07
Zr/Zr*	1.49	1.35	1.69	1.91	1.53	4.74	4.42	5.36	2.52	2.48	1.40
Hf/Hf*	1.50	1.31	1.69	1.88	1.61	4.63	4.73	5.67	2.39	2.62	1.58
Ti/Ti*	0.68	1.02	0.83	1.00	0.57	0.51	0.42	0.14	0.78	0.23	0.12

SAMPLE NAME	**JH18**	**JH28**	**MN22**	**MN23**	**MN37**	**MN43**	**BE478**	**BE482**	**BG266**	**IG220**	**ZW117**	**SR01**
depo age [Ga]	3.2	3.2	3.2	3.2	3.2	3.2	3.1	3.1	3.1	3	3	2.99
SiO2	98.03	101.79	79.21	99.06	78.39	81.93	95.98	99.35	81.99	95.28	82.04	87.48
TiO2	0.21	0.127	0.162	0.24	0.085	0.058	0.126	0.1	0.232	0.268	0.104	0.278
Al2O3	1.422	1.33	6.21	0.16	3.57	11.62	2.061	1.098	9.378	4.102	13.433	5.231
Fe2O3	0.29	0.091	14.68	2.19	17.76	5.31	1.401	0.292	1.325	0.046	1.067	3.077
MnO	-0.009	-0.013	0.28	-0.01	0.23	0.11	-0.008	-0.013	0.033	-0.012	-0.008	0.059
MgO	0.093	0.101	0.72	0.07	0.44	0.82	0.676	0.063	1.212	0.114	0.787	0.907
CaO	0.038	0.038	0.06	0.04	0.06	0.09	0.04	0.039	0.884	0.208	0.039	1.706
Na2O	0.039	0.039	0.02	0.01	0.07	0.05	0.085	0.091	2.851	0.094	0.149	0.853
K2O	0.364	0.326	0.00	0.00	0.01	0.28	0.082	0.219	2.032	0.362	4.215	0.64
P2O5	0.07	0.012	0.03	0.00	0.01	0.02	0.014	0.015	0.012	0.016	0.017	0.008
Total	101.3	101.6	100.7	100.5	101.1	101.1	101.3	99.9	100.5	101.8	100.5	100.3
P	273.75	49.34	111.38	19.86	51.60	87.73	32.54	49.60	42.56	63.44	33.72	38.77
Sc	2.56	1.42	6.30	0.43	5.00	7.77	1.69	0.63	3.55	5.71	0.81	3.23
Ti	997	498	598	4	661	1143	329	277	1101	1403	230	1188
V	8.80	5.11	21.57	1.11	34.14	35.60	6.78	4.92	17.43	11.20	4.11	29.03
Cr	717.11	495.08	93.00	3.36	76.19	109.81	79.77	51.79	325.06	46.38	5.35	18.38
Co	0.78	0.63	7.66	3.06	10.00	8.15	1.66	0.36	6.70	0.34	0.55	7.73
Ni	39.15	18.76	7.16	6.32	5.55	111.77	44.25	15.33	5.25	5.18	2.13	1.90
Rb	7.31	7.03	0.76	0.39	0.44	12.64	1.47	4.02	29.46	13.68	16.83	12.49
Sr	5.17	2.89	3.32	1.50	1.56	3.63	6.66	9.33	141.27	29.48	1.32	14.04
Y	24.50	17.82	11.03	0.43	7.45	15.14	3.94	2.94	7.66	11.10	5.82	1.51
Zr	256.89	91.60	64.24	0.65	52.10	86.16	30.70	32.05	82.51	188.59	26.55	27.98
Nb	9.52	7.54	4.66	0.07	1.19	6.33	1.11	1.04	4.40	5.80	0.65	0.69
Cs	0.04	0.05	0.04	0.01	0.02	0.17	0.05	0.09	0.58	0.39	0.40	0.27
Ba	17.45	25.43	18.96	3.23	10.46	152.83	16.66	90.74	335.42	224.64	101.38	63.79
La	45.62	20.93	24.61	0.43	14.78	34.85	9.41	5.02	12.31	19.02	3.89	5.07
Ce	80.09	34.20	40.59	0.74	25.36	57.68	16.41	9.12	20.62	34.57	7.66	10.64
Pr	8.22	3.32	4.05	0.10	2.56	5.77	1.65	0.96	2.77	3.53	0.89	1.18
Nd	30.84	12.16	14.07	0.31	8.71	19.56	5.76	3.65	10.43	12.77	3.46	4.55
Sm	5.22	2.02	2.40	0.05	1.49	3.02	0.84	0.59	2.08	2.11	0.66	0.78
Eu	0.32	0.17	0.33	0.02	0.24	0.52	0.15	0.10	0.72	0.42	0.17	0.18
Gd	4.29	2.38	1.89	0.08	1.32	2.51	0.31	0.23	1.33	1.60	0.88	0.57
Tb	0.72	0.46	0.35	0.01	0.22	0.46	0.12	0.08	0.31	0.28	0.12	0.08
Dy	4.48	3.00	2.10	0.07	1.32	2.82	0.76	0.53	1.72	1.84	0.80	0.40
Ho	0.94	0.59	0.40	0.01	0.26	0.57	0.15	0.11	0.30	0.43	0.16	0.07
Er	2.78	1.79	1.20	0.04	0.80	1.77	0.49	0.37	0.84	1.41	0.45	0.22
Tm	0.46	0.29	0.21	0.01	0.11	0.25	0.08	0.06	0.12	0.24	0.07	0.03
Yb	2.97	1.84	1.55	0.04	0.86	1.68	0.48	0.41	0.75	1.68	0.42	0.22
Lu	0.42	0.26	0.22	0.01	0.12	0.25	0.08	0.06	0.11	0.27	0.07	0.04
Hf	7.06	2.46	1.84	0.02	1.52	2.74	0.95	1.03	2.36	4.34	0.71	0.75
Ta	1.64	1.54	0.60	0.00	0.23	0.66	0.08	0.09	0.31	0.28	0.05	0.06
Th	29.48	8.90	14.05	0.03	9.19	16.18	2.64	1.90	4.04	5.18	2.07	0.93
U	7.55	4.05	5.25	0.13	4.91	3.12	0.46	0.64	0.81	1.15	0.26	0.25
Zr/Hf	36.36	37.18	34.86	35.77	34.27	31.50	32.46	31.16	34.94	43.40	37.24	37.12
Th/U	3.90	2.20	2.67	0.28	1.87	5.19	5.68	2.99	4.98	4.51	7.91	3.74
La/Ybn	10.43	7.73	10.78	8.29	11.65	14.12	13.32	8.33	11.22	7.71	6.34	15.57
La/Smn	5.46	6.46	6.40	4.94	6.21	7.20	7.02	5.31	3.69	5.64	3.68	4.06
Gd/Ybn	1.17	1.05	0.98	1.80	1.24	1.21	0.52	0.45	1.44	0.77	1.71	2.10
Ce/Ce*	1.00	0.99	0.98	0.87	1.00	0.98	1.01	1.01	0.85	1.02	1.00	1.05
Eu/Eu*	0.21	0.24	0.47	1.01	0.52	0.57	0.93	0.83	1.32	0.70	0.67	0.81
Nb/Nb*	0.09	0.19	0.09	0.21	0.04	0.09	0.08	0.12	0.22	0.20	0.08	0.11
Zr/Zr*	1.37	1.25	0.75	0.34	0.98	0.76	0.95	1.48	1.20	2.47	1.19	1.01
Hf/Hf*	1.40	1.25	0.80	0.36	1.06	0.90	1.08	1.76	1.28	2.11	1.19	1.01
Ti/Ti*	0.11	0.09	0.15	0.03	0.25	0.22	0.34	0.40	0.37	0.41	0.14	1.24

SAMPLE NAME	**SR03**	**SR07**	**SV12A**	**SV13**	**SV06**	**PP74**	**PP79**	**YK10**	**FT22**	**FT69**	**SV17**
depo age [Ga]	2.99	2.99	2.94	2.94	2.94	2.9	2.9	2.88	2.756	2.715	2.704
SiO2	90.09	74.76	74.36	84.15	78.81	79.69	81.98	71.41	80.63	74.03	65.39
TiO2	0.247	0.171	0.248	0.188	0.39	0.292	0.269	0.645	0.37	0.418	0.942
Al2O3	4.787	14.675	10.038	6.622	14.916	11.659	10.416	12.819	9.89	11.952	15.495
Fe2O3	2.681	1.863	4.06	2.458	0.22	1.313	1.089	6.609	3.559	5.192	6.577
MnO	0.01	0.04	0.226	0.102	-0.012	-0.005	-0.008	0.069	0.062	0.064	0.153
MgO	1.081	0.868	2.782	2.952	0.299	0.702	0.57	2.84	1.805	1.875	1.715
CaO	0.057	3.097	4.85	2.271	0.049	0.188	0.175	1.651	1.257	2.233	3.032
Na2O	0.932	3.503	1.806	0.971	0.105	2.621	2.478	2.176	0.859	3.633	4.565
K2O	0.434	2.584	2.737	1.892	4.508	3.039	2.71	1.463	1.622	2.525	2.136
P2O5	0.007	0.088	0.022	0.012	0.021	0.018	0.014	0.012	0.025	0.062	0.311
Total	101.7	100.2	101.1	101.6	99.3	99.5	99.7	99.7	100.1	102.0	100.3
P	37.80	345.51	83.79	55.82	103.73	53.98	78.15	53.27	135.20	372.72	937.16
Sc	3.62	4.62	7.30	5.90	6.54	3.76	4.36	4.29	10.83	12.27	7.85
Ti	1173	813	2202	944	1373	1429	1626	1259	2650	3323	3443
V	28.03	20.78	52.45	27.36	48.75	25.57	29.13	32.03	69.01	85.68	30.51
Cr	17.60	7.49	113.47	180.82	93.30	170.84	208.47	284.96	248.78	112.65	3.66
Co	6.26	4.08	0.59	9.67	11.75	2.53	4.04	7.89	15.42	21.41	4.43
Ni	19.07	9.35	55.74	44.44	10.64	21.15	8.59	56.64	5.65	23.70	18.38
Rb	8.94	51.94	105.71	43.60	49.47	106.36	126.97	41.77	95.88	101.29	34.17
Sr	10.96	61.21	11.10	54.15	77.47	113.21	123.21	63.81	37.35	125.29	253.73
Y	1.24	7.63	13.72	9.10	10.64	6.49	7.10	7.38	22.57	20.31	13.98
Zr	55.48	75.96	234.13	92.36	100.20	135.61	131.93	80.15	137.75	127.38	117.74
Nb	1.20	3.20	13.41	4.71	6.96	4.21	4.03	3.91	9.46	6.18	6.78
Cs	0.15	0.80	1.02	1.06	0.58	1.78	2.01	0.50	3.63	1.80	0.84
Ba	51.51	246.47	396.16	306.72	331.63	545.79	587.85	169.91	291.73	856.99	476.63
La	4.49	16.59	25.09	18.83	22.21	14.44	13.11	15.34	27.21	27.23	16.19
Ce	9.39	32.32	50.44	35.60	41.39	25.30	23.10	27.03	52.16	48.03	36.79
Pr	1.01	3.37	5.01	3.57	4.33	3.14	2.69	2.73	5.69	5.09	4.46
Nd	3.91	12.19	18.01	12.80	15.82	11.43	9.87	9.74	21.46	18.95	18.57
Sm	0.69	1.95	3.24	2.20	3.00	1.95	1.68	1.65	4.11	3.56	3.52
Eu	0.16	0.59	0.49	0.39	0.45	0.57	0.54	0.48	0.88	0.89	0.97
Gd	0.41	1.44	2.85	2.02	2.35	1.63	1.55	1.47	3.88	3.47	2.96
Tb	0.07	0.25	0.45	0.33	0.42	0.25	0.23	0.24	0.70	0.61	0.47
Dy	0.37	1.40	2.69	1.97	2.18	1.36	1.33	1.38	4.53	3.77	2.91
Ho	0.05	0.28	0.56	0.41	0.45	0.28	0.27	0.29	0.87	0.78	0.55
Er	0.16	0.85	1.74	1.23	1.31	0.80	0.81	0.83	2.58	2.42	1.53
Tm	0.03	0.12	0.26	0.18	0.20	0.11	0.11	0.12	0.38	0.35	0.22
Yb	0.19	0.78	1.76	1.26	1.22	0.78	0.75	0.87	2.34	2.12	1.46
Lu	0.04	0.11	0.28	0.20	0.17	0.13	0.12	0.14	0.37	0.35	0.20
Hf	1.52	2.08	6.32	3.02	2.83	3.48	3.05	2.25	3.92	3.58	3.04
Ta	0.07	0.33	1.06	0.50	0.50	0.30	0.26	0.35	1.13	0.66	0.32
Th	0.99	3.91	21.75	10.28	11.54	2.68	2.69	5.85	9.63	8.53	4.51
U	0.38	0.51	5.89	3.25	2.20	0.83	0.79	1.69	2.82	2.66	1.13
Zr/Hf	36.62	36.55	37.04	30.60	35.37	39.02	43.19	35.69	35.13	35.59	38.79
Th/U	2.63	7.73	3.69	3.16	5.24	3.22	3.40	3.46	3.41	3.21	4.00
La/Ybn	15.78	14.37	9.70	10.16	12.35	12.65	11.90	11.97	7.89	8.71	7.53
La/Smn	4.06	5.32	4.84	5.35	4.62	4.63	4.87	5.79	4.13	4.78	2.88
Gd/Ybn	1.71	1.49	1.31	1.30	1.55	1.70	1.68	1.37	1.34	1.32	1.64
Ce/Ce*	1.07	1.05	1.09	1.05	1.02	0.91	0.94	1.01	1.01	0.99	1.05
Eu/Eu*	0.94	1.07	0.49	0.56	0.52	0.98	1.02	0.94	0.67	0.77	0.91
Nb/Nb*	0.20	0.14	0.20	0.12	0.15	0.23	0.23	0.14	0.20	0.14	0.27
Zr/Zr*	2.29	1.06	2.08	1.18	0.99	1.95	2.20	1.35	0.99	1.05	0.99
Hf/Hf*	2.32	1.07	2.08	1.43	1.03	1.85	1.89	1.41	1.05	1.10	0.95
Ti/Ti*	1.51	0.29	0.40	0.24	0.31	0.48	0.57	0.44	0.32	0.46	0.59

SAMPLE NAME	SV25	SV26	BW355	BW98	FT61	RM10	YK04	YK07	UC02	UC12	UC14
depo age [Ga]	2.704	2.704	2.7	2.7	2.684	2.684	2.66	2.66	2.33	2.33	2.33
SiO2	71.72	65.91	79.31	79.34	84.83	96.02	73.52	65.87	93.36	71.00	71.11
TiO2	0.358	0.508	0.221	0.354	0.253	0.168	0.528	0.59	0.123	0.098	0.654
Al2O3	15.324	17.28	15.007	7.452	7.72	1.67	13.754	16.575	5.56	18.63	12.788
Fe2O3	3.244	5.042	0.623	6.195	0.978	2.771	4.993	5.364	0.198	0.709	6.604
MnO	0.034	0.048	0	0.129	0.007	-0.012	0.024	0.043	-0.008	0.006	0.071
MgO	1.229	3.218	0.282	1.781	0.307	0.066	1.975	2.73	0.232	0.678	2.818
CaO	2.183	3.398	0.21	2.366	0.793	0.043	2.032	0.344	0.058	0.141	1.637
Na2O	4.191	4.881	1.217	0.077	1.711	0.109	3.149	5.577	0.132	1.375	2.177
K2O	2.517	1.843	2.604	1.922	3.357	0.073	1.754	3.678	0.819	8.351	1.463
P2O5	0.087	0.16	0.069	0.031	0.025	0.027	0.073	0.126	0.019	0.033	0.014
Total	100.9	102.3	99.5	99.6	100.0	100.9	101.8	100.9	101.8	100.6	99.3
P	353.65	308.77	355.75	121.62	180.09	105.25	304.87	496.75	90.73	140.99	50.76
Sc	6.78	3.50	2.64	6.31	7.90	1.45	12.47	11.90	1.32	2.46	13.84
Ti	1857	991	1319	2031	1444	706	3062	3404	558	382	3862
V	48.33	28.81	16.73	48.23	77.73	12.74	89.55	92.04	10.57	2.40	109.79
Cr	41.02	23.08	8.59	188.07	148.01	81.33	119.45	128.71	11.84	5.41	251.64
Co	10.42	5.04	2.28	18.54	74.49	0.89	17.73	20.44	0.37	1.28	26.36
Ni	23.62	11.34	3.12	7.10	7.23	5.91	2.45	47.35	47.61	11.31	13.60
Rb	56.60	42.80	85.93	58.40	108.70	2.65	52.72	64.49	49.10	206.94	30.48
Sr	455.23	194.38	84.30	24.83	84.88	4.99	230.84	85.61	20.01	94.38	109.33
Y	5.91	3.32	3.95	6.36	9.07	17.06	10.99	12.96	6.43	7.21	4.30
Zr	102.33	37.04	96.07	89.02	58.54	79.59	103.62	135.93	104.76	48.26	465.29
Nb	3.90	1.60	2.92	3.52	2.93	2.29	5.47	6.04	3.40	3.56	19.57
Cs	2.61	3.12	4.09	1.89	1.59	0.19	2.47	0.36	0.48	2.21	0.82
Ba	632.75	223.19	464.83	113.15	1151.46	29.48	307.83	623.46	27.53	2570.67	7970.03
La	22.70	9.98	13.52	15.63	5.81	14.67	24.96	25.45	13.20	49.81	22.06
Ce	44.28	20.42	23.26	30.27	13.11	26.64	48.22	50.64	26.47	89.16	33.72
Pr	4.84	2.22	2.26	3.21	1.59	3.18	5.25	5.69	2.94	8.02	3.02
Nd	18.10	8.70	7.82	11.87	7.39	12.03	20.12	22.15	10.19	28.03	9.99
Sm	2.58	1.41	1.30	2.16	1.77	2.39	3.38	3.64	1.72	5.22	1.30
Eu	0.67	0.35	0.40	0.49	0.34	0.49	1.20	1.02	0.26	0.89	1.35
Gd	1.71	0.96	1.05	1.88	1.57	2.11	3.33	3.18	1.47	3.98	1.00
Tb	0.28	0.13	0.15	0.29	0.30	0.47	0.42	0.44	0.23	0.48	0.15
Dy	1.24	0.67	0.72	1.58	1.80	2.98	2.34	2.71	1.36	1.92	0.70
Ho	0.24	0.13	0.13	0.31	0.36	0.61	0.47	0.57	0.26	0.33	0.14
Er	0.66	0.41	0.39	0.88	1.12	1.92	1.32	1.55	0.79	0.78	0.47
Tm	0.09	0.05	0.05	0.12	0.20	0.29	0.18	0.22	0.12	0.09	0.07
Yb	0.69	0.34	0.34	0.85	1.19	2.00	1.31	1.46	0.77	0.57	0.64
Lu	0.10	0.05	0.05	0.13	0.22	0.31	0.18	0.22	0.11	0.08	0.13
Hf	2.97	0.87	2.29	2.45	1.70	2.08	2.91	3.69	3.23	1.90	10.78
Ta	0.31	0.08	0.20	0.24	0.26	0.18	0.34	0.35	0.41	0.29	0.69
Th	5.50	1.62	3.75	5.95	3.10	3.49	6.65	1.66	13.24	38.32	5.46
U	1.29	0.47	1.75	3.08	1.08	1.51	1.80	2.95	0.94	3.59	11.14
Zr/Hf	34.41	42.71	41.91	36.34	34.40	38.20	35.55	36.79	32.44	25.45	43.16
Th/U	4.26	3.45	2.14	1.93	2.88	2.31	3.69	0.56	14.06	10.67	0.49
La/Ybn	22.23	19.71	26.83	12.53	3.32	4.99	12.97	11.83	11.66	59.68	23.44
La/Smn	5.49	4.43	6.50	4.53	2.05	3.84	4.61	4.36	4.80	5.96	10.59
Gd/Ybn	1.99	2.26	2.48	1.79	1.07	0.85	2.06	1.76	1.55	5.68	1.26
Ce/Ce*	1.02	1.05	1.02	1.03	1.04	0.94	1.02	1.02	1.03	1.08	1.00
Eu/Eu*	0.97	0.91	1.04	0.75	0.62	0.66	1.09	0.91	0.50	0.60	3.61
Nb/Nb*	0.12	0.14	0.14	0.13	0.24	0.11	0.15	0.32	0.09	0.03	0.62
Zr/Zr*	1.02	0.72	2.05	1.19	1.10	1.01	0.85	1.03	1.70	0.27	8.76
Hf/Hf*	1.09	0.62	1.81	1.22	1.18	0.98	0.89	1.04	1.94	0.39	7.53
Ti/Ti*	0.64	0.62	0.76	0.59	0.43	0.14	0.55	0.58	0.20	0.07	2.32

SAMPLE NAME	**UC03**	**UC09**	**UC21**	**WY1**	**TC96**	**TC155**	**TC266**	**TC381**	**TC144**	**TC179**	**TC195**
depo age [Ga]	2.33	2.33	2.33	2.3	2.21	2.21	2.21	2.21	2.21	2.21	2.21
SiO2	71.77	72.31	95.35	92.74	92.19	94.07	100.31	100.40	93.37	71.42	90.61
TiO2	0.249	0.059	0.181	0.157	0.428	0.221	0.082	0.065	0.216	0.631	0.123
Al2O3	16.79	17.56	4.092	5.884	3.325	5.661	1.582	0.683	2.67	14.667	3.217
Fe2O3	3.174	0.7	0.154	0.903	4.826	0.47	0.302	0.043	3.413	7.935	5.417
MnO	0.054	-0.01	-0.01	0.004	-0.012	-0.011	-0.012	-0.011	0.01	0.019	0.023
MgO	0.994	0.31	0.136	2.254	0.077	0.198	0.12	0.074	0.706	2.699	0.608
CaO	1.528	1.37	0.049	0.124	0.042	0.046	0.038	0.038	0.05	0.212	0.117
Na2O	3.864	4.837	0.047	0.033	0.084	0.107	0.053	0.038	0.052	0.088	0.04
K2O	3.342	2.327	0.613	1.217	0.726	1.413	0.322	0.111	0.058	3.072	0.137
P2O5	0.072	0.015	0.015	0.073	0.018	0.035	0.006	0.007	0.02	0.129	0.033
Total	101.0	100.5	99.5	101.7	101.7	102.2	102.8	101.4	100.6	100.9	100.3
P	282.55	44.37	63.89	31.39	298.72	178.99	37.38	47.20	63.91	405.13	103.78
Sc	6.17	1.04	3.02	0.71	5.56	4.40	1.00	0.40	1.62	9.49	1.99
Ti	1238	319	889	151	2258	1538	245	142	773	2545	375
V	19.78	3.64	3.45	4.08	46.12	21.46	5.58	3.10	20.21	58.28	14.54
Cr	5.73	3.54	8.01	8.86	117.76	45.90	7.19	5.16	18.55	100.91	16.79
Co	6.87	0.63	0.39	0.86	0.47	1.10	0.21	0.26	2.65	7.08	3.59
Ni	7.43	17.77	3.77	34.87	5.15	48.64	16.05	8.23	20.43	15.07	28.54
Rb	81.75	29.60	14.49	39.62	35.74	38.25	11.97	4.01	1.98	111.28	5.41
Sr	168.29	109.09	31.35	10.50	24.10	63.70	2.85	4.42	3.30	8.77	6.98
Y	9.06	4.71	4.11	4.03	15.70	8.52	2.73	2.44	6.02	17.68	5.51
Zr	140.13	44.29	409.42	27.42	1408.07	115.95	35.76	23.82	268.18	195.12	28.91
Nb	8.12	1.55	5.09	0.67	7.52	3.87	1.13	0.67	3.10	9.22	1.56
Cs	0.51	0.82	0.14	0.24	1.33	1.99	0.41	0.12	0.31	5.55	0.39
Ba	602.59	2385.51	46.40	159.70	54.54	227.07	45.03	15.56	31.71	228.87	179.22
La	22.38	30.04	11.30	7.68	12.72	24.09	7.76	6.44	7.29	30.87	9.03
Ce	41.58	52.87	17.75	14.81	26.37	40.25	15.10	10.71	14.18	64.45	17.46
Pr	4.32	5.30	1.84	1.60	3.10	4.14	1.63	1.23	1.58	6.68	2.16
Nd	15.65	18.55	5.86	6.06	12.95	15.23	5.79	4.25	5.88	25.86	8.73
Sm	3.05	3.03	0.81	0.98	2.70	2.42	0.82	0.66	1.04	4.48	1.73
Eu	0.60	0.85	0.17	0.22	0.63	0.58	0.14	0.11	0.22	0.90	0.34
Gd	2.38	2.57	0.64	0.82	2.36	2.14	0.54	0.47	0.51	2.33	0.99
Tb	0.38	0.32	0.12	0.12	0.48	0.31	0.11	0.09	0.17	0.61	0.22
Dy	2.18	1.40	0.78	0.73	2.93	1.79	0.62	0.49	1.06	3.53	1.20
Ho	0.39	0.18	0.16	0.13	0.65	0.38	0.10	0.09	0.22	0.67	0.22
Er	1.10	0.43	0.58	0.42	2.07	1.04	0.32	0.28	0.74	2.03	0.59
Tm	0.15	0.04	0.10	0.05	0.35	0.17	0.04	0.03	0.12	0.29	0.08
Yb	0.92	0.22	0.89	0.37	2.67	1.09	0.29	0.23	0.85	1.96	0.56
Lu	0.13	0.04	0.16	0.06	0.43	0.17	0.04	0.03	0.15	0.30	0.07
Hf	4.13	1.53	10.99	0.82	32.93	3.59	1.04	0.66	5.78	4.89	0.87
Ta	0.35	0.03	0.55	0.09	0.71	0.36	0.16	0.10	0.27	0.66	0.11
Th	14.71	15.84	16.96	2.35	5.03	6.25	2.57	1.37	3.38	11.14	2.43
U	1.39	0.44	1.24	0.46	3.33	1.73	0.58	0.44	1.52	4.05	0.95
Zr/Hf	33.92	28.86	37.25	33.44	42.76	32.27	34.43	35.94	46.37	39.86	33.16
Th/U	10.58	36.20	13.67	5.11	1.51	3.61	4.43	3.14	2.23	2.75	2.56
La/Ybn	16.58	94.01	8.67	13.93	3.24	14.97	18.10	18.84	5.85	10.68	10.92
La/Smn	4.58	6.19	8.75	4.89	2.94	6.22	5.88	6.10	4.36	4.30	3.27
Gd/Ybn	2.10	9.57	0.58	1.77	0.72	1.59	1.51	1.63	0.49	0.96	1.43
Ce/Ce*	1.02	1.01	0.94	1.02	1.02	0.98	1.03	0.92	1.01	1.09	0.96
Eu/Eu*	0.68	0.93	0.73	0.75	0.76	0.77	0.64	0.59	0.91	0.84	0.79
Nb/Nb*	0.15	0.02	0.13	0.05	0.32	0.11	0.09	0.08	0.22	0.17	0.11
Zr/Zr*	1.38	0.40	12.77	0.76	16.16	1.30	1.11	0.96	7.34	1.23	0.51
Hf/Hf*	1.50	0.52	12.72	0.85	14.02	1.49	1.20	1.00	5.88	1.14	0.57
Ti/Ti*	0.27	0.08	0.64	0.10	0.43	0.39	0.21	0.15	0.53	0.45	0.17

SAMPLE NAME	**ZW5**	**ZW74**	**UK1**	**UK2**	**UK4**	**NF2**	**NF9**	**IR300**	**IR306**	**IR409**	**IR416**	**ISN1**
depo age [Ga]	2.2	2.2	1.9	1.1	1.1	0.6	0.6	0.6	0.6	0.6	0.6	0.595
SiO2	77.78	99.13	98.42	84.06	72.57	72.19	76.06	81.25	72.18	71.71	79.97	88.68
TiO2	0.225	0.078	0.119	0.237	0.98	0.601	0.32	0.372	0.713	0.594	0.422	0.296
Al2O3	12.197	1.715	1.108	8.75	12.264	14.025	13.482	9.988	15.03	15.36	8.913	6.729
Fe2O3	3.092	0.073	0.162	1.581	5.493	3.819	2.651	2.099	4.51	3.66	3.788	0.475
MnO	0.145	-0.014	0	0.005	0.112	0.067	0.046	0.012	0.032	0.077	0.113	0
MgO	1.98	0.175	0.086	0.38	1.594	1.431	0.619	0.657	1.19	0.77	1.574	0.428
CaO	2.873	0.038	0.041	0.266	2.086	2.312	0.544	0.067	0.24	1.16	0.991	0.161
Na2O	1.771	0.011	0.058	1.328	3.075	4.227	5.323	1.808	4.083	4.566	3.505	1.473
K2O	1.354	0.521	0.656	3.546	2.902	1.679	2.236	4.272	2.277	2.3	0.436	2.651
P2O5	0.013	0.009	0.005	0.02	0.142	0.083	0.037	0.025	0.091	0.082	0.066	0.079
Total	101.4	103.4	100.6	100.2	101.2	100.4	101.3	100.5	100.3	100.3	99.8	101.0
P	320.61	28.09	14.30	50.55	486.17	298.86	156.42	83.36	336.12	334.17	250.48	297.31
Sc	2.87	0.79	0.48	1.77	8.12	7.94	3.94	3.25	7.37	12.63	3.80	2.17
Ti	724	231	366	799	4724	2865	1499	1498	3243	2993	1953	1364
V	12.58	3.99	4.11	14.30	62.43	52.53	23.08	18.82	45.99	60.43	17.44	7.68
Cr	25.65	5.38	5.88	9.29	49.06	35.90	12.53	9.15	54.23	15.97	16.14	8.71
Co	4.77	0.66	0.40	1.91	6.59	6.52	5.30	2.54	7.08	5.45	7.25	0.61
Ni	17.44	52.95	21.30	14.49	31.13	28.63	1.60	4.37	13.07	75.25	39.83	9.03
Rb	33.19	16.17	7.95	77.52	63.94	47.00	45.19	122.33	77.91	84.37	13.89	56.86
Sr	10.65	1.31	7.56	40.15	315.74	221.79	171.77	17.81	55.28	55.29	26.52	32.75
Y	5.29	5.70	1.23	6.88	14.30	15.12	9.84	9.84	12.54	22.22	10.72	11.94
Zr	31.43	35.72	59.50	77.70	657.04	108.04	79.82	122.29	378.32	173.02	104.70	434.89
Nb	0.98	0.72	1.00	3.32	12.79	6.55	5.37	6.74	10.44	10.04	5.81	7.16
Cs	0.77	0.40	0.08	1.01	0.49	2.15	0.65	1.07	1.47	1.46	0.41	0.51
Ba	280.89	103.98	52.61	641.30	586.72	345.33	794.01	522.79	628.75	242.75	49.85	903.43
La	15.71	4.22	4.17	16.24	25.05	16.02	17.61	18.12	20.28	24.57	25.76	5.47
Ce	23.97	8.13	8.96	33.71	47.76	33.45	38.13	39.50	48.78	52.84	65.91	9.30
Pr	3.39	0.92	0.80	3.58	5.40	3.94	4.17	4.13	4.77	5.64	7.75	1.47
Nd	13.16	3.73	2.77	13.43	20.99	16.12	16.23	15.72	18.71	22.24	30.47	5.91
Sm	2.20	0.84	0.41	2.23	3.58	3.16	2.92	2.69	3.30	4.24	5.42	1.37
Eu	0.56	0.17	0.08	0.48	0.77	0.77	0.62	0.52	0.86	1.12	1.10	0.32
Gd	1.86	0.89	0.13	0.88	1.50	1.79	1.19	1.30	1.75	3.34	2.06	1.05
Tb	0.25	0.15	0.05	0.27	0.48	0.49	0.36	0.34	0.44	0.68	0.48	0.29
Dy	1.31	0.84	0.28	1.55	2.82	2.94	2.10	1.96	2.52	4.20	2.43	2.03
Ho	0.23	0.19	0.06	0.31	0.57	0.58	0.40	0.41	0.53	0.89	0.45	0.46
Er	0.63	0.56	0.16	0.90	1.73	1.73	1.16	1.24	1.58	2.64	1.33	1.45
Tm	0.07	0.08	0.03	0.14	0.27	0.27	0.18	0.19	0.23	0.38	0.18	0.23
Yb	0.49	0.49	0.17	0.91	1.91	1.74	1.17	1.32	1.52	2.68	1.25	1.65
Lu	0.07	0.09	0.03	0.14	0.31	0.26	0.18	0.19	0.23	0.42	0.20	0.26
Hf	0.92	1.09	1.76	2.18	11.54	3.07	2.30	3.03	7.58	4.41	2.90	7.84
Ta	0.07	0.06	0.05	0.20	0.62	0.36	0.33	0.43	0.52	0.57	0.33	0.37
Th	1.49	2.89	0.73	2.68	7.76	4.28	4.23	4.18	7.50	7.93	3.69	2.36
U	0.39	0.40	0.45	0.50	1.96	1.06	0.90	0.71	1.19	1.48	1.00	0.76
Zr/Hf	34.21	32.72	33.72	35.71	56.92	35.22	34.69	40.33	49.88	39.27	36.07	55.49
Th/U	3.82	7.22	1.62	5.36	3.96	4.02	4.73	5.84	6.29	5.35	3.69	3.13
La/Ybn	21.85	5.86	16.33	12.09	8.93	6.24	10.22	9.36	9.09	6.23	14.05	2.26
La/Smn	4.45	3.13	6.30	4.55	4.37	3.17	3.77	4.20	3.83	3.62	2.97	2.50
Gd/Ybn	3.09	1.47	0.61	0.78	0.64	0.83	0.82	0.80	0.93	1.01	1.34	0.51
Ce/Ce*	0.79	1.00	1.18	1.07	0.99	1.02	1.08	1.10	1.20	1.09	1.13	0.79
Eu/Eu*	0.84	0.61	1.01	1.04	1.01	0.99	1.01	0.85	1.09	0.91	1.00	0.81
Nb/Nb*	0.07	0.07	0.20	0.17	0.32	0.27	0.21	0.27	0.29	0.25	0.21	0.69
Zr/Zr*	0.40	1.37	3.77	0.96	5.14	1.03	0.79	1.27	3.26	1.21	0.55	10.38
Hf/Hf*	0.43	1.55	4.15	1.00	3.35	1.08	0.84	1.17	2.43	1.14	0.57	6.94
Ti/Ti*	0.23	0.13	0.95	0.34	1.15	0.63	0.48	0.47	0.78	0.40	0.44	0.47

SAMPLE NAME	**IS150**	**IS160**	**UKP4**	**UKP6**	**UKP8**	**ANG321**	**ANG331**	**NF28**	**NF32**	**NF33**	**IR363**
depo age [Ga]	0.595	0.595	0.5	0.5	0.5	0.5	0.5	0.43	0.41	0.41	0.4
SiO2	76.88	94.98	78.89	61.72	84.30	96.43	95.84	73.23	76.01	53.86	82.45
TiO2	0.428	0.265	0.502	0.817	0.27	0.285	0.283	0.54	0.453	1.193	0.711
Al2O3	9.051	5.151	9.756	14.912	6.602	2.935	2.722	10.782	12.097	17.299	9.03
Fe2O3	2.918	1.085	4.377	7.445	1.965	0.388	0.861	4.204	4.131	8.56	3.229
MnO	0.149	0.015	0.051	0.131	0.056	0	0	0.148	0.065	0.144	0.023
MgO	3.828	0.872	2.779	4.941	0.872	0.15	0.244	2.742	1.619	6.175	0.871
CaO	4.936	0.727	1.477	4.889	5.598	0.048	0.062	5.065	0.874	7.873	0.122
Na2O	0.107	0.136	1.604	1.92	0.471	0.018	0.283	2.587	3.81	3.425	2.395
K2O	3.026	2.053	2.013	2.955	0.178	0.743	0.656	1.858	2.032	1.253	1.26
P2O5	0.077	0.046	0.097	0.116	0.016	0.009	0.024	0.127	0.062	0.194	0.035
Total	101.4	105.3	101.5	99.8	100.3	101.0	101.0	101.3	101.1	100.0	100.1
P	293.75	153.36	358.19	372.99	55.94	29.97	92.91	364.49	197.48	607.39	123.39
Sc	4.76	1.49	7.43	10.66	3.09	1.76	1.87	6.26	8.15	16.32	4.91
Ti	2164	1011	2392	3710	1102	1113	1275	2121	1835	5474	3315
V	23.05	7.90	59.92	65.05	15.41	10.11	8.89	35.98	54.44	114.78	34.73
Cr	20.81	7.88	155.53	70.52	20.05	13.33	11.74	55.2	46.66	93.46	40.2
Co	5.33	0.86	9.71	27.98	3.12	0.24	0.78	7.07	5.95	21.82	4.3
Ni	3.21	6.49	2.57	8.71	2.48	6.05	19.96	13.17	5.7	14.27	17.49
Rb	92.16	46.11	68.69	98.35	6.82	18.48	19.79	53.62	34.83	25.23	37.96
Sr	59.47	12.73	73.64	443.1	280.16	6.87	11.7	103.66	123.87	365.15	36.18
Y	17.64	10.04	11.46	16.71	7.09	6.5	6.65	15.63	10.36	13.9	8.91
Zr	380.13	339.64	204.22	264.64	197.89	155.03	351.3	134.9	87.22	76.42	455.33
Nb	9.25	4.82	8.01	10.3	2.5	3.74	4.61	7.58	4.6	4.45	9.59
Cs	1.68	0.73	1.96	3.27	1.02	0.54	0.66	2.62	0.37	0.72	0.62
Ba	523.80	259.63	270.62	648.76	48.69	108.98	114.16	157.89	667.15	157.85	209.56
La	14.57	9.08	19.26	26.63	8.95	7.39	8.29	25.21	18.84	7.87	23.44
Ce	32.86	19.94	41.38	60.31	22.11	15.21	18.25	55.21	36.61	18.35	50.07
Pr	3.67	2.37	4.45	6.43	2.45	1.64	2.13	4.77	3.88	2.4	4.99
Nd	15.05	9.88	17.03	24.29	10.15	6.2	8.14	19.05	14.43	10.83	18.17
Sm	3.24	2.09	3.10	4.57	2.15	1.2	1.64	3.72	2.51	2.54	2.76
Eu	0.63	0.41	0.76	0.87	0.52	0.24	0.28	0.67	0.51	0.81	0.54
Gd	2.29	1.43	1.50	2.06	1.22	0.8	0.81	1.82	1.17	1.9	1.16
Tb	0.53	0.31	0.41	0.59	0.26	0.22	0.23	0.54	0.35	0.45	0.34
Dy	3.16	1.92	2.37	3.43	1.4	1.31	1.35	3.15	2.14	2.79	1.86
Ho	0.68	0.39	0.46	0.68	0.27	0.27	0.29	0.63	0.42	0.56	0.38
Er	2.07	1.23	1.39	2.03	0.75	0.75	0.87	1.76	1.3	1.6	1.11
Tm	0.31	0.18	0.20	0.31	0.1	0.12	0.13	0.26	0.19	0.23	0.17
Yb	2.06	1.27	1.32	1.92	0.68	0.76	0.95	1.71	1.31	1.45	1.17
Lu	0.30	0.20	0.20	0.29	0.1	0.11	0.15	0.25	0.19	0.22	0.18
Hf	7.43	6.53	4.68	5.77	4.62	3.45	6.77	3.54	2.36	1.99	8.54
Ta	0.50	0.27	0.46	0.54	0.14	0.2	0.24	0.43	0.26	0.26	0.46
Th	3.37	2.35	5.36	6.42	2.79	2.07	3.	5.03	6.18	1.59	10.23
U	0.96	0.63	1.65	1.71	0.58	0.45	0.8	1.28	1.43	0.67	1.08
Zr/Hf	51.17	51.98	43.67	45.84	42.83	44.89	51.92	38.12	36.93	38.49	53.31
Th/U	3.53	3.74	3.24	3.75	4.79	4.62	3.74	3.94	4.31	2.38	9.51
La/Ybn	4.80	4.84	9.94	9.44	8.97	6.61	5.95	10.	9.78	3.7	13.62
La/Smn	2.80	2.72	3.88	3.64	2.59	3.86	3.16	4.23	4.68	1.94	5.31
Gd/Ybn	0.90	0.91	0.92	0.87	1.46	0.85	0.69	0.86	0.73	1.06	0.8
Ce/Ce*	1.09	1.04	1.08	1.12	1.14	1.06	1.05	1.22	1.04	1.02	1.12
Eu/Eu*	0.71	0.73	1.08	0.87	0.98	0.75	0.73	0.79	0.9	1.13	0.92
Nb/Nb*	0.46	0.36	0.27	0.27	0.17	0.33	0.32	0.23	0.15	0.43	0.21
Zr/Zr*	3.69	5.08	1.91	1.7	2.87	3.86	6.52	1.09	0.98	0.99	4.37
Hf/Hf*	2.68	3.62	1.62	1.38	2.49	3.19	4.66	1.06	0.99	0.95	3.04
Ti/Ti*	0.40	0.31	0.64	0.7	0.42	0.55	0.61	0.44	0.58	1.19	1.14

SAMPLE NAME	**14HD2**	**14HD3**	**BRH2**	**BRH3**	**GRY**	**INBO**	**NSHR**
depo age [Ga]	0.1	0.1	0.1	0.1	0.1	0.1	0.1
SiO2	69.10	81.06	89.12	79.52	78.38	84.14	79.31
TiO2	0.519	0.256	0.122	0.128	0.405	0.311	0.291
Al2O3	17.172	12.002	6.543	5.619	12.462	8.776	12.742
Fe2O3	2.178	0.642	0.904	1.407	2.763	1.288	2.204
MnO	0.036	-0.012	0.011	0.242	0.04	0	0.011
MgO	0.989	0.228	0.253	0.417	0.856	0.455	0.646
CaO	3.584	0.106	0.125	11.628	0.715	0.514	0.181
Na2O	4.263	2.671	2.731	2.512	3.795	2.137	3.458
K2O	3.171	3.134	0.494	0.229	2.054	2.556	2.31
P2O5	0.096	0.039	0.019	0.036	0.06	0.035	0.033
Total	101.1	100.1	100.3	101.7	101.5	100.2	101.2
P	404.11	213.15	75.11	122.18	217.88	116.76	106.96
Sc	6.69	3.54	0.83	1.53	6.17	2.78	3.4
Ti	2868	1610	419	439	1887	1292	1152
V	32.87	23.12	4.33	8.31	37.48	17.16	19.62
Cr	7.63	16.18	14.45	66.01	32.79	24.76	28.59
Co	3.26	0.73	1.17	3.8	4.11	2.81	2.54
Ni	19.44	6.18	13.06	12.93	50.23	140.25	5.09
Rb	109.6	204.54	15.55	6.51	57.83	52.64	58.08
Sr	369.91	142.3	36.29	215.84	117.17	80.36	105.46
Y	18.88	21.62	5.48	6.54	14.42	7.57	7.67
Zr	653.33	174.01	50.81	43.92	93.54	311.89	111.73
Nb	13.48	13.32	2.28	1.88	5.74	4.51	4.4
Cs	9.04	6.75	0.35	0.21	1.81	0.88	1.21
Ba	548.61	954.47	65.66	35.26	433.72	389.	398.37
La	66.33	29.34	17.01	8.55	22.35	16.3	13.94
Ce	128.88	49.76	31.71	15.79	40.16	33.23	26.84
Pr	11.6	6.25	3.36	1.93	5.18	3.47	3.09
Nd	39.94	23.11	12.02	7.37	20.16	13.12	11.51
Sm	6.04	4.36	2.	1.4	3.98	2.2	2.02
Eu	1.1	0.64	0.41	0.48	0.78	0.44	0.44
Gd	1.82	2.15	0.76	0.82	2.09	0.84	0.91
Tb	0.65	0.58	0.23	0.19	0.55	0.27	0.27
Dy	3.75	3.9	1.16	1.2	3.18	1.57	1.58
Ho	0.72	0.83	0.22	0.23	0.59	0.31	0.31
Er	2.14	2.54	0.58	0.7	1.69	0.92	0.97
Tm	0.32	0.39	0.09	0.1	0.24	0.15	0.15
Yb	2.33	2.53	0.57	0.67	1.67	1.	1.01
Lu	0.39	0.38	0.09	0.1	0.24	0.16	0.16
Hf	14.11	5.4	1.56	1.35	2.82	6.97	2.87
Ta	0.85	0.76	0.16	0.11	0.36	0.24	0.26
Th	24.43	11.85	3.95	2.38	6.13	5.15	4.34
U	4.59	2.46	0.66	0.63	1.31	1.22	1.03
Zr/Hf	46.3	32.21	32.58	32.65	33.22	44.74	38.94
Th/U	5.32	4.81	5.98	3.79	4.68	4.22	4.24
La/Ybn	19.3	7.88	20.16	8.62	9.08	11.04	9.4
La/Smn	6.85	4.21	5.32	3.8	3.5	4.62	4.31
Gd/Ybn	0.63	0.69	1.07	0.99	1.01	0.68	0.73
Ce/Ce*	1.12	0.89	1.01	0.94	0.9	1.07	0.99
Eu/Eu*	1.01	0.64	1.01	1.36	0.82	0.99	0.99
Nb/Nb*	0.12	0.25	0.1	0.14	0.17	0.17	0.19
Zr/Zr*	2.85	1.18	0.7	0.93	0.71	3.94	1.57
Hf/Hf*	2.29	1.36	0.8	1.05	0.79	3.26	1.5
Ti/Ti*	0.55	0.28	0.23	0.22	0.37	0.56	0.48